

Institut für Chemie und Biologie des Meeres

Fakultät V

Carl-von-Ossietzky-Universität Oldenburg

**Community dynamics, genetic capacities, and  
polysaccharide degradation of marine bacteria over  
geographic, seasonal, and microdiversity scales**

**Habilitationsschrift**

Kumulative Arbeit

Zur Erlangung der *venia legendi*

für das Lehrgebiet

**Mikrobiologie**

Vorgelegt von Matthias Wietz, PhD

Oldenburg, Januar 2024

*für meine Eltern*

## Summary

Microbes are the fundamental drivers of Earth's biogeochemical cycles. Their enormous taxonomic, functional and metabolic diversity are of essential importance for ecosystem functioning – from cellular to community scales, over time and space. Among the multitude of microbial metabolisms in the oceans, polysaccharide degradation is one key process, featuring distinct substrate niches and bacteria-algae interactions. Nonetheless, many aspects regarding the distribution of polysaccharide-degrading taxa and their genetic regulation remain open. One central question is how hydrolytic abilities, and the diversity of metabolic functions in general, affect microbiome assembly over time. Studying temporal variability is especially important in vulnerable and changing systems such as the polar oceans, where the climate crisis exerts substantial pressure on biological communities.

This Habilitation summarizes my research on bacterial polysaccharide degradation, intraspecific diversity, and microbiome seasonality in the Arctic Ocean. The enclosed studies present interdisciplinary insights into the biogeography, identity, genetic repertoire, and regulatory dynamics of polysaccharide degraders on cellular, microhabitat and ocean-wide scales. Experimental incubations revealed distinct “hydrolytic community fingerprints” in the Atlantic, Pacific, and Southern Oceans. Furthermore, studying the genetic machinery and cellular regulation under both simple and complex substrate conditions, including dissolved and particulate polysaccharides, illuminated the microscale underpinnings of larger community dynamics. This integrated molecular and culture-based evidence contributes to a conceptual perspective on polysaccharide utilization in contrasting marine systems.

The establishment of model organisms was essential for studying genetic regulation and intraspecific diversity; addressing hydrolytic capacities and other traits including siderophore production, aromatics degradation, and metabolite secretion – mediators of central element cycles and chemical ecology. Connecting genotypes to niches furthermore contributed to broader eco-evolutionary concepts on species delineation and population assembly.

Finally, my research characterized microbial communities over seasonal and environmental gradients in the Arctic Ocean. Time-series observations via autonomous devices revealed community dynamics over polar day and night, and across different sea-ice and polar water regimes. This microbial inventory in the environmental context establishes a baseline of Arctic microbial ecology, and allows benchmarking future ecosystem shifts.

Overall, the presented research contributes important conclusions for the understanding of microbial diversity and biogeochemical functions in cellular, spatial and temporal dimensions, underlining the relevance of microbes for ecosystem functioning in the current and future ocean.

## Zusammenfassung

Mikroben sind die fundamentalen Treiber globaler biogeochemischer Kreisläufe. Ihre enorme taxonomische, funktionale und metabolische Diversität ist für marine Ökosysteme von zentraler Bedeutung – von der Zelle zur Gemeinschaft, über Zeit und Raum. Innerhalb der Vielfalt mikrobieller Stoffwechselwege ist der Abbau von Polysacchariden ein Schlüsselprozess, gekennzeichnet durch spezifische Nischen und Bakterien-Algen-Interaktionen. Dennoch bleiben viele Aspekte hinsichtlich polysaccharid-abbauender Taxa und ihrer genetischen Regulierung offen. Eine zentrale Frage ist, wie hydrolytische Fähigkeiten, und die Diversität von Stoffwechselfunktionen im Allgemeinen, zeitliche Dynamiken innerhalb des Mikrobioms beeinflussen. Das Verstehen zeitlicher Variabilität ist insbesondere wichtig in gefährdeten und sich verändernden Ökosystemen wie den polaren Ozeanen, in denen die Klimakrise erheblichen Druck auf biologische Gemeinschaften ausübt.

Diese Habilitationsschrift dokumentiert meine Forschung zum bakteriellen Polysaccharidabbau, zur intraspezifischen Diversität, und zur mikrobiellen Saisonalität im Arktischen Ozean. Die beigefügten Studien leisten interdisziplinäre Erkenntnisse zur Biogeographie, Identität, genetischen Vielfalt und regulatorischen Dynamik von Polysaccharidabbauern auf zellulärer, mikrophabitat-bezogener und ozeanweiter Ebene. Experimentelle Inkubationen zeigten spezifische "hydrolytische Fingerabdrücke" im Atlantik, Pazifik und Südpolarmeer. Die Untersuchung der genetischen Maschinerie und zellulären Regulation unter einfachen und komplexen Substratbedingungen, einschließlich gelöster und partikulärer Polysaccharide, beleuchtet die kleinskaligen Grundlagen übergeordneter Gemeinschaftsdynamiken. Die Kombination molekularer und kultivierungsbasierter Ergebnisse erweitert das Verständnis des Polysaccharidabbaus in unterschiedlichen marinen Systemen.

Die Etablierung von Modellorganismen ermöglichte die Untersuchung genetischer Regulierung und intraspezifischer metabolischer Vielfalt; sowohl hinsichtlich hydrolytischer Kapazitäten als auch Merkmalen wie Siderophorproduktion, Aromatenabbau und Metabolitsekretion – Elemente zentraler Stoffkreisläufe und chemischer Interaktionen. Die Verknüpfung von Genotypen und Nischen ergänzt umfassendere ökologisch-evolutionäre Konzepte, wie die Abgrenzung mikrobieller Arten und Assemblierung natürlicher Populationen.

Des Weiteren charakterisierte meine Forschung mikrobielle Gemeinschaften über saisonale und abiotische Gradienten im Arktischen Ozean. Zeitreihenuntersuchungen mittels autonomer Geräte beleuchteten die mikrobielle Dynamik über Polartag und Polarnacht, sowie unter verschiedenen Meereis- und Polarwasserbedingungen. Diese mikrobielle Bestandsaufnahme erzielte grundlegende Schlussfolgerungen über die mikrobielle Ökologie der Arktis, und ermöglicht die Bewertung zukünftiger Ökosystemveränderungen.

Zusammengefasst fördert die vorgestellte Forschung das Verständnis der mikrobiellen Vielfalt und biogeochemischen Funktionen in zellulären, räumlichen und zeitlichen Dimensionen, und unterstreicht die mikrobielle Bedeutung für Ökosystemfunktionen im heutigen und zukünftigen Ozean.

# Table of Content

## Summary

<b>1</b>	<b>Introduction</b>	<b>1</b>
1.1	Marine microbiomes and the cycling of polysaccharides	1
1.2	Geographic and seasonal components of microbial systems	4
1.3	Microbial ecology of the (changing) Arctic Ocean	7
<b>2</b>	<b>Polysaccharide degradation from cellular to oceanic scales</b>	<b>10</b>
2.1	The biogeography of polysaccharide degradation	10
2.2	The genetic machinery and cellular regulation of polysaccharide degradation	12
2.3	Polysaccharide microhabitats: sensing, utilization, and regulation	16
<b>3</b>	<b>Intraspecific diversity</b>	<b>19</b>
3.1	<i>Alteromonas</i> microdiversity and niche specialization	19
<b>4</b>	<b>Polar microbiomes, seasonality and the future Arctic Ocean</b>	<b>22</b>
4.1	Year-round microbial diversity in Arctic and Atlantic ecosystem states	23
4.2	Influence of “Arctic Atlantification” on microbial ecology and seasonality	25
<b>5</b>	<b>Synopsis and Outlook</b>	<b>26</b>
<b>6</b>	<b>References</b>	<b>29</b>
<b>7</b>	<b>Manuscripts summarized in this thesis</b>	<b>43</b>
<b>8</b>	<b>Complete publication list</b>	<b>44</b>
<b>9</b>	<b>Teaching</b>	<b>48</b>
<b>10</b>	<b>Acknowledgments</b>	<b>49</b>
	<b>Appendix</b>	<b>50</b>

## 1. INTRODUCTION

Microbial communities are vital for ecosystem health and functioning. Bacteria and archaea (herein referred to as prokaryotes) account for ~60% of the ocean's biomass, constituting approximately four gigatons of carbon [1]. The global amount of  $\sim 10^{29}$  prokaryotic cells by far outnumber stars in the universe. The enormous taxonomic and functional diversity within prokaryotic communities represents one major foundation of the marine food web, driving biogeochemical cycles and fueling higher trophic levels. These dynamics include a cascade of species, genes and interactions [2–4], mediating chemical transformations and ecosystem services worldwide – from polar sea-ice to the tropical oceans. The implications of geographic distance and environmental selection for biodiversity and biogeochemistry remains one key aspect in microbiological research. Furthermore, biological dynamics scale with the seasonal cycle, with particularly marked gradients in the polar regions. Ocean-wide, whole-community variability in metabolic capacities is underpinned by substantial microdiversity, with distinct traits and niches among individual strains of a taxon [5].

This Habilitation summarizes my research over the past decade, exploring the taxonomic and functional diversity of prokaryotes from global to intraspecific scales, with special emphasis on polysaccharide biogeochemistry and the seasonality of polar microbiomes. In three chapters, I present insights into (i) the community structure, genetic diversity, and cellular regulation of bacterial polysaccharide degradation; (ii) the intraspecific diversity and adaptations in *Alteromonas*; and (iii) the microbial ecology and seasonality in the Arctic Ocean. First, I summarize the key concepts, present knowledge, and open questions. The main part then encapsulates my corresponding research via a summary of nine publications.

### 1.1 Marine microbiomes and the cycling of polysaccharides

Microorganisms, including primary producers and heterotrophic recyclers, are the major drivers of marine biogeochemical cycles. They play a key role in the biological carbon pump, which mediates carbon supply, consumption, and storage in the oceans [6–8]. Over the past 20 years, molecular methodological advances have substantially improved the taxonomic and functional understanding of marine prokaryotes. Metabarcoding of marker genes (mostly 16S rRNA, but also metabolic genes) has revealed how communities assemble under specific environmental conditions, which organisms encode major metabolic pathways, and how these dynamics are rooted in the ecosystem context. Meta-omic sequencing has extended the understanding of microbial communities to a systemic level, illustrating the genetic diversity underpinning biogeochemical transformations and nutrient fluxes. Large-scale research endeavors have illuminated marine microbial diversity from surface to seafloor, global biogeographic patterns, responses to changing environmental conditions, as well as genetic adaptations [9–16]. Dedicated polar expeditions including MOSAiC and Tara Arctic [17–20] are invaluable indicators of polar oceans during the escalating climate crisis.

Prokaryotes possess an enormous taxonomic and functional diversity, encoding an almost infinite range of metabolic reactions for energy production and growth. Within this metabolic spectrum, heterotrophic bacteria rely on the oxidation of organic compounds. This reservoir is immense, encompassing both labile and recalcitrant compounds, with thousands of molecular

formulae detected by untargeted metabolomics of seawater [21]. This chemical diversity is enriched by the secretion of various organic compounds by microbial species [21, 22]. One important class of organic compounds are carbohydrates, constituting 15–50% of dissolved organic matter in the oceans, with spatial and seasonal variations [23–27]. In a review co-authored by myself [28], we have budgeted the sources and sinks of marine carbohydrates (Figure 1). The carbohydrate pool includes oligomers (typically <10 monomers) and polysaccharides (high-molecular, often branched chains), produced by algae and zooplankton. Phytoplankton and macroalgae synthesize a wide spectrum of polysaccharides, representing storage and structural components for the producing organism [29, 30] and fueling the heterotrophic food web [31]. Of the ~1.3 petagram atmospheric carbon fixed by marine macroalgae every year [32], up to half are converted into polysaccharides. Considering that macroalgae export ~40% of the fixed carbon into the surrounding water, either by exudation or cell death [33–35], there is a considerable flux of polysaccharides into the oceans. Typical macroalgal polysaccharides are laminarin, alginate, agar, ulvan, and carrageenan; compounds with different chemical composition and complexity [36]. In addition to algal polysaccharides, chitin produced by zooplankton and crustaceans constitutes a global amount of 100 billion tons [37, 38]. As detailed below, this immense carbon pool represents a central nutrient source for heterotrophic bacteria – from coastal waters to deep-sea sediments.

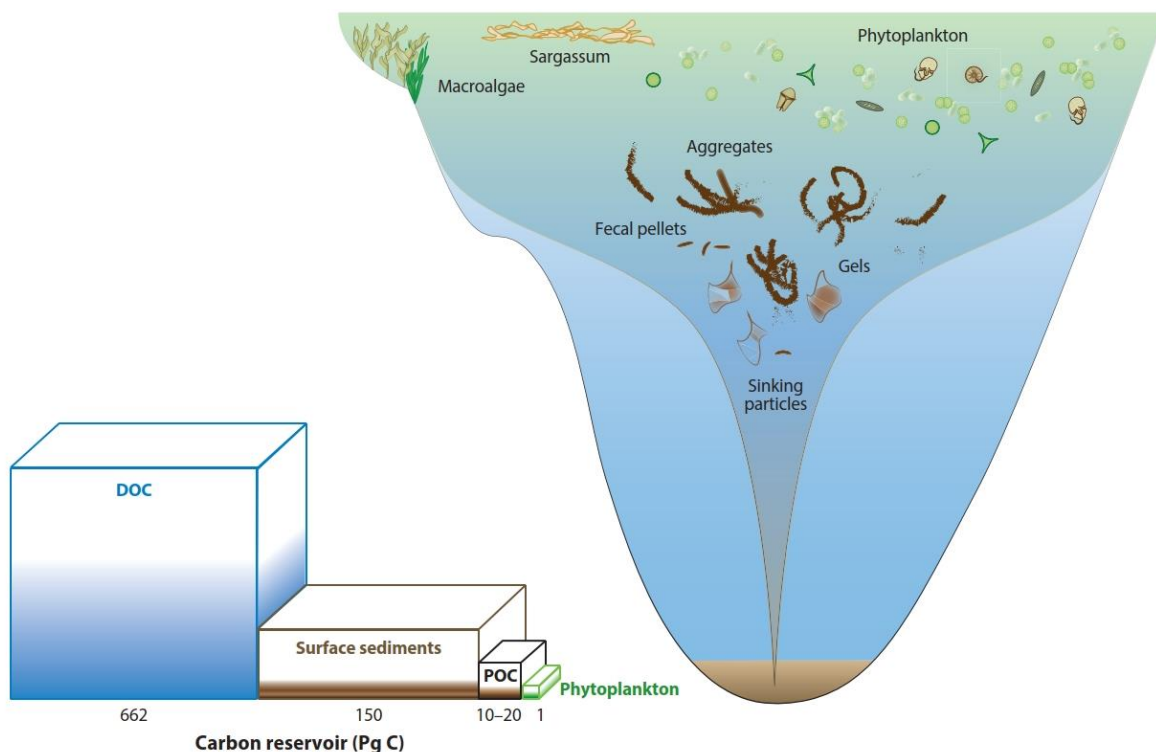


**Figure 1: Polysaccharide sources and reservoirs in the oceans.** Amounts are illustrated via box sizes and estimated quantities in petagram below. Transformation of photosynthesis-derived organic matter yields aggregates, gels, and particles that contribute to vertical export flux of organic matter, of which a minor fraction (symbolized by the narrowing funnel) reaches the seafloor. The shading of boxes illustrates the contribution of carbohydrates to the total carbon content per reservoir [28].

Polysaccharides are complex, often branched compounds with molecular weights of up to 500 kilodalton, with diverse modifications and decorations (e.g. sulfation or methylation). Polysaccharides occur in a spectrum of dissolved, particulate, colloidal and microgel forms; including relatively simple (e.g. laminarin) and complex polymers (e.g. alginate, fucoidan). Polysaccharides are challenging to quantify in their native conformation, and budgeting oceanic reservoirs so-far largely relied on estimates derived from acid-hydrolysis. Such approaches indicated that acidic polysaccharides constitute ~10% of particulate organic matter (POM) in the oceans [39]. Transparent exopolymer particles, a type of POM largely composed of acidic polysaccharides, represent hotspots of marine microbial activity [40–42]. The natural gelling properties of some polysaccharides, including alginate and agar, contribute to the formation of POM; a fraction of which reaches the seafloor via gravitational sinking. This vertical export from surface waters to the deep sea, termed benthopelagic coupling, is a major nutrient source for abyssal and benthic organisms. Yet, several elements of the carbohydrate cycle are only beginning to be resolved. Recent methodological advances using topical antibodies enable a refined quantification of specific polysaccharide classes, and the identity of enzymes that target these polymers [43–45]. Notably, some polysaccharides are highly resistant to microbial degradation, potentially fueling long-term carbon sequestration [43].

The identity of polysaccharide-degrading microbes is a focal point of research. Following pioneering studies on terrestrial hydrolytic bacteria [46–48], polysaccharides are now widely recognized as important nutrient source for marine bacteria. Bacteria degrade and metabolize polysaccharides via specialized enzymes, termed CAZymes [49], encoded by diverse phyla (Figure 2). CAZymes include glycosyl hydrolases (GHs), polysaccharide lyases (PLs), carbohydrate esterases (CEs) and carbohydrate-binding modules (CBMs), often encoded in polysaccharide utilization loci (PULs) facilitating the concerted degradation [50]. A recent global survey revealed highest CAZyme numbers in plant-associated bacteria [51], connected to the structural complexity of plant biopolymers. Macroalgae, the marine equivalent of land plants, are therefore an important habitat for hydrolytic bacteria. Nonetheless, supported by the ample horizontal gene transfer among bacteria, CAZymes occur across all marine ecosystem compartments, from host-associated microbiomes to the water column [51].

Marine CAZymes have been mainly studied in phylum Bacteroidota, including the species *Zobellia galactanivorans*, *Gramella forsetii*, and *Formosa agariphila* [52–56]. In Gammaproteobacteria, hydrolytic strains are found among *Alteromonas*, *Pseudoalteromonas*, and *Colwellia* [57–59]. Hydrolytic bacteria show different degrees of specialization depending on their CAZyme repertoire, and hence occupy narrow or broad “polysaccharide niches”. Furthermore, hydrolytic bacteria employ distinct ecological strategies; some utilizing the majority of substrate using a “selfish” mechanism, and some sharing monomers via cross-feeding [60]. These characteristics can vary between strains of single species [61], highlighting extensive microdiversity in hydrolytic potential [62]. Overall, simple glucose-based glycans like laminarin can be utilized by numerous microorganisms. In contrast, recalcitrant structures like sulfated fucans are only accessible to highly specialized taxa. For instance, fucoidan degradation by Verrucomicrobia requires approximately 100 enzymes, including a megaplasmid [63]. The diversity of ecological strategies and specializations often results in successional patterns of bacterial taxa and CAZymes during a phytoplankton bloom, stimulated by distinct suites of glycans from different algae [64–67].

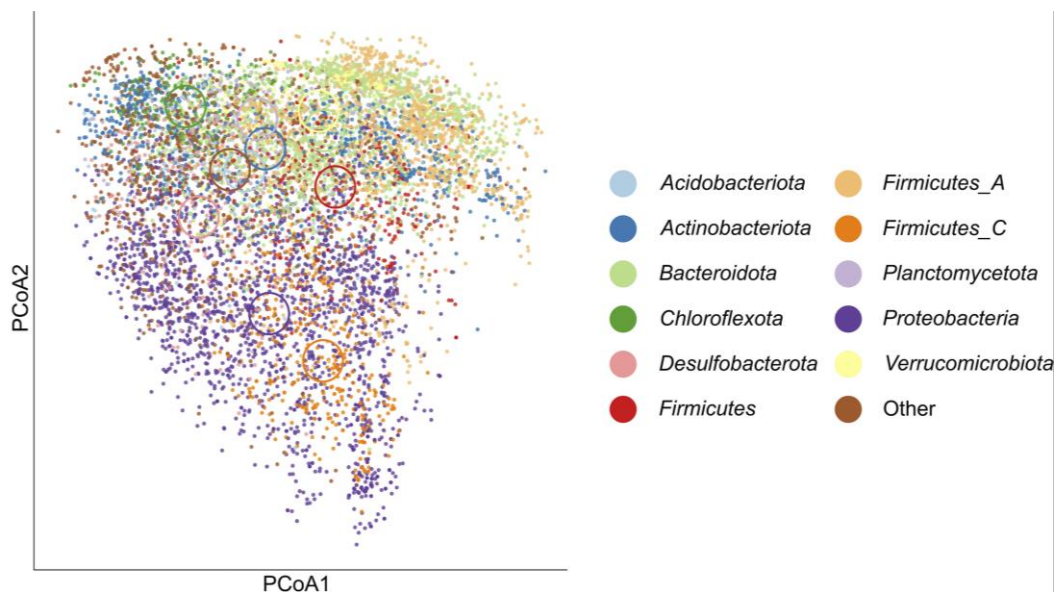


**Figure 2: Prevalence of CAZymes among bacteria.** Principal Coordinates Analyses of CAZymes within 9143 metagenome-assembled genomes from global locations [51].

## 1.2 Geographic and seasonal components of microbial systems

Marine microbial dynamics and biogeochemical processes, including polysaccharide degradation, show spatial and seasonal variation. Regional differences between biological communities, referred to as biogeography, is influenced by major gradients in environmental conditions. For instance, chlorophyll (as proxy for primary production) and nutrient regimes regionally differ in context of oceanographic features, helping to define biogeographic provinces [68–70]. Spatial variability occurs from micro- to macroscales; influenced by fronts, eddies, and oceanic currents [71–73]. Four major mechanisms – selection, drift, dispersal, and mutation – have been attributed to creating and maintaining microbial biogeography across ecological and evolutionary scales, including distance-decay relationships [74].

Remote sensing via satellites can track large-scale geographic contrasts in e.g. primary production. However, detailed insights into microbiome structure, interactions and activities – such as polysaccharide degradation – require *in situ* evidence. The Tara, Malaspina, BioGEO TRACES and Bio-GO-SHIP expeditions study microbial diversity and function across oceanic realms. Following the sequencing of environmental DNA (eDNA), the analysis of amplicon sequence variants (ASVs) and metagenome-assembled genomes (MAGs) can decipher microbial niches and adaptations [75]. Integrating biological and physicochemical information (Figure 3) contributes towards a mechanistic understanding of biodiversity and its response to environmental variation, from surface to deep waters [76]. For instance, a catalogue of 47 million microbial genes derived from Tara Oceans enabled quantitative insights into organismal turnover and gene expression changes [76]. Moreover, such datasets indicated considerable microdiversity; i.e. extensive variation in functional traits between closely related strains. This has been shown for the abundant cyanobacterium *Prochlorococcus* [75], but also less abundant but metabolically versatile taxa such as *Alteromonas* [77].

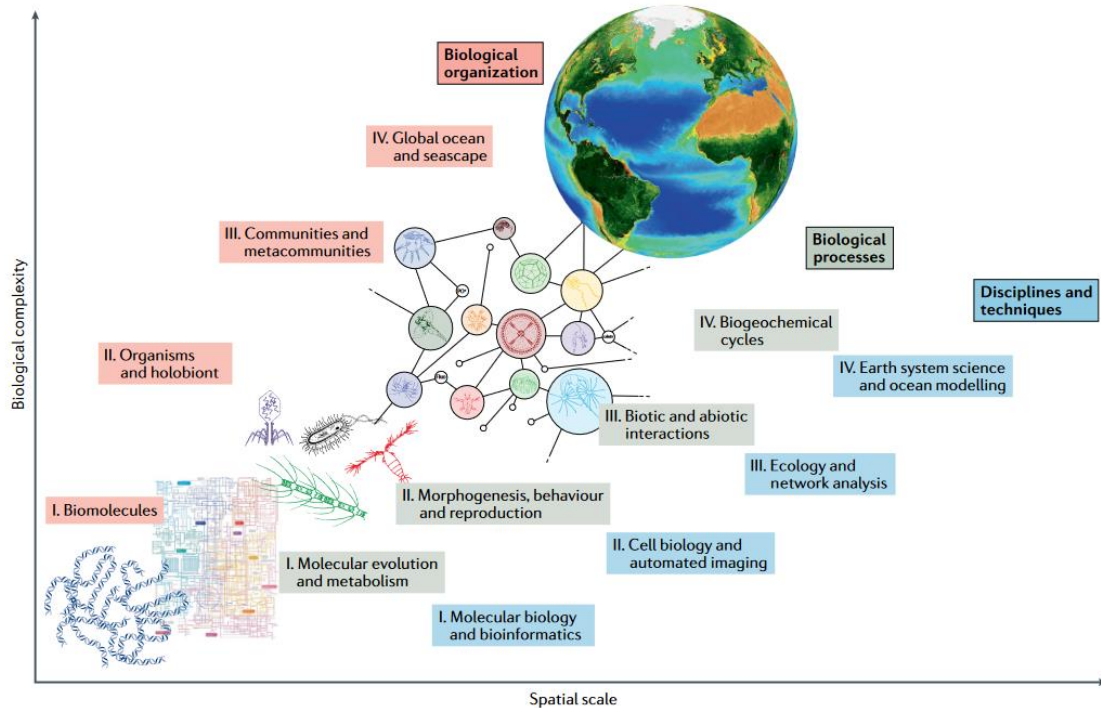


**Figure 3: Integrative analyses towards the systemic understanding of marine microbial ecology within the (a)biotic framework.** Scope of the planetary-scale dataset from Tara Oceans to reconstruct an eco-evolutionary framework, from genes to the biological carbon pump [76].

Transects along extended sections of the world’s oceans substantially contribute to the biogeographic understanding of marine microbiomes. For instance, high-resolution metagenomics across the Atlantic revealed peaking bacterial richness around 40° latitude at intermediate water temperatures, with regional variability of functional gene clusters mediating biochemical pathways. Distance-decay rates of gene profiles mostly related to biotic factors, whereas taxonomic distribution scaled with temperature and biogeographic province [78]. A related study across the Pacific Ocean, sampling along a transect of ~12,000 km between subantarctic and subarctic regions, showed that homogeneous selection contributed ~60% to microbial community structure in the epipelagic, whereas drift had the strongest influence on particle-associated communities in the upper mesopelagic [79].

However, biogeographic studies rarely address temporal dynamics. Tracking microbial dynamics and drivers over time requires recurrent samplings at the same location, which is infeasible across broad geographic ranges. Generally, microbial seasonality follows phytoplankton growth and the corresponding production of organic matter, inducing degradative cascades via heterotrophs, grazers and viruses that scale with latitude, coastal proximity, and stratification (Figure 4) [80]. Concurrent biological interactions, such as the exchange of metabolites, can stimulate short-term fluctuations [81]. Marine biological observatories (for instance SPOT, BATS, HOTS, Helgoland Roads) have been established worldwide, mostly at coastal locations to ensure consistent records. However, continuous monitoring of microbial communities through eDNA sequencing has only started in recent years. Time-series studies are indispensable for discerning the dynamics and drivers of marine microbiomes – from days to

decades, and across ecological and biogeochemical gradients [80, 82–84]. Sampling resolution has a major influence, as microbial dynamics can be rapid (e.g. transcriptional responses within minutes after a nutrient pulse) as well as long-term along broad seasonal gradients [85–87]. Decadal records of key ecological indicators, like phytoplankton cell numbers and chlorophyll concentrations, are to date mostly available from warmer waters. In contrast, such records are rare from the polar oceans, where continuous samplings are challenged by harsh environmental conditions. However, such evidence is essential in view of climate change and its impact on biological communities.

Key for successful long-term observations is the international coordination and integration, along the FAIR principles of science – ensuring a comprehensive understanding of the state and health of the oceans, fostered by global initiatives like the UN Ocean Decade [88]. For instance, collaborative approaches should emphasize the establishment of common bioindicators, streamlined protocols and synchronized observations, allowing to systematically assess phenomena of scientific and societal relevance.

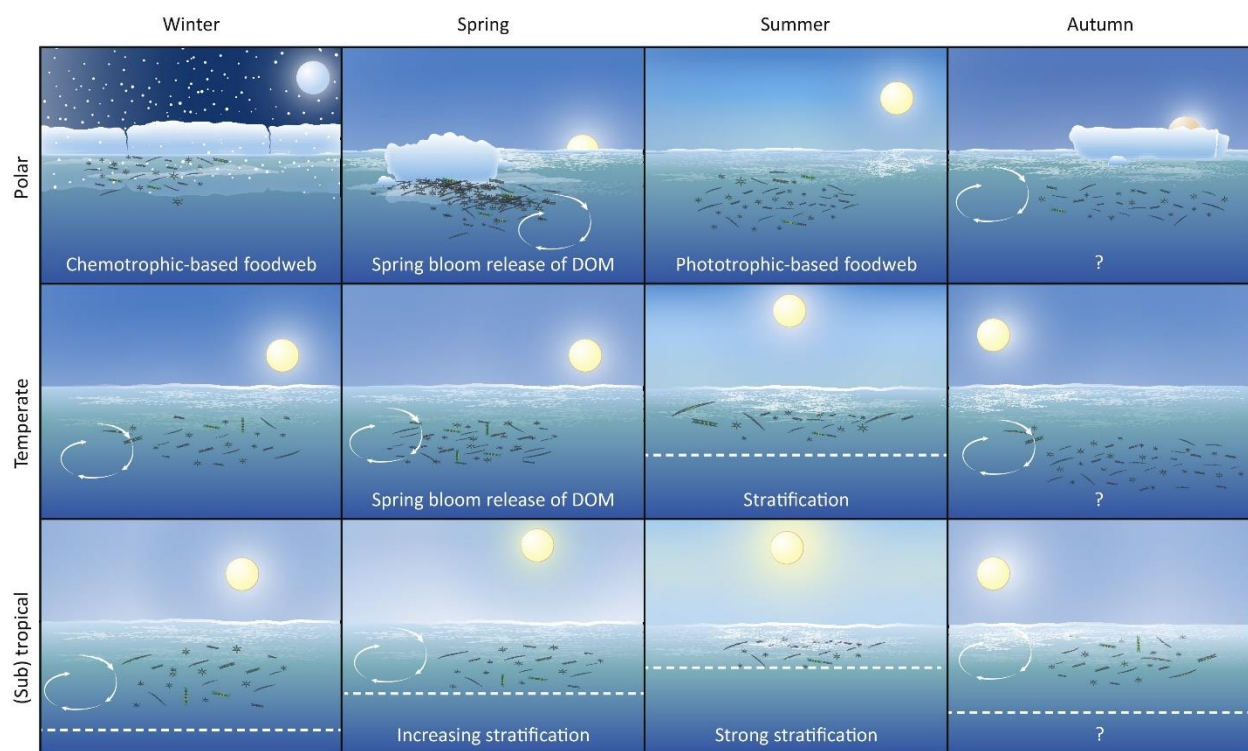


**Figure 4: Principles of microbial seasonality in polar, temperate and tropical oceans.** In polar regions, wintertime darkness limits phytoplankton growth, followed by a short productive season (see sections 1.3 and 4.1 for more details). Temperate oceans typically feature an overturn of the water column in autumn and winter, followed by a marked spring phytoplankton bloom and summertime stratification; with concurrent successional shifts of microbial taxa. In tropical regions, offshore waters are often mixed by wind or ocean currents, compared to upwelling of nutrient-rich water at the coasts. During summer, water masses are stratified at shallow depths, and temperatures are high in surface waters. Periods with limited data coverage are indicated by question marks. Figure from [80].

### 1.3 Microbial ecology of the (changing) Arctic Ocean

The polar oceans show unique physicochemical and biological signatures; shaped by daylight, water column stratification, and nutrient availability. Polar day and night – with intense gradients in solar radiation and sea-ice cover – are key determinants of life. Furthermore, the permanently cold water temperatures require specific cellular adaptations, especially for organisms living in sea-ice. These factors explain the presence of distinct biological communities in polar habitats, featuring latitudinal diversity gradients and “bipolar taxa” occurring in both Arctic and Antarctic waters [89–92]. The biological carbon pump and its microbial underpinnings show special characteristics across the diverse ecosystem compartments (Figure 5). In the Arctic Ocean, microbial ecology and biogeochemical functions are fundamentally determined by the short productive season, with elevated photosynthesis followed by aggregate formation and organic matter export to the deep sea. The polar winter is little studied due to logistic constraints and limited accessibility; however, it becomes increasingly clear that this period is not biologically inactive but harbors diverse microbial metabolisms and strategies, for instance driving nutrient recycling during vertical mixing [93]. Other organisms overwinter in dormancy [94], but quickly awake with even minimal solar radiation [95].

Sea-ice is a fascinating element of polar ecology, with relevance across trophic levels (Figure 5). The porous matrix of sea-ice brine channels is highly productive, constituting the basis of an ice-associated food web comprising diatoms, heterotrophic bacteria, protists (ciliates, flagellates, foraminifera), and meiofauna (nematodes, copepods, rotifers, polychaetes). Especially the lower section and the underside of ice are biologically active, featuring elevated cell numbers and primary production fueled by nutrients from the underlying ocean. In turn, ice-derived organic matter can enter the water, and stimulate rapid microbial responses [96, 97]. Furthermore, sizeable mats of filamentous algae growing on bottom ice are released during the melting season and quickly sink to the seafloor. This seeding has important ecological consequences for both pelagic and benthic organisms; scaling with the origin and characteristics of sea-ice that often varies between years [98–100]. Regional differences in hydrography and sea-ice cover, for instance between the transpolar drift and the Arctic-Atlantic interface, are important factors for the biological carbon pump. For instance, surface waters across the Fram Strait – the major gateway between the North Atlantic and the central Arctic Ocean – harbour distinct microbial communities in vertical and horizontal dimensions, shaped by sea-ice cover and polar water proportions [101]. Furthermore, local variability around submesoscale features and near the sea-ice margin – with strong environmental gradients over short spatial scales – can substantially influence microbial patterns [102, 103].

Surface production eventually results in the transfer of energy to deeper waters via sinking particles. In the Fram Strait, diatom-rich aggregates in ice-covered regions mediated two-fold higher carbon export, coincident with increased export of microbes to the deep sea [104]. The magnitude of export events can differ by year and region, scaling with phytoplankton bloom phenologies and primary productivity; including the ratio of diatoms and mixotrophic flagellates [105–108]. In addition, microbial ecology and activities can respond to specific perturbations. For instance, a warm-water anomaly in Fram Strait resulted in markedly changing microbiomes on sinking particles – signifying that the dynamics of benthopelagic coupling are sensitive to environmental change [109].

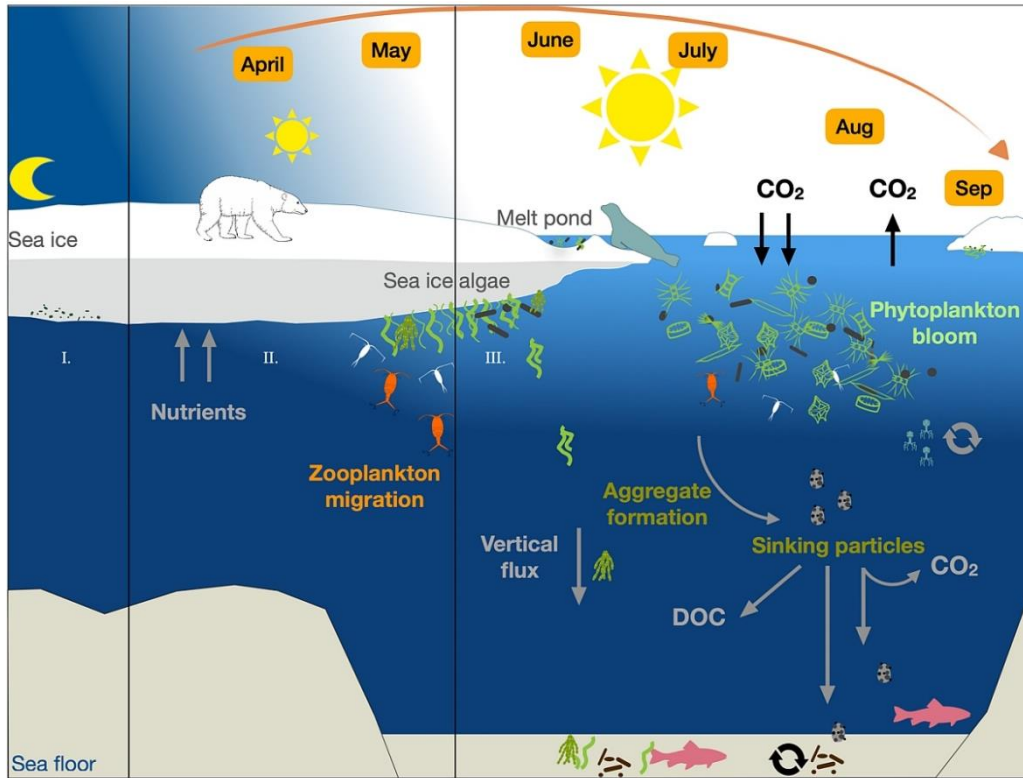


**Figure 5: The Arctic biological carbon pump.** The seasonal growth of phytoplankton stimulates heterotrophic bacteria, grazers, and the viral shunt. In autumn, organic matter is exported to deeper waters via sinking particles and vertical migration of zooplankton. A fraction of the exported carbon is sequestered for centuries to millennia. Nutrient replenishment during winter mixing fuels the following productive season [110].

Yet, broad assessments of Arctic microbiome structure and function in the environmental context remain sparse, largely owing to logistic challenges and the inaccessibility during polar night. The recent MOSAiC and Tara Arctic expeditions are establishing baseline catalogues of microbial diversity across Arctic regions (Figure 6), showing considerable horizontal and vertical contrasts in microbiome structure and function [19, 20]. Specific follow-up studies on e.g. ice-binding proteins [111] inform about essential microbial adaptations, and allow benchmarking future changes. The Arctic warms fourfold faster than the global average, coincident with rapidly declining sea-ice over the past decades [112]. Climate change significantly alters polar ecosystems across physical, chemical, and biological scales [113, 114]. Future projections suggest frequent ice-free summers by 2050, especially in the Eurasian Arctic alongside the expanding influence of Atlantic waters [115]. Associated hydrographic and physicochemical changes, termed Atlantification, facilitate the northward expansion of temperate organisms and will likely result in the establishment of new biological communities [116–118]. For instance, temperate cyanobacteria like *Synechococcus* have been recently detected near Svalbard [119]. Longer ice-free periods and thinner ice stimulate primary production, considerably affecting the organic matter pool and nutrient availability [120, 121]. Accelerated and amplified ice melt furthermore modifies the vertical export of organic matter: strong melt events result in intense

stratification, trapping organic material at the surface – i.e. limiting benthopelagic coupling and long-term carbon storage in the ocean’s interior [122–124]. The observation of concurrently weakened microbial connectivity between surface and deeper waters [124] substantiates the notion of lower export efficiency during sea-ice loss, likely affecting both local and global biogeochemical cycles.

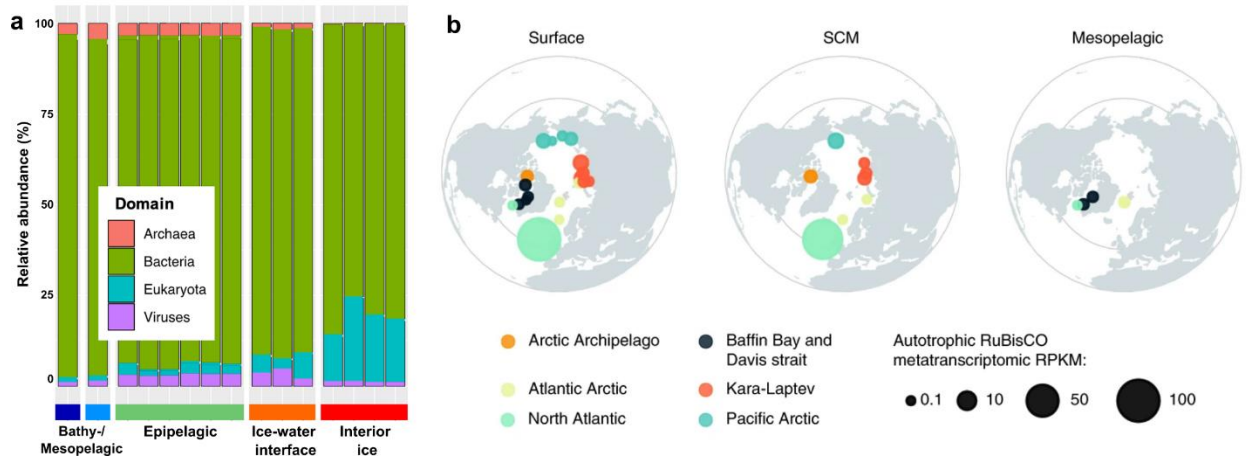


**Figure 6: Microbial patterns in different Arctic ecosystems. A:** Abundances of major microbial groups across the central Arctic Ocean, with a notable enrichment of eukaryotes versus an absence of archaea in interior sea ice [19]. **B:** Transcript abundances of RuBisCO genes (ortholog K01601 in the KEGG database) in different water layers, colour-coded by region [20].

Studying the ecological consequences of environmental variation is essential to assess the current and future functioning of polar ecosystems. To meet this goal, ecosystem structure and inhabiting organisms need to be studied over time. Available studies have shown variable numbers, activities and communities in polar habitats over time and space [125–127], yet with limited temporal resolution – especially in pelagic waters and across natural gradients, such as the Arctic-Atlantic interface in Fram Strait. Assessing ecosystem shifts requires continuous monitoring programs under different environmental conditions. While sea-ice cover and chlorophyll concentrations are trackable via satellites [128, 129], the dynamics of pelagic communities are only discernable through *in situ* observations [82, 130, 131]. Only few multiannual records are available from the polar oceans to date, for instance from the Antarctic Peninsula [89, 132, 133]. In the Arctic Ocean, the FRAM and HAUSGARTEN long-term observatories study microbiology and oceanography over the year, towards a mechanistic understanding of the biological carbon pump in context of declining sea-ice and Atlantification. FRAM studies have shown that Atlantic-influenced waters are more productive and feature stronger seasonal contrasts, with central implications for benthopelagic coupling [104, 123, 134, 135]. New autonomous technologies are a key advance in this regard, recently providing the first year-round records in the Arctic and Antarctic Oceans [122, 136–139]. Such approaches can identify transition phases in the seasonal interplay between ocean physics and the ecosystem, for instance the onset of the spring bloom and how biophysical processes contribute to nutrient replenishment in winter [93, 94, 140, 141].

## 2. POLYSACCHARIDE DEGRADATION FROM CELLULAR TO OCEANIC SCALES

There is still limited understanding of the cellular regulation of polysaccharide degradation in marine bacteria, and how hydrolytic activities are embedded in the community and ecosystem context. Answering key open questions requires a conceptual view that embraces cellular, microhabitat, and ocean-wide dimensions – contextualizing the identity, distribution, genetic repertoire, and regulatory dynamics of polysaccharide degraders. For instance, linking the biogeography and genetics of hydrolytic bacteria can assess functional redundancy in polysaccharide degradation between oceanic regions. Here, I present six key studies investigating bacterial community dynamics, ecophysiology, and gene regulation under both simple and complex substrate regimes: when encountering a single polysaccharide in dissolved or particulate form, in comparison to encountering mixtures of dissolved and particulate polysaccharides. These complementary insights contribute towards the understanding of polysaccharide utilization in natural, highly heterogeneous marine systems. Of particular importance was the establishment of model strains from the genus *Alteromonas*, including *Alteromonas macleodii*.

### 2.1 The biogeography of polysaccharide degradation

**Appendix 1:** [Wietz M](#), Wemheuer B, Simon H, Giebel H-A, Seibt MA, Daniel R, Brinkhoff T, Simon M (2015). Bacterial community dynamics during polysaccharide degradation at contrasting sites in the Southern and Atlantic Oceans. *Environ. Microbiol.* 17:3822–3831. [doi:10.1111/1462-2920.12842](https://doi.org/10.1111/1462-2920.12842)

My research on bacterial polysaccharide degradation founds on two expeditions with RV Polarstern to the Southern and Atlantic Oceans in 2011 and 2012, during which we performed microcosm experiments with polysaccharide amendments. In 2016, similar experiments were conducted along a Pacific Ocean transect. This ocean-scale approach revealed specific ‘hydrolytic community fingerprints’ in contrasting oceanic biomes, i.e. that bacterial communities from distinct regions harbor different potentials to utilize polysaccharides. This predominance of location-specific patterns advanced the spatial understanding of polysaccharide cycling in the world’s oceans. Concurrently, I established several model organisms to support community fingerprints with physiological and genomic evidence.

The Polarstern expeditions (ANT28-2 and ANT28-5) were the first performing polysaccharide degradation experiments in contrasting oceans (Figure 7). Amending natural seawater with alginate, agarose or chitin, followed by amplicon sequencing and substrate quantification, revealed markedly different responding taxa. These patterns were attributed to distinct, site-specific biological and hydrographic conditions. Both the Polar Front and Antarctic Ice Shelf featured strong responses of Bacteroidota to chitin amendment, with up to 24% higher cell numbers. At the Patagonian Continental Shelf, alginate and agarose degradation covaried with elevated abundances of distinct *Alteromonadaceae* populations, each with specific temporal dynamics. At the Mauritanian Upwelling, only the alginate monomer guluronate was consumed, coincident with increasing abundances of *Alteromonadaceae*. The genus *Reichenbachiella* (Bacteroidota) was stimulated by chitin at all cold/temperate stations, suggesting comparable ecological roles over wide geographical scales. An important complement was the isolation of bacteria from these microcosms, using selective media with polysaccharides as sole carbon

source. From a collection of ~60 strains, following tests in liquid minimal media identified three with marked hydrolytic potential: *Alteromonas macleodii* 83-1, *Alteromonas* sp. 76-1 and *Maribacter dokdonensis* 62-1, subsequently investigated in detailed physiological and genetic studies (see section 2.2). Establishing *Alteromonas* strains as model polysaccharide degraders was a key outcome, since hydrolytic Gammaproteobacteria are little studied to date.

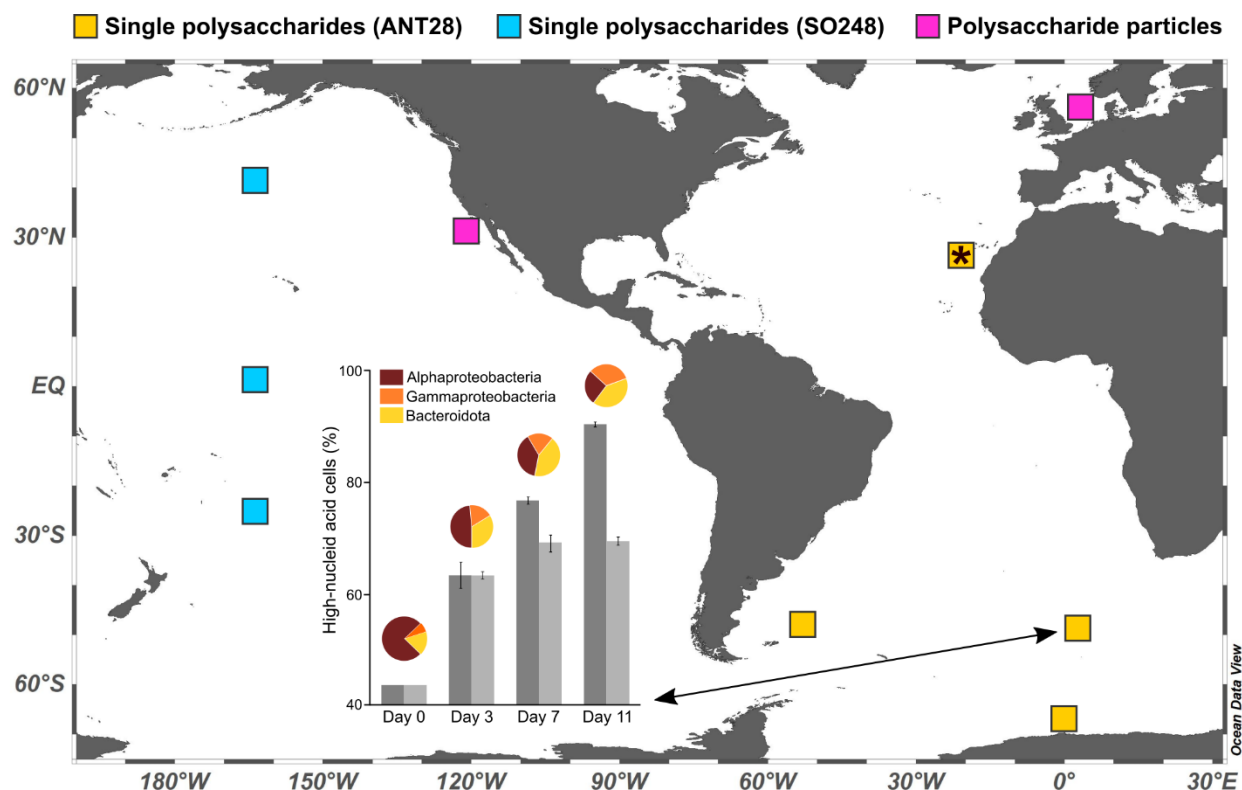


**Figure 7: Biogeography of polysaccharide degradation, studied via experimental incubations.** Locations of microcosms with addition of single or particulate polysaccharides. Insert: percentage of high-nucleic acid cells with chitin (dark bars) vs. alginate/agarose addition (light bars), and proportions of major bacterial classes with chitin (circles) at the southern polar front. *A. macleodii* strain 83-1 from the Mauritanian upwelling (marked by asterisk) was established as model organism for gammaproteobacterial polysaccharide degradation.

Considering the alginolytic abilities of the new model isolates, together with the widespread occurrence of alginate in macroalgae where it can constitute half of dry weight [36], my subsequent research focused on alginate degradation. On expedition SO248 with RV Sonne, traversing the Pacific Ocean from New Zealand to Alaska along the 180° meridian, we incubated natural seawater with alginate, alongside the quantification of various oceanographic and biogeochemical parameters [142]. Comparable to varied patterns between Atlantic Ocean provinces, we observed biogeographic variability of hydrolytic communities. Here, additional isolates were obtained; including each one *A. macleodii* strain from the South Subtropical Gyre, Equatorial Upwelling, and Northern Polar Front. Notably, the genomes of Pacific strains were almost identical to the genome of *A. macleodii* 83-1 from the Mauritanian upwelling. This finding was essential for my studies on intraspecific diversity (see Chapter 3).

## 2.2 The genetic machinery and cellular regulation of polysaccharide degradation

**Appendix 2:** Neumann A, Balmonte JP, Berger M, Giebel H-A, Arnosti C, Voget S, Brinkhoff T, Simon M, Wietz M (2015). Different utilization of alginate and other algal polysaccharides by marine *Alteromonas macleodii* ecotypes. *Environ. Microbiol.* 17:3857–3868. [doi:10.1111/1462-2920.12862](https://doi.org/10.1111/1462-2920.12862)

**Appendix 3:** Koch H, Dürwald A, Schweder T, Noriega-Ortega B, Vidal-Melgosa S, Hehemann J-H, Dittmar T, Freese HM, Becher D, Simon M, Wietz M (2019). Biphasic cellular adaptations and ecological implications of *Alteromonas macleodii* degrading a mixture of algal polysaccharides. *ISME J.* 13:92–103. [doi:10.1038/s41396-018-0252-4](https://doi.org/10.1038/s41396-018-0252-4)

**Appendix 4:** Koch H, Freese HM, Hahnke RL, Simon M, Wietz M (2019). Adaptations of *Alteromonas* sp. 76-1 to polysaccharide degradation: A CAZyme plasmid for ulvan degradation and two alginolytic systems. *Front. Microbiol.* 10:504. [doi:10.3389/fmicb.2019.00504](https://doi.org/10.3389/fmicb.2019.00504)

Model isolates are a valuable, yet sometimes overlooked resource in the times of high-throughput sequencing. While providing a wealth of genomic information, ‘omics studies often remain speculative since functional assessments rely on the prediction of gene functions by sequence homology, mostly without experimental verification. Hence, molecular studies only indirectly inform about bacterial traits, based on taxon and gene abundances under specific environmental conditions. Traditional isolation of bacterial strains is low-throughput and challenging, since only a fraction of bacteria can be cultured. Nonetheless, isolation offers the potential to obtain strains that represent taxa with abundance *in situ*, whose metabolic and phenotypic traits can then be tested in the laboratory – important to achieve ecological conclusions. My research established the strains *Alteromonas* 83-1, *Alteromonas* 76-1 and *Maribacter* 62-1 as model organisms with closed genomes; enabling detailed physiological and genomic support for molecular evidence. For *Alteromonas* 83-1, a matching 16S rRNA amplicon was found abundant in metabarcoding data from the Pacific, underlining how laboratory studies can strengthen ecological conclusions. Here, I present results from the two *Alteromonas* strains, able to degrade alginate, laminarin, xylan, pullulan, and ulvan. By combining genomics, transcriptomics, proteomics and culturing, we established key insights into hydrolytic Gammaproteobacteria and their PULs.

This initial study on *Alteromonas* strain 83-1, in collaboration with University of Chapel Hill, investigated alginate utilization via growth curves, HPLC quantification of monomers, and comparative genomics (Appendix 2). Real-time quantitative PCR showed considerable upregulation of alginate lyases when grown with alginate compared to glucose (Figure 8), accordant with decreasing concentrations of alginate monomers. We optimized hydrolysis and quantification protocols to measure concentrations of the constituent monomers mannuronate and guluronate; highlighting that hydrolyzed polymers were indeed metabolized. Genomic analysis identified 83-1 as a strain of the species *Alteromonas macleodii*. This finding facilitated comparative studies, as ~15 related genomes from worldwide locations are publicly available. During the time, *A. macleodii* strains were distinguished into “surface“ and “deep ecotype“, and we found that only the “surface ecotype“ encodes alginate lyases. This finding matches the subsequent reclassification of deep-ecotype strains as *A. mediterranea*, showing that both phenotype and genotype contribute to species delineation. Furthermore, incubations with

fluorescently labelled polysaccharides demonstrated that 83-1 also hydrolyzes xylan, pullulan and laminarin. The identification of *A. macleodii* as versatile polysaccharide degrader substantially advances the knowledge about the metabolic adaptations of this taxon, and provided important avenues for subsequent studies.

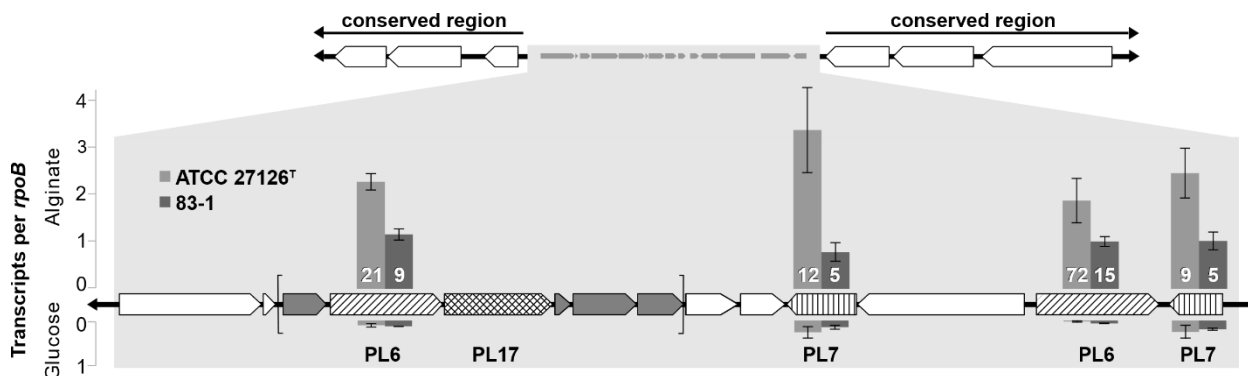


**Figure 8:** The first alginolytic operon in marine Gammaproteobacteria described in detail, using real-time quantitative PCR with newly developed specific primers. This showed that alginate lyases from families PL6 and PL7 are upregulated in *Alteromonas macleodii* 83-1 and the type strain ATCC 27126 with alginate vs. glucose as sole carbon source.

Studying gene expression when degrading a single polysaccharide helps understanding an organism's ecology when encountering algal substrates in the natural habitat, as this requires swift transcriptional responses. The distinct upregulation is one potential explanation why *Alteromonas* species often respond quickly to nutrient availability. Despite being considered copiotrophic, commonly found abundant in experimental incubations with addition of organic matter, our evidence shows that *A. macleodii* strains not merely respond indiscriminately to any kind of substrate, but feature distinct adaptations which probably underpin their fast metabolic responses.

However, this study determined growth on a single substrate – an unfeasible scenario in natural systems. Algae comprise different polysaccharides that are likely released simultaneously, in addition to the diverse organic matter pool exuded via the microbial loop. Hence, the oceans comprise a diverse mix of organic matter, requiring that bacteria possess specific adaptations to find their niche, including fine-scale means of intraspecific resource partitioning [143]. Considering the ability of *A. macleodii* strain 83-1 to degrade different polysaccharides, we investigated its phenotype within a mix of substrates – a likely scenario during natural phytoplankton blooms, which comprise diverse algal taxa and organic matter types. We hypothesized that hydrolytic activities in 83-1 are regulated by a complex transcriptional machinery within mixed polysaccharide pools, attributed to substrate preferences and catabolite repression. The phenomenon of sequential substrate utilization has been intensively studied in terrestrial and enteric bacteria [144], but rarely in marine taxa. To contribute to these aspects, we characterized strain 83-1 when degrading a mix of laminarin, alginate and pectin. Transcriptomic, proteomic and exometabolomic profiling revealed substrate prioritization, with initial degradation of laminarin followed by the simultaneous degradation of alginate and pectin (Figure 9).

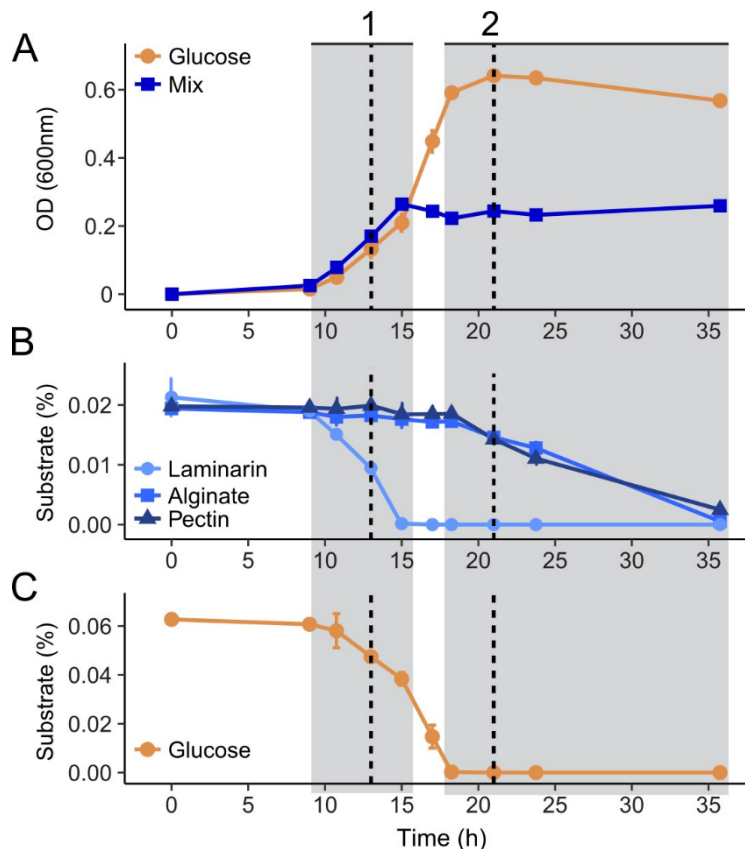


**Figure 9: Bacterial physiology when degrading mixed polysaccharide pools.** Biphasic phenotype of *Alteromonas macleodii* 83-1 (A) and corresponding substrate concentrations in polysaccharide mix (B) and glucose (C). Both phases (shaded) were characterized using transcriptomics, proteomics and exometabolomics at the time points indicated.

This biphasic phenotype coincided with marked shifts in protein abundance and metabolite secretion, mainly involving CAZymes within PULs (Appendix 3). In addition, our experiment showed temporal changes in exometabolome composition, including the secretion of pyrroloquinoline quinone during alginate/pectin utilization. Hence, degrading a polysaccharide mixture can also shape chemical crosstalk within the community. The ecological relevance of cellular adaptations was underlined by chemical evidence that globally widespread marine macroalgae release rhamnogalacturonan (contained in pectin) as well as alginate. Moreover, analyzing CAZyme microdiversity among *Alteromonas* spp. illustrated that hydrolytic traits are linked to the existence of 'carbohydrate utilization types' with different ecological strategies. Considering the substantial primary productivity of algae on global scales, these insights contribute to the understanding of bacteria-algae interactions and the remineralization of chemically diverse polysaccharide pools – key elements of marine carbon cycling.

This combined evidence allowed reconstructing the complete degradation pathways for the three polysaccharides (Figure 10), which has only been done in few other Gammaproteobacteria to date. Ultimately, this evidence furthermore helped curating the metabolic model for the *A. macleodii* type strain [145], [available in BioCyc](#) as community resource for metabolic reconstructions.

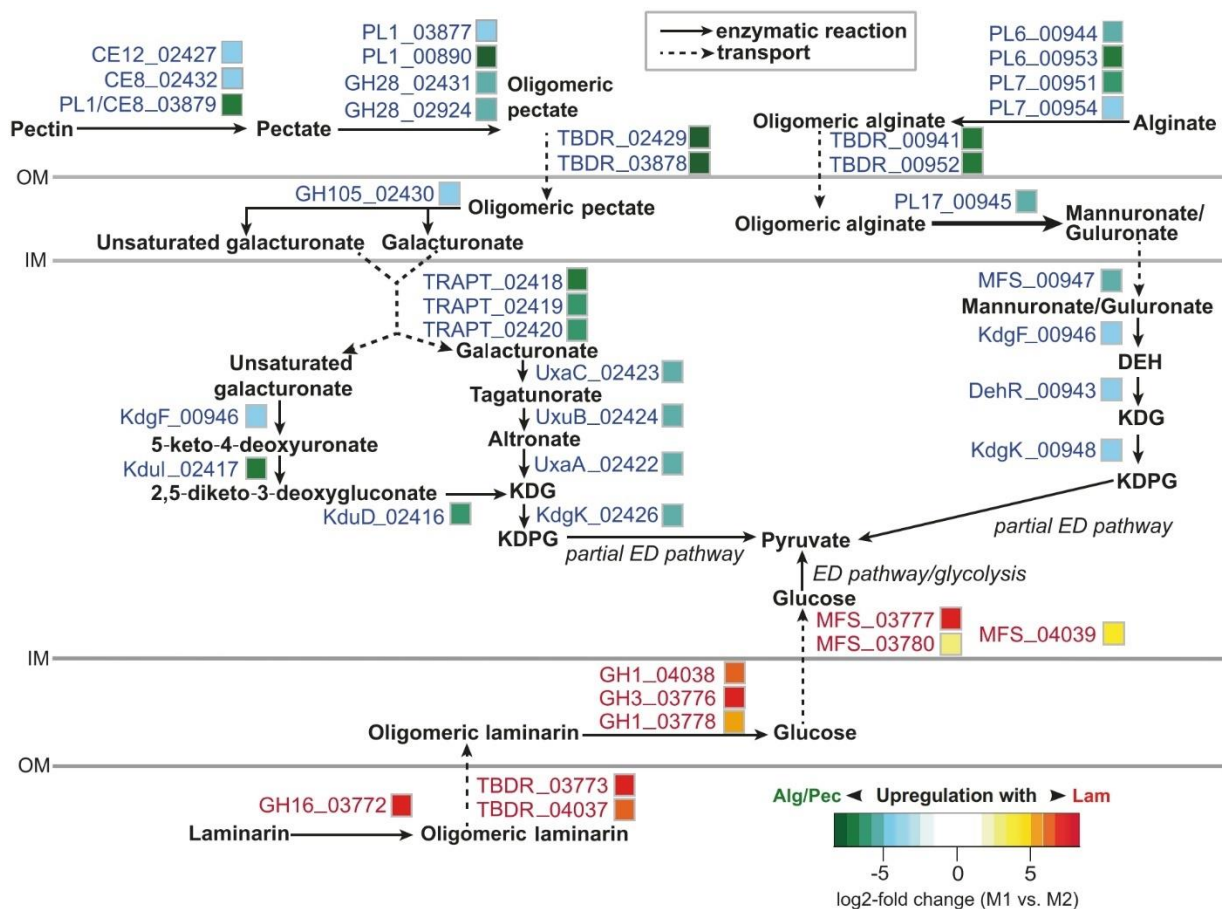


**Figure 10: Metabolic pathways for laminarin, alginate and pectin degradation in *A. macleodii* reconstructed from transcriptomic and proteomic evidence.** Upregulation during laminarin (yellow/red colors) and simultaneous alginate / pectin degradation (blue/green colors) was observed in various genes; encoding CAZymes (PL, GH, CE), transporters (TBDR, MFS, TRAPT), and downstream pathways (DehR, KdgFK, KduDI, UxaAC, UxB). ED: Entner-Doudoroff pathway; IM: inner membrane; OM: outer membrane.

My research also addressed other hydrolytic strains among *Alteromonas*. During expedition ANT28-5, we isolated *Alteromonas* sp. 76-1 from the Patagonian Continental Shelf (Figure 7). This strain, related to *Alteromonas naphthalenivorans*, has several distinct features. Strain 76-1 harbors a more complex alginolytic machinery than *A. macleodii* 83-1, as well as a plasmid dedicated for degrading the green algal polysaccharide ulvan (Appendix 4). Opposed to 83-1, strain 76-1 harbors two alginate-targeting PULs with different genes and structural organization. We hypothesize this might facilitate the utilization of different alginate structures in nature, e.g. being specific to varying polymer lengths, or the ratio between mannuronate and guluronate residues. Notably, ulvan degradation is attributed to a 126 Kb plasmid, encoding several ulvan lyases and monomer-processing genes. The plasmid-related adaptation to ulvan has never been reported to date. Hence, mobile PUL can mediate eco-evolutionary processes by providing access to certain “polysaccharide niches”, similar to fucoidan-degrading *Verrucomicrobia* [63]. Transfer of such plasmids between strains can contribute to metabolic diversification. Indeed, we

found related sequences in bacteria from distant locations, suggesting the plasmid as efficient vehicle to exchange hydrolytic capacities and establish new niches for receiving strains. Due to the extensive and versatile CAZyme repertoire, 76-1 showed substantial growth on polysaccharides, with comparable doubling times with alginate (2 h) and ulvan (3 h) in relation to glucose (3 h). Overall, the demonstrated CAZyme repertoire substantiates the role of *Alteromonas* in polysaccharide degradation, and how PUL exchange influences the ecophysiology of this ubiquitous marine taxon.

### 2.3 Polysaccharide microhabitats: sensing, utilization, and regulation

**Appendix 5:** Mitulla M, Dinasquet J, Guillemette R, Simon M, Azam F, Wietz M (2016). Response of bacterial communities from California coastal waters to alginate particles and an alginolytic *Alteromonas macleodii* strain. *Environ. Microbiol.* 18:4369–4377. [doi:10.1111/1462-2920.13314](https://doi.org/10.1111/1462-2920.13314)

**Appendix 6:** Bunse C, Koch H, Breider S, Simon M, Wietz M (2021). Sweet spheres: Succession and CAZyme expression of marine bacterial communities colonizing a mix of alginate and pectin particles. *Environ. Microbiol.* 23:3130–3148. [doi:10.1111/1462-2920.15536](https://doi.org/10.1111/1462-2920.15536)

Hydrolytic activities on cellular level should be considered in the bigger ecological context, as microbial cells live within a diverse consortium of competitors and cooperators. Ultimately, the combined effect of the countless interactions among cells, populations and communities has large-scale biogeochemical consequences. A central question is how bacteria sense and access polysaccharide substrates, given that the ocean is quite heterogeneous at the microscale [146]. Due to their considerable abundance in transparent exopolymer particles and the “oceanic gel phase” [147], polysaccharides are often present as localized nutrient hotspots, and hydrolytic bacteria possibly require chemosensory abilities to access these resources [148–150]. Polysaccharide microhabitats are a fascinating but poorly characterized niche for studying bacterial behavior and foraging strategies on small spatial scales. The ability of anionic polysaccharides like alginate and pectin to self-assemble into microgels is ecologically relevant, since these particles represent nutrient-rich scaffolds for attachment and growth of diverse microbes [151]. Furthermore, the possibility for controlled fabrication of such particles in reproducible size and polymer content allows dedicated laboratory experiments.

My research has illuminated different aspects of bacterial dynamics in connection with polysaccharide microhabitats. One paper evidenced that alginate particles are quickly colonized by distinct populations (Appendix 5). Three- to eightfold higher bacterial abundances on alginate particles corresponded to enrichment of *Cryomorphaceae*, *Saprospiraceae* and *Phaeobacter*, as shown by 16S rRNA amplicon sequencing. Concurrently, alginate-attached cells were significantly more productive than those in the surrounding water (Figure 11). In a parallel experiment using the same set-up but with the addition of *A. macleodii* 83-1, this strain outcompeted other taxa, indicating that its alginolytic activity does not benefit non-alginolytic strains by potential cross-feeding on alginate monomers or other metabolic products. Instead, strain 83-1 apparently employs a selfish strategy [152], utilizing all resources for its own growth. Considering the extensive biomass of alginate-containing macroalgae in temperate seas worldwide, the observed bacterial dynamics promote the understanding of carbon cycling in macroalgae-rich habitats.

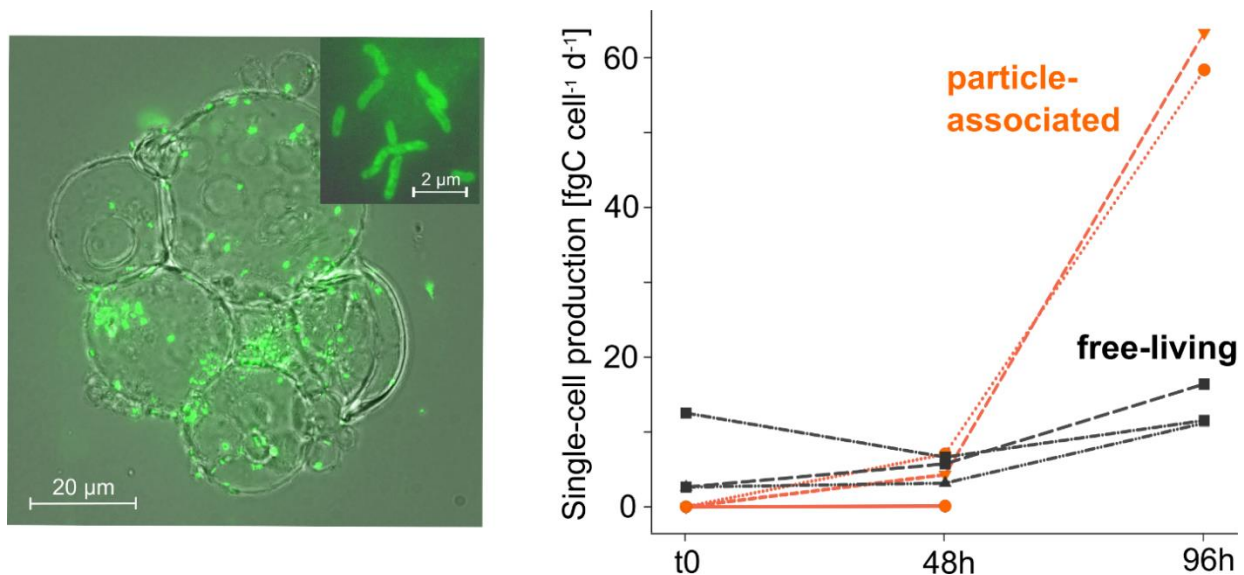


**Figure 11: Bacteria on alginate particle microhabitats.** Alginate particles colonized by bacteria (left; SYBR-stained cells in green). The insert highlights the considerable size (3-4 μm) of alginolytic cells of *Alteromonas* 83-1, indicating that a considerable amount of carbon was converted into biomass. Colonization concurred with higher cell-specific production on particles compared to free-living bacteria (right).

While this study investigated the utilization of single particle types, the ocean is highly heterogeneous [146]. Connected to the sheer diversity of polymers and their structural-chemical modifications, marine gels comprise a variety of types [147]. This especially applies to macroalgae-rich temperate seas, which harbor a variety of brown, red and green algae that produce diverse gelling compounds (alginate, carrageenan, agar, pectinous substrates). However, substrate-specific bacterial dynamics in mixtures of particle types with different polysaccharide composition, as likely occurring in natural habitats, are largely undescribed. Especially the Cordero and Polz labs have illuminated central mechanisms of community assembly and succession on model marine particles [153–155], with implications for microbial dynamics on natural particles and their role in the biological carbon pump [156]. We contributed to these aspects by studying the structure, functional diversity, and gene expression of marine microbiomes encountering a mix of polysaccharide particles (Appendix 6). Specifically, we incubated seawater collected near macroalgal forests at Helgoland Island with different combinations of magnetic/non-magnetic alginate and pectin particles; disentangling substrate-specific dynamics in terms of bacterial composition (amplicons), metabolic potential (metagenomics), and gene expression (metatranscriptomics). Magnetic particles provided an invaluable benefit, allowing to separate particle types and identify polymer-specific responses. This addressed key open questions – do bacterial communities segregate when encountering mixed particle resources, as a function of genetic capacities or substrate preferences? Do the predominant responders express particle-specific enzyme repertoires? We revealed distinct communities on particles compared to their free-living counterparts, with predominant utilization of alginate particles. Unexpectedly, bacterial communities on alginate and pectin particles overlapped in the most abundant taxa, comprising *Tenacibaculum*, *Colwellia*, *Psychrobium*, and

*Psychromonas* ASVs. Metagenomics and metatranscriptomics revealed that corresponding MAGs harbor PULs encoding alginate lyases, glycoside hydrolases and carbohydrate-binding modules, with specific upregulation (Figure 12). In contrast, only a single MAG showed elevated transcript abundances of pectin-degrading enzymes. The free-living fraction was dominated by a *Glaciecola* ASV. A corresponding MAG showed expression of a carbohydrate-related gene cluster, suggesting responses to carbohydrate monomers or other metabolic intermediates released from particle-associated taxa. Upregulation of ammonium uptake and metabolism indicated that nitrogen availability and cycling are important when degrading carbon-rich particles. These multifaceted responses underline the existence of complex dynamics around polysaccharide microhabitats [153, 157, 158]. The bacterial preference for alginate, whereas pectin primarily served as colonization scaffold, illuminated microbial substrate preferences and niche specialization, linking microscale ecology with major biogeochemical cycles.

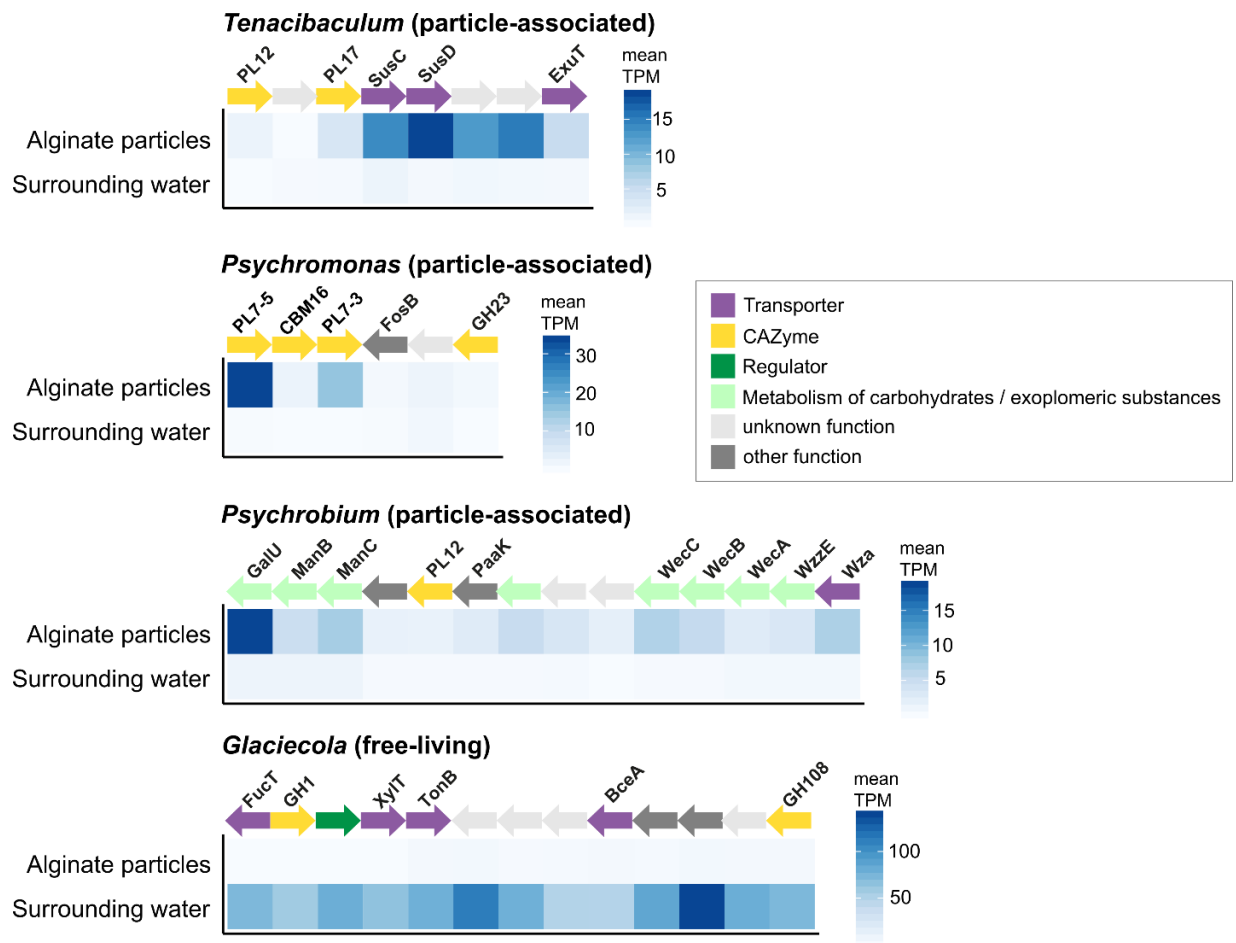


**Figure 12: Structure and expression of PULs in co-incubations with alginate and pectin particles.** TPM values show expression on alginate particles and in the surrounding water. From top to bottom: *susCD* and a pair of PL12-PL17 alginate lyases (*Tenacibaculum*); PL7 genes from different subfamilies co-localized with a CBM16 gene (*Psychromonas*); PL12 and exopolysaccharide-related genes (*Psychrobium*); unique GH108 adjacent to GH1 and carbohydrate transporter genes (*Glaciecola*). See Appendix 6 for details.

### 3. INTRASPECIFIC DIVERSITY

Metabolic variability is a major element in the ecological differentiation among bacterial taxa, influencing adaptive strategies and consequently their niche space [5]. Considerable functional diversity among closely related strains has implications for bacterial diversification and distribution, illustrated by genomic and geographic heterogeneity among strains of the cyanobacterium *Prochlorococcus* [159, 160]. The accessory genome (i.e. genes shared by multiple strains of a given taxon) and the unique genome (i.e. genes limited to specific strains of a given taxon) are primary drivers of ecological differentiation. This so-called flexible genome is often encoded in genomic islands, regions of preferential horizontal gene transfer and recombination events that are important drivers of niche specialization across the bacterial kingdom [161]. For instance, flexible genomic islands mediate intraspecific variability in carbon use, siderophore synthesis, and pilus assembly in *Alteromonas macleodii* [77]. Plasmids and other mobile genetic elements can enhance such adaptive-evolutionary processes, promoting diversification on short time scales [162]. The diversity of strain-specific ecological strategies is not necessarily reflected in current metrics of species delineation, such as 16S rRNA or core-genome phylogenies. For instance, ~400 *Vibrio cholerae* strains were shown to possess distinct intraspecific variability in bioluminescence, zooplankton colonization, and polysaccharide degradation [61]. Among marine *Salinispora*, comparable microdiversity occurs regarding secondary metabolism and phage defense [163, 164], with implications for strain-specific antagonism. Furthermore, marine *Polaribacter* strains colonize distinct niches based on their specialization for different polysaccharides [66, 165]. Microdiversity patterns also raise overarching questions: What defines a species, and how many strains constitute a natural bacterial population? Do currently known strains of any taxon represent stable genotypes or merely snapshots in evolutionary time, randomly captured from a continuum of strains that appear and vanish? A recent study substantially advanced these concepts by sequencing 138 *Salinibacter* isolates from the same site, followed by comparisons with metagenomes that were obtained in parallel. Although the 138 isolates represented about 80% of the *Salinibacter* population, the total population was estimated to constitute 5000-11000 genomovars, most of them rare [166]. These findings provide a glimpse into the population structure of closely related strains, likely featuring a high degree of genetic exchange and rapid diversification.

#### 3.1 *Alteromonas* microdiversity and niche specialization

**Appendix 7:** Koch H, Germscheid N, Freese HM, Noriega-Ortega B, Lücking D, Berger M, Qiu G, Marzinelli E, Campbell A, Steinberg P, Overmann J, Dittmar T, Simon M, Wietz M (2020). Genomic, metabolic and phenotypic variability shapes ecological differentiation and intraspecies interactions of *Alteromonas macleodii*. *Sci. Rep.* 10:809. [doi:10.1038/s41598-020-57526-5](https://doi.org/10.1038/s41598-020-57526-5)

My research has contributed to connecting genotypes to ecological niches in *Alteromonas macleodii* by studying intraspecific diversity among a collection of isolates with sequenced genomes, allowing to link genomic capacities with phenotypic traits. The available ~15 closed genomes were derived from various marine systems and geographic regions – underlining *A. macleodii* as an excellent model for studying the ecological implications of strain-level heterogeneity. One major benefit was the available genomic and physiological evidence from studying strains 83-1, BGP6, BGP9 and BGP14 (see Chapter 2). Expanding on the shown

intraspecific diversity in hydrolytic abilities, we here evidenced that a variety of other traits differ among *A. macleodii* strains, and contribute to intraspecific diversification. Contextualizing pangenomic, exometabolomic and physiological information illuminated adaptive strategies of carbon metabolism, microbial interactions, cellular communication, and iron acquisition (Figure 13). For this purpose, collaborating scientists Daniel Sher, Steven Biller and Erik Zinser kindly shared live cultures for physiological tests, for instance allowing to demonstrate strain-specific production of siderophores and homoserine lactones. These differences were reflected in genomic content and arrangement; including a dysfunctional siderophore-encoding cluster in MIT1002 due to a genomic insertion, disrupting the operon. Amino acid secretion, demonstrated by ultrahigh-resolution FT-ICR mass spectrometry, might promote the association of strain MIT1002 with *Prochlorococcus* through alleviating resource limitations [167]. Notably, strain 83-1 and the three BGP isolates featured clonal genomes despite originating from distant locations; resembling the isolation of *A. mediterranea* strains with less than 100 polymorphisms from distant locations and years [168].

In cooperation with Peter Steinberg, Ezequiel Marzinelli and colleagues at University of New South Wales (Australia), our study furthermore tested whether alginolytic capacities have implications for algal health, using the green macroalga *Ecklonia* as model system. For this purpose, we incubated live algae with *A. macleodii* for several days, without observing any detrimental effects or algal tissue disintegration. This result indicates that *A. macleodii* is not harmful for living macroalgae, but may rather utilize polysaccharides from dead algal biomass, or particles forming from algal exudates.

Unexpectedly, we discovered that several strains grow on aromatic compounds as sole carbon source. Strain MIT1002 showed the unique ability to degrade phenol, which might benefit associations with cyanobacteria. This scenario is substantiated by the upregulation of phenol hydroxylases in co-culture with *Prochlorococcus*, the common production of phenolics by cyanobacteria, and the presence of a homologous gene cluster in strains with comparable association to phototrophs [169–171]. Growth on toluene and xylene, mediated via a plasmid syntenic to terrestrial *Pseudomonas*, was unique to strain EZ55 (Figure 13). The ecological underpinnings are unclear, since these substrates are rare in marine habitats. Alternatively, related genes might target related aromatic compounds, for instance cyanobacterial derivatives of benzoate or cinnamate [172]. Benzoate degradation by strain EC673 was attributed to a chromosomal gene cluster shared with the plasmid of *A. mediterranea* EC615, highlighting how mobile genetic elements contribute to bacterial adaptations.

Another key outcome was the development of qPCR primers targeting unique genes of individual strains, identified using a pangenomic approach. These primers allowed tracking the growth of individual strains in co-culture, showing that certain strains grow faster and might have a competitive advantage in natural mixed populations. Despite being >99% identical at the 16S rRNA gene level, the demonstrated phenotypic, metabolic and genomic diversity indicate the existence of functionally distinct entities and specific niches within the *A. macleodii* species boundary. The finding of “ecological microdiversity” helps understanding the widespread occurrence of *A. macleodii*, with wider implications for the perception of bacterial niche specialization, population ecology, and biogeochemical roles.

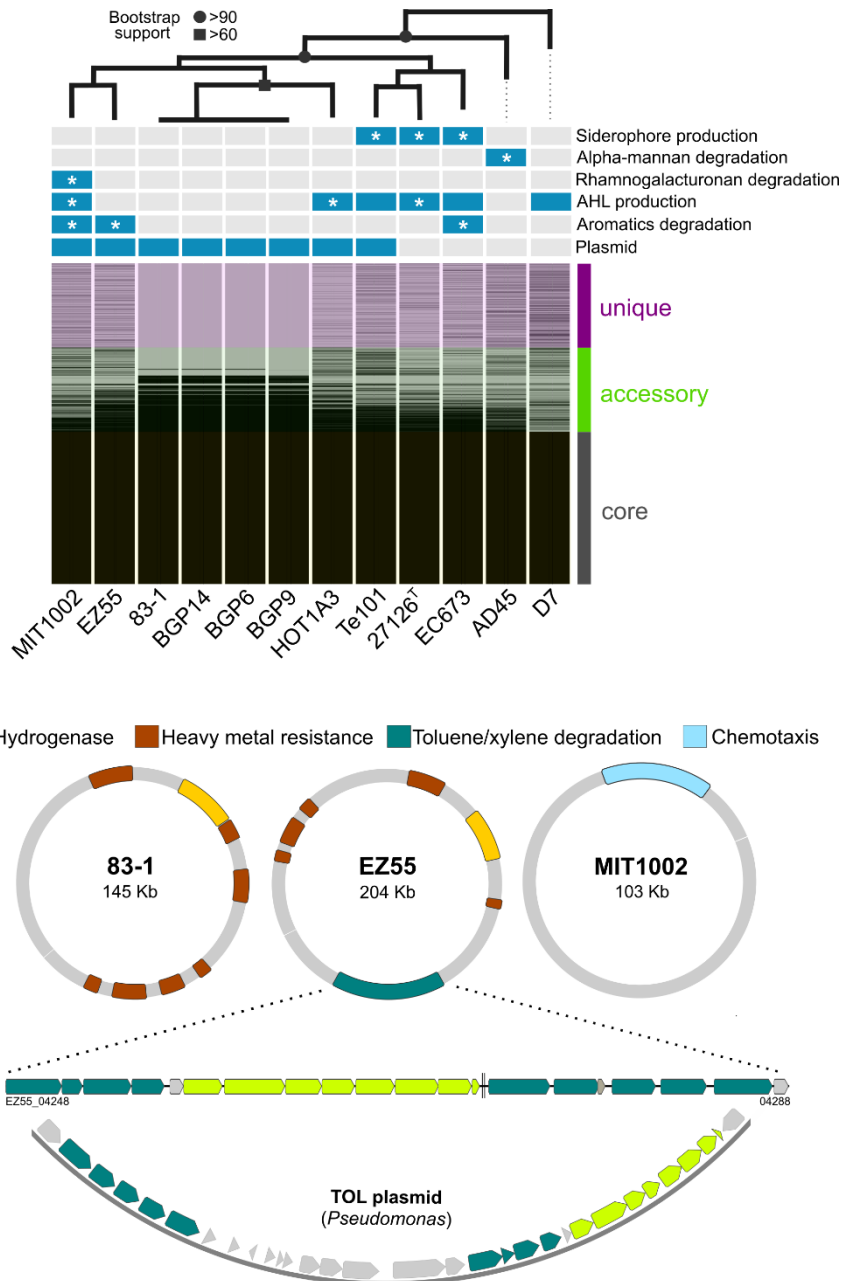


**Figure 13: Intraspecific diversity among *Alteromonas macleodii*.** **A:** Maximum-likelihood phylogeny and pangenome structure, showing presence (blue) and absence (gray) of specific genomic features. Phylogenetic analysis was based on 92 single-copy housekeeping genes. Asterisks designate phenotypic features experimentally verified in the present study. Bootstrap support values are indicated by symbols; unlabeled branches have <50% support. **B:** Structural diversity of plasmids in strains 83-1, EZ55 and MIT1002. Cassettes encoding hydrogenase and heavy metal resistance were found in different organization, whereas the MIT1002 plasmid harbored a unique chemotaxis-related cluster. The EZ55 plasmid furthermore contains a unique insertion syntenic to the *Pseudomonas* TOL plasmid (blue-green: toluene/xylene hydroxylases and transporters; green: catechol meta-cleavage pathway; gray: non-homologous genes).

#### 4. POLAR MICROBIOMES, SEASONALITY AND THE FUTURE ARCTIC OCEAN

The polar oceans are experiencing unprecedented changes during the climate crisis. The progressing, rapid warming of the Arctic [112] has major consequences for inhabiting organisms and ecosystem functioning. Yet, there is still limited understanding of polar ecology over environmental gradients, both human-influenced and natural. The polar oceans harbor distinct microbial communities and adaptations, with marked differences to warmer waters attributed to unique environmental conditions and selection pressures. Large-scale genomic surveys, such as MOSAiC and Tara Arctic, are beginning to establish detailed inventories of the taxonomic and functional diversity in polar oceans, including numerous MAGs – providing unique insights into genetic features and adaptations [19, 20]. In addition, repeated expeditions to the central Arctic Ocean over the past decades have illuminated the microbial diversity in seawater and sea-ice, the role of under-ice algae in benthopelagic coupling, melt ponds as biological hotspots, the connectivity between ocean and atmosphere, and various other aspects of the biological carbon pump [98, 123, 134, 173–176].

Nonetheless, literally only the tip of the iceberg has been characterized. The taxonomic and functional diversity of Arctic microbes across natural (e.g. solar irradiation) and human-influenced (e.g. accelerated sea-ice decline) gradients remains poorly resolved. Particularly little is known about biodiversity along contrasting daylight, temperature and stratification conditions between polar day and night [94]. Understanding the temporal assembly of microbial communities, in context of their (a)biotic surrounding, is central for deciphering Arctic ecosystem functionality. Such insights require continuous observations, ideally in high resolution to capture short-lived ecological events [177]. However, due to extreme winter conditions and remoteness, continuous records are rare to date, or restricted to coastal areas [100, 178]. Recently, the MOSAiC expedition has published a 12-month dataset in weekly resolution, accompanied by the sampling of localized “special events” (e.g. the short-term formation of leads, ridges, melt ponds, and freshwater lenses). This information – integrating metabarcoding, metagenomics, metatranscriptomics and environmental monitoring – helps understanding biodiversity over the seasonal cycle [19].

Autonomous samplers and sensors are indispensable for continuous *in situ* observations, collecting information in high temporal resolution irrespective of environmental conditions. For instance, robotic vehicles can record hydrography and nutrients in ice-covered waters [17, 18]. The FRAM Observatory in the Arctic Fram Strait performs annual (since 1999) and year-round (since 2015) samplings across the northward, ice-free West Spitsbergen Current (WSC) and the southward, ice-covered East Greenland Current (EGC), including the productive marginal ice zone. The available record of primary production, deep-sea ecology, microbiology and biogeochemistry in summertime [105–108, 179–181] is now expanded by continuous studies through moored devices, which autonomously collect seawater and sinking particles over the annual cycle. The resulting biodiversity assessments via eDNA sequencing establish a yet unknown seasonal perspective. Annual records also promote the understanding of biological responses to Atlantification, which propagates through the entire food web [182]. These aspects have important links to polysaccharide degradation, since the longer productive season and enhanced phytoplankton growth in thinner ice (including under-ice-blooms) result in higher organic matter production.

#### 4.1 Year-round microbial diversity in Arctic and Atlantic ecosystem states

**Appendix 8:** [Wietz M](#), [Bienhold C](#), [Metfies K](#), [Torres-Valdés S](#), [von Appen W-J](#), [Salter I](#), [Boetius A](#) (2021). The polar night shift: Seasonal dynamics and drivers of Arctic Ocean microbiomes revealed by autonomous sampling. *ISME Commun.* 1:76. [doi:10.1038/s43705-021-00074-4](https://doi.org/10.1038/s43705-021-00074-4)

This study provided the first year-round portrait of microbial diversity in the open Arctic Ocean, across diverse environmental conditions – only possible through autonomous sampling. The Atlantic-influenced WSC showed strong seasonality (Figure 14), with marked separation of the productive summer (dominated by diatoms and carbohydrate-degrading bacteria) and recycling-gearred winter (dominated by eukaryotic parasites, radiolarians, chemoautotrophic bacteria, and archaea). Depletion of the major nutrients nitrate and phosphate during autumn coincided with specific diatoms (*Coscinodiscophyceae*) and bacteria with known oligotrophic adaptations, including *Rhodobacteraceae* and SAR116. Winter harbored a unique microbiome including Rhodospirillales and Dadabacteriales, likely contributing to nutrient replenishment by chemoautotrophic capacities, e.g. converting ammonium to nitrate. This was highlighted by metagenomic evidence from a following study (section 4.2). Hence, bacterial activities in winter are likely an important contributor (in addition to physical mixing) to fuel the following phytoplankton bloom. Spring and summer featured successional patterns among phytoplankton and bacteria, comparable to temperate seas: abundance peaks of *Phaeocystis*, *Grammonema*, and *Thalassiosira* coincided with ephemeral peaks of the flavobacteria *Aurantivirga*, *Formosa*, and *Polaribacter*. Considering the flavobacterial role in polysaccharide degradation, these observations likely correspond to polysaccharide-driven metabolic relationships – expanding my biogeographic research on hydrolytic bacteria to the Arctic Ocean.

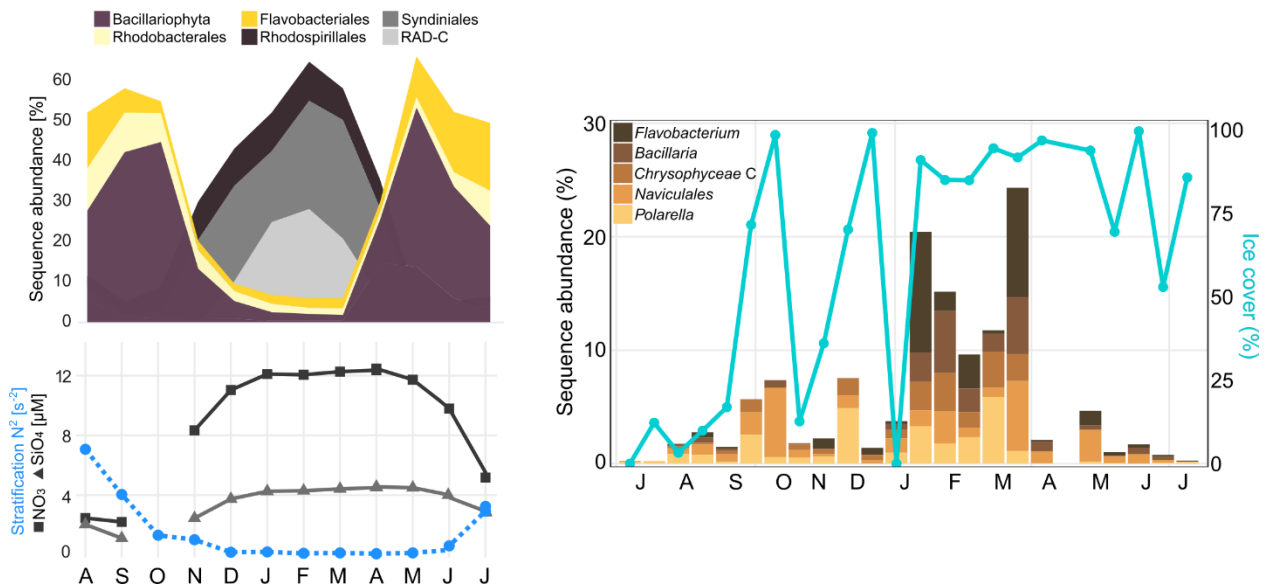


**Figure 14: Year-round biodiversity and physicochemistry in the Arctic Ocean.** In the West Spitsbergen Current, polar day and night showed markedly different microbial composition, nitrate/silicate concentrations, and stratification (right). The East Greenland Current featured a specific winter microbiome after a sea-ice low in January (right).

In the Arctic-influenced EGC, the presence of sea-ice and polar Arctic water masses concurred with weaker seasonality and a stronger heterotrophic signature. A specific winter microbiome, likely related to seeding from ice (Figure 14), included the known sea-ice diatoms *Bacillaria* and *Naviculales* [183, 184]. Ice algae produce copious amounts of storage polysaccharides and extracellular polymers, fueling bacterial growth in the underlying water [97, 185, 186]. The parallel peak of an ASV related to *Flavobacterium frigidarium*, a bacterium with laminarin-degrading abilities [187] found on ice-algal aggregates [123], indicates bacterial utilization of ice-algal carbohydrates. Such an ice-driven microbial loop could have major biogeochemical consequences during accelerated ice melt [188].

We are continuing the time-series observations in Fram Strait, aiming at a systemic understanding of microbial seasonality and polar night ecology in the Arctic Ocean. In ongoing studies, we found that microbial dynamics in the WSC show considerable annual recurrence (Figure 15). Analyses include novel mathematical approaches on metagenomic and metabarcoding data, fostered by a collaboration with University of Düsseldorf (see [189] for methodology). For instance, calculating oscillation signals and combined ASV-gene networks revealed fine-tuned community assembly and recurrent microbial modules over four annual cycles, shaped by environmental conditions and microbial interactions. This study includes 47 PacBio long-read metagenomes, covering all seasonal states in high resolution – an unprecedented inventory of microbial functions in the Arctic Ocean.

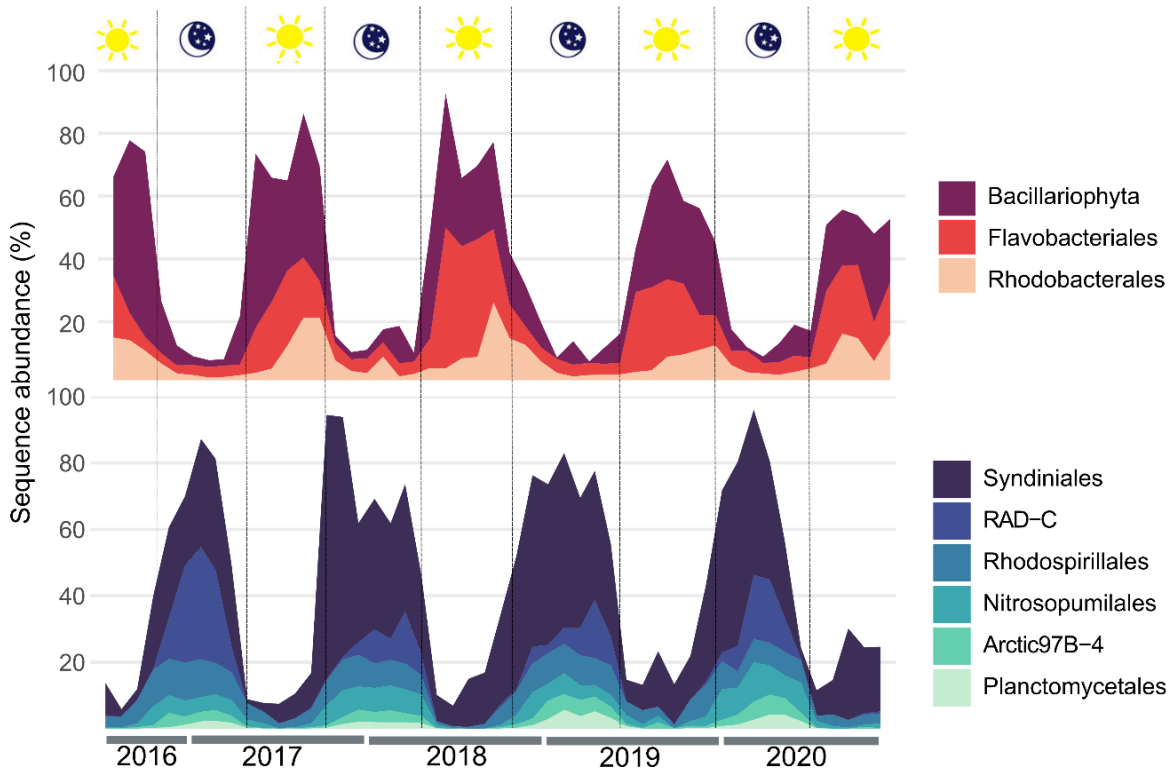


**Figure 15:** Recurrent microbial succession over four annual cycles in the West Spitsbergen Current, showing the predominant bacterial, archaeal and microeukaryotic taxa over polar day (top) and polar night (bottom).

## 4.2 Influence of “Arctic Atlantification” on microbial ecology and seasonality

**Appendix 9:** Priest T, von Appen W-J, Oldenburg E, Popa O, Torres-Valdés S, Bienhold C, Metfies K, Boulton W, Mock T, Fuchs BM, Amann R, Boetius A, Wietz M (2023). Atlantic water influx and sea-ice cover drive taxonomic and functional shifts in Arctic marine bacterial communities. *ISME J* 17:1612–1626. [doi:10.1038/s41396-023-01461-6](https://doi.org/10.1038/s41396-023-01461-6)

The shown impact of sea-ice and hydrography on microbial dynamics in the EGC motivated a detailed temporal analysis under different degrees of Atlantic influence. A four-year amplicon time-series was contextualized with nine PacBio long-read metagenomes, sampled over a gradient from 0-100% ice cover and Atlantic water influx. We identified bacterial signature populations of specific environmental conditions, with consistent dynamics across the wider Arctic. Densely ice-covered waters harbored a stable “core” microbiome, including signature ASVs from *Thioglobus* that were found at similar environmental conditions during Tara Arctic. In contrast, Atlantic water and low sea-ice favoured populations with seasonal variability, for instance *Thiotrichaceae* (Figure 16). These dynamics resembled a “replacement” process via advection, mixing, and environmental selection. Associated shifts in biogeochemical pathways included carbohydrate and osmolyte metabolism (e.g. targeting the phytoplankton compounds DMSP and methanethiol) enriched at low-ice cover (Figure 16), underlining that Atlantification concurs with higher primary production and associated release of carbohydrates. Hence, microbial dynamics and adaptations shaped by polysaccharide availability will become more prominent in the future Arctic Ocean. Periods of high-ice cover were characterized by a greater community potential to utilize terrestrial and inorganic compounds, including ketones and inorganic sulphur substrates, signifying that “true” polar microbiomes are fueled by substrates independent from primary production. Notably, we also detected pathways for degradation of bacterial detritus, supporting the predominance of recycling processes under winter and polar conditions. Overall, our study established a baseline catalogue of polar microbial metabolism. In context with datasets from the central Arctic [19], this evidence contributes to assessing biological conditions of the future Arctic Ocean under progressing Atlantification.

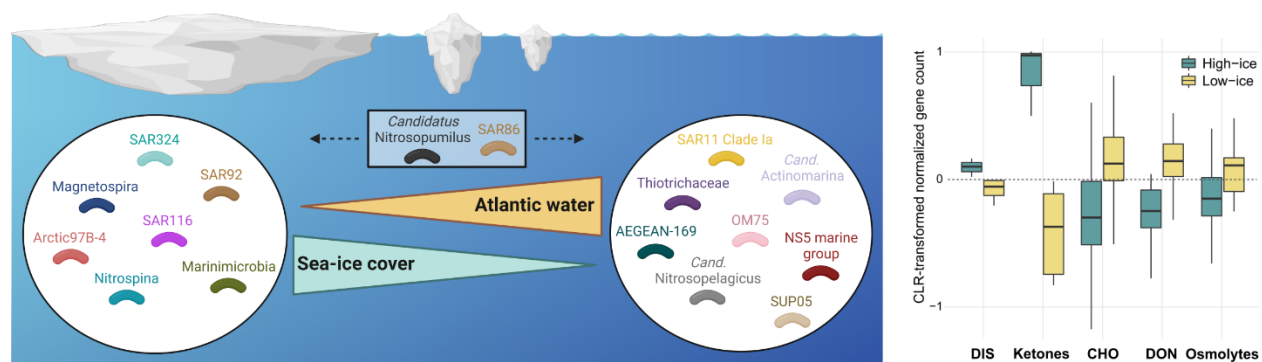


**Figure 16: Taxonomic and functional diversity under contrasting sea-ice and hydrographic conditions in the East Greenland Current.** Abundances of specific taxa scaled with the extent of sea-ice cover and Atlantic water (left), coincident with differential enrichment of genes involved in the metabolism of dissolved organic sulfur (DIS), ketones, carbohydrates (CHO), dissolved organic nitrogen (DON), and osmolytes (right).

## 5. SYNOPSIS AND OUTLOOK

My research on biogeographic, genetic, regulatory and metabolic signatures has refined the current state and future directions in marine polysaccharide research; summarized in a recent review which I have co-authored [28]. The establishment of *Alteromonas macleodii* as model organism benefits the scientific community, recently contributing to the collaborative metabolic curation of this species during an interactive workshop at Haifa University [145]. In parallel, the findings on *A. macleodii* ecology and evolution have been summarized in a recent “microbe profile” [190], written by invitation from the Microbiology Society (United Kingdom). My research in the Arctic Ocean promotes the understanding of the still essentially uncharted microbial biodiversity in the polar oceans, including novel hydrolytic bacteria.

Still, many exciting future avenues remain. CAZyme repertoires and PUL machineries, sometimes with multiple PULs targeting the same substrate in a single strain, should be researched from multiple viewpoints; combining transcriptomics, proteomics and the chemical complexity of polysaccharides. For example, do strains with multiple PULs for the same polysaccharide – like *Alteromonas* sp. 76-1 – have the potential to occupy more niches? In the case of strain 76-1, the two alginolytic machines might be specific to different alginate architectures (e.g. different polymer lengths or ratios between mannuronate and guluronate monomers). Transcriptomics when degrading different alginate types could identify new ecological strategies, including specific adaptations to distinct algal taxa or physiologies, as alginate content and monomer ratio can vary by taxon and growth stage [191–193]. Ultimately, these aspects need to be transferred to the community context for overarching conclusions on eco-evolutionary scales. New methods for the *in situ* quantification of polysaccharides, e.g. via topical antibodies, are important for a holistic view – contextualizing production and recycling with the contrasting accessibility of polysaccharides to microbial utilization, and how these dynamics are linked with carbon sequestration.

The finding of extensive CAZyme diversity has implications for the perception of (intra)specific variability among taxa, genes and traits. How does metabolic versatility determine niche specialization, and why are *Alteromonas* rare in nature despite their extensive metabolic repertoire? *A. macleodii* and related taxa often dominate incubation experiments, and similar events might happen in the oceans – but on very short timescales, or being restricted to spatially separated niches. A recent study revealed ephemeral “blooms” of *Alteromonas* populations, which would be missed by traditional single-point sampling [194]. Viral activity and rapid grazing might be controlling factors, and immediately diminish emerging populations. However, the underlying drivers remain unknown. Has *A. macleodii* ‘prioritized’ metabolic versatility over defense mechanisms, and how does this influence carbon and nutrient fluxes? Studying such questions under pulses of different polysaccharides, for instance during phytoplankton blooms, could provide important clues. Potentially, *Alteromonas* rather occurs on macroalgal surfaces or in the surrounding water, where exudation of algal polysaccharides yields the formation of gel particles that serve as colonization scaffolds. Alternatively, pelagic macroalgae with substantial alginate content, for instance *Sargassum*, might represent a habitat for alginolytic *Alteromonas* strains. At any rate, the finding of conserved PULs in *Alteromonas* members from distant locations, together with the substrate-dependent regulation of related CAZymes, suggests considerable ecological relevance.

Overarching questions include how intraspecific metabolic diversity translates to population structure. Natural *A. macleodii* assemblages can be dominated by single strains via competitive exclusion [195–197], to which my research contributed through co-culturing experiments. Strains 83-1, 27126 and MIT1002 – the two former encoding the same alginolytic machineries – differed in growth dynamics when co-cultured on glucose, with MIT1002 emerging as dominant strain (Figure 17). Hence, one could hypothesize that MIT1002 outcompetes the other strains in a natural community upon glucose availability. Transcriptomic studies with different combinations of strains and substrates, resembling mixed substrate conditions as found in nature, could illuminate how genetic diversity and regulation underpin growth and competitiveness in marine systems. Finally, these aspects have a broader eco-evolutionary dimension [198–200]: what defines a bacterial species, how to incorporate microdiversity in species delineation, and how do intraspecific interactions shape the structure of natural populations? Combining evidence from extensive samplings at single sites – including metagenomes, high-quality MAGs, and isolates with >99.5% rRNA gene identity – can help assessing linkages between bacterial (sub)species diversity, environmental conditions, and microbial interactions.

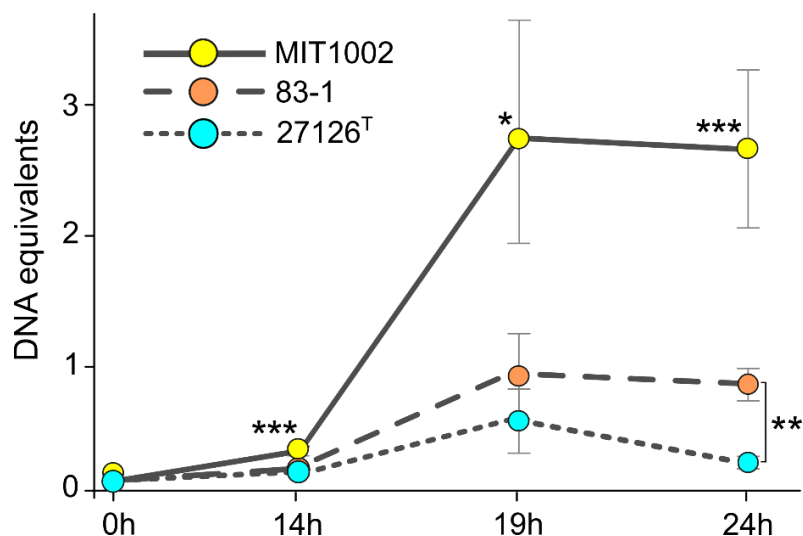


**Figure 17: Ecophysiological implications of strain-specific variability in *Alteromonas macleodii*.** Different growth of strains MIT1002, 83-1 and 27126 in co-culture, determined by quantitative PCR of unique genes (\* $p < 0.01$ ; \*\* $p < 0.001$ ; \*\*\* $p < 0.0001$ ).

My research on polysaccharide degradation and *Alteromonas* is integrally connected to my studies in the polar oceans. For instance, it is puzzling why *Alteromonas* spp. are rarely found in polar oceans, despite their diverse metabolic repertoire. Potentially, *Alteromonas* species lack cold adaptations, or colonize very narrow niches. Our evidence from a just published paper supports the latter scenario: across a five-year time-series, *Alteromonas* ASVs were only found during the summer-autumn transition, and only in the ice-covered western Fram Strait [201]. Connected to the seeding of ice-derived substrates during that time [97], *Alteromonas* might rely on ice-seeded proteins via proteolytic activities [202], as seen in related *Alteromonadaceae* [97]. This observation furthermore underlines the relevance of repeated samplings to identify ephemeral but potentially important dynamics.

My research on microbial dynamics over environmental gradients emphasizes the key importance of continuous observations. High-resolution samplings are indispensable for a mechanistic understanding, and how the future Arctic Ocean might respond to climate change [203, 204]. The found taxonomic and functional diversity across spatial and temporal scales provided unprecedented insights into Arctic ecology, the major dynamics and drivers of seasonality, and effects of Atlantification – central to assess the future biological carbon pump [205–207]. Elevated photosynthesis and corresponding polysaccharide availability might accelerate the microbial loop at the expense of chemoautotrophic and ice-specific metabolisms [208, 209], with yet unknown consequences. Another interesting direction is the comparison between Arctic and Antarctic seasonality. Whether overlapping environmental pressures, most notably the seasonal extremes in daylight, result in similar biological communities is a long-standing question [89, 210, 211]. On the other hand, Arctic and Antarctic Oceans substantially differ in topography and hydrography. Nonetheless, some taxa have been found at similar seasonal states in both hemispheres [137]. Specifically, *Aurantivirga* and SAR92 appeared in early spring, indicating comparable temporal niches at both poles. My new project using [autonomous sampling in the Weddell Sea](#) will address these questions by identifying unique and shared seasonal dynamics. Overall, interdisciplinary and joint studies are essential to achieve systemic insights into ecosystem functionality. For instance, a collaborative paper to which I have contributed [122] harnessed the expertise of 26 scientists and engineers from diverse fields (oceanography, biogeochemistry, microbiology, biology, physics, bio-optics, acoustics, modeling). This integrative approach was vital to elucidate benthopelagic coupling between contrasting sea-ice conditions (Figure 18).

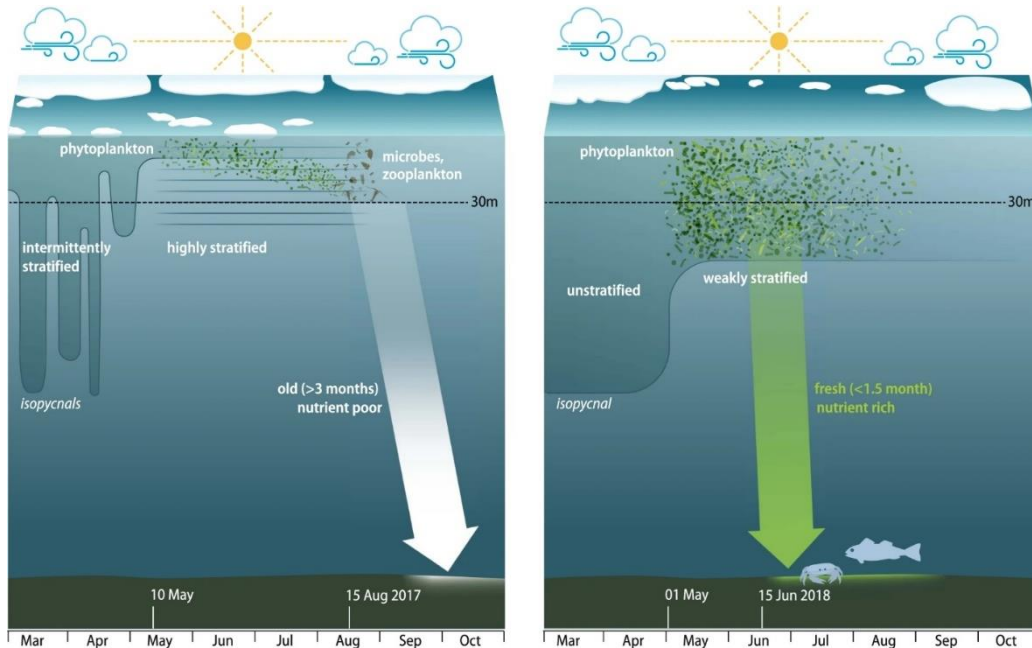


**Figure 18: The biological carbon pump under different sea-ice conditions.** Near-ice, meltwater-stratified waters hosted vertically constrained, longer blooms (left). Well-mixed waters distant from the ice edge hosted higher biomass and shorter, intense export of algal detritus, supporting denser megafauna on the seafloor (right). Hence, meltwater-induced stratification constitutes a retention system, whereas a mixed upper layer is an export system [212–214].

To conclude, I would like to share some personal thoughts and values that are elemental to my academic journey. The research culminated in this Habilitation has immensely benefited from numerous collaborations and continuous exchange within the scientific community. Only the teamwork with diverse scientists from multiple disciplines and backgrounds can yield a holistic understanding of processes with broad ecological implications. The tireless work and essential contributions by engineers and technicians shall be emphasized here. Furthermore, understanding (polar) microbial ecology and its environmental drivers are important beyond academia [215]. Outreach is one emphasis of my academic life. For instance, in the regular YouTube livestreams “[Wissenschaft fürs Wohnzimmer](#)” (*Sitting Room Science*), our team hosts scientists across disciplines to present their research, and discuss interactively with the online community. Here I have presented my research on [Arctic microbial seasonality](#) and [ocean-atmosphere interactions](#). We have shared our experiences in science communication, including recommendations for peers interested in own outreach activities, in a dedicated paper [216]. Furthermore, both science and society should have FAIR access to all knowledge generated. In this context, we have established the interactive website “[polarDNAexplorer](#)” to visualize results from eDNA studies in the polar oceans. My research, teaching and mentoring will continue along these principles of open, collaborative, and interdisciplinary science.

## 6. REFERENCES

1. Bar-On YM, Milo R. The biomass composition of the oceans: a blueprint of our blue planet. *Cell* 2019; **179**: 1451–1454.
2. Sunagawa S, Coelho LP, Chaffron S, Kultima JR, Labadie K, Salazar G, et al. Structure and function of the global ocean microbiome. *Science* 2015; **348**: 1261359.
3. Guidi L, Chaffron S, Bittner L, Eveillard D, Larhlimi A, Roux S, et al. Plankton networks driving carbon export in the oligotrophic ocean. *Nature* 2016; **532**: 465–470.
4. Falkowski PG, Fenchel T, Delong EF. The microbial engines that drive earth’s biogeochemical cycles. *Science* 2008; **320**: 1034–1039.
5. Larkin AA, Martiny AC. Microdiversity shapes the traits, niche space, and biogeography of microbial taxa. *Environ Microbiol Rep* 2017; **9**: 55–70.
6. Iversen MH. Carbon export in the ocean: A biologist’s perspective. *Annu Rev Mar Sci* 2023; **15**: 357–381.
7. Boyd PW, Claustre H, Levy M, Siegel DA, Weber T. Multi-faceted particle pumps drive carbon sequestration in the ocean. *Nature* 2019; **568**: 327–335.
8. Dall’Olmo G, Dingle J, Polimene L, Brewin RJW, Claustre H. Substantial energy input to the mesopelagic ecosystem from the seasonal mixed-layer pump. *Nat Geosci* 2016; **9**: 820–823.
9. Acinas SG, Sánchez P, Salazar G, Cornejo-Castillo FM, Sebastián M, Logares R, et al. Deep ocean metagenomes provide insight into the metabolic architecture of bathypelagic microbial communities. *Commun Biol* 2021; **4**: 604.
10. Chaffron S, Delage E, Budinich M, Vintache D, Henry N, Nef C, et al. Environmental vulnerability of the global ocean epipelagic plankton community interactome. *Sci Adv* 2021; **7**: eabg1921.

11. Cordier T, Angeles IB, Henry N, Lejzerowicz F, Berney C, Morard R, et al. Patterns of eukaryotic diversity from the surface to the deep-ocean sediment. *Sci Adv* 2022; **8**: eabj9309.
12. de Vargas C, Audic S, Henry N, Decelle J, Mahé F, Logares R, et al. Ocean plankton. Eukaryotic plankton diversity in the sunlit ocean. *Science* 2015; **348**: 1261605.
13. Paoli L, Ruscheweyh H-J, Forneris CC, Hubrich F, Kautsar S, Bhushan A, et al. Biosynthetic potential of the global ocean microbiome. *Nature* 2022; **607**: 111–118.
14. Frémont P, Gehlen M, Vrac M, Leconte J, Delmont TO, Wincker P, et al. Restructuring of plankton genomic biogeography in the surface ocean under climate change. *Nat Clim Change* 2022; **12**: 393–401.
15. Larkin AA, Garcia CA, Garcia N, Brock ML, Lee JA, Ustick LJ, et al. High spatial resolution global ocean metagenomes from Bio-GO-SHIP repeat hydrography transects. *Sci Data* 2021; **8**: 107.
16. Pierella Karlusich JJ, Ibarbalz FM, Bowler C. Phytoplankton in the Tara Ocean. *Ann Rev Mar Sci* 2020; **12**: 233–265.
17. Rabe B, Heuzé C, Regnery J, Aksenov Y, Allerholt J, Athanase M, et al. Overview of the MOSAiC expedition: Physical oceanography. *Elem Sci Anth* 2022; **10**: 00062.
18. Clark MS, Hoffman JI, Peck LS, Bargelloni L, Gande D, Havermans C, et al. Multi-omics for studying and understanding polar life. *Nat Commun* 2023; **14**: 7451.
19. Mock T, Boulton W, Balmonte J-P, Barry K, Bertilsson S, Bowman J, et al. Multiomics in the central Arctic Ocean for benchmarking biodiversity change. *PLoS Biol* 2022; **20**: e3001835.
20. Royo-Llonch M, Sánchez P, Ruiz-González C, Salazar G, Pedrós-Alió C, Sebastián M, et al. Compendium of 530 metagenome-assembled bacterial and archaeal genomes from the polar Arctic Ocean. *Nat Microbiol* 2021; **6**: 1561–1574.
21. Bercovici SK, Dittmar T, Niggemann J. The detection of bacterial exometabolites in marine dissolved organic matter through ultrahigh-resolution mass spectrometry. *Limnol Oceanogr Meth* 2022; **20**: 350–360.
22. Wienhausen G, Noriega-Ortega BE, Niggemann J, Dittmar T, Simon M. The exometabolome of two model strains of the *Roseobacter* group: a marketplace of microbial metabolites. *Front Microbiol* 2017; **8**: 1985–1985.
23. Benner R, Pakulski JD, McCarthy M, Hedges JI, Hatcher PG. Bulk chemical characteristics of dissolved organic matter in the ocean. *Science* 1992; **255**: 1561–1564.
24. McCarthy M, Hedges J, Benner R. Major biochemical composition of dissolved high molecular weight organic matter in seawater. *Mar Chem* 1996; **55**: 281–297.
25. Hung C-C, Guo L, Santschi PH, Alvarado-Quiroz N, Haye JM. Distributions of carbohydrate species in the Gulf of Mexico. *Mar Chem* 2003; **81**: 119–135.
26. Lin P, Guo L. Spatial and vertical variability of dissolved carbohydrate species in the northern Gulf of Mexico following the Deepwater Horizon oil spill, 2010–2011. *Mar Chem* 2015; **174**: 13–25.
27. Myklestad SM, Børsheim KY. Dynamics of carbohydrates in the Norwegian Sea inferred from monthly profiles collected during 3 years at 66°N, 2°E. *Mar Chem* 2007; **107**: 475–485.

28. Arnosti C, Wietz M, Brinkhoff T, Hehemann J-H, Probandt D, Zeugner L, et al. The biogeochemistry of marine polysaccharides: sources, inventories, and bacterial drivers of the carbohydrate cycle. *Annu Rev Mar Sci* 2021; **13**: 81–108.
29. Biersmith A, Benner R. Carbohydrates in phytoplankton and freshly produced dissolved organic matter. *Mar Chem* 1998; **63**: 131–144.
30. Becker S, Tebben J, Coffinet S, Wiltshire K, Iversen MH, Harder T, et al. Laminarin is a major molecule in the marine carbon cycle. *Proc Natl Acad Sci USA* 2020; **117**: 6599–6607.
31. Field CB, Behrenfeld MJ, Randerson JT, Falkowski P. Primary production of the biosphere: Integrating terrestrial and oceanic components. *Science* 1998; **281**: 237–240.
32. Krause-Jensen D, Duarte CM. Substantial role of macroalgae in marine carbon sequestration. *Nat Geosci* 2016; **9**: 737–742.
33. Thornton DCO. Dissolved organic matter (DOM) release by phytoplankton in the contemporary and future ocean. *Eur J Phycol* 2014; **49**: 20–46.
34. Lopez-Sandoval DC, Rodriguez-Ramos T, Cermeno P, Maranon E. Exudation of organic carbon by marine phytoplankton: dependence on taxon and cell size. *Mar Ecol Progr Ser* 2013; **477**: 53–60.
35. Mühlenbruch M, Grossart H-P, Eigemann F, Voss M. Mini-review: Phytoplankton-derived polysaccharides in the marine environment and their interactions with heterotrophic bacteria. *Environ Microbiol* 2018; **20**: 2671–2685.
36. Mabeau S, Kloareg B. Isolation and analysis of the cell walls of brown algae: *Fucus spiralis*, *F. ceranoides*, *F. vesiculosus*, *F. serratus*, *Bifurcaria bifurcata* and *Laminaria digitata*. *J Exp Bot* 1987; **38**: 1573–1580.
37. Gooday GW. The ecology of chitin degradation. *Advances in Microbial Ecology*. 1990. pp 387–430.
38. Souza CP, Almeida BC, Colwell RR, Rivera IN. The importance of chitin in the marine environment. *Mar Biotechnol* 2011; **13**: 823–30.
39. Panagiotopoulos C, Sempéré R. The molecular distribution of combined aldoses in sinking particles in various oceanic conditions. *Mar Chem* 2005; **95**: 31–49.
40. Passow U. Transparent exopolymer particles (TEP) in aquatic environments. *Prog Oceanogr* 2002; **55**: 287–333.
41. Alldredge AL, Passow U, Logan BE. The abundance and significance of a class of large, transparent organic particles in the ocean. *Deep Sea Res I* 1993; **40**: 1131–1140.
42. Decho AW. Microbial exopolymer secretions in ocean environments: their role(s) in food webs and marine processes. *Oceanogr Mar Biol* 2015; **28**: 73–153.
43. Vidal-Melgosa S, Sichert A, Francis TB, Bartosik D, Niggemann J, Wichels A, et al. Diatom fucan polysaccharide precipitates carbon during algal blooms. *Nat Commun* 2021; **12**: 1150.
44. Vidal-Melgosa S, Pedersen HL, Schückel J, Arnal G, Dumon C, Amby DB, et al. A new versatile microarray-based method for high throughput screening of carbohydrate-active enzymes. *J Biol Chem* 2015; **290**: 9020–9036.
45. Priest T, Vidal-Melgosa S, Hehemann J-H, Amann R, Fuchs BM. Carbohydrates and carbohydrate degradation gene abundance and transcription in Atlantic waters of the Arctic. *ISME Commun* 2023; **3**: 1–13.

46. Cuskin F, Lowe EC, Temple MJ, Zhu Y, Cameron EA, Pudlo NA, et al. Human gut *Bacteroidetes* can utilize yeast mannan through a selfish mechanism. *Nature* 2015; **517**: 165–169.
47. Martens EC, Koropatkin NM, Smith TJ, Gordon JI. Complex glycan catabolism by the human gut microbiota: the *Bacteroidetes* Sus-like paradigm. *J Biol Chem* 2009; **284**: 24673–7.
48. Wardman JF, Bains RK, Rahfeld P, Withers SG. Carbohydrate-active enzymes (CAZymes) in the gut microbiome. *Nat Rev Microbiol* 2022; **20**: 542–556.
49. Hehemann J-H, Boraston AB, Czjzek M. A sweet new wave: structures and mechanisms of enzymes that digest polysaccharides from marine algae. *Curr Opin Struct Biol* 2014; **28**: 77–86.
50. Grondin JM, Tamura K, Déjean G, Abbott DW, Brumer H. Polysaccharide Utilization Loci: Fuelling microbial communities. *J Bacteriol* 2017; **199**: JB.00860-16.
51. López-Mondéjar R, Tláškal V, da Rocha UN, Baldrian P. Global distribution of carbohydrate utilization potential in the prokaryotic tree of life. *mSystems* 2022; **7**: e00829-22.
52. Barbeyron T, Thomas F, Barbe V, Teeling H, Schenowitz C, Dossat C, et al. Habitat and taxon as driving forces of carbohydrate catabolism in marine heterotrophic bacteria: example of the model algae-associated bacterium *Zobellia galactanivorans* Dsij<sup>T</sup>. *Environ Microbiol* 2016; **18**: 4610–4627.
53. Hehemann J-H, Correc G, Thomas F, Bernard T, Barbeyron T, Jam M, et al. Biochemical and structural characterization of the complex agarolytic enzyme system from the marine bacterium *Zobellia galactanivorans*. *J Biol Chem* 2012; **287**: 30571–30584.
54. Thomas F, Bordron P, Eveillard D, Michel G. Gene expression analysis of *Zobellia galactanivorans* during the degradation of algal polysaccharides reveals both substrate-specific and shared transcriptome-wide responses. *Front Microbiol* 2017; **8**: 1808–1808.
55. Kabisch A, Otto A, König S, Becher D, Albrecht D, Schüler M, et al. Functional characterization of polysaccharide utilization loci in the marine *Bacteroidetes* 'Gramella forsetii' KT0803. *ISME J* 2014; **8**: 1492–1502.
56. Reisky L, Stanetty C, Mihovilovic MD, Schweder T, Hehemann J-H, Bornscheuer UT. Biochemical characterization of an ulvan lyase from the marine flavobacterium *Formosa agariphila* KMM 3901<sup>T</sup>. *Appl Microbiol Biotechnol* 2018; **102**: 6987–6996.
57. Hehemann J-H, Truong LV, Unfried F, Welsch N, Kabisch J, Heiden SE, et al. Aquatic adaptation of a laterally acquired pectin degradation pathway in marine gammaproteobacteria. *Environ Microbiol* 2017; **19**: 2320–2333.
58. Francis B, Urich T, Mikolasch A, Teeling H, Amann R. North Sea spring bloom-associated Gammaproteobacteria fill diverse heterotrophic niches. *Environ Microbiome* 2021; **16**: 15.
59. Christiansen L, Bech PK, Schultz-Johansen M, Martens HJ, Stougaard P. *Colwellia echini* sp. nov., an agar- and carrageenan-solubilizing bacterium isolated from sea urchin. *Int J Syst Evol Microbiol* 2018; **68**: 687–691.
60. Reintjes G, Arnosti C, Fuchs B, Amann R. Selfish, sharing and scavenging bacteria in the Atlantic Ocean: a biogeographical study of bacterial substrate utilisation. *ISME J* 2019; **13**: 1119–1132.
61. Hehemann J-H, Arevalo P, Datta MS, Yu X, Corzett CH, Henschel A, et al. Adaptive radiation by waves of gene transfer leads to fine-scale resource partitioning in marine microbes. *Nat Commun* 2016; **7**: 12860.

62. Zimmerman AE, Martiny AC, Allison SD. Microdiversity of extracellular enzyme genes among sequenced prokaryotic genomes. *ISME J* 2013; **7**: 1187–1199.
63. Sichert A, Corzett CH, Schechter MS, Unfried F, Markert S, Becher D, et al. Verrucomicrobia use hundreds of enzymes to digest the algal polysaccharide fucoidan. *Nat Microbiol* 2020; **5**: 1026–1039.
64. Teeling H, Fuchs BM, Becher D, Klockow C, Gardebrecht A, Bennke CM, et al. Substrate-controlled succession of marine bacterioplankton populations induced by a phytoplankton bloom. *Science* 2012; **336**: 608–611.
65. Teeling H, Fuchs BM, Bennke CM, Krüger K, Chafee M, Kappelmann L, et al. Recurring patterns in bacterioplankton dynamics during coastal spring algae blooms. *eLife* 2016; **5**: e11888.
66. Avcı B, Krüger K, Fuchs BM, Teeling H, Amann RI. Polysaccharide niche partitioning of distinct *Polaribacter* clades during North Sea spring algal blooms. *ISME J* 2020; **14**: 1369–1383.
67. Kappelmann L, Krüger K, Hehemann J-H, Harder J, Markert S, Unfried F, et al. Polysaccharide utilization loci of North Sea *Flavobacteriia* as basis for using SusC/D-protein expression for predicting major phytoplankton glycans. *ISME J* 2019; **13**: 76–91.
68. Longhurst A. Seasonal cycles of pelagic production and consumption. *Science* 1995; **36**: 77–167.
69. Longhurst AR. *Ecological Geography of the Sea*. 1998. Academic Press, San Diego.
70. Oliver MJ, Irwin AJ. Objective global ocean biogeographic provinces. *Geophys Res Lett* 2008; **35**: L15601.
71. Richter DJ, Watteaux R, Vannier T, Leconte J, Frémont P, Reygondeau G, et al. Genomic evidence for global ocean plankton biogeography shaped by large-scale current systems. *eLife* 2022; **11**: e78129.
72. Perelman JN, Ladroit Y, Escobar-Flores P, Firing E, Drazen JC. Eddies and fronts influence pelagic communities across the eastern Pacific Ocean. *Prog Oceanogr* 2023; **211**: 102967.
73. Hörstmann C, Raes EJ, Buttigieg PL, Lo Monaco C, John U, Waite AM. Hydrographic fronts shape productivity, nitrogen fixation, and microbial community composition in the southern Indian Ocean and the Southern Ocean. *Biogeosciences* 2021; **18**: 3733–3749.
74. Hanson CA, Fuhrman JA, Horner-Devine MC, Martiny JBH. Beyond biogeographic patterns: processes shaping the microbial landscape. *Nat Rev Microbiol* 2012; **10**: 497.
75. Thompson AW, Kouba K, Ahlgren NA. Niche partitioning of low-light adapted *Prochlorococcus* subecotypes across oceanographic gradients of the North Pacific Subtropical Front. *Limnol Oceanogr* 2021; **66**: 1548–1562.
76. Sunagawa S, Acinas SG, Bork P, Bowler C, Eveillard D, Gorsky G, et al. Tara Oceans: towards global ocean ecosystems biology. *Nat Rev Microbiol* 2020; **18**: 428–445.
77. López-Pérez M, Rodríguez-Valera F. Pangenome evolution in the marine bacterium *Alteromonas*. *Genome Biol Evol* 2016; **8**: 1556–1570.
78. Dlugosch L, Poehlein A, Wemheuer B, Pfeiffer B, Badewien TH, Daniel R, et al. Significance of gene variants for the functional biogeography of the near-surface Atlantic Ocean microbiome. *Nat Commun* 2022; **13**: 456.

79. Milke F, Wagner-Doebler I, Wienhausen G, Simon M. Selection, drift and community interactions shape microbial biogeographic patterns in the Pacific Ocean. *ISME J* 2022; **16**: 2653–2665.
80. Bunse C, Pinhassi J. Marine bacterioplankton seasonal succession dynamics. *Trends Microbiol* 2017; **25**: 494–505.
81. Needham DM, Fichot EB, Wang E, Berdjeb L, Cram JA, Fichot CG, et al. Dynamics and interactions of highly resolved marine plankton via automated high-frequency sampling. *ISME J* 2018; **12**: 2417–2432.
82. Buttigieg PL, Fadeev E, Bienhold C, Hehemann L, Offre P, Boetius A. Marine microbes in 4D - using time series observation to assess the dynamics of the ocean microbiome and its links to ocean health. *Curr Opin Microbiol* 2018; **43**: 169–185.
83. Cram JA, Chow C-ET, Sachdeva R, Needham DM, Parada AE, Steele JA, et al. Seasonal and interannual variability of the marine bacterioplankton community throughout the water column over ten years. *ISME J* 2015; **9**: 563–580.
84. Gilbert JA, Steele JA, Caporaso JG, Steinbrück L, Reeder J, Temperton B, et al. Defining seasonal marine microbial community dynamics. *ISME J* 2012; **6**: 298–308.
85. Chafee M, Fernández-Guerra A, Buttigieg PL, Gerdtts G, Eren AM, Teeling H, et al. Recurrent patterns of microdiversity in a temperate coastal marine environment. *ISME J* 2018; **12**: 237–252.
86. Bunse C, Israelsson S, Baltar F, Bertos-Fortis M, Fridolfsson E, Legrand C, et al. High frequency multi-year variability in Baltic Sea microbial plankton stocks and activities. *Front Microbiol* 2019; **9**: 3296.
87. Auladell A, Barberán A, Logares R, Garcés E, Gasol JM, Ferrera I. Seasonal niche differentiation among closely related marine bacteria. *ISME J* 2021; 1–12.
88. Révelard A, Tintoré J, Verron J, Bahurel P, Barth JA, Belbéoch M, et al. Ocean Integration: the needs and challenges of effective coordination within the Ocean Observing System. *Front Mar Sci* 2022; **8**: 737671.
89. Sul WJ, Oliver TA, Ducklow HW, Amaral-Zettler LA, Sogin ML. Marine bacteria exhibit a bipolar distribution. *Proc Natl Acad Sci USA* 2013; **110**: 2342–2347.
90. Meng L, Delmont TO, Gaïa M, Pelletier E, Fernández-Guerra A, Chaffron S, et al. Genomic adaptation of giant viruses in polar oceans. *bioRxiv* 2023; 2023.02.09.527846.
91. Boetius A, Anesio AM, Deming JW, Mikucki JA, Rapp JZ. Microbial ecology of the cryosphere: Sea ice and glacial habitats. *Nat Rev Microbiol* 2015; **13**: 677–690.
92. Fuhrman JA, Steele JA, Hewson I, Schwalbach MS, Brown MV, Green JL, et al. A latitudinal diversity gradient in planktonic marine bacteria. *Proc Natl Acad Sci USA* 2008; **105**: 7774–7778.
93. Müller O, Wilson B, Paulsen ML, Rumińska A, Armo HR, Bratbak G, et al. Spatiotemporal dynamics of ammonia-oxidizing Thaumarchaeota in distinct Arctic water masses. *Front Microbiol* 2018; **9**: 24.
94. Berge J, Renaud PE, Darnis G, Cottier F, Last K, Gabrielsen TM, et al. In the dark: A review of ecosystem processes during the Arctic polar night. *Prog Oceanogr* 2015; **139**: 258–271.
95. Hoppe CJM. Always ready? Primary production of Arctic phytoplankton at the end of the polar night. *Limnol Oceanogr Letters* 2022; **7**: 167–174.

96. Niemi A, Meisterhans G, Michel C. Response of under-ice prokaryotes to experimental sea-late DOM enrichment. *Aquat Microb Ecol* 2014; **73**: 17–28.
97. Underwood GJC, Michel C, Meisterhans G, Niemi A, Belzile C, Witt M, et al. Organic matter from Arctic sea-ice loss alters bacterial community structure and function. *Nat Clim Change* 2019; **9**: 170–176.
98. Boetius A, Albrecht S, Bakker K, Bienhold C, Felden J, Fernández-Méndez M, et al. Export of algal biomass from the melting Arctic sea ice. *Science* 2013; **339**: 1430–1432.
99. Koenig Z, Muilwijk M, Sandven H, Lundesgaard Ø, Assmy P, Lind S, et al. From winter to late summer in the northwestern Barents Sea Shelf: impacts of seasonal progression of sea ice and upper ocean on nutrient and phytoplankton dynamics. *Progr Oceanogr* 2023; 103174.
100. Assmy P, Fernández-Méndez M, Duarte P, Meyer A, Randelhoff A, Mundy CJ, et al. Leads in Arctic pack ice enable early phytoplankton blooms below snow-covered sea ice. *Sci Rep* 2017; **7**: 40850.
101. Fadeev E, Salter I, Schourup-Kristensen V, Nöthig E-M, Metfies K, Engel A, et al. Microbial communities in the east and west Fram Strait during sea ice melting season. *Front Mar Sci* 2018; **5**: 429.
102. Fadeev E, Wietz M, Appen W-J von, Iversen MH, Nöthig E-M, Engel A, et al. Submesoscale physicochemical dynamics directly shape bacterioplankton community structure in space and time. *Limnol Oceanogr* 2021; **66**: 2901–2913.
103. Jacquemot L, Vigneron A, Tremblay J-É, Lovejoy C. Contrasting sea ice conditions shape microbial food webs in Hudson Bay (Canadian Arctic). *ISME Commun* 2022; **2**: 104.
104. Fadeev E, Rogge A, Ramondenc S, Nöthig E-M, Wekerle C, Bienhold C, et al. Sea ice presence is linked to higher carbon export and vertical microbial connectivity in the Eurasian Arctic Ocean. *Commun Biol* 2021; **4**: 1–13.
105. Nöthig E-M, Bracher A, Engel A, Metfies K, Niehoff B, Peeken I, et al. Summertime plankton ecology in Fram Strait—a compilation of long- and short-term observations. *Polar Res* 2015; **34**: 23349.
106. Nöthig E-M, Ramondenc S, Haas A, Hehemann L, Walter A, Bracher A, et al. Summertime chlorophyll *a* and particulate organic carbon standing stocks in surface waters of the Fram Strait and the Arctic Ocean (1991–2015). *Front Mar Sci* 2020; **7**: 350.
107. Engel A, Bracher A, Dinter T, Endres S, Grosse J, Metfies K, et al. Inter-annual variability of organic carbon concentration in the eastern Fram Strait during summer (2009–2017). *Front Mar Sci* 2019; **6**: 187.
108. Metfies K, Bauerfeind E, Wolf C, Sprong P, Frickenhaus S, Kaleschke L, et al. Protist communities in moored long-term sediment traps (Fram Strait, Arctic)—Preservation with mercury chloride allows for PCR-based molecular genetic analyses. *Front Mar Sci* 2017; **4**: 301.
109. Cardozo-Mino M, Salter I, Nöthig E-M, Metfies K, Ramondenc S, Wekerle C, et al. A decade of microbial community dynamics on sinking particles during high carbon export events in the eastern Fram Strait. *Front Mar Sci* 2023; **10**: 1173384.
110. Cardozo-Mino, M. Temporal and spatial dynamics of marine microorganisms in ice-covered seas. *PhD thesis* 2022.

111. Winder JC, Boulton W, Salamov A, Eggers SL, Metfies K, Moulton V, et al. Genetic and structural diversity of prokaryotic ice-binding proteins from the central Arctic Ocean. *Genes* 2023; **14**: 363.
112. Rantanen M, Karpechko AY, Lipponen A, Nordling K, Hyvärinen O, Ruosteenoja K, et al. The Arctic has warmed nearly four times faster than the globe since 1979. *Commun Earth Environ* 2022; **3**: 1–10.
113. Kwok R. Arctic sea ice thickness, volume, and multiyear ice coverage: losses and coupled variability (1958–2018). *Environ Res Lett* 2018; **13**: 105005.
114. AMAP. Snow, water, ice and permafrost in the Arctic (SWIPA). 2017. Oslo, Norway.
115. Årthun M, Eldevik T, Smedsrud LH, Skagseth Ø, Ingvaldsen RB. Quantifying the influence of Atlantic heat on Barents sea ice variability and retreat. *J Clim* 2012; **25**: 4736–4743.
116. Oziel L, Baudena A, Ardyna M, Massicotte P, Randelhoff A, Sallée J-B, et al. Faster Atlantic currents drive poleward expansion of temperate phytoplankton in the Arctic Ocean. *Nature Communications* 2020; **11**: 1–8.
117. Neukermans G, Oziel L, Babin M. Increased intrusion of warming Atlantic water leads to rapid expansion of temperate phytoplankton in the Arctic. *Global Change Biol* 2018; **24**: 2545–2553.
118. Woodgate RA. Increases in the Pacific inflow to the Arctic from 1990 to 2015, and insights into seasonal trends and driving mechanisms from year-round Bering Strait mooring data. *Progr Oceanogr* 2018; **160**: 124–154.
119. Paulsen ML, Doré H, Garczarek L, Seuthe L, Müller O, Sandaa R-A, et al. *Synechococcus* in the Atlantic Gateway to the Arctic Ocean. *Front Mar Sci* 2016; **3**.
120. Ardyna M, Arrigo KR. Phytoplankton dynamics in a changing Arctic Ocean. *Nat Clim Chang* 2020; **10**: 892–903.
121. Lewis KM, Dijken GL van, Arrigo KR. Changes in phytoplankton concentration now drive increased Arctic Ocean primary production. *Science* 2020; **369**: 198–202.
122. von Appen W-J, Waite AM, Bergmann M, Bienhold C, Boebel O, Bracher A, et al. Sea-ice derived meltwater stratification slows the biological carbon pump: results from continuous observations. *Nat Commun* 2021; **12**: 7309.
123. Rapp JZ, Fernández-Méndez M, Bienhold C, Boetius A. Effects of ice-algal aggregate export on the connectivity of bacterial communities in the central Arctic Ocean. *Front Microbiol* 2018; **9**: 1035.
124. Fadeev E, Rogge A, Ramondenc S, Nöthig E-M, Wekerle C, Bienhold C, et al. Sea ice presence is linked to higher carbon export and vertical microbial connectivity in the Eurasian Arctic Ocean. *Commun Biol* 2021; **4**: 1–13.
125. Grzymalski JJ, Riesenfeld CS, Williams TJ, Dussaq AM, Ducklow H, Erickson M, et al. A metagenomic assessment of winter and summer bacterioplankton from Antarctica Peninsula coastal surface waters. *ISME J* 2012; **6**: 1901–15.
126. Freyria NJ, Joli N, Lovejoy C. A decadal perspective on north water microbial eukaryotes as Arctic Ocean sentinels. *Sci Rep* 2021; **11**: 8413.
127. Sandaa R-A, E Storesund J, Olesin E, Lund Paulsen M, Larsen A, Bratbak G, et al. Seasonality drives microbial community structure, shaping both eukaryotic and prokaryotic host-viral relationships in an Arctic marine ecosystem. *Viruses* 2018; **10**: 715.

128. Horvat C, Jones DR, Iams S, Schroeder D, Flocco D, Feltham D. The frequency and extent of sub-ice phytoplankton blooms in the Arctic Ocean. *Sci Adv* 2017; **3**: e1601191.
129. Frey KE, Comiso JC, Stock LV, Young LNC, Cooper LW, Grebmeier JM. A comprehensive satellite-based assessment across the Pacific Arctic Distributed Biological Observatory shows widespread late-season sea surface warming and sea ice declines with significant influences on primary productivity. *PLOS ONE* 2023; **18**: e0287960.
130. Grebmeier JM, Moore SE, Cooper LW, Frey KE. The Distributed Biological Observatory: A change detection array in the Pacific Arctic – An introduction. *Deep Sea Res II* 2019; **162**: 1–7.
131. Solan M, Archambault P, Renaud PE, März C. The changing Arctic Ocean: consequences for biological communities, biogeochemical processes and ecosystem functioning. *Philos Trans R Soc A* 2020; **378**: 20200266.
132. Luria CM, Amaral-Zettler LA, Ducklow HW, Repeta DJ, Rhyne AL, Rich JJ. Seasonal shifts in bacterial community responses to phytoplankton-derived dissolved organic matter in the western Antarctic Peninsula. *Front Microbiol* 2017; **8**: 2117.
133. Kim HH, Bowman JS, Luo Y-W, Ducklow HW, Schofield OM, Steinberg DK, et al. Modeling polar marine ecosystem functions guided by bacterial physiological and taxonomic traits. *Biogeosciences* 2022; **19**: 117–136.
134. Flores H, David C, Ehrlich J, Hardge K, Kohlbach D, Lange BA, et al. Sea-ice properties and nutrient concentration as drivers of the taxonomic and trophic structure of high-Arctic protist and metazoan communities. *Polar Biol* 2019; **42**: 1377–1395.
135. Ramondenc S, Nöthig E-M, Hufnagel L, Bauerfeind E, Busch K, Knüppel N, et al. Effects of Atlantification and changing sea-ice dynamics on zooplankton community structure and carbon flux between 2000 and 2016 in the eastern Fram Strait. *Limnol Oceanogr* 2022; **68**: S39–S53.
136. Wietz M, Bienhold C, Metfies K, Torres-Valdés S, von Appen W-J, Salter I, et al. The polar night shift: seasonal dynamics and drivers of Arctic Ocean microbiomes revealed by autonomous sampling. *ISME Commun* 2021; **1**: 76.
137. Liu Y, Blain S, Crispi O, Rembauville M, Obernosterer I. Seasonal dynamics of prokaryotes and their associations with diatoms in the Southern Ocean as revealed by an autonomous sampler. *Environ Microbiol* 2020; **22**: 3968–3984.
138. Randelhoff A, Lacour L, Marec C, Leymarie E, Lagunas J, Xing X, et al. Arctic mid-winter phytoplankton growth revealed by autonomous profilers. *Sci Adv* 2020; **6**: eabc2678.
139. Priest T, von Appen W-J, Oldenburg E, Popa O, Torres-Valdés S, Bienhold C, et al. Atlantic water influx and sea-ice cover drive taxonomic and functional shifts in Arctic marine bacterial communities. *ISME J* 2023; **17**: 1612–1625.
140. Randelhoff A, Reigstad M, Chierici M, Sundfjord A, Ivanov V, Cape M, et al. Seasonality of the physical and biogeochemical hydrography in the inflow to the Arctic Ocean through Fram Strait. *Front Mar Sci* 2018; **5**: 224.
141. Johnsen G, Leu E, Gradinger R. Marine Micro- and Macroalgae in the Polar Night. In: Berge J, Johnsen G, Cohen JH (eds). *Polar Night Marine Ecology: Life and Light in the Dead of Night*. 2020. Springer International Publishing, Cham, pp 67–112.

142. Giebel H-A, Arnosti C, Badewien TH, Bakenhus I, Balmonte JP, Billerbeck S, et al. Microbial growth and organic matter cycling in the Pacific Ocean along a latitudinal transect between subarctic and subantarctic waters. *Front Mar Sci* 2021; **8**: 764383.
143. Yu XA, McLean C, Hehemann J-H, Angeles-Albores D, Wu F, Muszyński A, et al. Low-level resource partitioning supports coexistence among functionally redundant bacteria during successional dynamics. *ISME J* 2024; **18**: wrad013.
144. Görke B, Stülke J. Carbon catabolite repression in bacteria: many ways to make the most out of nutrients. *Nat Rev Microbiol* 2008; **6**: 613–624.
145. Sher D, George EE, Wietz M, Gifford SM, Zoccaratto L, Weissberg O, et al. Collaborative metabolic curation of an emerging model marine bacterium, *Alteromonas macleodii* ATCC 27126. *bioRxiv* 2023; 2023.12.13.571488.
146. Stocker R. Marine microbes see a sea of gradients. *Science* 2012; **338**: 628–633.
147. Verdugo P. Marine microgels. *Annu Rev Mar Sci* 2012; **4**: 375–400.
148. Konishi H, Hio M, Kobayashi M, Takase R, Hashimoto W. Bacterial chemotaxis towards polysaccharide pectin by pectin-binding protein. *Sci Rep* 2020; **10**: 3977.
149. Smriga S, Fernandez VI, Mitchell JG, Stocker R. Chemotaxis toward phytoplankton drives organic matter partitioning among marine bacteria. *Proc Natl Acad Sci USA* 2016; **113**: 1576–1581.
150. Clerc EE, Raina J-B, Keegstra JM, Landry Z, Pontrelli S, Alcolombri U, et al. Strong chemotaxis by marine bacteria towards polysaccharides is enhanced by the abundant organosulfur compound DMSP. *Nat Commun* 2023; **14**: 8080.
151. Cordero OX, Datta MS. Microbial interactions and community assembly at microscales. *Curr Opin Microbiol* 2016; **31**: 227–234.
152. Reintjes G, Arnosti C, Fuchs BM, Amann R. An alternative polysaccharide uptake mechanism of marine bacteria. *ISME J* 2017; **11**: 1640–1650.
153. Ebrahimi A, Schwartzman J, Cordero OX. Cooperation and spatial self-organization determine rate and efficiency of particulate organic matter degradation in marine bacteria. *Proc Natl Acad Sci USA* 2019; **116**: 23309–23316.
154. Enke TN, Datta MS, Schwartzman J, Cermak N, Schmitz D, Barrere J, et al. Modular assembly of polysaccharide-degrading marine microbial communities. *Curr Biol* 2019; **29**: 1528-1535.e6.
155. Enke TN, Leventhal GE, Metzger M, Saavedra JT, Cordero OX. Microscale ecology regulates particulate organic matter turnover in model marine microbial communities. *Nat Commun* 2018; **9**: 2743.
156. Stephens BM, Durkin CA, Sharpe G, Nguyen TTH, Albers J, Estapa ML, et al. Direct observations of microbial community succession on sinking marine particles. *ISME J* 2024; **18**: wrad010.
157. Pontrelli S, Szabo R, Pollak S, Schwartzman J, Ledezma-Tejeida D, Cordero OX, et al. Metabolic cross-feeding structures the assembly of polysaccharide degrading communities. *Sci Adv* 2022; **8**: eabk3076.
158. Sichert A, Cordero OX. Polysaccharide-bacteria interactions from the lens of evolutionary ecology. *Front Microbiol* 2021; **12**: 705082.

159. Coleman ML, Sullivan MB, Martiny AC, Steglich C, Barry K, Delong EF, et al. Genomic islands and the ecology and evolution of *Prochlorococcus*. *Science* 2006; **311**: 1768–1770.
160. Johnson ZI, Zinser ER, Coe A, McNulty NP, Woodward EMS, Chisholm SW. Niche partitioning among *Prochlorococcus* ecotypes along ocean-scale environmental gradients. *Science* 2006; **311**: 1737–1740.
161. McDaniel LD, Young E, Delaney J, Ruhnau F, Ritchie KB, Paul JH. High frequency of horizontal gene transfer in the oceans. *Science* 2010; **330**: 50.
162. MacLean RC, San Millan A. Microbial evolution: towards resolving the plasmid paradox. *Curr Biol* 2015; **25**: R764–R767.
163. Ziemert N, Lechner A, Wietz M, Millan-Aguinaga N, Chavarria KL, Jensen PRR. Diversity and evolution of secondary metabolism in the marine actinomycete *Salinispora*. *Proceedings of the National Academy of Sciences USA* 2014; **111**: E1130–E1139.
164. Wietz M, Millan-Aguinaga N, Jensen PR. CRISPR-Cas systems in the marine actinomycete *Salinispora*: Linkages with phage defense, microdiversity and biogeography. *BMC Genomics* 2014; **15**: 1–10.
165. Xing P, Hahnke RL, Unfried F, Markert S, Huang S, Barbeyron T, et al. Niches of two polysaccharide-degrading *Polaribacter* isolates from the North Sea during a spring diatom bloom. *ISME J* 2015; **9**: 1410–1422.
166. Viver T, Conrad RE, Rodriguez-R LM, Ramírez AS, Venter SN, Rocha-Cárdenas J, et al. Towards estimating the number of strains that make up a natural bacterial population. *Nat Commun* 2024; **15**: 544.
167. Biller SJ, Coe A, Roggensack SE, Chisholm SW. Heterotroph interactions alter *Prochlorococcus* transcriptome dynamics during extended periods of darkness. *mSystems* 2018; **3**: e00040-18.
168. López-Pérez M, Gonzaga A, Rodriguez-Valera F. Genomic diversity of ‘deep ecotype’ *Alteromonas macleodii* isolates: evidence for pan-mediterranean clonal frames. *Genome Biol Evol* 2013; **5**: 1220–32.
169. Fiore CL, Longnecker K, Kido Soule MC, Kujawinski EB. Release of ecologically relevant metabolites by the cyanobacterium *Synechococcus elongatus* CCMP 1631. *Environ Microbiol* 2015; **17**: 3949–3963.
170. Biller SJ, Coe A, Chisholm SW. Torn apart and reunited: impact of a heterotroph on the transcriptome of *Prochlorococcus*. *ISME J* 2016; **10**: 2831–2843.
171. Green DH, Bowman JP, Smith EA, Gutierrez T, Bolch CJS. *Marinobacter algicola* sp. nov., isolated from laboratory cultures of paralytic shellfish toxin-producing dinoflagellates. *Int J Syst Evol Microbiol* 2006; **56**: 523–527.
172. Zyszka-Haberecht B, Niemczyk E, Lipok J. Metabolic relation of cyanobacteria to aromatic compounds. *Appl Microbiol Biotechnol* 2019; **103**: 1167–1178.
173. Cau A, Ennas C, Moccia D, Mangoni O, Bolinesi F, Saggiomo M, et al. Particulate organic matter release below melting sea ice (Terra Nova Bay, Ross Sea, Antarctica): Possible relationships with zooplankton. *J Mar Sys* 2021; 103510.
174. Yubin F, Dong LI, Jun Z, Jianming P, Haisheng Z, Zhengbing H, et al. Effects of sea ice melt water input on phytoplankton biomass and community structure in the eastern Amundsen Sea. *Adv Polar Sci* 2022; **33**: 14–27.

175. Fernández-Méndez M, Turk-Kubo KA, Buttigieg PL, Rapp JZ, Krumpfen T, Zehr JP, et al. Diazotroph diversity in the sea ice, melt ponds, and surface waters of the Eurasian Basin of the central Arctic Ocean. *Front Microbiol* 2016; **7**: 1884–1884.
176. Uhlig C, Damm E, Peeken I, Krumpfen T, Rabe B, Korhonen M, et al. Sea ice and water mass influence dimethylsulfide concentrations in the central Arctic Ocean. *Front Earth Sci* 2019; **7**: 179.
177. Alonso-Sáez L, Zeder M, Harding T, Pernthaler J, Lovejoy C, Bertilsson S, et al. Winter bloom of a rare betaproteobacterium in the Arctic Ocean. *Front Microbiol* 2014; **5**: 425.
178. Hegseth EN, Assmy P, Wiktor JM, Wiktor J, Kristiansen S, Leu E, et al. Phytoplankton seasonal dynamics in Kongsfjorden, Svalbard and the adjacent shelf. In: Hop H, Wiencke C (eds). *The Ecosystem of Kongsfjorden, Svalbard*. 2019. Springer International Publishing, Cham, pp 173–227.
179. Soltwedel T, Bauerfeind E, Bergmann M, Bracher A, Budaeva N, Busch K, et al. Natural variability or anthropogenically-induced variation? Insights from 15 years of multidisciplinary observations at the arctic marine LTER site HAUSGARTEN. *Ecol Indicators* 2016; **65**: 89–102.
180. von Jackowski A, Grosse J, Nöthig E-M, Engel A. Dynamics of organic matter and bacterial activity in the Fram Strait during summer and autumn. *Philos Trans R Soc A* 2020; **378**: 20190366.
181. Cardozo-Mino MG, Fadeev E, Salman-Carvalho V, Boetius A. Spatial distribution of Arctic bacterioplankton abundance is linked to distinct water masses and summertime phytoplankton bloom dynamics (Fram Strait, 79°N). *Front Microbiol* 2021; **12**: 658803.
182. Polyakov IV, Pnyushkov AV, Alkire MB, Ashik IM, Baumann TM, Carmack EC, et al. Greater role for Atlantic inflows on sea-ice loss in the Eurasian Basin of the Arctic Ocean. *Science* 2017; **356**: 285–291.
183. Stecher A, Neuhaus S, Lange B, Frickenhaus S, Beszteri B, Kroth PG, et al. rRNA and rDNA based assessment of sea ice protist biodiversity from the central Arctic Ocean. *Eur J Phycol* 2016; **51**: 31–46.
184. Leeuwe M van, Tedesco L, Arrigo KR, Assmy P, Campbell K, Meiners KM, et al. Microalgal community structure and primary production in Arctic and Antarctic sea ice: A synthesis. *Elem Sci Anth* 2018; **6**: 4.
185. Lalande C, Nöthig E-M, Somavilla R, Bauerfeind E, Shevchenko V, Okolodkov Y. Variability in under-ice export fluxes of biogenic matter in the Arctic Ocean. *Glob Biogeochem Cyc* 2014; **28**: 571–583.
186. Hoffmann K, Hassenrück C, Salman-Carvalho V, Holtappels M, Bienhold C. Response of bacterial communities to different detritus compositions in Arctic deep-sea sediments. *Front Microbiol* 2017; **8**: 266.
187. Humphry DR, George A, Black GW, Cummings SP. *Flavobacterium frigidarium* sp. nov., an aerobic, psychrophilic, xylanolytic and laminarinolytic bacterium from Antarctica. *Int J Syst Evol Microbiol* 2001; **51**: 1235–1243.
188. Ardyna M, Mundy CJ, Mayot N, Matthes LC, Oziel L, Horvat C, et al. Under-ice phytoplankton blooms: shedding light on the “invisible” part of Arctic primary production. *Front Mar Sci* 2020; **7**: 608032.

189. Oldenburg E, Popa O, Wietz M, von Appen W-J, Torres-Valdes S, Bienhold C, et al. Sea-ice melt determines seasonal phytoplankton dynamics and delimits the habitat of temperate Atlantic taxa as the Arctic Ocean atlantifies. *bioRxiv* 2023; 2023.05.04.539293.
190. Wietz M, López-Pérez M, Sher D, Biller SJ, Rodriguez-Valera F. Microbe Profile: *Alteromonas macleodii* - a widespread, fast-responding, 'interactive' marine bacterium. *Microbiology* 2022; **168**: 001236.
191. Rosado-Espinosa LA, Freile-Pelegrín Y, Hernández-Nuñez E, Robledo D. A comparative study of *Sargassum* species from the Yucatan Peninsula coast: morphological and chemical characterisation. *Phycologia* 2020; **59**: 261–271.
192. Haug A, Larsen B, Smidsrød O. Uronic acid sequence in alginate from different sources. *Carbohydr Res* 1974; **32**: 217–225.
193. Davis D, Simister R, Campbell S, Marston M, Bose S, McQueen-Mason SJ, et al. Biomass composition of the golden tide pelagic seaweeds *Sargassum fluitans* and *S. natans* (morphotypes I and VIII) to inform valorisation pathways. *Sci Total Environ* 2021; **762**: 143134.
194. Roth Rosenberg D, Haber M, Goldford J, Lalzar M, Aharonovich D, Al-Ashhab A, et al. Particle-associated and free-living bacterial communities in an oligotrophic sea are affected by different environmental factors. *Environ Microbiol* 2021; **23**: 4295–4308.
195. Gonzaga A, Martin-Cuadrado A-BB, López-Pérez M, Mizuno CM, García-Heredia I, Kimes NE, et al. Polyclonality of concurrent natural populations of *Alteromonas macleodii*. *Genome Biol Evol* 2012; **4**: 1360–1374.
196. Hibbing ME, Fuqua C, Parsek MR, Peterson SBB. Bacterial competition: surviving and thriving in the microbial jungle. *Nat Rev Microbiol* 2010; **8**: 15–25.
197. Kimes NE, López-Pérez M, Ausó E, Ghai R, Rodriguez-Valera F. RNA sequencing provides evidence for functional variability between naturally co-existing *Alteromonas macleodii* lineages. *BMC Genomics* 2014; **15**: 938–938.
198. Farrant GK, Doré H, Cornejo-Castillo FM, Partensky F, Ratin M, Ostrowski M, et al. Delineating ecologically significant taxonomic units from global patterns of marine picocyanobacteria. *Proc Natl Acad Sci USA* 2016; **113**: E3365–E3374.
199. Riley MA, Lizotte-Waniewski M. Population genomics and the bacterial species concept. *Methods Mol Biol* 2009; **532**: 367–77.
200. Shapiro BJ, Friedman J, Cordero OX, Preheim SP, Timberlake SC, Szabó G, et al. Population genomics of early events in the ecological differentiation of bacteria. *Science* 2012; **335**: 48–51.
201. Wietz M, Engel A, Ramondenc S, Niwano M, von Appen W-J, Priest T, et al. The Arctic summer microbiome across Fram Strait: Depth, longitude, and substrate concentrations structure microbial diversity in the euphotic zone. *Environ Microbiol* 2024; **in press**.
202. Park HJ, Lee YM, Kim S, Wi AR, Han SJ, Kim H-W, et al. Identification of proteolytic bacteria from the Arctic Chukchi Sea expedition cruise and characterization of cold-active proteases. *J Microbiol* 2014; **52**: 825–833.
203. Lannuzel D, Tedesco L, van Leeuwe M, Campbell K, Flores H, Delille B, et al. The future of Arctic sea-ice biogeochemistry and ice-associated ecosystems. *Nat Clim Change* 2020; **10**: 983–992.

204. Carter-Gates M, Balestreri C, Thorpe SE, Cottier F, Baylay A, Bibby TS, et al. Implications of increasing Atlantic influence for Arctic microbial community structure. *Sci Rep* 2020; **10**: 19262.
205. Comeau AM, Li WK, Tremblay JE, Carmack EC, Lovejoy C. Arctic Ocean microbial community structure before and after the 2007 record sea ice minimum. *PLOS ONE* 2011; **6**: e27492.
206. Lalande C, Bauerfeind E, Nöthig E-M, Beszczynska-Möller A. Impact of a warm anomaly on export fluxes of biogenic matter in the eastern Fram Strait. *Prog Oceanogr* 2013; **109**: 70–77.
207. Dybwad C, Assmy P, Olsen LM, Peeken I, Nikolopoulos A, Krumpen T, et al. Carbon export in the seasonal sea ice zone north of Svalbard from winter to late summer. *Front Mar Sci* 2021; **7**: 525800.
208. Glud RN, Rysgaard S, Turner G, McGinnis DF, Leakey RJG. Biological- and physical-induced oxygen dynamics in melting sea ice of the Fram Strait. *Limnol Oceanogr* 2014; **59**: 1097–1111.
209. Shiozaki T, Ijichi M, Fujiwara A, Makabe A, Nishino S, Yoshikawa C, et al. Factors regulating nitrification in the Arctic Ocean: potential impact of sea ice reduction and ocean acidification. *Glob Biogeochem Cyc* 2019; **33**: 1085–1099.
210. Ghiglione J-FJF, Galand PE, Pommier T, Pedros-Alio C, Maas EW, Bakker K, et al. Pole-to-pole biogeography of surface and deep marine bacterial communities. *Proc Natl Acad Sci USA* 2012; **109**: 17633–17638.
211. Cao S, Zhang W, Ding W, Wang M, Fan S, Yang B, et al. Structure and function of the Arctic and Antarctic marine microbiota as revealed by metagenomics. *Microbiome* 2020; **8**: 47.
212. Olli K, Halvorsen E, Vernet M, Lavrentyev PJ, Franzè G, Sanz-Martin M, et al. Food web functions and interactions during spring and summer in the Arctic water inflow region: investigated through inverse modeling. *Front Mar Sci* 2019; **6**: 244.
213. Wassmann P. Retention versus export food chains: processes controlling sinking loss from marine pelagic systems. *Hydrobiologia* 1997; **363**: 29–57.
214. Svensen C, Halvorsen E, Vernet M, Franzè G, Dmoch K, Lavrentyev PJ, et al. Zooplankton communities associated with new and regenerated primary production in the Atlantic inflow north of Svalbard. *Front Mar Sci* 2019; **6**: 293.
215. Cavicchioli R, Ripple WJ, Timmis KN, Azam F, Bakken LR, Baylis M, et al. Scientists' warning to humanity: microorganisms and climate change. *Nat Rev Microbiol* 2019; **17**: 569–586.
216. Stoll N, Wietz M, Juricke S, Pausch F, Peter C, Seifert M, et al. "Wissenschaft fürs Wohnzimmer" – 2 years of weekly interactive, scientific livestreams on YouTube. *Polarforschung* 2023; **91**: 31–43.

## 7. Manuscripts summarized in this thesis (chronological order)

- **Wietz M**, Wemheuer B, Simon H, Giebel H-A, Seibt MA, Daniel R, Brinkhoff T, Simon M (2015). Bacterial community dynamics during polysaccharide degradation at contrasting sites in the Southern and Atlantic Oceans. *Environ. Microbiol.* 17:3822–3831. *Own contribution: field and laboratory work, molecular analyses, data evaluation and visualization, writing.*
- Neumann A, Balmonte JP, Berger M, Giebel H-A, Arnosti C, Voget S, Brinkhoff T, Simon M, **Wietz M** (2015). Different utilization of alginate and other algal polysaccharides by marine *Alteromonas macleodii* ecotypes. *Environ. Microbiol.* 17:3857–3868. *Own contribution: Project design, student supervision, genomic analyses, data evaluation and visualization, writing.*
- Mitulla M, Dinasquet J, Guillemette R, Simon M, Azam F, **Wietz M** (2016). Response of bacterial communities from California coastal waters to alginate particles and an alginolytic *Alteromonas macleodii* strain. *Environ. Microbiol.* 18:4369–4377. *Own contribution: Project design, student supervision, amplicon analyses, data evaluation and visualization, writing.*
- Koch H, Freese HM, Hahnke RL, Simon M, **Wietz M** (2019). Adaptations of *Alteromonas* sp. 76-1 to polysaccharide degradation: A CAZyme plasmid for ulvan degradation and two alginolytic systems. *Front. Microbiol.* 10:504. *Own contribution: Project design, supervision, genomic analyses, data evaluation and visualization, writing.*
- Koch H, Dürwald A, Schweder T, Noriega-Ortega B, Vidal-Melgosa S, Hehemann J-H, Dittmar T, Freese HM, Becher D, Simon M, **Wietz M** (2019). Biphasic cellular adaptations and ecological implications of *Alteromonas macleodii* degrading a mixture of algal polysaccharides. *ISME J.* 13:92–103. *Own contribution: Project design, supervision, genomic analyses, laboratory work, data evaluation and visualization, writing.*
- Koch H, Germscheid N, Freese HM, Noriega-Ortega B, Lücking D, Berger M, Qiu G, Marzinelli E, Campbell A, Steinberg P, Overmann J, Dittmar T, Simon M, **Wietz M** (2020). Genomic, metabolic and phenotypic variability shapes ecological differentiation and intraspecies interactions of *Alteromonas macleodii*. *Sci. Rep.* 10:809. *Own contribution: Project design, supervision, genomic analyses, laboratory work, data evaluation and visualization, writing.*
- Bunse C, Koch H, Breider S, Simon M, **Wietz M** (2021). Sweet spheres: Succession and CAZyme expression of marine bacterial communities colonizing a mix of alginate and pectin particles. *Environ. Microbiol.* 23:3130–3148. *Own contribution: Project design, fieldwork, supervision, amplicon analyses, data evaluation and visualization, writing.*
- **Wietz M**, Bienhold C, Metfies K, Torres-Valdes S, von Appen W-J, Salter I, Boetius A (2021). The polar night shift: Seasonal dynamics and drivers of Arctic Ocean microbiomes revealed by autonomous sampling. *ISME Commun.* 1:76. *Own contribution: Project design, amplicon analyses, data evaluation and visualization, writing.*
- Priest T, von Appen W-J, Oldenburg E, Popa O, Torres-Valdés S, Bienhold C, Metfies K, Boulton W, Mock T, Fuchs B, Amann R, Boetius A, **Wietz M** (2023). Atlantic water influx and sea-ice cover drive taxonomic and functional shifts in Arctic marine bacterial communities. *ISME J* 17:1612–1625. *Own contribution: Project design, sequence analyses, data evaluation and visualization, writing.*

## 8. Complete publication list

Total publications: 39 (14x first author; 9x senior author)

Citations: 1620 h-index: 19 i10-index: 26

Conference contributions / Invited presentations: 28 / 8

\*(co-)supervised students

- **Wietz M**, Engel A, Ramondenc S, Niwano M, von Appen W-J, Priest T, von Jackowski A, Metfies K, Bienhold C, Boetius A (2024). The Arctic summer microbiome across Fram Strait: depth, region and substrate concentrations structure microbial diversity in the euphotic zone. *Environ. Microbiol.* in press. [doi:10.1111/1462-2920.16568](https://doi.org/10.1111/1462-2920.16568)
- Priest T, von Appen W-J, Oldenburg E, Popa O, Torres-Valdés S, Bienhold C, Metfies K, Boulton W, Mock T, Fuchs BM, Amann R, Boetius A, **Wietz M** (2023). Atlantic water influx and sea-ice cover drive taxonomic and functional shifts in Arctic marine bacterial communities. *ISME J* 17:1612–1625. [doi:10.1038/s41396-023-01461-6](https://doi.org/10.1038/s41396-023-01461-6)
- Gros V, Bonsang B, Sarda-Estève R, Nikolopoulos A, Metfies K, **Wietz M**, Peeken I (2023). Concentrations of dissolved dimethyl sulfide (DMS), methanethiol and other trace gases in context of microbial communities from the temperate Atlantic to the Arctic Ocean. *Biogeosciences* 20:851–867. [doi:10.5194/bg-20-851-2023](https://doi.org/10.5194/bg-20-851-2023)
- Rahlff J, **Wietz M**, Giebel H-A, Bayfield O, Nilsson E, Bergstroem K, Kieft K, Anantharaman K, Ribas-Ribas M, Wurl O, Hoetzinger M, Antson A, Holmfeldt K (2023). Ecogenomics and cultivation reveal distinctive viral-bacterial communities in the surface microlayer of a Baltic Sea slick. *ISME Commun.* 3:97. [doi:10.1038/s43705-023-00307-8](https://doi.org/10.1038/s43705-023-00307-8)
- Fadeev E, Bastos CC, Hennenfeind J, Biller SJ, Sher D, **Wietz M**, Herndl GJ (2023). Characterization of membrane vesicles in *Alteromonas macleodii* indicates potential roles in their copiotrophic lifestyle. *microLife* 4:1–11. [doi:10.1093/femsml/uqac025](https://doi.org/10.1093/femsml/uqac025)
- Stoll N, **Wietz M**, Juricke S, Pausch F, Peter C, Massing JC, Seifert M, Zeising M, Käß M, McPherson R, Suckow B. “Wissenschaft fürs Wohnzimmer” – two years of interactive, scientific livestreams weekly on YouTube. *Polarforschung* 91, 31–43. [doi:10.5194/polf-91-31-2023](https://doi.org/10.5194/polf-91-31-2023)
- **Wietz M**, Metfies K, Bienhold C, Wolf C, Janssen F, Salter I, Boetius A (2022). Impact of preservation method and storage period on ribosomal metabarcoding of marine microbes: Implications for remote automated samplings. *Front. Microbiol.* 13:999925. [doi:10.3389/fmicb.2022.999925](https://doi.org/10.3389/fmicb.2022.999925)
- **Wietz M**, López-Pérez M, Sher D, Biller SJ, Rodriguez-Valera F (2022). *Alteromonas macleodii* – A widespread, fast-responding, “interactive” marine bacterium. *Microbiology* 168:001236. [doi:10.1099/mic.0.00123](https://doi.org/10.1099/mic.0.00123)
- von Jackowski A, Becker K, Zäncker B, **Wietz M**, Bienhold C, Nöthig E-M, Engel A (2022). Variations of microbial communities and substrate regimes in the eastern Fram Strait between summer and fall. *Environ. Microbiol.* 24:4124–4136. [doi:10.1111/1462-2920.16036](https://doi.org/10.1111/1462-2920.16036)
- **Wietz M**, Bienhold C, Metfies K, Torres-Valdes S, von Appen W-J, Salter I, Boetius A (2021). The polar night shift: Seasonal dynamics and drivers of Arctic Ocean microbiomes revealed by autonomous sampling. *ISME Commun.* 1:76. [doi:10.1038/s43705-021-00074-4](https://doi.org/10.1038/s43705-021-00074-4)

- von Appen W-J, Waite A, Bergmann M, Bienhold C, Boebel O, Bracher A, Cisewski B, Hagemann J, Hoppema M, Iversen M, Konrad C, Krumpfen T, Lochthofen N, Metfies K, Niehoff B, Nöthig E-M, Purser A, Salter I, Schaber M, Scholz D, Soltwedel T, Torres-Valdés S, Wekerle C, Wenzhoefer F, **Wietz M**, Boetius A (2021). Sea-ice derived meltwater stratification slows the biological carbon pump: results from continuous observations. *Nat. Comm.* 12:7309. [doi:10.1038/s41467-021-26943-z](https://doi.org/10.1038/s41467-021-26943-z)
- Arnosti C, **Wietz M**, Brinkhoff T, Hehemann J-H, Probandt D, Zeugner L, Amann R (2021). The biogeochemistry of marine polysaccharides: sources, inventories, and bacterial drivers of the carbohydrate cycle. *Annu. Rev. Mar. Sci.* 13:81–108. [doi:10.1146/annurev-marine-032020-012810](https://doi.org/10.1146/annurev-marine-032020-012810)
- Fadeev E, **Wietz M**, von Appen W-J, Iversen MH, Nöthig E-M, Engel A, Grosse J, Graeve M, Boetius A (2021). Submesoscale physicochemical dynamics directly shape bacterioplankton community structure in space and time. *Limnol. Oceanogr.* 66:2901–2913. [doi:10.1002/lno.11799](https://doi.org/10.1002/lno.11799)
- Bunse C, Koch H, Breider S, Simon M, **Wietz M** (2021). Sweet spheres: Succession and CAZyme expression of marine bacterial communities colonizing a mix of alginate and pectin particles. *Environ. Microbiol.* 23:3130–3148. [doi:10.1111/1462-2920.15536](https://doi.org/10.1111/1462-2920.15536)
- Wolter LA\*, Mitulla M, Kalem J, Daniel R, Simon M, **Wietz M** (2021). CAZymes in *Maribacter dokdonensis* 62-1 from the Patagonian shelf: Genomics and physiology compared to related flavobacteria and a co-occurring *Alteromonas* strain. *Front. Microbiol.* 12:628055. [doi:10.3389/fmicb.2021.628055](https://doi.org/10.3389/fmicb.2021.628055)
- Wolter LA\*, **Wietz M**, Ziesche L, Breider S, Leinberger J, Poehlein A, Daniel R, Schulz S, Brinkhoff T (2021). *Pseudoceanicola algae* sp. nov., isolated from the marine macroalga *Fucus spiralis*, shows genomic and physiological adaptations for an algae-associated lifestyle. *Syst. Appl. Microbiol.* 44:126166. [doi:10.1016/j.syapm.2020.126166](https://doi.org/10.1016/j.syapm.2020.126166)
- Giebel H-A, Arnosti C, Badewien TH, Bakenhus I, Balmonte JP, Billerbeck S, Dlugosch L, Henkel R, Kuerzel B, Meyerjürgens J, Milke F, Voss D, Wienhausen G, **Wietz M**, Winkler H, Wolterink M, Simon M (2021). Microbial growth and organic matter cycling in the Pacific Ocean along a latitudinal transect between subarctic and subantarctic waters. *Front. Mar. Sci.* 8:764383. [doi:10.3389/fmars.2021.764383](https://doi.org/10.3389/fmars.2021.764383)
- Koch H, Germscheid N\*, Freese HM, Noriega-Ortega B, Lücking D\*, Berger M, Qiu G, Marzinelli EM, Campbell AH, Steinberg PD, Overmann J, Dittmar T, Simon M, **Wietz M** (2020). Genomic, metabolic and phenotypic variability shapes ecological differentiation and intraspecies interactions of *Alteromonas macleodii*. *Sci. Rep.* 10:809. [doi:10.1038/s41598-020-57526-5](https://doi.org/10.1038/s41598-020-57526-5)
- **Wietz M**, Lau SC, Harder T (2019). Editorial: Socio-ecology of microbes in a changing ocean. *Front. Mar. Sci.* 6:190. [doi:10.3389/fmars.2019.00190](https://doi.org/10.3389/fmars.2019.00190)
- Koch H, Freese HM, Hahnke RL, Simon M, **Wietz M** (2019). Adaptations of *Alteromonas* sp. 76-1 to polysaccharide degradation: A CAZyme plasmid for ulvan degradation and two alginolytic systems. *Front. Microbiol.* 10:504. [doi:10.3389/fmicb.2019.00504](https://doi.org/10.3389/fmicb.2019.00504)
- Koch H, Dürwald A, Schweder T, Noriega-Ortega B, Vidal-Melgosa S, Hehemann J-H, Dittmar T, Freese HM, Becher D, Simon M, **Wietz M** (2019). Biphasic cellular adaptations and ecological implications of *Alteromonas macleodii* degrading a mixture of algal polysaccharides. *ISME J.* 13:92–103. [doi:10.1038/s41396-018-0252-4](https://doi.org/10.1038/s41396-018-0252-4)

- Bakenhus I\*, Dlugosch L, Giebel H-A, Beardsley C, Simon M, **Wietz M** (2018). Distinct biogeographic patterns of bacterioplankton composition and single-cell activity between the subtropics and Antarctica. *Environ. Microbiol.* 20:3100–3108. [doi:10.1111/1462-2920.14383](https://doi.org/10.1111/1462-2920.14383)
- Klotz F, Brinkhoff T, Freese HM, **Wietz M**, Teske A, Simon M, Giebel H-A (2018). Description of *Tritonibacter horizontis* gen. nov., sp. nov., a new member of the *Rhodobacteraceae*, isolated from the Deepwater Horizon oil spill. *Int. J. Syst. Evol. Microbiol.* 68:736–744. [doi:10.1099/ijsem.0.002573](https://doi.org/10.1099/ijsem.0.002573)
- Mitulla M\*, Dinasquet J, Guillemette R, Simon M, Azam F, **Wietz M**. (2016). Response of bacterial communities from California coastal waters to alginate particles and an alginolytic *Alteromonas macleodii* strain. *Environ. Microbiol.* 18:4369–4377. [doi:10.1111/1462-2920.13314](https://doi.org/10.1111/1462-2920.13314)
- Neumann A\*, Balmonte JP, Berger M, Giebel H-A, Arnosti C, Voget S, Brinkhoff T, Simon M, **Wietz M** (2015). Different utilization of alginate and other algal polysaccharides by marine *Alteromonas macleodii* ecotypes. *Environ. Microbiol.* 17:3857–3868. [doi:10.1111/1462-2920.12862](https://doi.org/10.1111/1462-2920.12862)
- **Wietz M**, Wemheuer B, Simon H, Giebel H-A, Seibt MA, Daniel R, Brinkhoff T, Simon M (2015). Bacterial community dynamics during polysaccharide degradation at contrasting sites in the Southern and Atlantic Oceans. *Environ. Microbiol.* 17:3822–3831. [doi:10.1111/1462-2920.12842](https://doi.org/10.1111/1462-2920.12842)
- **Wietz M**, Millán-Aguíñaga N, Jensen PR (2014) CRISPR-Cas systems in the marine actinomycete *Salinispora*: linkages with phage defense, microdiversity and biogeography. *BMC Genomics* 9:536. [doi:10.1186/1471-2164-15-936](https://doi.org/10.1186/1471-2164-15-936)
- Ziemert N, Lechner A, **Wietz M**, Millán-Aguíñaga N, Chavarria KL, Jensen PR (2014). Diversity and evolution of secondary metabolism in the marine actinomycete genus *Salinispora*. *Proc. Natl. Acad. Sci. USA* 111:E1130–1139. [doi:10.1073/pnas.1324161111](https://doi.org/10.1073/pnas.1324161111)
- **Wietz M**, Duncan K, Patin N, Jensen PR (2013). Antagonistic interactions mediated by marine bacteria: the role of small molecules. *J. Chem. Ecol.* 9:879–891. [doi:10.1007/s10886-013-0316-x](https://doi.org/10.1007/s10886-013-0316-x)
- **Wietz M**, Månsson M, Vynne NG, Gram L (2013). Small-molecule antibiotics from marine bacteria and strategies to prevent rediscovery of known compounds. In “Marine Microbiology: Bioactive Compounds and Biotechnological Applications“ (Ed. Se-Kwon Kim), Wiley-VCH, Weinheim. [doi:10.1002/9783527665259.ch08](https://doi.org/10.1002/9783527665259.ch08)
- Nielsen A, Månsson M, **Wietz M**, Varming AN, Phipps RK, Larsen TO, Gram L, Ingmer H (2012). Nigribactin, a novel siderophore from *Vibrio nigripulchritudo*, modulates *Staphylococcus aureus* virulence gene expression. *Mar. Drugs* 10:2584–2595. [doi:10.3390/md10112584](https://doi.org/10.3390/md10112584)
- **Wietz M**, Månsson M, Bowman JS, Blom N, Ng Y, Gram L (2012). Wide distribution of closely related, antibiotic-producing *Arthrobacter* strains throughout the Arctic Ocean. *Appl. Environ. Microbiol.* 78:2039–2042. [doi:10.1128/AEM.07096-11](https://doi.org/10.1128/AEM.07096-11)
- **Wietz M**, Månsson M, Gram L (2011). Chitin stimulates production of the antibiotic andrimid in a *Vibrio coralliilyticus* strain. *Environ. Microbiol. Rep.* 3:559–564. [doi:10.1111/j.1758-2229.2011.00259.x](https://doi.org/10.1111/j.1758-2229.2011.00259.x)
- Månsson M, Nielsen A, Kjaerulff L, Gotfredsen C, **Wietz M**, Ingmer H, Gram L, Larsen TO (2011). Inhibition of virulence gene expression in *Staphylococcus aureus* by novel

depsipeptides from a marine *Photobacterium*. *Mar. Drugs* 9:2537–2552. [doi:10.3390/md9122537](https://doi.org/10.3390/md9122537)

- **Wietz M**, Gram L, Jørgensen B, Schramm A (2010). Latitudinal patterns in the abundance of major marine bacterioplankton groups. *Aquat. Microb. Ecol.* 61:179–189. [doi:10.3354/ame01443](https://doi.org/10.3354/ame01443)
- **Wietz M**, Månsson M, Gotfredsen C, Larsen TO, Gram L (2010). Antibacterial compounds from marine *Vibrionaceae* isolated on a global expedition. *Mar. Drugs* 8:2946–2960. [doi: 10.3390/md8122946](https://doi.org/10.3390/md8122946)
- **Wietz M**, Hall MR, Høj L (2009). Effects of seawater ozonation on biofilm development in aquaculture tanks. *Syst. Appl. Microbiol.* 32:266–277. [doi: 10.1016/j.syapm.2009.04.001](https://doi.org/10.1016/j.syapm.2009.04.001)
- Payne MS, Høj L, **Wietz M**, Hall MR, Sly L, Bourne DG (2008). Microbial diversity of mid-stage Palinurid phyllosoma from Great Barrier Reef waters. *J. Appl. Microbiol.* 105:340–350. [doi:10.1111/j.1365-2672.2008.03749.x](https://doi.org/10.1111/j.1365-2672.2008.03749.x)

## 9. TEACHING

### Lectures and exercises

- Methods in Aquatic Microbial Ecology (UOL, 2022–2023) **PC**
  - Microbial Diversity (UOL, 2022–2023) **VL**
  - Genome to Phylogeny, Function and Ecology (HS Bremerhaven; 2022–2023) **PC**
  - *Marmic* (MPI Bremen; 2019–2022) **PC**
  - Microbial Diversity (UOL; 2014–2018) **VL**
  - Biological Oceanography (UOL; 2016) **VL**
  - Ecology of Marine Microorganisms (UOL; 2015) **PC**
  - Scientific Writing and Practice (UOL; 2014) **VL**
  - Experimental Applied Biodiversity (Technical University of Denmark; 2011) **PC**
  - Bacterial Diversity in Fresh and Marine Waters (Technical University of Denmark; 2010) **PC**
- VL:** lecture / Vorlesung; **PC:** practical course / Praktikum

### Student supervision and mentoring

- Ruben Schulte-Hillen (AWI; 2023). MSc thesis
- Tabea Platz (AWI; 2023). Student assistantship
- Miriam Sternel (AWI; 2022). MSc project
- Matomo Niwano (AWI; 2021). BSc project
- Jovan Kalem (AWI; 2020). Virtual internship
- Magda Cardozo Mino (AWI; 2019). PhD co-supervision
- Nora Germscheid (UOL; 2018). MSc thesis
- Dominik Lücking (UOL; 2018). Student assistantship
- Antoine Ng (UOL; 2018). MSc thesis
- Zain Albezra (UOL; 2017). MSc project
- Mara Heinrichs (UOL; 2016). MSc project
- Nadine Gerlach (UOL; 2016). MSc thesis
- Dennis Tebbe, Julius Degenhardt (UOL; 2015). MSc project
- Maximilian Mitulla (UOL; 2015). MSc thesis
- Anna Neumann (UOL; 2014). MSc thesis
- Robert Strodel, Anna Moskva (UOL; 2014). BSc project
- Maximilian Mitulla (UOL; 2014). BSc project
- Martin Mierzejewski (UOL; 2013). BSc project
- Kamilla Spanggaard, Anja Sander (DTU; 2010). MSc thesis
- Sine Fredslund (DTU; 2010). MSc thesis
- Mentor; “Buddy Program” ISME18, Switzerland (2022)
- High school project (AWI "HighSea" program; 2022 – received [Hans Riegel Award](#))
- Mentor, ASLO Multicultural Program, Ocean Sciences Meeting (2022)
- Student Presentation Evaluation Program, Ocean Sciences Meeting (2020 & 2022)
- Reviewer for “Annette Barthelt Prize” awarding outstanding marine PhD theses (2019)

## 10. ACKNOWLEDGMENTS

So many people, from all around the world, have tremendously enriched my academic and personal journey. Thank you so much for the good times, exciting science, stimulating discussions, cultivating ideas, exploring places, and being friends.

To Meinhard Simon, Lone Gram, Antje Boetius, Lone Høj, Paul Jensen, Christina Bienhold, and Thorsten Brinkhoff – my heartfelt gratitude for your dedicated and diverse roles.

Many thanks to the Simon, Cypionka, Dittmar, Rabus, Könnecke and Meren labs, everyone at ICBM and collaborators; foremost Hanna Koch, Heike Simon, Rolf Weinert, Helge-Ansgar Giebel, Carina Bunse, Mathias Wolterink, Carol Arnosti, and JP Balmonte.

Many thanks to the Deep-Sea Group at AWI / MPI, everyone in FRAM and collaborators; foremost Taylor Priest, Wilken-Jon von Appen, Katja Metfies, Ellen Oldenburg, Ovidiu Popa, Morten Iversen, Ulli Hoge, Jakob Barz, Bernhard Fuchs, Rudi Amann, Thomas Soltwedel, Sinhué Torres-Valdés, Eddie Fadeev, and Eva-Maria Nöthig.

Many thanks to crews and colleagues at sea (ANT28-2, ANT28-5, PS121, PS138, SO248, LOMROG-II, Cape Ferguson), TROPOS, and AWIPEV.

Many thanks to the Jensen, Azam, Bowman, Moore, Fenical, and Rouse labs at Scripps; Maria Månsson and Nete Bernbom at DTU; David Bourne and Michael Hall at AIMS; all of my students; AWIs4Future; as well as DFG, DAAD, Helmholtz Association, Max Planck Society, Oldenburg University, and SPP1158 for financial support.

Beyond academic endeavors, I am forever grateful for love and laughter: Laura Wolter, Annelies Weyn, Natalie Millán-Aguiñaga, my band and football mates, and all dear friends near and far.

Finally, and foremost: thank you, Mama und Papa, for everything. Thank you, my brother, Olli, and the entire family for holding a special place in my life.

## Appendix 1

### **Bacterial community dynamics during polysaccharide degradation at contrasting sites in the Southern and Atlantic Oceans**

Wietz M, Wemheuer B, Simon H, Giebel H-A, Seibt MA, Daniel R, Brinkhoff T, Simon M

*Environmental Microbiology* (2015), 17:3822–3831

# Bacterial community dynamics during polysaccharide degradation at contrasting sites in the Southern and Atlantic Oceans

Matthias Wietz,<sup>1\*</sup> Bernd Wemheuer,<sup>2</sup> Heike Simon,<sup>1</sup> Helge-Ansgar Giebel,<sup>1</sup> Maren A. Seibt,<sup>3</sup> Rolf Daniel,<sup>2</sup> Thorsten Brinkhoff<sup>1</sup> and Meinhard Simon<sup>1</sup>

<sup>1</sup>Institute for Chemistry and Biology of the Marine Environment, University of Oldenburg, Oldenburg 26129, Germany.

<sup>2</sup>Genomic and Applied Microbiology and Göttingen Genomics Laboratory, Institute of Microbiology and Genetics, University of Göttingen, Göttingen 37077, Germany.

<sup>3</sup>ICBM-MPI Bridging Group for Marine Geochemistry, Institute for Chemistry and Biology of the Marine Environment, University of Oldenburg, Oldenburg 26129, Germany.

## Summary

The bacterial degradation of polysaccharides is central to marine carbon cycling, but little is known about the bacterial taxa that degrade specific marine polysaccharides. Here, bacterial growth and community dynamics were studied during the degradation of the polysaccharides chitin, alginate and agarose in microcosm experiments at four contrasting locations in the Southern and Atlantic Oceans. At the Southern polar front, chitin-supplemented microcosms were characterized by higher fractions of actively growing cells and a community shift from *Alphaproteobacteria* to *Gammaproteobacteria* and *Bacteroidetes*. At the Antarctic ice shelf, chitin degradation was associated with growth of *Bacteroidetes*, with 24% higher cell numbers compared with the control. At the Patagonian continental shelf, alginate and agarose degradation covaried with growth of different *Alteromonadaceae* populations, each with specific temporal growth patterns. At the Mauritanian upwelling, only the alginate hydrolysis product guluronate was consumed, coincident with increasing abundances of *Alteromonadaceae* and possibly cross-feeding SAR11. 16S rRNA gene amplicon librar-

ies indicated that growth of the *Bacteroidetes*-affiliated genus *Reichenbachiella* was stimulated by chitin at all cold and temperate water stations, suggesting comparable ecological roles over wide geographical scales. Overall, the predominance of location-specific patterns showed that bacterial communities from contrasting oceanic biomes have members with different potentials to hydrolyse polysaccharides.

## Introduction

Polysaccharides constitute a considerable fraction of dissolved and particulate organic matter in the oceans (Cowie and Hedges, 1984; Tanoue and Handa, 1987; Benner *et al.*, 1992). Thus, polysaccharides are a central component of marine carbon cycles and a major nutrient source for heterotrophic bacteria (Azam and Malfatti, 2007). Bacterial uptake of polysaccharides requires initial hydrolysis to oligo- and monomers, which is performed by excreted hydrolytic enzymes with different substrate specificities (Zimmerman *et al.*, 2013). The phylum *Bacteroidetes* has been consistently linked to the utilization of biopolymers (Cottrell and Kirchman, 2000; Fernández-Gómez *et al.*, 2013; Kabisch *et al.*, 2014), but the capacity for hydrolytic enzyme production is also found among other marine bacterial taxa, including *Gammaproteobacteria* (Tang *et al.*, 2012; Zimmerman *et al.*, 2013).

The degradation of marine polysaccharides and other high-molecular weight organic matter is related to bacterial biomass (Piontek *et al.*, 2011), respiration rates (Amon and Benner, 1994) and community structure (Haynes *et al.*, 2007; Murray *et al.*, 2007). A number of studies have provided insights into the succession of taxa, metabolic pathways, and chemical transformations during biopolymer degradation (McCarren *et al.*, 2010; Sharma *et al.*, 2013). In the Mediterranean Sea, the community dynamics observed during the degradation of dissolved organic matter suggested functional redundancy for polymer degradation at different taxonomic levels (Landa *et al.*, 2013). Moreover, taxa that normally constitute only a minor part of the community, for instance *Reinekea* (Teeling *et al.*, 2012) or *Alteromonas* spp. (McCarren

Received 7 October, 2014; revised 4 March, 2015; accepted 4 March, 2015. \*For correspondence. E-mail matthias.wietz@uni-oldenburg.de; Tel. +49-441-7983637; Fax +49-441-7983438.

*et al.*, 2010; Sarmiento and Gasol, 2012), can also be stimulated by the availability of biopolymers.

Despite the insights into bacterial biopolymer degradation afforded by these studies, less is known about the bacterial lineages that degrade specific polysaccharides. In the Southern Ocean, microcosms supplemented with starch and agarose were dominated by *Gammaproteobacteria* and *Bacteroidetes* (Simon *et al.*, 2012), and the same taxa were stimulated by cellulose in the Irish Sea (Edwards *et al.*, 2010). A series of studies on six marine polysaccharides revealed that both the hydrolysable range of substrates as well as summed hydrolysis rates were higher in equatorial than in polar oceans (Arnosti *et al.*, 2011). Hydrolysis of the same substrates also varied between biogeographic provinces (Arnosti *et al.*, 2012), deep versus surface waters (D'Ambrosio *et al.*, 2014), and estuarine versus coastal sites (Steen *et al.*, 2008). However, these analyses of hydrolysis rates and enzymatic substrate specificities did not include detailed characterization of bacterial community dynamics.

The present study used quantitative microbiological and chemical techniques to investigate the development of bacterial community structure and cell numbers during the degradation of the polysaccharides chitin, alginate and agarose. All three polysaccharides can be utilized by marine bacteria (Souza *et al.*, 2011; Chi *et al.*, 2012; Thomas *et al.*, 2012) and are widespread in marine systems. Chitin, which consists of  $\beta$ -1,4-linked *N*-Acetyl glucosamine monomers, is the most abundant marine polymer with a global amount of about  $10^{11}$  tons (Gooday, 1990), being mostly bound in crustacean exoskeletons, zooplankton and diatom surfaces (Durkin *et al.*, 2009). Alginate and agarose are structural polymers from benthic macroalgae and can constitute up to 40% of their biomass (Davis *et al.*, 2003). Alginate consists of the uronic acids guluronate and mannuronate, which are (1,4)-linked and arranged in homo- or heteropolymeric blocks. Agarose is made up of  $\alpha$ -(1,3) and  $\beta$ -(1,4)-linked agarobiose units, each consisting of a galactose and galactopyranose monomer. We studied the degradation of chitin, alginate and agarose in microcosms at four contrasting locations in the Southern and Atlantic Oceans, including subantarctic frontal zones, perennially ice-covered waters, temperate shelf systems and subtropical upwelling regions. As each site lies within a distinct oceanic biome (Longhurst, 1998), this study illuminates bacterial community dynamics during polysaccharide degradation in markedly different biogeographic provinces of the ocean.

We hypothesized that polysaccharide availability creates ecological niches with specialized populations. These populations might encompass known degraders, taxa not yet linked to polysaccharide utilization, and non-hydrolytic opportunists that benefit from released hydroly-

sis products. Better understanding of bacterial community dynamics during the degradation of polysaccharides will help illuminate the factors controlling carbon cycling in contrasting marine habitats.

## Results and discussion

### *Characteristics of stations*

Bacterial community dynamics during polysaccharide degradation were investigated in polysaccharide-supplemented microcosms at the Southern polar front (PF), the Antarctic ice shelf (AS), the Patagonian continental shelf (PS) and the Mauritanian upwelling (MU). The stations are located in contrasting oceanic biomes and biogeographic provinces (Longhurst, 1998), as reflected in distinct variability among temperature and to a lesser extent salinity (Table S1). The frontal system at station PF is a region of high biological activity at the transition between subantarctic and Antarctic waters, featuring the highest chlorophyll concentrations of all stations (Table S1). The perennially ice-covered waters of station AS, directly adjacent to the Ekström ice shelf within the Antarctic Coastal Current, were low in chlorophyll and subject to ice breaking prior to sampling, which potentially influenced observed community dynamics. Station PS is situated in a highly productive temperate shelf region influenced by nutrient-rich subantarctic waters. Station MU in the subtropical Eastern Atlantic at the border of the Mauritanian upwelling was characterized by a relatively high salinity of 36 psu compared with  $\leq 34$  psu for the other stations (Table S1).

### *Response of bacterioplankton communities to polysaccharide addition*

Samples from triplicate polysaccharide-supplemented and control microcosms were analysed for bacterial community composition, cell numbers and carbohydrate concentrations. Community fingerprinting by denaturing gradient gel electrophoresis (DGGE) and non-metric multidimensional scaling of resulting banding patterns revealed four distinct clusters according to station ( $P < 0.05$ ), but there was no substrate-dependent grouping across the sites. In contrast, separate analysis by site revealed a considerable effect of polysaccharide addition, with significantly different community compositions between polysaccharide and control treatments at stations AS, PS and MU ( $P < 0.01$ ) (Fig. S1). At station PF, polysaccharide addition yielded differences between treatments in bacterial activities instead of different community structures (see below). The finding of location-specific polysaccharide effects illustrated the point that contrasting oceanic biomes harbour distinct bacterial

**Table 1.** Similarities (%) of DGGE banding patterns among triplicate polysaccharide-supplemented and control treatments at stations PF, AS, PS and MU.

Station	Control	Chitin	Agarose	Alginate
PF	97	74	87	75
AS	86	89	88	85
PS	57	75	89	90
MU	65	70	57	14

communities with specific 'hydrolytic potentials', which is consistent with prior observations of geographic variability in polysaccharide degradation (Arnosti *et al.*, 2011).

Clustering analyses of DGGE banding patterns from triplicate incubations per treatment demonstrated similarities of > 70% in 12 of 16 treatments (Table 1), which supported the biological significance of observed effects. In all but one case, lower similarities were due to deviating communities in single replicates, whereas the other two replicates were comparable. Only in the alginate treatment at station MU did all three replicates harbour different bacterial communities. However, RNA-based community analyses differed less between triplicates (see below). Some of the variability may thus have been attributed to DNA extraction or polymerase chain reaction (PCR) bias (von Wintzingerode *et al.*, 1997), although extractions, PCR and DGGE from a given station were done in parallel.

The 'starter communities' in the original seawater samples as well as 'end communities' in one end-point replicate per treatment were characterized by 454 pyrosequencing of 16S rRNA gene amplicons. Community fingerprints of 'starter' and 'end' communities (Fig. S2) were used to identify possible trends in community development upon polysaccharide addition. These indications were then used to design targeted quantitative microbiological (catalyzed reporter deposition-fluorescence *in situ* hybridization (CARD-FISH), flow cytometry) and chemical analyses [carbohydrate high-performance liquid chromatography (HPLC)] on all three replicates per treatment. This approach permitted statistical evaluation of community responses during polysaccharide degradation at each of the four stations. Given that most effects were site specific, we describe one specific effect of polysaccharide addition on community dynamics per station.

#### Effects of chitin at the polar front

At station PF, flow cytometry revealed that chitin treatments harboured a significantly higher fraction of cells with high-nucleic acid content (HNA) than alginate and agarose treatments on days 7 and 11 (Fig. 1, Table S2). As HNA cells are considered actively growing (Lebaron *et al.*, 2001), the PF community has a greater capacity for chitin utilization compared with the macroalgal

substrates. The increase of HNA cells was associated with significantly increasing abundances of *Gammaproteobacteria* and *Bacteroidetes* as determined by CARD-FISH ( $P < 0.01$ ), which largely replaced *Alphaproteobacteria* (Fig. 1). These shifts in abundance suggest that chitinolytic strains among the *Gammaproteobacteria* and *Bacteroidetes* outcompeted non-hydrolytic *Alphaproteobacteria*.

Although chitin elicited the strongest bacterial activity, the fraction of HNA cells also increased in alginate and agarose treatments (Fig. 1). As alginate and agarose concentrations remained constant (Tables S3 and S4), this increase may have related to hydrolytic activities below the detection limit or other effects of polysaccharide addition, such as alterations of the physicochemical water characteristics (e.g. changes in viscosity, surfactant effects or trace metal binding by polysaccharidic microgels). In addition, HPLC detected approximately 0.5  $\mu\text{M}$  of other carbohydrates (Table S5) that were either already present in the ambient seawater or introduced as impurities from polysaccharide preparations. Although decreasing significantly in only a few cases (Table S5), these carbohydrates may have contributed to the observed community dynamics. Overall, the effects may also have been influenced by other factors in addition to carbohydrate availability, such as biological factors (grazing, phage infections, antagonistic and synergistic bacterial interactions) as well as bottle effects (Guixa-Boixereu *et al.*, 1999).

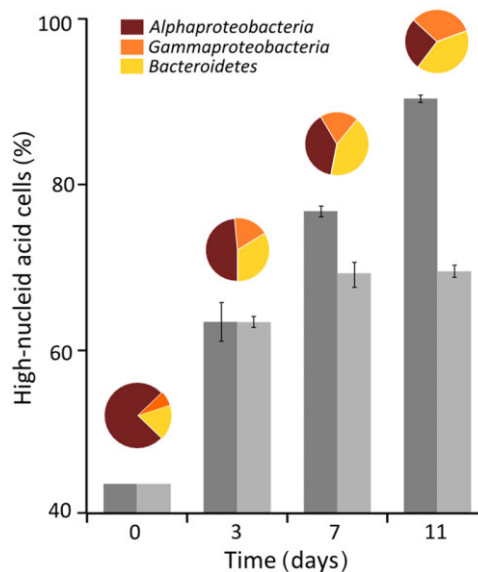


**Fig. 1.** Percentages of high-nucleic acid cells in chitin (dark grey bars) versus alginate and agarose treatments (mean; light grey bars) and relative proportions of *Alphaproteobacteria*, *Gammaproteobacteria* and *Bacteroidetes* in chitin treatments (inserts above) at station PF.

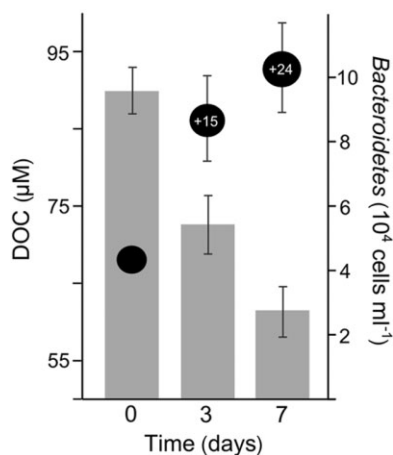


**Fig. 2.** DOC concentrations (grey bars) and *Bacteroidetes* cell numbers (black circles) in the chitin treatment at station AS. Increases of *Bacteroidetes* cells relative to the control are shown as numbers in the black circles.

#### Effects of chitin at the Antarctic ice shelf

At station AS, CARD-FISH demonstrated increasing abundances of *Bacteroidetes* in chitin treatments, with 15% and 24% higher cell numbers compared with the control on days 3 and 7, respectively. This increase was correlated with a 30% decrease in dissolved organic carbon (DOC) concentrations (Fig. 2). Concentrations of DOC served as a proxy for chitin, as chitin was not amenable to different acid and enzymatic hydrolysis protocols we tested for quantification by HPLC. The enrichment of *Bacteroidetes* with chitin was observed at all cold and temperate water stations (PF, AS and PS), with an average of 45% higher abundances on day 7 compared with the control. 16S rRNA gene amplicon libraries indicated that approximately half of *Bacteroidetes* in the 'end communities' at stations PF, AS and PS were represented by the genus *Reichenbachiella* (class *Cytophagia*/family *Flammeovirgaceae*), corresponding to a relative abundance of about 20% in the total community (Fig. S2). The consistent stimulation of *Reichenbachiella* by chitin in contrasting habitats with distinct starter communities suggests that certain taxa with wide distribution may have similar ecological roles over broad spatial scales. As there is no specific *Reichenbachiella* FISH probe available, we could not quantify *Reichenbachiella* directly. Moreover, the general CF319a probe may have underestimated *Reichenbachiella* abundances, since SILVA probecheck demonstrated poor coverage of CF319a for this genus (Quast *et al.*, 2013).

#### Effects of alginate and agarose at the Patagonian continental shelf

At station PS, 16S rRNA gene amplicon libraries indicated that the gammaproteobacterial *Alteromonadaceae* family

reached abundances of up to 80% in alginate and agarose treatments (Fig. S2). CARD-FISH subsequently demonstrated specific temporal growth patterns of *Alteromonadaceae* during alginate and agarose degradation, whereas abundances in the control treatment did not increase (Fig. 3A). In alginate treatments, increasing *Alteromonadaceae* cell numbers between days 3 and 7 coincided with significantly decreasing alginate concentrations (Fig. 3B, Tables S3 and S4). The associated doubling times were as short as 15 h and thus considerably shorter than normally observed for marine bacteria (Kirchman, 2008). 16S rRNA gene amplicon libraries indicated that the *Alteromonadaceae* population was dominated by a single operational taxonomic unit (OTU) related to *Alteromonas macleodii*, which constituted a relative abundance of > 50% (Fig. S2). The potential contribution of this OTU to alginate hydrolysis is supported by the pronounced ability of *A. macleodii* isolates to grow with alginate as sole carbon source (Neumann *et al.*, 2015).

In agarose treatments, increasing *Alteromonadaceae* cell numbers between days 7 and 11 coincided with significantly decreasing agarose concentrations (Fig. 3, Tables S3 and S4). Comparable with alginate, 16S rRNA

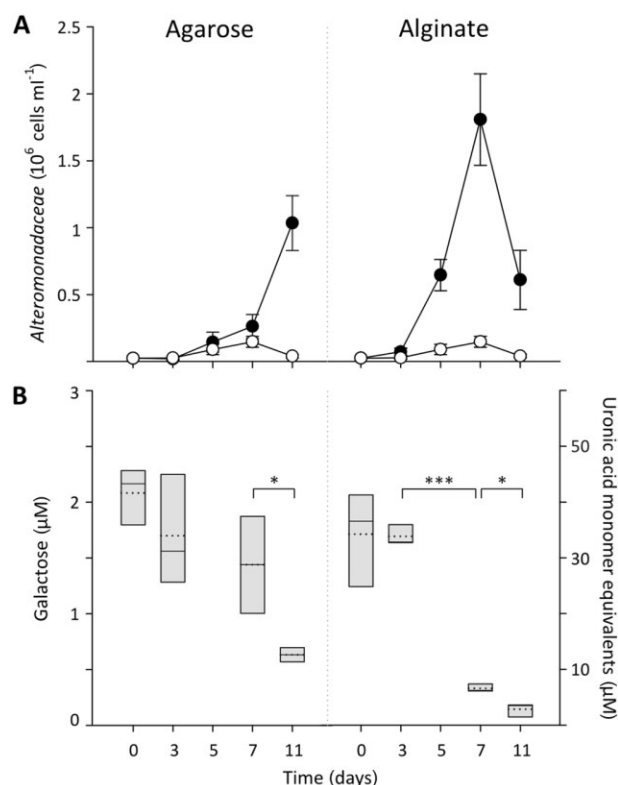


**Fig. 3.** (A) *Alteromonadaceae* cell numbers in agarose (black circles), alginate (black circles) and control (white circles) treatments at station PS. (B) Concentrations of galactose and uronic acid monomer equivalents (solid line: median, dotted line: mean), with significantly different concentrations between two time points indicated (\* $P < 0.05$ , \*\*\* $P < 0.001$ ).

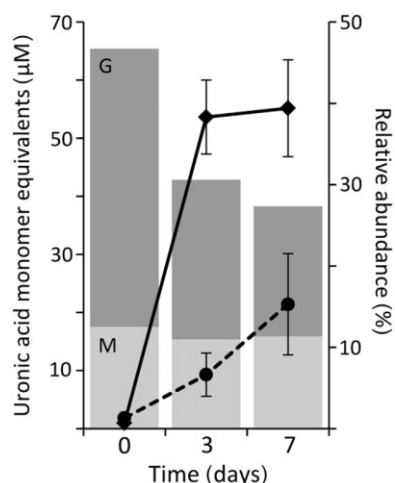


**Fig. 4.** Concentrations of the alginate monomers mannuronate (M) and guluronate (G) and relative abundances of SAR11 (diamonds) and *Alteromonadaceae* (circles) in alginate treatments at station MU.

gene amplicon libraries indicated that the majority of *Alteromonadaceae* were represented by a single OTU with a relative abundance of > 60% (Fig. S2). The potential contribution of this OTU to agarose hydrolysis was supported by 99% 16S rRNA gene similarity to the known agarolytic strain *Glaciecola agarilytica* (Yong *et al.*, 2007). The stimulation of *Alteromonadaceae* by different macroalgal substrates attests to the metabolic versatility among this bacterial family (Allers *et al.*, 2008; Tada *et al.*, 2011; Nelson and Carlson, 2012; Pedler *et al.*, 2014). Consequently, hydrolytic capacities may contribute to the commonly observed dominance of *Alteromonadaceae* in confined experimental settings (Pukall *et al.*, 1999; Eilers *et al.*, 2000a; Schäfer *et al.*, 2001).

#### Effects of alginate at the Mauritanian upwelling

We hypothesized that polysaccharide availability may have secondary effects in addition to stimulating taxa that can hydrolyse these substrates. For instance, non-hydrolytic strains may benefit from monosaccharides and/or other metabolic products released by hydrolytic bacteria. Such interspecies 'cross-feeding' has been shown for e.g. chitinolytic bacteria, where non-hydrolytic *r* strategists could even outcompete chitin degraders (Beier and Bertilsson, 2013). At station MU, 16S rRNA gene amplicon libraries indicated that abundances of both SAR11 and *Alteromonadaceae* increased in alginate relative to control treatments, indicating a specific effect of the polysaccharide (Fig. S2). CARD-FISH confirmed that their relative abundances increased from initially < 5% to > 35% (SAR11) and 15% (*Alteromonadaceae*) respectively (Fig. 4). As strains of SAR11 most likely do

not produce extracellular hydrolytic enzymes (Malmstrom *et al.*, 2005) but possess the Entner-Doudoroff pathway required for assimilation of alginate monomers (Giovannoni *et al.*, 2005; Schwalbach *et al.*, 2010), the stimulation of SAR11 may have been attributed to cross-feeding on alginate monomers and other metabolic products released by alginolytic *Alteromonadaceae*. Interestingly, only a single alginate monomer, guluronate, significantly decreased in concentration (Fig. 4). This may reflect selective utilization of guluronate, or the predominant action of guluronate-specific alginate lyases (Doubet and Quatrano, 1982; Lange *et al.*, 1989).

## Experimental procedures

### Microcosm experiments with polysaccharide substrates

Seawater samples were obtained at four stations (Table S1) from 20 m depth using each Niskin bottle holds 12 l mounted on a rosette sampler equipped with a conductivity-temperature-depth (CTD) sensor. Per replicate, 2 l of seawater were transferred to an acid-washed 2 l of glass bottle and supplemented with either 0.001% of sterile colloidal chitin, sodium alginate or agarose. Colloidal chitin was prepared according to Weyland and colleagues (1970) from practical grade chitin (Sigma P7170) by treatment with ice-cold 37% HCl for 20 min. The solution was stirred at 37°C until clear and poured into 4 l of dH<sub>2</sub>O for settlement overnight at 4°C. The supernatant was aspirated, chitin resuspended in 2 l of dH<sub>2</sub>O and collected by centrifugation (4000 g for 12 min). Chitin was resuspended in 1 l of dH<sub>2</sub>O and the pH adjusted to 7 using potassium hydroxide (KOH) pellets. The solution was homogenized using an Ultra-Turrax (IKA, Staufen, Germany) and autoclaved. The chitin concentration of the resulting preparation was determined from a dried (70°C overnight) subsample. Stock solutions of alginate (1%) and agarose (0.1%) were filter sterilized. Triplicate microcosms were set up per treatment, including triplicate bottles without substrate addition as controls. Bottles were incubated on roller systems at approximately 6 rpm for 7 (stations AS and MU) or 11 days (stations PF and PS) at temperatures similar to the original seawater temperature (Table S1), i.e. 4°C (station PF), 8°C (station PS) and 20°C (station MU). Due to logistical constraints, bottles from station AS were incubated at 4°C instead of below zero temperatures.

### Flow cytometry

Per sampling point, 4.6 ml was taken from each replicate, fixed with glutardialdehyde (final concentration 1%, v/v) for 30 min at room temperature, and stored at -20°C. Cell numbers were determined by flow cytometry using an Accuri C6 (BD Biosciences, San Jose, CA) using SYBR Green I staining and the internal fluidics calibration. Volume verification was done using TruCount beads (BD) as described previously (Giebel *et al.*, 2009). Data were processed by C-FLOW software v1.026421 (BD). Pyrophosphate and ultrasonication sample pretreatments were tested to dissolve cell aggregates

that might have been present, but these treatments did not influence cell counts.

#### *DGGE and statistical evaluation*

Approximately 1000 ml of each original seawater sample ('starter community') and 1000 ml from each replicate after incubation ('end community') were filtered onto 47 mm polycarbonate filters (0.2 µm pore size), transferred to sterile microcentrifuge tubes, and stored at -80°C. DNA was extracted in a modification after Zhou and colleagues (1996) by bead beating, phenol-chloroform-isoamyl alcohol purification, isopropanol/sodium acetate precipitation and ethanol washing. DGGE was carried out on bacterial 16S rRNA gene fragments that were amplified using primers 341F-GC and 907RM and separated on an IngenyPhor DGGE system in 8% polyacrylamide gels with a 40–70% denaturing gradient (Giebel *et al.*, 2009). Similarities of banding patterns were evaluated using GELCOMPAR (<http://www.applied-maths.com/gelcompar-ii>) by calculating an Unweighted Pair Group Method with Arithmetic Mean (UPGMA) similarity matrix of presence/absence of bands in relation to a reference banding pattern. Similarities of banding patterns and significant differences between samples and treatments were analysed using the metaMDS and envfit functions within the VEGAN package (Oksanen *et al.*, 2013) implemented in R (R Core Team, 2012).

#### *454 pyrosequencing of 16S rRNA gene amplicons*

Extracted DNA from starter communities and one end-point replicate per treatment were subjected to PCR of the hypervariable regions V3 to V5 of bacterial 16S rRNA genes. Each reaction mixture (50 µl) contained 25 µl of Phusion High-Fidelity PCR Master Mix with HF buffer (Thermo Scientific, Waltham, MA), 0.5 µM of each primer, 3% dimethylsulphoxide, 30 µg BSA and 50 ng template. Primer sequences included the Roche pyrosequencing adaptors (underlined), a key (TCAG) and a variable multiplex identifier (MID) consisting of 10 bases. Primers used were V3for 5'-CCATCTCATCCCTGCGTGTCTCCGAC-TCAG-MID-TACGGRAGGCAGCAG-3' (Liu *et al.*, 2007) and V5rev 5'-CCTATCCCCTGTGTGCCTTGGCAGTC-TCAG-CCGTCAAATTCM TTTGAGT-3' (Wang and Qian, 2009). Each sample was amplified in three parallel PCR runs (95°C for 4 min; 30 cycles of 45 s at 95°C, 1 min at 58°C, and 45 s at 72°C; 5 min at 72°C). Products were electrophoresed for 1 h at 80 V and gel-purified using the PeqGold Gel Extraction Kit (Peqlab, Erlangen, Germany). PCR products from parallel runs were pooled and quantified using the Quant-iT dsDNA HS assay kit and a Qubit fluorometer (Invitrogen, Carlsbad, CA). 16S rRNA gene amplicons were sequenced using a GS-FLX 454 pyrosequencer and titanium chemistry (Roche, Branford, CT).

#### *Processing and taxonomic analysis of pyrosequencing data*

Amplicon sequences shorter than 300 bp, with an average quality value below 25, possessing long homopolymer

stretches (> 8 bp) or > 5 primer mismatches were removed using QIIME v1.6 (Caporaso *et al.*, 2010). Sequences were denoised using ACACIA (Bragg *et al.*, 2012) and remaining primer sequences truncated using CUTADAPT (Martin, 2011). Chimeric sequences were removed using UCHIME in reference mode with the most recent SILVA SSU database as reference (SSURef 115 NR) (Edgar *et al.*, 2011; Quast *et al.*, 2013). Processed sequences were combined, sorted by decreasing length and clustered employing the UCLUST algorithm using the optimal variant (Edgar, 2010). Sequences were clustered in OTUs at 80%, 97% and 99% genetic similarity according to Wemheuer and colleagues (2013). Phylogenetic composition was determined using the QIIME assign\_taxonomy.py script and a BLAST alignment against the SILVA SSURef 115 NR database. Rarefaction curves (Fig. S3) were calculated with QIIME according to Wemheuer and colleagues (2013), indicating that the diversity was sufficiently covered at 80%, 97% and 99% genetic similarity. The processed sequence data have been deposited at NCBI under BioProject PRJNA246186.

#### *Catalysed reporter deposition-fluorescence in situ hybridization (CARD-FISH)*

Per sampling point, 50 ml was taken from each replicate and fixed with particle-free formaldehyde (final concentration 2%, v/v) for 1–24 h at 4°C in the dark. Fixed samples were filtered onto 47 mm polycarbonate filters (0.2 µm pore size), washed with MilliQ water and stored at -20°C. Based on 16S rRNA gene amplicon libraries, selected taxa were quantified by CARD-FISH according to Perenthaler and colleagues (2004) using probes ALF968 (Neef, 1997), GAM42a (Manz *et al.*, 1992), CF319a (Manz *et al.*, 1996), ALT1413 (Eilers *et al.*, 2000b) and SAR11-441 (Morris *et al.*, 2002). The SILVA TestProbe application (<http://www.arb-silva.de/search/testprobe>) was used to confirm that applied probes target OTUs from 16S rRNA gene amplicon libraries. Per hybridization, at least 500 4',6-diamidino-2-phenylindole (DAPI)-stained cells and the respective fraction of hybridized cells were counted in ≥ 10 randomly selected microscopic fields. Relative abundances were corrected by subtraction of counts with probe NON338 (Wallner *et al.*, 1993) and transformed into absolute abundances using flow cytometric cell counts. Significant differences in abundances between sampling days were determined using the Mann–Whitney *U*-test.

#### *Quantification of polysaccharide degradation*

Per sampling point, 10 ml were taken from each replicate, filtered through 0.22 µm Acrodisc filters into combusted glass vials, and frozen at -20°C. Agarose and alginate concentrations were determined by HPLC and pulsed amperometric detection according to Mopper and colleagues (1992) after acid hydrolysis (20 h, 100°C, 0.1 M HCl) to their monomeric components (galactose and mannuronate/gulonate respectively) in combusted and sealed glass ampoules. The hydrolysate was neutralized with 6 N NaOH. Galactose samples were desalted using a 1:1 mixture of AG 2-X8 and AG 50W-X8 resins (Bio-Rad, Hercules, CA) (Borch and Kirchman, 1997) and eluted with 18 mM NaOH. Uronic acid samples were desalted using DionexOnGuard II Ag/H

cartridges (Thermo Scientific) and eluted with 100 mM sodium acetate tri-hydrate in 100 mM NaOH. HPLC separation was done using a CarboPac PA1 column (Dionex, Sunnyvale, CA). For validation of methodological accuracy (e.g. sample loss or pH shifts due to desalting) and to control for analytical variation in replicate HPLC analyses, one additional sample per triplicate was measured with an internal replicate, showing a maximum variance of 13%. Blanks with dH<sub>2</sub>O were included with every HPLC run, confirming that no contaminations were present. Calibration was done using a mixture of arabinose, fucose, galactose, glucose, mannose, rhamnose and xylose (each at 100 µM) for galactose and a hydrolysed 1% alginate solution containing a 3:2 mixture of mannuronate : guluronate for alginate. In addition to polysaccharides, the concentrations of free and combined carbohydrates were measured to assess the potential contribution of ambient carbohydrate substrates to community dynamics. Changes in mean carbohydrate concentrations between sampling days were evaluated using Student's *t*-test and the Mann–Whitney *U*-test. Several chemical and enzymatic hydrolysis protocols were tested in order to determine chitin concentrations by HPLC, but no satisfactory results were obtained when checking against an HPLC standard of the chitin monomer *N*-Acetyl glucosamine. Instead, chitin degradation was assessed from DOC concentrations in chitin vs. control treatments using samples that were filtered through combusted 0.7 µm glass fiber filters (Whatman) and acidified to pH 2 using 25% HCl. DOC analysis was carried out by high temperature catalytic oxidation (HTCO) on a Shimadzu TOC-VCPH/CPN Total Organic Carbon Analyzer equipped with an ASI-V autosampler. Acidified samples were purged with synthetic air to remove inorganic carbon compounds. Calibration was done using L-arginine solutions (25 to 500 µM C L<sup>-1</sup>). Deep Atlantic seawater reference material (DSR, D.A. Hansell, University of Miami, FL) and an in-house North Sea water reference sample were measured repeatedly during each run to control for instrument precision and accuracy (5 and 7% respectively). Only samples from station AS were available for DOC measurements.

## Conclusions

The location-specific stimulation of certain bacterial taxa during polysaccharide degradation illustrates the point that contrasting oceanic biomes harbour distinct bacterial communities with specific 'hydrolytic potentials'. Thus, the effects of polysaccharide addition are a function of the structure and 'hydrolytic enzyme fingerprint' of a given community, which varies between biogeographic provinces. These aspects may also relate to natural patterns of polysaccharide abundances. For instance, chitin production by zooplankton and krill can vary by region and season (Jeuniaux and Voss-Foucart, 1991), and bacterial communities in regions with commonly higher chitin abundances may respond more strongly to a chitin pulse. Nonetheless, the stimulation of *Reichenbachiella* at three distant stations showed that some hydrolytic taxa are widespread and respond to the same stimulus over wide geographical scales. Furthermore, the observed growth of taxa that have not been linked to polymer utilization to date, such as *Alteromonadaceae*, demonstrated that polysaccharide degradation may be performed by more bac-

terial community members than commonly thought. Stimulation of non-hydrolytic taxa indicates that polysaccharides likely also benefit non-hydrolytic strains. These complex linkages of bacterial community dynamics and polysaccharide degradation contribute to our understanding of bacterial hydrolytic activities in contrasting biomes, important aspects of global marine carbon cycling.

## Acknowledgements

We thank the captain, crew and scientists of RV *Polarstern* cruises ANTXXVIII/2 and ANTXXVIII/5, in particular Mascha Wurst, Birgit Kürzel, Helena Osterholz, Christine Beardsley and John Vollmers, for experimental assistance onboard. Rolf Weinert, Andrea Thürmer, Frauke-Dorothee Meyer, Mathias Wolterink, Regina Gohl and Matthias Friebe are gratefully acknowledged for technical assistance. This work was supported by grants WI3888/1-1 (to MW; Temporary Position for Principal Investigators), NI1366/1-1, and TRR51 (German Research Foundation, DFG).

## References

- Allers, E., Niesner, C., Wild, C., and Pernthaler, J. (2008) Microbes enriched in seawater after addition of coral mucus. *Appl Environ Microbiol* **74**: 3274–3278.
- Amon, R.M.W., and Benner, R. (1994) Rapid cycling of high-molecular-weight dissolved organic matter in the ocean. *Nature* **369**: 549–552.
- Arnosti, C., Steen, A.D., Zierovogel, K., Ghobrial, S., and Jeffrey, W.H. (2011) Latitudinal gradients in degradation of marine dissolved organic carbon. *PLoS ONE* **6**: e28900.
- Arnosti, C., Fuchs, B.M., Amann, R., and Passow, U. (2012) Contrasting extracellular enzyme activities of particle-associated bacteria from distinct provinces of the North Atlantic Ocean. *Front Microbiol* **3**: 425.
- Azam, F., and Malfatti, F. (2007) Microbial structuring of marine ecosystems. *Nat Rev Microbiol* **5**: 782–791.
- Beier, S., and Bertilsson, S. (2013) Bacterial chitin degradation – mechanisms and ecophysiological strategies. *Front Microbiol* **4**: 149.
- Benner, R., Pakulski, J., McCarthy, M., Hedges, J., and Hatcher, P. (1992) Bulk chemical characteristics of dissolved organic matter in the ocean. *Science* **255**: 1561–1564.
- Borch, N.H., and Kirchman, D.L. (1997) Concentration and composition of dissolved combined neutral sugars (polysaccharides) in seawater determined by HPLC-PAD. *Mar Chem* **57**: 85–95.
- Bragg, L., Stone, G., Imelfort, M., Hugenholtz, P., and Tyson, G.W. (2012) Fast, accurate error-correction of amplicon pyrosequences using Acacia. *Nat Methods* **9**: 425–426.
- Caporaso, J.G., Kuczynski, J., Stombaugh, J., Bittinger, K., Bushman, F.D., Costello, E.K., *et al.* (2010) QIIME allows analysis of high-throughput community sequencing data. *Nat Methods* **7**: 335–336.
- Chi, W.-J., Chang, Y.-K., and Hong, S.-K. (2012) Agar degradation by microorganisms and agar-degrading enzymes. *Appl Microbiol Biotechnol* **94**: 917–930.
- Cottrell, M.T., and Kirchman, D.L. (2000) Natural assemblages of marine proteobacteria and members of the

- Cytophaga-Flavobacter cluster consuming low- and high-molecular-weight dissolved organic matter. *Appl Environ Microbiol* **66**: 1692–1697.
- Cowie, G.L., and Hedges, J.I. (1984) Carbohydrate sources in a coastal marine environment. *Geochim Cosmochim Acta* **48**: 2075–2087.
- Davis, T.A., Volesky, B., and Mucci, A. (2003) A review of the biochemistry of heavy metal biosorption by brown algae. *Water Res* **37**: 4311–4330.
- D'Ambrosio, L., Zierovogel, K., Macgregor, B., Teske, A., and Arnosti, C. (2014) Composition and enzymatic function of particle-associated and free-living bacteria: a coastal/offshore comparison. *ISME J* **8**: 2167–2179.
- Doubet, R.S., and Quatrano, R.S. (1982) Isolation of marine bacteria capable of producing specific lyases for alginate degradation. *Appl Environ Microbiol* **44**: 754–756.
- Durkin, C.A., Mock, T., and Armbrust, E.V. (2009) Chitin in diatoms and its association with the cell wall. *Eukaryot Cell* **8**: 1038–1050.
- Edgar, R.C. (2010) Search and clustering orders of magnitude faster than BLAST. *Bioinformatics* **26**: 2460–2461.
- Edgar, R.C., Haas, B.J., Clemente, J.C., Quince, C., and Knight, R. (2011) UCHIME improves sensitivity and speed of chimera detection. *Bioinformatics* **27**: 2194–2200.
- Edwards, J.L., Smith, D.L., Connolly, J., McDonald, J.E., Cox, M.J., Joint, I., et al. (2010) Identification of carbohydrate metabolism genes in the metagenome of a marine biofilm community shown to be dominated by Gammaproteobacteria and Bacteroidetes. *Genes* **1**: 371–384.
- Eilers, H., Pernthaler, J., and Amann, R. (2000a) Succession of pelagic marine bacteria during enrichment: a close look at cultivation-induced shifts. *Appl Environ Microbiol* **66**: 4634–4640.
- Eilers, H., Pernthaler, J., Glöckner, F., and Amann, R. (2000b) Culturability and *in situ* abundance of pelagic bacteria from the North Sea. *Appl Environ Microbiol* **66**: 3044–3051.
- Fernández-Gómez, B., Richter, M., Schüller, M., Pinhassi, J., Acinas, S.G., González, J.M., and Pedrós-Alió, C. (2013) Ecology of marine *Bacteroidetes*: a comparative genomics approach. *ISME J* **7**: 1026–1037.
- Giebel, H.A., Brinkhoff, T., Zwisler, W., Selje, N., and Simon, M. (2009) Distribution of *Roseobacter* RCA and SAR11 lineages and distinct bacterial communities from the subtropics to the Southern Ocean. *Environ Microbiol* **11**: 2164–2178.
- Giovannoni, S.J., Tripp, H.J., Givan, S., Podar, M., Vergin, K.L., Baptista, D., et al. (2005) Genome streamlining in a cosmopolitan oceanic bacterium. *Science* **309**: 1242–1245.
- Gooday, G.W. (1990) The ecology of chitin degradation. *Adv Microb Ecol* **11**: 387–430.
- Guixa-Boixereu, N., Lysnes, K., and Pedros-Alio, C. (1999) Viral lysis and bacterivory during a phytoplankton bloom in a coastal water microcosm. *Appl Environ Microbiol* **65**: 1949–1958.
- Haynes, K., Hofmann, T.A., Smith, C.J., Ball, A.S., Underwood, G.J.C., and Osborn, A.M. (2007) Diatom-derived carbohydrates as factors affecting bacterial community composition in estuarine sediments. *Appl Environ Microbiol* **73**: 6112–6124.
- Jeuniaux, C., and Voss-Foucart, M.F. (1991) Chitin biomass and production in the marine environment. *Biochem Syst Ecol* **19**: 347–356.
- Kabisch, A., Otto, A., König, S., Becher, D., Albrecht, D., Schüller, M., et al. (2014) Functional characterization of polysaccharide utilization loci in the marine *Bacteroidetes* 'Gramella forsetii' KT0803. *ISME J* **8**: 1492–1502.
- Kirchman, D.L. (2008) *Microbial Ecology of the Oceans*. New York, NJ, USA: John Wiley & Sons.
- Landa, M., Cottrell, M.T., Kirchman, D.L., Kaiser, K., Medeiros, P.M., Tremblay, L., et al. (2013) Phylogenetic and structural response of heterotrophic bacteria to dissolved organic matter of different chemical composition in a continuous culture study. *Environ Microbiol* **16**: 1668–1681.
- Lange, B., Wingender, J., and Winkler, U.K. (1989) Isolation and characterization of an alginate lyase from *Klebsiella aerogenes*. *Arch Microbiol* **152**: 302–308.
- Lebaron, P., Servais, P., Agogué, H., Courties, C., and Joux, F. (2001) Does the high nucleic acid content of individual bacterial cells allow us to discriminate between active cells and inactive cells in aquatic systems? *Appl Environ Microbiol* **67**: 1775–1782.
- Liu, Z., Lozupone, C., Hamady, M., Bushman, F.D., and Knight, R. (2007) Short pyrosequencing reads suffice for accurate microbial community analysis. *Nucleic Acids Res* **35**: e120.
- Longhurst, A.R. (1998) *Ecological Geography of the Sea*. San Diego, CA, USA: Academic Press.
- McCarren, J., Becker, J.W., Repeta, D.J., Shi, Y., Young, C.R., Malmstrom, R.R., et al. (2010) Microbial community transcriptomes reveal microbes and metabolic pathways associated with dissolved organic matter turnover in the sea. *Proc Natl Acad Sci USA* **107**: 16420–16427.
- Malmstrom, R.R., Cottrell, M.T., Elifantz, H., and Kirchman, D.L. (2005) Biomass production and assimilation of dissolved organic matter by SAR11 bacteria in the Northwest Atlantic Ocean. *Appl Environ Microbiol* **71**: 2979–2986.
- Manz, W., Amann, R., Ludwig, W., Wagner, M., and Schleifer, K.H. (1992) Phylogenetic oligodeoxynucleotide probes for the major subclasses of proteobacteria – problems and solutions. *Syst Appl Microbiol* **15**: 593–600.
- Manz, W., Amann, R., Ludwig, W., Vancanneyt, M., and Schleifer, K.-H. (1996) Application of a suite of 16S rRNA-specific oligonucleotide probes designed to investigate bacteria of the phylum Cytophaga-Flavobacter-Bacteroides in the natural environment. *Microbiology* **142**: 1097–1106.
- Martin, M. (2011) Cutadapt removes adapter sequences from high-throughput sequencing reads. *EMBnet Journal* **17**: 10–12.
- Mopper, K., Schultz, C.A., Chevolut, L., Germain, C., Revuelta, R., and Dawson, R. (1992) Determination of sugars in unconcentrated seawater and other natural waters by liquid chromatography and pulsed amperometric detection. *Environ Sci Technol* **26**: 133–138.
- Morris, R.M., Rappe, M.S., Connon, S.A., Vergin, K.L., Siebold, W.A., Carlson, C.A., and Giovannoni, S.J. (2002) SAR11 clade dominates ocean surface bacterioplankton communities. *Nature* **420**: 806–810.

- Murray, A., Arnosti, C., De La Rocha, C., Grossart, H.-P., and Passow, U. (2007) Microbial dynamics in autotrophic and heterotrophic seawater mesocosms. II. Bacterioplankton community structure and hydrolytic enzyme activities. *Aquat Microb Ecol* **49**: 123–141.
- Neef, A. (1997) Anwendung der in situ Einzelzell-Identifizierung von Bakterien zur Populationsanalyse in komplexen mikrobiellen Biozönosen. PhD thesis. Munich, Germany: Technische Universität München.
- Nelson, C.E., and Carlson, C.A. (2012) Tracking differential incorporation of dissolved organic carbon types among diverse lineages of Sargasso Sea bacterioplankton. *Environ Microbiol* **14**: 1500–1516.
- Neumann, A.M., Balmonte, J.P., Berger, M., Giebel, H.-A., Arnosti, C., Voget, S., *et al.* (2015) Different utilization of alginate and other algal polysaccharides by marine *Alteromonas macleodii* ecotypes. *Environ Microbiol* accepted.
- Oksanen, J., Blanchet, F.G., Kindt, R., Legendre, P., Minchin, P.R., O'Hara, R.B., *et al.* (2013) Vegan: community ecology package.
- Pedler, B.E., Aluwihare, L.I., and Azam, F. (2014) Single bacterial strain capable of significant contribution to carbon cycling in the surface ocean. *Proc Natl Acad Sci USA* **111**: 7202–7207.
- Pernthaler, A., Pernthaler, J., and Amann, R. (2004) Sensitive multi-color fluorescence in situ hybridization for the identification of environmental microorganisms. In *Molecular Microbial Ecology Manual*. Kowalchuk, G.A., de Bruijn, F.J., Head, I.M., Akkermans, A.D., and van Elsas, J. (eds). Dordrecht, Netherlands: Kluwer Academic Publishers, pp. 2613–2627.
- Piontek, J., Handel, N., De Bodt, C., Harlay, J., Chou, L., and Engel, A. (2011) The utilization of polysaccharides by heterotrophic bacterioplankton in the Bay of Biscay (North Atlantic Ocean). *J Plankton Res* **33**: 1719–1735.
- Pukall, R., Päuker, O., Buntetuß, D., Ulrichs, G., Lebaron, P., Bernard, L., *et al.* (1999) High sequence diversity of *Alteromonas macleodii*-related cloned and cellular 16S rDNAs from a Mediterranean seawater mesocosm experiment. *FEMS Microbiol Ecol* **28**: 335–344.
- Quast, C., Pruesse, E., Yilmaz, P., Gerken, J., Schweer, T., Yarza, P., *et al.* (2013) The SILVA ribosomal RNA gene database project: improved data processing and web-based tools. *Nucleic Acids Res* **41**: D590–D596.
- R Core Team (2012) *R: A Language and Environment for Statistical Computing*. Vienna, Austria: R Foundation for Statistical Computing.
- Sarmiento, H., and Gasol, J.M. (2012) Use of phytoplankton-derived dissolved organic carbon by different types of bacterioplankton. *Environ Microbiol* **14**: 2348–2360.
- Schäfer, H., Bernard, L., Courties, C., Lebaron, P., Servais, P., Pukall, R., *et al.* (2001) Microbial community dynamics in Mediterranean nutrient-enriched seawater mesocosms: changes in the genetic diversity of bacterial populations. *FEMS Microbiol Ecol* **34**: 243–253.
- Schwalbach, M.S., Tripp, H.J., Steindler, L., Smith, D.P., and Giovannoni, S.J. (2010) The presence of the glycolysis operon in SAR11 genomes is positively correlated with ocean productivity. *Environ Microbiol* **12**: 490–500.
- Sharma, A.K., Becker, J.W., Ottesen, E.A., Bryant, J.A., Duhamel, S., Karl, D.M., *et al.* (2013) Distinct dissolved organic matter sources induce rapid transcriptional responses in coexisting populations of *Prochlorococcus*, *Pelagibacter* and the OM60 clade. *Environ Microbiol* **16**: 2815–2830.
- Simon, M., Billerbeck, S., Kessler, D., Selje, N., and Schlingloff, A. (2012) Bacterioplankton communities in the Southern Ocean: composition and growth response to various substrate regimes. *Aquat Microb Ecol* **68**: 13–28.
- Souza, C.P., Almeida, B.C., Colwell, R.R., and Rivera, I.N. (2011) The importance of chitin in the marine environment. *Mar Biotechnol* **13**: 823–830.
- Steen, A.D., Hamdan, L.J., and Arnosti, C. (2008) Dynamics of dissolved carbohydrates in the Chesapeake Bay: insights from enzyme activities, concentrations, and microbial metabolism. *Limnol Oceanogr* **53**: 936–947.
- Tada, Y., Taniguchi, A., Nagao, I., Miki, T., Uematsu, M., Tsuda, A., and Hamasaki, K. (2011) Differing growth responses of major phylogenetic groups of marine bacteria to natural phytoplankton blooms in the western North Pacific Ocean. *Appl Environ Microbiol* **77**: 4055–4065.
- Tang, K., Jiao, N., Liu, K., Zhang, Y., and Li, S. (2012) Distribution and functions of TonB-dependent transporters in marine bacteria and environments: implications for dissolved organic matter utilization. *PLoS ONE* **7**: e41204.
- Tanoue, E., and Handa, N. (1987) Monosaccharide composition of marine particles and sediments from the Bering Sea and northern North Pacific. *Oceanol Acta* **10**: 91–99.
- Teeling, H., Fuchs, B.M., Becher, D., Klockow, C., Gardebrecht, A., Bennke, C.M., *et al.* (2012) Substrate-controlled succession of marine bacterioplankton populations induced by a phytoplankton bloom. *Science* **336**: 608–611.
- Thomas, F., Barbeyron, T., Tonon, T., Génicot, S., Czjzek, M., and Michel, G. (2012) Characterization of the first alginolytic operons in a marine bacterium: from their emergence in marine *Flavobacteriia* to their independent transfers to marine *Proteobacteria* and human gut *Bacteroides*. *Environ Microbiol* **14**: 2379–2394.
- von Wintzingerode, F., Göbel, U.B., and Stackebrandt, E. (1997) Determination of microbial diversity in environmental samples: pitfalls of PCR-based rRNA analysis. *FEMS Microbiol Rev* **21**: 213–229.
- Wallner, G., Amann, R., and Beisker, W. (1993) Optimizing fluorescent in situ hybridization with rRNA-targeted oligonucleotide probes for flow cytometric identification of microorganisms. *Cytometry* **14**: 133–141.
- Wang, Y., and Qian, P.-Y. (2009) Conservative fragments in bacterial 16S rRNA genes and primer design for 16S ribosomal DNA amplicons in metagenomic studies. *PLoS ONE* **4**: e7401.
- Wemheuer, B., Güllert, S., Billerbeck, S., Giebel, H.-A., Voget, S., Simon, M., and Daniel, R. (2013) Impact of a phytoplankton bloom on the diversity of the active bacterial community in the southern North Sea as revealed by metatranscriptomic approaches. *FEMS Microbiol Ecol* **87**: 378–389.

- Weyland, H., Ruger, H.-J., and Schwarz, H. (1970) Zur Isolierung und Identifizierung mariner Bakterien. Ein Beitrag zur Standardisierung und Entwicklung adäquater Methoden. *Veröff Inst Meeresforsch Bremerhaven* **12**: 269–296.
- Yong, J.-J., Park, S.-J., Kim, H.-J., and Rhee, S.-K. (2007) *Glaciecola agarilytica* sp. nov., an agar-digesting marine bacterium from the East Sea, Korea. *Int J Syst Evol Microbiol* **57**: 951–953.
- Zhou, J., Bruns, M., and Tiedje, J. (1996) DNA recovery from soils of diverse composition. *Appl Environ Microbiol* **62**: 316–322.
- Zimmerman, A.E., Martiny, A.C., and Allison, S.D. (2013) Microdiversity of extracellular enzyme genes among sequenced prokaryotic genomes. *ISME J* **7**: 1187–1199.

### Supporting information

Additional Supporting Information may be found in the online version of this article at the publisher's web-site:

**Fig. S1.** Non-metric multidimensional scaling (NMDS) analysis of DGGE banding pattern similarities (UPGMA clustering) calculated using Gelcompar.

**Fig. S2.** OTUs with > 5% relative abundance in 'starter' (t0) and 'end' communities (CTR: control, CHI: chitin, AGA: agarose, ALG: alginate) at stations PF, AS, PS, and MU as determined by 454 pyrosequencing of 16S rRNA gene

amplicons. Data originates from one replicate per treatment and was used to identify trends in community dynamics and to design quantitative analyses on all three replicates per treatment.

**Fig. S3.** Rarefaction analysis comparing the number of OTUs with the number of sequences at (A) 80%, (B) 97%, and (C) 99% genetic similarity in 'starter' (t0) and 'end' communities (CTR: control, CHI: chitin, AGA: agarose, ALG: alginate) at stations PF, AS, PS, and MU. The saturation of curves indicates that the diversity has been sufficiently covered at all three genetic similarity levels.

**Table S1.** Origin, biome/province assignment, and physicochemical parameters of seawater from stations PF, AS, PS, and MU used for microcosm experiments.

**Table S2.** Cell numbers and fraction of high-nucleic acid cells (HNA; %) as determined by flow cytometry.

**Table S3.** Mean concentrations [ $\mu\text{M}$ ] of the agarose monomer galactose and the alginate monomers guluronate/mannuronate in triplicate microcosms at stations PF, AS, PS, and MU.

**Table S4.** *P* values of significantly decreasing mean concentrations of alginate and agarose monomers between sampling days.

**Table S5.** Concentrations of combined carbohydrates [ $\mu\text{M}$ ; mean of triplicates  $\pm$  standard deviation] in control (= ambient carbohydrates) as well as agarose/alginate treatments (= ambient carbohydrates and polysaccharide impurities). Red: carbohydrates with significantly lower concentrations compared to day 0.

## Appendix 2

### **Different utilization of alginate and other algal polysaccharides by marine *Alteromonas macleodii* ecotypes**

Neumann A, Balmonte JP, Berger M, Giebel H-A, Arnosti C, Voget S, Brinkhoff T, Simon M, Wietz M

*Environmental Microbiology* (2015), 17:3857–3868

# Different utilization of alginate and other algal polysaccharides by marine *Alteromonas macleodii* ecotypes

Anna M. Neumann,<sup>1</sup> John P. Balmonte,<sup>2</sup>  
Martine Berger,<sup>1</sup> Helge-Ansgar Giebel,<sup>1</sup>  
Carol Arnosti,<sup>2</sup> Sonja Voget,<sup>3</sup> Meinhard Simon,<sup>1</sup>  
Thorsten Brinkhoff<sup>1</sup> and Matthias Wietz<sup>1\*</sup>

<sup>1</sup>Institute for Chemistry and Biology of the Marine Environment, University of Oldenburg, Oldenburg 26129, Germany.

<sup>2</sup>Department of Marine Sciences, University of North Carolina, 3117 Venable Hall, Chapel Hill, NC, USA.

<sup>3</sup>Genomic and Applied Microbiology and Göttingen Genomics Laboratory, Institute of Microbiology and Genetics, University of Göttingen, Göttingen 37077, Germany.

## Summary

The marine bacterium *Alteromonas macleodii* is a copiotrophic *r*-strategist, but little is known about its potential to degrade polysaccharides. Here, we studied the degradation of alginate and other algal polysaccharides by *A. macleodii* strain 83-1 in comparison to other *A. macleodii* strains. Cell densities of strain 83-1 with alginate as sole carbon source were comparable to those with glucose, but the exponential phase was delayed. The genome of 83-1 was found to harbour an alginolytic system comprising five alginate lyases, whose expression was induced by alginate. The alginolytic system contains additional CAZymes, including two TonB-dependent receptors, and is part of a 24 kb genomic island unique to the *A. macleodii* 'surface clade' ecotype. In contrast, strains of the 'deep clade' ecotype contain only a single alginate lyase in a separate 7 kb island. This difference was reflected in an eightfold greater efficiency of surface clade strains to grow on alginate. Strain 83-1 furthermore hydrolysed laminarin, pullulan and xylan, and corresponding polysaccharide utilization loci were detected in the genome. *Alteromonas macleodii* alginate lyases were predominantly detected in Atlantic Ocean

metagenomes. The demonstrated hydrolytic capacities are likely of ecological relevance and represent another level of adaptation among *A. macleodii* ecotypes.

## Introduction

Macroalgae represent a substantial fraction of biomass in coastal oceans and contain a wealth of polysaccharides, which function as structural components and storage compounds (Kraan, 2012). Macroalgal polysaccharides also provide distinct niches for heterotrophic bacteria, including hydrolytic populations that can utilize algal compounds (Martin *et al.*, 2014). One abundant marine algal polysaccharide is alginate, which can account for > 50% of the dry weight of brown macroalgae (Mabeau and Kloareg, 1987) and represents a nutrient source for different marine bacteria (Thomas *et al.*, 2012).

The alginate polymer is composed of the uronic acids  $\beta$ -D-mannuronate and  $\alpha$ -L-guluronate, which are arranged in alternating homo- or heteropolymeric blocks. Bacterial alginate utilization requires hydrolysis by alginate lyases and subsequent conversion via several oligosaccharide and monosaccharide intermediates to the final product 2-keto-3-deoxy-6-phosphogluconate (KDPG), which can be assimilated through the Entner–Doudoroff pathway (Preiss and Ashwell, 1962a,b). According to the carbohydrate-active enzyme (CAZyme) classification system (Lombard *et al.*, 2014), polysaccharide lyase (PL) families 5–7, 14, 15, 17 and 18 are classified as alginate lyases (Garron and Cygler, 2010; Vincent *et al.*, 2010). In bacterial genomes, alginate lyases and other CAZymes are often clustered in operon-like 'polysaccharide utilization loci' (PUL), which have been initially described in human gut *Bacteroidetes* (Shipman *et al.*, 2000) and are thought to enable the orchestrated degradation of polysaccharides (Martens *et al.*, 2009).

Also in marine systems, PUL have been mainly described among *Bacteroidetes*, which reflects their designation as key marine polymer degraders (Bauer *et al.*, 2006; Fernández-Gómez *et al.*, 2013). For instance, the marine flavobacterium *Zobellia galactanivorans* contains two PUL with seven alginate lyases that are induced by the presence of alginate (Thomas *et al.*, 2012).

Received 19 January, 2015; accepted 29 March, 2015. \*For correspondence. E-mail matthias.wietz@uni-oldenburg.de; Tel. +49 441 7983637; Fax +49 441 7983438.

Polysaccharide utilization loci with similar genomic arrangements are also found in the related flavobacteria *Gramella forsetii* (Kabisch *et al.*, 2014) and *Formosa agariphila* (Mann *et al.*, 2013), illustrating considerable conservation or even horizontal transfer between taxa (Thomas *et al.*, 2012). *Gramella forsetii* and *F. agariphila* also contain PUL for the degradation of other algal polysaccharides, including laminarin and xylan. While these studies promoted the understanding of the structural and functional diversity of marine bacterial CAZymes (Hehemann *et al.*, 2014), a considerable number of hydrolytic enzymes may potentially be discovered, for instance among *Gammaproteobacteria* (Michel and Czjzek, 2013; Zimmerman *et al.*, 2013). This notion is consistent with the ability of different *Alteromonadales* to degrade complex algal polysaccharides (Akagawa-Matsushita *et al.*, 1992; Sawabe *et al.*, 1997).

The marine bacterium *Alteromonas macleodii* is a copiotrophic *r*-strategist and often dominates bacterial blooms when organic nutrients are available (Allers *et al.*, 2008; McCarren *et al.*, 2010; Sarmiento and Gasol, 2012). *Alteromonas macleodii* is globally distributed in temperate surface oceans and occurs at all depths of the Mediterranean Sea (Ivars-Martínez *et al.*, 2008). Isolates of *A. macleodii* are separated into two ecotypes – the surface clade and the deep clade – with presumably different niches. Their proposed adaptations include different substrate spectra and a preference for colonizing smaller versus larger organic particles respectively (Ivars-Martínez *et al.*, 2008). Despite > 98% 16S rRNA gene sequence similarity, surface and deep clade have recently been proposed as separate species, with deep clade strains to be reclassified as *Alteromonas mediterranea* (Ivanova *et al.*, 2015).

While it has been observed that *A. macleodii* utilizes easily accessible substrates such as glucose (Allers *et al.*, 2007), less is known about its potential to degrade complex polymeric compounds. McCarren and colleagues (2010) provided initial evidence for hydrolytic capacities, as the growth of *A. macleodii* was stimulated by addition of high molecular weight organic matter to natural seawater. In addition, *A. macleodii* was recently shown to constitute > 60% of the bacterial community during the degradation of alginate in microcosm experiments, suggesting a major contribution to alginate hydrolysis in environmental microbiota (Wietz *et al.*, 2015).

Here, we report the utilization of alginate and other algal polysaccharides by *A. macleodii* strain 83-1 isolated from an alginate-supplemented microcosm with Atlantic seawater. The considerable hydrolytic capacities of strain 83-1 match those in key marine polysaccharide degraders, supporting the notion that *Alteromonas* spp. can contribute significantly to biogeochemical processes (Pedler *et al.*, 2014). In addition, comparative analyses showed

that hydrolytic activities provide another level of niche differentiation between *A. macleodii* surface and deep clade ecotypes.

## Results and discussion

### *Alginate utilization by A. macleodii* strain 83-1

*Alteromonas macleodii* strain 83-1 was isolated from a microcosm with alginate-supplemented surface seawater from the Mauritanian upwelling region in the eastern Atlantic (Wietz *et al.*, 2015). In order to investigate the polysaccharide degradation potential of strain 83-1, we studied the utilization of alginate and other marine polysaccharides as sole carbon sources in comparison to glucose.

With glucose, *A. macleodii* strain 83-1 started exponential growth 9 h after inoculation and reached the stationary phase after 18 h (Fig. 1A). In contrast, alginate-supplemented cultures featured a lag phase of up to 32 h, although cells were pre-cultured on alginate and thus adapted to the substrate. The formation of cell aggregates (as confirmed by epifluorescence microscopy) and concurrently decreasing alginate concentrations, however, indicated that exponential growth started after 21 h (Fig. 1B). While final cell densities and generation times during exponential growth were comparable, high-performance liquid chromatography (HPLC) analyses suggested that a greater fraction of the available alginate (97%) than glucose (56%) was consumed (Fig. 1). Nonetheless, the culture may have still contained poly- or oligomeric alginate that was not depolymerized by the acid treatment to be measurable by HPLC. The cessation of growth on glucose prior to complete substrate consumption may reflect a lack of some essential element or cell stress at high cell densities that can be associated with the excretion of metabolites (Goo *et al.*, 2012). The observed production of foam in glucose cultures indeed points to a substantial excretion of metabolites. In contrast, alginate cultures did not produce foam but did exhibit a light-yellow pigmentation (data not shown). While other marine *Alteromonas* spp. are known to degrade polysaccharides (Akagawa-Matsushita *et al.*, 1992; Sawabe *et al.*, 1997), this is the first report of substantial alginolytic capacities among *A. macleodii*. The cell densities of strain 83-1 on alginate were in our experiments approximately twofold higher compared with other alginate-degrading bacteria (Ueno, 2009).

### *Alginolytic system in 83-1 and other strains of the A. macleodii* surface clade

The genome of *A. macleodii* strain 83-1 was investigated for alginate-related gene content and compared with 11

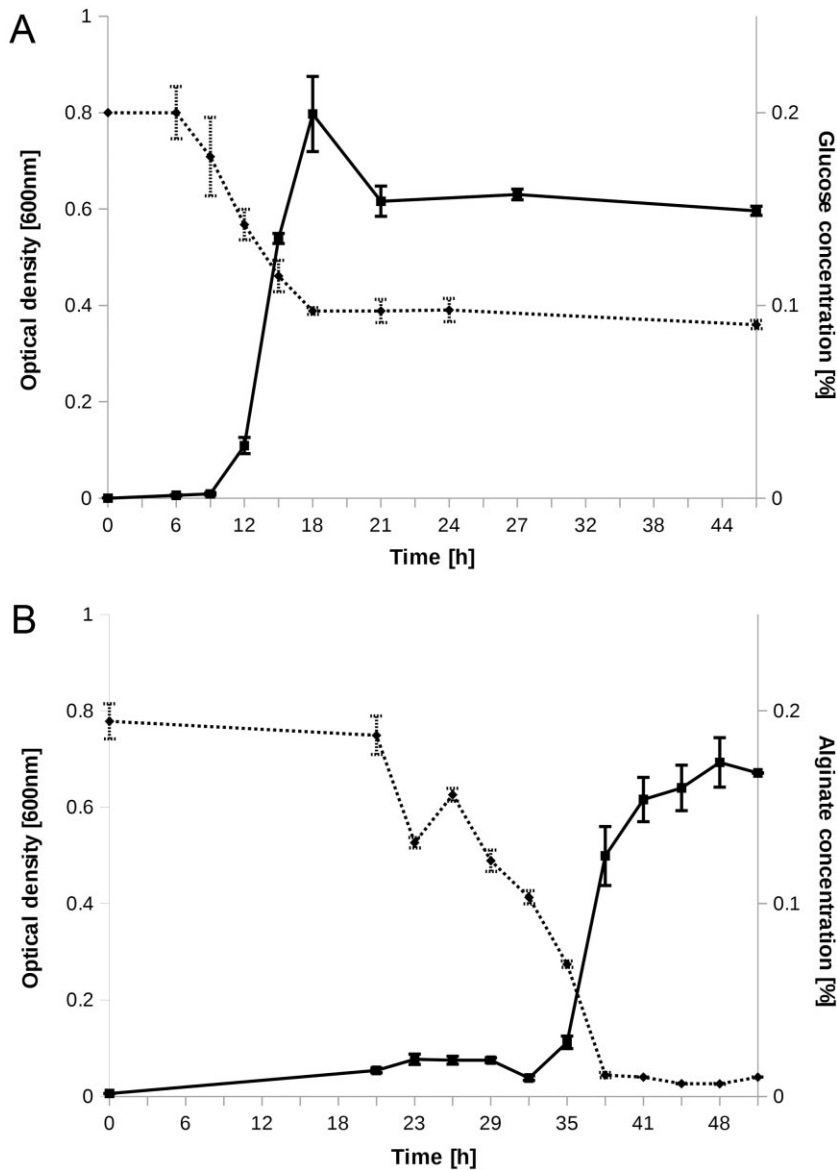


**Fig. 1.** Growth and substrate utilization of *Alteromonas macleodii* strain 83-1 with glucose (A) or alginate (B) as sole carbon source as determined by optical densities (solid lines) and HPLC quantification of glucose or guluronate/mannuronate (dotted lines) respectively.

other *A. macleodii* strains from the surface and deep clade (Table S1). BLASTp with known alginate lyases revealed that strain 83-1 harbours an alginolytic system (AS) within a 24 kb genomic island, which comprises five putative alginate lyases and other CAZymes (Fig. 2, Table S2) and thus matches the typical characteristics of a PUL. Bidirectional BLAST within IMG/ER revealed nearly identical AS at corresponding genomic loci in strains ATCC 27126<sup>T</sup> and AD45 from the *A. macleodii* surface clade, while deep clade strains did not contain the AS. Together with phylogenetic analysis of 2340 *A. macleodii* core genes (Fig. S1) and average nucleotide identities of > 97%, strain 83-1 was clearly placed within the *A. macleodii* surface clade.

The five predicted alginate lyases were identified as belonging to CAZy polysaccharide lyase families PL6 (2

genes), PL7 (2 genes) and PL17 (1 gene). These families have been originally characterized in *Pseudomonas* (Maki *et al.*, 1993; Yamasaki *et al.*, 2004) and *Saccharophagus* (Weiner *et al.*, 2008) species respectively. The diversity of PL families in *A. macleodii* indicates an exquisite adaptation to alginate degradation (Thomas *et al.*, 2013). The PL7 alginate lyase (IMG Gene ID 2562022990) is homologous to AlyA5 in *Zobellia galactanivorans* (Table S2) and may thus have a similar mode of action based on exolytic cleaving at the non-reducing end of oligo-alginates (Thomas *et al.*, 2013). The PL6 and PL17 alginate lyases (IMG Gene IDs 2562022980 and 81) plus adjacent cupin-domain, sugar permease, sugar kinase and isobutyrate dehydrogenase genes (Fig. 2) form the core of the AS, which is highly conserved among surface clade strains (99% nucleotide sequence identity) despite their origin

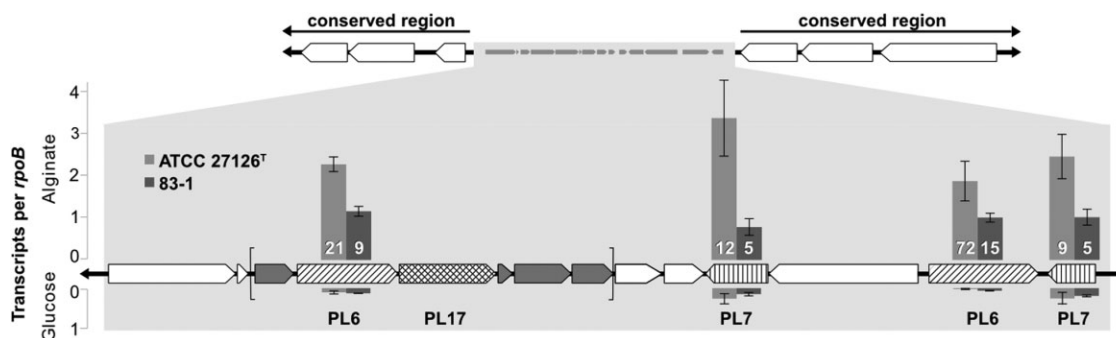


**Fig. 2.** Alginolytic system (AS) within a genomic island specific to strain 83-1 and other *Alteromonas macleodii* surface clade strains, as well as relative expression of alginate lyases in strains 83-1 and ATCC 27126<sup>T</sup>. The up- and downstream boundaries of the AS are conserved among all *A. macleodii* strains. Putative alginate lyases are designated following their CAZy classification. Alginate lyases PL6, PL17 and adjacent cupin-domain, sugar permease, sugar kinase and isobutyrate dehydrogenase genes (gray) represent the core of the AS (as indicated by square brackets). Bars indicate the relative expression of alginate lyases compared with *rpoB*, with numbers designating *n*-fold induction with alginate in comparison to glucose. As PL6 and PL17 from the AS core are directly adjacent and orientated in the same direction, we presume that expression levels are similar.

from distant locations (Table S1). The AS core is also present in the *Alteromonadales* species *Pseudoalteromonas haloplanktis* (67%), *Pseudoalteromonas marina* (62%) and *Shewanella waksmanii* (57% nucleotide sequence identity) (Fig. S2), suggesting comparable functionality. The alginate lyase families PL6, 7 and 17 are also those found in *F. agariphila* (Mann *et al.*, 2013) and *G. forsetii* (Kabisch *et al.*, 2014), but AS architectures vary between *A. macleodii* and the *Flavobacteriaceae* (Fig. S2). This indicates that alginate depolymerization proceeds similarly, while the evolutionary history of involved genes is different. Nonetheless, considerable sequence similarities in four AS core genes between *A. macleodii* and *Z. galactanivorans* (Table S2) support the notion that CAZymes have been transferred between phyla (Thomas *et al.*, 2012).

Strains of the *A. macleodii* deep clade only possess a single PL6 alginate lyase, with 50% nucleotide sequence identity to the PL6 core lyase in surface clade strains (IMG Gene ID 2562022980). This lyase is part of a deep clade-specific genomic island, which is much smaller (seven kb/seven genes) and located in a different genomic context but also contains several CAZymes (Fig. S3A). Comparative analyses with strains 83-1 (surface clade) versus U7 (deep clade) confirmed that the different content in alginate lyases relates to different alginolytic capacities. While growth on glucose was similar, strain 83-1 reached eightfold higher cell densities than U7 when grown on alginate (Fig. S3B). Overall, the physiological and genomic differences in alginolytic capacities support the delineation of *A. macleodii* into surface and deep ecotypes as well as their specific adaptations (Ivars-Martinez *et al.*, 2008). Likewise, differences would be consistent with the proposed reclassification into two species (Ivanova *et al.*, 2015). However, as this reclassification has not been validated yet, the present

study maintains the distinction into two ecotypes instead of species.

#### Expression of alginate lyases in surface clade strains

A quantitative real-time polymerase chain reaction (PCR) protocol was designed to study the expression of predicted alginate lyases (Table S2) in *A. macleodii* strains 83-1 and ATCC 27126<sup>T</sup> when grown on alginate compared with glucose. In both strains the expression of alginate lyases was upregulated between 5- and 72-fold in the presence of alginate (Fig. 2), which supported the involvement in alginate hydrolysis. The probable alginolytic activity was underlined by biochemical confirmation that purified homologous enzymes in *Z. galactanivorans* indeed hydrolyse alginate (Thomas *et al.*, 2012). The expression level of ATCC 27126<sup>T</sup> was 1.8 to 4.7-fold higher and associated with a higher induction compared with strain 83-1 (Fig. 2), which mirrors previously observed transcriptional differences among deep clade strains (Kimes *et al.*, 2014). However, ribonucleic acid (RNA) of strains 83-1 and ATCC 27126<sup>T</sup> has been extracted at slightly different cell densities, possibly affecting profiles of gene expression. In contrast to observations in *Z. galactanivorans*, the alternating forward/reverse orientation of several genes in the AS of *A. macleodii* would prevent a potential transcription as polycistronic messenger RNA. This gene organization might, however, allow differential transcriptional regulation within the AS.

#### Degradation of other algal polysaccharides and natural substrates by *A. macleodii* strain 83-1

Six fluorescently labelled marine polysaccharides, i.e. laminarin, pullulan, xylan, chondroitin, fucoidan and arabinogalactan (Arnosti, 1996; 2003), were used to test

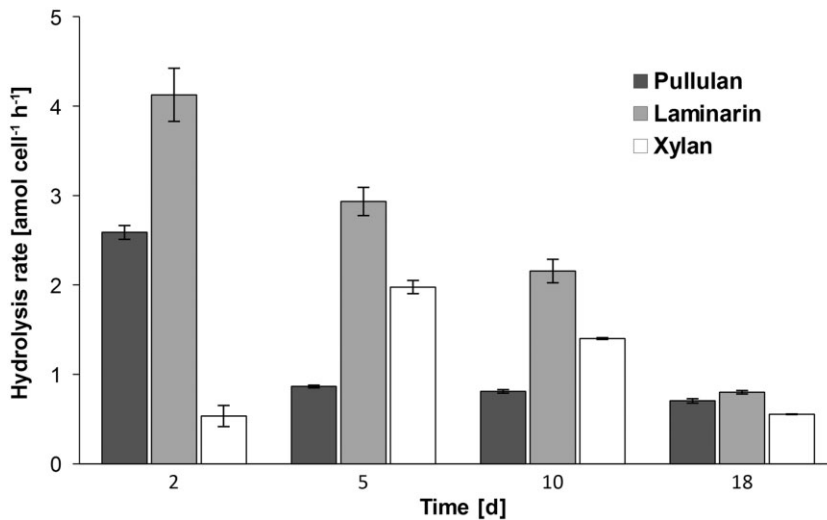


**Fig. 3.** Cell-specific hydrolysis rates of pullulan, laminarin and xylan by *Alteromonas macleodii* strain 83-1 over a period of 18 days. Rates were calculated as change in substrate molecular weight due to hydrolysis and normalized to cell counts determined by flow cytometry.

whether *A. macleodii* strain 83-1 can hydrolyse a broader range of structurally diverse marine polysaccharides. Strain 83-1 hydrolysed laminarin, pullulan and xylan, each with different temporal utilization patterns (Fig. 3). Hydrolysis of laminarin and pullulan were maximal after 2 days, and xylan hydrolysis after 5 days of incubation. Normalized to cell counts, laminarin hydrolysis at day 2 was nearly twice as high as maximal pullulan or xylan hydrolysis (Fig. 3). The maximum rates on a per-cell basis were approx. 1.5 to fivefold higher compared with those observed in near-shore waters and approx. two to eightfold lower compared with offshore waters near the North Carolina coast (D'Ambrosio *et al.*, 2014). Overall, the observed capacities to degrade structurally diverse algal polysaccharides match those of prime polymer degraders such as the *Bacteroidetes* (Mann *et al.*, 2013; Kabisch *et al.*, 2014).

The ability of strain 83-1 to degrade laminarin, pullulan and xylan was linked with the presence of  $\beta$ -glucanase, pullulanase and xylanase genes, respectively, within separate PUL that ranged between 21 and 40 kb in size (Table S3). The xylan-related PUL harboured a  $\beta$ -xylosidase with 70% similarity to *xyIB* in *Z. galactanivorans*, but the latter possesses a total of four xylan-related loci (Caspi *et al.*, 2014) compared with the single PUL in strain 83-1. In contrast, chondroitin, fucoidan and arabinogalactan were not measurably hydrolysed.

In addition, we tested growth of *A. macleodii* strain 83-1 on an exudate from the marine *Synechococcus* strain RCC2527 that originates from the same Atlantic province. The exudate may represent a substrate pool that strain 83-1 might encounter in its natural habitat, also considering that *Synechococcus* spp. constituted approximately a third of the bacterial community from which strain 83-1 was isolated (Wietz *et al.*, 2015). Strain 83-1 was con-

firmed to grow with RCC2527 exudate as sole nutrient source, with final cell densities of  $3 \times 10^6$  cells ml<sup>-1</sup> (Fig. S4) but four to fivefold longer generation times compared with growth on alginate and glucose respectively. While the exudate may contain more monomeric than polymeric compounds (Baran *et al.*, 2010), it likely contains polysaccharides, as 70% of the > 10 KDa fraction of *Synechococcus* spp. exudates can be polysaccharides (Biersmith and Benner, 1998).

#### *Biogeography of A. macleodii* alginate lyases and homologues from other taxa

The broad hydrolytic capacities of *A. macleodii* strain 83-1 suggest an ecological relevance in the natural habitat. Although the occurrence of *A. macleodii* has been examined in different marine systems (Garcia-Martinez *et al.*, 2002; Ivars-Martínez *et al.*, 2008; Gonzaga *et al.*, 2012), prior studies did not specifically address biogeographic patterns of surface clade strains and associated hydrolytic traits. Hence, we searched *A. macleodii* alginate lyases (Table S2) in metagenomes from the Malaspina expedition (deep waters), Global Ocean Sampling (surface waters) and different other marine habitats around the world (Table S4). All searched alginate lyases were detected in deep waters near Cabo Verde, the Canary Islands, Brazil and Madagascar (Fig. 4A). In contrast, the majority of deep Pacific and Indian Ocean waters either possessed only short fragments of *A. macleodii* alginate lyases or none at all (Fig. 4A). Lyases were neither detected in Global Ocean Sampling metagenomes, although surface waters were previously found to contain larger *A. macleodii* gene fragments (López-Pérez *et al.*, 2012). Surface waters and other marine habitats only contained homologous lyases from other bacteria (Fig. 4A and B). The fact that these were detected when querying

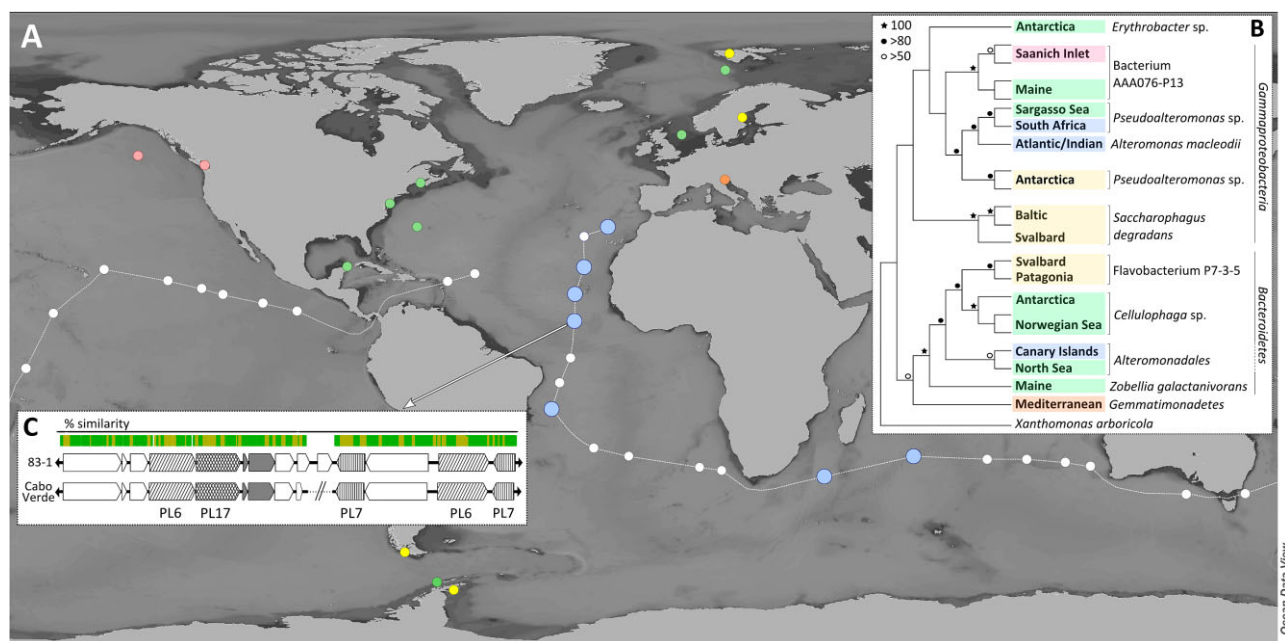


**Fig. 4.** (A) Occurrence of *Alteromonas macleodii* alginolytic systems in metagenomes from different marine habitats. *Alteromonas macleodii* alginolytic systems were only detected in some Atlantic and Indian Ocean metagenomes (large blue circles) along the global Malaspina expedition (broken white line). Other habitats (green: surface waters, yellow: sediments, red: oxygen minimum zones, orange: sponge) only contained homologous systems from other taxa. (B) Maximum likelihood phylogeny of detected PL17 alginolytic systems. Phylogenetic analyses demonstrated that PL17 alginolytic systems from *A. macleodii* are found in a variety of other taxa with the closest sequence relative indicated next to the branches. Colour codes correspond to habitat type as designated in A, with the closest sequence relative indicated next to the branches. (C) Recruitment of *A. macleodii* alginolytic system from a deep-water metagenome. BLAST and sequence alignments detected an almost complete alginolytic system on two metagenome contigs obtained from 4000 m depth near Cabo Verde (arrow). Sequence similarities are indicated by colours above (yellow: > 95%; green: 100%).

with *A. macleodii* sequences at high stringency ( $1^{-50}$ ) highlights considerable sequence conservation or even horizontal exchange between taxa (Thomas *et al.*, 2012). Phylogenetic analyses revealed that PL17 alginolytic system homologues from *A. macleodii* are found in a variety of *Alphaproteobacteria*, *Bacteroidetes* and *Gemmatimonadetes*. Potential horizontal exchange was corroborated by two *Alteromonadales*-affiliated systems grouping with *Bacteroidetes* sequences (Fig. 4B). An almost complete AS with 98.8% nucleotide sequence identity was retrieved from a Cabo Verde metagenome from 4000 m depth (Fig. 4C). BLAST analyses showed that this metagenome also comprised 71% of the 2340 *A. macleodii* core genes at > 99% sequence identity. These findings strongly suggest the presence of *A. macleodii* in this sample, indicating that the species likewise occurs in cold deep waters and is not limited by low temperatures, as reported previously (López-Pérez and Rodríguez-Valera, 2014).

#### Genomic microdiversity suggests potential *A. macleodii* 'sub-ecotypes'

In addition to the distinction into *A. macleodii* surface and deep ecotypes reported here and previously

(Ivars-Martinez *et al.*, 2008; López-Pérez *et al.*, 2012), we investigated specific adaptations that may define microniche speciation among related (and sometimes co-occurring) *A. macleodii* strains. In this context, comparative genomics demonstrated that strains EC673 and BS11 do not possess an AS, despite having the conserved genomic boundaries at the respective AS insertion sites and being clearly affiliated with the surface clade (Fig. S1). This microdiversity mirrors strain-specific variations in flexible genomic islands (López-Pérez *et al.*, 2012) and suggests the presence of 'sub-ecotypes' within the surface and deep clade (Klochko *et al.*, 2012), which possibly reflect specific adaptations to a certain habitat or niche.

Some 'sub-ecotype' features were shared between selected strains from the surface and deep clades. For instance, the co-occurrence of the xylan-related PUL among surface and deep clade strains (Table S3) suggests that their niches overlap with respect to the utilization of certain substrates. Among the deep clade, the xylan-related PUL was restricted to a single lineage containing strains AltDE1, UM4b and UM7 (Fig. S1), illustrating that 'sub-ecotype' features can be linked with phylogenetic relationships. Lineage-specific traits were also detected in non-carbohydrate related features.

For instance, a predicted siderophore biosynthetic gene cluster was restricted to strains 83-1, ATCC 27126<sup>T</sup> and EC673 (Fig. S1), mirroring the phylogenetic restriction of other biosynthetic capacities among *A. macleodii* strains (Mizuno *et al.*, 2013). In addition, a hydrogenase-related gene cluster present in most deep clade strains was also detected in strain 83-1 (IMG gene IDs 2562026286-296) while being absent from other surface clade strains. This cluster encodes for one of the most oxygen-resistant hydrogenases described to date (Vargas *et al.*, 2011) and may provide strain 83-1 a location-specific adaptation to microaerophilic conditions. The occurrence of such 'mixed genotypes' support the notion of gene exchange and recombination events among *A. macleodii* strains (Ivars-Martínez *et al.*, 2008; López-Pérez *et al.*, 2013), possibly illustrating a snapshot of ongoing evolutionary and adaptive processes.

#### Ecological conclusions

The utilization of structurally diverse algal polysaccharides by *A. macleodii* strain 83-1 and the associated complex PUL match the characteristics of prime marine polymer degraders, such as the *Bacteroidetes*. As only 6% of the genome-sequenced *Gammaproteobacteria* but 15% of *Flavobacteriaceae* possess an AS (Thomas *et al.*, 2012), alginolytic abilities in *A. macleodii* may represent a largely unobserved specialization among the *Gammaproteobacteria*. The ability to hydrolyse pullulan may provide a specific niche, as the polymer-specialized algal associates *F. agariphila*, *G. forsetii* and *Z. galactanivorans* lack pullulan-related genes (Markowitz *et al.*, 2014). The presence of multiple hydrolytic traits suggests that *A. macleodii* frequently encounters algal substrates. However, *A. macleodii* primarily occurs in pelagic waters but is not a typical associate of alginate-producing coastal macroalgae (Sawabe *et al.*, 2000; Staufenberger *et al.*, 2008; Goecke *et al.*, 2010). Potentially, *A. macleodii* may encounter alginate and other polysaccharides in form of open-ocean macroalgal genera such as *Sargassum*, which can have an alginate content of up to 45% (Davis *et al.*, 2003). Hypothetically, alginolytic abilities may also contribute to the degradation of 'marine gels', which contain uronic acids (Hung *et al.*, 2003; Verdugo *et al.*, 2004) and possibly also alginate, especially considering its gelling properties. As *A. macleodii* is commonly found in particle-associated bacterial communities (López-Pérez and Rodríguez-Valera, 2014), acidic marine gels could provide a niche for specialized pelagic hydrolysers including *A. macleodii*. The relevance of hydrolytic capacities in the ecophysiology of *A. macleodii* represents a promising prospect for further study.

## Experimental procedures

### Bacterial strains

*Alteromonas macleodii* strain 83-1 was isolated from a microcosm with Mauritanian upwelling surface seawater (20.70889 N, 21.17194 W) amended with 0.001% sodium alginate. The *A. macleodii* type strain (ATCC 27126<sup>T</sup>) and *A. macleodii* strain U7 were obtained from the German Collection of Microorganisms and Cell Cultures to compare strain 83-1 with other *A. macleodii* strains from the surface and deep clade respectively. *Synechococcus* sp. RCC2527, a cyanobacterial strain also originating from the Mauritanian upwelling (21.6833 N, 17.8333 W; 20 m), was obtained from the Roscoff Culture Collection (<http://www.roscoff-culture-collection.org/rcc-strain-details/2527>).

### Alginate utilization in surface and deep clade *A. macleodii* strains

Alginate utilization was analysed in seawater minimal medium (SWM) (Zech *et al.*, 2009) supplemented with 0.2% alginate (61:39% mannuronate:guluronate; Sigma A2158, St. Louis, MO) as sole carbon source. SWM supplemented with 0.2% glucose served as monosaccharide comparison. Pre-cultures were grown from single colonies for 24 h (glucose) or 48 h (alginate) and used to inoculate main cultures at 1% (v/v) of pre-culture diluted to an optical density (OD<sub>600</sub>) of 0.1. Cultures were incubated at 20°C and 140 r.p.m. in triplicate. Growth was determined photometrically (OD<sub>600</sub>), and cultures were diluted if necessary to measure within the linear range (OD<sub>600</sub> of < 0.4). Subsamples of 5 ml for determination of substrate concentrations were filtered through 0.22 µm polycarbonate filters into combusted glass vials and stored at -20°C. Alginate concentrations were measured by HPLC of its monomeric components guluronate and mannuronate obtained by chemical hydrolysis (20 h, 100°C, 0.1 M HCl) in combusted and sealed glass ampoules. Samples were neutralized with 6 N NaOH, desalted using DionexOnGuard II Ag/H cartridges (Thermo Scientific, Waltham, MA) and eluted with 100 mM sodium acetate tri-hydrate in 100 mM NaOH. Concentrations were determined in three dilutions per sample (0.01, 0.002, 0.001%) using a CarboPac PA 1 column (Thermo Scientific) and pulsed amperometric detection according to Mopper and colleagues (1992). A calibration curve was generated using hydrolysed 1% alginate solution ( $R^2 = 0.97$ ). Glucose concentrations were measured using samples diluted to 0.001% with MilliQ water followed by HPLC with NaOH (18 mM) as eluent and a CarboPac PA 1 column (Thermo Scientific). A calibration curve was generated using 24 concentrations from 0.025–10 µM glucose ( $R^2 = 0.99$ ).

### Utilization of other marine polysaccharides and natural substrates

Six commercially available polysaccharides (laminarin, pullulan, xylan, fucoidan, chondroitin and arabinogalactan) were fluorescently labelled as described previously (Arnosti, 1996; 2003). Strain 83-1 was pre-cultured and inoculated as described above in SWM with 3.5 µM monomer equivalent of

each labelled polysaccharide. Incubations were conducted in triplicate at 20°C in the dark, with an additional autoclaved dead control to exclude potential polysaccharide autolysis. Subsamples of 2 ml were taken over a period of 18 days, filtered through 0.2 µm surfactant-free cellulose acetate filters and stored at -20°C until analysis according to Arnosti (2003). Additional subsamples of 500 µL for flow cytometric cell counts were fixed with 1% glutaraldehyde (v/v) for 30 min at room temperature and stored at -20°C. Cyanobacterial exudates were prepared by sterile filtration of a culture of *Synechococcus* sp. RCC2527 grown for 10 days in f/2 medium at 20°C under a light/dark cycle. Strain 83-1 was inoculated, and subsamples for flow cytometry were processed as described above. Cell numbers were determined on an Accuri C6 flow cytometer (BD, San Jose, CA) using SYBR Green I staining and the internal fluidics calibration. Volume verification was conducted using TruCount beads (BD) following Giebel and colleagues (2009). Data were processed by BD ACCURIC6 software v.1.0.264.21.

### Genome analysis

Genomic DNA of strain 83-1 was extracted using the PeqGold DNA Isolation Kit (PEQLAB, Erlangen, Germany) according to the manufacturer's instructions. The genome was sequenced with Illumina technology using a GAIIx sequencing platform at the Göttingen Genomics Laboratory (Germany) on paired-end libraries prepared with the Nextera XT DNA Kit (Illumina, San Diego, CA). A total of 6 293 142 paired-end reads of 112 bp were assembled *de novo* into 31 contigs (mean coverage 134) between 3.3 kb and 615 kb using the SPADES ASSEMBLER v3.0 (Bankevich *et al.*, 2012), followed by error correction using BayesHammer (Nikolenko *et al.*, 2013). Gene prediction and functional annotation were done using the automatic pipeline of the IMG database (Markowitz *et al.*, 2012). The relationship of strain 83-1 to other *A. macleodii* strains (Table S1) was determined using 2340 single-copy core genes identified using GET\_HOMOLOGUES (Contreras-Moreira and Vinuesa, 2013). Genes were concatenated using GENEIOUS PRO v7.1 (available from <http://www.geneious.com>) and aligned using MAFFT (FFT-NS-2 algorithm, 1PAM/κ = 2 scoring matrix, Unalignlevel = 0, gappy regions included) (Katoh *et al.*, 2002). The manually curated alignment of 2 381 187 bp was used to compute a maximum likelihood phylogeny using RAxML (GTR + G model, 1000 bootstrap replicates) implemented on the CIPRES Science Gateway (Miller *et al.*, 2010). Average nucleotide identities between strain 83-1 and other *A. macleodii* strains were calculated using <http://www.enve-omics.ce.gatech.edu/ani/index>.

### Identification of polysaccharide-related gene content

Putative alginate-related genes in strain 83-1 were identified by searching for homologues of AS genes from *Z. galactanivorans* (Thomas *et al.*, 2012) as well as predicted alginate lyases from *A. macleodii* (Lombard *et al.*, 2014) using custom BLASTp implemented in GENEIOUS PRO v7.1. Identified candidate genes and associated domains were classified using the CAZy database (Lombard *et al.*, 2014). The occurrence of candidate genes in other bacteria was

analysed using IMG/ER (Markowitz *et al.*, 2009), MetaCyc (Caspi *et al.*, 2014) and NCBI BLASTp. *Alteromonas macleodii* strains EC615 and U4 were excluded from comparative analyses, as the genome of EC615 was not adequately annotated due to possible sequencing errors (comprising ~400 genes with frame shifts), and the genome of U4 was marked as erroneous in the IMG database at the time of analysis. A pseudochromosome of strain 83-1 was created using the CONTIGUATOR Web Server (Galardini *et al.*, 2011), and the closed genome of *A. macleodii* strain AD45 as reference. Twenty-seven of the 31 contigs (99% of the genome in bp) were mapped, allowing the comparison of genomic structures between strain 83-1 and other *A. macleodii* strains. Genes of strain 83-1 putatively involved in the hydrolysis of fluorescently labelled marine polysaccharides were identified by searching for homologues in the CAZy database. Following the delimiting criterion by Mann and colleagues (2013), clusters associated with candidate genes were defined as PUL if containing at least one TonB-dependent receptor plus CAZymes.

### Quantitative real-time PCR of alginate lyases

*Alteromonas macleodii* strains 83-1 and ATCC 27126<sup>T</sup> were grown in 30 ml SW supplemented with either 0.2% alginate or glucose in 100 ml Erlenmeyer flasks at 140 r.p.m. and 20°C in triplicate. Cells were harvested in exponential phase at mean ODs of 0.18 ± 0.01 (alginate)/0.32 ± 0.03 (glucose) for strain 83-1 and 0.32 ± 0.01 (alginate)/0.36 ± 0.03 (glucose) for strain ATCC 27126<sup>T</sup> respectively. For analysis of gene expression, total RNA was extracted using the High Pure RNA Isolation Kit (Roche, Basel, Switzerland) according to the manufacturer's instructions. Primer sets were designed for all five predicted alginate lyases (Table S5) using the Roche Universal Probe Library (<http://www.tinyurl.com/roche-upl>). Quantitative real-time PCR was performed using a LIGHTCYCLER 480 (Roche) as described by Berger and colleagues (2011). Copy numbers of alginate lyases were set in relation to copy numbers of *rpoB*.

### Distribution of *A. macleodii* alginate lyases in marine metagenomes

Amino acid sequences of *A. macleodii* alginate lyases (Table S2) were searched against a selection of metagenomes deposited in IMG/M (Markowitz *et al.*, 2014) using BLASTp (e-value of 1<sup>-50</sup>). The search focused on global surface and deep ocean metagenomes obtained from the Global Ocean Sampling (<http://www.tinyurl.com/sorcerer-II>) and Malaspina expeditions (<http://www.scientific.expedicionmalaspina.es>), as both applied a consistent experimental approach to a large number of samples. In addition, a selection of metagenomes from other habitats was searched (Table S4). Hits were subjected to BLASTp to support their affiliation with *A. macleodii* or to determine whether they represent homologous lyases from other taxa. Detected amino acid sequences related to the PL17 alginate lyase were aligned using MAFFT (Katoh *et al.*, 2002) within GENEIOUS PRO v7.1, followed by manual curation of poorly aligned regions. MEGA6 (Tamura *et al.*, 2013) was used to determine the best substitution model (LG + G) and to

compute a maximum likelihood phylogeny with 1000 bootstrap replicates. An alginate lyase of *Xanthomonas arboricola* (GenBank accession number WP\_024938635) was used as outgroup.

## Acknowledgements

We thank Rolf Weinert, Katrin Klapproth, Maren Seibt and Birgit Kürzel for chemical analyses. Martin Mierzejewski, Robert Strodel and Lisa-Marie Moskwa are thanked for laboratory assistance. This work was supported by grants WI3888/1-1 (to MW) and the Transregional Collaborative Research Centre 'Roseobacter' (TRR 51), both from the German Research Foundation (DFG). JPB and CA received support from the U.S. National Science Foundation (OCE-1332881); CA additionally received a fellowship from the Hanse-Wissenschaftskolleg (Delmenhorst, Germany).

## References

- Akagawa-Matsushita, M., Matsuo, M., Koga, Y., and Yamasato, K. (1992) *Alteromonas atlantica* sp. nov. and *Alteromonas carrageenovora* sp. nov., bacteria that decompose algal polysaccharides. *Int J Syst Evol Microbiol* **42**: 621–627.
- Allers, E., Gómez-Consarnau, L., Pinhassi, J., Gasol, J.M., Simek, K., and Pernthaler, J. (2007) Response of *Alteromonadaceae* and *Rhodobacteriaceae* to glucose and phosphorus manipulation in marine mesocosms. *Environ Microbiol* **9**: 2417–2429.
- Allers, E., Niesner, C., Wild, C., and Pernthaler, J. (2008) Microbes enriched in seawater after addition of coral mucus. *Appl Environ Microbiol* **74**: 3274–3278.
- Arnosti, C. (1996) A new method for measuring polysaccharide hydrolysis rates in marine environments. *Org Geochem* **25**: 105–115.
- Arnosti, C. (2003) Fluorescent derivatization of polysaccharides and carbohydrate-containing biopolymers for measurement of enzyme activities in complex media. *J Chromatogr B Analyt Technol Biomed Life Sci* **793**: 181–191.
- Bankevich, A., Nurk, S., Antipov, D., Gurevich, A.A., Dvorkin, M., Kulikov, A.S., et al. (2012) SPAdes: a new genome assembly algorithm and its applications to single-cell sequencing. *J Comput Biol* **19**: 455–477.
- Baran, R., Bowen, B.P., Bouskill, N.J., Brodie, E.L., Yannone, S.M., and Northen, T.R. (2010) Metabolite identification in *Synechococcus* sp. PCC 7002 using untargeted stable isotope assisted metabolite profiling. *Anal Chem* **82**: 9034–9042.
- Bauer, M., Kube, M., Teeling, H., Richter, M., Lombardot, T., Allers, E., et al. (2006) Whole genome analysis of the marine *Bacteroidetes* "*Gramella forsetii*" reveals adaptations to degradation of polymeric organic matter. *Environ Microbiol* **8**: 2201–2213.
- Berger, M., Neumann, A., Schulz, S., Simon, M., and Brinkhoff, T. (2011) Tropodithietic acid production in *Phaeobacter gallaeciensis* is regulated by *N*-Acyl homoserine lactone-mediated quorum sensing. *J Bacteriol* **193**: 6576–6585.
- Biersmith, A., and Benner, R. (1998) Carbohydrates in phytoplankton and freshly produced dissolved organic matter. *Mar Chem* **63**: 131–144.
- Caspi, R., Altman, T., Billington, R., Dreher, K., Foerster, H., Fulcher, C.A., et al. (2014) The MetaCyc database of metabolic pathways and enzymes and the BioCyc collection of Pathway/Genome Databases. *Nucleic Acids Res* **42**: D459–D471.
- Contreras-Moreira, B., and Vinuesa, P. (2013) GET\_HOMOLOGUES, a versatile software package for scalable and robust microbial pangenome analysis. *Appl Environ Microbiol* **79**: 7696–7701.
- D'Ambrosio, L., Zievelogel, K., MacGregor, B., Teske, A., and Arnosti, C. (2014) Composition and enzymatic function of particle-associated and free-living bacteria: a coastal/offshore comparison. *ISME J* **8**: 2167–2179.
- Davis, T.A., Volesky, B., and Mucci, A. (2003) A review of the biochemistry of heavy metal biosorption by brown algae. *Water Res* **37**: 4311–4330.
- Fernández-Gómez, B., Richter, M., Schüller, M., Pinhassi, J., Acinas, S.G., González, J.M., and Pedrós-Alió, C. (2013) Ecology of marine *Bacteroidetes*: a comparative genomics approach. *ISME J* **7**: 1026–1037.
- Galardini, M., Biondi, E.G., Bazzicalupo, M., and Mengoni, A. (2011) CONTIGuator: a bacterial genomes finishing tool for structural insights on draft genomes. *Source Code Biol Med* **6**: 11.
- García-Martínez, J., Acinas, S.G., Massana, R., Rodríguez-Valera, F., García-Martínez, J., and Rodríguez-Valera, F. (2002) Prevalence and microdiversity of *Alteromonas macleodii*-like microorganisms in different oceanic regions. *Environ Microbiol* **4**: 42–50.
- Garron, M.-L., and Cygler, M. (2010) Structural and mechanistic classification of uronic acid-containing polysaccharide lyases. *Glycobiology* **20**: 1547–1573.
- Giebel, H.-A., Brinkhoff, T., Zwisler, W., Selje, N., and Simon, M. (2009) Distribution of *Roseobacter* RCA and SAR11 lineages and distinct bacterial communities from the subtropics to the Southern Ocean. *Environ Microbiol* **11**: 2164–2178.
- Goecke, F., Labes, A., Wiese, J., and Imhoff, J.F. (2010) Chemical interactions between marine macroalgae and bacteria. *Mar Ecol Progr Ser* **409**: 267–299.
- Gonzaga, A., Martín-Cuadrado, A.-B., López-Pérez, M., Megumi Mizuno, C., García-Heredia, I., Kimes, N.E., et al. (2012) Polyclonality of concurrent natural populations of *Alteromonas macleodii*. *Genome Biol Evol* **4**: 1360–1374.
- Goo, E., Majerczyk, C.D., An, J.H., Chandler, J.R., Seo, Y.-S., Ham, H., et al. (2012) Bacterial quorum sensing, cooperativity, and anticipation of stationary-phase stress. *Proc Natl Acad Sci USA* **109**: 19775–19780.
- Hehmann, J.-H., Boraston, A.B., and Czjzek, M. (2014) A sweet new wave: structures and mechanisms of enzymes that digest polysaccharides from marine algae. *Curr Opin Struct Biol* **28**: 77–86.
- Hung, C.-C., Guo, L., Santschi, P.H., Alvarado-Quiroz, N., and Haye, J.M. (2003) Distributions of carbohydrate species in the Gulf of Mexico. *Mar Chem* **81**: 119–135.
- Ivanova, E.P., López-Pérez, M., Zabalos, M., Nguyen, S.H., Webb, H.K., Ryan, J., et al. (2015) Ecophysiological diversity of a novel member of the genus *Alteromonas*, and

- description of *Alteromonas mediterranea* sp. nov. *Antonie Van Leeuwenhoek* **107**: 119–132.
- Ivars-Martínez, E., D'Auria, G., Rodríguez-Valera, F., Sánchez-Porro, C., Ventosa, A., Joint, I., and Mühling, M. (2008) Biogeography of the ubiquitous marine bacterium *Alteromonas macleodii* determined by multilocus sequence analysis. *Mol Ecol* **17**: 4092–4106.
- Ivars-Martínez, E., Martín-Cuadrado, A.-B., D'Auria, G., Mira, A., Ferrera, S., Johnson, J., et al. (2008) Comparative genomics of two ecotypes of the marine planktonic copiotroph *Alteromonas macleodii* suggests alternative lifestyles associated with different kinds of particulate organic matter. *ISME J* **2**: 1194–1212.
- Kabisch, A., Otto, A., König, S., Becher, D., Albrecht, D., Schüler, M., et al. (2014) Functional characterization of polysaccharide utilization loci in the marine *Bacteroidetes* 'Gramella forsetii' KT0803. *ISME J* **8**: 1492–1502.
- Katoh, K., Misawa, K., Kuma, K., and Miyata, T. (2002) MAFFT: a novel method for rapid multiple sequence alignment based on fast Fourier transform. *Nucleic Acids Res* **30**: 3059–3066.
- Kimes, N.E., López-Pérez, M., Ausó, E., Ghai, R., and Rodríguez-Valera, F. (2014) RNA sequencing provides evidence for functional variability between naturally co-existing *Alteromonas macleodii* lineages. *BMC Genomics* **15**: 938.
- Klochko, V., Zelena, L., Voychuk, S., and Ostapchuk, A. (2012) Peculiarities of *Alteromonas macleodii* strains reflects their deep/surface habitation rather than geographical distribution. *J Gen Appl Microbiol* **58**: 129–135.
- Kraan, S. (2012) Algal polysaccharides, novel applications and outlook. In *Carbohydrates – Comprehensive Studies on Glycobiology and Glycotechnology*. Chang, C.-F. (ed.). Rijeka, Croatia: InTech, pp. 489–532.
- López-Pérez, M., and Rodríguez-Valera, F. (2014) *The family Alteromonadaceae*. In *The Prokaryotes*. Rosenberg, E., DeLong, E.F., Lory, S., Stackebrandt, E., and Thompson, F. (eds). Berlin, Germany: Springer, pp. 69–92.
- López-Pérez, M., Gonzaga, A., Martín-Cuadrado, A.-B., Onyshchenko, O., Ghavidel, A., Ghai, R., and Rodríguez-Valera, F. (2012) Genomes of surface isolates of *Alteromonas macleodii*: the life of a widespread marine opportunistic copiotroph. *Sci Rep* **2**: 696.
- López-Pérez, M., Gonzaga, A., and Rodríguez-Valera, F. (2013) Genomic diversity of 'deep ecotype' *Alteromonas macleodii* isolates: evidence for Pan-Mediterranean clonal frames. *Genome Biol Evol* **5**: 1220–1232.
- Lombard, V., Golaconda Ramulu, H., Drula, E., Coutinho, P.M., and Henrissat, B. (2014) The carbohydrate-active enzymes database (CAZy) in 2013. *Nucleic Acids Res* **42**: D490–D495.
- Mabeau, S., and Kloareg, B. (1987) Isolation and Analysis of the Cell Walls of Brown Algae: *Fucus spiralis*, *F. ceranoides*, *F. vesiculosus*, *F. serratus*, *Bifurcaria bifurcata* and *Laminaria digitata*. *J Exp Bot* **38**: 1573–1580.
- McCarren, J., Becker, J.W., Repeta, D.J., Shi, Y., Young, C.R., Malmstrom, R.R., et al. (2010) Microbial community transcriptomes reveal microbes and metabolic pathways associated with dissolved organic matter turnover in the sea. *Proc Natl Acad Sci USA* **107**: 16420–16427.
- Maki, H., Mori, A., Fujiyama, K., Kinoshita, S., and Yoshida, T. (1993) Cloning, sequence analysis and expression in *Escherichia coli* of a gene encoding an alginate lyase from *Pseudomonas* sp. OS-ALG-9. *J Gen Microbiol* **139**: 987–993.
- Mann, A.J., Hahnke, R.L., Huang, S., Werner, J., Xing, P., Barbeyron, T., et al. (2013) The genome of the alga-associated marine flavobacterium *Formosa agariphila* KMM 3901<sup>T</sup> reveals a broad potential for degradation of algal polysaccharides. *Appl Environ Microbiol* **79**: 6813–6822.
- Markowitz, V.M., Mavromatis, K., Ivanova, N.N., Chen, I., Min, A., Chu, K., and Kyripides, N.C. (2009) IMG ER: a system for microbial genome annotation expert review and curation. *Bioinformatics* **25**: 2271–2278.
- Markowitz, V.M., Chen, I.-M.A., Palaniappan, K., Chu, K., Szeto, E., Grechkin, Y., et al. (2012) IMG: the Integrated Microbial Genomes database and comparative analysis system. *Nucleic Acids Res* **40**: D115–D122.
- Markowitz, V.M., Chen, I.-M.A., Chu, K., Szeto, E., Palaniappan, K., Pillay, M., et al. (2014) IMG/M 4 version of the integrated metagenome comparative analysis system. *Nucleic Acids Res* **42**: D568–D573.
- Martens, E.C., Koropatkin, N.M., Smith, T.J., and Gordon, J.I. (2009) Complex glycan catabolism by the human gut microbiota: the *Bacteroidetes* Sus-like paradigm. *J Biol Chem* **284**: 24673–24677.
- Martin, M., Portetelle, D., Michel, G., and Vandenberg, M. (2014) Microorganisms living on macroalgae: diversity, interactions, and biotechnological applications. *Appl Microbiol Biotechnol* **98**: 2917–2935.
- Michel, G., and Czjzek, M. (2013) Polysaccharide-degrading enzymes from marine bacteria. In *Marine Enzymes for Biocatalysis*. Trincone, A. (ed.). Cambridge, UK: Woodhead Publishing, pp. 429–464.
- Miller, M., Pfeiffer, W., and Schwartz, T. (2010) Creating the CIPRES science gateway for inference of large phylogenetic trees. In *Proceedings of the Gateway Computing Environments Workshop (GCE)*. New York, USA: IEEE, pp. 1–8.
- Mizuno, C.M., Kimes, N.E., López-Pérez, M., Ausó, E., Rodríguez-Valera, F., and Ghai, R. (2013) A hybrid NRPS-PKS gene cluster related to the bleomycin family of antitumor antibiotics in *Alteromonas macleodii* strains. *PLoS ONE* **8**: e76021.
- Mopper, K., Schultz, C.A., Chevolut, L., Germain, C., Revuelta, R., and Dawson, R. (1992) Determination of sugars in unconcentrated seawater and other natural waters by liquid chromatography and pulsed amperometric detection. *Environ Sci Technol* **26**: 133–138.
- Nikolenko, S.I., Korobeynikov, A.I., and Alekseyev, M.A. (2013) BayesHammer: Bayesian clustering for error correction in single-cell sequencing. *BMC Genomics* **14** (Suppl. 1): S7.
- Pedler, B.E., Aluwihare, L.I., and Azam, F. (2014) Single bacterial strain capable of significant contribution to carbon cycling in the surface ocean. *Proc Natl Acad Sci USA* **111**: 7202–7207.
- Preiss, J., and Ashwell, G. (1962a) Alginic acid metabolism in bacteria. I. Enzymatic formation of unsaturated oligosaccharides and 4-deoxy-l-erythro-5-hexoseulose uronic acid. *J Biol Chem* **237**: 309–316.

- Preiss, J., and Ashwell, G. (1962b) Alginic acid metabolism in bacteria. II. The enzymatic reduction of 4-deoxy-L-erythro-5-hexoseulose uronic acid to 2-keto-3-deoxy-D-gluconic acid. *J Biol Chem* **237**: 317–321.
- Sarmiento, H., and Gasol, J.M. (2012) Use of phytoplankton-derived dissolved organic carbon by different types of bacterioplankton. *Environ Microbiol* **14**: 2348–2360.
- Sawabe, T., Ohtsuka, M., and Ezura, Y. (1997) Novel alginate lyases from marine bacterium *Alteromonas* sp. strain H-4. *Carbohydr Res* **304**: 69–76.
- Sawabe, T., Tanaka, R., Iqbal, M.M., Tajima, K., Ezura, Y., Ivanova, E.P., and Christen, R. (2000) Assignment of *Alteromonas elyakovii* KMM 162<sup>T</sup> and five strains isolated from spot-wounded fronds of *Laminaria japonica* to *Pseudoalteromonas elyakovii* comb. nov. and the extended description of the species. *Int J Syst Evol Microbiol* **50**: 265–271.
- Shipman, J.A., Berlenman, J.E., and Salyers, A.A. (2000) Characterization of four outer membrane proteins involved in binding starch to the cell surface of *Bacteroides thetaiotaomicron*. *J Bacteriol* **182**: 5365–5372.
- Staufenberger, T., Thiel, V., Wiese, J., and Imhoff, J.F. (2008) Phylogenetic analysis of bacteria associated with *Laminaria saccharina*. *FEMS Microbiol Ecol* **64**: 65–77.
- Tamura, K., Stecher, G., Peterson, D., Filipiński, A., and Kumar, S. (2013) MEGA6: Molecular Evolutionary Genetics Analysis version 6.0. *Mol Biol Evol* **30**: 2725–2729.
- Thomas, F., Barbeyron, T., Tonon, T., Génicot, S., Czjzek, M., and Michel, G. (2012) Characterization of the first alginolytic operons in a marine bacterium: from their emergence in marine *Flavobacteriia* to their independent transfers to marine *Proteobacteria* and human gut *Bacteroides*. *Environ Microbiol* **14**: 2379–2394.
- Thomas, F., Lundqvist, L.C.E., Jam, M., Jeudy, A., Barbeyron, T., Sandström, C., *et al.* (2013) Comparative characterization of two marine alginate lyases from *Zobellia galactanivorans* reveals distinct modes of action and exquisite adaptation to their natural substrate. *J Biol Chem* **288**: 23021–23037.
- Ueno, R. (2009) A method of in situ screening for bacteria capable of producing alginate-degrading enzyme from aquatic fields. *J Food Agric Environ* **7**: 731–735.
- Vargas, W.A., Weyman, P.D., Tong, Y., Smith, H.O., and Xu, Q. (2011) [NiFe] hydrogenase from *Alteromonas macleodii* with unusual stability in the presence of oxygen and high temperature. *Appl Environ Microbiol* **77**: 1990–1998.
- Verdugo, P., Alldredge, A.L., Azam, F., Kirchman, D.L., Passow, U., and Santschi, P.H. (2004) The oceanic gel phase: a bridge in the DOM–POM continuum. *Mar Chem* **92**: 67–85.
- Vincent, L., Thomas, B., Corinne, R., Harry, B., Pedro, M.C., and Bernard, H. (2010) A hierarchical classification of polysaccharide lyases for glycogenomics. *Biochem J* **432**: 437–444.
- Weiner, R.M., Taylor, L.E., Henrissat, B., Hauser, L., Land, M., Coutinho, P.M., *et al.* (2008) Complete genome sequence of the complex carbohydrate-degrading marine bacterium, *Saccharophagus degradans* strain 2–40 T. *PLoS Genet* **4**: e1000087.
- Wietz, M., Wemheuer, B., Simon, H., Giebel, H.-A., Seibt, M.A., Daniel, R., *et al.* (2015) Bacterial community dynamics during polysaccharide degradation at contrasting sites in the Southern and Atlantic Oceans. *Environ Microbiol* doi:10.1111/1462-2920.12842; in press.
- Yamasaki, M., Moriwaki, S., Miyake, O., Hashimoto, W., Murata, K., and Mikami, B. (2004) Structure and function of a hypothetical *Pseudomonas aeruginosa* protein PA1167 classified into family PL-7: a novel alginate lyase with a beta-sandwich fold. *J Biol Chem* **279**: 31863–31872.
- Zech, H., Thole, S., Schreiber, K., Kalthöfer, D., Voget, S., Brinkhoff, T., *et al.* (2009) Growth phase-dependent global protein and metabolite profiles of *Phaeobacter gallaeciensis* strain DSM 17395, a member of the marine *Roseobacter*-clade. *Proteomics* **9**: 3677–3697.
- Zimmerman, A.E., Martiny, A.C., and Allison, S.D. (2013) Microdiversity of extracellular enzyme genes among sequenced prokaryotic genomes. *ISME J* **7**: 1187–1199.

### Supporting information

Additional Supporting Information may be found in the online version of this article at the publisher's web-site:

**Fig. S1.** Maximum likelihood phylogeny of 12 *Alteromonas macleodii* strains based on a 2.3 Mb alignment of 2340 single-copy core genes, confirming the affiliation of strain 83-1 with the *A. macleodii* surface clade. Circles indicate nodes with >95% bootstrap support in 1000 replicates.

**Fig. S2.** Comparison of alginolytic systems (AS) in *Alteromonas macleodii* strain 83-1, other *Alteromonadales*, as well as the flavobacteria *Gramella forsetii* and *Formosa agariphila*. Gene designations in strain 83-1 correspond to IMG locus tags shown in Table S2. As indicated by the gray box and gray-shaded genes, *Pseudoalteromonas haloplanktis*, *Pseudoalteromonas marina* and *Shewanella waksmanii* all contain the 'AS core' consisting of alginate lyases PL6 and PL17 and adjacent cupin-domain, sugar permease, sugar kinase and isobutyrate dehydrogenase genes (Table S2).

**Fig. S3.** (A) Alginolytic system in genomic island specific to the *Alteromonas macleodii* deep clade. Alginolytic system containing a PL6 alginate lyase, three other CAZymes (1: putative 4-hydroxy-2-oxoglutarate aldolase; 2/3: putative ketodeoxygluconokinases), a putative diguanylate cyclase (DGC), a hypothetical protein (HP), as well as a GntR-family transcriptional regulator (GntR). (B) Growth of surface versus deep clade strains with alginate. The presence of only a single alginate lyase in comparison to five lyases in surface clade strains (Fig. 2) was reflected in substantially lower alginolytic capacities, as illustrated by an eightfold lower cell density of deep clade strain U7 in comparison to strain 83-1 after cultivation for 48 h with alginate as sole carbon source.

**Fig. S4.** Growth of *Alteromonas macleodii* strain 83-1 with an exudate of *Synechococcus* sp. RCC2527 (solid line) in comparison to sterile f/2 medium as negative control (dotted line).

**Table S1.** Origin and genome characteristics of *Alteromonas macleodii* strains analysed in the present study.

**Table S2.** Alginolytic system in *Alteromonas macleodii* strain 83-1 and homologous genes in *Zobellia galactanivorans* Dsij<sup>T</sup> (Thomas *et al.*, 2012).

**Table S3.** Polysaccharide utilization loci (PUL) in *Alteromonas macleodii* strain 83-1 associated with the degradation of xylan, laminarin and pullulan.

**Table S4.** Metagenomes in the Integrated Microbial Metagenome (IMG/M) database searched for alginate lyases from *Alteromonas macleodii*.

**Table S5.** Primer and probes used for RT-qPCR of alginate lyases and the *rpoB* reference gene.

## Appendix 3

### **Biphasic cellular adaptations and ecological implications of *Alteromonas macleodii* degrading a mixture of algal polysaccharides**

Koch H, Dürwald A, Schweder T, Noriega-Ortega B, Vidal-Melgosa S, Hehemann J-H, Dittmar T, Freese HM, Becher D, Simon M, Wietz M

*The ISME Journal* (2019), 13:92–103



# Biphasic cellular adaptations and ecological implications of *Alteromonas macleodii* degrading a mixture of algal polysaccharides

Hanna Koch<sup>1,8</sup> · Alexandra Dürwald<sup>2,3</sup> · Thomas Schweder<sup>1,2,3</sup> · Beatriz Noriega-Ortega<sup>4</sup> · Silvia Vidal-Melgosa<sup>5</sup> · Jan-Hendrik Hehemann<sup>5</sup> · Thorsten Dittmar<sup>4</sup> · Heike M. Freese<sup>6</sup> · Dörte Becher<sup>2,7</sup> · Meinhard Simon<sup>1</sup> · Matthias Wietz<sup>1</sup>

Received: 9 May 2018 / Revised: 10 July 2018 / Accepted: 19 July 2018 / Published online: 16 August 2018  
© International Society for Microbial Ecology 2018

## Abstract

Algal polysaccharides are an important bacterial nutrient source and central component of marine food webs. However, cellular and ecological aspects concerning the bacterial degradation of polysaccharide mixtures, as presumably abundant in natural habitats, are poorly understood. Here, we contextualize marine polysaccharide mixtures and their bacterial utilization in several ways using the model bacterium *Alteromonas macleodii* 83-1, which can degrade multiple algal polysaccharides and contributes to polysaccharide degradation in the oceans. Transcriptomic, proteomic and exometabolomic profiling revealed cellular adaptations of *A. macleodii* 83-1 when degrading a mix of laminarin, alginate and pectin. Strain 83-1 exhibited substrate prioritization driven by catabolite repression, with initial laminarin utilization followed by simultaneous alginate/pectin utilization. This biphasic phenotype coincided with pronounced shifts in gene expression, protein abundance and metabolite secretion, mainly involving CAZymes/polysaccharide utilization loci but also other functional traits. Distinct temporal changes in exometabolome composition, including the alginate/pectin-specific secretion of pyrroloquinoline quinone, suggest that substrate-dependent adaptations influence chemical interactions within the community. The ecological relevance of cellular adaptations was underlined by molecular evidence that common marine macroalgae, in particular *Saccharina* and *Fucus*, release mixtures of alginate and pectin-like rhamnogalacturonan. Moreover, CAZyme microdiversity and the genomic predisposition towards polysaccharide mixtures among *Alteromonas* spp. suggest polysaccharide-related traits as an ecophysiological factor, potentially relating to distinct ‘carbohydrate utilization types’ with different ecological strategies. Considering the substantial primary productivity of algae on global scales, these insights contribute to the understanding of bacteria–algae interactions and the remineralization of chemically diverse polysaccharide pools, a key step in marine carbon cycling.

**Electronic supplementary material** The online version of this article (<https://doi.org/10.1038/s41396-018-0252-4>) contains supplementary material, which is available to authorized users.

✉ Matthias Wietz  
matthias.wietz@uni-oldenburg.de

- <sup>1</sup> Institute for Chemistry and Biology of the Marine Environment, University of Oldenburg, Oldenburg, Germany
- <sup>2</sup> Institute of Marine Biotechnology, Greifswald, Germany
- <sup>3</sup> Institute of Pharmacy, University of Greifswald, Greifswald, Germany
- <sup>4</sup> ICBM-MPI Bridging Group for Marine Geochemistry, University of Oldenburg, Oldenburg, Germany

## Introduction

Algae constitute a major fraction of biomass in the oceans and are rich in chemically diverse polysaccharides [1, 2]. Algal polysaccharides are vital structural and storage components, whose composition can vary by species and season

- <sup>5</sup> MARUM-MPI Bridge Group for Marine Glycobiology, University of Bremen, Bremen, Germany
- <sup>6</sup> Leibniz Institute DSMZ–German Collection of Microorganisms and Cell Cultures, Braunschweig, Germany
- <sup>7</sup> Institute of Microbiology, University of Greifswald, Greifswald, Germany
- <sup>8</sup> Present address: Department of Microbiology, Radboud University Nijmegen, Nijmegen, The Netherlands

[3]. Polysaccharides released by exudation or decay [4] are an important carbon source for heterotrophic bacteria, which hydrolyze and metabolize polymeric carbohydrates via carbohydrate-active enzymes (CAZymes) [5]. CAZymes with or without carbohydrate-binding modules (CBM) include polysaccharide lyases (PL), glycoside hydrolases (GH), carbohydrate esterases (CE), glycosyl transferases (GT) plus a range of auxiliary enzymes [6], many having been biochemically characterized in detail [7].

Flavobacteria are pivotal polysaccharide degraders in marine systems [8, 9], but diverse CAZyme repertoires are also found in *Gammaproteobacteria* [10], *Verrucomicrobia* [11] and *Planctomycetes* [12]. CAZymes are often clustered in polysaccharide utilization loci (PUL) that allow the concerted degradation from polymer to monomer [13], with up to 50 PUL for a range of substrates in some bacteria [14]. Structure and expression of PUL have been described in several marine bacteria, but only considering one substrate at a time [15–19].

Despite the insights afforded by these studies, a conceptual investigation of bacterial polysaccharide degradation should consider that marine polysaccharide pools are chemically diverse and variable mixtures [20] and that competitive access to these resources is likely facilitated by dedicated cellular adaptations. In the environment, bacterial adaptive responses to varying polysaccharide pools are reflected by temporal changes in CAZyme abundance and diversity during the succession of phytoplankton blooms [21, 22] that produce diverse polysaccharides [23, 24]. We hypothesize that the structuring influence of marine polysaccharide mixtures on bacterial dynamics resembles processes among human gut microbiota, including sequential substrate utilization through catabolite repression and regulatory networks [25–27], with ecological implications on cellular and community levels [28, 29]. Indeed, a recent study in marine systems revealed that sequential degradation of alginate and laminarin in *Bacillus* coincides with temporal regulation of the respective PUL [30]. The ecological relevance of such adaptations is highlighted by substrate-controlled regulation of hydrolytic machineries for brown/green/red algae polysaccharides in *Zobellia galactanivorans* [31] and sophisticated laminarin uptake systems [32].

Here, we present three complementary perspectives on polysaccharide mixtures and their utilization by marine bacteria. First, transcriptomic, proteomic and exometabolomic analyses of *Alteromonas macleodii* strain 83-1 growing on laminarin, alginate and pectin illuminate bacterial adaptations to polysaccharide mixtures on cellular level. Second, molecular evidence that macroalgae release polysaccharide mixtures indicates that cellular adaptations are important in the environment. Third, microdiversity of hydrolytic capacities among *Alteromonas* spp.

suggests different ecological strategies related to polysaccharide utilization. *A. macleodii* strain 83-1 has been isolated from an alginate-enriched microcosm and represents an ecologically relevant model organism, as *A. macleodii* degrades the algal polysaccharides laminarin, alginate, pectin, xylan and pullulan [33], dominates polysaccharide degradation in some marine regions [34–36] and occurs globally [37]. These traits may also contribute to the close associations and metabolic interactions of *A. macleodii* with phototrophs, including diatoms [38], prymnesiophyceae [39] and cyanobacteria [40–42].

The polysaccharides investigated in the present study are chemically diverse and ecologically relevant. Laminarin, composed of  $\beta$ -(1–3)-glucose with  $\beta$ -(1–6) branches, is the major intracellular polysaccharide of macroalgae and diatoms [43] and occurs at up to 0.5 mg L<sup>-1</sup> in the North Sea [44]. Accordingly, laminarinases are found in coastal to pelagic bacteria worldwide [45, 46]. Alginate, comprising homo- or heteropolymeric blocks of  $\beta$ -D-mannuronate and  $\alpha$ -L-guluronate, can constitute >50% of benthic and pelagic brown macroalgae [47]. The environmental importance of alginate is reflected by the occurrence of alginate lyases in various bacterial taxa [48]. Pectin, largely composed of  $\alpha$ -(1–4)-galacturonate, is abundant in terrestrial plants, but the presence of complex pectinolytic operons in marine bacteria [49] and up to 0.3  $\mu$ M galacturonate during phytoplankton blooms [50] suggest that pectinous substrates are common in marine systems as well. Due to their gelling capacities, alginate and pectin may also occur in transparent exopolymer particles [50, 51]. These particulate forms of polysaccharide mixtures are attractive microhabitats for bacteria, including *A. macleodii* that colonizes gels derived from macroalgae [34] and diatoms [35].

Overall, our multifaceted perspective on polysaccharide mixture utilization contributes to understanding bacterial gene regulation under substrate regimes that occur during phytoplankton blooms or macroalgae decay. Considering the substantial primary productivity of micro- and macroalgae on global scales [52, 53] and the importance of polysaccharides in biogeochemical cycles [54], these insights are relevant for carbon fluxes and bacteria–algae interactions in the oceans.

## Materials and methods

### Cultivation and sampling regime

All cultivations were carried out in seawater minimal medium (SWM) [55] supplemented with sterile-filtered polysaccharide mix or glucose as sole carbon sources. Polysaccharides included laminarin from *Laminaria digitata* (L9634; Sigma-Aldrich, St. Louis, MO), alginate from

brown algae (A2158; Sigma-Aldrich) and apple pectin (76282; Fluka, Switzerland). For all experiments, *A. macleodii* 83-1 was precultured in SWM+0.1% glucose at 20 °C with shaking at 140 rpm for 24 h, washed twice with sterile SWM and diluted to an optical density (OD<sub>600</sub>) of 0.1 (corresponding to approximately  $8 \times 10^7$  colony-forming units per mL as determined by plating on marine agar). Main cultures were inoculated in 2 L Erlenmeyer flasks containing each 400 mL SWM (supplemented with 0.06% glucose or 0.02% of each polysaccharide to provide equal amounts of carbon source per treatment) with diluted preculture at 0.5% (v/v) in triplicate. Cultures were incubated at 20 °C with shaking at 140 rpm. Growth (OD<sub>600</sub>; diluted if >0.4) and substrate utilization (high-performance liquid chromatography (HPLC); see below) were determined in regular intervals. Samples for transcriptomics and proteomics were taken after 13 and 21 h. Samples for exometabolomics were taken after 13, 21 and 36 h (end of the incubation). In addition, utilization of single substrates was tested in 100 mL Erlenmeyer flasks containing each 20 mL SWM supplemented with glucose, pectin or laminarin (0.05%, respectively) or methanol (0.1 and 0.3%), which were incubated as described above.

### Carbohydrate quantification

At each OD measurement, subsamples of 3 mL were filtered through 0.22 µm mixed cellulose ester filters into combusted glass vials and stored at -20 °C until analysis. Polysaccharide mix samples were diluted 1:3, chemically hydrolyzed in 1.275 M H<sub>2</sub>SO<sub>4</sub> for 3 h at 100 °C in combusted and sealed glass ampoules and neutralized with 1.75 M calcium carbonate. Samples were diluted 1:2000 (glucose) or 1:100 (hydrolyzed polysaccharides) with MilliQ before quantification by pulsed amperometric detection [56, 57] using a CarboPac PA 1 column (Thermo Fisher, Waltham, MA). Eluents were 18 mM NaOH (for glucose/laminarin) or 135 mM NaOH (alginate/pectin). Calibration curves were generated for all substrates, with five data points for glucose and seven for polysaccharides ( $R^2 > 0.994$ ).

### Genome sequencing and analysis

The genome of *A. macleodii* 83-1 was sequenced using PacBio RSII technology (Supplementary Methods). CAZymes were identified using dbCan [58], only considering hits with  $e < 10^{-23}$  and >80% query coverage. Detailed annotation of selected genes was performed using Pfam, UniprotKB, InterPro, TCBD and MEROPS databases [59–61]. For the predicted GH16 (Alt831\_03772) a structure-based sequence alignment was done using the ENDscript server with default parameters [62]. ZgLamA

(PDBid 4BQ1) from *Zobellia galactanivorans* [63] was used to guide the alignment, followed by alignment with biochemically characterized GH16 β-1,3-glucanases (CAZY accession numbers AAC25554.2, AAC69707.1, ADN02324.1 and AAD35118.1) [6].

### Transcriptomics

At each sampling point, two 5 mL subsamples from each replicate were centrifuged for 3 min at 8000 × *g* at room temperature (RT). Cell pellets were immediately flash-frozen in liquid nitrogen and stored at -80 °C until RNA extraction. Total nucleic acids were extracted from one subsample per replicate using the MasterPure RNA purification kit (Epicentre, Madison, WI). DNA digestion using the Turbo DNA-free Kit (Thermo Fisher) was confirmed by 16S rRNA gene PCR. RNA was quantified using the Qubit RNA BR Assay Kit (Thermo Fisher) and stored at -80 °C before shipping on dry ice to the Earlham Institute (<http://www.earlham.ac.uk>; Norwich, UK) for sequencing. Library preparation, quality control, sequencing and bioinformatic analysis were done following standard procedures (Supplementary Methods). Differential expression analysis of quality-checked Illumina reads as mean of three biological replicates is reported in Table S1. Changes of ≥2 log<sub>2</sub> fold and an adjusted *P* value of <0.001 calculated using DESeq2 [64] were considered significant.

### Proteomics

At each sampling point, a 20 mL subsample from each replicate was centrifuged for 5 min at 6500 × *g* at RT. Extracellular proteins in the supernatant were processed with StrataClean resin (Agilent, Santa Clara, CA). Cell pellets were washed with phosphate-buffered saline, centrifuged again, immediately flash-frozen in liquid nitrogen and stored at -80 °C until analysis (Supplementary Methods). Briefly, extracted proteins were separated by sodium dodecyl sulfate–polyacrylamide gel electrophoresis, obtained peptide fractions digested using trypsin and separated via liquid chromatography. Protein abundances determined by tandem mass spectrometry (MS/MS) were semi-quantified using calculated normalized spectral abundance factor (%NSAF) values [65].

### Exometabolomics

At each sampling point, a 20 mL subsample from each replicate was centrifuged for 20 min at 3500 × *g* at 4 °C. In addition, three sterile media blanks per substrate regime were incubated and processed in the same manner. Exometabolites were purified from supernatants using solid-phase cartridges containing modified styrene-divinylbenzene polymer sorbents

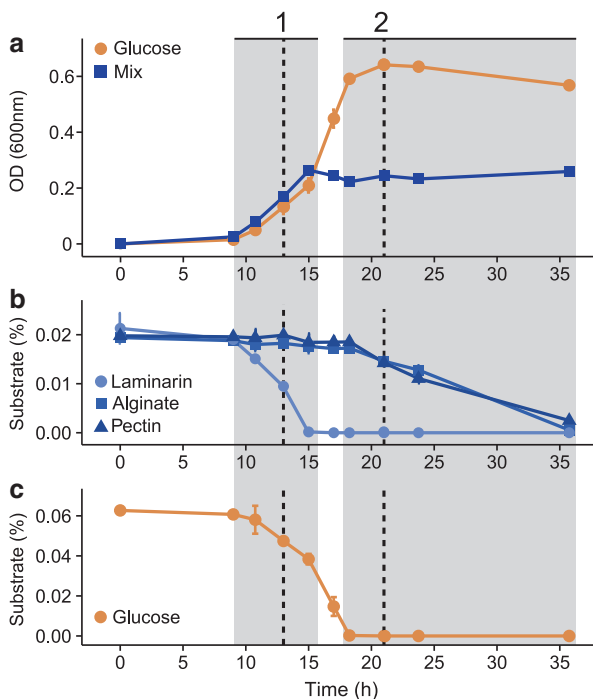


**Fig. 1** Growth and substrate utilization. Biphasic phenotype of *Alteromonas macleodii* 83-1 (**a**) and utilization of polysaccharide mix (**b**) and glucose (**c**) based on three biological replicates  $\pm$  standard deviation. Both phases (shaded) were characterized using transcriptomics, proteomics and exometabolomics at the time points indicated

[66] and analyzed by ultrahigh resolution mass spectrometry [67] (Supplementary Methods). Briefly, extracted exometabolites were analyzed on a 15 T Solarix Fourier transform ion cyclotron resonance mass spectrometer (FT-ICR-MS) coupled to electrospray ionization (Bruker, Germany) in negative mode. Two technical replicates per biological replicate were measured, only considering peaks detected in both runs. Furthermore, obtained spectra were calibrated and denoised using strict procedures to ensure that only bacterial metabolites were evaluated.

### Carbohydrate microarrays of macroalgal exudates

Fresh macroalgal specimens were collected from rocky tidal areas on the Isle of Helgoland (North Sea) in June 2017. Algae were placed inside dialysis devices with 3.5–5 kDa membranes (Float-A-Lyzer G2; SpectrumLabs, Rancho Domingo, CA). Devices were filled with 10 mL ambient seawater and placed in sterile-filtered seawater for 6 days in the dark. Each 5 mL of dialyzed samples was filtered through 0.2  $\mu$ m Acrodisc filters (Pall, Port Washington, NY) into combusted HPLC vials and stored at 4 °C. Samples were printed as microarrays in triplicate and probed with 28 carbohydrate-specific probes [68] (Supplementary Methods).

### Comparative genomics

*Alteromonas* draft genomes assembled from metagenomes were annotated using Prokka [69]. We furthermore included 33 complete genomes from *Alteromonas* isolates [70–73] deposited at the Integrated Microbial Genomes (IMG) database [74]. CAZymes were classified using the CAZY database [6] and dbCan [58], only considering hits with  $e < 10^{-23}$  and  $>80\%$  query coverage. Syntenic PUL were identified using MultiGeneBLAST [75], only considering hits with  $>50\%$  amino acid identity and  $>70\%$  query coverage. For taxonomic comparisons, amino acid sequences of 20 core genes identified using BPGA [76] were aligned using muscle [77]. A phylogenetic tree was constructed using FastTree with 1000 replications [78] implemented on CIPRES [79]. Homologs of *A. macleodii* 83-1 genes putatively involved in catabolite repression were searched against marine metatranscriptomes deposited at IMG, only considering hits with  $>90\%$  amino acid identity and  $>60\%$  query coverage.

### Results and discussion

*A. macleodii* 83-1 cultivated on a mixture of laminarin, alginate and pectin showed a biphasic phenotype relating to polysaccharide preferences (Fig. 1). Initial exponential growth during laminarin utilization until its complete consumption (phase M1) was followed by simultaneous utilization of alginate and pectin, but without net growth (phase M2).

Phases M1 and M2 coincided with major temporal shifts in gene expression, protein abundance and metabolite secretion (Figs 2–4; S1–2), involving 1–2 PUL per polysaccharide plus additional gene clusters (Table S3). These adaptations match those of pivotal polysaccharide degraders such as *Zobellia galactanivorans* [31], substantiating the relevance of *A. macleodii* for the remineralization of algal polysaccharides [33, 34]. The prioritization of laminarin over alginate was diametric to *Bacillus weihaiensis* [30], possibly indicative of different ecological niches. *B. weihaiensis* has been isolated from macroalgae and hence regularly encounters alginate from cell walls, whereas *A. macleodii* is rarely found on macrophytes and may primarily target storage laminarin released by exudation or decay.

The biphasic phenotype resembled sequential polysaccharide degradation through catabolite repression in human gut microbiota [25, 81, 82]. Related candidate genes in *A. macleodii* include CreA (Alt831\_00877), two putative cAMP receptors (02509/03405), a partial phosphoenolpyruvate phosphotransferase system (01559) and one hybrid two-component system (02433), but none with differential expression between growth phases. Although this indicates a different mode of catabolite repression than in other

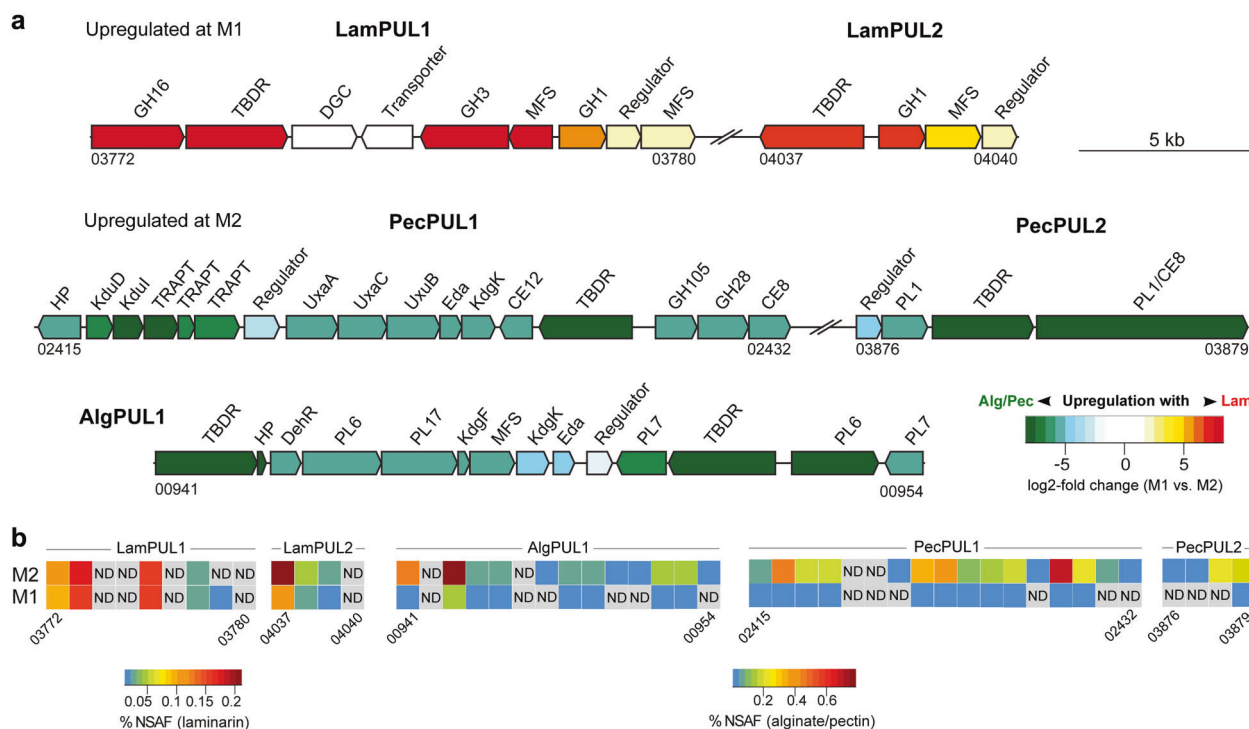


**Fig. 2** Temporal changes in the expression of PUL for laminarin, alginate and pectin degradation. **a** Upregulation of genes during laminarin (phase M1; yellow/red colors) and alginate/pectin degradation (phase M2; blue/green colors) based on three biological replicates per sample (average log<sub>2</sub>-fold changes  $\geq 2$ ;  $P_{\text{adj}} < 0.001$ ). **b** Corresponding abundances of proteins (%NSAF; note the different scales for laminarin vs. alginate/pectin-related proteins). PUL encode CAZymes (PL poly-saccharide lyase, GH glycoside hydrolase, CE carbohydrate esterase; numbers designating CAZyme families), transporters (TBDR TonB-dependent receptor, MFS major facilitator superfamily transporter,

TRAPT tripartite ATP-independent transporter) and monomer utilization genes (DehR 4-deoxy-L-erythro-5-hexoseulose uronate reductase, Eda 2-keto-3-deoxy-6-phosphogluconate aldolase, KdgF protein for uronate linearization, KdgK 2-keto-3-deoxy-D-gluconate kinase, KduD 2-deoxy-D-gluconate 3-dehydrogenase, KduI 4-deoxy-L-threo-5-hexosulose-uronate ketol-isomerase, UxaA altronate dehydratase, UxaC glucuronate isomerase, UxuB fructuronate reductase). Numbers below PUL correspond to IMG locus tags (prefix Alt831\_ omitted). DGC diguanylate cyclase, HP protein of unknown function, ND not detected, %NSAF normalized spectral abundance factor

marine bacteria [83–85], the detection of all candidate genes in metatranscriptomes from the Atlantic, Pacific and Indian Oceans indicated that substrate-controlled gene expression influences the ecophysiology of *Alteromonas*. This notion was supported by detection of all transcripts near the original isolation site of strain 83-1 (Table S4). Substrate specialization can provide a competitive advantage in natural communities, but also promotes niche partitioning and the stable co-existence of bacterial taxa [29, 86].

## Cellular adaptations during sequential degradation of polysaccharides

### Laminarin utilization (phase M1)

Exponential growth during laminarin utilization was accompanied by upregulation of 253 genes compared to phase M2. Genes encoding laminarin hydrolases, including GH16, GH1 and GH3 located in LamPUL1 and LamPUL2, were among the highest upregulated genes (Figs. 2, 3; Table S3). The colocalization of GH16- and GH3-encoding genes resembles PUL organization in marine *Bacteroidetes* [9, 16], whereas

that of GH16 and GH1 is reminiscent of *Bacillus* [30]. Homology with biochemically characterized endolytic  $\beta$ -(1–3)-glucanases (Fig. S3A) [63, 87] in combination with the spectrometric detection of several laminarin oligomers (Fig. S3B) suggested endolytic activity of the predicted GH16 (Alt831\_03772). The exclusive upregulation of LamPUL1 and LamPUL2 with laminarin but not glucose indicated fine-tuned sensing of polymeric vs. monomeric glucose, comparable to *Gramella forsetii* [16]. In this context, only laminarin induced the upregulation of gene cluster Alt831\_00338–47 (Table S3) encoding three xylose/glucose isomerases, two glucose oxidoreductases and a gluconate 2-dehydrogenase, suggesting that only polymeric glucose is partially channeled into oxidative degradation to generate additional reducing equivalents [88].

### Alginate/pectin utilization (phase M2)

The switch to alginate/pectin utilization was mirrored by induction of the respective degradation pathways (Figs. 2, 3), with 290 upregulated genes compared to M1 and an enrichment of alginate/pectin-related proteins (Fig. S2B).

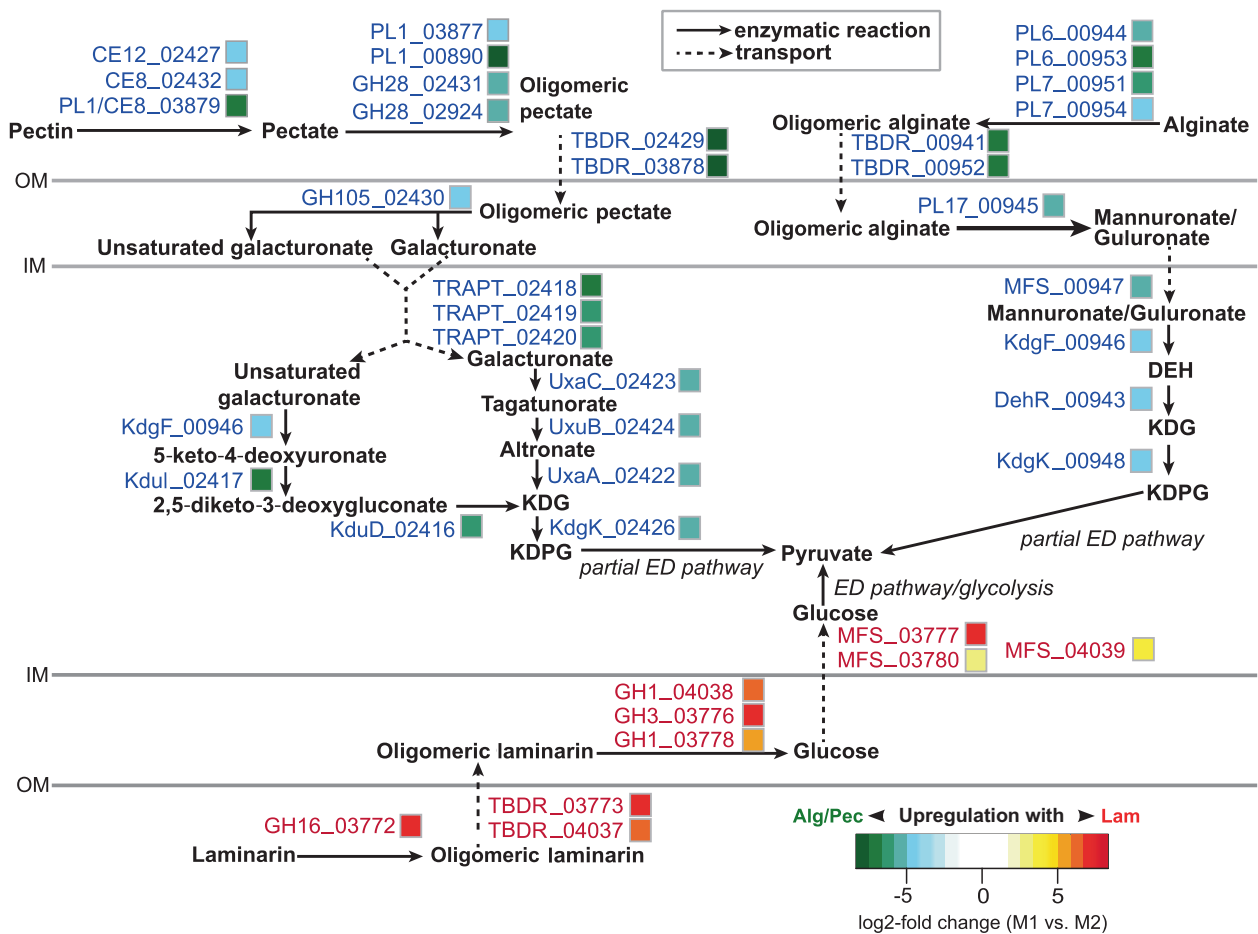


**Fig. 3** Gene expression of metabolic pathways related to laminarin, alginate and pectin. Upregulation during laminarin (phase M1; yellow/red colors) and alginate/pectin degradation (phase M2; blue/green colors) based on three biological replicates per sample (average log<sub>2</sub>-fold change ≥|2|; *P*<sub>adj</sub> < 0.001). Degradation via central intermediates (DEH 4-deoxy-L-erythro-5-hexoseulose uronate, KDG 2-keto-3-deoxy-D-gluconate, KDGP 2-keto-3-deoxy-6-phosphogluconate) is related to CAZymes (PL polysaccharide lyase, GH glycoside hydrolase, CE carbohydrate esterase; with numbers designating CAzyme families), transporters (TBDR TonB-dependent receptor, MFS major

facilitator superfamily transporter, TRAPT tripartite ATP-independent transporter) and monomer utilization genes (DehR DEH reductase, KdgF protein for uronate linearization, KdgK KDG kinase, KduD 2-deoxy-D-gluconate 3-dehydrogenase, KduI 4-deoxy-L-threo-5-hexosulose-uronate ketol-isomerase, UxaA altronate dehydratase, UxaC glucuronate isomerase, UxuB fructuronate reductase). Enzyme names and IMG locus tags of encoding genes (separated by underscore; prefix Alt831\_ omitted) are shown next to each step. ED Entner–Doudoroff pathway, IM inner membrane, OM outer membrane

Pectin degradation was related to three genomic loci. PecPUL1 only encodes enzymes for processing pectin intermediates, whereas the three PL1 enzymes for initial hydrolysis are encoded separately: two in a second PUL (PecPUL2) and one distantly without adjacent CAZymes (Alt831\_00890). Although our sampling procedure cannot exclude some carry-over between intra- and extracellular protein fractions, PL1\_00890 was enriched 25-fold in the culture supernatant and hence likely secreted (Table S5). Similarities to the extracellular AlyA1 of *Z. galactanivorans*, which is likewise not inside a PUL and essential for attacking alginate gels and cell walls [89], indicate comparable roles as extracellular actors towards complex matrices of gelling polysaccharides. However, the effectivity of PL1\_00890 may be limited by missing a CBM, as

present in the otherwise homologous PelB pectate lyase of *Pseudoalteromonas haloplanktis* [49]. Pectin degradation is most likely regulated comparably via a LacI type repressor encoded in PecPUL1 and associated palindromic binding motif TGCCACCGGTGGCA upstream of genes encoding KduD, UxaA and GH28 (PecPUL1), a TonB-dependent receptor (PecPUL2) and a distant GH28 (Alt831\_02924), respectively. Additional binding motifs with one mismatch were identified upstream of genes encoding the separate PL1, the GH105 in PecPUL1 and the transcriptional regulator in PecPUL2, respectively. An ecological relevance of pectin degradation has been supported by micromolar galacturonate concentrations during phytoplankton blooms, which positively correlated with abundances of *Gamma-proteobacteria* [50].

Alginate degradation was related to AlgPUL1, which has been characterized in detail before [33]. The enzyme KdgF (Alt831\_00946) essential for both pectin and alginate degradation [90] is encoded in AlgPUL1 and hence potentially shared by both pathways. In contrast, both pathways possess a dedicated KdgK enzyme comparable to *Saccharophagus degradans* [91]. Despite the significant upregulation in phase M2, proteomic detection of several AlgPUL1 enzymes in M1 (e.g., PL6 but not PL7 alginate lyases) indicated that induction of alginolytic systems started earlier, possibly yielding the accumulation of oligomers before their consumption in M2.

Missing net growth in phase M2 was surprising, as *A. macleodii* 83-1 grows exponentially on alginate/pectin when inoculated freshly (Fig. S4). Bacteriostasis from accumulation of KDPG, the key intermediate from both pathways, was hence unlikely [92]. We can also disregard growth-repressive pH changes during laminarin utilization, as laminarin supports growth at even higher concentrations (Fig. S4). One possible scenario is an initiation of maintenance metabolism [93] reflected by the upregulation of isocitrate lyase, a central enzyme in the glyoxylate shunt and mediator of slow growth [94]. Potential fermentative processes cannot be assessed, as putative inhibitory fermentation products (e.g., acetate) were outside the analytical window of FT-ICR-MS. The missing upregulation of flagellar synthesis (Alt831\_01034–58/01083–01107), chemotaxis (00310–00315) and oxidative stress response (e.g., 00915/01232/02447) compared to glucose-grown stationary cells (Table S1) showed that M2 was no stationary phase and that processes related to exploitation of new niches were less expressed. This persistence-like but metabolically active phenotype [95] may provide adaptation to changing nutrient regimes and benefit the survivability of *Alteromonas* in the oceans.

## Ecological implications

### Exometabolome diversity

Laminarin and alginate/pectin utilization coincided with major changes in exometabolome composition, with 138 and 143 molecular masses unique to phases M1 vs. M2, respectively (Fig. 4a) and a decreasing relative fraction of phosphorous and oxygen among exometabolites (Table S2). The production of specific exometabolites with different polysaccharides likely influences chemical interactions with other bacteria [96]. A particular example is pyrroloquinoline quinone (PQQ), whose molecular mass (329.00522 Da) was exclusively detected at the end of phase M2 coincident with induction of the PQQ biosynthetic operon (Tables S2–S3). Identification of PQQ was corroborated by MS/MS fragmentation, yielding three fragment ions (285.016030, 241.026120 and 197.036170 Da) corresponding to loss of

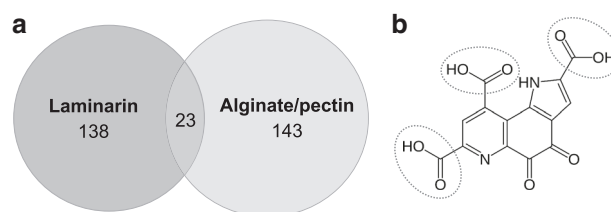


**Fig. 4** Exometabolome analyses by FT-ICR-MS. **a** Number of molecular masses exclusively detected during laminarin and alginate/pectin utilization. **b** Structure of pyrroloquinoline quinone, with carboxylic groups with  $\text{CO}_2$  losses in MS/MS fragmentation encircled

	FCP (BAM1)	RGI (INRA-RU1)	AGP (JIM13)	GlcA in AGP (LM2)	Alginate (BAM7)
<i>Laminaria digitata</i>	0	7	7	0	6
<i>Saccharina latissima</i>	88	0	0	100	18
<i>Fucus serratus</i>	7	0	9	0	20
<i>Porphyra</i> sp.	0	0	7	0	0

**Fig. 5** Exudation of polysaccharide mixtures by macroalgae. Mean spot signal intensities in carbohydrate microarrays of four macroalgal exudates, only showing those of the 28 polysaccharide-specific probes with a positive signal (name indicated in parentheses; see Supplementary Methods). FCP fucose-containing polysaccharide, RGI rhamnogalacturonan I, AGP arabinogalactan-protein glycan, GlcA glucuronic acid

one, two and three  $\text{CO}_2$  (Fig. 4b). PQQ likely served as cofactor for alcohol dehydrogenases (ADHs) to convert methanol released during pectin deesterification, mirrored by upregulation of an adjacent PQQ-dependent ADH and other ADHs (Table S3). However, the further metabolic fate of methanol remains unclear. One possible route is oxidation to formate, but methylenetetrahydrofolate dehydrogenase (Alt831\_02739) was not upregulated in M2. Missing growth on methanol as sole energy source (data not shown) and the absence of relevant genes also question potential assimilation via the serine cycle, although a recent study has suggested methylotrophy for a closely related *A. macleodii* [41]. Nonetheless, PQQ-/methanol-related traits may play a role in microbial interactions [97], as methanol is secreted by marine phytoplankton [98] and one mediator of *A. macleodii* interactions with cyanobacteria [41]. The fact that *Alteromonas* genomes vary in their content of PQQ-dependent ADHs (Table S6) indicates different ecological strategies related to alcohol metabolism.

### Cellular adaptations in light of polysaccharide release by macroalgae

Using carbohydrate microarrays, we demonstrated release of polysaccharide mixtures by natural brown and red macroalgae, suggesting that cellular adaptations as found in *A. macleodii* 83-1 are environmentally relevant. Four of six

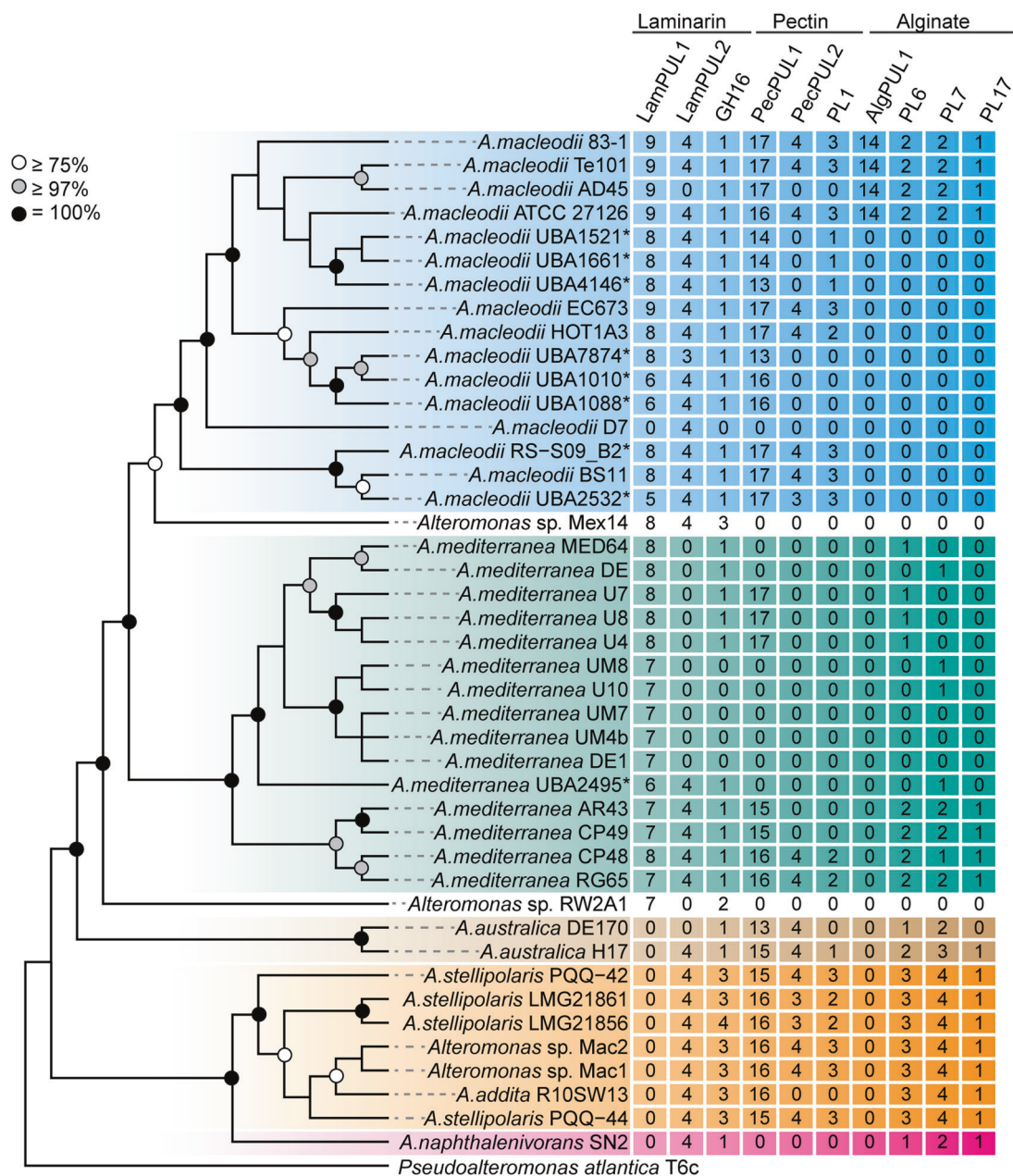


**Fig. 6** Distribution and abundance of CAZymes among *Alteromonas* in relation to phylogeny. Numbers correspond to gene count in synthetic PUL compared to *A. macleodii* 83-1. In addition, total numbers of CAZymes for laminarin (GH16), pectin (PL1) and alginate degradation (PL6/7/17) are listed separately, as some are encoded outside of

PUL. Tree bases on alignment of 20 core proteins with *Pseudoalteromonas atlantica* T6c as outgroup (branch support values indicated by circles). Genomes shaded blue: *A. macleodii*; green: *A. mediterranea*; brown/yellow/pink/white: other *Alteromonas*. Asterisks indicate metagenome-assembled genomes

algal species, in particular the brown algae *Saccharina latissima* and *Fucus serratus*, released varying levels of fucoidan, arabinogalactan, rhamnogalacturonan and alginate (Fig. 5), highlighting the ecological relevance of our cultivation experiment. *S. latissima*, *F. serratus* and related species are dominant macroalgae in temperate rocky habitats, with a global standing stock of 200 million tons [99] of which >50% can be polysaccharides [100]. Hence, polysaccharides released by these algae may contribute

sizably to secondary production in coastal zones worldwide. The detection of rhamnogalacturonan supports the notion that pectinous compounds are present in marine algae and that cellular adaptations thereto play an ecological role. The detection of released alginate is important in view of polysaccharide microhabitats, as dissolved alginate self-assembles into microgels that are rapidly colonized by marine bacteria, including *A. macleodii* [34]. Whereas commonly applied hydrolysis techniques only allow

indirect conclusions on the native polymers, our method provides direct insights into the composition of macroalgae-derived polysaccharide mixtures.

### Potential for polysaccharide mixture utilization among *Alteromonas* spp.

To broadly assess the predisposition towards polysaccharide mixtures, we compared CAZyme content of *A. macleodii* 83-1 with 33 closed and 9 metagenome-assembled *Alteromonas* genomes (Table S7) from diverse marine regions [101, 102]. Presence of the complete PUL repertoire in *A. macleodii* strains ATCC27126<sup>T</sup>, Te101 and AD45 isolated from distant locations (Fig. 6) indicated that polysaccharide mixture utilization is relevant in different habitats. Missing PUL expression in Te101 during co-culture with nitrogen-fixing *Trichodesmium* cyanobacteria [70] underlined that PUL are substrate regulated, and furthermore showed that polysaccharides are rarely secreted by healthy *Trichodesmium*. However, increasing TEP production when *Trichodesmium* blooms demise [103] indicates that polysaccharide-related traits may become important at other stages of their interaction.

The wide occurrence of laminarin-related genes highlights the importance of laminarin as bacterial substrate [45]. Homologs of the GH16 were found in >85% of *Alteromonas* genomes, but not all possessing both complete laminarin PUL (Fig. 6). Due to the broad substrate ranges of CAZyme families such as GH16, some homologs may however target other polysaccharides. For instance, *A. stellipolaris*, *A. addita* and strains Mac1/Mac2 encode a second GH16 with 99% sequence similarity to a  $\beta$ -agarase [104], probably opening further ‘substrate niches’ during degradation of algal biomass.

The occurrence of pectin-related CAZymes in *Alteromonas* and *Pseudoalteromonas* [49] supports the notion that pectinous substrates are indeed ecologically relevant in marine systems. Over 80% of *Alteromonas* genomes possess homologs of PecPUL1 enabling the metabolism of pectin oligomers, but PL1 enzymes needed for initial polymer hydrolysis are often absent. Consequently, strains like *A. mediterranea* U7 are unable to grow on polymeric pectin (Fig. S5) but may scavenge pectin oligomers from PL1-encoding strains, being reminiscent of interactions between pioneers, harvesters and scavengers [105]. A similar scenario may apply to alginate degradation. Whereas only four strains harbor the complete AlgPUL1, other *Alteromonas* spp. possess alginate lyases as well, which are clustered within two PUL (*A. stellipolaris*), in one PUL plus additional scattered lyases (*A. australica*) or completely dispersed (*A. mediterranea*). These genomic differences may influence alginolytic potentials and contribute to ecological speciation, as seen in alginolytic vibrios [105]. The observed microdiversity in enzymatic features, sometimes

in strains from distant locations and habitats (e.g., subclade BS11, RS-S09 and UBA2532), indicates different ‘carbohydrate utilization ecotypes’ among *Alteromonas* adapted to distinct substrate niches [106, 107].

## Conclusions

Although being a simplified approximation to processes in natural habitats, the demonstrated bacterial adaptations to polysaccharide mixtures provide a window into organismal and functional dynamics associated with successive ‘polysaccharide niches’ during phytoplankton blooms [21, 22] where bacteria with varying hydrolytic potentials and substrate preferences compete. Together with the shown release of polysaccharide mixtures by macroalgae and the genomic predisposition of *Alteromonas* towards such mixtures, we provide comprehensive cellular and environmental perspectives on the recycling of algal biomass, a key step in marine carbon cycling. Considering the substantial abundance and primary productivity of micro- and macroalgae, these insights are relevant for carbon fluxes and bacteria–algae interactions in the oceans.

## Data accessibility

The closed and annotated genome of *A. macleodii* 83-1 is publicly available under IMG accession #2716884210. Raw transcriptomic reads from all biological replicates have been deposited at the Gene Expression Omnibus under GSE107306. Proteomics data from all biological replicates have been deposited to the ProteomeXchange Consortium via PRIDE [80] under PXD008280. The complete FT-ICR-MS data are shown in Table S2.

**Acknowledgements** We gratefully acknowledge technical assistance by Rolf Weinert (HPLC), Katrin Klaproth, Maren Zark, Helena Osterholz and Jutta Niggemann (FT-ICR-MS), Sebastian Grund, Frank Unfried and Stephanie Markert (proteomics), and Cathrin Spröer (genome sequencing). The Biological Institute Helgoland of the Alfred Wegener Institute, in particular Antje Wichels, Eva-Maria Brodte, Gunnar Gerdt and Uwe Nettelmann, are thanked for excellent scientific support. RNA sequencing was expertly performed by the Earlham Institute (Norwich, UK). This work was funded by the German Research Foundation (DFG) through grants WI3888/1-2 (to MW), SCHW595/9-1 (to TS), the Emmy Noether program (to J-HH) and the Collaborative Research Centre TRR51. HK was supported by Volkswagen Foundation under VW-Vorab grant ‘Marine Biodiversity across Scales’ (MarBAS; ZN3112).

## Compliance with ethical standards

**Conflict of interest** The authors declare that they have no conflict of interest.

## References

- Kraan S. Algal polysaccharides, novel applications and outlook. In: Chang C-F, editor. Carbohydrates - comprehensive studies on glycobiology and glycotecnology. Rijeka: InTech; 2012. p. 489–532. .
- Rossi F, De Philippis R. Exocellular polysaccharides in microalgae and cyanobacteria: chemical features, role and enzymes and genes involved in their biosynthesis. The physiology of microalgae. Eds. Borowitzka MA, Beardall J, Raven JA. Cham: Springer International Publishing; 2016. p. 565–90.
- Fletcher HR, Biller P, Ross AB, Adams JMM. The seasonal variation of fucoxanthin within three species of brown macroalgae. *Algal Res.* 2017;22:79–86.
- Thornton DCO. Dissolved organic matter (DOM) release by phytoplankton in the contemporary and future ocean. *Eur J Phycol.* 2014;49:20–46.
- Hehemann J-H, Boraston AB, Czjzek M. A sweet new wave: structures and mechanisms of enzymes that digest polysaccharides from marine algae. *Curr Opin Struct Biol.* 2014;28:77–86.
- Lombard V, Golaconda Ramulu H, Drula E, Coutinho PM, Henrissat B. The carbohydrate-active enzymes database (CAZy) in 2013. *Nucleic Acids Res.* 2014;42:D490–5.
- Michel G, Czjzek M. Polysaccharide-degrading enzymes from marine bacteria. In: Trincone A, editor. Marine Enzymes for Biocatalysis. Cambridge: Woodhead Publishing; 2013. p. 429–64.
- Fernández-Gómez B, Richter M, Schüller M, Pinhassi J, Acinas SG, González JM, et al. Ecology of marine *Bacteroidetes*: a comparative genomics approach. *ISME J.* 2013;7:1026–37.
- Bennke CM, Krüger K, Kappellmann L, Huang S, Gobet A, Schüller M, et al. Polysaccharide utilisation loci of *Bacteroidetes* from two contrasting open ocean sites in the North Atlantic. *Environ Microbiol.* 2016;18:4456–70.
- Weiner RM, Taylor LE, Henrissat B, Hauser L, Land M, Coutinho PM, et al. Complete genome sequence of the complex carbohydrate-degrading marine bacterium, *Saccharophagus degradans* strain 2-40T. *PLoS Genet.* 2008;4:e1000087.
- Martinez-Garcia M, Brazel DM, Swan BK, Arnosti C, Chain PSG, Reitenga KG, et al. Capturing single cell genomes of active polysaccharide degraders: an unexpected contribution of Verrucomicrobia. *PLoS ONE.* 2012;7:e35314.
- Lage OM, Bondoso J. Planctomycetes and macroalgae, a striking association. *Front Microbiol.* 2014;5:267.
- Grondin JM, Tamura K, Déjean G, Abbott DW, Brumer H. Polysaccharide utilization loci: fueling microbial communities. *J Bacteriol.* 2017;199:e00860–16.
- Barbeyron T, Thomas F, Barbe V, Teeling H, Schenowitz C, Dossat C, et al. Habitat and taxon as driving forces of carbohydrate catabolism in marine heterotrophic bacteria: example of the model algae-associated bacterium *Zobellia galactanivorans* Dsij<sup>T</sup>. *Environ Microbiol.* 2016;18:4610–27.
- Ficko-Blean E, Préchoux A, Thomas F, Rochat T, Larocque R, Zhu Y, et al. Carrageenan catabolism is encoded by a complex regulon in marine heterotrophic bacteria. *Nat Commun.* 2017; 8:1685.
- Kabisch A, Otto A, König S, Becher D, Albrecht D, Schüller M, et al. Functional characterization of polysaccharide utilization loci in the marine *Bacteroidetes* 'Gramella forsetii' KT0803. *ISME J.* 2014;8:1492–502.
- Tang K, Lin Y, Han Y, Jiao N. Characterization of potential polysaccharide utilization systems in the marine *Bacteroidetes* *Gramella flava* JLT2011 using a multi-omics approach. *Front Microbiol.* 2017;8:220.
- Thomas F, Barbeyron T, Tonon T, Génicot S, Czjzek M, Michel G. Characterization of the first alginolytic operons in a marine bacterium: from their emergence in marine *Flavobacteriia* to their independent transfers to marine *Proteobacteria* and human gut *Bacteroides*. *Environ Microbiol.* 2012;14:2379–94.
- Xing P, Hahnke RL, Unfried F, Markert S, Huang S, Barbeyron T, et al. Niches of two polysaccharide-degrading *Polaribacter* isolates from the North Sea during a spring diatom bloom. *ISME J.* 2015;9:1410–22.
- Verdugo P, Alldredge AL, Azam F, Kirchman DL, Passow U, Santschi PH. The oceanic gel phase: a bridge in the DOM-POM continuum. *Mar Chem.* 2004;92:67–85.
- Teeling H, Fuchs BM, Becher D, Klockow C, Gardebrecht A, Bennke CM, et al. Substrate-controlled succession of marine bacterioplankton populations induced by a phytoplankton bloom. *Science.* 2012;336:608–11.
- Teeling H, Fuchs BM, Bennke CM, Krüger K, Chafee M, Kappellmann L, et al. Recurring patterns in bacterioplankton dynamics during coastal spring algae blooms. *elife.* 2016;5: e11888.
- Nelson CE, Goldberg SJ, Wegley Kelly L, Haas AF, Smith JE, Rohwer F, et al. Coral and macroalgal exudates vary in neutral sugar composition and differentially enrich reef bacterioplankton lineages. *ISME J.* 2013;7:962–79.
- Villacorte LO, Ekowati Y, Neu TR, Kleijn JM, Winters H, Amy G, et al. Characterisation of algal organic matter produced by bloom-forming marine and freshwater algae. *Water Res.* 2015;73:216–30.
- Rogers TE, Pudlo NA, Koropatkin NM, Bell JSK, Moya Balasch M, Jasker K, et al. Dynamic responses of *Bacteroides thetaiotaomicron* during growth on glycan mixtures. *Mol Microbiol.* 2013;88:876–90.
- Schwalm ND, Townsend GE, Groisman EA. Prioritization of polysaccharide utilization and control of regulator activation in *Bacteroides thetaiotaomicron*. *Mol Microbiol.* 2017;104:32–45.
- Tuncil YE, Xiao Y, Porter NT, Reuhs BL, Martens EC, Hamaker BR. Reciprocal prioritization to dietary glycans by gut bacteria in a competitive environment promotes stable coexistence. *mBio.* 2017;8:e01068–17.
- Cuskin F, Lowe EC, Temple MJ, Zhu Y, Cameron EA, Pudlo NA, et al. Human gut *Bacteroidetes* can utilize yeast mannan through a selfish mechanism. *Nature.* 2015;517:165–9.
- Goyal A, Dubinkina V, Maslov S. Microbial community structure predicted by the stable marriage problem. Preprint at <http://arxiv.org/abs/1712.06042> (2017). Accessed 12 Apr 2018).
- Zhu Y, Chen P, Bao Y, Men Y, Zeng Y, Yang J, et al. Complete genome sequence and transcriptomic analysis of a novel marine strain *Bacillus weihaiensis* reveals the mechanism of brown algae degradation. *Sci Rep.* 2016;6:38248.
- Thomas F, Bordron P, Eveillard D, Michel G. Gene expression analysis of *Zobellia galactanivorans* during the degradation of algal polysaccharides reveals both substrate-specific and shared transcriptome-wide responses. *Front Microbiol.* 2017;8:1808.
- Reintjes G, Arnosti C, Fuchs BM, Amann R. An alternative polysaccharide uptake mechanism of marine bacteria. *ISME J.* 2017;11:1640–50.
- Neumann AM, Balmonte JP, Berger M, Giebel H-A, Arnosti C, Brinkhoff T, et al. Different utilization of alginate and other algal polysaccharides by marine *Alteromonas macleodii* ecotypes. *Environ Microbiol.* 2015;17:3857–68.
- Mitulla M, Dinasquet J, Guillemette R, Simon M, Azam F, Wietz M. Response of bacterial communities from California coastal waters to alginate particles and an alginolytic *Alteromonas macleodii* strain. *Environ Microbiol.* 2016;18:4369–77.
- Taylor JD, Cunliffe M. Coastal bacterioplankton community response to diatom-derived polysaccharide microgels. *Environ Microbiol Rep.* 2017;9:151–7.

36. Wietz M, Wemheuer B, Simon H, Giebel H-A, Seibt MA, Daniel R, et al. Bacterial community dynamics during polysaccharide degradation at contrasting sites in the Southern and Atlantic Oceans. *Environ Microbiol.* 2015;17:3822–31.
37. Ivars-Martínez E, D'Auria G, Rodríguez-Valera F, Sánchez-Porro C, Ventosa A, Joint I, et al. Biogeography of the ubiquitous marine bacterium *Alteromonas macleodii* determined by multilocus sequence analysis. *Mol Ecol.* 2008;17:4092–106.
38. Diner RE, Schwenck SM, McCrow JP, Zheng H, Allen AE. Genetic manipulation of competition for nitrate between heterotrophic bacteria and diatoms. *Front Microbiol.* 2016;7:880.
39. Wu S, Zhou J, Xin Y, Xue S. Nutritional stress effects under different nitrogen sources on the genes in microalga *Isochrysis zhangjiangensis* and the assistance of *Alteromonas macleodii* in releasing the stress of amino acid deficiency. *J Phycol.* 2015;51:885–95.
40. Aharonovich D, Sher D. Transcriptional response of *Prochlorococcus* to co-culture with a marine *Alteromonas*: differences between strains and the involvement of putative infochemicals. *ISME J.* 2016;10:2892–906.
41. Lee MD, Walworth NG, McParland EL, Fu F-X, Mincer TJ, Levine NM, et al. The *Trichodesmium* consortium: conserved heterotrophic co-occurrence and genomic signatures of potential interactions. *ISME J.* 2017;11:1813–24.
42. Morris JJ, Johnson ZI, Szul MJ, Keller M, Zinser ER. Dependence of the cyanobacterium *Prochlorococcus* on hydrogen peroxide scavenging microbes for growth at the ocean's surface. *PLoS ONE.* 2011;6:e16805.
43. Beattie A, Hirst EL, Percival E. Studies on the metabolism of the *Chrysophyceae*. Comparative structural investigations on leucosin (chrysolaminarin) separated from diatoms and laminarin from the brown algae. *Biochem J.* 1961;79:531–7.
44. Becker S, Scheffel A, Polz MF, Hehemann J-H. Accurate quantification of laminarin in marine organic matter with enzymes from marine microbes. *Appl Environ Microbiol.* 2017;83:e03389–16.
45. Arnosti C, Steen AD, Ziervogel K, Ghobrial S, Jeffrey WH. Latitudinal gradients in degradation of marine dissolved organic carbon. *PLoS ONE.* 2011;6:e28900.
46. Planas A. Bacterial 1,3-1,4- $\beta$ -glucanases: structure, function and protein engineering. *Biochim Biophys Acta.* 2000;1543:361–82.
47. Davis TA, Volesky B, Mucci A. A review of the biochemistry of heavy metal biosorption by brown algae. *Water Res.* 2003;37:4311–30.
48. Ertesvåg H. Alginate-modifying enzymes: biological roles and biotechnological uses. *Front Microbiol.* 2015;6:523.
49. Hehemann J-H, Truong L Van, Unfried F, Welsch N, Kabisch J, Heiden SE, et al. Aquatic adaptation of a laterally acquired pectin degradation pathway in marine gammaproteobacteria. *Environ Microbiol.* 2017;19:2320–33.
50. Sperling M, Piontek J, Engel A, Wiltshire KH, Niggemann J, Gerds G, et al. Combined carbohydrates support rich communities of particle-associated marine bacterioplankton. *Front Microbiol.* 2017;08:65.
51. Passow U. Transparent exopolymer particles (TEP) in aquatic environments. *Prog Oceanogr.* 2002;55:287–333.
52. Duarte CM, Cebrián J. The fate of marine autotrophic production. *Limnol Oceanogr.* 1996;41:1758–66.
53. Steneck RS, Graham MH, Bourque BJ, Corbett D, Erlandson JM, Estes JA, et al. Kelp forest ecosystems: biodiversity, stability, resilience and future. *Environ Conserv.* 2003;29:436–59.
54. Benner R, Pakulski J, McCarthy M, Hedges J, Hatcher P. Bulk chemical characteristics of dissolved organic matter in the ocean. *Science.* 1992;255:1561–4.
55. Zech H, Thole S, Schreiber K, Kalhöfer D, Voget S, Brinkhoff T, et al. Growth phase-dependent global protein and metabolite profiles of *Phaeobacter gallaeciensis* strain DSM 17395, a member of the marine *Roseobacter*-clade. *Proteomics.* 2009;9:3677–97.
56. Hahnke S, Brock NL, Zell C, Simon M, Dickschat JS, Brinkhoff T. Physiological diversity of *Roseobacter* clade bacteria co-occurring during a phytoplankton bloom in the North Sea. *Syst Appl Microbiol.* 2013;36:39–48.
57. Mopper K, Schultz CA, Chevolut L, Germain C, Revuelta R, Dawson R. Determination of sugars in unconcentrated seawater and other natural waters by liquid chromatography and pulsed amperometric detection. *Environ Sci Technol.* 1992;26:133–8.
58. Yin Y, Mao X, Yang J, Chen X, Mao F, Xu Y. dbCAN: a web resource for automated carbohydrate-active enzyme annotation. *Nucleic Acids Res.* 2012;40:W445–51.
59. Finn RD, Clements J, Arndt W, Miller BL, Wheeler TJ, Schreiber F, et al. HMMER web server: 2015 update. *Nucleic Acids Res.* 2015;43:W30–8.
60. Saier MH, Reddy VS, Tsu BV, Ahmed MS, Li C, Moreno-Hagelsieb G. The Transporter Classification Database (TCDB): recent advances. *Nucleic Acids Res.* 2016;44:D372–9.
61. Finn R, Attwood TK, Babbitt PC, Bateman A, Bork P, Bridge AJ, et al. InterPro in 2017 — beyond protein family and domain annotations. *Nucleic Acids Res.* 2017;45:D190–9.
62. Robert X, Gouet P. Deciphering key features in protein structures with the new ENDscript server. *Nucleic Acids Res.* 2014;42:W320–4.
63. Labourel A, Jam M, Jeudy A, Hehemann J-H, Czjzek M, Michel G. The  $\beta$ -glucanase ZgLamA from *Zobellia galactanivorans* evolved a bent active site adapted for efficient degradation of algal laminarin. *J Biol Chem.* 2014;289:2027–42.
64. Love MI, Huber W, Anders S. Moderated estimation of fold change and dispersion for RNA-seq data with DESeq2. *Genome Biol.* 2014;15:550.
65. Zybaïlov B, Mosley AL, Sardi ME, Coleman MK, Florens L, Washburn MP. Statistical analysis of membrane proteome expression changes in *Saccharomyces cerevisiae*. *J Proteome Res.* 2006;5:2339–47.
66. Dittmar T, Koch B, Hertkorn N, Kattner G. A simple and efficient method for the solid-phase extraction of dissolved organic matter (SPE-DOM) from seawater. *Limnol Oceanogr Methods.* 2008;6:230–5.
67. Seidel M, Beck M, Riedel T, Waska H, Suryaputra IGNA, Schnetger B, et al. Biogeochemistry of dissolved organic matter in an anoxic intertidal creek bank. *Geochim Cosmochim Acta.* 2014;140:418–34.
68. Vidal-Melgosa S, Pedersen HL, Schückel J, Arnal G, Dumon C, Amby DB, et al. A new versatile microarray-based method for high throughput screening of carbohydrate-active enzymes. *J Biol Chem.* 2015;290:9020–36.
69. Seemann T. Prokka: rapid prokaryotic genome annotation. *Bioinformatics.* 2014;30:2068–9.
70. Hou S, López-Pérez M, Pfreundt U, Belkin N, Stüber K, Huettel B, et al. Benefit from decline: the primary transcriptome of *Alteromonas macleodii* str. Te101 during *Trichodesmium* demise. *ISME J.* 2018;12:981–96.
71. Ivars-Martínez E, Martín-Cuadrado A-B, D'Auria G, Mira A, Ferreira S, Johnson J, et al. Comparative genomics of two ecotypes of the marine planktonic copiotroph *Alteromonas macleodii* suggests alternative lifestyles associated with different kinds of particulate organic matter. *ISME J.* 2008;2:1194–212.
72. López-Pérez M, Gonzaga A, Martín-Cuadrado A-B, Onyshchenko O, Ghavidel A, Ghai R, et al. Genomes of surface isolates of *Alteromonas macleodii*: the life of a widespread marine opportunistic copiotroph. *Sci Rep.* 2012;2:696.
73. López-Pérez M, Gonzaga A, Rodríguez-Valera F. Genomic diversity of 'deep ecotype' *Alteromonas macleodii* isolates:

- evidence for Pan-Mediterranean clonal frames. *Genome Biol Evol.* 2013;5:1220–32.
74. Chen I-MA, Markowitz VM, Chu K, Palaniappan K, Szeto E, Pillay M, et al. IMG/M: integrated genome and metagenome comparative data analysis system. *Nucleic Acids Res.* 2017;45:D507–16.
  75. Medema MH, Takano E, Breitling R. Detecting sequence homology at the gene cluster level with MultiGeneBlast. *Mol Biol Evol.* 2013;30:1218–23.
  76. Chaudhari NM, Gupta VK, Dutta C. BPGA- an ultra-fast pan-genome analysis pipeline. *Sci Rep.* 2016;6:24373.
  77. Edgar RC. MUSCLE: multiple sequence alignment with high accuracy and high throughput. *Nucleic Acids Res.* 2004;32:1792–7.
  78. Price MN, Dehal PS, Arkin AP. FastTree: computing large minimum evolution trees with profiles instead of a distance matrix. *Mol Biol Evol.* 2009;26:1641–50.
  79. Miller M, Pfeiffer W, Schwartz T. (2010). Creating the CIPRES science gateway for inference of large phylogenetic trees. In: *Proceedings of the Gateway Computing Environments Workshop*. New Orleans: IEEE; 2010. p. 1–8. <http://toc.proceedings.com/10226webtoc.pdf>
  80. Vizcaíno JA, Csordas A, del-Toro N, Dianas JA, Griss J, Lavidas I, et al. 2016 update of the PRIDE database and its related tools. *Nucleic Acids Res.* 2016;44:D447–56.
  81. Görke B, Stülke J. Carbon catabolite repression in bacteria: many ways to make the most out of nutrients. *Nat Rev Microbiol.* 2008;6:613–24.
  82. Lynch JB, Sonnenburg JL. Prioritization of a plant polysaccharide over a mucus carbohydrate is enforced by a *Bacteroides* hybrid two-component system. *Mol Microbiol.* 2012;85:478–91.
  83. Blokesch M. Chitin colonization, chitin degradation and chitin-induced natural competence of *Vibrio cholerae* are subject to catabolite repression. *Environ Microbiol.* 2012;14:1898–912.
  84. Ensor LA, Stosz SK, Weiner RM. Expression of multiple complex polysaccharide-degrading enzyme systems by marine bacterium strain 2-40. *J Ind Microbiol Biotechnol.* 1999;23:123–6.
  85. Furusawa G, Lau N-S, Suganthi A, Amirul AA-A. Agarolytic bacterium *Persicobacter* sp. CCB-QB2 exhibited a diauxic growth involving galactose utilization pathway. *MicrobiologyOpen.* 2017;6:e00405.
  86. Baran R, Brodie EL, Mayberry-Lewis J, Hummel E, Da Rocha UN, Chakraborty R, et al. Exometabolite niche partitioning among sympatric soil bacteria. *Nat Commun.* 2015;6:8289.
  87. Labourel A, Jam M, Legentil L, Sylla B, Hehemann J-H, Ferrières V, et al. Structural and biochemical characterization of the laminarinase Zg Lam<sub>GH16</sub> from *Zobellia galactanivorans* suggests preferred recognition of branched laminarin. *Acta Crystallogr Sect D Biol Crystallogr.* 2015;71:173–84.
  88. Buurman ET, ten Voorde GJ, Teixeira de Mattos MJ. The physiological function of periplasmic glucose oxidation in phosphate-limited chemostat cultures of *Klebsiella pneumoniae* NCTC 418. *Microbiology.* 1994;140:2451–8.
  89. Zhu Y, Thomas F, Larocque R, Li N, Duffieux D, Cladière L, et al. Genetic analyses unravel the crucial role of a horizontally acquired alginate lyase for brown algal biomass degradation by *Zobellia galactanivorans*. *Environ Microbiol.* 2017;19:2164–81.
  90. Hobbs JK, Lee SM, Robb M, Hof F, Barr C, Abe KT, et al. KdgF, the missing link in the microbial metabolism of uronate sugars from pectin and alginate. *Proc Natl Acad Sci USA.* 2016;113:6188–93.
  91. Takagi T, Morisaka H, Aburaya S, Tatsukami Y, Kuroda K, Ueda M. Putative alginate assimilation process of the marine bacterium *Saccharophagus degradans* 2-40 based on quantitative proteomic analysis. *Mar Biotechnol.* 2016;18:15–23.
  92. Fuhrman LK, Wanken A, Nickerson KW, Conway T. Rapid accumulation of intracellular 2-keto-3-deoxy-6-phosphogluconate in an Entner-Doudoroff aldolase mutant results in bacteriostasis. *FEMS Microbiol Lett.* 1998;159:261–6.
  93. van Bodegom P. Microbial maintenance: a critical review on its quantification. *Microb Ecol.* 2007;53:513–23.
  94. Beste DJV, McFadden J. System-level strategies for studying the metabolism of *Mycobacterium tuberculosis*. *Mol Biosyst.* 2010;6:2363–72.
  95. Haruta S, Kanno N. Survivability of microbes in natural environments and their ecological impacts. *Microbes Environ.* 2015;30:123–5.
  96. Chodkowski JL, Shade A. A synthetic community system for probing microbial interactions driven by exometabolites. *mSystems.* 2017;2:e00129.
  97. Toyama H. Pyrroloquinoline quinone (PQQ). Vandamme EJ, Revuelta JL. In: *Industrial biotechnology of vitamins, biopigments, and antioxidants*. Weinheim: Wiley-VCH; 2016. p. 367–88.
  98. Mincer TJ, Aicher AC. Methanol production by a broad phylogenetic array of marine phytoplankton. *PLoS ONE.* 2016;11:e0150820.
  99. Carpenter LJ, Liss PS. On temperate sources of bromoform and other reactive organic bromine gases. *J Geophys Res Atmos.* 2000;105:20539–47.
  100. Mabeau S, Kloareg B. Isolation and analysis of the cell walls of brown algae: *Fucus spiralis*, *F. ceranoides*, *F. vesiculosus*, *F. serratus*, *Bifurcaria bifurcata* and *Laminaria digitata*. *J Exp Bot.* 1987;38:1573–80.
  101. Haroon MF, Thompson LR, Parks DH, Hugenholtz P, Stingl U. A catalogue of 136 microbial draft genomes from Red Sea metagenomes. *Sci Data.* 2016;3:160050.
  102. Parks DH, Rinke C, Chuvochina M, Chaumeil P-A, Woodcroft BJ, Evans PN, et al. Recovery of nearly 8,000 metagenome-assembled genomes substantially expands the tree of life. *Nat Microbiol.* 2017;2:1533–42.
  103. Berman-Frank I, Rosenberg G, Levitan O, Haramaty L, Mari X. Coupling between autocatalytic cell death and transparent exopolymeric particle production in the marine cyanobacterium *Trichodesmium*. *Environ Microbiol.* 2007;9:1415–22.
  104. Chi W-J, Park DY, Seo YB, Chang YK, Lee S-Y, Hong S-K. Cloning, expression, and biochemical characterization of a novel GH16  $\beta$ -agarase AgaG1 from *Alteromonas* sp. GNUM-1. *Appl Microbiol Biotechnol.* 2014;98:4545–55.
  105. Hehemann J-HH, Arevalo P, Datta MS, Yu X, Corzett CH, Henschel A, et al. Adaptive radiation by waves of gene transfer leads to fine-scale resource partitioning in marine microbes. *Nat Commun.* 2016;7:12860.
  106. Zimmerman AE, Martiny AC, Allison SD. Microdiversity of extracellular enzyme genes among sequenced prokaryotic genomes. *ISME J.* 2013;7:1187–99.
  107. Sheridan-PO, Martin JC, Lawley TD, Browne HP, Harris HMB, Bernalier-Donadille A, et al. Polysaccharide utilization loci and nutritional specialization in a dominant group of butyrate-producing human colonic *Firmicutes*. *Microb Genom.* 2016;2:e000043.

## Appendix 4

### **Adaptations of *Alteromonas* sp. 76-1 to polysaccharide degradation: A CAZyme plasmid for ulvan degradation and two alginolytic systems**

Koch H, Freese HM, Hahnke RL, Simon M, Wietz M

*Frontiers in Microbiology* (2019), 10:504



OPEN ACCESS

**Edited by:**

Martin G. Klotz,  
Washington State University,  
United States

**Reviewed by:**

Christopher Fields,  
University of Illinois  
at Urbana–Champaign, United States  
William Helbert,  
Centre National de la Recherche  
Scientifique (CNRS), France  
Phil B. Pope,  
Norwegian University of Life Sciences,  
Norway

**\*Correspondence:**

Matthias Wietz  
matthias.wietz@uni-oldenburg.de;  
matthias.wietz@awi.de

**† Present address:**

Hanna Koch,  
Department of Microbiology,  
Radboud University Nijmegen,  
Nijmegen, Netherlands  
Matthias Wietz,  
Alfred Wegener Institute Helmholtz  
Centre for Polar and Marine  
Research, Bremerhaven, Germany

**Specialty section:**

This article was submitted to  
Microbial Physiology and Metabolism,  
a section of the journal  
Frontiers in Microbiology

**Received:** 28 September 2018

**Accepted:** 27 February 2019

**Published:** 18 March 2019

**Citation:**

Koch H, Freese HM, Hahnke RL,  
Simon M and Wietz M (2019)  
Adaptations of *Alteromonas* sp. 76-1  
to Polysaccharide Degradation:  
A CAZyme Plasmid for Ulvan  
Degradation and Two Alginolytic  
Systems. *Front. Microbiol.* 10:504.  
doi: 10.3389/fmicb.2019.00504

# Adaptations of *Alteromonas* sp. 76-1 to Polysaccharide Degradation: A CAZyme Plasmid for Ulvan Degradation and Two Alginolytic Systems

Hanna Koch<sup>1†</sup>, Heike M. Freese<sup>2</sup>, Richard L. Hahnke<sup>2</sup>, Meinhard Simon<sup>1</sup> and Matthias Wietz<sup>1\*†</sup>

<sup>1</sup> Institute for Chemistry and Biology of the Marine Environment, University of Oldenburg, Oldenburg, Germany, <sup>2</sup> Leibniz Institute DSMZ – German Collection of Microorganisms and Cell Cultures, Braunschweig, Germany

Studying the physiology and genomics of cultured hydrolytic bacteria is a valuable approach to decipher the biogeochemical cycling of marine polysaccharides, major nutrients derived from phytoplankton and macroalgae. We herein describe the profound potential of *Alteromonas* sp. 76-1, isolated from alginate-enriched seawater at the Patagonian continental shelf, to degrade the algal polysaccharides alginate and ulvan. Phylogenetic analyses indicated that strain 76-1 might represent a novel species, distinguished from its closest relative (*Alteromonas naphthalenivorans*) by adaptations to their contrasting habitats (productive open ocean vs. coastal sediments). Ecological distinction of 76-1 was particularly manifested in the abundance of carbohydrate-active enzymes (CAZymes), consistent with its isolation from alginate-enriched seawater and elevated abundance of a related OTU in the original microcosm. Strain 76-1 encodes multiple alginate lyases from families PL6, PL7, PL17, and PL18 largely contained in two polysaccharide utilization loci (PUL), which may facilitate the utilization of different alginate structures in nature. Notably, ulvan degradation relates to a 126 Kb plasmid dedicated to polysaccharide utilization, encoding several PL24 and PL25 ulvan lyases and monomer-processing genes. This extensive and versatile CAZyme repertoire allowed substantial growth on polysaccharides, showing comparable doubling times with alginate (2 h) and ulvan (3 h) in relation to glucose (3 h). The finding of homologous ulvanolytic systems in distantly related *Alteromonas* spp. suggests CAZyme plasmids as effective vehicles for PUL transfer that mediate niche gain. Overall, the demonstrated CAZyme repertoire substantiates the role of *Alteromonas* in marine polysaccharide degradation and how PUL exchange influences the ecophysiology of this ubiquitous marine taxon.

**Keywords:** alginate, ulvan, polysaccharide utilization loci, unique genes, niche specialization

## INTRODUCTION

Polysaccharides from phytoplankton and macroalgae represent a major fraction of organic matter in the oceans (Benner et al., 1992; Kraan, 2012; Rossi and De Philippis, 2016), especially in systems with high primary production such as continental shelves (Acha et al., 2004; Thomas et al., 2004). Algal polysaccharides are an important nutrient source for heterotrophic bacteria, as demonstrated by molecular studies of bacterial hydrolysis rates (Arnosti et al., 2011), population dynamics (Wietz et al., 2015), functional genomics (Martinez-Garcia et al., 2012; Matos et al., 2016) and cellular uptake processes (Reintjes et al., 2017) associated with polysaccharide degradation.

Cultured bacterial strains are a vital resource to study the genomic and ecophysiological basis of polysaccharide degradation, providing fundamental understanding of environmentally relevant processes. Culture-based studies were pivotal in revealing the functionality of carbohydrate-active enzymes (CAZymes) and their common localization in polysaccharide utilization loci (PUL), which allows the concerted degradation of polysaccharides (Hehemann et al., 2014; Grondin et al., 2017). To date, such studies have identified 322 families of polysaccharide lyases (PL), glycoside hydrolases (GH), carbohydrate-binding modules (CBM), carbohydrate esterases (CE), glycosyl transferases (GT) and auxiliary carbohydrate-active oxidoreductases (Lombard et al., 2014). CAZymes are commonly subject to horizontal gene transfer, the primary driver of strain-specific differences in hydrolytic capacities (Hehemann et al., 2016).

The continuously increasing number of sequenced bacterial genomes suggests that CAZymes are effective mechanisms of adaptation. For instance, the flavobacterium *Zobellia galactanivorans* is adapted to life on macroalgae through 50 PUL, providing numerous insights into PUL structure (Thomas et al., 2012), CAZyme biochemistry (Hehemann et al., 2012; Labourel et al., 2014), substrate-specific gene expression (Ficko-Blean et al., 2017; Thomas et al., 2017) and regulatory networks (Zhu et al., 2017). Comparable features in many *Bacteroidetes* (Mann et al., 2013; Kabisch et al., 2014) underline their predisposition toward polysaccharide degradation (Fernández-Gómez et al., 2013), but proficient hydrolytic capacities also occur among *Gammaproteobacteria* (Hehemann et al., 2017), *Verrucomicrobia* (Martinez-Garcia et al., 2012) and *Bacilli* (Zhu et al., 2016). Members of these taxa degrade a variety of polysaccharides produced by micro- and macroalgae, including laminarin, alginate, ulvan and pectin (Ekborg et al., 2005; Foran et al., 2017; Corzett et al., 2018).

To expand the understanding of bacterial CAZyme diversity and its role in ecological specialization, so-far understudied taxa can provide valuable insights. The gammaproteobacterial genus *Alteromonas* has been recently identified as important contributor to polysaccharide degradation in natural habitats, utilizing both dissolved (Wietz et al., 2015; Taylor and Cunliffe, 2017) and particulate substrates (Mitulla et al., 2016). Studies of model isolates have connected this functionality to diverse hydrolytic enzymes encoded in complex gene clusters (Chi et al., 2014; Neumann et al., 2015), whose expression is

controlled by substrate availability (Koch et al., 2019). Although *Gammaproteobacteria* do not encode SusC/D proteins, the hallmark of PUL in *Bacteroidetes*, the finding of comparable functionality suggests these clusters can be designated PUL as well. Overall, model isolates provide conceptual understanding of ecophysiological adaptations that influence complex environmental processes, such as the succession of bacterial taxa during phytoplankton blooms (Teeling et al., 2012, 2016).

Here, we report the whole genome and physiology of a novel *Alteromonas* strain (designated 76-1) with pronounced potential for utilizing alginate and ulvan, structurally diverse polysaccharides that can constitute >50% of brown and green algae, respectively (Michel and Czjzek, 2013). Strain 76-1 has been isolated from an alginate-supplemented microcosm at the Patagonian continental shelf, a region with high primary productivity and hence regular availability of polysaccharides (Acha et al., 2004; Garcia et al., 2008). 16S rRNA gene amplicon sequencing showed that an OTU with 99% rRNA sequence identity was abundant in the original microcosm (Wietz et al., 2015), suggesting strain 76-1 as an environmentally relevant polysaccharide degrader. Genomic machineries for degradation of alginate and ulvan were compared to the closest relative (*Alteromonas naphthalenivorans* SN2<sup>T</sup>) and other *Alteromonas* strains, establishing an eco-evolutionary perspective into CAZyme-related niche specialization among *Alteromonas* and its connection to biogeochemical processes.

## MATERIALS AND METHODS

### Isolation and Cultivation of Strain 76-1

*Alteromonas* sp. 76-1 was isolated in April 2012 from a microcosm with surface seawater collected at the Patagonian continental shelf (47° 56'41''S 61° 55'23''W) amended with 0.001% (w/v) sodium alginate (Wietz et al., 2015). Purity was confirmed by 16S rRNA gene PCR after several rounds of subculturing. Polysaccharide utilization was analyzed in seawater minimal medium (SWM) (Zech et al., 2009) supplemented with 0.1% sodium alginate (cat. no. A2158; Sigma-Aldrich, St. Louis, MO, United States) or 0.2% ulvan (cat. no. YU11689; Carbosynth, United Kingdom) as sole carbon sources in comparison to SWM + 0.1% glucose. All cultures were incubated in triplicates at 20°C and 100 rpm with regular photometric determination of growth (diluted if OD<sub>600</sub> >0.4) followed by calculation of maximal growth rate ( $\mu_{\max}$ ) and doubling time ( $\ln 2/\mu_{\max}$ ). In addition, hydrolysis of 18 AZO-CL labeled polymers was tested according to Pansch et al. (2016). Briefly, AZO-CL substrates (Megazyme, Ireland) were distributed to individual microtiter wells in triplicate. To each well, 100  $\mu$ L HaHa medium (Hahnke and Harder, 2013) were added, plus each 100  $\mu$ L of a starved culture or 100  $\mu$ L medium as control. Cultures were incubated at 25°C for up to 14 days and evaluated for hydrolytic activity on the basis of color change.

### Genome Sequencing and Taxonomy

Genomic DNA was extracted with the Genomic-tip 100/G kit (Qiagen, Hilden, Germany). After shearing using g-tubes

(Covaris, Woburn, MA, United States) and monitoring the size range by pulse field gel electrophoresis, DNA fragments were end-repaired and ligated to hairpin adapters using P6 chemistry (Pacific Biosciences, Menlo Park, CA, United States). SMRT sequencing was carried out on a PacBio RSII instrument (Pacific Biosciences). PacBio reads were assembled *de novo* using the RS\_HGAP\_Assembly.3 protocol in the SMRT Portal v2.3. Indel errors were corrected using 5,759,952 paired-end reads of 112 bp from prior Illumina GAIIX sequencing on Nextera XT libraries (Illumina, San Diego, CA, United States) performed at Göttingen Genomics Laboratory (Germany). Illumina reads were mapped using the Burrows-Wheeler Aligner (Li and Durbin, 2009) followed by variant detection using VarScan v2.3.6 (Koboldt et al., 2012), consensus calling using GATK 3.1-1 (McKenna et al., 2010), and trimming of the final assembly. Chromosome and plasmid were circularized (in total 4,817,656 bp) and uploaded to both ENA<sup>1</sup> and IMG<sup>2</sup> under accession numbers PRJEB28726 and 2784132050, respectively. Phylogenetic analysis was carried out with 92 core genes identified using the UBCG pipeline (Na et al., 2018) including *Pseudoalteromonas atlantica* T6c as outgroup (RefSeq NC\_008228.1). The concatenated nucleotide alignment was manually curated and the best substitution model (GTR+G) computed using jModelTest2 (Darriba et al., 2012). A maximum-likelihood phylogeny with 1000 bootstrap replicates was calculated using RaxML (Stamatakis, 2014) implemented on CIPRES (Miller et al., 2010).

## Comparative Genomics

Genomes of strain 76-1 and publicly available *Alteromonas* spp. (Supplementary Table S1) were compared using a variety of bioinformatic tools. Average amino acid identities and genome-to-genome distances were calculated using the Enveomics (Rodriguez-R and Konstantinidis, 2016) and GGDC (Meier-Kolthoff et al., 2013) web applications, respectively. Unique genes were identified using BPGA (Chaudhari et al., 2016) with a threshold of 50% amino acid identity, only considering proteins > 50 amino acids (Supplementary Table S2). CAZymes were identified using dbCAN2 (Zhang et al., 2018), only considering hits with  $e < 10^{-23}$  and >80% query coverage. Annotations of selected genes were checked using UniprotKB-Swissprot, KAAS and MEROPS databases (Moriya et al., 2007; The UniProt Consortium, 2017; Rawlings et al., 2018). Genomic regions were visualized using genoPlotR (Guy et al., 2010) and Circos (Krzywinski et al., 2009) followed by manual inspection. Homologous PUL in related strains were identified using MultiGeneBlast (Medema et al., 2013), only considering proteins with >50% amino acid identity and >50% sequence coverage. Completeness of draft genomes used for comparative analyses was estimated using CheckM (Parks et al., 2015).

## Phylogeny and Annotation of Polysaccharide Lyases

Polysaccharide lyases of strain 76-1 were compared to enzymes deposited in the curated databases CAZY (Lombard et al., 2014)

and PDB (Berman et al., 2000). In addition, related sequences deposited at NCBI were identified by BLASTp, only considering hits with >90% query coverage and >60% amino acid identity. PL sequences were aligned using ProbCons (Do et al., 2005) followed by manual inspection. Protein substitution models (WAG+G+F best for all alignments) were calculated using Modeltest-NG<sup>3</sup>, an improved successor of ProtTest3 (Darriba et al., 2011). Phylogenies were computed using RaxML with 1000 bootstrap replicates (Stamatakis, 2014). To determine the occurrence of PL transcripts in marine habitats, one PL from each alginolytic system (alt76\_01684, alt76\_03417) was searched against 272 marine metatranscriptomes publicly available at IMG (Supplementary Table S3). Only a co-detection of PL homologs with >70% amino acid identity was considered positive.

## Test for Antibacterial Activity and Siderophore Production

Two grams of XAD-16 resin (Dow Chemical Company, Midland, MI, United States) were washed several times with dH<sub>2</sub>O and methanol, concentrated on a metal filter, resuspended in 100 mL dH<sub>2</sub>O, and autoclaved. Strain 76-1 was precultured in sea salt medium (4% Sigma sea salts, 0.3% casamino acids, and 0.4% glucose) for 16 h at 20°C. Preculture was inoculated at 2% (v/v) into 100 mL sea salt medium mixed with 100 mL XAD-16 solution and cultivated at 20°C and 100 rpm for 24 h. Resin was collected by filtration and extracted with methanol:dH<sub>2</sub>O (80:20). Extracts were concentrated in a rotary evaporator using a two-step vacuum (337 mbar, 100 mbar) and heating to 40°C. Concentrated extract was tested for antimicrobial activity in a well-diffusion assay (Hjelm et al., 2004) with *Alteromonas macleodii* D7 as target strain and methanol:dH<sub>2</sub>O (80:20) as negative control. Siderophore production was tested with sterile-filtered supernatant from overnight cultures in both iron-deplete and iron-replete minimal medium using a modified CAS assay (Schwyn and Neilands, 1987; Alexander and Zuberer, 1991). Positive and negative controls were deferoxamine mesylate and sterile medium, respectively.

## RESULTS AND DISCUSSION

### General Characteristics of *Alteromonas* sp. 76-1

Strain 76-1 was isolated from alginate-supplemented seawater collected at the Patagonian continental shelf (Wietz et al., 2015) on solid media containing alginate as sole carbon source. Colonies appear round and cream-colored, assuming a tough surface after several days. Cells are motile as confirmed by light microscopy. Whole-genome sequencing revealed a chromosome of 4.7 Mb and a 126 Kb plasmid, encoding a total of 4100 proteins (Table 1). Core genome phylogeny demonstrated close relationship with *Alteromonas naphthalenivorans*, with 95.5% average amino acid identity

<sup>1</sup><https://www.ebi.ac.uk/ena>

<sup>2</sup><https://img.jgi.doe.gov>

<sup>3</sup><https://github.com/ddarriba/modeltest>

(AAI) to *A. naphthalenivorans* SN2<sup>T</sup> but only 63.5% DNA-DNA relatedness. Hence, strain 76-1 can only be assigned to genus level and might represent a novel *Alteromonas* species. Strains 76-1 and SN2 form a phylogenetic clade with *A. stellipolaris* and *A. addita* (89% AAI), separated from the more distant relatives *A. australica*, *A. macleodii*, and *A. mediterranea* (75–77% AAI) (Figure 1).

The unclear taxonomic affiliation motivated an initial comparison of strain 76-1 with the closest relative, *A. naphthalenivorans* SN2<sup>T</sup>. In addition to a shared core of 3401 genes, strains 76-1 and SN2 encode 621 and 793 unique genes relating to their contrasting habitats (Table 1 and Supplementary Table S2). Notably, the origin of strain 76-1 from pelagic waters with high primary production and carbohydrate availability (Acha et al., 2004; Garcia et al., 2008) is reflected by a third of unique genes belonging to KEGG class “Carbohydrate Metabolism” (Figure 2A) and a diverse CAZyme repertoire (Figure 2B). Strain 76-1 encodes a total of 96 CAZymes, including thirteen polysaccharide lyases from six families and 41 glycoside hydrolases from 20 families (Table 2 and Figure 2B). This CAZyme content approximates that of algae-associated *Flavobacteriia* (Mann et al., 2013) whereas most other *Alteromonas* encode lower numbers (Supplementary Table S1).

Based on these observations, this study focuses on the genomics and ecophysiology of polysaccharide degradation, as detailed below, but 76-1 features further unique adaptations. Specifically, unique gene clusters for siderophore synthesis and methylamine metabolism (Supplementary Figure S1) could sustain iron and nitrogen supply under limiting conditions in pelagic habitats (Boiteau et al., 2016; Taubert et al., 2017). The siderophore cluster is co-localized with polyketide-nonribosomal peptide (PKS-NRPS)-encoding genes that may enhance competitive abilities (Patin et al., 2017). We experimentally confirmed functionality of these clusters by showing iron scavenging and antibacterial activity using CAS and well-diffusion assays (Supplementary Figure S1). Homology of the PKS-NRPS to tyrocidine/gramicidin-related gene clusters in *Bacillus* (Mootz and Marahiel, 1997) and differing G+C content compared to the chromosome (38 vs. 44%) suggest horizontal acquisition from low-GC Gram-positive bacteria. In contrast, proteins for naphthalene and urea degradation (Math et al., 2012; Jin et al., 2016) as well as conjugal transfer (Supplementary Table S2) are unique to *A. naphthalenivorans*

SN2<sup>T</sup> and probably facilitate adaptation to higher anthropogenic input (Cozzi et al., 2014) and genetic exchange (Fuchsman et al., 2017) in coastal sediments. The lower numbers and diversity of CAZymes (Figure 2) suggests a minor role of polysaccharide degradation in the habitat of SN2 (Math et al., 2012).

## Proficiency of *Alteromonas* sp. 76-1 to Degrade Different Algal Polysaccharides

A comprehensive CAZyme inventory of *Alteromonas* sp. 76-1 revealed genetic machineries for degradation of alginate, ulvan and xylan, common polysaccharides from marine algae (Michel and Czjzek, 2013) and potentially contained in algal-derived microgels (Aluwihare and Repeta, 1999). Furthermore, we identified functional genes for the degradation of different glucans with simpler molecular structure.

Alginate degradation of strain 76-1 relates to two separate alginate lytic systems (designated AS1 and AS2) encoding PL6 and PL7 alginate lyases, TonB-dependent receptors, MFS transporters and enzymes for monomer processing (Figure 3A). Additional alginate lyases from families PL7, PL17, and PL18 are located outside of AS1 and AS2 (Figure 3B and Supplementary Table S2). The role of these enzymes in alginate degradation is supported by distinct homologies to biochemically characterized alginate lyases (Table 3 and Supplementary Figure S2) and co-localization of genes for downstream processing. Alginate lyases encoded in AS1 are probably exolytic, including alt76\_01689 with homology to a PL6 from *Paraglaciecola chathamensis* (Xu et al., 2017) and alt76\_01684 with homology to a PL7 from *Zobellia galactanivorans* that is specifically upregulated in the presence of alginate (Thomas et al., 2017). AS2 encodes another exolytic candidate PL6 and two homologs of endolytic PL7 from *Vibrio splendidus* releasing trisaccharides (Lyu et al., 2018). In line with other studies, the separate PL17 (alt76\_2604) probably degrades released oligomers, exemplified by distinct similarity to PL17\_4NEI from *Saccharophagus degradans* (Park et al., 2014). The separate PL18 (alt76\_00345) shares >50% amino acid similarity to PL18\_4Q8L from *Pseudoalteromonas* sp. 0524 with complete conservation of the seven central residues, indicating endolytic release of di- and trisaccharides (Dong et al., 2014). The PL18 furthermore harbors two predicted CBMs from families 16 and 32, which may enable binding different alginate motifs (Sim et al., 2017) or contribute to protein maturation (Dong et al., 2014).

Accordingly, strain 76-1 grew proficiently with alginate as sole carbon source (Figure 4). Faster growth than with glucose was notable, as degradation of the complex alginate polymer (comprising heterogeneous blocks of mannuronate and guluronate) involves more enzymatic steps and induces a prolonged lag phase in other *Alteromonas* strains (Neumann et al., 2015). Utilization may be boosted by FabG-like enzymes encoded in both AS (Supplementary Figure S3) with homology to alginate-specific reductases in *Flavobacteriia* (Inoue et al., 2015). These enzymes possibly accelerate the central downstream conversion of 4-deoxy-L-erythro-5-hexoseulose uronate to 2-keto-3-deoxy-D-gluconate and hence prevent

**TABLE 1** | Genome features of *Alteromonas* strains 76-1 and SN2.

Feature	76-1	SN2
Chromosome size (bp)	4,731,105	4,972,148
Plasmid size (bp)	125,985	not present
Average G+C content (%)	43.4	43.5
Protein-coding sequences (CDS)	4100	4335
rRNA genes	15	15
Strain-specific proteins <sup>#</sup>	621	793

<sup>#</sup>based on 50% amino acid identity.

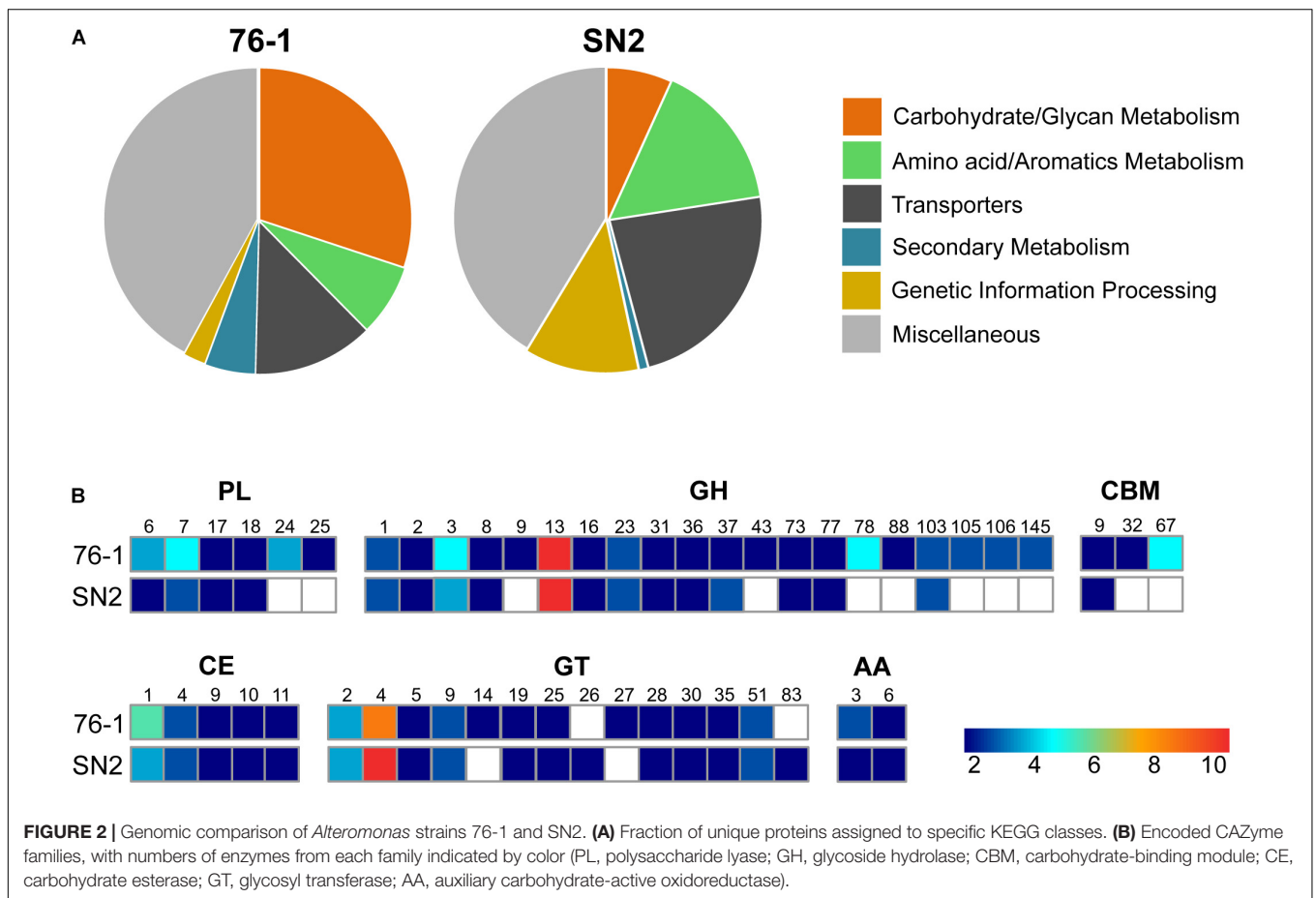
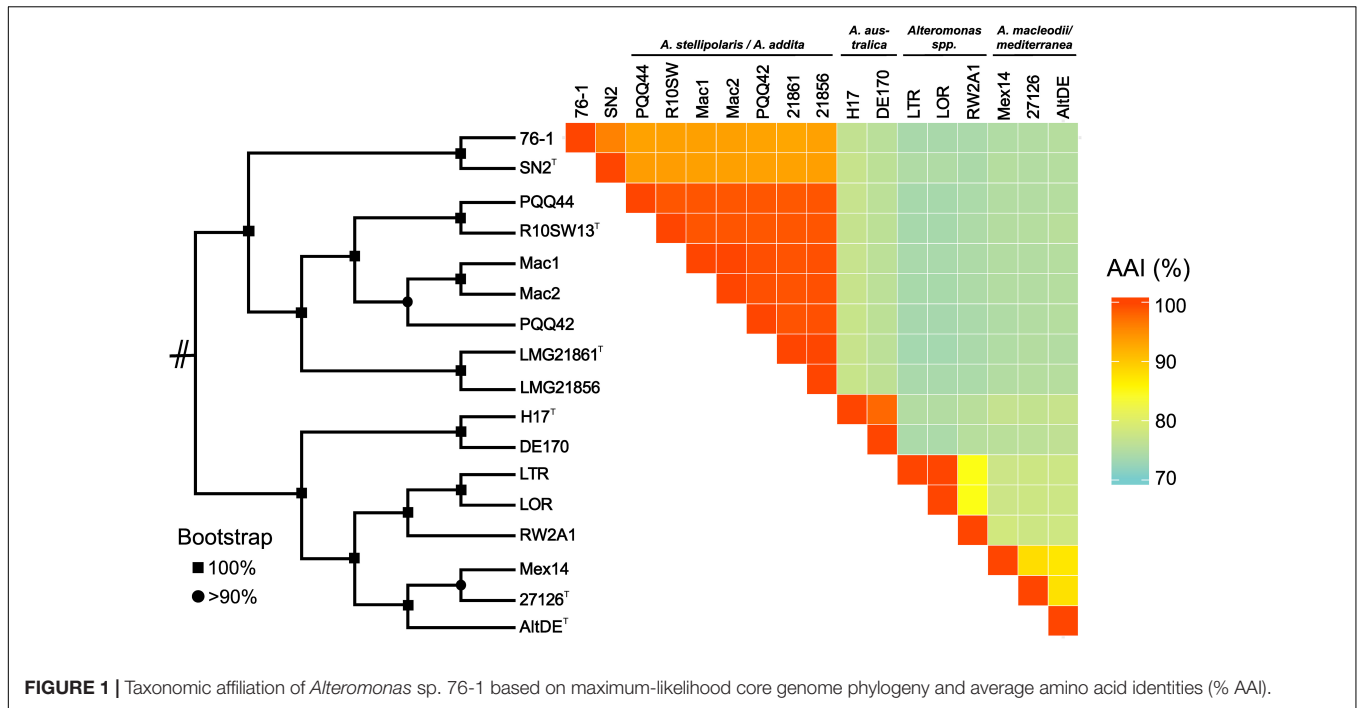


**TABLE 2** | CAZyme families encoded on chromosome and plasmid of *Alteromonas* sp. 76-1 as predicted by dbCAN2.

Class <sup>#</sup>	Families on chromosome	Families on plasmid
PL	6 7 17 18	24 25
GH	1 2 3 8 9 13 16 23 31 36 37 73 77 103	43 78 88 105 106 145
CBM	9 32	67
CE	1 4 9 10 11	
GT	2 4 5 9 14 19 25 27 28 30 35 51	
AA	3 6	

<sup>#</sup>PL, polysaccharide lyase; GH, glycoside hydrolase; CBM, carbohydrate-binding module; CE, carbohydrate esterase; GT, glycosyl transferase; AA, auxiliary carbohydrate-active oxidoreductase.

bacteriostasis from accumulation of metabolic intermediates (Fuhrman et al., 1998).

The alginolytic machinery of 76-1 is found in several *Alteromonas* strains, indicating a broader distribution of alginate degradation among this taxon than previously assumed. AS1 and the separate PL17/18 are conserved in the phylogenetic clade

comprising strain 76-1, *A. naphthalenivorans*, *A. stellipolaris*, and *A. addita* (Figure 1 and Supplementary Figure S3). AS1 also occurs in the next related species (*A. australica*) but including the PL17 that is encoded separately in 76-1 (Figure 3B). AS2 shows greater structural variability between strains; with three genes including a putative TBDR plug domain (The UniProt Consortium, 2017) missing in 76-1 and a further reduced version in *A. australica* and some *A. mediterranea* (Figure 3B). Different PUL architectures and PL rearrangements are consistent with *Alteromonas* genome plasticity (López-Pérez et al., 2017) and may confer ecological differentiation, as lyase copy number correlates with enzymatic activity due to gene dosage effect (Hehemann et al., 2016). In the broader eco-evolutionary context, the alginolytic machinery of 76-1 might play an important role, allowing degradation of different alginate structures (Peteiro, 2018) and natural polysaccharide pulses that frequently occur at the productive Patagonian shelf (Acha et al., 2004; Romero et al., 2006). Accordingly, an OTU with 99% 16S rRNA gene similarity was abundant in the alginate-supplemented microcosm from which 76-1 was isolated (Wietz et al., 2015). The

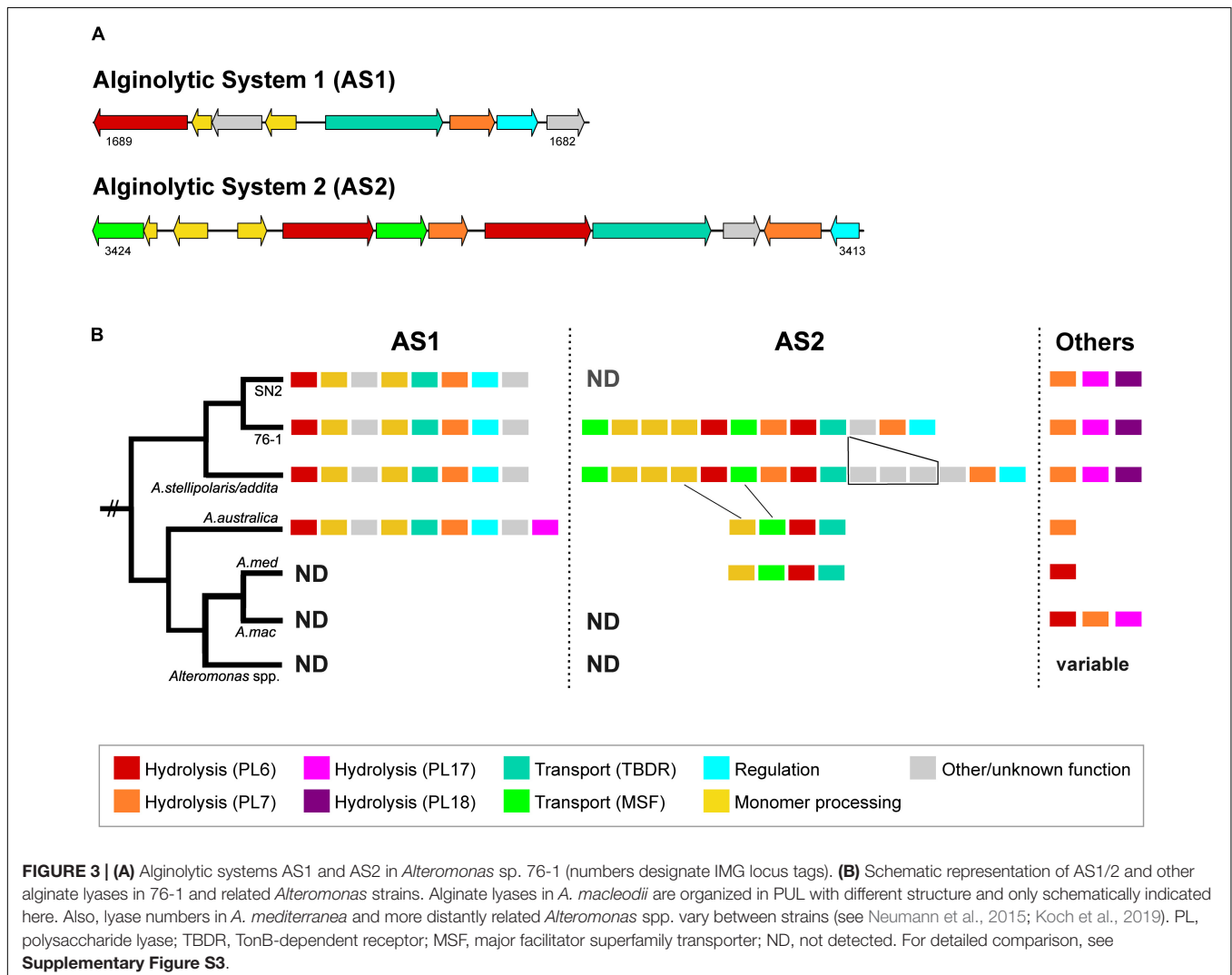


**TABLE 3** | Similarities of polysaccharide lyases of *Alteromonas* sp. 76-1 to biochemically characterized enzymes in the PDB database.

Gene (alt76_)	CAZyme family	PDB	Organism	% ID/coverage	Function	Reference
00345	PL18, CBM16, CBM32	4Q8L	<i>Pseudoalteromonas</i> sp. SMO524	54/41	endolytic alginate lyase (M-M, G-G)	Dong et al., 2014
01684	PL7	4BE3	<i>Zobellia galactanivorans</i>	36/88	exolytic alginate lyase (M-M, M-G, G-G)	Thomas et al., 2013
01689	PL6	5GKD	<i>Paraglaciecola chathamensis</i>	49/90	exolytic alginate lyase (G-G)	Xu et al., 2017
02604	PL17	4NEI	<i>Saccharophagus degradans</i>	39/99	cleaves oligosaccharide	Park et al., 2014
03213	PL7	4BE3	<i>Zobellia galactanivorans</i>	34/62	exolytic alginate lyase (M-M, M-G, G-G)	Thomas et al., 2013
03414	PL7, CBM32	5ZU5	<i>Vibrio splendidus</i>	51/57	alginate lyase (M-M and G-G)	Lyu et al., 2018
03417	PL6	nd	nd	nd	nd	nd
03418	PL7	5ZU5	<i>Vibrio splendidus</i>	53/82	alginate lyase (M-M and G-G)	Lyu et al., 2018
03420	PL6	5GKD	<i>Paraglaciecola chathamensis</i>	59/93	exolytic alginate lyase (G-G)	Xu et al., 2017
04143	PL24	6BYP	<i>Alteromonas</i> sp. LOR	46/92	ulvan lyase (Rha3S-GlcA)	Kopel et al., 2016; Ulaganathan et al., 2018
04144	PL24	6BYP	<i>Alteromonas</i> sp. LOR	88/95	ulvan lyase (Rha3S-GlcA)	Kopel et al., 2016; Ulaganathan et al., 2018
04173	PL25	5UAM	<i>Pseudoalteromonas</i> sp. PLSV	77/92	ulvan lyase (Rha3S-GlcA, Rha3S-IdoA)	Ulaganathan et al., 2017
04188	PL24	6BYP	<i>Alteromonas</i> sp. LOR	67/49	ulvan lyase (Rha3S-GlcA)	Kopel et al., 2016; Ulaganathan et al., 2018

PL, polysaccharide lyase; CBM, carbohydrate-binding module; M, mannuronate; G, guluronate; Rha3S, 3-sulfated rhamnose; GlcA, glucuronic acid; IdoA, iduronic acid; nd, no homolog detected with >30% identity/query coverage.

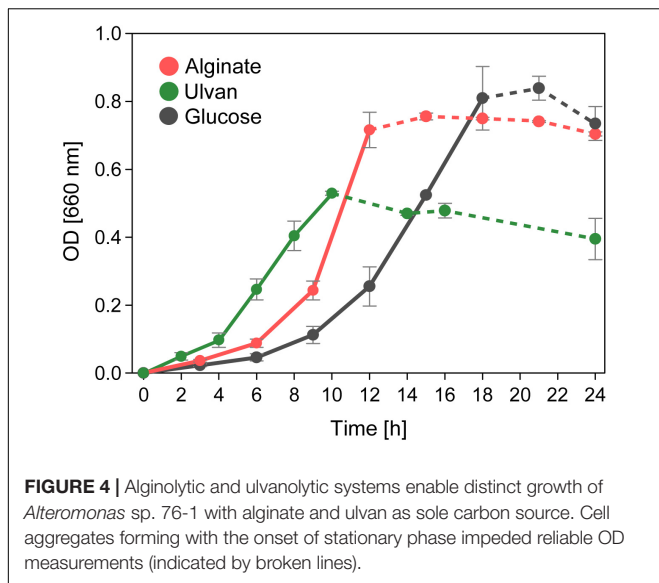
ecological relevance was underlined by co-detecting transcripts of alginate lyases from both AS near the original isolation site (**Supplementary Table S3**), suggesting active roles in natural habitats.

## A CAZyme Plasmid for Ulvan Degradation

The plasmid of *Alteromonas* sp. 76-1 is markedly devoted to polysaccharide degradation (**Figure 5A** and **Table 2**). Twenty percent of plasmid genes encode CAZymes (plus additional sulfatase and monomer-processing genes) in comparison to 2% CAZymes on the chromosome. This CAZyme condensation essentially denotes the plasmid as an extrachromosomal PUL, matching the size of the largest PUL hitherto described in marine bacteria (Schultz-Johansen et al., 2018). Comparison to characterized CAZymes suggest that the plasmid is linked to degradation of ulvan, a common polysaccharide of green algae (Michel and Czjzek, 2013) mainly consisting of 3-sulfated rhamnose, iduronic acid, glucuronic acid and xylose. Accordingly, strain 76-1 showed distinct growth on ulvan as sole carbon source, with doubling times comparable to glucose (**Figure 4**). This activity relates to three PL24 and two PL25 ulvan lyases, multiple GHs including predicted rhamnosidases, as well as transporters and monomer-processing genes in the plasmid-encoded ulvanolytic system (**Figure 5A**). Highly homologous proteins in similar organization also occur in *Alteromonas* sp. LOR and *Pseudoalteromonas* sp. PLSV

(Kopel et al., 2016; Foran et al., 2017), and several of these homologs have been characterized biochemically (**Table 3**). All encoded PL24 of strain 76-1 are homologous to the PL24\_6BYP ulvan lyase from *Alteromonas* sp. LOR, although phylogenetic clustering of alt76\_04143 with flavobacterial PLs suggests another evolutionary origin (**Figure 5B**). The proposed functionality of the ulvanolytic system is supported by structural alignments (**Figure 5C**), showing conservation in residues essential for endolytic ulvan cleavage (Ulaganathan et al., 2017, 2018). Activity assays in strains LOR and PLSV have illustrated potential routes of downstream degradation, showing release of two uronic tetrasaccharides by PL24\_6BYP (Ulaganathan et al., 2018) which were in turn degraded by PL25\_5UAM from strain PLSV (Qin et al., 2018). Considering sizeable genomic similarities and physiological evidence, we assume similar action by the homologous enzymes in 76-1.

Although regulatory mechanisms remain to be determined, the rapid initiation of growth indicates that the plasmid localization accelerates ulvan degradation, as plasmids are less affected by DNA supercoiling (Dorman and Dorman, 2016) and early-replicating regions (due to the proximity of lyases and origin of replication) are characterized by higher expression (Oliveira et al., 2017). Moreover, the common induction of PUL by substrate availability (Thomas et al., 2017; Koch et al., 2019) suggests that enzymes are only produced in presence of ulvan, reducing fitness costs and the risk of plasmid loss (MacLean and San Millan, 2015). Intriguingly, the encoding contigs in *Alteromonas* sp. LOR and *Pseudoalteromonas* sp.

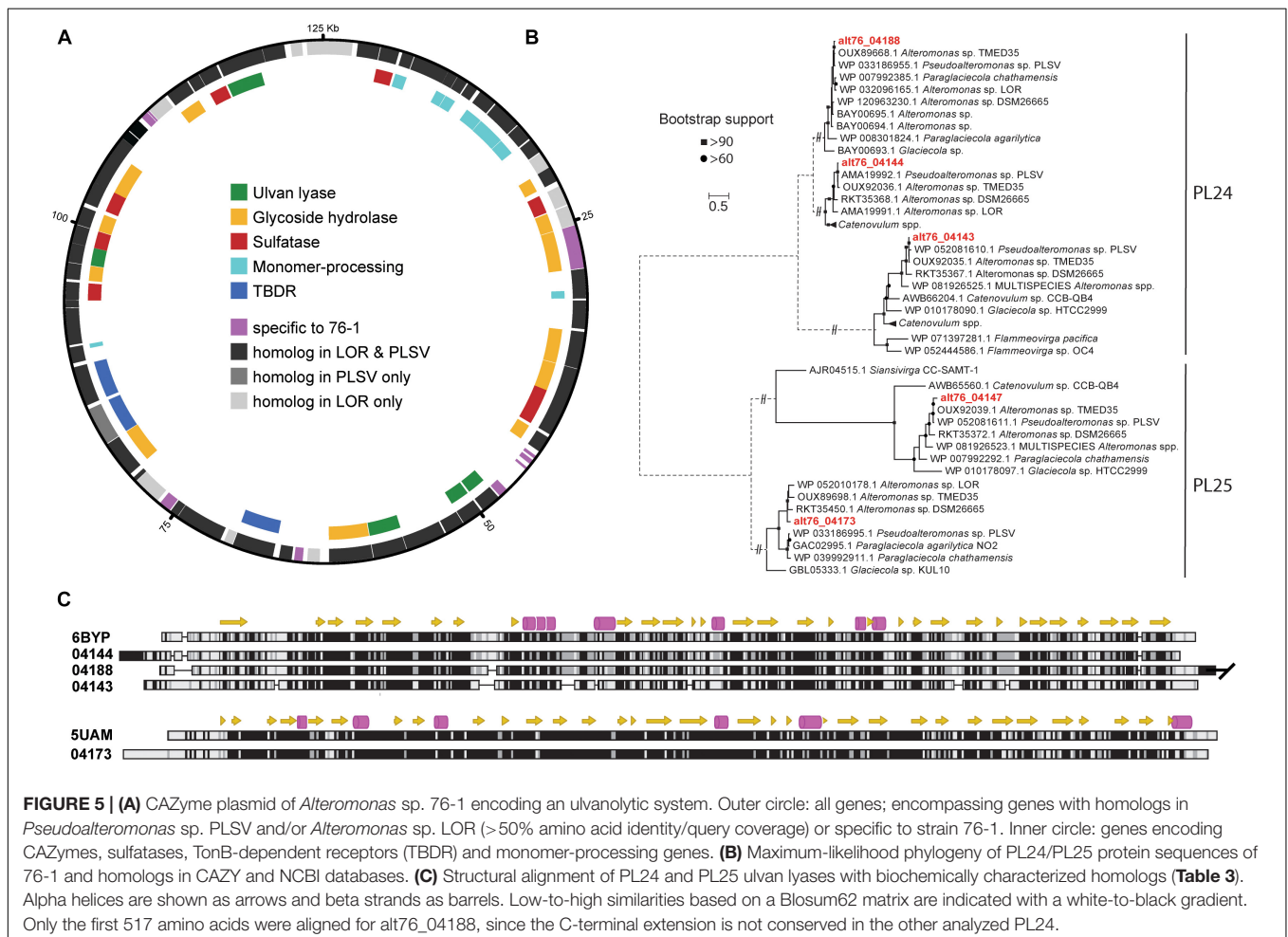


PLSV (estimated completeness of draft genomes >99%) harbor partitioning proteins with 83% identity to those on the 76-1

plasmid (alt76\_04111–12), suggesting equivalent localization on plasmids acquired in separate horizontal transfer events. Strains LOR and PLSV originate from sea slugs feeding on ulvan-rich macroalgae, indicating ecological relevance of ulvan degradation in host-microbe interactions (Gobet et al., 2018a; Konasani et al., 2018). Isolation of LOR/PLSV from the Brittany coast and hence the opposite side of the Atlantic suggest that ulvanolytic plasmids are distributed over wide geographic scales and maintained in strains from certain niches. Although PUL on plasmids are known in marine bacteria (Zhong et al., 2001) this is only the second report of a plasmid almost fully dedicated to polysaccharide metabolism (Gobet et al., 2018b). Mobile CAZyme elements are likely an important eco-evolutionary factor, representing efficient vehicles of PUL that provide recipient strains with access to specific “polysaccharide niches” on short time scales (Hülter et al., 2017).

### Degradation of Other Polysaccharides

The predisposition of *Alteromonas* sp. 76-1 toward polysaccharides was underlined by testing hydrolysis of 18 AZO-CL labeled substrates (Pansch et al., 2016). Strain 76-1 hydrolyzed diverse glucans with  $\alpha$ -(1–4),  $\beta$ -(1–3), and  $\beta$ -(1–4)



bonds, including amylose, pullulan, pachyman and barley  $\beta$ -glucan (**Supplementary Table S4**). Amylase and pullulanase activity likely relates to a gene cluster with four GH13 enzymes plus an additional GH13 in a distant genomic location. Pachyman and barley  $\beta$ -glucan are probably hydrolyzed by the same endo- $\beta$ -(1-3,4)-glucanase from family GH16. Commonly described xylanase families (GH10, GH30, GH67, and GH115) were not detected in the genome, but xylanolytic activity likely corresponds to a unique chromosomal cluster harboring a GH3  $\beta$ -(1-4)-xylosidase, a GH9 and several xylose-processing genes (**Supplementary Table S4**). Proteolytic activity exemplified by casein hydrolysis demonstrated that 76-1 also utilizes other polymer types, attributed to 97 encoded peptidases and proteases predicted by MEROPS (**Supplementary Table S2**). However, this number is only about half compared to related *Alteromonas* such as *A. macleodii*, which in turn encode less CAZymes (**Supplementary Table S1**). This observation indicates differing preferences between *Alteromonas* lineages toward polysaccharides and proteins.

## CONCLUSION

The presence of diverse polysaccharide lyases, two alginolytic systems and a plasmid dedicated to ulvan degradation demonstrate a marked adaptation of *Alteromonas* sp. 76-1 toward polysaccharides from algae, potentially allowing considerable hydrolytic activity in marine systems. The plasmid-mediated adaptation to ulvan is unprecedented to date, illustrating that mobile PUL can provide access to certain “polysaccharide niches” and represent an important eco-evolutionary factor. It remains to be determined whether the predisposition of 76-1 toward algal polysaccharides corresponds to occurrence on macroalgae, although *Alteromonas* spp. are seldom reported as algal epibionts to date and may rather target polysaccharides derived from exudation or decay (Koch et al., 2019). Considering the substantial primary production of algae on global scales and the relevance of polysaccharides in marine food webs, these insights contribute to the understanding of niche specialization among marine *Alteromonas* and how their CAZyme repertoire influences the biogeochemical cycling of abundant algal polysaccharides.

## AUTHOR CONTRIBUTIONS

MW, HK, and MS designed the research and wrote the manuscript. HK and MW conducted the genomic analyses and growth experiments. HF performed the complete genome assembly with error correction and annotation. RH conducted the AZO-CL assay. All authors contributed to the final version of the manuscript.

## FUNDING

MW and HF were supported by the German Research Foundation (DFG) through grants WI3888/1-2 and TRR

51/2-3 TA07, respectively. HK was supported by Volkswagen Foundation under VW-Vorab grant “Marine Biodiversity across Scales” (MarBAS; ZN3112) and the Radboud Excellence Initiative.

## ACKNOWLEDGMENTS

We thank Zain Albezra, Martine Berger, Malien Laurien, Antoine Olivier Nguelefack, Matthias Schröder, Rolf Weinert, and Martin Mierzejewski for excellent laboratory and bioinformatic assistance. The captain and crew of RV *Polarstern* expedition ANTXXXVIII/5 are thanked for professional support. Cathrin Spröer, Anja Poehlein, and Sonja Voget are gratefully acknowledged for PacBio and Illumina sequencing. Thorsten Brinkhoff and Jan-Hendrik Hehemann are thanked for helpful advice.

## SUPPLEMENTARY MATERIAL

The Supplementary Material for this article can be found online at: <https://www.frontiersin.org/articles/10.3389/fmicb.2019.00504/full#supplementary-material>

**FIGURE S1** | Unique gene clusters in *Alteromonas* sp. 76-1. **(A)** hybrid biosynthetic gene cluster encoding a functional siderophore (insert depicting CAS assay including positive and negative control) and active antibacterial compound (insert depicting inhibition of *A. macleodii* D7 in well-diffusion agar assay; marked in yellow). **(B)** gene cluster for methylamine metabolism (mau, methylamine dehydrogenase; cyt, cytochrome). Numbers below clusters designate IMG locus tags.

**FIGURE S2** | Amino acid-based maximum-likelihood phylogeny of PL6 alginate lyases of *Alteromonas* sp. 76-1 (red label), related *Alteromonas* spp. and deposited sequences at the CAZY database. Only relevant subtrees are shown; labeled with locus tags/NCBI gene identifiers, strain and annotation.

**FIGURE S3** | Detailed overview of AS1 and AS2 in *Alteromonas* sp. 76-1 and related strains. PL, polysaccharide lyase; TBDR, TonB-dependent receptor; MSF, major facilitator superfamily transporter; KdgF, protein for uronate linearization; DehR, 4-deoxy-L-erythro-5-hexoseulose uronate (DEH) reductase; FabG, oxidoreductase with similarity to DEH reductase; Nrapm, metal-ion transporter; HP, protein of unknown function. Numbers below clusters designate IMG locus tags.

**TABLE S1** | List of *Alteromonas* genomes analyzed, including gene and CAZyme count.

**TABLE S2** | Sheet Alt761\_CDS: Complete list of protein-coding sequences of *Alteromonas* sp. 76-1 including CAZyme prediction using dbCAN2, KEGG annotation using KAAS, and protease/peptidase prediction using MEROPS. Sheet Uniques\_Alt761\_SN2: Unique genes and associated KEGG classifications in *Alteromonas* strains 76-1 and SN2, including CAZyme prediction using dbCAN2 and KEGG annotation using KAAS.

**TABLE S3** | Detection of transcripts homologous to alginate lyases PL7\_AS1 (alt76\_01684) and PL6\_AS2 (alt76\_03417) from *Alteromonas* sp. 76-1 in marine metatranscriptomes. Red label: co-detection of both transcripts in the same metatranscriptome. The picture insert illustrates origin of 76-1 and co-detection of alginate lyases in metatranscriptomes from nearby locations.

**TABLE S4** | Hydrolysis of AZO-CL polymers by *Alteromonas* sp. 76-1 and proposedly involved genes.

## REFERENCES

- Acha, E. M., Mianzan, H. W., Guerrero, R. A., Favero, M., and Bava, J. (2004). Marine fronts at the continental shelves of austral South America: physical and ecological processes. *J. Mar. Syst.* 44, 83–105. doi: 10.1016/j.jmarsys.2003.09.005
- Alexander, D. B., and Zuberer, D. A. (1991). Use of chrome azurol S reagents to evaluate siderophore production by rhizosphere bacteria. *Biol. Fertility Soils* 12, 39–45. doi: 10.1007/BF00369386
- Aluwihare, L. I., and Repeta, D. J. (1999). A comparison of the chemical characteristics of oceanic DOM and extracellular DOM produced by marine algae. *Mar. Ecol. Prog. Ser.* 186, 105–117. doi: 10.3354/meps186105
- Arnosti, C., Steen, A. D., Ziervogel, K., Ghobrial, S., and Jeffrey, W. H. (2011). Latitudinal gradients in degradation of marine dissolved organic carbon. *PLoS One* 6:e28900. doi: 10.1371/journal.pone.0028900
- Benner, R., Pakulski, J. D., Mccarthy, M., Hedges, J. I., and Hatcher, P. G. (1992). Bulk chemical characteristics of dissolved organic matter in the ocean. *Science* 255, 1561–1564. doi: 10.1126/science.255.5051.1561
- Berman, H. M., Westbrook, J., Feng, Z., Gilliland, G., Bhat, T. N., Weissig, H., et al. (2000). The protein data bank. *Nucleic Acids Res.* 28, 235–242. doi: 10.1093/nar/28.1.235
- Boiteau, R. M., Mende, D. R., Hawco, N. J., Mcilvin, M. R., Fitzsimmons, J. N., Saito, M. A., et al. (2016). Siderophore-based microbial adaptations to iron scarcity across the eastern Pacific Ocean. *Proc. Natl. Acad. Sci. U.S.A.* 113, 14237–14242. doi: 10.1073/pnas.1608594113
- Chaudhari, N. M., Gupta, V. K., and Dutta, C. (2016). BPGA- an ultra-fast pan-genome analysis pipeline. *Sci. Rep.* 6:24373. doi: 10.1038/srep24373
- Chi, W.-J., Park, D. Y., Seo, Y. B., Chang, Y. K., Lee, S.-Y., and Hong, S.-K. (2014). Cloning, expression, and biochemical characterization of a novel GH16  $\beta$ -agarase AgaG1 from *Alteromonas* sp. GNUM-1. *Appl. Microbiol. Biotechnol.* 98, 4545–4555. doi: 10.1007/s00253-014-5510-4
- Corzett, C. H., Elsherbini, J., Chien, D. M., Hehemann, J.-H., Henschel, A., Preheim, S. P., et al. (2018). Evolution of a vegetarian vibrio: metabolic specialization of *V. breoganii* to macroalgal substrates. *J. Bacteriol.* 200:e00020-18. doi: 10.1128/JB.00020-18
- Cozzi, S., Mistarò, A., Sparnocchia, S., Colugnati, L., Bajt, O., and Toniatti, L. (2014). Anthropogenic loads and biogeochemical role of urea in the Gulf of Trieste. *Sci. Total Environ.* 493, 271–281. doi: 10.1016/j.scitotenv.2014.05.148
- Darriba, D., Taboada, G. L., Doallo, R., Posada, D. (2011). ProtTest 3: fast selection of best-fit models of protein evolution. *Bioinformatics* 27, 1164–1165. doi: 10.1093/bioinformatics/btr088
- Darriba, D., Taboada, G. L., Doallo, R., and Posada, D. (2012). jModelTest 2: more models, new heuristics and parallel computing. *Nat. Methods* 9, 772–772. doi: 10.1038/nmeth.2109
- Do, C. B., Mahabhashyam, M. S. P., Brudno, M., and Batzoglou, S. (2005). ProbCons: probabilistic consistency-based multiple sequence alignment. *Genome Res.* 15, 330–340. doi: 10.1101/gr.2821705
- Dong, S., Wei, T.-D., Chen, X.-L., Li, C.-Y., Wang, P., Xie, B.-B., et al. (2014). Molecular insight into the role of the n-terminal extension in the maturation, substrate recognition, and catalysis of a bacterial alginate lyase from polysaccharide lyase family 18. *J. Biol. Chem.* 289, 29558–29569. doi: 10.1074/jbc.M114.584573
- Dorman, C. J., and Dorman, M. J. (2016). DNA supercoiling is a fundamental regulatory principle in the control of bacterial gene expression. *Biophys. Rev.* 8, 89–100. doi: 10.1007/s12551-016-0238-2
- Ekborg, N. A., Gonzalez, J. M., Howard, M. B., Taylor, L. E., Hutcheson, S. W., and Weiner, R. M. (2005). *Saccharophagus degradans* gen. nov., sp. nov., a versatile marine degrader of complex polysaccharides. *Int. J. Syst. Evol. Microbiol.* 55, 1545–1549. doi: 10.1099/ijss.0.63627-0
- Fernández-Gómez, B., Richter, M., Schüler, M., Pinhasi, J., Acinas, S. G., González, J. M., et al. (2013). Ecology of marine *Bacteroidetes*: a comparative genomics approach. *ISME J.* 7, 1026–1037. doi: 10.1038/ismej.2012.169
- Ficko-Blean, E., Préchoux, A., Thomas, F., Rochat, T., Larocque, R., Zhu, Y., et al. (2017). Carrageenan catabolism is encoded by a complex regulon in marine heterotrophic bacteria. *Nat. Commun.* 8:1685. doi: 10.1038/s41467-017-01832-6
- Foran, E., Buravenkov, V., Kopel, M., Mizrahi, N., Shoshani, S., Helbert, W., et al. (2017). Functional characterization of a novel “ulvan utilization loci” found in *Alteromonas* sp. LOR genome. *Algal Res.* 25, 39–46. doi: 10.1016/j.algal.2017.04.036
- Fuchsman, C. A., Collins, R. E., Rocap, G., and Brazelton, W. J. (2017). Effect of the environment on horizontal gene transfer between bacteria and archaea. *PeerJ* 5:e3865. doi: 10.7717/peerj.3865
- Fuhrman, L. K., Wanken, A., Nickerson, K. W., and Conway, T. (1998). Rapid accumulation of intracellular 2-keto-3-deoxy-6-phosphogluconate in an Entner-Doudoroff aldolase mutant results in bacteriostasis. *FEMS Microbiol. Lett.* 159, 261–266. doi: 10.1111/j.1574-6968.1998.tb12870.x
- García, V. M. T., García, C. A. E., Mata, M. M., Pollery, R. C., Piola, A. R., Signorini, S. R., et al. (2008). Environmental factors controlling the phytoplankton blooms at the Patagonia shelf-break in spring. *Deep Sea Res. I* 55, 1150–1166. doi: 10.1016/j.dsr.2008.04.011
- Gobet, A., Barbeyron, T., Matard-Mann, M., Magdelenat, G., Vallenet, D., Duchaud, E., et al. (2018a). Evolutionary evidence of algal polysaccharide degradation acquisition by *Pseudoalteromonas carrageenovora* 9T to adapt to macroalgal niches. *Front. Microbiol.* 9:2740. doi: 10.3389/fmicb.2018.02740
- Gobet, A., Mest, L., Perennou, M., Dittami, S. M., Caralp, C., Coulombet, C., et al. (2018b). Seasonal and algal diet-driven patterns of the digestive microbiota of the European abalone *Haliotis tuberculata*, a generalist marine herbivore. *Microbiome* 6:60. doi: 10.1186/s40168-018-0430-7
- Grondin, J. M., Tamura, K., Déjean, G., Abbott, D. W., and Brumer, H. (2017). Polysaccharide utilization loci: fuelling microbial communities. *J. Bacteriol.* 199:e00860-16. doi: 10.1128/JB.00860-16
- Guy, L., Roat Kultima, J., and Andersson, S. G. E. (2010). genoPlotR: comparative gene and genome visualization in R. *Bioinformatics* 26, 2334–2335. doi: 10.1093/bioinformatics/btq413
- Hahnke, R. L., and Harder, J. (2013). Phylogenetic diversity of *Flavobacteria* isolated from the North Sea on solid media. *Syst. Appl. Microbiol.* 36, 497–504. doi: 10.1016/j.syapm.2013.06.006
- Hehemann, J.-H., Boraston, A. B., and Czjzek, M. (2014). A sweet new wave: structures and mechanisms of enzymes that digest polysaccharides from marine algae. *Curr. Opin. Struct. Biol.* 28, 77–86. doi: 10.1016/j.sbi.2014.07.009
- Hehemann, J.-H., Correc, G., Thomas, F., Bernard, T., Barbeyron, T., Jam, M., et al. (2012). Biochemical and structural characterization of the complex agarolytic enzyme system from the marine bacterium *Zobellia galactanivorans*. *J. Biol. Chem.* 287, 30571–30584. doi: 10.1074/jbc.M112.377184
- Hehemann, J.-H., Truong, L. V., Unfried, F., Welsch, N., Kabisch, J., Heiden, S. E., et al. (2017). Aquatic adaptation of a laterally acquired pectin degradation pathway in marine gammaproteobacteria. *Environ. Microbiol.* 19, 2320–2333. doi: 10.1111/1462-2920.13726
- Hehemann, J.-H. H., Arevalo, P., Datta, M. S., Yu, X., Corzett, C. H., Henschel, A., et al. (2016). Adaptive radiation by waves of gene transfer leads to fine-scale resource partitioning in marine microbes. *Nat. Commun.* 7:12860. doi: 10.1038/ncomms12860
- Hjelm, M., Bergh, I., Riazia, A., Nielsen, J., Melchiorson, J., Jensen, S., et al. (2004). Selection and identification of autochthonous potential probiotic bacteria from turbot larvae (*Scophthalmus maximus*) rearing units. *Syst. Appl. Microbiol.* 27, 360–371. doi: 10.1078/0723-2020-00256
- Hülter, N., Ilhan, J., Wein, T., Kadibalban, A. S., Hammerschmidt, K., and Dagan, T. (2017). An evolutionary perspective on plasmid lifestyle modes. *Curr. Opin. Microbiol.* 38, 74–80. doi: 10.1016/j.mib.2017.05.001
- Inoue, A., Nishiyama, R., Mochizuki, S., and Ojima, T. (2015). Identification of a 4-deoxy-L-erythro-5-hexoseulose uronic acid reductase, FRed, in an alginate lyase bacterium *Flavobacterium* sp. strain UMI-01. *Mar. Drugs* 13, 493–508. doi: 10.3390/md13010493
- Jin, H. M., Jeong, H. I., Kim, K. H., Hahn, Y., Madsen, E. L., and Jeon, C. O. (2016). Genome-wide transcriptional responses of *Alteromonas naphthalenivorans* SN2 to contaminated seawater and marine tidal flat sediment. *Sci. Rep.* 6:21796. doi: 10.1038/srep21796
- Kabisch, A., Otto, A., König, S., Becher, D., Albrecht, D., Schüler, M., et al. (2014). Functional characterization of polysaccharide utilization loci in the marine *Bacteroidetes* ‘Gramella forsetii’ KT0803. *ISME J.* 8, 1492–1502. doi: 10.1038/ismej.2014.4
- Koboldt, D. C., Zhang, Q., Larson, D. E., Shen, D., Mclellan, M. D., Lin, L., et al. (2012). VarScan 2: somatic mutation and copy number alteration discovery in

- cancer by exome sequencing. *Genome Res.* 22, 568–576. doi: 10.1101/gr.129684.111
- Koch, H., Dürwald, A., Schweder, T., Noriega-Ortega, B., Vidal-Melgosa, S., Hehemann, J.-H., et al. (2019). Biphasic cellular adaptations and ecological implications of *Alteromonas macleodii* degrading a mixture of algal polysaccharides. *ISME J.* 13, 92–103. doi: 10.1038/s41396-018-0252-4
- Konasani, V. R., Jin, C., Karlsson, N. G., and Albers, E. (2018). A novel ulvan lyase family with broad-spectrum activity from the ulvan utilisation loci of *Formosa agariphila* KMM 3901. *Sci. Rep.* 8:14713. doi: 10.1038/s41598-018-32922-0
- Kopel, M., Helbert, W., Belnik, Y., Buravenkov, V., Herman, A., and Banin, E. (2016). New family of ulvan lyases identified in three isolates from the alteromonadales order. *J. Biol. Chem.* 291, 5871–5878. doi: 10.1074/jbc.M115.673947
- Kraan, S. (2012). “Algal polysaccharides, novel applications and outlook,” in *Carbohydrates*, ed. C.-F. Chang (Rijeka: InTech).
- Krzywinski, M., Schein, J., Birol, I., Connors, J., Gascoyne, R., Horsman, D., et al. (2009). Circos: an information aesthetic for comparative genomics. *Genome Res.* 19, 1639–1645. doi: 10.1101/gr.092759.109
- Labourel, A., Jam, M., Jeudy, A., Hehemann, J.-H., Czjzek, M., and Michel, G. (2014). The  $\beta$ -glucanase ZgLamA from *Zobellia galactanivorans* evolved a bent active site adapted for efficient degradation of algal laminarin. *J. Biol. Chem.* 289, 2027–2042. doi: 10.1074/jbc.M113.538843
- Li, H., and Durbin, R. (2009). Fast and accurate short read alignment with Burrows-Wheeler transform. *Bioinformatics* 25, 1754–1760. doi: 10.1093/bioinformatics/btp324
- Lombard, V., Golaconda Ramulu, H., Drula, E., Coutinho, P. M., and Henrissat, B. (2014). The carbohydrate-active enzymes database (CAZy) in 2013. *Nucleic Acids Res.* 42, D490–D495. doi: 10.1093/nar/gkt1178
- López-Pérez, M., Ramon-Marco, N., and Rodríguez-Valera, F. (2017). Networking in microbes: conjugative elements and plasmids in the genus *Alteromonas*. *BMC Genomics* 18:36. doi: 10.1186/s12864-016-3461-0
- Lyu, Q., Zhang, K., Zhu, Q., Li, Z., Liu, Y., Fitzek, E., et al. (2018). Structural and biochemical characterization of a multidomain alginate lyase reveals a novel role of CBM32 in CAZymes. *Biochim. Biophys. Acta Gen. Subj.* 1862, 1862–1869. doi: 10.1016/j.bbagen.2018.05.024
- MacLean, R. C., and San Millan, A. (2015). Microbial evolution: towards resolving the plasmid paradox. *Curr. Biol.* 25, R764–R767. doi: 10.1016/J.CUB.2015.07.006
- Mann, A. J., Hahnke, R. L., Huang, S., Werner, J., Xing, P., Barbeyron, T., et al. (2013). The genome of the alga-associated marine flavobacterium *Formosa agariphila* KMM 3901<sup>T</sup> reveals a broad potential for degradation of algal polysaccharides. *Appl. Environ. Microbiol.* 79, 6813–6822. doi: 10.1128/AEM.01937-13
- Martinez-Garcia, M., Brazel, D. M., Swan, B. K., Arnosti, C., Chain, P. S. G., Reitenga, K. G., et al. (2012). Capturing single cell genomes of active polysaccharide degraders: an unexpected contribution of Verrucomicrobia. *PLoS One* 7:e35314. doi: 10.1371/journal.pone.0035314
- Math, R. K., Jin, H. M., Kim, J. M., Hahn, Y., Park, W., Madsen, E. L., et al. (2012). Comparative genomics reveals adaptation by *Alteromonas* sp. SN2 to marine tidal-flat conditions: cold tolerance and aromatic hydrocarbon metabolism. *PLoS One* 7:e35784. doi: 10.1371/journal.pone.0035784
- Matos, M. N., Lozada, M., Anselmino, L. E., Musumeci, M. A., Henrissat, B., Jansson, J. K., et al. (2016). Metagenomics unveils the attributes of the alginolytic guilds of sediments from four distant cold coastal environments. *Environ. Microbiol.* 18, 4471–4484. doi: 10.1111/1462-2920.13433
- McKenna, A., Hanna, M., Banks, E., Sivachenko, A., Cibulskis, K., Kernysky, A., et al. (2010). The genome analysis toolkit: a MapReduce framework for analyzing next-generation DNA sequencing data. *Genome Res.* 20, 1297–1303. doi: 10.1101/gr.107524.110
- Medema, M. H., Takano, E., and Breitling, R. (2013). Detecting sequence homology at the gene cluster level with MultiGeneBlast. *Mol. Biol. Evol.* 30, 1218–1223. doi: 10.1093/molbev/mst025
- Meier-Kolthoff, J. P., Auch, A. F., Klenk, H.-P., and Göker, M. (2013). Genome sequence-based species delimitation with confidence intervals and improved distance functions. *BMC Bioinformatics* 14:60. doi: 10.1186/1471-2105-14-60
- Michel, G., and Czjzek, M. (2013). “Polysaccharide-degrading enzymes from marine bacteria,” in *Marine Enzymes for Biocatalysis*, ed. A. Trincone (Cambridge: Woodhead Publishing).
- Miller, M. A., Pfeiffer, W., and Schwartz, T. (2010). “Creating the CIPRES science gateway for inference of large phylogenetic trees,” in *Proceedings of the Gateway Computing Environments Workshop (GCE)*, (New Orleans), 1–8. doi: 10.1109/GCE.2010.5676129
- Mitulla, M., Dinasquet, J., Guillemette, R., Simon, M., Azam, F., and Wietz, M. (2016). Response of bacterial communities from California coastal waters to alginate particles and an alginolytic *Alteromonas macleodii* strain. *Environ. Microbiol.* 18, 4369–4377. doi: 10.1111/1462-2920.13314
- Mootz, H. D., and Marahiel, M. A. (1997). The tyrocidine biosynthesis operon of *Bacillus brevis*: complete nucleotide sequence and biochemical characterization of functional internal adenylation domains. *J. Bacteriol.* 179, 6843–6850. doi: 10.1128/jb.179.21.6843-6850.1997
- Moriya, Y., Itoh, M., Okuda, S., Yoshizawa, A. C., and Kanehisa, M. (2007). KAA5: an automatic genome annotation and pathway reconstruction server. *Nucleic Acids Res.* 35, W182–W185. doi: 10.1093/nar/gkm321
- Na, S.-I., Kim, Y. O., Yoon, S.-H., Ha, S.-M., Baek, I., and Chun, J. (2018). UBCG: up-to-date bacterial core gene set and pipeline for phylogenomic tree reconstruction. *J. Microbiol.* 56, 281–285. doi: 10.1007/s12275-018-8014-6
- Neumann, A. M., Balmonte, J. P., Berger, M., Giebel, H. A., Arnosti, C., Brinkhoff, T., et al. (2015). Different utilization of alginate and other algal polysaccharides by marine *Alteromonas macleodii* ecotypes. *Environ. Microbiol.* 17, 3857–3868. doi: 10.1111/1462-2920.12862
- Oliveira, P. H., Touchon, M., Cury, J., and Rocha, E. P. C. (2017). The chromosomal organization of horizontal gene transfer in bacteria. *Nat. Commun.* 8:41. doi: 10.1038/s41467-017-00808-w
- Pansch, I., Huang, S., Meier-Kolthoff, J. P., Tindall, B. J., Rohde, M., Verburg, S., et al. (2016). Comparing polysaccharide decomposition between the type strains *Gramella echinicola* KMM 6050<sup>T</sup> (DSM 19838<sup>T</sup>) and *Gramella portivictoriae* UST040801-001<sup>T</sup> (DSM 23547<sup>T</sup>), and emended description of *Gramella echinicola*. *Stand. Gen. Sci.* 11, 1–16. doi: 10.1186/s40793-016-0163-9
- Park, D., Jagtap, S., and Nair, S. K. (2014). Structure of a PL17 family alginate lyase demonstrates functional similarities among exotype depolymerases. *J. Biol. Chem.* 289, 8645–8655. doi: 10.1074/jbc.M113.531111
- Parks, D. H., Imelfort, M., Skennerton, C. T., Hugenholtz, P., and Tyson, G. W. (2015). CheckM: assessing the quality of microbial genomes recovered from isolates, single cells, and metagenomes. *Genome Res.* 25, 1043–1055. doi: 10.1101/gr.186072.114
- Patin, N. V., Schorn, M., Aguinaldo, K., Lincecum, T., Moore, B. S., and Jensen, P. R. (2017). Effects of actinomycete secondary metabolites on sediment microbial communities. *Appl. Environ. Microbiol.* 83:e2676-16. doi: 10.1128/AEM.02676-16
- Peteiro, C. (2018). “Alginate production from marine macroalgae, with emphasis on kelp farming,” in *Alginates and Their Biomedical Applications*, eds B. A. H. Rehm and M. Fata Moradali (Singapore: Springer), 27–66.
- Qin, H.-M., Xu, P., Guo, Q., Cheng, X., Gao, D., Sun, D., et al. (2018). Biochemical characterization of a novel ulvan lyase from *Pseudoalteromonas* sp. strain PLSV. *RSC Adv.* 8, 2610–2615. doi: 10.1039/C7RA12294B
- Rawlings, N. D., Barrett, A. J., Thomas, P. D., Huang, X., Bateman, A., and Finn, R. D. (2018). The MEROPS database of proteolytic enzymes, their substrates and inhibitors in 2017 and a comparison with peptidases in the PANTHER database. *Nucleic Acids Res.* 46, D624–D632. doi: 10.1093/nar/gkx1134
- Reintjes, G., Arnosti, C., Fuchs, B. M., and Amann, R. (2017). An alternative polysaccharide uptake mechanism of marine bacteria. *ISME J.* 11, 1640–1650. doi: 10.1038/ismej.2017.26
- Rodríguez-R, L. M., and Konstantinidis, K. T. (2016). The envomics collection: a toolbox for specialized analyses of microbial genomes and metagenomes. *PeerJ Preprints* 4:e1900v1. doi: 10.7287/PEERJ.PREPRINTS.1900V1
- Romero, S. I., Piola, A. R., Charo, M., and Garcia, C. A. E. (2006). Chlorophyll *a* variability off Patagonia based on SeaWiFS data. *J. Geophys. Res.* 111:C05021. doi: 10.1029/2005JC003244
- Rossi, F., and De Philippis, R. (2016). “Exocellular polysaccharides in microalgae and cyanobacteria: chemical features, role and enzymes and genes involved in their biosynthesis,” in *The Physiology of Microalgae*, eds M. A. Borowitzka, J. Beardall, and J. A. Raven (New York, NY: Springer International Publishing), 565–590.
- Schultz-Johansen, M., Bech, P. K., Hennessy, R. C., Glaring, M. A., Barbeyron, T., Czjzek, M., et al. (2018). A novel enzyme portfolio for red algal polysaccharide degradation in the marine bacterium *Paraglaciicola hydrolytica* S66<sup>T</sup> encoded

- in a sizeable polysaccharide utilization locus. *Front. Microbiol.* 9:839. doi: 10.3389/fmicb.2018.00839
- Schwyn, B., and Neilands, J. B. (1987). Universal chemical assay for the detection and determination of siderophores. *Anal. Biochem.* 160, 47–56. doi: 10.1016/0003-2697(87)90612-9
- Sim, P.-F., Furusawa, G., and Teh, A.-H. (2017). Functional and structural studies of a multidomain alginate lyase from *Persicobacter* sp. CCB-QB2. *Sci. Rep.* 7:13656. doi: 10.1038/s41598-017-13288-1
- Stamatakis, A. (2014). RAxML version 8: a tool for phylogenetic analysis and post-analysis of large phylogenies. *Bioinformatics* 30, 1312–1313. doi: 10.1093/bioinformatics/btu033
- Taubert, M., Grob, C., Howat, A. M., Burns, O. J., Pratscher, J., Jehmlich, N., et al. (2017). Methylamine as a nitrogen source for microorganisms from a coastal marine environment. *Environ. Microbiol.* 19, 2246–2257. doi: 10.1111/1462-2920.13709
- Taylor, J. D., and Cunliffe, M. (2017). Coastal bacterioplankton community response to diatom-derived polysaccharide microgels. *Environ. Microbiol. Rep.* 9, 151–157. doi: 10.1111/1758-2229.12513
- Teeling, H., Fuchs, B. M., Becher, D., Klockow, C., Gardebrecht, A., Bennis, C. M., et al. (2012). Substrate-controlled succession of marine bacterioplankton populations induced by a phytoplankton bloom. *Science* 336, 608–611. doi: 10.1126/science.1218344
- Teeling, H., Fuchs, B. M., Bennis, C. M., Krüger, K., Chafee, M., Kappelmann, L., et al. (2016). Recurring patterns in bacterioplankton dynamics during coastal spring algae blooms. *eLife* 5:e11888. doi: 10.7554/eLife.11888
- The UniProt Consortium (2017). UniProt: the universal protein knowledgebase. *Nucleic Acids Res.* 45, D158–D169. doi: 10.1093/nar/gkw1099
- Thomas, F., Barbeyron, T., Tonon, T., Génicot, S., Czjzek, M., and Michel, G. (2012). Characterization of the first alginolytic operons in a marine bacterium: from their emergence in marine *Flavobacteriia* to their independent transfers to marine *Proteobacteria* and human gut *Bacteroides*. *Environ. Microbiol.* 14, 2379–2394. doi: 10.1111/j.1462-2920.2012.02751.x
- Thomas, F., Bordron, P., Eveillard, D., and Michel, G. (2017). Gene expression analysis of *Zobellia galactanivorans* during the degradation of algal polysaccharides reveals both substrate-specific and shared transcriptome-wide responses. *Front. Microbiol.* 8:1808. doi: 10.3389/fmicb.2017.01808
- Thomas, F., Lundqvist, L. C., Jam, M., Jeudy, A., Barbeyron, T., Sandstrom, C., et al. (2013). Comparative characterization of two marine alginate lyases from *Zobellia galactanivorans* reveals distinct modes of action and exquisite adaptation to their natural substrate. *J. Biol. Chem.* 288, 23021–23037. doi: 10.1074/jbc.M113.467217
- Thomas, H., Bozec, Y., Elkalay, K., and De Baar, H. J. W. (2004). Enhanced open ocean storage of CO<sub>2</sub> from shelf sea pumping. *Science* 304, 1005–1008. doi: 10.1126/science.1095491
- Ulaganathan, T., Boniecki, M. T., Foran, E., Buravenkov, V., Mizrachi, N., Banin, E., et al. (2017). New ulvan-degrading polysaccharide lyase family: structure and catalytic mechanism suggests convergent evolution of active site architecture. *ACS Chem. Biol.* 12, 1269–1280. doi: 10.1021/acscchembio.7b00126
- Ulaganathan, T., Helbert, W., Kopel, M., Banin, E., and Cygler, M. (2018). Structure-function analyses of a PL24 family ulvan lyase reveal key features and suggest its catalytic mechanism. *J. Biol. Chem.* 293, 4026–4036. doi: 10.1074/jbc.RA117.001642
- Wietz, M., Wemheuer, B., Simon, H., Giebel, H. A., Seibt, M. A., Daniel, R., et al. (2015). Bacterial community dynamics during polysaccharide degradation at contrasting sites in the Southern and Atlantic Oceans. *Environ. Microbiol.* 17, 3822–3831. doi: 10.1111/1462-2920.12842
- Xu, F., Dong, F., Wang, P., Cao, H. Y., Li, C. Y., Li, P. Y., et al. (2017). Novel molecular insights into the catalytic mechanism of marine bacterial alginate lyase AlyGC from polysaccharide lyase family 6. *J. Biol. Chem.* 292, 4457–4468. doi: 10.1074/jbc.M116.766030
- Zech, H., Thole, S., Schreiber, K., Kalthöfer, D., Voget, S., Brinkhoff, T., et al. (2009). Growth phase-dependent global protein and metabolite profiles of *Phaeobacter gallaeciensis* strain DSM 17395, a member of the marine *Roseobacter*-clade. *Proteomics* 9, 3677–3697. doi: 10.1002/pmic.2009.00120
- Zhang, H., Yohe, T., Huang, L., Entwistle, S., Wu, P., Yang, Z., et al. (2018). dbCAN2: a meta server for automated carbohydrate-active enzyme annotation. *Nucleic Acids Res.* 46, W95–W101. doi: 10.1093/nar/gky418
- Zhong, Z., Toukdarian, A., Helinski, D., Knauf, V., Sykes, S., Wilkinson, J. E., et al. (2001). Sequence analysis of a 101-kilobase plasmid required for agar degradation by a *Microscilla* isolate. *Appl. Environ. Microbiol.* 67, 5771–5779. doi: 10.1128/AEM.67.12.5771-5779.2001
- Zhu, Y., Chen, P., Bao, Y., Men, Y., Zeng, Y., Yang, J., et al. (2016). Complete genome sequence and transcriptomic analysis of a novel marine strain *Bacillus weihaiensis* reveals the mechanism of brown algae degradation. *Sci. Rep.* 6:38248. doi: 10.1038/srep38248
- Zhu, Y., Thomas, F., Larocque, R., Li, N., Duffieux, D., Cladière, L., et al. (2017). Genetic analyses unravel the crucial role of a horizontally acquired alginate lyase for brown algal biomass degradation by *Zobellia galactanivorans*. *Environ. Microbiol.* 19, 2164–2181. doi: 10.1111/1462-2920.13699

**Conflict of Interest Statement:** The authors declare that the research was conducted in the absence of any commercial or financial relationships that could be construed as a potential conflict of interest.

Copyright © 2019 Koch, Freese, Hahnke, Simon and Wietz. This is an open-access article distributed under the terms of the Creative Commons Attribution License (CC BY). The use, distribution or reproduction in other forums is permitted, provided the original author(s) and the copyright owner(s) are credited and that the original publication in this journal is cited, in accordance with accepted academic practice. No use, distribution or reproduction is permitted which does not comply with these terms.

## Appendix 5

### **Response of bacterial communities from California coastal waters to alginate particles and an alginolytic *Alteromonas macleodii* strain**

Mitulla M, Dinasquet J, Guillemette R, Simon M, Azam F, Wietz M  
*Environmental Microbiology* (2016), 18:4369–4377

# Response of bacterial communities from California coastal waters to alginate particles and an alginolytic *Alteromonas macleodii* strain

Maximilian Mitulla,<sup>1</sup> Julie Dinasquet,<sup>2,3</sup>  
Ryan Guillemette,<sup>2</sup> Meinhard Simon,<sup>1</sup>  
Farooq Azam<sup>2</sup> and Matthias Wietz<sup>1\*</sup>

<sup>1</sup>Institute for Chemistry and Biology of the Marine Environment, University of Oldenburg, 26129 Oldenburg, Germany.

<sup>2</sup>Marine Biology Research Division, Scripps Institution of Oceanography, University of California San Diego, La Jolla, CA 92037, USA.

<sup>3</sup>Laboratoire d'Océanographie Microbienne (LOMIC), Observatoire Océanologique de Banyuls sur mer, Sorbonne Universités, UPMC, France.

## Summary

Alginate is a major cell wall polysaccharide from marine macroalgae and nutrient source for heterotrophic bacteria. Alginate can form gel particles in contact with divalent cations as found in seawater. Here, we tested the hypothesis that alginate gel particles serve as carbon source and microhabitat for marine bacteria by adding sterile alginate particles to microcosms with seawater from coastal California, a habitat rich in alginate-containing macroalgae. Alginate particles were rapidly colonized and degraded, with three- to eightfold higher bacterial abundances and production among alginate particle-associated (PA) bacteria. 16S rRNA gene amplicon sequencing showed that alginate PA bacteria were enriched in OTUs related to *Cryomorpaceae*, *Saprospiraceae* (*Bacteroidetes*) and *Phaeobacter* (*Alphaproteobacteria*) towards the end of the experiment. In microcosms amended with alginate particles and the proficient alginolytic bacterium *Alteromonas macleodii* strain 83-1, this strain dominated the community and outcompeted *Cryomorpaceae*, *Saprospiraceae* and *Phaeobacter*, and PA hydrolytic activities were over 50% higher. Thus, alginolytic activity by strain 83-1 did not benefit

non-alginolytic strains by cross-feeding on alginate hydrolysis or other metabolic products. Considering the global distribution and extensive biomass of alginate-containing macroalgae, the observed bacterial dynamics associated with the utilization and remineralization of alginate microhabitats promote the understanding of carbon cycling in macroalgae-rich waters worldwide.

## Introduction

Particulate organic matter (POM) can be both nutrient source and habitat for heterotrophic marine bacteria. The remineralization of POM is a major process in oceanic carbon fluxes (Azam and Malfatti, 2007), and comprehensive knowledge on bacterial POM colonization and degradation is important to elucidate the cycling of organic carbon within the microbial loop (Azam, 1998). POM often accounts for the majority of bacterial production (Alldredge *et al.*, 1995; Riemann *et al.*, 2000) and harbors distinct communities that differ from planktonic counterparts (Simon *et al.* 2002; Simon *et al.*, 2014), probably due to adaptive traits of particle colonizers including hydrolytic enzyme activities, chemotaxis, and motility (Stocker, 2012). However, the relationship between the degradation of specific POM substrates and bacterial community dynamics is not well understood.

POM contains a substantial amount of polysaccharides (Lampitt *et al.*, 1993) that can serve as nutrient source for different bacterial taxa (Gómez-Pereira *et al.*, 2012; Michel and Czjzek, 2013; Cardman *et al.*, 2014). In coastal marine waters, a considerable fraction of POM-bound polysaccharides may be derived from macroalgae, where they function as major structural and storage compounds (Mabeau and Kloareg, 1987). One of the most abundant macroalgal polysaccharides is alginate, which consists of the uronic acids  $\beta$ -(1-4)-D-mannuronate and its C5 epimer  $\alpha$ -(1-4)-L-guluronate and can represent up to 60% of brown macroalgae dry weight (Draget *et al.*, 2005). With an estimated global standing crop of 30 Gt brown macroalgae

Received 16 February, 2016; accepted 23 March, 2016. \*For correspondence. E-mail matthias.wietz@uni-oldenburg.de; Tel. +49-441-7983637; Fax +49-441-7983438.

(De Vooy, 1979; Zemke-White and Ohno, 1999), the global steady-state amount of alginate may constitute up to 15 Gt, representing a central component of the carbon budget. However, despite the global distribution of brown macroalgae and their diverse microbial associates (Martin *et al.*, 2014), detailed insights into bacterial community dynamics during the degradation of alginate are still scarce. For instance, contrasting marine regions have been shown to feature specific bacterial community patterns during alginate degradation, including a stimulation of *Alteromonas* spp. in the southern Atlantic (Wietz *et al.*, 2015). The pronounced alginolytic potential among flavobacterial (Thomas *et al.*, 2012; Mann *et al.*, 2013; Kabisch *et al.*, 2014) and gammaproteobacterial (Jagtap *et al.*, 2014; Neumann *et al.*, 2015) strains suggests an ecological relevance of alginolytic traits, warranting further studies on bacterial alginate degradation *in situ*.

Alginate can form gel-like particles in contact with divalent cations as found in seawater, such as  $\text{Ca}^{2+}$  and  $\text{Mg}^{2+}$ . Supported by the notion that marine organic matter can naturally assemble into gels (Chin *et al.*, 1998) that are productive microbial microhabitats (Verdugo, 2012) and can contain uronic acids (Hung *et al.*, 2003), we hypothesize that alginate particles may represent colonization and nutrient 'hot spots' for marine bacteria. In the present study, this hypothesis was tested by adding laboratory-made sterile alginate particles to a natural community from coastal Southern California, a habitat rich in alginate-containing macroalgae (Steneck *et al.*, 2003). The use of sterile alginate particles allowed identifying specific bacterial responses to the defined substrate, which would be challenging to study with natural POM that is of mixed composition and rapidly colonized by microbial populations (Grossart *et al.*, 2003).

In a parallel experiment, we investigated whether addition of alginate particles also stimulates non-alginolytic taxa that grow by 'cross-feeding' on uronic acids or other metabolites released by alginolytic strains. For this purpose, we added alginate particles and the proficient alginolytic bacterium *Alteromonas macleodii* strain 83-1 to the California coastal community. *A. macleodii* strain 83-1 has an extensive genomic repertoire for alginate degradation (Neumann *et al.*, 2015), and related strains were shown to be enriched during alginate degradation *in situ* (Wietz *et al.*, 2015).

Considering the global distribution and extensive biomass of alginate-containing macroalgae, the observed patterns in bacterial abundances, production, and community composition during alginate particle utilization substantially advance the understanding of biogeochemical processes that are essential to coastal carbon cycles worldwide.

## Results and discussion

### Characteristics of alginate particles

Microscopic analyses revealed that the stock solution contained 245,079 alginate particles  $\text{ml}^{-1}$ , with an average particle size of  $33 \pm 8 \mu\text{m}$ . Carbon and HPLC analyses showed that this number corresponded to 55.9  $\mu\text{g}$  particulate organic carbon (POC) and 100  $\mu\text{g}$  alginate  $\text{ml}^{-1}$  respectively. These data allowed calculating the amount of alginate per particle, yielding comparable results (0.4 ng by HPLC and 1.3 ng by POC analysis). At lower densities as used in microcosm experiments, the majority of particles were monodisperse. Higher particle densities, as present in the stock solution or as used in pure culture incubations, repeatedly resulted in the spontaneous agglomeration of particles, which may influence the dynamics of bacterial particle utilization.

### Microcosm experiments with alginate particles in California-coastal seawater

**Bacterial abundance.** Sterile alginate particles added to California seawater were rapidly colonized and degraded by the natural bacterial community as well as the alginolytic model bacterium *Alteromonas macleodii* strain 83-1 (Fig. 1). These findings support the notion that alginate particles are suitable bacterial microenvironments and carbon source. To each microcosm incubation, approximately 200,000 alginate particles were added, corresponding to a total amount of ca. 82  $\mu\text{g}$  alginate. The bacterial utilization of these particles was highlighted by increasing cell numbers in alginate-amended microcosm experiments AP and AP-ALT (Fig. 2) and concurrently decreasing concentrations of total organic carbon (TOC) (Fig. 3). In treatment AP, abundances of both free-living (FL) and particle-associated (PA) bacteria peaked after 24 h and remained constant until 48 h. FL outnumbered PA bacteria in ratios of approximately 3:2 (24 h) and 2:1 (48 h). In treatment AP-ALT, abundances of FL bacteria peaked after 24 h whereas abundances of PA bacteria peaked after 48 h (Fig. 2; Table S1), which coincided with substantially shifting ratios of FL:PA bacteria from 4:1 (24 h) to 1:1 (48 h). In both treatments AP and AP-ALT, FL and PA bacterial abundances declined to initial values after 72 h. In the control treatment CTR, FL bacterial abundances remained almost constant, and PA bacteria were only detected from 48 h onward.

**Bacterial production and TOC concentrations.** The addition of alginate particles stimulated total bacterial production up to fourfold ( $p = 0.02$ ; repeated-measure ANOVA), with a peak after 48 h in both treatments AP and AP-ALT (Fig. 3). TOC analysis revealed that addition of alginate particles introduced 10.5  $\mu\text{M}$  of organic carbon

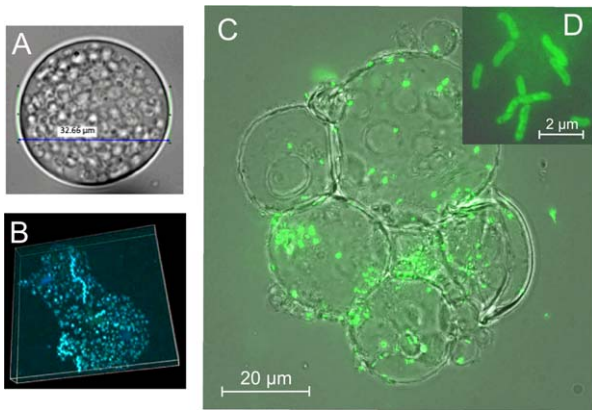


**Fig. 1.** Sterile alginate particles (A) were subsequently colonized and degraded by bacterial communities from California coastal seawater (B). SYBR Green staining revealed extensive attachment of alginolytic *Alteromonas macleodii* strain 83-1 to alginate particles (C), with cell sizes of  $>3 \mu\text{m}$  (D).

(Table S2), which was respired to  $\text{CO}_2$  in different amounts depending on the treatment. In treatment AP, 60% of the alginate-derived carbon was respired after 48 h and 66% after 96 h. In contrast, in treatment AP-ALT the added carbon was completely respired after 48 h. Among FL bacteria, all three treatments showed only minor fluctuations in cell-specific production, averaging at around  $10 \text{ fgC cell}^{-1} \text{ day}^{-1}$ , which is  $\sim 50\%$  of the biomass per cell of FL bacteria (Simon and Azam, 1989). Among PA bacteria, a strong increase in cell-specific production occurred after 96 h in both alginate-amended treatments, peaking at approximately  $60 \text{ fgC cell}^{-1} \text{ d}^{-1}$  (Fig. 4, Table S1). These numbers are equivalent to the biomass per cell of larger PA bacteria (Simon and Azam, 1989; Fig. 4, Table S1) and indicate generation times of around 2 days (FL bacteria) and 1 day (PA bacteria) respectively. Overall, concurrently decreasing TOC concentrations and increasing bacterial

cell numbers reflect a combined effect of respiration and biomass production by the community. TOC measurements indicated that bacterial growth in treatment AP required less carbon compared to AP-ALT, probably reflecting that the large and up to fourfold carbon-richer *Alteromonas* cells in treatment AP-ALT can metabolize a greater amount of carbon per cell (Pedler *et al.*, 2014). As the growth efficiency of bacteria acting on alginate particles is critical for the carbon budget, we calculated bacterial growth efficiency (BGE) following del Giorgio and Cole (1998). BGEs were overall similar in treatments AP and AP-ALT (39%), with a peak of 56% in treatment AP between 48 and 96 h, representing high values compared to recent BGE reports of 12–20% (del Giorgio *et al.*, 2011).

**Bacterial community composition.** The ambient ‘starter community’ ( $t_0$ ) as well as each replicate incubation per treatment were subjected to 16S rRNA gene amplicon sequencing to analyze community composition (FL and PA fractions combined). Rarefaction curves indicated that the diversity was covered sufficiently in most amplicon libraries (Fig. S1), with between 6,000 and 17,000 sequences of 250 nt after quality-filtering (Table S3). The biological significance of results was highlighted by overall low standard deviations between the replicates (Table S4). Non-metric multidimensional scaling (NMDS) showed that community compositions differed between  $t_0$  and each of the treatments ( $P < 0.01$ ), demonstrating that alginate amendment as well as the presence of strain 83-1 significantly influenced community dynamics (Fig. 5A and B). These patterns were related to changes in bacterial diversity and richness, which increased in treatments CTR and AP but decreased in AP-ALT (Table S3). The considerable changes in community composition upon alginate degradation were consistent with previous studies (Wietz *et al.*, 2015).

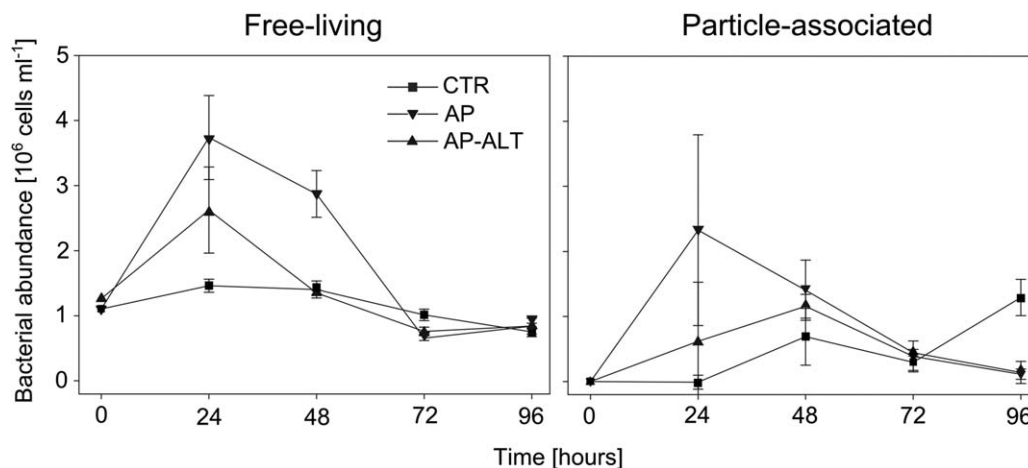


**Fig. 2.** Abundances of free-living and particle-associated bacteria in microcosm experiments CTR, AP and AP-ALT over 96 h.

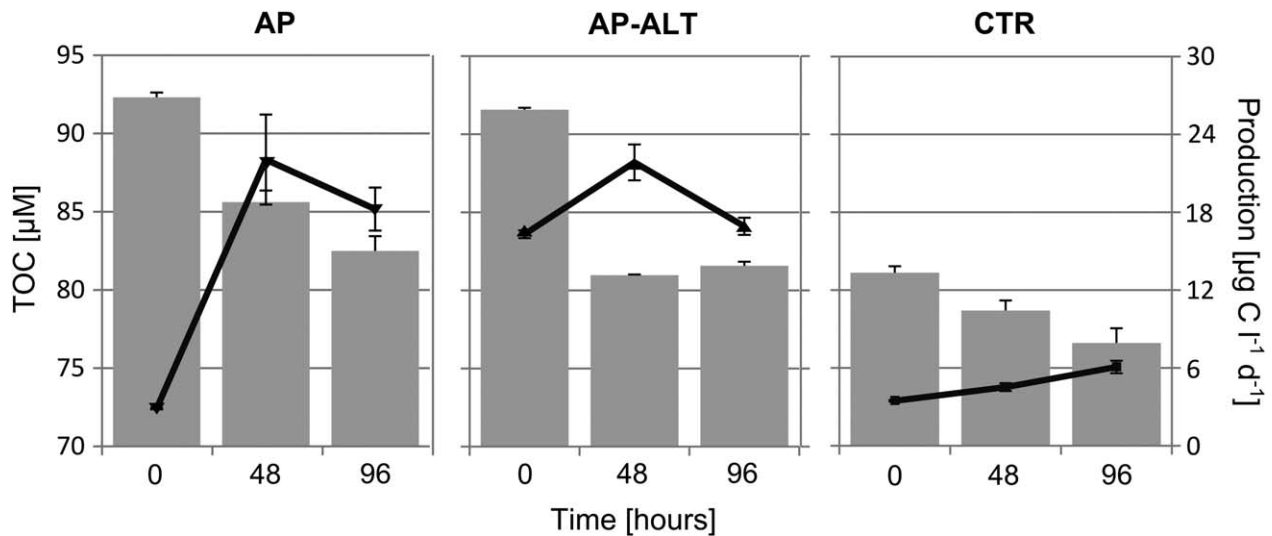


**Fig. 3.** Bacterial production (lines) and concentrations of total organic carbon (TOC; bars) in microcosm experiments CTR, AP and AP-ALT over 96 h.

Treatment AP was enriched approximately twofold in *Roseobacter* clade-affiliated bacteria albeit relative abundances of *Alphaproteobacteria* overall decreased by ~20%, indicating distinct changes among alphaproteobacterial subpopulations. The higher abundance of *Roseobacter*-affiliated OTUs with alginate particles may reflect the PA lifestyle of several roseobacters (Slightom and Buchan, 2009), however, polysaccharide degradation has been reported only rarely among this taxon (Hahnke *et al.*, 2013; Christie-Oleza *et al.*, 2015). BLAST of abundant OTU sequences revealed that the *Roseobacter*-affiliated genus *Phaeobacter* was significantly enriched (constituting  $3.3 \pm 0.6\%$ ), while taxa such as *Nereida* and SAR116 largely disappeared (Fig. 5C, Table 1). The abundant *Phaeobacter*-related OTU shares 99% 16S rRNA gene similarity to a macroalgae-derived *Phaeobacter* isolate from our culture collection (strain I 8.25; Genbank accession number KJ786471), and cultivation of this related strain with alginate as sole carbon source showed low but viable growth by microscopic analyses (data not shown). The AP-specific increase in *Bacteroidetes* was largely attributed to a *Cryomorphaceae*-related OTU ( $3\% \pm 0.8\%$ ) and the *Saprospiraceae* family ( $2.5\% \pm 0.3\%$ ), being enriched between 5- and 11-fold compared to CTR and AP-ALT regimes respectively (Fig. 5C). The stimulation of *Bacteroidetes* reflects the common occurrence of hydrolytic traits among this phylum (Fernández-Gómez *et al.*, 2013; Zimmerman *et al.*, 2013). The emergence of *Saprospiraceae* is possibly related to their known glycolytic abilities and association with macroalgae (Chen *et al.*, 2014). Treatment AP furthermore harbored higher abundances of OTUs affiliated with the *Sphingomonadales* (*Alphaproteobacteria*) as well as *Thalassomonas* and *Psychromonas*

spp. (*Gammaproteobacteria*) (Table 1). In contrast, SAR11 and OM1 clades decreased by about 50% compared to t0, CTR and AP-ALT (Fig. 5C).

In treatment AP-ALT, *Alteromonas macleodii* strain 83-1 was added to the starter community at  $5 \times 10^5$  cells ml<sup>-1</sup>, which corresponds to a relative abundance of ~10%. BLAST confirmed that the final *Alteromonas* abundance of  $20\% \pm 0.7\%$  was in fact attributed to *A. macleodii*. However, *A. macleodii* was also enriched in AP and CTR treatments, albeit at lower abundances of 2–3%. *A. macleodii* prevented the stimulation of most taxa that occurred in treatment AP, but *Colwellia* spp. established in

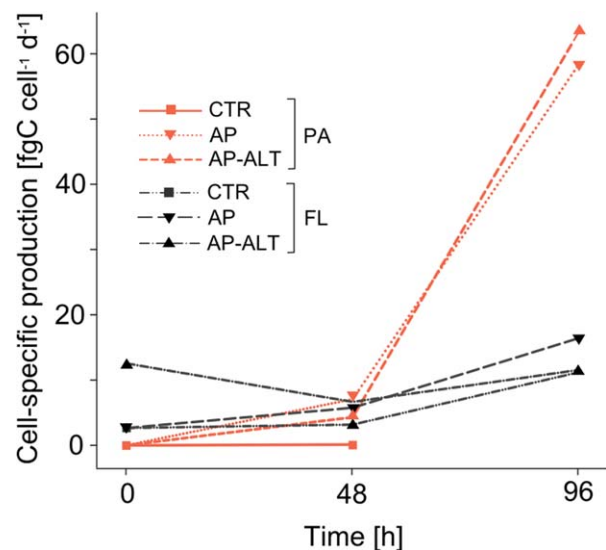


**Fig. 4.** Cell-specific production of free-living (FL) and particle-associated (PA) bacteria in microcosm experiments CTR, AP and AP-ALT over 96 h.



Changes that occurred in all treatments suggest the existence of substrate-independent bottle effects. Such effects were exemplified by the disappearance of e.g. *Nereida* spp. as well as the enrichment in *Gammaproteobacteria* across all treatments (Fig. 5B). All communities shared a stable 'core' of taxa that were neither diminished nor stimulated by the added alginate, including several *Rhodobacteraceae* lineages (Table S4).

## Conclusions

Macroalgae constitute a substantial amount of biomass in coastal oceans worldwide (Hulatt *et al.*, 2009), but the contribution of macroalgal polysaccharides to POM and their degradation by marine bacteria remain largely unknown. The present study showed that alginate particles represent highly accessible carbon 'hot spots' for heterotrophic marine bacteria. With elevated growth and production rates comparable to those in marine snow (Alldredge and Youngbluth, 1985; Simon *et al.* 2002), alginate particles were identified as attractive microhabitat and POM substrate for bacterial communities from coastal seawater. The successively increasing production of PA bacteria indicate migration of alginolytic bacteria to alginate particles, mirroring previous observations of bacterial attraction to nutrient-rich microenvironments (Stocker, 2012). Considering the global distribution and extensive biomass of alginate-containing macroalgae, the observed dynamics of bacterial alginate utilization substantially advance the understanding of fundamental biogeochemical processes in coastal waters worldwide.

## Experimental procedures

### Production and characteristics of alginate particles

Sterile alginate particles (Fig. 1A) were produced after a modification of Safariková *et al.* (2003). Sterile 1% alginate solution was prepared by slowly adding sodium alginate (Sigma Aldrich cat. no. 9005-38-3) to Milli-Q water at 60°C while stirring, followed by filter sterilization. Two millilitre of 1% alginate solution and 60 mg SDS were vortexed at maximum speed in a 15 ml reaction tube until SDS was completely dissolved. Eight millilitre of 1-pentanol was added and the solution vortexed for 5 min. The contents were transferred into a 50 ml reaction tube containing 10 ml of autoclaved 5% CaCl<sub>2</sub> solution and vortexed for 2 min. Particles were allowed to settle for 15 min, centrifuged at 5,000 *g* for 3 min, and the supernatant was decanted. Particles were washed five times with 20 ml of 5% CaCl<sub>2</sub> solution, filtered through a sterile 100 µm strainer (BD, San Jose, CA), and stored in autoclaved 5% CaCl<sub>2</sub> solution at 4°C until use. Stability and sterility of alginate particles was tested by incubation at 22°C in autoclaved artificial seawater or 5% CaCl<sub>2</sub> solution for 5 days, without notable disintegration of the alginate particles or bacterial growth respectively (data not shown). Alginate particle number and dispersity were determined by light microscopy. The alginate concentration of the particle stock solution was determined

using an established HPLC protocol (Neumann *et al.*, 2015). In addition, POC was measured in the stock solution after filtration onto combusted 25mm GF/F filters, drying for 2 h at 60°C, and exposing to the fume of concentrated HCl for 12 h to remove carbonates. Filters were transferred into tin capsules and analyzed for POC using a FlashEA 1112 CHN-analyzer (Thermo Scientific, Waltham, MA) at a combustion temperature of 1,000°C and a column temperature of 35°C. Concentrations were calculated by an external calibration curve with methionine. We also evaluated staining of alginate particles with alcian blue (Passow and Alldredge, 1995) and ruthenium red. Ruthenium red solution was prepared by dissolving ruthenium red in PBS under sonication (2 min) to 1.3 mM followed by filter sterilization. Particles were filtered on 3 µm polycarbonate filters and stained by incubation with 100 µl of ruthenium red solution for 10 min. Excessive ruthenium red solution was removed and particles were washed twice with 1 ml Milli-Q water before evaluation by light microscopy. Ruthenium red was superior to alcian blue, yielding much brighter staining and negligible interference with fluorescent DNA-binding dyes such as DAPI or SYBR Green.

### Cultivation of *Alteromonas macleodii* strain 83-1

*Alteromonas macleodii* strain 83-1 (Neumann *et al.*, 2015) was cultivated in sterile Zobell medium (5 g l<sup>-1</sup> peptone, 1 g l<sup>-1</sup> yeast extract, 80% filtered seawater and 20% dH<sub>2</sub>O) for 17 h. Two ml of cell suspension were centrifuged at 3,500 *g* for 5 min, the pellet was re-suspended in the same volume of filtered autoclaved seawater, and the washing procedure repeated five times to ensure that no residual Zobell medium was carried over into the subsequent experimental manipulations.

### Microcosm experiments with alginate particles

On October 6th 2014, 15 l of coastal surface seawater (21.37°C, 33.55 PSU, 0.89 µg l<sup>-1</sup> chlorophyll *a*) were collected from a depth of 0.5 m off Scripps Pier, La Jolla, CA (32° 52.0188 N 117° 15.4350 W) using a 20 l acid-rinsed polyethylene container. Within 1 h after sampling, seawater was filtered through a 50 µm screen (Nitex), enriched with inorganic nutrients (10 µM NaNO<sub>3</sub>, 1 µM NaH<sub>2</sub>PO<sub>4</sub>) to prevent growth-limiting conditions, and distributed in 1 l aliquots into autoclaved glass bottles. Three experiments were set up in triplicate, (i) seawater without further amendments (control treatment CTR), (ii) seawater plus 818 µl alginate particle solution corresponding to ~82 µg alginate according to HPLC (treatment AP), and (iii) seawater plus 818 µl alginate particle solution plus 5 × 10<sup>5</sup> cells ml<sup>-1</sup> *Alteromonas macleodii* strain 83-1 (treatment AP-ALT). The concentration of *A. macleodii* added was chosen to constitute ~10% of the total bacterial abundance. Bottles were incubated at 130 rpm at 23°C in the dark. Bacterial colonization of alginate particles was studied by DAPI or SYBR Green staining followed by confocal laser microscopy (A1R; Nikon, Tokyo, Japan).

### Bacterial abundance

Each day at the same hour, 2 ml were sampled aseptically from each bottle. One subsample of 1 ml was prefiltered

through 3.0 µm polycarbonate syringe filters to remove alginate particles, fixed with 0.2 µm filtered formaldehyde (2% final concentration), and filtered onto 0.2 µm polycarbonate filters to capture the FL fraction only. In the second subsample, alginate particles were dissolved by adding SDS (35 mM) and EDTA (25 mM) and vortexing before filtering on 0.2 µm polycarbonate filters to capture both PA and FL cells. The difference between the total abundance (PA + FL) and FL abundance was used to calculate the PA abundance. Quantification was done via enumeration of DAPI-stained cells using an BX51 epifluorescence microscope (Olympus, Tokyo, Japan) by counting 20 fields of view or 200 cells, ensuring a standard deviation of < 10%.

### Bacterial production

Total and cell-specific bacterial production for both FL and PA fractions was measured via the [<sup>3</sup>H]-leucine incorporation method (Kirchman *et al.*, 1985; Simon and Azam, 1989) modified for microcentrifugation (Smith and Azam, 1992). Triplicate 1.7 ml aliquots were incubated with [<sup>3</sup>H]-Leucine (20 nM final concentration, 125 Ci mmol<sup>-1</sup>/2.78<sup>17</sup> dpm mol<sup>-1</sup> specific activity) in sterile 2.0 ml polypropylene tubes for 1 h at 16°C in the dark. Samples with 5% trichloroacetic acid added prior to isotope served as blanks. Leucine incorporation was converted to carbon production assuming 3.1 kg C mol<sup>-1</sup> leucine (Simon and Azam, 1989).

### Bacterial community analysis

Fifty millilitre of the original seawater sample were filtered onto 0.2 µm polycarbonate filters to characterize the composition of the natural bacterial assemblage ('starter community'). At the end of the experiment, 250 ml of each triplicate were filtered onto 0.2 µm polycarbonate filters and the filters stored at -20°C until DNA extraction in a modification after Delbès *et al.* (2001) including bead-beating, phenol-chloroform-isomyl alcohol purification, isopropanol/sodium acetate precipitation and ethanol washing. DNA was sent to Eurofins Genomics (Ebersberg, Germany) for PCR amplification of the V3–V5 region using primer 319F and sequencing of amplicons using Illumina MiSeq with v3 chemistry. Raw sequence data has been deposited at NCBI under BioProject PRJNA289311. For community analyses, raw sequence data was processed by trimming of low-quality segments using Trimmomatic (Bolger *et al.*, 2014), quality-filtering, dereplication and singleton removal using Usearch (Edgar, 2010), and chimera detection, OTU classification, as well as rarefaction analyses using the SILVAngs web server (<https://www.arb-silva.de/ngs>) with SILVA database release 119.1. Alpha and beta diversity indices were estimated after randomized subsampling to 6,039 reads to accommodate to the lowest number of reads found in a sample. Observed OTUs as well as Chao1, Shannon and Simpson indices were calculated using QIIME v.1.9.1 (Caporaso *et al.*, 2010). Beta diversity was analyzed using the Primer v6 software package (Clarke and Gorley, 2006). Bacterial community composition between treatments was compared by means of Bray-Curtis similarities of cluster analyses followed by NMDS on a log X + 1 transformed dataset. 16S rRNA gene amplicon data were analyzed using Tax4Fun (Aßhauer *et al.*, 2015) and compared using the

Wilcoxon rank-sum test to predict functional capabilities of bacterial communities.

### Acknowledgements

We thank Yanyan Zhou, Francesca Malfatti, Lihini Aluwihare, Magali Porrachia, Insa Bakenhus, Marco Dogs, Rolf Weinert, Andrea Schlingloff, Nirav Patel, and Natalie Millán-Aguíñaga for advice and technical assistance. This work was supported by grants WI3888/1-1 (to MW) and the Transregional Collaborative Research Centre TRR 51 *Roseobacter*, both from the German Research Foundation (DFG). This research is funded in part by the Gordon and Betty Moore Foundation through Grant GBMF#2758 to FA. JD was supported by a Marie Curie Actions–International Outgoing Fellowship (PIOF-GA-2013-629378).

### References

- Allredge, A.L., Gotschalk, C., Passow, U., and Riebesell, U. (1995) Mass aggregation of diatom blooms: Insights from a mesocosm study. *Deep Sea Res Part II Top Stud Oceanogr* **42**: 9–27.
- Allredge, A.L., and Youngbluth, M.J. (1985) The significance of macroscopic aggregates (marine snow) as sites for heterotrophic bacterial production in the mesopelagic zone of the subtropical Atlantic. *Deep Sea Res Part A Oceanogr Res Pap* **32**: 1445–1456.
- Aßhauer, K.P., Wemheuer, B., Daniel, R., and Meinicke, P. (2015) Tax4Fun: Predicting functional profiles from metagenomic 16S rRNA data. *Bioinformatics* **31**: 2882–2884.
- Azam, F. (1998) Microbial control of oceanic carbon flux: The plot thickens. *Science* **280**: 694–696.
- Azam, F. and Malfatti, F. (2007) Microbial structuring of marine ecosystems. *Nat Rev Microbiol* **5**: 782–791.
- Bolger, A.M., Lohse, M., and Usadel, B. (2014) Trimmomatic: A flexible trimmer for Illumina sequence data. *Bioinformatics* **30**: 2114–2120.
- Caporaso, J.G., Kuczynski, J., Stombaugh, J., Bittinger, K., Bushman, F.D., Costello, E.K., *et al.* (2010) QIIME allows analysis of high-throughput community sequencing data. *Nat Method* **7**: 335–336.
- Cardman, Z., Arnosti, C., Durbin, A., Ziervogel, K., Cox, C., Steen, A.D., and Teske, A. (2014) *Verrucomicrobia* are candidates for polysaccharide-degrading bacterioplankton in an Arctic fjord of Svalbard. *Appl Environ Microbiol* **80**: 3749–3756.
- Chen, Z., Lei, X., Lai, Q., Li, Y., Zhang, B., Zhang, J., *et al.* (2014) *Phaeodactylibacter xiamenensis* gen. nov., sp. nov., a member of the family *Saprospiraceae* isolated from the marine alga *Phaeodactylum tricorutum*. *Int J Syst Evol Microbiol* **64**: 3496–3502.
- Chin, W.-C., Orellana, M. V., and Verdugo, P. (1998) Spontaneous assembly of marine dissolved organic matter into polymer gels. *Nature* **391**: 568–572.
- Christie-Oleza, J.A., Scanlan, D.J., and Armengaud, J. (2015) 'You produce while I clean up', a strategy revealed by exoproteomics during *Synechococcus-Roseobacter* interactions. *Proteomics* **15**: 3454–3462.
- Clarke, K., and Gorley, R. (2006) PRIMER v6: User Manual/ Tutorial.

- De Voys, C. (1979) Primary production in aquatic environments. In *The Global Carbon Cycle*. Bolin, B., Degens, E.T., Kempe, S., Ketner, P. (eds). New York: Wiley.
- del Giorgio, P.A., and Cole, J.J. (1998) Bacterial growth efficiency in natural aquatic ecosystems. *Annu Rev Ecol Syst* **29**: 503–541.
- del Giorgio, P.A., Condon, R., Bouvier, T., Longnecker, K., Bouvier, C., Sherr, E., and Gasol, J.M. (2011) Coherent patterns in bacterial growth, growth efficiency, and leucine metabolism along a northeastern Pacific inshore-offshore transect. *Limnol Oceanogr* **56**: 1–16.
- Delbès, C., Moletta, R., and Godon, J.-J. (2001) Bacterial and archaeal 16S rDNA and 16S rRNA dynamics during an acetate crisis in an anaerobic digester ecosystem. *FEMS Microbiol Ecol* **35**: 19–26.
- Dragnet, K.I., Smidsrød, O., and Skjåk-Bræk, G. (2005) Alginates from algae. *Biopolym Online* **6**: 215–224.
- Edgar, R.C. (2010) Search and clustering orders of magnitude faster than BLAST. *Bioinformatics* **26**: 2460–2461.
- Fernández-Gómez, B., Richter, M., Schüller, M., Pinhassi, J., Acinas, S.G., González, J.M., and Pedrós-Alió, C. (2013) Ecology of marine *Bacteroidetes*: A comparative genomics approach. *ISME J* **7**: 1026–1037.
- Gómez-Pereira, P.R., Schüller, M., Fuchs, B.M., Bennke, C., Teeling, H., Waldmann, J., et al. (2012) Genomic content of uncultured *Bacteroidetes* from contrasting oceanic provinces in the North Atlantic Ocean. *Environ Microbiol* **14**: 52–66.
- Grossart, H.-P., Kiorboe, T., Tang, K., and Ploug, H. (2003) Bacterial colonization of particles: Growth and interactions. *Appl Environ Microbiol* **69**: 3500–3509.
- Hahnke, S., Brock, N.L., Zell, C., Simon, M., Dickschat, J.S., and Brinkhoff, T. (2013) Physiological diversity of *Roseobacter* clade bacteria co-occurring during a phytoplankton bloom in the North Sea. *Syst Appl Microbiol* **36**: 39–48.
- Hulatt, C.J., Thomas, D.N., Bowers, D.G., Norman, L., and Zhang, C. (2009) Exudation and decomposition of chromophoric dissolved organic matter (CDOM) from some temperate macroalgae. *Estuar Coast Shelf Sci* **84**: 147–153.
- Hung, C.-C., Guo, L., Santschi, P.H., Alvarado-Quiroz, N., and Haye, J.M. (2003) Distributions of carbohydrate species in the Gulf of Mexico. *Mar Chem* **81**: 119–135.
- Jagtap, S.S., Hehemann, J.-H., Polz, M.F., Lee, J.-K., and Zhao, H. (2014) Comparative biochemical characterization of three exolytic oligoalginatase lyases from *Vibrio splendidus* reveals complementary substrate scope, temperature, and pH adaptations. *Appl Environ Microbiol* **80**: 4207–4214.
- Kabisch, A., Otto, A., König, S., Becher, D., Albrecht, D., Schüller, M., et al. (2014) Functional characterization of polysaccharide utilization loci in the marine *Bacteroidetes* 'Gramella forsetii' KT0803. *ISME J* **8**: 1492–1502.
- Kirchman, D., K'nees, E., and Hodson, R. (1985) Leucine incorporation and its potential as a measure of protein synthesis by bacteria in natural aquatic systems. *Appl Environ Microbiol* **49**: 599–607.
- Lampitt, R.S., Wishner, K.F., Turley, C.M., and Angel, M. V. (1993) Marine snow studies in the Northeast Atlantic Ocean: Distribution, composition and role as a food source for migrating plankton. *Mar Biol* **116**: 689–702.
- Mabeau, S., and Kloareg, B. (1987) Isolation and analysis of the cell walls of brown algae: *Fucus spiralis*, *F. ceranoides*, *F. vesiculosus*, *F. serratus*, *Bifurcaria bifurcata* and *Laminaria digitata*. *J Exp Bot* **38**: 1573–1580.
- Mann, A.J., Hahnke, R.L., Huang, S., Werner, J., Xing, P., Barbeyron, T., et al. (2013) The genome of the alga-associated marine Flavobacterium *Formosa agariphila* KMM 3901<sup>T</sup> reveals a broad potential for degradation of algal polysaccharides. *Appl Environ Microbiol* **79**: 6813–6822.
- Martin, M., Portetelle, D., Michel, G., and Vandenberg, M. (2014) Microorganisms living on macroalgae: Diversity, interactions, and biotechnological applications. *Appl Microbiol Biotechnol* **98**: 2917–2935.
- Michel, G., and Czjzek, M. (2013) Polysaccharide-degrading enzymes from marine bacteria. In *Marine Enzymes for Biocatalysis*. Trincone, A. (ed). Cambridge, UK: Woodhead Publishing, pp. 429–464.
- Neumann, A.M., Balmonte, J.P., Berger, M., Giebel, H.-A., Arnosti, C., Voget, S., et al. (2015) Different utilization of alginate and other algal polysaccharides by marine *Alteromonas macleodii* ecotypes. *Environ Microbiol* **17**: 3857–3856.
- Passow, U., and Alldredge, A.L. (1995) A dye-binding assay for the spectrophotometric measurement of transparent exopolymer particles (TEP). *Limnol Oceanogr* **40**: 1326–1335.
- Pedler, B.E., Aluwihare, L.I., and Azam, F. (2014) Single bacterial strain capable of significant contribution to carbon cycling in the surface ocean. *Proc Natl Acad Sci USA* **111**: 7202–7207.
- Riemann, L., Steward, G.F., and Azam, F. (2000) Dynamics of bacterial community composition and activity during a mesocosm diatom bloom. *Appl Environ Microbiol* **66**: 578–587.
- Safariková, M., Roy, I., Gupta, M.N., and Safarik, I. (2003) Magnetic alginate microparticles for purification of alpha-amylases. *J Biotechnol* **105**: 255–260.
- Simon, M., and Azam, F. (1989) Protein content and protein synthesis rates of planktonic marine bacteria. *Mar Ecol Prog Ser* **51**: 201–213.
- Simon, M., Grossart, H.-P., Schweitzer, B., and Ploug, H. (2002) Microbial ecology of organic aggregates in aquatic ecosystems. *Aquat Microb Ecol* **28**: 175–211.
- Simon, H.M., Smith, M.W., and Herfort, L. (2014) Metagenomic insights into particles and their associated microbiota in a coastal margin ecosystem. *Front Microbiol* **5**: 466.
- Slightom, R.N., and Buchan, A. (2009) Surface colonization by marine roseobacters: Integrating genotype and phenotype. *Appl Environ Microbiol* **75**: 6027–6037.
- Smith, D.C., and Azam, F. (1992) A simple, economical method for measuring bacterial protein synthesis rates in seawater using 3<sup>H</sup>-leucine. *Mar Microb Food Webs* **6**: 107–114.
- Steneck, R.S., Graham, M.H., Bourque, B.J., Corbett, D., Erlandson, J.M., Estes, J.A., and Tegner, M.J. (2003) Kelp forest ecosystems: Biodiversity, stability, resilience and future. *Environ Conserv* **29**: 436–459.
- Stocker, R. (2012) Marine microbes see a sea of gradients. *Science* **338**: 628–633.
- Thomas, F., Barbeyron, T., Tonon, T., Génicot, S., Czjzek, M., and Michel, G. (2012) Characterization of the first alginolytic operons in a marine bacterium: From their emergence in marine *Flavobacteriia* to their independent transfers to marine *Proteobacteria* and human gut *Bacteroides*. *Environ Microbiol* **14**: 2379–2394.
- Verdugo, P. (2012) Marine microgels. *Annu Rev Mar Sci* **4**: 375–400.

- Wietz, M., Wemheuer, B., Simon, H., Giebel, H.-A., Seibt, M.A., Daniel, R., *et al.* (2015) Bacterial community dynamics during polysaccharide degradation at contrasting sites in the Southern and Atlantic Oceans. *Environ Microbiol* **17**: 3822–3831.
- Zemke-White, W.L. and Ohno, M. (1999) World seaweed utilisation: An end-of-century summary. *J Appl Phycol* **11**: 369–376.
- Zimmerman, A.E., Martiny, A.C., and Allison, S.D. (2013) Microdiversity of extracellular enzyme genes among sequenced prokaryotic genomes. *ISME J* **7**: 1187–1199.

### Supporting information

Additional Supporting Information may be found in the online version of this article at the publisher's web-site:

**Fig. S1.** Rarefaction analysis comparing the number of OTUs and sequences at 97% genetic similarity in the

'starter community' (t0) and replicates 1–3 in microcosm experiments CTR, AP and AP-ALT.

**Table S1.** Bacterial cell numbers and cell-specific production among free-living and particle-associated populations in microcosm experiments CTR, AP and AP-ALT over 96 h.

**Table S2.** Total bacterial production and total organic carbon concentrations in microcosm experiments CTR, AP and AP-ALT over 96 h.

**Table S3.** Number of sequences, community richness (OTUs, Chao1), and community diversity (Shannon/Simpson indices) in the starter community (t0) and replicates 1–3 of microcosm experiments CTR, AP and AP-ALT after 96 h.

**Table S4.** Relative abundances (%) and taxonomic classification of OTUs in the starter community (t0) and replicates 1–3 of microcosm experiments CTR, AP and AP-ALT after 96 h.

## Appendix 6

### **Sweet spheres: Succession and CAZyme expression of marine bacterial communities colonizing a mix of alginate and pectin particles**

Bunse C, Koch H, Breider S, Simon M, Wietz M

*Environmental Microbiology* (2021), 23:3130–3148

# Sweet spheres: succession and CAZyme expression of marine bacterial communities colonizing a mix of alginate and pectin particles

Carina Bunse <sup>1,2†</sup> Hanna Koch <sup>3,4†</sup> Sven Breider,<sup>3</sup> Meinhard Simon <sup>1,3</sup> and Matthias Wietz <sup>2,3\*</sup>

<sup>1</sup>Helmholtz Institute for Functional Marine Biodiversity at the University of Oldenburg, Oldenburg, Germany.

<sup>2</sup>Alfred Wegener Institute Helmholtz Centre for Polar and Marine Research, Bremerhaven, Germany.

<sup>3</sup>Institute for Chemistry and Biology of the Marine Environment, University of Oldenburg, Oldenburg, Germany.

<sup>4</sup>Department of Microbiology, Radboud University Nijmegen, Nijmegen, The Netherlands.

## Summary

**Polysaccharide particles are important substrates and microhabitats for marine bacteria. However, substrate-specific bacterial dynamics in mixtures of particle types with different polysaccharide composition, as likely occurring in natural habitats, are undescribed. Here, we studied the composition, functional diversity and gene expression of marine bacterial communities colonizing a mix of alginate and pectin particles. Amplicon, metagenome and metatranscriptome sequencing revealed that communities on alginate and pectin particles significantly differed from their free-living counterparts. Unexpectedly, microbial dynamics on alginate and pectin particles were similar, with predominance of amplicon sequence variants (ASVs) from *Tenacibaculum*, *Colwellia*, *Psychrobium* and *Psychromonas*. Corresponding metagenome-assembled genomes (MAGs) expressed diverse alginate lyases, several colocalized in polysaccharide utilization loci. Only a single, low-abundant MAG showed elevated transcript abundances of pectin-degrading enzymes. One specific *Glaciecola* ASV dominated the free-living fraction, possibly persisting on particle-derived oligomers through different glycoside hydrolases. Elevated ammonium uptake and metabolism**

**signified nitrogen as an important factor for degrading carbon-rich particles, whereas elevated methylcitrate and glyoxylate cycles suggested nutrient limitation in surrounding waters. The bacterial preference for alginate, whereas pectin primarily served as colonization scaffold, illuminates substrate-driven dynamics within mixed polysaccharide pools. These insights expand our understanding of bacterial niche specialization and the biological carbon pump in macroalgae-rich habitats.**

## Introduction

Polysaccharides produced by marine macroalgae and phytoplankton are important ecological and biogeochemical agents, serving as structural and storage components for the algae as well as nutrient source for heterotrophic bacteria (Armosti *et al.*, 2021). A considerable fraction of algal polysaccharides is bound in particles, hotspots of microbial activity with central implications for the biological carbon pump (Stocker, 2012). Hydrogels and transparent exopolymer particles (TEP), a subset of polysaccharide particles forming by self-assembly of anionic polysaccharides in seawater, constitute a global amount of ~70 gigatons and are indispensable for the study of particle–microbe interactions (Verdugo *et al.*, 2004; Verdugo, 2012; Cordero and Datta, 2016). The building blocks of marine hydrogels largely originate from macroalgae, in which anionic gelling polysaccharides such as alginate can constitute >50% of the biomass (Mabeau and Kloareg, 1987). In addition, phytoplankton produce anionic polymers and contribute to the marine hydrogel pool (Mühlenbruch *et al.*, 2018). Natural processes of decay or exudation, such as the release of alginate and rhamnogalacturonan from widespread macroalgae (Koch *et al.*, 2019a), presumably result in the formation of hydrogel scaffolds that represent hotspots for microbial life. These events potentially play an ecological role at rocky coasts of temperate seas, which harbor dense forests of macroalgae.

The chemical and structural complexity of marine hydrogels challenges the identification of specific

Received 23 February, 2021; revised 6 April, 2021; accepted 15 April, 2021. \*For correspondence. E-mail matthias.wietz@awi.de; Tel. +49-471-48311454; Fax. +49-471-48311776. †These authors contributed equally to this work.

particle–microbe relationships. To reduce this complexity, exposing synthetic model particles to natural bacterioplankton helps understanding the dynamics and drivers of particle colonization. Such approaches have identified hydrogels and other polysaccharide particles as active microbial microhabitats, which harbor distinct communities compared to the surrounding water (Mitulla *et al.*, 2016; Sperling *et al.*, 2017; Zäncker *et al.*, 2019). Furthermore, attached microbes can undergo a temporal succession of primary degraders and opportunistic taxa (Datta *et al.*, 2016; Enke *et al.*, 2018, 2019). The main indicator of hydrolytic capacities is the presence and diversity of carbohydrate-active enzymes (CAZymes), foremost polysaccharide lyases (PLs) and glycoside hydrolases (GHs), in bacterial genomes (Hehemann *et al.*, 2014). CAZymes are commonly clustered in polysaccharide utilization loci (PUL), operon-like regions facilitating efficient hydrolysis (Grondin *et al.*, 2017). CAZyme numbers, diversity and genomic organization can distinguish bacteria in primary degraders for initial polymer breakdown, and secondary consumers utilizing oligosaccharides, monosaccharides or other compounds released by primary degraders. These types occur across taxonomic boundaries and also within single species (Hehemann *et al.*, 2016; Koch *et al.*, 2020).

Nonetheless, it remains enigmatic how bacterial particle utilization proceeds within the natural ‘particlescape’ – presumably containing a mixture of particle types with different polysaccharide composition – and how these processes are shaped by the taxonomic and functional diversity of the ambient microbiota. The co-availability of hydrogels with different polysaccharide composition might initiate a segregation of bacterial populations by substrate preferences, comparable to hydrolyzing model isolates (Zhu *et al.*, 2016; Koch *et al.*, 2019a). In this context, the CAZyme repertoire is considered to be a stronger driver of niche specialization than phylogenetic relationships (Hehemann *et al.*, 2016; Wolter *et al.*, 2021a). The colonization and utilization of particle resources might also include interactions with free-living microbes, which might benefit from oligosaccharides and other compounds released into the surrounding water. In addition, microbial competition and cooperation can coincide with successional patterns and specific interactions (Ebrahimi *et al.*, 2019; Gralka *et al.*, 2020).

To evaluate particle-specific bacterial dynamics in a mixture of hydrogels, the present study co-exposed alginate and pectin particles to bacterioplankton communities from Helgoland, an island in the southern North Sea surrounded by dense macroalgal forests (Bartsch and Kuhlenkamp, 2000; Uhl *et al.*, 2016). Due to the gelling capacities of alginate and pectin and their demonstrated release from Helgoland macroalgae (Koch *et al.*, 2019a), we assume that related particles occur in this habitat and

constitute microhabitats for specialized microbiota. The co-incubation followed by magnetic separation allowed deciphering community composition, functional potential and gene expression depending on particle type and in relation to the free-living fraction. Opposed to our original hypothesis that alginate and pectin particles are utilized by different members of the ambient community, we observed similar compositional and functional patterns with predominant expression of alginate lyases. The identification of alginate as preferred substrate, whereas pectin primarily served as colonization scaffold, illuminates bacterial microhabitat ecology and substrate cycling in macroalgae-rich habitats with diverse polysaccharide budgets.

## Results and discussion

We studied taxonomic diversity, functional capacities and gene expression of particle-attached (PA) marine bacterial communities on alginate (AlgP) and pectin (PecP) particles in comparison to their free-living (FL) counterparts. For this purpose, synthetic AlgP and PecP were co-exposed to bacterioplankton collected near Helgoland Island, surrounded by dense macroalgal forests and hence considerable polysaccharide budgets (Supplementary Fig. 1A). The ambient water was sequentially filtered through 100 and 20  $\mu\text{m}$  before AlgP/PecP addition to exclude naturally occurring particles and larger organisms. For the targeted separation of communities, we then carried out triplicate co-incubations in different combinations of magnetic and non-magnetic particles: (i) magnetic AlgP and non-magnetic PecP, (ii) non-magnetic AlgP and magnetic PecP, and (iii) controls without particles. Applying magnetic force allowed the specific recovery of each particle type (Supplementary Video 1). The FL fraction was obtained by 5  $\mu\text{m}$  filtration to remove non-magnetic particles and collecting the flow-through on 0.2  $\mu\text{m}$  filters (Supplementary Fig. 1B).

### *Do AlgP, PecP and FL harbour specific communities with temporal variability?*

Amplicon sequencing of bacterial 16S rRNA genes revealed significant differences between PA and FL communities (PERMANOVA,  $p < 0.001$ ) but substantial overlap between AlgP and PecP (Fig. 1A, Supplementary Fig. 2A). FL communities from both particle combinations were congruent as expected (Fig. 1A), and FL data were thus combined in subsequent analyses. Furthermore, significant compositional differences of PA and FL communities to those in the ambient seawater and controls without added particles (PERMANOVA,  $p < 0.001$ ) confirmed the observations as true biological dynamics.

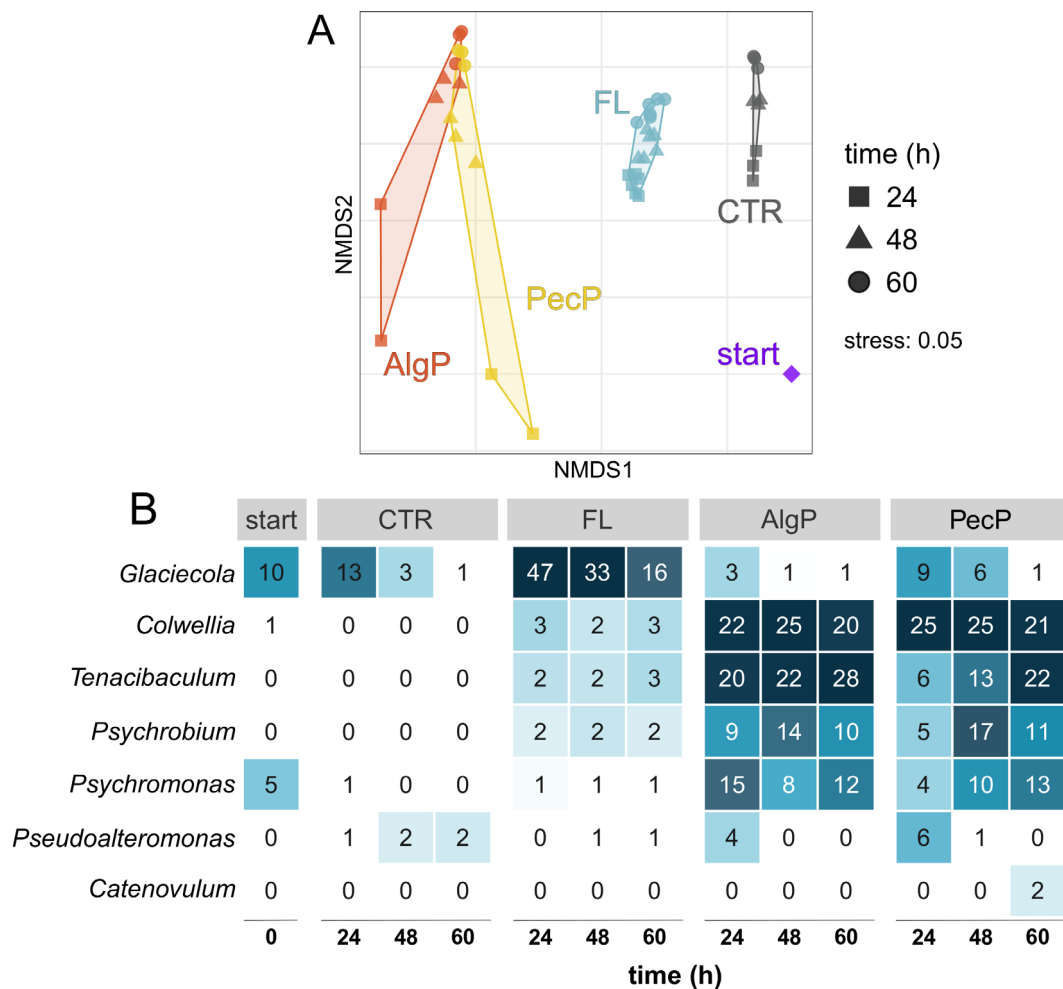


**Fig 1.** Bacterial community composition based on amplicon sequence variants.

A. Non-metric multidimensional scaling reveals different communities on alginate (AlgP) and pectin particles (PecP) compared to the free-living fraction (FL), control without particles (CTR), and the ambient seawater (start).

B. Relative abundances of dominant genera on AlgP and PecP in comparison to FL, CTR and start communities.

Amplicon sequence variants (ASVs) affiliated with *Tenacibaculum* (*Bacteroidetes*: *Flavobacteriales*), *Colwellia*, *Psychromonas* and *Psychrobium* (*Gammaproteobacteria*: *Alteromonadales*) constituted up to 60% of both AlgP and PecP communities (Fig. 1B), with significant enrichment compared to the FL fraction (Kruskal–Wallis test,  $p < 0.001$ ). Hence, particle colonization largely related to few dominant taxa, comparable to other marine polysaccharide particles (Datta *et al.*, 2016; Enke *et al.*, 2019). The finding of related strains with considerable CAZyme repertoires on marine macroalgae (Dong *et al.*, 2012; Martin *et al.*, 2015; Gobet *et al.*, 2018; Christiansen *et al.*, 2020) supports the ecological relevance of our observations. Notably, both *Colwellia* and *Tenacibaculum* can be enriched on decaying algae (Fernandes *et al.*, 2012; Zhu *et al.*, 2017) and hence under circumstances when algal polysaccharides might be released and self-assemble into particles. Furthermore,

*Tenacibaculum* and *Psychromonas* frequently occur during phytoplankton blooms near Helgoland, when bacterial dynamics are largely driven by algal carbohydrates (Teeling *et al.*, 2012; Kappelmann *et al.*, 2019; Krüger *et al.*, 2019). High adaptability and metabolic rates, illustrated by the rapid stimulation of multiple *Colwellia* ASVs from nearly undetectable levels in the ambient community (Supplementary Fig. 3), could be a competitive advantage during such events.

*Glaciecola* (*Alteromonadales*) dominated the FL community (Kruskal–Wallis test;  $p < 0.0003$ ), with an average abundance of >30% during the first 48 h with low alpha-diversity (Fig. 1B, Supplementary Fig. 2B). Notably, the *Glaciecola* population was dominated by a single ASV (Supplementary Fig. 3), suggesting that nutrient scarcity in FL favoured highly competitive genotypes. This finding underlined that specific biogeochemical conditions can

stimulate the predominance of single community members (Pedler *et al.*, 2014). We hypothesize that *Glaciecola* largely persisted as secondary consumer of particle-derived substrates, supported by genomic evidence from the major corresponding MAG (see below).

The substantial overlap between AlgP and PecP microbiomes contradicted our original hypothesis that the ambient community segregates by particle type. Furthermore, there was little temporal variability in community composition, although we possibly missed rapid successional dynamics as observed in related studies (Datta *et al.*, 2016; Enke *et al.*, 2019). One exception was *Pseudoalteromonas*, whose sole occurrence at 24 h on both particle types (Fig. 1B; Kruskal–Wallis test,  $p = 0.002$ ) signifies a polysaccharide pioneer (Hehemann *et al.*, 2016). This notion is supported by alginolytic and pectinolytic capacities of various *Pseudoalteromonas* species, which generally respond quickly to nutrient input (Ivanova *et al.*, 2014; Hehemann *et al.*, 2017). The AlgP microbiota established within the first 24 h and then remained unchanged, whereas *Tenacibaculum* established with temporal delay on PecP with peak abundances at 60 h (Fig. 1B; Kruskal–Wallis test,  $p = 0.04$ ). Faster stabilization of the AlgP community indicates that alginate was the major nutrient source, as discussed below in context of metagenomic and metatranscriptomic evidence. One notable exception was *Catenovulum* (*Alteromonadales*), which solely established on PecP after 60 h (Fig. 1B; Kruskal–Wallis test,  $p = 0.01$ ) and was the only taxon linked to pectin degradation (see below).

#### *Do AlgP, PecP and FL communities differ in functional diversity and gene expression?*

As taxonomic and metagenomic richness are overall connected (Salazar *et al.*, 2019), we expected contrasting functional potentials in PA and FL communities, whereas metabolic capacities of AlgP and PecP communities should be largely congruent. However, AlgP and PecP microbiomes might differ in gene expression patterns, as these can be independent from taxonomic composition (Salazar *et al.*, 2019). For instance, certain taxa encode both alginate and pectate lyases (Koch *et al.*, 2019a) and might express the corresponding genes differentially depending on particle type. To evaluate these aspects, we analyzed the metagenome (24 and 60 h) and metatranscriptome (60 h) of AlgP and PecP communities in relation to the FL fraction (Supplementary Table 1). This approach included both community-wide and genome-centric perspectives through MAGs.

The metagenomic library of 21 gigabases comprised ~192 000 genes predicted by Prokka, 47% of which

were functionally annotated using UniProtKB, KEGG and/or COG databases. Two percent of all genes were predicted to encode CAZymes according to dbCAN2 (Supplementary Table 2). We first assessed overarching differences between PA (i.e. occurring on both AlgP and PecP) and FL communities to identify general signatures of planktonic and attached niches. Transcripts from the citric acid cycle, glycolysis/gluconeogenesis and amino acid metabolism were abundant in both PA and FL metatranscriptomes but numerous pathways differed (Supplementary Table 3). Overall, ~60% of all transcripts were differentially abundant between PA and FL communities (Fig. 2A, Supplementary Table 3), matching metatranscriptomic evidence in other marine ecosystems (Satinsky *et al.*, 2014). Transcript abundances of glutamine synthetase, one key enzyme of bacterial nitrogen assimilation converting ammonium into glutamine, peaked in PA communities (Fig. 2B). This observation suggests considerable ammonium uptake to meet the nitrogen demand for fuelling polysaccharide-derived carbon into protein biosynthesis, supported by abundant transcripts of related transporter and regulator genes (Fig. 2B; Wilcoxon rank-sum test,  $p < 0.05$ ). Notably, the biosynthesis of valine, leucine and isoleucine peaked in PA, but their degradation in FL communities (Supplementary Table 3; Wilcoxon rank-sum test,  $p < 0.01$ ). We interpret this observation as provision of amino acids from actively growing PA to substrate-limited FL bacteria. In this context, leucine exchange between bacteria on polysaccharide particles and the surrounding water (Enke *et al.*, 2019) might be a stabilizing component of their interactions (Johnson *et al.*, 2020). Glyoxylate, dicarboxylate and pyruvate metabolism peaked in FL communities (Supplementary Table 3). Furthermore, induction of the methylcitrate cycle and the glyoxylate shunt (Fig. 2B; Wilcoxon rank-sum test,  $p < 0.01$ ) supports the notion of substrate limitation in the FL niche, matching transcriptomic responses of starved bacterioplankton (Kaberdin *et al.*, 2015). These pathways likely promoted persistence by generating energy from short-chain fatty acids but might also alleviate iron limitation or oxidative stress (Palovaara *et al.*, 2014; Ahn *et al.*, 2016; Dolan *et al.*, 2018; Koedooder *et al.*, 2018; Serafini *et al.*, 2019). In *Alteromonas macleodii*, similar expression patterns were interpreted as maintenance metabolism (van Bodegom, 2007; Beste and McFadden, 2010; Koch *et al.*, 2019b).

Next, we specifically compared AlgP and PecP to identify polysaccharide-specific patterns. Communities on AlgP and PecP only slightly differed in functional potential and gene expression (Fig. 2A), compliant with their compositional overlap (Fig. 1). Only 2% of transcripts were differentially abundant, without community-wide patterns

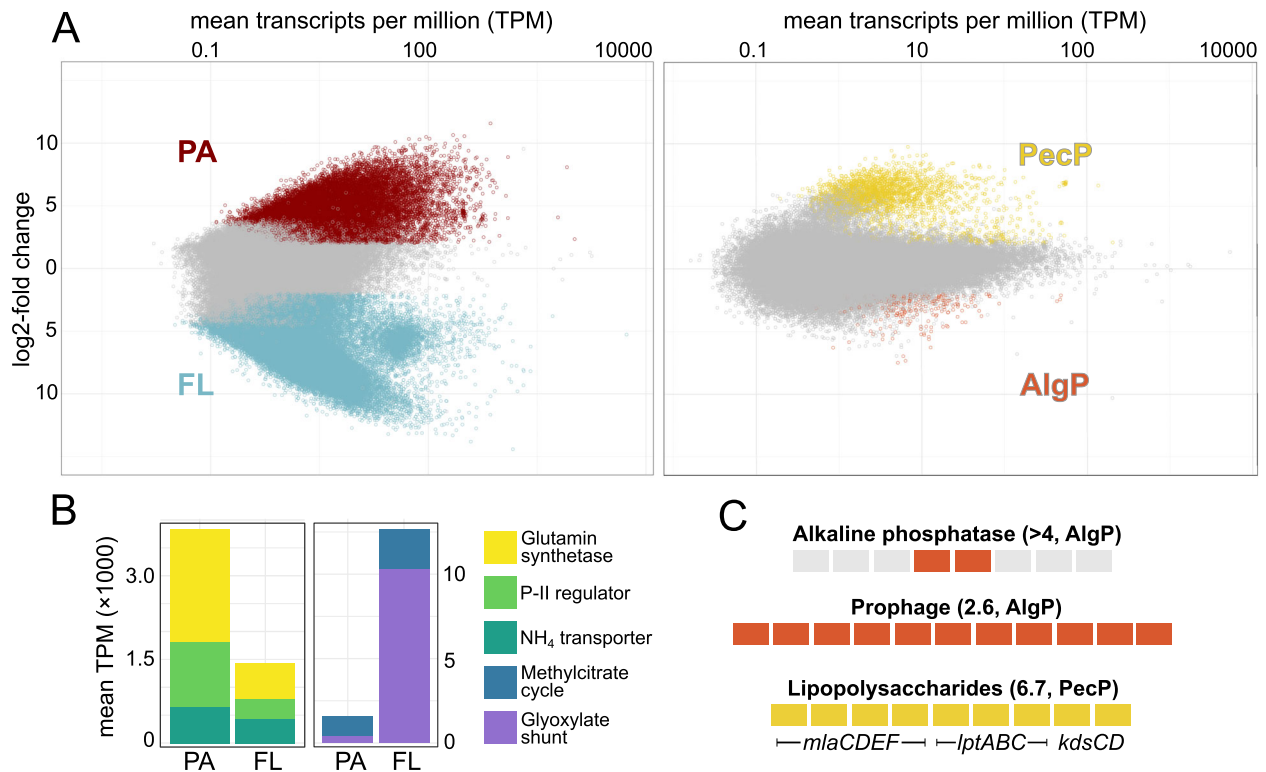


**Fig 2.** General metagenomic and metatranscriptomic patterns.

A. Differential transcript abundances in PA (both particle types) versus FL (left panel); and in AlgP versus PecP communities (right panel). Coloured dots designate genes with DESeq2 log<sub>2</sub>-fold changes >2 and  $\rho_{\text{adj}} < 0.001$ .

B. Selected genes and pathways with higher transcript abundances in PA or FL, including glutamine synthetase (EC number 6.3.1.2) and ammonium transporters (homologs of AmtB (Saier *et al.*, 2016)). ‘Methylcitrate cycle’ is the sum of methyl-isocitrate lyase, methyl-aconitate isomerase, methyl-citrate synthase and aconitate hydratase genes (COG2513, COG2828, COG0372, COG1048). ‘Glyoxylate shunt’ is the sum of isocitrate lyase and malate synthase genes (EC numbers 4.1.3.1 and 2.3.3.9). P-II regulator: Nitrogen regulatory protein P-II (COG0347). C: Selected gene clusters with higher transcript abundances on AlgP (orange-colored) or PecP (yellow-colored), encoding alkaline phosphatases (locus tags 41274–41275), a predicted prophage (38698–38711) and lipopolysaccharide-related *mla*, *lpt* and *kds* pathways (73039–73048). Values in parentheses designate the mean log<sub>2</sub>-fold change of genes.

in specific functional categories (Supplementary Table 3). On AlgP, higher transcript abundances of alkaline phosphatase genes possibly counteracted beginning phosphate limitation, comparable to late stages of natural TEP colonization (Berman-Frank *et al.*, 2016). Furthermore, higher transcript abundances of predicted prophages (Fig. 2C, Supplementary Table 3) indicates the induction of lytic cycles and corresponding release of organic matter (Breitbart *et al.*, 2018). These events potentially stimulated secondary consumers such as *Aureispira*, which only appeared after 60 h (Kruskal–Wallis test,  $p = 0.01$ ). This predatory taxon can feed on metabolic products or cell debris from other bacteria, fuelled by its capacity to adhere to anionic polysaccharides (Furusawa *et al.*, 2015). On PecP, a single MAG related to *Catenovulum* accounted for the vast majority of differentially abundant transcripts, supporting the predisposition of this taxon towards pectin (see below). The PecP-specific upregulation of lipopolysaccharide-related *mla*, *lpt* and *kds*

genes presumably stimulated biofilm formation, an important advantage for colonization and assimilation of particulate substrates (Sivadon *et al.*, 2019).

#### Community-level diversity and expression of CAZymes

Similarities between AlgP and PecP extended to comparable CAZyme profiles, dominated by PL6 and PL7 alginate lyase genes on both particle types (Supplementary Table 2). PL7 genes for the initial depolymerization of alginate, approximately half including a CBM32 carbohydrate-binding domain, peaked in both copy numbers and transcript abundances (Fig. 3A, Supplementary Table 2). PL15, PL17 and PL18 genes encoding the processing of released oligomers were less numerous but considerably transcribed (e.g. locus tags 183566 and 114168), with the highest transcript abundance of all CAZymes in a PL18 gene (locus tag 127388). The alginate content of >50% in brown macroalgae like

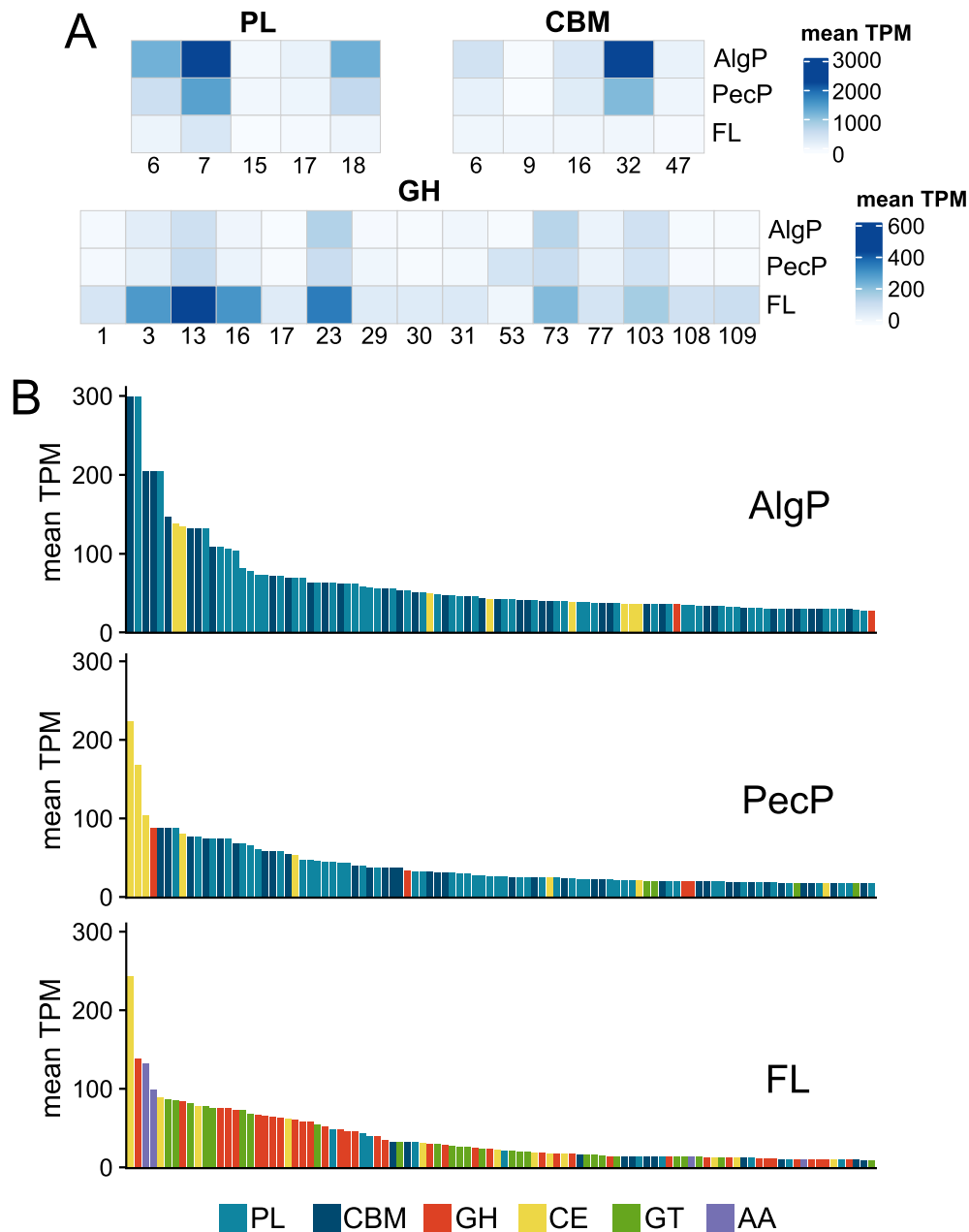


**Fig 3.** Community-wide diversity and expression of CAZymes.

A. Average transcript abundances of polysaccharide lyases (PL), carbohydrate-binding modules (CBM) and glycoside hydrolases (GH) with mean TPM >50.

B. Top100 CAZymes with the highest expression in the different bacterial fractions.

*Saccharina* and *Fucus*, which are abundant in our sampling area and release alginate into the water column (Koch *et al.*, 2019a), offers an explanation why alginate-degrading genes and organisms predominated. In contrast, we only detected three PL1 pectate lyases and few other pectin-related genes (CE8, GH28, GH105). These results indicate that pectin is not a prime bacterial substrate in kelp forests, although pectinolytic bacteria occur in diverse marine habitats (Van Truong *et al.*, 2001;

Hehemann *et al.*, 2017; Hobbs *et al.*, 2019) and pectinous substrates are exuded by Helgoland macroalgae (Koch *et al.*, 2019a). Instead, we hypothesise that PecP primarily served as colonization scaffolds for alginolytic bacteria. We propose that the predominant taxa are generally adapted to life on (polysaccharide) particles, favoring cross-particle colonization especially as AlgP were available nearby. The fast sinking of the relatively large particles (diameter ~200  $\mu\text{m}$ ) resulted in a loose bottom

layer, with close spatial contact of both particle types. This ‘particulatescape’ potentially allowed cross-particle interactions and utilization of alginate, even if attached to PecP. Nonetheless, significantly higher abundances of alginate lyase transcripts on AlgP (Wilcoxon rank-sum test,  $p = 0.0002$  to  $10^{-16}$ ) indicates that PecP associates were less alginolytic, possibly attributed to diffusion losses.

The FL community showed a completely different CAZyme signature, with elevated transcript abundances of GHs (Fig. 3A and B). Predominance of families GH3, GH13, GH16 and GH23 (Fig. 3A) matches the hydrolase repertoire of FL bacteria during phytoplankton blooms around Helgoland (Teeling *et al.*, 2016; Kappelmann *et al.*, 2019). Hence, our observations resemble responses of natural bacterioplankton to oligosaccharide mixtures. Although these GH families are mainly associated with  $\alpha$ -1,4-glucan,  $\beta$ -1,3-glucan or peptidoglycan degradation (Lombard *et al.*, 2014), our observations indicate a broader range including oligomers of anionic polysaccharides.

#### CAZymes and PUL on genomic level

Analysis of five near-complete MAGs (>90% completeness at <5% contamination) supported the genomic and ecological differentiation between PA and FL communities (Table 1, Supplementary Table 4). Core-gene phylogeny demonstrated that these MAGs represent the major PA and FL members *Colwellia*, *Tenacibaculum*, *Psychrobium*, *Psychromonas* and *Glaciecola* (Fig. 4A, Supplementary Fig. 4). Accordingly, their normalized coverage matched amplicon-based abundances (Fig. 4B).

Approximately 3% of genes in the major PA-MAGs were annotated as CAZymes (Table 1), mostly PL6, PL7 and PL18 alginate lyases with CBM32, CBM16 or CBM6 domains (Fig. 5). Considerable transcript abundances of alginate lyase and monomer-processing genes *kdgA*, *kdgF*, *kdgK* and *dehR* illustrate the complete metabolism of alginate (Fig. 5, Supplementary Table 4, Supplementary Fig. 5). Approximately half of CAZymes

from *Colwellia*, *Psychrobium* and *Psychromonas* MAGs harbour predicted signal peptides (Supplementary Table 4) and were hence likely secreted, although we cannot discern whether these were indeed free enzymes or anchored to the cell membrane. Presumably, CAZyme secretion into the polysaccharide matrix facilitated particle utilization, enhancing polymer hydrolysis and subsequent oligomer uptake (Vetter *et al.*, 1998). MAG Gla-32 affiliated with the dominant FL taxon *Glaciecola* encoded only three PLs but 18 GHs, with the highest transcript abundances of families GH3, GH13 and GH23 (Fig. 5). The lower fraction of signal peptides in its CAZymes (30%) indicates that secreted enzymes are less relevant when free-living, pointing towards opportunistic interactions with primary hydrolyzers.

Overall, only some CAZymes of each MAG’s repertoire showed elevated transcript abundances (Fig. 5). We assume that the ‘silent’ CAZymes enable the degradation of other carbohydrates. For instance, the *Colwellia*-MAG Col-24 encodes a homolog of the rarely described PL29 family (locus tag 50313), potentially activated in presence of chondroitin sulfate, dermatan sulfate or hyaluronic acid (Ndeh *et al.*, 2018). Although Col-24 clusters with the hydrolytic model isolate *Colwellia echini* A3 (Fig. 4A) at 80% average nucleotide identity (ANI), a BLASTp survey revealed that CAZymes targeting agar, carrageenan and furcellaran are not shared with strain A3 (Supplementary Table 4). Divergent CAZyme repertoires in related *Colwellia* spp. presumably reflect their different habitats (Christiansen *et al.*, 2020).

*MAG-specific polysaccharide utilization loci.* We detected several PUL in the *Tenacibaculum*-MAG Ten-26. For instance, one PUL encodes PL12 and PL17 alginate lyase plus SusCD transporter genes, the hallmark of flavobacterial PUL (Fig. 6A, Supplementary Fig. 6). In contrast, CAZyme genes in gammaproteobacterial MAGs were largely scattered throughout the genomes, although PUL-like operons occur in related taxa (Neumann *et al.*, 2015; Schultz-Johansen *et al.*, 2018; Christiansen *et al.*, 2020). The *Psychromonas*-MAG Psym-73 encodes

**Table 1.** Characteristics of near-complete metagenome-assembled genomes.

MAG	Taxonomy (GTDB-tk)	Completeness	Contamination	Size (Mbp)	Genes	CAZymes	PLs/GHs
Col-24	<i>Alteromonadaceae</i> ; <i>Colwellia</i>	90	3.0	3.27	2886	91	16/18
Ten-26	<i>Flavobacteriaceae</i> ; <i>Tenacibaculum</i>	97	2.0	3.06	2781	65	17/9
Gla-32	<i>Alteromonadaceae</i> ; <i>Glaciecola</i>	96	0.6	2.77	2575	49	3/18
Psyb-57	<i>Psychrobiaceae</i> ; <i>Psychrobium</i>	95	0.9	2.99	2690	61	16/10
Psym-73	<i>Psychromonadaceae</i> ; <i>Psychromonas</i>	94	1.0	3.69	3337	110	22/34

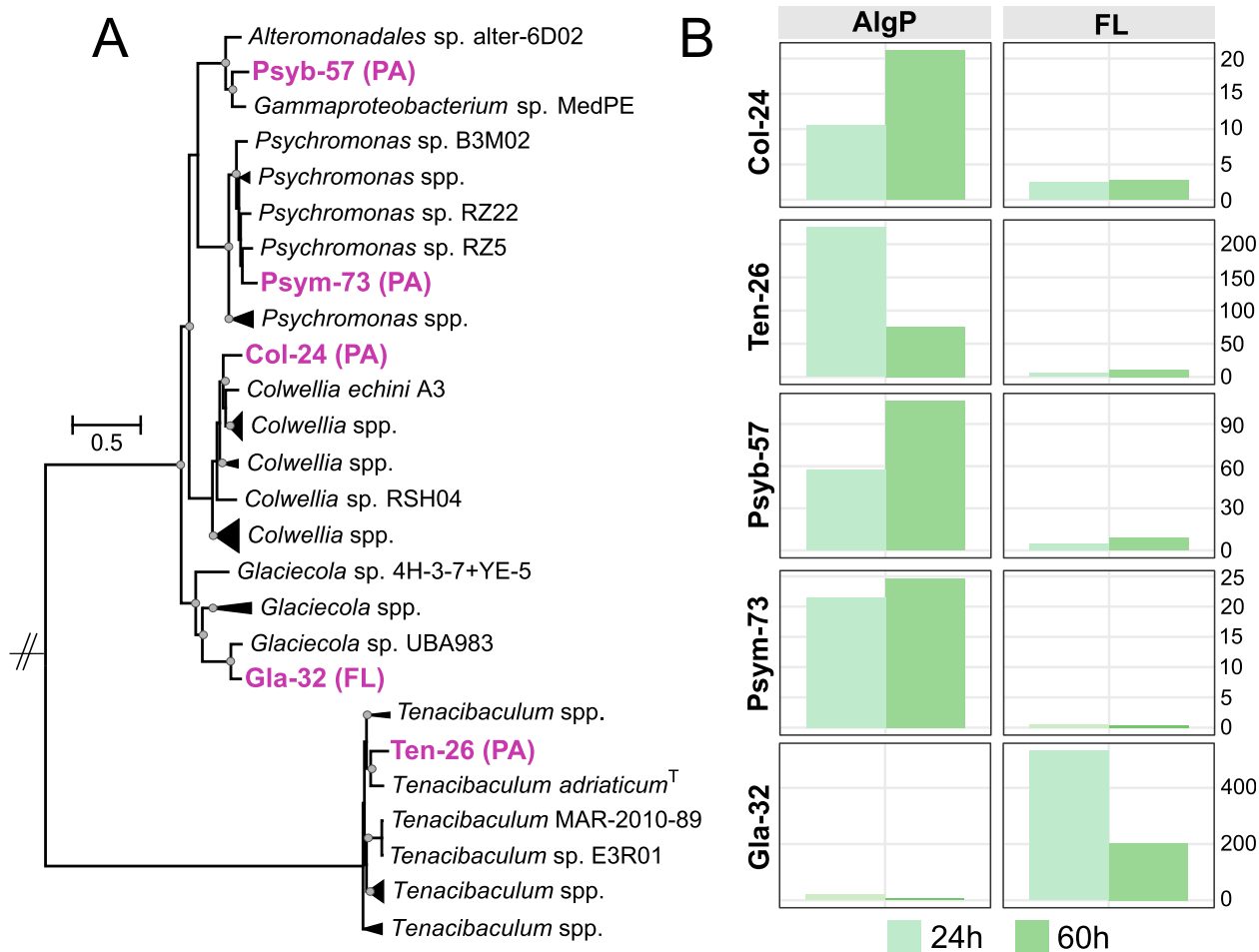


**Fig 4.** Phylogeny and abundance of metagenome-assembled genomes (MAGs).

A. Maximum-likelihood phylogeny based on 92 single-copy core genes in the context of related genomes. Dots designate nodes with >90% bootstrap support. Supplementary Fig. 4 shows an extended tree including medium-quality MAGs and additional related genomes.

B. Normalized coverage in metagenomes at 24 and 60 h. The scales of y-axes differ for better visualization.

two PL7 from subfamilies 5 and 3, each harboring a CBM16 and CBM32 domain (Fig. 6B, Supplementary Table 4). Together with the adjacent CBM16 gene, this combination indicates efficient binding and processing of different alginate architectures (Sim *et al.*, 2017; Hu *et al.*, 2019). The *Psychrobium*-MAG Psyb-57 encodes a PL12, a candidate novel variant of alginate lyases shared with other bacteria from Helgoland (Kappelmann *et al.*, 2019). Colocalization of this PL12 with exopolysaccharide-related genes (Fig. 6C) might link polysaccharide degradation and biosynthesis, considering the regulation of exopolysaccharide metabolism via PLs (Bakkevig *et al.*, 2005; Köseoğlu *et al.*, 2015). A comparable gene arrangement in an alginolytic *Maribacter* strain from the south Atlantic (Wolter *et al.*, 2021b) supports the potential implications for particle colonization.

A GH108 gene unique to *Glaciecola*-MAG Gla-32, colocalized with GH1 and carbohydrate transporter

genes (Fig. 6D), might allow scavenging oligomers released from particles. Gla-32 is related to the deep-sea isolate *Glaciecola* sp. 4H-3-7 + YE-5 (Fig. 4A), and their share of 40 CAZymes including a GH13 pair and adjacent GH77 (locus tags 06167–06169) indicates ecological relevance in diverse habitats (Klippel *et al.*, 2011). We detected transcripts of PL6 and PL7 lyases as well as the monomer processing pathway in Gla-32 (Fig. 5, Supplementary Table 4), indicating a general ability for alginate depolymerization. However, its incomplete alginate operon compared to known alginate degraders (Supplementary Fig. 7A) might signify inefficient alginolytic activity that limits particle colonization.

*Diversity of PL7 homologues in Psym-73.* The presence of 14 PL7 genes in the *Psychromonas*-MAG Psym-73 signifies a marked specialization towards alginate, as

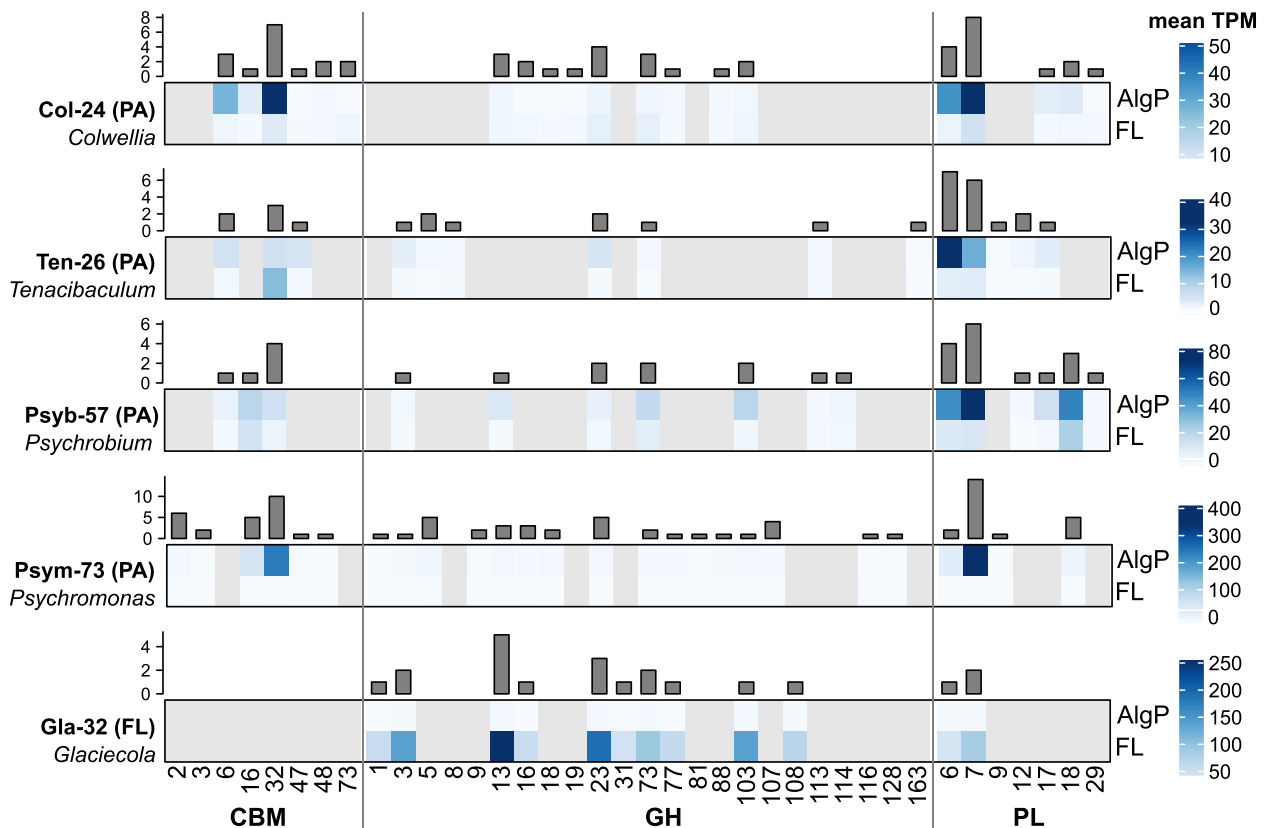


**Fig 5.** Diversity and expression of CAZymes in metagenome-assembled genomes. Mean transcript abundance (heatmaps) and number (bars) of CAZyme-encoding genes in MAGs affiliated with the dominant PA and FL community members.

hydrolytic activity scales with CAZyme number (Hehemann *et al.*, 2016). Two of these homologs (locus tags 20477 and 38641) exhibited the highest transcript abundances of all PL7 genes in our dataset (Supplementary Table 4). Both are related to biochemically characterized lyases from *Vibrio* strains (Supplementary Fig. 8) isolated from macroalgae or seawater (Roux *et al.*, 2009; Badur *et al.*, 2015; Sun *et al.*, 2019). For instance, PL7\_38641 has 72% amino acid identity to AlyD of *Vibrio splendidus*, an endolytic lyase releasing three oligomer fractions from guluronate-rich sections (Badur *et al.*, 2015). Prediction of a Lipo signal peptide while lacking a CBM indicates that PL7\_38641 is anchored as outer membrane lipoprotein (Supplementary Table 4), comparable to AlyA5 from *Zobellia galactanivorans* (Thomas *et al.*, 2013).

The two adjacent PL7 genes from different subfamilies (Fig. 6B) possess predicted Sec and Lipo signal peptides respectively (Supplementary Table 4), indicating complementary membrane-bound versus secreted localization to maximize alginate utilization. Homologues of PL7\_75913 with >50% amino acid identity also occur in *Simiduia* (Cellvibrionales), *Reichenbachiella* and *Marinoscillum*

(*Cytophagales*), indicating wide ecological relevance (Spring *et al.*, 2015). PL7\_75915 from the poorly described subfamily 3 has 55% amino acid identity to a structurally resolved lyase from *Persicobacter* (*Sphingobacteriales*) specialized towards alginate of high molecular weight (Sim *et al.*, 2017), suggesting a role in initial depolymerization. We hypothesize that the two PL variants originate from separate horizontal acquisition events with subsequent insertion into the same genomic locus, considering their low similarity and different branching in the phylogenetic tree (Supplementary Fig. 8). Overall, highly variable transcript abundances of PL7 genes (Supplementary Fig. 8) suggest that different variants are activated by specific biochemical conditions, for instance, different alginate characteristics (e.g. polymer length; dissolved or particulate form; or the ratio of mannuronate to guluronate monomers).

*Taxa with recurrent occurrence on alginate particles.* We compared MAGs Psym-73 and Ten-26 with the genomes of *Psychromonas* sp. B3M02 and *Tenacibaculum* sp. E3R01 respectively; strains isolated in a comparable study on alginate particles (Enke *et al.*, 2019). Supported by ~80% ANI and core-gene phylogeny (Fig. 4A), these

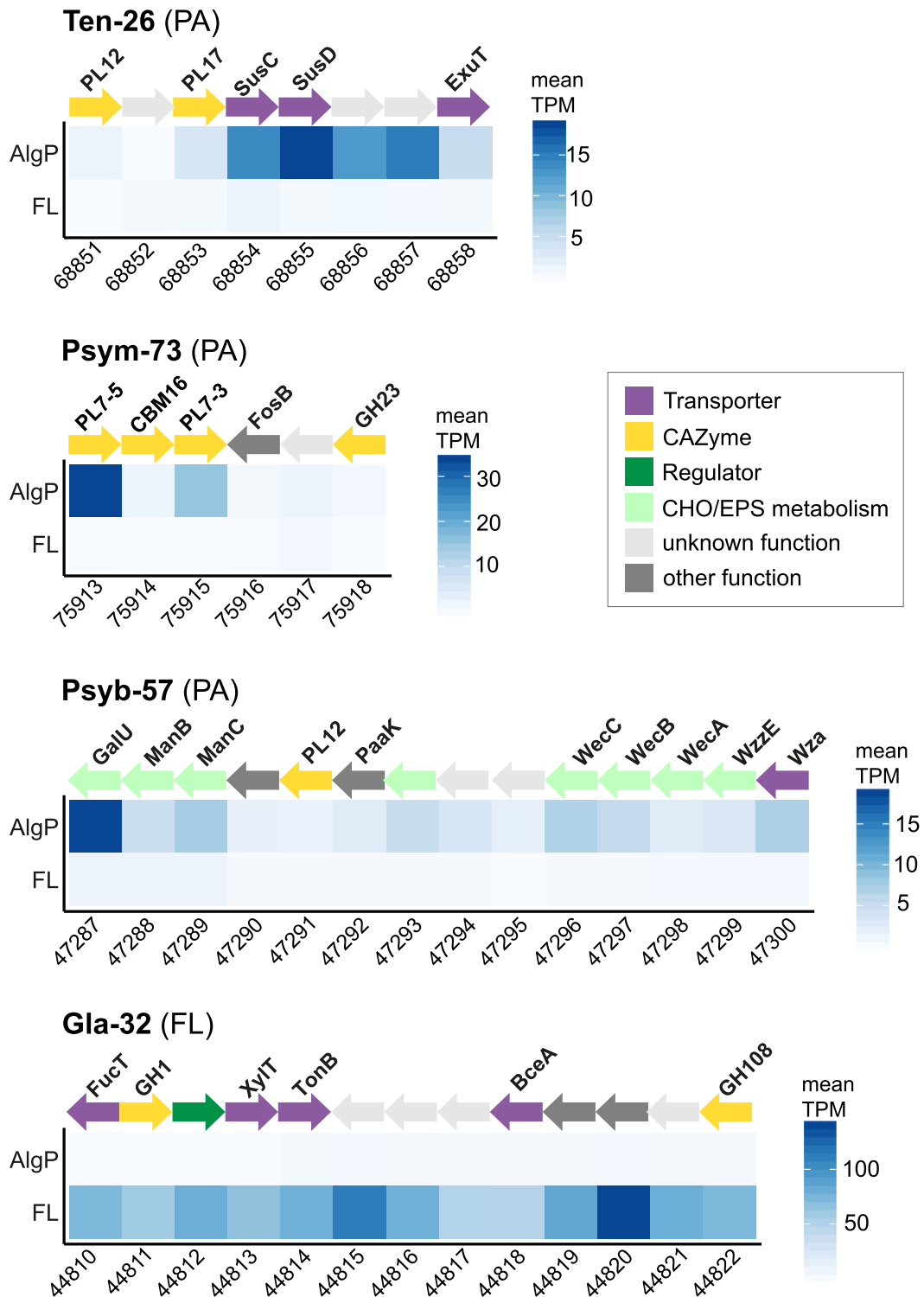


**Fig 6.** Structure and expression of PUL in MAGs.

A. PUL encoding SusCD and a PL12-PL17 gene pair in *Tenacibaculum*-MAG Ten-26.

B. PL7 genes from different subfamilies colocalized with a CBM16 gene in *Psychromonas*-MAG Psym-73.

C. PL12 and exopolysaccharide-related genes (green) in *Psychrobium*-MAG Psyb-57.

D. Unique GH108 adjacent to GH1 and carbohydrate transporter genes in *Glaciecola*-MAG Gla-32. Supplementary Table 4 and Supplementary Fig. 6 show detailed gene annotations and PUL architectures. EPS: exopolysaccharide; CHO: carbohydrate.

represent related species with presumably wide ecological relevance on polysaccharide particles. Psym-73 and strain B3M02 share nine homologous PLs (Supplementary Table 5), however, encoded in different genomic contexts. This variable organization, together with the higher PL count in Psym-73, indicates considerable CAZyme diversity and genomic rearrangements among hydrolytic *Psychromonas*. Ten-26 and strain E3R01 share 29 homologous CAZymes. However, no PLs were detected in E3R01 while Ten-26 encodes 17 (Supplementary Table 5). These observations indicate CAZyme-related niche specialization among *Tenacibaculum* species, consistent with CAZyme variability in *Tenacibaculum* type strains ranging from eight PLs in *T. jejuense* to none in *T. mesophilum* (Lombard *et al.*, 2014).

*A single, rare pectin degrader.* Despite the compelling evidence that alginate was the preferred bacterial substrate, MAG21 is a candidate for pectin utilization. MAG21 accounted for ~95% of differentially abundant transcripts on PecP (Fig. 7A), contributing to significantly elevated GH abundances and normalized coverage compared to AlgP (Fig. 7B, Kruskal–Wallis test,  $p < 10^{-16}$ ). MAG21 encodes several genes for galacturonate degradation and processing of pectin monomers. A GH53 endo-galactanase gene with the fourth-highest transcript abundance of all CAZymes on PecP (locus tag 118003) might cleave galacturonate-rich side chains from pectinous substrates by endolytic activity (Benoit *et al.*, 2012). Moreover, colocalized GH53 and GH2 plus two carbohydrate transporter genes (Fig. 7B) resemble a galacturonan-related PUL in *Bacteroides thetaiotaomicron* (Luis *et al.*, 2018). Thus, MAG21 might utilize oligomeric side chains of pectin, processing the resulting galacturonate via tagaturonate and altronate to 2-keto-3-deoxy-D-gluconate through UxuABC (Supplementary Table 4, Supplementary Fig. 5). Genome-based taxonomy assigned MAG21 to the uncultured taxon GCA-2401725, whereas the majority of CAZymes possess homologs in *Catenovulum* spp. (Supplementary Table 4), recently described for pectinolytic capacities (Furusawa *et al.*, 2021). Growth of the *Catenovulum* isolate CCB-QB4 on unsaturated galacturonate has been linked to GH28 and GH105 enzymes, which are also encoded by MAG21 (Supplementary Table 4). Together with the restriction of *Catenovulum* ASVs to PecP (Fig. 1C) we propose that MAG21 is taxonomically and functionally related to *Catenovulum* and degrades galacturonate. The medium quality of MAG21 (76% estimated completeness) may explain why pectate lyases are missing compared to CCB-QB4. Alternatively, MAG21 indeed only encodes an incomplete degradation cascade, only accessing oligomeric side chains or

oligomers released by the activity of primary degraders that encode pectate lyases.

An additional PecP-specific pattern occurred in *Psychromonas*-MAG Psym-73, with significantly higher transcript abundances of a hybrid gene cluster for the biosynthesis of a siderophore as well as spermidine (Supplementary Table 3, Supplementary Fig. 7B). Homologues of the siderophore-encoding section have been identified in diverse marine bacteria with shown iron-chelating activity (Koch *et al.*, 2019b), indicating a similar functionality in Psym-73. The upstream spermidine-related section has ~40% amino acid similarity to the polyamine synthesis pathway of *Vibrio*, indicating a PecP-specific role in biofilm formation (Lee *et al.*, 2009).

### Ecological conclusions

The predominance of alginolytic pathways demonstrates alginate particles as preferred microbial substrate, whereas pectin was primarily a colonization scaffold. The establishment of similar communities contradicted our original hypothesis of community segregation by substrate preferences. On the contrary, the expression of alginate lyases when attached to pectin signify the concept of a ‘particlescape’ encompassing cross-particle interactions. Such a scenario might resemble natural processes when algal polysaccharide exudates enter the water column, self-assemble into particles and sink to the seafloor. Under such circumstances, bacteria might utilize alginate even if attached to neighboring microhabitats, e.g. by secreting extracellular CAZymes or exploiting hydrolytic activity of co-occurring microbes. The predominance of few taxa indicates that polysaccharide availability stimulates only certain community members, outcompeting most other strains by their extensive CAZyme repertoire. Nonetheless, identification of a single MAG with pectin-specific dynamics suggests that numerically rare but competitive bacteria can establish in specific niches. Single-particle incubations and the application of  $^{13}\text{C}$ -labelled substrates followed by NanoSIMS or stable isotope probing might answer these open questions in future studies. Altogether, our study illuminates central elements of the biological carbon pump in macroalgae-rich habitats, with implications for microscale ecology, niche specialization and bacteria–algae interactions.

### Experimental procedures

#### *Characteristics of polysaccharide particles*

Custom polysaccharide particles consisting of alginate (CAS #9005-38-3) or pectin (CAS #9000-69-5), approximately 200  $\mu\text{m}$  in diameter, were fabricated by geniaLab

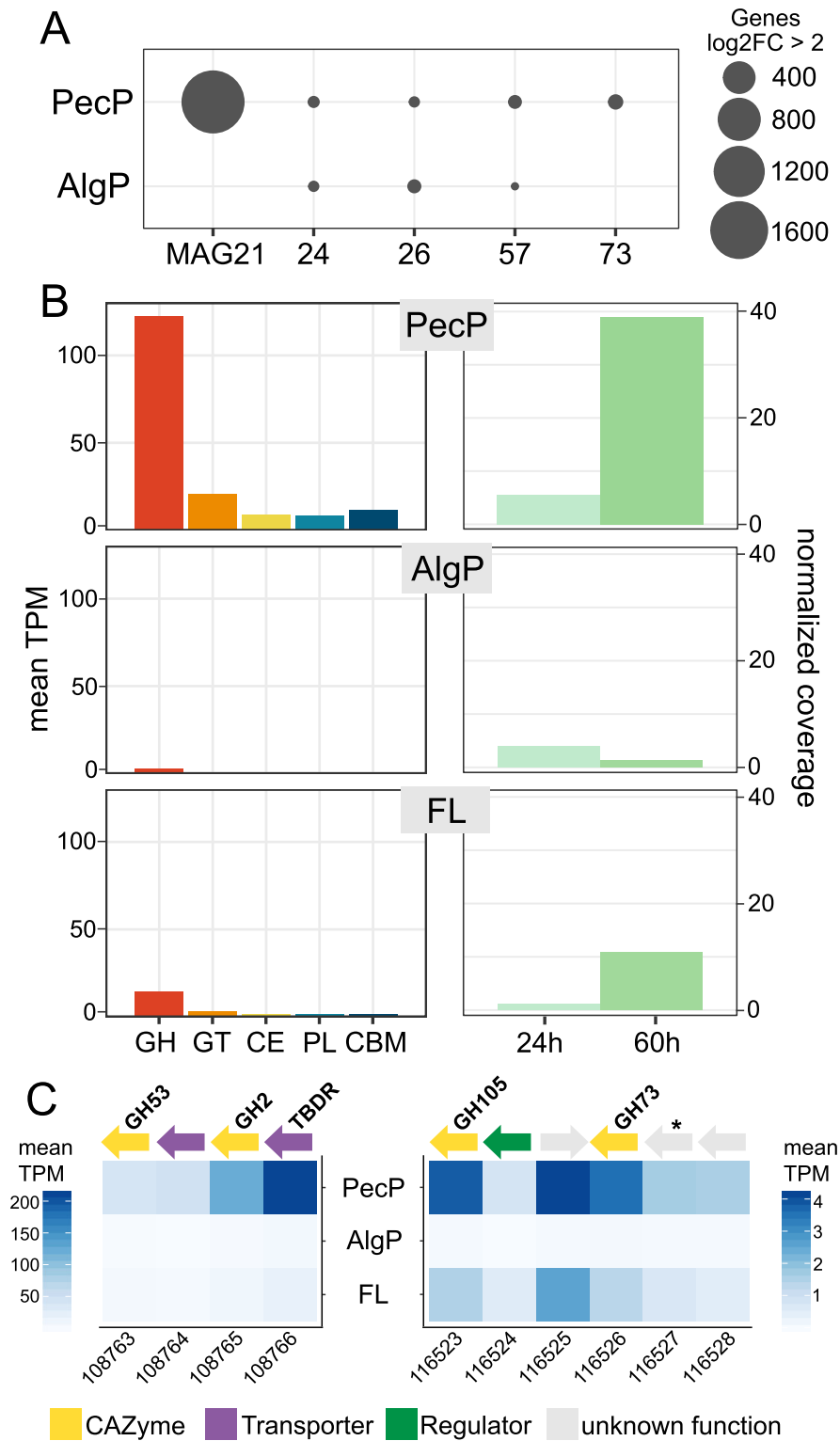


**Fig 7.** MAG21 as candidate for pectin degradation.

A. Numbers of differentially abundant transcripts compared to the major PA-MAGs on PecP versus AlgP.

B. Elevated transcript abundances of glycoside hydrolase genes on PecP. C, left panel: PUL with similarities to the pectinolytic operon BT4667–4673 in *Bacteroides thetaiotaomicron*. C, right panel: PUL encoding GH105 and GH73 genes plus a hypothetical protein with 60% amino acid identity to an alpha-amylase from *Paraglaciecola arctica* (UniProtKB accession K6ZD77; indicated by asterisk).

(Braunschweig, Germany) by immersing polysaccharide in calcium chloride solution containing metallic beads (Supplementary Methods). Four different versions were produced: magnetic alginate and pectin particles (polysaccharide coated on magnetite core) as well as non-magnetic alginate and pectin particles (polysaccharide coated on ferrous iron core). Particles contained on average 4% polysaccharide (Supplementary Table 6), approximating the 1:100 solid:solvent ratio in natural hydrogels (Verdugo *et al.*, 2004). Magnetic and non-magnetic particles of each polysaccharide allowed co-incubation of both polysaccharides and hence similar selection pressures per treatment (i.e. always two available particle types, only varying in magnetism). Applying external magnetic force (Supplementary File 1) subsequently allowed the targeted sampling of particle types.

#### Seawater sampling and experimental set-up

Seawater was sampled from approx. 1 m depth above macroalgal forests at Helgoland Island (54.190556 N, 7.866667 E) in June 2017. Seawater was filtered through a 100 µm mesh, brought to the lab within 2 h, and filtered again through a 20 µm mesh to remove larger particles and organisms. Each 12 L of filtered seawater were distributed into 20 L Clearboy bottles (Nalgene, Rochester, NY) previously rinsed with the same seawater. Per bottle, 10 µM NaNO<sub>3</sub> and 1 µM NaH<sub>2</sub>PO<sub>4</sub> (wt./vol.) were added as additional nitrogen and phosphorous source to avoid limitation. Three experiments were set up in triplicate: (i) magnetic alginate particles and non-magnetic pectin particles, (ii) non-magnetic alginate particles and magnetic pectin particles, and (iii) control without particles (Supplementary Fig. 1). Each particle type was added at 3500 L<sup>-1</sup>, resulting in ~42 000 particles per bottle. Bottles were incubated statically at 15°C (approx. *in situ* temperature) in the dark.

#### Sampling and nucleic acid extraction of particle-associated and free-living cells

250 ml of the original seawater were filtered onto 0.2 µm polycarbonate filters for determination of the ambient *in situ* community (start). Filters were flash-frozen in liquid nitrogen and stored at -80°C. Incubations were sampled after 24, 48 and 60 h. At each sampling point, bottles were mixed by inversion and ca. 550 ml withdrawn into rinsed measuring cylinders. Each sample was distributed (2 × 250 ml) into sterile RNase-free Nunc tubes (cat. no. 376814; Thermo Fisher Scientific, Waltham, MA). Particle-associated communities on magnetic AlgP or PecP were sampled by holding a neodymium magnet (cat. no. Q-40-10-10-N; Supermagnete, Gottmadingen, Germany) next to the tube. AlgP and PecP were washed

with sterile seawater (filtered through 100 and 20 µm; mixed 3:1 with ddH<sub>2</sub>O to prevent salt precipitation during autoclavation for 20 min at 121°C) and transferred to 2 ml RNase-free microcentrifuge tubes. The supernatant was transferred to a separate tube and non-magnetic particles were removed by filtration through 5 µm polycarbonate filters. The flow-through was captured on 0.2 µm polycarbonate filters to obtain the FL community. All samples were directly flash-frozen in liquid nitrogen and stored at -80°C. Simultaneous extraction of DNA and RNA was done using a modification of Schneider *et al.* (2017). Purified DNA and RNA were sent on dry ice to DNASense (Aalborg, Denmark) for quality control and sequencing. For particles, several subsamples per replicate were pooled to obtain sufficient DNA and RNA (Supplementary Table 1).

#### 16S rRNA gene amplicon sequencing

Briefly, the V3–V4 region of bacterial 16S rRNA genes was sequenced using primers 341F-806R (Sundberg *et al.*, 2013) with MiSeq technology (Illumina, San Diego, CA). Internal company standards worked as expected (Supplementary Methods). Reads were classified into ASVs using DADA2 (Callahan *et al.*, 2016) and taxonomically assigned using SILVA v132 (Quast *et al.*, 2013). Rarefaction analysis showed that diversity was reasonably covered (Supplementary Fig. 9). Replicates were congruent per treatment and time, without significant differences in Bray–Curtis dissimilarities (PERMANOVA;  $p = 0.72$  to 0.98). Furthermore, FL communities from AlgP and PecP were congruent as expected, and FL data combined in subsequent analyses. Alpha-diversity indices (richness, Shannon and inverse Simpson) were calculated using R package iNEXT (Hsieh *et al.*, 2016).

#### Metagenomics

As amplicon data confirmed the consistency of replicates, DNA from the three AlgP, PecP and FL replicates at 24 and 60 h were pooled respectively. DNA was quantified using Qubit (Thermo Fisher Scientific) and fragmented to ~550 bp using M220 using microTUBE AFA fibre screw tubes (Covaris, Woburn, MA) for 45 s at 20°C with duty factor 20%, peak/displayed power 50 W, and cycles/burst 200. Libraries were prepared using the NEB Next Ultra II kit (New England Biotech, Ipswich, MA) and paired-end sequenced (2 × 150 bp) on a NextSeq system (Illumina). Adaptors were removed using cutadapt v1.10 (Martin, 2011) and reads assembled using SPAdes v3.7.1 (Bankevich *et al.*, 2012). Genes were predicted using Prokka (Seemann, 2014) and assigned to KEGG categories using KAAS-SBH-GhostX (Moriya *et al.*, 2007). CAZymes were predicted using dbCAN2

with CAZyDB v8 (Zhang *et al.*, 2018), only considering hits with >80% coverage. Ammonium transporters were predicted by BLASTp of AmtB (P69681) in the Transporter Classification Database (Saier *et al.*, 2016).

### Metatranscriptomics

RNA was quantified in duplicate per sample using the Qubit BR RNA assay (Thermo Fisher Scientific). RNA quality and integrity were confirmed using TapeStation with RNA ScreenTape (Agilent, Santa Clara, CA). rRNA was depleted using the Ribo-Zero Magnetic kit (Illumina) and residual DNA removed using the DNase MAX kit (Qiagen, Hilden, Germany). Following sample cleaning and concentrating using the RNeasy MinElute Cleanup kit (Qiagen), rRNA removal was confirmed using TapeStation HS RNA ScreenTapes (Agilent). Sequencing libraries were prepared using the TruSeq Stranded Total RNA kit (Illumina), quantified using the Qubit HS DNA assay (Thermo Fisher Scientific) and size-estimated using TapeStation D1000 ScreenTapes (Agilent). For RNA from particle samples, four to five subsamples per replicate were pooled in equimolar concentrations and sequenced on a HiSeq2500 in a 1 × 50 bp Rapid Run (Illumina). As the first sequencing run did not deliver sufficient data for seven metatranscriptomes, a second run was performed on the same library. PCA confirmed consistent sequencing runs (data not shown), and read counts were subsequently aggregated. Raw fastq sequence reads were trimmed using USEARCH v10.0.2132 (Edgar, 2010) using -fastq\_filter and settings -fastq\_minlen 45 -fastq\_truncqual 20. rRNA reads were removed using BBDuk (<http://jgi.doe.gov/data-and-tools/bb-tools>) using the SILVA database as reference (Quast *et al.*, 2013). Reads were mapped to the predicted genes using Minimap2, discarding reads with sequence identities <0.98. Relative transcript abundances were obtained by dividing raw counts by the length of each gene (RPK) and normalized by per-million scaling factors. Resulting transcripts per million (TPM) were summed per gene annotation (Supplementary Table 2). Differential transcript abundances were calculated on raw read counts using the default DESeq2 workflow in R v3.6 (Love *et al.*, 2014; R Core Team, 2018) in RStudio (<https://rstudio.com>), only considering log<sub>2</sub>-fold changes >2 with  $p_{\text{adj}} < 0.001$  (Supplementary Table 3).

### MAG binning and analysis

MAGs were binned using MetaBat2 and mmgenome2 (Karst *et al.*, 2016; Kang *et al.*, 2019). Reads were mapped back to the assembly using Minimap2 v2.5 (Li, 2018), and the average coverage of each bin was calculated using mmgenome2 (weighted by scaffold

sizes). Based on results from CheckM and GTDB-Tk (Parks *et al.*, 2015; Chaumeil *et al.*, 2020), we selected five near-complete MAGs (≥90% estimated genome completeness and <5% genome contamination) representing the major taxa in amplicon data (Table 1, Supplementary Table 4). Whole-genome comparison with type strains was carried out using the MiGA web application (Rodriguez-R *et al.*, 2018). Normalized coverage in metagenomic data was calculated following Poghosyan *et al.* (2020) after multiplying the coverage of each MAG in every sample with a normalization factor (sequencing depth of the largest sample divided by the sequencing depth of each individual sample). A maximum-likelihood phylogeny based on 92 core genes identified using the UBCG pipeline (Na *et al.*, 2018), including medium-quality MAGs (>70% estimated completeness/<10% contamination) assigned to the same genus plus related genomes from public databases, was calculated using RaxMLHPC-Hybrid v8.2.12 with the GTRGAMMA substitution model and 1000 bootstrap replicates on the CIPRES Science Gateway v3.3 (Miller *et al.*, 2010; Stamatakis, 2014). Genes were assigned to KEGG categories using KAAS, and pathways reconstructed from these predictions using KEGG Pathway Mapper (Moriya *et al.*, 2007; Kanehisa and Sato, 2020). Gene annotations were refined using UniProtKB/Swiss-Prot (Boutet *et al.*, 2016) by custom-BLAST in Geneious v7 (<https://www.geneious.com>). Genes for processing alginate and pectin monomers were predicted based on the fully reconstructed pathways in *A. macleodii* and *Gramella forsetii* (Kabisch *et al.*, 2014; Koch *et al.*, 2019a). For comparative purposes, CAZymes of strains B3M02 and E3R01 (Enke *et al.*, 2019) were re-annotated with dbCAN2 v8.0 and compared to MAGs Ten-26 and Psym-73 using custom-BLAST in Geneious, only considering hits with >30% query coverage and >40% amino acid identity. ANIs between genomes were calculated using enveomics (Rodriguez-R and Konstantinidis, 2016). Prophages and biosynthetic gene clusters were predicted using PHASTER and antiSMASH 5.0 respectively (Arndt *et al.*, 2016; Blin *et al.*, 2019). Amino acid sequences of PL7 genes from Psym-73 were aligned using the MAFFT E-INS-i algorithm with default parameters (Katoch *et al.*, 2002). A maximum-likelihood phylogeny with 500 bootstrap replicates was calculated using RaxML v8.0 (Stamatakis, 2014) and the WAG+G + F substitution model determined using ModelTest-NG (Darriba *et al.*, 2020), both run on CIPRES (Miller *et al.*, 2010).

### Data availability

All sequencing data have been deposited at NCBI under BioProject PRJEB38771 (see Supplementary Table 1 for accession numbers of each sequence file). Annotated

metagenome contigs and near-complete MAGs, genes and translations, metatranscriptomic counts and the DNA–RNA extraction protocol are available at <https://doi.org/10.5281/zenodo.4171148>. Rscripts and additional input files for reproducing the analysis are available at <https://github.com/matthiaswietz/sweet-spheres>. Major R packages used for analysis and visualization included phyloseq, ampvis2, tidyverse, ComplexHeatmap, gtools and PNWColors (McMurdie and Holmes, 2013; Gu et al., 2016; Andersen et al., 2018; Wickham et al., 2019; Lawlor, 2020; Warnes et al., 2020).

## Acknowledgements

We are indebted to Antje Wichels, Eva-Maria Brodte, Gunnar Gerds and Uwe Nettelmann (Biological Department Helgoland) for exceptional scientific and logistic support during the experimental work. Mara Heinrichs, Felix Milke and Mathias Wolterink are gratefully acknowledged for excellent technical assistance. Many thanks to genialLab (Braunschweig), in particular Ulli Jahnz, for their exceptional service and helpful discussions in the preparation of custom polysaccharide particles. Sequencing was carried out by DNASense (Aalborg), with professional support by Mads Albertsen, Thomas Yssing Michaelsen, Rasmus H. Kirkegaard and Martin Hjorth Andersen. We thank Jan-Hendrik Hehemann, Silvia Vidal-Melgosa and Agata Mystkowska for valuable discussions. C.B. was supported by HIFMB, a collaboration between the Alfred Wegener Institute Helmholtz Centre for Polar and Marine Research and the Carl-von-Ossietzky University Oldenburg, initially funded by the Ministry for Science and Culture of Lower Saxony and the Volkswagen Foundation through the ‘Niedersächsisches Vorab’ program (grant number ZN3285). H.K. was supported by Volkswagen Foundation under VW-Vorab grant ‘Marine Biodiversity across Scales’ (MarBAS; ZN3112) and by the Netherlands Organization for Scientific Research (NWO Talent Programme grant VI.Veni.192.086). M.W. was supported by grant WI3888/1-2 from the German Research Foundation.

## References

Ahn, S., Jung, J., Jang, I.-A., Madsen, E.L., and Park, W. (2016) Role of glyoxylate shunt in oxidative stress response. *J Biol Chem* **291**: 11928–11938.

Andersen, K.S.S., Kirkegaard, R.H., Karst, S.M., and Albertsen, M. (2018) ampvis2: an R package to analyse and visualise 16S rRNA amplicon data. *bioRxiv* **299537**.

Arndt, D., Grant, J.R., Marcu, A., Sajed, T., Pon, A., Liang, Y., and Wishart, D.S. (2016) PHASTER: a better, faster version of the PHAST phage search tool. *Nucleic Acids Res* **44**: W16–W21.

Arnosti, C., Wietz, M., Brinkhoff, T., Hehemann, J.-H., Probandt, D., Zeugner, L., and Amann, R. (2021) The biogeochemistry of marine polysaccharides: sources, inventories, and bacterial drivers of the carbohydrate cycle. *Ann Rev Mar Sci* **13**: 81–108.

Badur, A.H., Jagtap, S.S., Yalamanchili, G., Lee, J.-K., Zhao, H., and Rao, C.V. (2015) Alginate lyases from alginate-degrading *Vibrio splendidus* 12B01 are endolytic. *Appl Environ Microbiol* **81**: 1865–1873.

Bakkevig, K., Sletta, H., Gimmetstad, M., Aune, R., Ertesvåg, H., Degnes, K., et al. (2005) Role of the *Pseudomonas fluorescens* alginate lyase (AlgL) in clearing the periplasm of alginates not exported to the extracellular environment. *J Bacteriol* **187**: 8375–8384.

Bankevich, A., Nurk, S., Antipov, D., Gurevich, A.A., Dvorkin, M., Kulikov, A.S., et al. (2012) SPAdes: a new genome assembly algorithm and its applications to single-cell sequencing. *J Comput Biol* **19**: 455–477.

Bartsch, I., and Kuhlenkamp, R. (2000) The marine macroalgae of Helgoland (North Sea): an annotated list of records between 1845 and 1999. *Helgol Mar Res* **54**: 160–189.

Benoit, I., Coutinho, P.M., Schols, H.A., Gerlach, J.P., Henrissat, B., and de Vries, R.P. (2012) Degradation of different pectins by fungi: correlations and contrasts between the pectinolytic enzyme sets identified in genomes and the growth on pectins of different origin. *BMC Genomics* **13**: 321.

Berman-Frank, I., Spungin, D., Rahav, E., Van Wambeke, F., Turk-Kubo, K., and Moutin, T. (2016) Dynamics of transparent exopolymer particles (TEP) during the VAHINE mesocosm experiment in the new Caledonian lagoon. *Biogeosciences* **13**: 3793–3805.

Beste, D.J.V., and McFadden, J. (2010) System-level strategies for studying the metabolism of *Mycobacterium tuberculosis*. *Mol Biosyst* **6**: 2363–2372.

Blin, K., Shaw, S., Steinke, K., Villebro, R., Ziemert, N., Lee, S.Y., et al. (2019) antiSMASH 5.0: updates to the secondary metabolite genome mining pipeline. *Nucleic Acids Res* **47**: W81–W87.

Boutet, E., Lieberherr, D., Tognolli, M., Schneider, M., Bansal, P., Bridge, A.J., et al. (2016) UniProtKB/Swiss-Prot, the manually annotated section of the UniProt KnowledgeBase: how to use the entry view. *Methods Mol Biol*: **1374**, 23–54.

Breitbart, M., Bonnain, C., Malki, K., and Sawaya, N.A. (2018) Phage puppet masters of the marine microbial realm. *Nat Microbiol* **3**: 754–766.

Callahan, B.J., McMurdie, P.J., Rosen, M.J., Han, A.W., Johnson, A.J.A., and Holmes, S.P. (2016) DADA2: high-resolution sample inference from Illumina amplicon data. *Nat Methods* **13**: 581–583.

Chaumeil, P.-A., Mussig, A.J., Hugenholtz, P., and Parks, D.H. (2020) GTDB-Tk: a toolkit to classify genomes with the genome taxonomy database. *Bioinformatics* **36**: 1925–1927.

Christiansen, L., Pathiraja, D., Bech, P.K., Schultz-Johansen, M., Hennessy, R., Teze, D., et al. (2020) A multifunctional polysaccharide utilization gene cluster in *Colwellia echini* encodes enzymes for the complete degradation of  $\kappa$ -carrageenan,  $\iota$ -carrageenan, and hybrid  $\beta$ - $\kappa$ -carrageenan. *mSphere* **5**: e00792-19.

Cordero, O.X., and Datta, M.S. (2016) Microbial interactions and community assembly at microscales. *Curr Opin Microbiol* **31**: 227–234.

Core Team, R. (2018) *R: A Language and Environment for Statistical Computing*. Vienna, Austria: R Foundation for Statistical Computing.

- Darriba, D., Posada, D., Kozlov, A.M., Stamatakis, A., Morel, B., and Flouri, T. (2020) ModelTest-NG: a new and scalable tool for the selection of DNA and protein evolutionary models. *Mol Biol Evol* **37**: 291–294.
- Datta, M.S., Sliwerska, E., Gore, J., Polz, M.F., and Cordero, O.X. (2016) Microbial interactions lead to rapid micro-scale successions on model marine particles. *Nat Commun* **7**: 11965.
- Dolan, S.K., Wijaya, A., Geddis, S.M., Spring, D.R., Silva-Rocha, R., and Welch, M. (2018) Loving the poison: the methylcitrate cycle and bacterial pathogenesis. *Microbiology* **164**: 251–259.
- Dong, S., Yang, J., Zhang, X.-Y., Shi, M., Song, X.-Y., Chen, X.-L., and Zhang, Y.-Z. (2012) Cultivable alginate Lyase-excreting bacteria associated with the Arctic brown alga *Laminaria*. *Mar Drugs* **10**: 2481–2491.
- Ebrahimi, A., Schwartzman, J., and Cordero, O.X. (2019) Cooperation and spatial self-organization determine rate and efficiency of particulate organic matter degradation in marine bacteria. *Proc Natl Acad Sci U S A* **116**: 23309–23316.
- Edgar, R.C. (2010) Search and clustering orders of magnitude faster than BLAST. *Bioinformatics* **26**: 2460–2461.
- Enke, T.N., Datta, M.S., Schwartzman, J., Cermak, N., Schmitz, D., Barrere, J., et al. (2019) Modular assembly of polysaccharide-degrading marine microbial communities. *Curr Biol* **29**: 1528–1535.e6.
- Enke, T.N., Leventhal, G.E., Metzger, M., Saavedra, J.T., and Cordero, O.X. (2018) Microscale ecology regulates particulate organic matter turnover in model marine microbial communities. *Nat Commun* **9**: 2743.
- Fernandes, N., Steinberg, P., Rusch, D., Kjelleberg, S., and Thomas, T. (2012) Community structure and functional gene profile of bacteria on healthy and diseased thalli of the red seaweed *Delisea pulchra*. *PLoS One* **7**: e50854.
- Furusawa, G., Azami, N.A., and Teh, A.-H. (2021) Genes for degradation and utilization of uronic acid-containing polysaccharides of a marine bacterium *Catenovulum* sp. CCB-QB4. *PeerJ* **9**: e10929.
- Furusawa, G., Hartzell, P.L., and Navaratnam, V. (2015) Calcium is required for ixotrophy of *Aureispira* sp. CCB-QB1. *Microbiology* **161**: 1933–1941.
- Gobet, A., Mest, L., Perennou, M., Dittami, S.M., Caralp, C., Coulombet, C., et al. (2018) Seasonal and algal diet-driven patterns of the digestive microbiota of the European abalone *Haliotis tuberculata*, a generalist marine herbivore. *Microbiome* **6**: 60.
- Gralka, M., Szabo, R., Stocker, R., and Cordero, O.X. (2020) Trophic interactions and the drivers of microbial community assembly. *Curr Biol* **30**: R1176–R1188.
- Grondin, J.M., Tamura, K., Déjean, G., Abbott, D.W., and Brumer, H. (2017) Polysaccharide Utilization Loci: fuelling microbial communities. *J Bacteriol* **199**: e00860-16.
- Gu, Z., Eils, R., and Schlesner, M. (2016) Complex heatmaps reveal patterns and correlations in multi-dimensional genomic data. *Bioinformatics* **32**: 2847–2849.
- Hehemann, J.-H., Arevalo, P., Datta, M.S., Yu, X., Corzett, C.H., Henschel, A., et al. (2016) Adaptive radiation by waves of gene transfer leads to fine-scale resource partitioning in marine microbes. *Nat Commun* **7**: 12860.
- Hehemann, J.-H., Boraston, A.B., and Czjzek, M. (2014) A sweet new wave: structures and mechanisms of enzymes that digest polysaccharides from marine algae. *Curr Opin Struct Biol* **28**: 77–86.
- Hehemann, J.-H., Truong, L.V., Unfried, F., Welsch, N., Kabisch, J., Heiden, S.E., et al. (2017) Aquatic adaptation of a laterally acquired pectin degradation pathway in marine gammaproteobacteria. *Environ Microbiol* **19**: 2320–2333.
- Hobbs, J.K., Hettle, A.G., Vickers, C., and Boraston, A.B. (2019) Biochemical reconstruction of a metabolic pathway from a marine bacterium reveals its mechanism of pectin depolymerization. *Appl Environ Microbiol* **85**: e02114–e02118.
- Hsieh, T.C., Ma, K.H., and Chao, A. (2016) iNEXT: an R package for rarefaction and extrapolation of species diversity (Hill numbers). *Methods Ecol Evol* **7**: 1451–1456.
- Hu, F., Zhu, B., Li, Q., Yin, H., Sun, Y., Yao, Z., and Ming, D. (2019) Elucidation of a unique pattern and the role of carbohydrate binding module of an alginate lyase. *Mar Drugs* **18**: 32.
- Ivanova, E., Ng, H.J., and Webb, H.K. (2014) The family *Pseudoalteromonadaceae*. In *The Prokaryotes*. Berlin: Springer.
- Johnson, W.M., Alexander, H., Bier, R.L., Miller, D.R., Muscarella, M.E., Pitz, K.J., and Smith, H. (2020) Auxotrophic interactions: a stabilizing attribute of aquatic microbial communities? *FEMS Microbiol Ecol* **96**: fiaa115.
- Kaberdin, V.R., Montánchez, I., Parada, C., Orruño, M., Arana, I., and Barcina, I. (2015) Unveiling the metabolic pathways associated with the adaptive reduction of cell size during *Vibrio harveyi* persistence in seawater microcosms. *Microb Ecol* **70**: 689–700.
- Kabisch, A., Otto, A., König, S., Becher, D., Albrecht, D., Schöler, M., et al. (2014) Functional characterization of polysaccharide utilization loci in the marine *Bacteroidetes* ‘*Gramella forsetii*’ KT0803. *ISME J* **8**: 1492–1502.
- Kanehisa, M., and Sato, Y. (2020) KEGG mapper for inferring cellular functions from protein sequences. *Protein Sci* **29**: 28–35.
- Kang, D.D., Li, F., Kirton, E., Thomas, A., Egan, R., An, H., and Wang, Z. (2019) MetaBAT 2: an adaptive binning algorithm for robust and efficient genome reconstruction from metagenome assemblies. *PeerJ* **7**: e7359.
- Kappelmann, L., Krüger, K., Hehemann, J.-H., Harder, J., Markert, S., Unfried, F., et al. (2019) Polysaccharide utilization loci of North Sea *Flavobacteriia* as basis for using SusC/D-protein expression for predicting major phytoplankton glycans. *ISME J* **13**: 76–91.
- Karst, S.M., Kirkegaard, R.H., and Albertsen, M. (2016) mmgenome: a toolbox for reproducible genome extraction from metagenomes. *bioRxiv* **059121**.
- Katoh, K., Misawa, K., Kuma, K., and Miyata, T. (2002) MAFFT: a novel method for rapid multiple sequence alignment based on fast Fourier transform. *Nucleic Acids Res* **30**: 3059–3066.
- Klippel, B., Lochner, A., Bruce, D.C., Davenport, K.W., Dettler, C., Goodwin, L.A., et al. (2011) Complete genome sequence of the marine cellulose- and xylan-degrading bacterium *Glaciecola* sp. strain 4H-3-7+YE-5. *J Bacteriol* **193**: 4547–4548.

- Koch, H., Dürwald, A., Schweder, T., Noriega-Ortega, B., Vidal-Melgosa, S., Hehemann, J.-H., et al. (2019a) Biphasic cellular adaptations and ecological implications of *Alteromonas macleodii* degrading a mixture of algal polysaccharides. *ISME J* **13**: 92–103.
- Koch, H., Freese, H.M., Hahnke, R., Simon, M., and Wietz, M. (2019b) Adaptations of *Alteromonas* sp. 76-1 to polysaccharide degradation: a CAZyme plasmid for ulvan degradation and two alginolytic systems. *Front Microbiol* **10**: 504.
- Koch, H., Germscheid, N., Freese, H.M., Noriega-Ortega, B., Lücking, D., Berger, M., et al. (2020) Genomic, metabolic and phenotypic variability shapes ecological differentiation and intraspecies interactions of *Alteromonas macleodii*. *Sci Rep* **10**: 809.
- Koedooder, C., Guéneuguès, A., Van Geersdaële, R., Vergé, V., Bouget, F.-Y., Labreuche, Y., et al. (2018) The role of the glyoxylate shunt in the acclimation to iron limitation in marine heterotrophic bacteria. *Front Mar Sci* **5**: 435.
- Köseoğlu, V.K., Heiss, C., Azadi, P., Topchiy, E., Güvener, Z.T., Lehmann, T.E., et al. (2015) *Listeria monocytogenes* exopolysaccharide: origin, structure, biosynthetic machinery and c-di-GMP-dependent regulation. *Mol Microbiol* **96**: 728–743.
- Krüger, K., Chafee, M., Ben Francis, T., Glavina del Rio, T., Becher, D., Schweder, T., et al. (2019) In marine *Bacteroidetes* the bulk of glycan degradation during algae blooms is mediated by few clades using a restricted set of genes. *ISME J* **13**: 2800–2816.
- Lawlor, J. (2020) PNWColors. <https://github.com/jakelawlor/PNWColors>
- Lee, J., Sperandio, V., Frantz, D.E., Longgood, J., Camilli, A., Phillips, M.A., and Michael, A.J. (2009) An alternative polyamine biosynthetic pathway is widespread in bacteria and essential for biofilm formation in *Vibrio cholerae*. *J Biol Chem* **284**: 9899–9907.
- Li, H. (2018) Minimap2: pairwise alignment for nucleotide sequences. *Bioinformatics* **34**: 3094–3100.
- Lombard, V., Golaconda Ramulu, H., Drula, E., Coutinho, P. M., and Henrissat, B. (2014) The carbohydrate-active enzymes database (CAZy) in 2013. *Nucleic Acids Res* **42**: D490–D495.
- Love, M.I., Huber, W., and Anders, S. (2014) Moderated estimation of fold change and dispersion for RNA-seq data with DESeq2. *Genome Biol* **15**: 550.
- Luis, A.S., Briggs, J., Zhang, X., Farnell, B., Ndeh, D., Labourel, A., et al. (2018) Dietary pectic glycans are degraded by coordinated enzyme pathways in human colonic *Bacteroides*. *Nat Microbiol* **3**: 210–219.
- Mabeau, S., and Kloareg, B. (1987) Isolation and analysis of the cell walls of brown algae: *Fucus spiralis*, *F. ceranoides*, *F. vesiculosus*, *F. serratus*, *Bifurcaria bifurcata* and *Laminaria digitata*. *J Exp Bot* **38**: 1573–1580.
- Martin, M. (2011) Cutadapt removes adapter sequences from high-throughput sequencing reads. *EMBnetjournal* **17**: 10–12.
- Martin, M., Barbeyron, T., Martin, R., Portetelle, D., Michel, G., and Vandenbol, M. (2015) The cultivable surface microbiota of the brown alga *Ascophyllum nodosum* is enriched in macroalgal-polysaccharide-degrading bacteria. *Front Microbiol* **6**: 1487.
- McMurdie, P.J., and Holmes, S. (2013) Phyloseq: An R package for reproducible interactive analysis and graphics of microbiome census data. *PLoS One* **8**: e61217.
- Miller, M.A., Pfeiffer, W., and Schwartz, T. (2010) Creating the CIPRES science gateway for inference of large phylogenetic trees. Proceedings of the Gateway Computing Environments Workshop, pp. 1–8.
- Mitulla, M., Dinasquet, J., Guillemette, R., Simon, M., Azam, F., and Wietz, M. (2016) Response of bacterial communities from California coastal waters to alginate particles and an alginolytic *Alteromonas macleodii* strain. *Environ Microbiol* **18**: 4369–4377.
- Moriya, Y., Itoh, M., Okuda, S., Yoshizawa, A.C., and Kanehisa, M. (2007) KAAS: an automatic genome annotation and pathway reconstruction server. *Nucleic Acids Res* **35**: W182–W185.
- Mühlenbruch, M., Grossart, H.-P., Eigemann, F., and Voss, M. (2018) Mini-review: phytoplankton-derived polysaccharides in the marine environment and their interactions with heterotrophic bacteria. *Environ Microbiol* **20**: 2671–2685.
- Na, S.-I., Kim, Y.O., Yoon, S.-H., Ha, S., Baek, I., and Chun, J. (2018) UBCG: up-to-date bacterial core gene set and pipeline for phylogenomic tree reconstruction. *J Microbiol* **56**: 281–285.
- Ndeh, D., Munoz, J.M., Cartmell, A., Bulmer, D., Wills, C., Henrissat, B., and Gray, J. (2018) The human gut microbe *Bacteroides thetaiotaomicron* encodes the founding member of a novel glycosaminoglycan-degrading polysaccharide lyase family PL29. *J Biol Chem* **293**: 17906–17916.
- Neumann, A.M., Balmonte, J.P., Berger, M., Giebel, H.A., Arnosti, C., Brinkhoff, T., et al. (2015) Different utilization of alginate and other algal polysaccharides by marine *Alteromonas macleodii* ecotypes. *Environ Microbiol* **17**: 3857–3868.
- Palovaara, J., Akram, N., Baltar, F., Bunse, C., Forsberg, J., Pedrós-Alió, C., et al. (2014) Stimulation of growth by proteorhodopsin phototrophy involves regulation of central metabolic pathways in marine planktonic bacteria. *Proc Natl Acad Sci U S A* **111**: E3650–E3658.
- Parks, D.H., Imelfort, M., Skennerton, C.T., Hugenholtz, P., and Tyson, G.W. (2015) CheckM: assessing the quality of microbial genomes recovered from isolates, single cells, and metagenomes. *Genome Res* **25**: 1043–1055.
- Pedler, B.E., Aluwihare, L.I., and Azam, F. (2014) Single bacterial strain capable of significant contribution to carbon cycling in the surface ocean. *Proc Natl Acad Sci U S A* **111**: 7202–7207.
- Poghosyan, L., Koch, H., Frank, J., van Kessel, M.A.H.J., Cremers, G., van Alen, T., et al. (2020) Metagenomic profiling of ammonia- and methane-oxidizing microorganisms in two sequential rapid sand filters. *Water Res* **185**: 116288.
- Quast, C., Pruesse, E., Yilmaz, P., Gerken, J., Schweer, T., Yarza, P., et al. (2013) The SILVA ribosomal RNA gene database project: improved data processing and web-based tools. *Nucleic Acids Res* **41**: D590–D596.
- Rodriguez-R, L.M., Gunturu, S., Harvey, W.T., Rosselló-Mora, R., Tiedje, J.M., Cole, J.R., and Konstantinidis, K.T.

- (2018) The microbial genomes atlas (MiGA) webserver: taxonomic and gene diversity analysis of *Archaea* and *Bacteria* at the whole genome level. *Nucleic Acids Res* **46**: W282–W288.
- Rodriguez-R, L.M., and Konstantinidis, K.T. (2016) The enveomics collection: a toolbox for specialized analyses of microbial genomes and metagenomes. *PeerJ Preprints*: 4: e1900v1.
- Roux, F.L., Zouine, M., Chakroun, N., Binesse, J., Saulnier, D., Bouchier, C., *et al.* (2009) Genome sequence of *Vibrio splendidus*: an abundant planktonic marine species with a large genotypic diversity. *Environ Microbiol* **11**: 1959–1970.
- Saier, M.H., Reddy, V.S., Tsu, B.V., Ahmed, M.S., Li, C., and Moreno-Hagelsieb, G. (2016) The transporter classification database (TCDB): recent advances. *Nucleic Acids Res* **44**: D372–D379.
- Salazar, G., Paoli, L., Alberti, A., Huerta-Cepas, J., Ruscheweyh, H.-J., Cuenca, M., *et al.* (2019) Gene expression changes and community turnover differentially shape the global ocean metatranscriptome. *Cell* **179**: 1068–1083.e21.
- Satinsky, B.M., Zielinski, B.L., Doherty, M., Smith, C.B., Sharma, S., Paul, J.H., *et al.* (2014) The Amazon continuum dataset: quantitative metagenomic and metatranscriptomic inventories of the Amazon River plume, June 2010. *Microbiome* **2**: 17.
- Schneider, D., Wemheuer, F., Pfeiffer, B., and Wemheuer, B. (2017) Extraction of total DNA and RNA from marine filter samples and generation of a cDNA as universal template for marker gene studies. *Methods Mol Biol* **1539**: 13–22.
- Schultz-Johansen, M., Bech, P.K., Hennessy, R.C., Glaring, M.A., Barbeyron, T., Czjzek, M., and Stougaard, P. (2018) A novel enzyme portfolio for red algal polysaccharide degradation in the marine bacterium *Paraglaciacola hydrolytica* S66<sup>T</sup> encoded in a sizeable polysaccharide utilization locus. *Front Microbiol* **9**: 839.
- Seemann, T. (2014) Prokka: rapid prokaryotic genome annotation. *Bioinformatics* **30**: 2068–2069.
- Serafini, A., Tan, L., Horswell, S., Howell, S., Greenwood, D. J., Hunt, D.M., *et al.* (2019) *Mycobacterium tuberculosis* requires glyoxylate shunt and reverse methylcitrate cycle for lactate and pyruvate metabolism. *Mol Microbiol* **112**: 1284–1307.
- Sim, P.-F., Furusawa, G., and Teh, A.-H. (2017) Functional and structural studies of a multidomain alginate lyase from *Persicobacter* sp. CCB-QB2. *Sci Rep* **7**: 13656.
- Sivodon, P., Barnier, C., Urios, L., and Grimaud, R. (2019) Biofilm formation as a microbial strategy to assimilate particulate substrates. *Environ Microbiol Rep* **11**: 749–764.
- Sperling, M., Piontek, J., Engel, A., Wiltshire, K.H., Niggemann, J., Gerdt, G., and Wichels, A. (2017) Combined carbohydrates support rich communities of particle-associated marine Bacterioplankton. *Front Microbiol* **8**: 65.
- Spring, S., Scheuner, C., Göker, M., and Klenk, H.-P. (2015) A taxonomic framework for emerging groups of ecologically important marine gammaproteobacteria based on the reconstruction of evolutionary relationships using genome-scale data. *Front Microbiol* **6**: 281.
- Stamatakis, A. (2014) RAxML version 8: a tool for phylogenetic analysis and post-analysis of large phylogenies. *Bioinformatics* **30**: 1312–1313.
- Stocker, R. (2012) Marine microbes see a sea of gradients. *Science* **338**: 628–633.
- Sun, X., Shen, W., Gao, Y., Cai, M., Zhou, M., and Zhang, Y. (2019) Heterologous expression and purification of a marine alginate lyase in *Escherichia coli*. *Protein Expr Purif* **153**: 97–104.
- Sundberg, C., Al-Soud, W.A., Larsson, M., Alm, E., Yekta, S. S., Svensson, B.H., *et al.* (2013) 454 pyrosequencing analyses of bacterial and archaeal richness in 21 full-scale biogas digesters. *FEMS Microbiol Ecol* **85**: 612–626.
- Teeling, H., Fuchs, B.M., Becher, D., Klockow, C., Gardebrecht, A., Bennke, C.M., *et al.* (2012) Substrate-controlled succession of marine bacterioplankton populations induced by a phytoplankton bloom. *Science* **336**: 608–611.
- Teeling, H., Fuchs, B.M., Bennke, C.M., Krüger, K., Chafee, M., Kappelmann, L., *et al.* (2016) Recurring patterns in bacterioplankton dynamics during coastal spring algae blooms. *eLife* **5**: e11888.
- Thomas, F., Lundqvist, L.C.E., Jam, M., Jeudy, A., Barbeyron, T., Sandström, C., *et al.* (2013) Comparative characterization of two marine alginate lyases from *Zobellia galactanivorans* reveals distinct modes of action and exquisite adaptation to their natural substrate. *J Biol Chem* **288**: 23021–23037.
- Uhl, F., Bartsch, I., and Oppelt, N. (2016) Submerged kelp detection with hyperspectral data. *Remote Sens* **8**: 487.
- van Bodegom, P. (2007) Microbial maintenance: a critical review on its quantification. *Microb Ecol* **53**: 513–523.
- Van Truong, L., Tuyen, H., Helmke, E., Binh, L.T., and Schweder, T. (2001) Cloning of two pectate lyase genes from the marine Antarctic bacterium *Pseudoalteromonas haloplanktis* strain ANT/505 and characterization of the enzymes. *Extremophiles* **5**: 35–44.
- Verdugo, P. (2012) Marine microgels. *Ann Rev Mar Sci* **4**: 375–400.
- Verdugo, P., Alldredge, A.L., Azam, F., Kirchman, D.L., Passow, U., and Santschi, P.H. (2004) The oceanic gel phase: a bridge in the DOM–POM continuum. *Mar Chem* **92**: 67–85.
- Vetter, Y.A., Deming, J.W., Jumars, P.A., and Krieger-Brockett, B.B. (1998) A predictive model of bacterial foraging by means of freely released extracellular enzymes. *Microb Ecol* **36**: 75–92.
- Warnes, G., Bolker, B., and Lumley, T. (2020). gtools package. <https://rdrr.io/cran/gtools/>
- Wickham, H., Averick, M., Bryan, J., Chang, W., McGowan, L.D., François, R., *et al.* (2019) Welcome to the Tidyverse. *J Open Source Softw* **4**: 1686.
- Wolter, L.A., Mitulla, M., Kalem, J., Daniel, R., Simon, M., and Wietz, M. (2021b) CAZymes in *Maribacter dokdonensis* 62-1 from the Patagonian shelf: genomics and physiology compared to related flavobacteria and a co-occurring *Alteromonas* strain. *Front Microbiol* **12**: 628055.
- Wolter, L.A., Wietz, M., Ziesche, L., Breider, S., Leinberger, J., Poehlein, A., *et al.* (2021a) *Pseudoceanicola algae* sp. nov., isolated from the marine macroalga *Fucus spiralis*, shows genomic and physiological adaptations for an algae-associated lifestyle. *Syst Appl Microbiol* **44**: 126166.

- Zäncker, B., Engel, A., and Cunliffe, M. (2019) Bacterial communities associated with individual transparent exopolymer particles (TEP). *J Plankton Res* **41**: 561–565.
- Zhang, H., Yohe, T., Huang, L., Entwistle, S., Wu, P., Yang, Z., et al. (2018) dbCAN2: a meta server for automated carbohydrate-active enzyme annotation. *Nucleic Acids Res* **46**: W95–W101.
- Zhu, Y., Chen, P., Bao, Y., Men, Y., Zeng, Y., Yang, J., et al. (2016) Complete genome sequence and transcriptomic analysis of a novel marine strain *Bacillus weihaiensis* reveals the mechanism of brown algae degradation. *Sci Rep* **6**: 38248.
- Zhu, Y., Thomas, F., Larocque, R., Li, N., Duffieux, D., Cladière, L., et al. (2017) Genetic analyses unravel the crucial role of a horizontally acquired alginate lyase for brown algal biomass degradation by *Zobellia galactanivorans*. *Environ Microbiol* **19**: 2164–2181.

## Supporting Information

Additional Supporting Information may be found in the online version of this article at the publisher's web-site:

**Supplementary Fig. 1.** A. Sampling location (cross) near Helgoland Island above dense macroalgal forests; schematically depicted in green. B. Conceptual overview of experimental setup using custom polysaccharide particles (insert). Magnetic particles were separated from their non-magnetic counterparts by magnetic selection (Supplementary Video 1) and frozen in cryotubes. FL communities were sampled by size-fractionated filtration of the supernatant (5 µm followed by 0.2 µm). Ambient seawater (start) and control samples (CTR) were directly filtered on 0.2 µm. Amplicon (0, 24, 48 and 60 h), metagenomic (24 and 60 h), and meta-transcriptomic sequence data (60 h) were generated after different intervals of incubation.

**Supplementary Fig. 2.** Relative abundances of bacterial genera (top) and inverse Simpson alpha-diversity index (bottom) on alginate (AlgP) and pectin particles (PecP), in the free-living fraction (FL), control incubations (CTR) and the ambient *in situ* community (start). Only genera with abundances >4% are shown.

**Supplementary Fig. 3.** Relative abundances of *Colwellia* and *Glaciecola* ASVs in PA and FL communities. Each colour corresponds to a distinct ASV.

**Supplementary Fig. 4.** Maximum-likelihood phylogeny of MAGs based on 92 single-copy core genes, including the five near-complete MAGs (>90% completeness, <10% contamination), medium-quality MAGs (>70% completeness, <10% contamination) assigned to the same genus, and other related genomes.

**Supplementary Fig. 5.** Degradation of alginate and pectin based on Hobbs *et al.*, 2019 and Koch *et al.*, 2019a. TBDR: TonB-dependent receptor; MFS: major facilitator superfamily transporter; TRAP: tripartite ATP-independent transporter; DehR: DEH reductase; KdgK: KDG kinase; KdgA: KDG aldolase; KdgF: responsible for uronate linearisation; Kdul: 4-deoxy-L-threo-5-hexosulose-uronate ketol-isomerase; KduD: 2-deoxy-D-gluconate 3-dehydrogenase; UxaA: altronate dehydratase; UxaB: fructuronate reductase; UxaC: glucuronate isomerase; DEH: 4-deoxy-L-erythro-5-hexoseulose uronate; KDG: 2-keto-3-deoxy-D-gluconate; KDGP 2-keto-3-deoxy-6-phosphogluconate.

**Supplementary Fig. 6.** Detailed architecture of PUL in MAGs.

**Supplementary Fig. 7.** A: Truncated alginolytic operon in *Glaciecola*-MAG Gla-32 compared to the functionally characterized PUL in *Alteromonas macleodii* 83–1. BLASTp confirmed that missing genes were not encoded on other Gla-32 contigs. B: Hybrid biosynthetic gene cluster in *Psychromonas*-MAG Psym-73 encoding a siderophore homologous to a functional cluster in *Alteromonas* sp. 76–1 (left section) as well as spermidine-related genes homologous to VC1623 and VC1624 in *Vibrio cholerae* (right section). Locus tags are shown inside the first and last gene.

**Supplementary Fig. 8.** Maximum-likelihood phylogeny of PL7 genes from *Psychromonas*-MAG Psym-73, using BAB03312.1 from *Sphingomonas* as outgroup. Only some homologues showed substantial transcript abundances (right insert).

**Supplementary Fig. 9.** Rarefaction and coverage analysis of amplicon reads.

**Supplementary Table 1.** Metadata, sampling strategy, and statistics from amplicon, metagenome and meta-transcriptome sequencing.

**Supplementary Table 2.** Complete overview of metagenomic genes, their abundance in metatranscriptomes (transcripts per million), and their assignment to CAZyme and KEGG categories.

**Supplementary Table 3.** Complete overview of differential transcript abundance analysis.

**Supplementary Table 4.** Complete overview of metagenome-assembled genomes.

**Supplementary Table 5.** Comparison of *Tenacibaculum*-MAG Ten-26 and *Psychromonas*-MAG Psym-73 with *Psychromonas* sp. B3M02 and *Tenacibaculum* sp. E3R01 from Enke *et al.* 2019 (<https://doi.org/10.1016/j.cub.2019.03.047>).

**Supplementary Table 6.** Composition of alginate and pectin particles.

**Supplementary Video 1.** Magnetic polysaccharide particles.

## Appendix 7

### **Genomic, metabolic and phenotypic variability shapes ecological differentiation and intraspecies interactions of *Alteromonas macleodii***

Koch H, Germscheid N, Freese HM, Noriega-Ortega B, Lücking D, Berger M, Qiu G, Marzinelli E, Campbell A, Steinberg P, Overmann J, Dittmar T, Simon M, Wietz M

*Scientific Reports* (2020), 10:809

OPEN

# Genomic, metabolic and phenotypic variability shapes ecological differentiation and intraspecies interactions of *Alteromonas macleodii*

Hanna Koch<sup>1,8,14</sup>, Nora Germscheid<sup>1,14</sup>, Heike M. Freese<sup>2</sup>, Beatriz Noriega-Ortega<sup>3,9</sup>, Dominik Lücking<sup>1</sup>, Martine Berger<sup>1</sup>, Galaxy Qiu<sup>4,10</sup>, Ezequiel M. Marzinelli<sup>4,5,6,11</sup>, Alexandra H. Campbell<sup>4,12</sup>, Peter D. Steinberg<sup>4,5,6</sup>, Jörg Overmann<sup>2,7</sup>, Thorsten Dittmar<sup>3</sup>, Meinhard Simon<sup>1</sup> & Matthias Wietz<sup>1,13\*</sup>

Ecological differentiation between strains of bacterial species is shaped by genomic and metabolic variability. However, connecting genotypes to ecological niches remains a major challenge. Here, we linked bacterial geno- and phenotypes by contextualizing pangenomic, exometabolomic and physiological evidence in twelve strains of the marine bacterium *Alteromonas macleodii*, illuminating adaptive strategies of carbon metabolism, microbial interactions, cellular communication and iron acquisition. In *A. macleodii* strain MIT1002, secretion of amino acids and the unique capacity for phenol degradation may promote associations with *Prochlorococcus* cyanobacteria. Strain 83-1 and three novel Pacific isolates, featuring clonal genomes despite originating from distant locations, have profound abilities for algal polysaccharide utilization but without detrimental implications for *Ecklonia* macroalgae. Degradation of toluene and xylene, mediated via a plasmid syntenic to terrestrial *Pseudomonas*, was unique to strain EZ55. Benzoate degradation by strain EC673 related to a chromosomal gene cluster shared with the plasmid of *A. mediterranea* EC615, underlining that mobile genetic elements drive adaptations. Furthermore, we revealed strain-specific production of siderophores and homoserine lactones, with implications for nutrient acquisition and cellular communication. Phenotypic variability corresponded to different competitiveness in co-culture and geographic distribution, indicating linkages between intraspecific diversity, microbial interactions and biogeography. The finding of "ecological microdiversity" helps understanding the widespread occurrence of *A. macleodii* and contributes to the interpretation of bacterial niche specialization, population ecology and biogeochemical roles.

<sup>1</sup>Institute for Chemistry and Biology of the Marine Environment, University of Oldenburg, Oldenburg, Germany.

<sup>2</sup>Leibniz Institute DSMZ - German Collection of Microorganisms and Cell Cultures, Braunschweig, Germany. <sup>3</sup>ICBM-MPI Bridging Group for Marine Geochemistry, University of Oldenburg, Oldenburg, Germany. <sup>4</sup>Centre for Marine Science and Innovation, University of New South Wales, Kensington, Australia. <sup>5</sup>Singapore Centre for Environmental Life Sciences Engineering, Nanyang Technological University, Singapore, Singapore. <sup>6</sup>Sydney Institute of Marine Science, Mosman, Australia. <sup>7</sup>Braunschweig University of Technology, Braunschweig, Germany. <sup>8</sup>Present address: Radboud University Nijmegen, Nijmegen, The Netherlands. <sup>9</sup>Present address: Leibniz Institute of Freshwater Ecology and Inland Fisheries, Berlin, Germany. <sup>10</sup>Present address: Western Sydney University, Hawkesbury, Australia. <sup>11</sup>Present address: University of Sydney, Camperdown, Australia. <sup>12</sup>Present address: University of Sunshine Coast, Sunshine Coast, Australia. <sup>13</sup>Present address: Alfred Wegener Institute Helmholtz Centre for Polar and Marine Research, Bremerhaven, Germany. <sup>14</sup>These authors contributed equally: Hanna Koch and Nora Germscheid. \*email: [matthias.wietz@awi.de](mailto:matthias.wietz@awi.de)

Metabolic variability is a major driver of ecological differentiation within bacterial taxa, shaping adaptive strategies and hence the niche space of related strains<sup>1</sup>. With the increasing number of sequenced genomes, substantial functional diversity is being discovered among closely related strains<sup>2</sup>, with implications for bacterial species concepts<sup>3</sup>. This diversity can be investigated by interrogating the pangenome of a taxonomic group (i.e. their entire repertoire of core and variable genes) for genotypic variants with ecological implications<sup>4</sup>. Ecological differentiation within a taxon mainly relates to two flexible genomic categories: the accessory genome (shared by several strains) and the unique genome (restricted to individual strains). This variable repertoire is often encoded in genomic islands, hotspots of genetic exchange<sup>5</sup> known to influence niche specialization in cyanobacteria, actinobacteria and roseobacters<sup>6–8</sup>. Flexible genomic islands, located at equivalent loci in different strains of the same taxon, can provide or replace genetic information and are important factors for intraspecific heterogeneity<sup>9,10</sup>, for instance governing carbon utilization, siderophore production and pilus assembly<sup>11</sup>. These adaptive-evolutionary processes are often amplified by plasmids and other mobile genetic elements, driving horizontal gene transfer (HGT) and diversification on short time scales<sup>12–14</sup>. Bacterial adaptations can also relate to single-nucleotide exchanges via homologous recombination or mutations<sup>15,16</sup>.

Current approaches to species delineation, such as 16S rRNA or core-genome phylogenies, do not always reflect the diversity of strain-specific ecological strategies. For instance, the analysis of ~400 *Vibrio cholerae* strains has revealed distinct intraspecific variability in genes mediating bioluminescence and colonization of zooplankton<sup>17</sup>. Closely related vibrios also show substantial divergence in polysaccharide degradation<sup>18</sup> and particle colonization<sup>19</sup>. Comparable diversity has been observed for biosynthetic capacities within marine *Salinispora* species<sup>20</sup>, with implications for strain-specific competitive abilities<sup>21</sup>. Also the degree of carbohydrate utilization can vary between strains of the same species<sup>22</sup>. Recently, these aspects have been extended to the metapangenomic dimension, revealing linkages of genomic and geographic variability among *Prochlorococcus* strains<sup>23</sup>.

The marine gammaproteobacterium *Alteromonas macleodii* is an excellent model to study the ecological consequences of strain-level variability, as multiple genome-sequenced isolates from diverse habitats and locations are available. The occupation of different niches<sup>24</sup>, varied interactions with other organisms<sup>25–27</sup> and utilization of diverse substrates<sup>28,29</sup> suggests the existence of functionally distinct entities within the *A. macleodii* species boundary, despite being >99% identical on 16S rRNA gene level. This notion is supported by the diverse flexible genome and a high degree of genetic exchange between *A. macleodii* and the “sister species” *A. mediterranea*<sup>13,30</sup>. Consequently, genomic islands and mobile genetic elements are major drivers of genetic and metabolic variability within *Alteromonas*, influencing surface-associated vs. free-living lifestyles<sup>31</sup>, exopolysaccharide production<sup>30</sup>, heavy metal resistance<sup>32</sup> and polysaccharide utilization<sup>33</sup>. Notably, co-occurring *Alteromonas* strains have been postulated to colonize distinct microniches based on specific genomic features<sup>34</sup> and competitive abilities<sup>35</sup>. For instance, *A. mediterranea* strains differ in motility and glucose utilization, potentially influencing patterns of co-occurrence or mutual exclusion<sup>35</sup>. Despite these ecological implications of genome plasticity, phenotypic and genetic variability have not been comprehensively linked in *Alteromonas* to date, largely because few putative traits have been experimentally verified.

The present study investigated strain-level phenotypic and genomic variability in twelve strains of *A. macleodii* with completely sequenced genomes, including three novel isolates from a Pacific Ocean transect. Supported by exometabolomic evidence and targeted physiological assays, we show how accessory and unique features shape ecological differentiation and result in “microdiversity” of phenotypic traits<sup>1,36</sup>. Co-culturing experiments linked these observations to strain-specific competitiveness, a factor that may influence ecophysiological roles and biogeographic distribution. The finding of diverse metabolic potentials within a narrow taxonomic range, whose members may co-occur or compete depending on prevailing conditions, contributes to the functional interpretation of bacterial species and populations. The shown intraspecific diversity in adaptive strategies helps understanding the widespread occurrence of *A. macleodii* in the oceans, with broader implications for bacterial population ecology and niche specialization.

## Results and Discussion

This study combines genomic and phenotypic evidence to illuminate mechanisms of ecological differentiation within *Alteromonas macleodii*, a bacterium with widespread distribution and biogeochemical importance in the oceans<sup>24</sup>. The study focused on twelve *A. macleodii* strains with closed genomes, featuring average nucleotide identities (ANI) of 96.5–99.9% and 16S rRNA gene similarities of >99% (Fig. 1; Table S1). Despite this clear association to a single genospecies<sup>37</sup>, underlined by 3002 core genes, we detected considerable strain-level diversity related to 1662 accessory and 1659 unique gene clusters (Table S2). This is consistent with the pronounced diversity of the flexible genome in *A. macleodii* and the “sister species” *A. mediterranea*, as described previously<sup>30</sup>. Intraspecific differences were highlighted by a diverse pan-exometabolome of 138 core, 1796 accessory and 2096 unique molecular masses secreted during late exponential growth (Table S3). In the following, we contextualize (pan)genomic and phenotypic evidence to characterize how genome plasticity shapes interactions with cyanobacteria and macroalgae, degradation of aromatics and polysaccharides, chemical communication, iron acquisition, and intraspecific competition. These insights expand structural-genomic and evolutionary aspects of the *Alteromonas* pangenome<sup>30,32,34,38,39</sup> by ecological perspectives on niche specialization, competitive abilities and biogeography.

**Plasmids and genomic rearrangements.** As niche specialization is often mediated by mobile genetic elements<sup>40</sup>, we first characterized occurrence and function of plasmids. Eight out of twelve *A. macleodii* strains, including MIT1002 and EZ55 whose genomes were re-sequenced and closed herein, were found to contain a plasmid (Figs. 1, S1). Synteny of plasmids from *A. macleodii* Te101 and *A. mediterranea* DE1 corroborates the role of plasmids for niche specialization within and across species boundaries<sup>13,41</sup>.

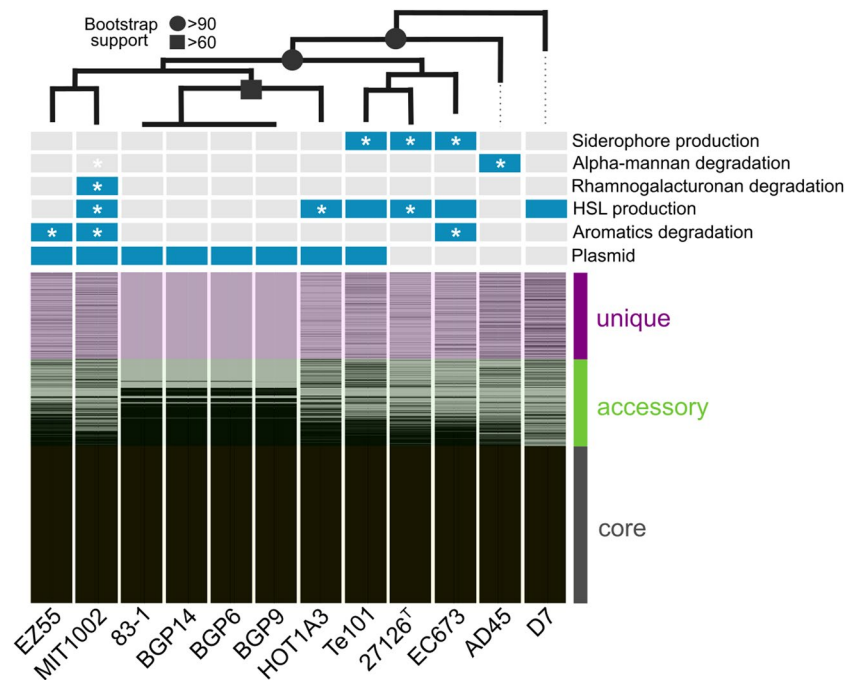


**Figure 1.** Maximum-likelihood phylogeny and pangenome structure of *Alteromonas macleodii*, showing presence (blue) and absence (gray) of specific genomic features. Phylogenetic analysis was based on 92 single-copy housekeeping genes identified using the UBCG pipeline<sup>119</sup>. Asterisks designate phenotypic features experimentally verified in the present study. Bootstrap support values are indicated by symbols; unlabeled branches have <50% support.

The plasmids of six strains display a similar functional profile, harboring metal resistance and [NiFe] hydrogenase cassettes (Fig. 2A) that have been described in *Alteromonas* before<sup>42,43</sup> and provide increased resistance compared to strains lacking these cassettes<sup>43</sup>. As homologous cassettes in *A. mediterranea* are encoded in a chromosomal genomic island<sup>30,32,44</sup>, plasmids possibly mediate their transfer between Alteromonadales<sup>13</sup>. Notably, number and arrangement of cassettes differed between strains (Fig. 2A), which may result in varying expression levels and hence different resistance profiles<sup>45</sup>. In strain MIT1002, hydrogenase and resistance cassettes have been inserted into the chromosome, and a unique chemotaxis-related plasmid has been acquired (Fig. 2B). This event may enhance chemosensory abilities and provide a competitive advantage to access nutrient patches<sup>46</sup>.

The plasmid of strain EZ55 harbors a unique 20 Kb insert, enabling aerobic degradation of the aromatic hydrocarbons toluene and xylene (Figs. 2; S2) as rarely described in marine microbes to date<sup>47,48</sup>. The insert is overall homologous to the TOL plasmid from *Pseudomonas putida* (Fig. 2A), a hydrocarbon-degrading Gammaproteobacterium from soil<sup>49</sup>. However, closer examination using MultiGeneBlast<sup>50</sup> suggests assembly during separate horizontal transfer events. Specifically, the downstream section (locus tags 04282–04290) has highest similarity to TOL plasmids from *Pseudomonas* strains, with amino acid identities between 70 to 86% (Fig. 3A). In contrast, the upstream section including the catechol meta-cleavage pathway (locus tags 04248–04260) has highest similarity to homologous clusters in *Marinobacter* followed by *Pseudomonas* spp., with amino acid identities between 52 and 98% (Fig. 3A). Considering multiple adjacent transposases and recombinases (locus tags 04244, 04264, 04266, 04267, 04270, 04273, 04279, 04291) and the fact that *Alteromonas*, *Pseudomonas* and *Marinobacter* co-occur during oil spills where toluene and xylene are present<sup>51</sup>, we hypothesize exchange of these clusters at contaminated sites. Alternatively, *Marinobacter* might constitute a “vehicle” between soil and seawater due to its occurrence in saline lakes and intertidal areas<sup>52</sup> and known acquisition of aromatic-degrading genes from *Pseudomonas*<sup>53</sup>. Considering the common association of *Marinobacter* spp. with phototrophs<sup>54,55</sup>, the cluster might likewise enable degradation of ecologically more relevant aromatics from cyanobacteria, e.g. derivatives of benzoate or cinnamate<sup>56</sup>.

***Alteromonas* and *Prochlorococcus*.** In addition to plasmids, ecological differentiation also relates to varying abilities for microbial interactions<sup>57</sup>. In this context, strains MIT1002 and EZ55 are naturally associated with *Prochlorococcus* cyanobacteria, to whom they establish mutualistic relationships by alleviating oxidative stress or nutrient limitation during extended periods of darkness<sup>58–61</sup>. Here, we demonstrate additional features that may support their co-existence. Specifically, only MIT1002 harbors a gene cluster encoding the potential for phenol metabolism (Figs. 4A; S2). This ability appears ecologically relevant considering upregulation of phenol hydroxylases in co-culture with *Prochlorococcus* (Table S4 with data from<sup>62</sup>), the common production of phenolics by cyanobacteria<sup>63</sup>, and presence of a homologous gene cluster in *Marinobacter algicola* with comparable association to phototrophs<sup>54</sup>. The *Alteromonas-Prochlorococcus* interplay may be further strengthened by metabolic interrelations, as FT-ICR-MS revealed that MIT1002 and EZ55 secrete ecologically relevant exometabolites

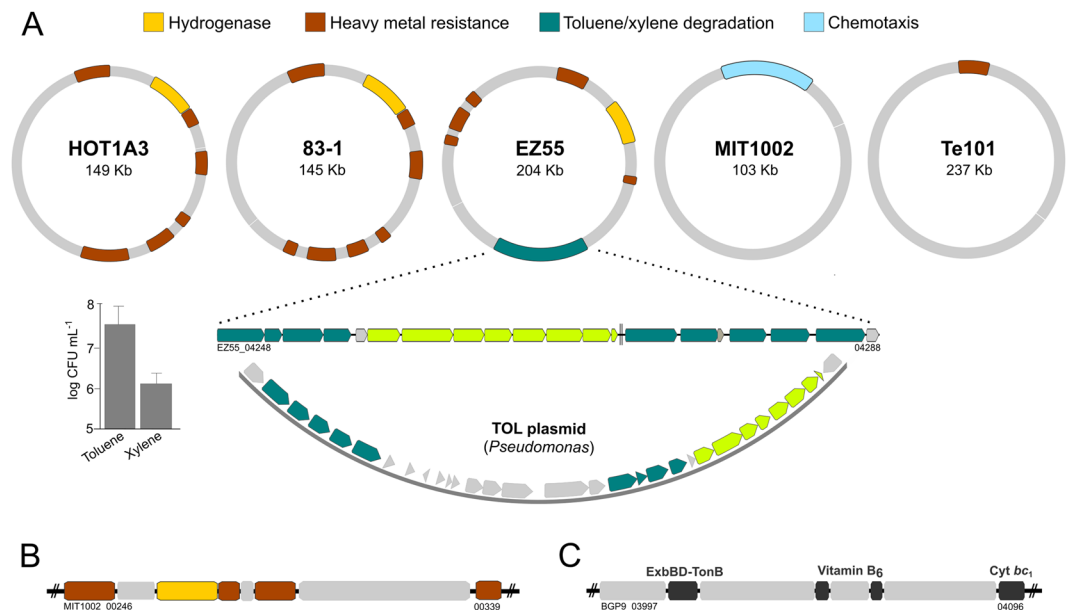


**Figure 2.** Structural diversity of plasmids in *Alteromonas macleodii*. **(A)** Functionally similar plasmids in strains HOT1A3, 83-1 and EZ55 encoding hydrogenase and heavy metal resistance cassettes, however with different organization. The plasmid of EZ55 furthermore contains a unique insertion syntenic to the *Pseudomonas* TOL plasmid (blue-green: toluene/xylene hydroxylases and transporters; green: catechol meta-cleavage pathway; gray: non-homologous genes) allowing growth with toluene and xylene as sole carbon source (insert). The plasmid of strain Te101 is structurally different and encodes only one resistance cassette. **(A,B)** Strain MIT1002 harbors a unique chemotaxis-related plasmid, whereas an 80 Kb region encoding hydrogenase and resistance cassettes has been translocated to the chromosome. **(C)** Strain BGP9 features a chromosome-plasmid translocation of a 90 Kb region harboring a TonB/ExbBD membrane system, a cytochrome  $bc_1$  complex and vitamin  $B_6$  synthesis genes.

(Table 1). Secretion of methyl-tryptophan and methyl-indolepyruvate may explain the differential regulation of tryptophan biosynthesis in *Prochlorococcus* when co-cultured with *A. macleodii*<sup>64,65</sup>, especially under restricted photosynthesis<sup>59</sup>. Secretion of asparagine and glutamine (Table 1) indicates exchange of further amino acids, coincident with upregulation of related importers in *Prochlorococcus* when co-cultured<sup>64</sup>. Possible cross-feeding is supported by the potential for mixotrophy<sup>66</sup> and considerable usage of exogenous amino acids<sup>67</sup> in environmental *Prochlorococcus* assemblages. Hence, these compounds are possible drivers of varied prokaryotic<sup>68,69</sup> but also interkingdom interactions, as *A. macleodii* can likewise counteract amino acid deficiency in microalgae<sup>25</sup>.

Comparison with prior transcriptomic data<sup>59</sup> showed that interactions of MIT1002 with *Prochlorococcus* involve several unique genes (Table S4). For instance, differential regulation of unique chemotaxis-, motility- and biofilm-related genes in co-culture may strengthen physical associations<sup>70</sup> whereas upregulation of a phytase gene might enhance phosphorus acquisition<sup>71</sup>. Overall, the array of interactive features suggests that MIT1002 and EZ55 are adapted to a mutualistic niche with *Prochlorococcus*, a relevant notion considering the cyanobacterium's reduced metabolic repertoire and importance for biogeochemical cycles<sup>72,73</sup>.

***Alteromonas*, macroalgae and algal polysaccharides.** We herein isolated *A. macleodii* strains BGP6, BGP9 and BGP14 from algalinate-supplemented microcosms in the south, equatorial and north Pacific Ocean (Table S1) using analogous procedures that yielded the alginolytic strain *A. macleodii* 83-1 from the Atlantic<sup>33</sup>. Strikingly, the new isolates and strain 83-1 are clonal, featuring only four polymorphisms in 4,801,369 core sites despite being isolated over wide geographic and temporal scales. These observations resemble the isolation of *A. mediterranea* strains with less than 100 polymorphisms from distant locations and years apart<sup>30,38</sup>. In addition, two *A. australica* strains with 99% ANI have been retrieved from opposite global locations<sup>44</sup>, illustrating that highly similar *Alteromonas* spp. are widely distributed over time and space.

The four clonal *A. macleodii* strains encode numerous carbohydrate-active enzymes (CAZymes) and other enzymes involved in carbohydrate-related KEGG categories (Fig. S3A; Table S2), enabling the degradation of various algal polysaccharides<sup>74</sup> and indicating association with plants<sup>75</sup>. To examine whether these features trigger direct interactions with algae, *A. macleodii* 83-1 was incubated with tissue from the marine macroalga *Ecklonia radiata*, which contains >50% algalinate and hence a preferred substrate<sup>33</sup>. However, no significant tissue degradation was observed (Fig. S3B) although epibiotic bacteria cause visible digestion of *Ecklonia* and other macroalgae<sup>76-78</sup>. These observations suggest that *A. macleodii* has limited abilities to attack macroalgal tissue, and potentially utilizes polysaccharide exudates released directly by the macroalga<sup>74</sup> or by co-metabolizing bacteria<sup>18</sup>. This proposed lifestyle is supported by low *Alteromonas* abundances on wild macroalgae<sup>79</sup>. Alternatively, colonization might occur in a neutral manner, comparable to other *Alteromonas* spp. with a similar CAZyme profile<sup>80</sup>.

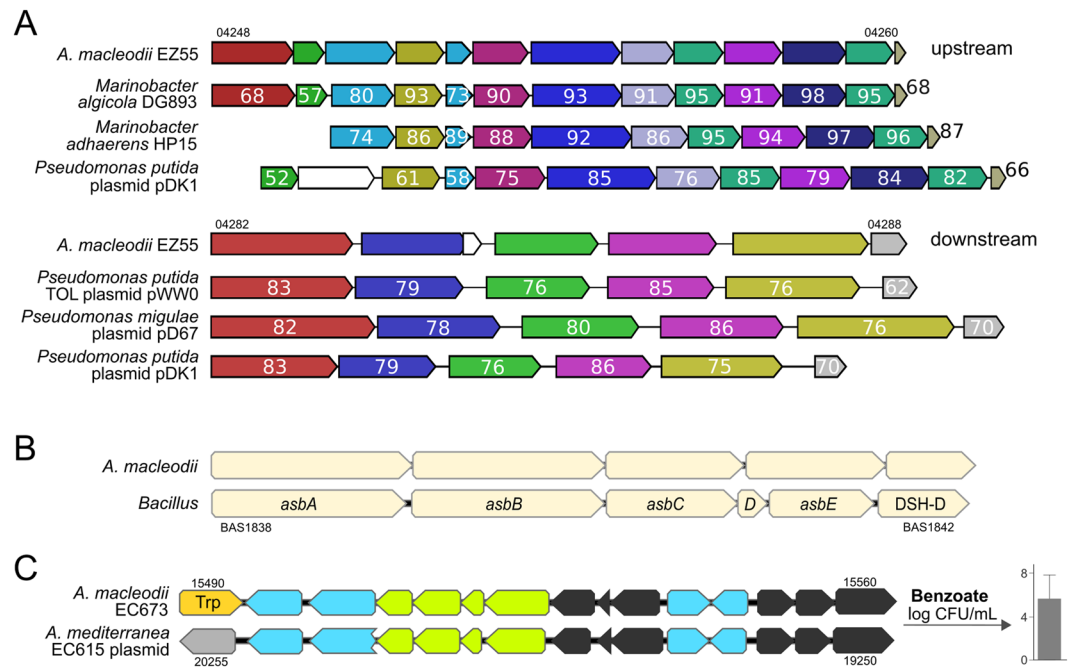


**Figure 3.** Comparative analysis of selected gene clusters in *Alteromonas macleodii* and other bacteria. **(A)** Gene cluster for toluene/xylene degradation in strain EZ55 plus closest relatives of upstream (locus tags 04248–04260) and downstream (04282–04288) cluster sections. Colors illustrate homologs as determined by MultiGeneBlast, with numbers designating % amino acid similarities. **(B)** Homology of the siderophore-encoding cluster of strains ATCC27126<sup>T</sup>, EC673 and Te101 with the petrobactin operon *asbABCDE* plus adjacent dehydroshikimate dehydratase (DHS-D) from *Bacillus* spp. **(C)** Gene cluster for benzoate degradation in strain EC673, encoding benzoate dioxygenases (green), the catechol ortho-cleavage pathway (black) and transporters/regulators (blue), allowing growth with benzoate as sole carbon source (right insert). A homologous cluster is encoded on the plasmid of *A. mediterranea* EC615. Trp: transposase; gray: non-homologous gene.

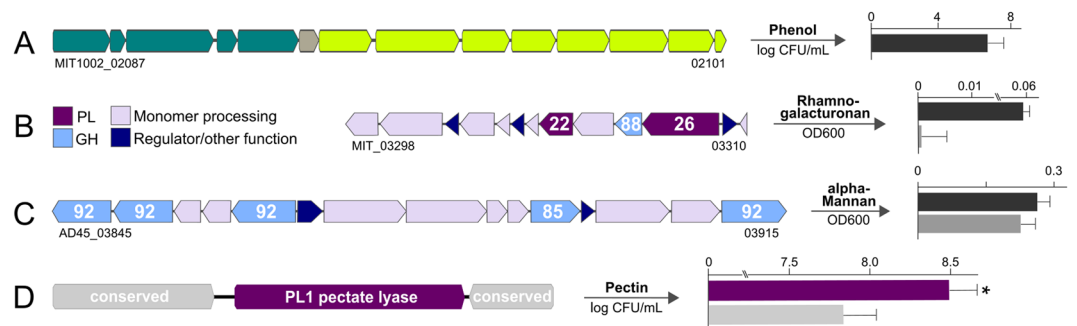


**Figure 4.** Features of *Alteromonas macleodii* relating to interactions with cyanobacteria and macroalgae. **(A)** Unique gene cluster in strain MIT1002 encoding phenol hydroxylases (blue-green) and the catechol meta-cleavage pathway (green), allowing growth with phenol as sole carbon source. **(B,C)** Unique polysaccharide utilization loci in strains MIT1002 and AD45 allowing growth with rhamnogalacturonan and alpha-mannan as sole carbon source (MIT1002: dark gray, AD45: light gray). Numbers designate encoded glycoside hydrolase and polysaccharide lyase families. **(D)** Several strains encode an additional PL1 pectate lyase within a conserved region, enhancing growth with pectin as sole carbon source (purple: strain 83-1 with additional PL1; gray: strain HOT1A3 without). \* $p < 0.05$ .

Considering nucleotide substitution rates of ca.  $10^{-8}$  per site/year in related *Gammaproteobacteria*<sup>81</sup>, the four clonal strains probably diverged only recently followed by rapid geographic spread, comparable to *Phaeobacter* strains from the same Pacific transect<sup>82</sup>. However, some features illustrate the beginning of differentiation. In BGP9, a 91 Kb region harboring a TonB/ExbBD membrane system and vitamin B<sub>6</sub> synthesis genes was translocated from chromosome to plasmid (Fig. 2C), which may influence iron and vitamin metabolism<sup>83,84</sup>. The transposed region also harbors the strain's sole cytochrome *bc<sub>1</sub>* complex, although essential genes are uncommon on plasmids<sup>85</sup>. At an estimated plasmid loss of  $\sim 10^{-3}$  per cell and generation<sup>86</sup>, this event may pose a considerable risk for survival.

Exact mass (Da)	Predicted compound	Detected in
216.066647	methyl-indolepyruvate	MIT1002
217.098241	methyl-tryptophan	EZ55
131.046208	asparagine	EZ55
145.061869	glutamine	EZ55
198.186345	dodecanamide (fatty acid moiety of 3-oxo-C12-HSL)	MIT1002
296.186680	<i>N</i> -3-oxododecanoyl-homoserine lactone (3-oxo-C12-HSL)	HOT1A3
198.113576	<i>N</i> -hexanoyl-L-homoserine lactone (C6-HSL)	27126 <sup>T</sup>

**Table 1.** Selected exometabolites of *Alteromonas macleodii* strains.

Specific adaptations to algal polysaccharide degradation were also found in strains MIT1002 and AD45, mediated by unique polysaccharide utilization loci (PUL)<sup>87</sup>. Specifically, only MIT1002 harbors a PUL encoding PL22 and PL26 polysaccharide lyases, a GH88 rhamnogalacturonyl hydrolase and several rhamnose-processing genes, allowing growth with rhamnogalacturonan as sole carbon source (Fig. 4B). A PL26-GH88 pair also occurs in the rhamnogalacturonan-degrading flavobacterium *Gramella flava*<sup>88</sup>, indicating co-functionality towards rhamnose-rich polysaccharides. As rhamnogalacturonan is present in widespread marine macroalgae<sup>74</sup>, degradative abilities may strengthen associations between MIT1002 and phototrophs. Homologous PUL in *A. australica* with 80% nucleotide identity (data not shown) demonstrates independent acquisition of these genes by other *Alteromonas* species, comparable to PUL targeting ulvan from green algae<sup>89,90</sup>. Strain AD45 harbors a unique PUL encoding GH85 and GH92 mannosidases and grows with alpha-mannan as sole carbon source (Fig. 4C), but comparable growth of MIT1002 indicates that mannosidase activity also occurs via other encoded GHs (Fig. S3A). Opposed to mannan-degrading marine flavobacteria<sup>91</sup>, strain AD45 does not encode sulfatases and may hence primarily target terrestrial mannans, corresponding to its coastal origin<sup>92</sup> and the lower degree of sulfatation in terrestrial polysaccharides<sup>93</sup>. A speculative link relates to the isolation of AD45 from the vicinity of aquaculture facilities, where mannan oligosaccharides are increasingly used as feed additive<sup>94</sup>. Overall, presence in diverse terrestrial and aquatic bacteria (Fig. S3C) suggests the PUL as a widespread niche-defining feature.

Finally, we found that adaptation towards algal polysaccharide degradation is also linked to numerical variation in CAZymes, in context of gene dosage effect and substrate affinity<sup>18</sup>. Specifically, *A. macleodii* strains that encode three PL1 pectate lyases grow significantly better on pectin than strains with only two lyases (Figs. 4D; S3A). Enrichment of the third lyase in the exoproteome of strain 83-1<sup>74</sup> suggests a role in extracellular substrate recognition and initial hydrolysis. Enhanced degradation through higher lyase numbers is consistent with observations in *Zobellia galactanivorans*, a common macroalgal associate and proficient polysaccharide degrader<sup>78</sup>. Overall, the patchy distribution of rhamnogalacturonan, mannan and pectin degradation discriminates *A. macleodii* into specific “polysaccharide utilization types” with distinct ecophysiological roles<sup>95</sup>.

**Cellular communication.** Ecological differentiation can also coincide with the potential to coordinate behavior at population level. In this context, we found that *A. macleodii* strains vary in their ability to synthesize homoserine lactones (HSL) for intraspecific communication via quorum sensing<sup>96</sup>. Two gene variants encoding *N*-acyl amino acid synthase occur in *A. macleodii* (Fig. 5A), but masses corresponding to C6-HSL, 3-oxo-C12-HSL and dodecanamide (the fatty acid moiety of 3-oxo-C12-HSL) were only detected in exometabolomes of strains 27126<sup>T</sup>, HOT1A3 and MIT1002 (Table 1). The restriction of HSL production to these strains is supported by antimash<sup>97</sup>, which only predicts their sequence variant as functional synthase (Table S1). Accordingly, the autoinducer domain of producers and non-producers has <80% sequence identity (data not shown). Synthase sequences of 27126<sup>T</sup>, HOT1A3 and MIT1002 contain different substitutions (Fig. 5A), which potentially explains the observation of HSLs with differing chain lengths<sup>98</sup>. HSLs were only detectable using highly sensitive FT-ICR-MS but not standard bacterial monitor assays<sup>99</sup>, but HSLs can influence chemical interactions and surface attachment even at low concentrations<sup>96,100</sup>. Intraspecific HSL diversity has also been described among symbiotic *Vibrio*<sup>101</sup>, suggesting variable potential for chemical communication as common discriminator of closely related strains.

**Iron acquisition.** Successful niche colonization also depends on efficient acquisition of limiting micronutrients, including iron<sup>102</sup>. In this context, only strains 27126<sup>T</sup>, EC673 and Te101 harbor a gene cluster for siderophore synthesis with demonstrated iron-scavenging activity (Fig. 5B), likely providing an advantage during iron limitation<sup>103</sup>. The gene cluster is homologous to the petrobactin operon of *Bacillus* spp. (Fig. 3B; 35% amino acid identity) and also occurs in other marine bacteria, suggesting broad ecological relevance<sup>104</sup>. In strain EC673 from the English Channel, the siderophore might support growth with benzoate as sole carbon source (Figs. 3C, S2) by counteracting iron limitation of benzoate breakdown<sup>105</sup>. This scenario could be advantageous considering the anthropogenic input of benzoate in its original habitat<sup>106</sup>. The benzoate cluster is located in a genomic island<sup>32</sup> and flanked by a transposase, underlining the importance of flexible loci for phenotypic variability. Notably, also *A. mediterranea* EC615 from the English Channel harbors the benzoate-related cluster (Fig. 3C), but encoded on a plasmid<sup>38</sup>. These observations indicate common occurrence and exchange of these genes via mobile genetic elements in habitats where certain chemicals may prevail.

Strain MIT1002 harbors a truncated siderophore cluster, where synthases have been separated by metal-resistance cassettes during the translocation from plasmid to genome (see above). This integration

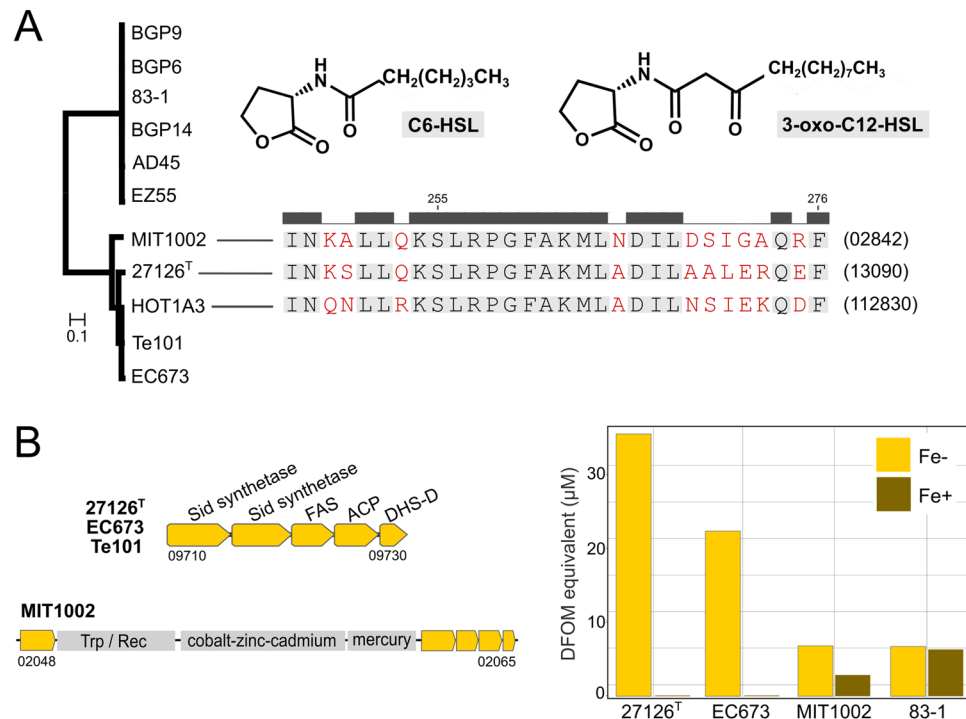


**Figure 5.** Cellular communication and iron acquisition in *Alteromonas macleodii*. **(A)** Phylogenetic analysis reveals two sequence variants of *N*-acyl amino acid synthase in producers (lower) and non-producers (upper) of homoserine lactones (HSL). Accordingly, molecular masses relating to C6-HSL and 3-oxo-C12-HSL were only secreted by strains 27126<sup>T</sup>, MIT1002 and HOT1A3 (see Table 1). Strain-specific amino acid substitutions (red) may explain differential HSL production (synthase locus tags in parentheses). **(B)** Gene cluster unique to strains 27126<sup>T</sup>, EC673 and Te101 encoding a functional siderophore (locus tags from type strain), with iron-scavenging activity under iron-deplete (Fe<sup>-</sup>) but not iron-replete (Fe<sup>+</sup>) conditions in relation to deferoxamine mesylate (DFOM) standard. MIT1002 harbors a nonfunctional cluster after insertion of gene cassettes for cobalt-zinc-cadmium and mercury resistance. Weak signals in MIT1002 and negative control 83-1 under both conditions signify iron-unrelated effects. Sid: siderophore; FAS: fatty acid synthase; ACP: acyl carrier protein; DHS-D: 3-dehydroshikimate dehydratase; Trp: transposase; Rec: recombinase.

abolished iron-scavenging activity (Fig. 5B), showing that genetic exchange and restructuring of genomic islands can also be disadvantageous.

**Implications for intraspecific interactions and biogeography.** To address broader eco-evolutionary implications, we asked whether strain-level variability affects population dynamics, competitive abilities and biogeographic distribution<sup>107,108</sup>. For instance, it is known that natural populations of *A. macleodii* can be dominated by specific strains through competitive exclusion<sup>34,109</sup>. To evaluate these aspects, three *A. macleodii* strains with comparable growth in monoculture (Fig. S4) were co-cultured with glucose as sole carbon source, and individual population sizes determined by quantitative PCR of unique genes (Table S5). The tripartite co-culture was dominated by strain MIT1002, which outcompeted both 83-1 and 27126<sup>T</sup> over a period of 24 h ( $p < 0.01$ ). Furthermore, strain 83-1 outcompeted 27126<sup>T</sup> in late exponential phase ( $p < 0.001$ ) (Fig. 6A). Comparable intraspecific differences were also observed in *A. mediterranea*, where greater competitive abilities coincided with higher motility<sup>35</sup>. The putative importance of motility in microbial interactions is supported by upregulation of related genes in MIT1002 when co-cultured with *Prochlorococcus*<sup>62</sup>.

Higher competitiveness of MIT1002 on glucose may provide an advantage in the environment, as glucose is one of the major marine carbohydrates<sup>110</sup>. Accordingly, MIT1002 showed a wider geographic distribution in TARA Ocean metagenomes (Fig. 6B, Table S6), indicating linkages between metabolic abilities and biogeography. Contact with diverse microbiota in different locations may also explain why unique genes of MIT1002 have been acquired from a wider taxonomic range (Fig. 6C; Table S7). These patterns may be amplified by association with *Prochlorococcus*, considering the wide occurrence of the cyanobacterium and higher genetic exchange in host-associated niches<sup>111,112</sup>. In contrast, 27126<sup>T</sup> has been isolated from oligotrophic waters with less biological activity and genetic exchange<sup>113</sup>, and lower growth efficiency on glucose may indicate a *k*-strategist lifestyle. Future co-culturing systems could address how co-existence or competitive exclusion proceed in more complex ecological scenarios, for instance pioneer-scavenger relationships during polysaccharide degradation<sup>18</sup>.

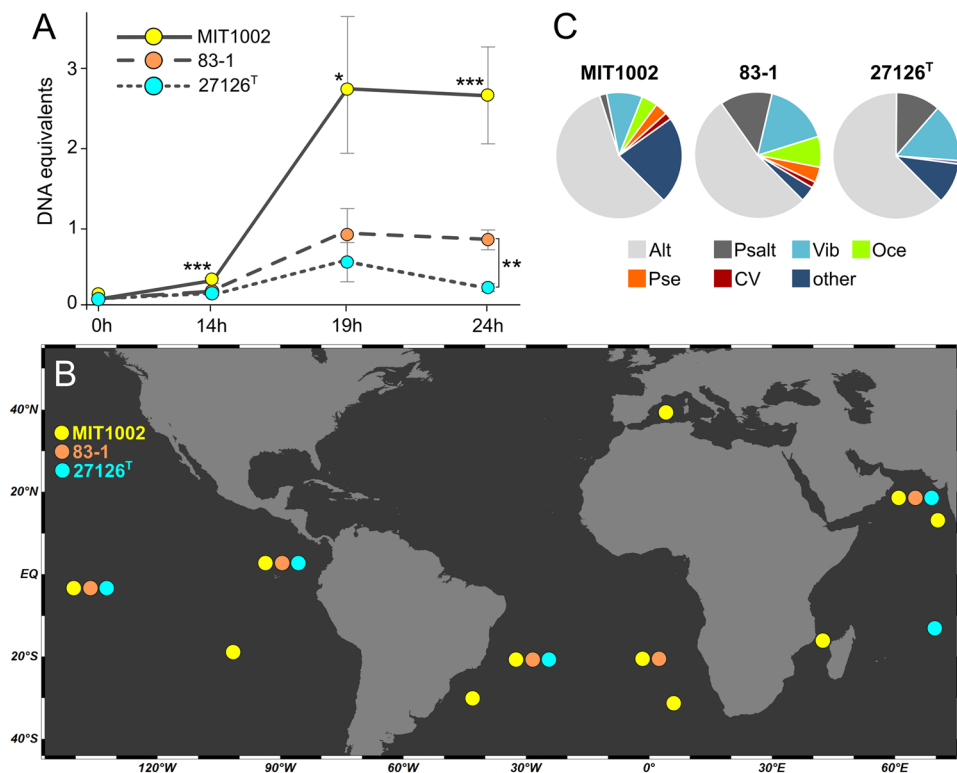


**Figure 6.** Ecological implications of strain-specific variability in *Alteromonas macleodii*. **(A)** Varying competitiveness of strains MIT1002, 83-1 and 27126<sup>T</sup> in a tripartite co-culture, determined by quantitative PCR of unique genes (\* $p < 0.01$ ; \*\* $p < 0.001$ ; \*\*\* $p < 0.0001$ ). **(B)** Occurrence of strains MIT1002, 83-1 and 27126<sup>T</sup> in TARA Ocean metagenomes based on BLAST of unique genes (see Table S6 for details). **(C)** Closest relatives of unique genes from strains MIT, 83-1 and 27126<sup>T</sup> based on BLAST against NCBI RefSeq. Alt: *Alteromonadaceae*; Psalt: *Pseudoalteromonadaceae*; Vib: *Vibrionaceae*; Oce: *Oceanospirillaceae*; Pse: *Pseudomonadaceae*; CV: Cellvibrionales (see Table S7 for details).

## Conclusions

Here, we extend existing knowledge on (pan)genome evolution and structure in *Alteromonas* by functional perspectives on genome plasticity in twelve *A. macleodii* strains. The shown range of ecological strategies demonstrates that single genospecies can encompass considerable diversity of adaptive features, underlining the importance of polyphasic studies that link bacterial genotypes and phenotypes<sup>114</sup>. The “ecological microdiversity” among strains with >99% 16S rRNA gene identity should be emphasized in microbial diversity studies, which are only beginning to explore the extent of fine-scale variability in natural communities<sup>36</sup>. Notably, phylogenetic relationships only partially corresponded to ecological similarity, illustrated by the patchy distribution of niche-defining metabolic features. Hence, in line with common recombination and genetic exchange<sup>30</sup>, *A. macleodii* appears to perform constant “pathway sampling” that has not (yet) manifested in divergence of specific clades. Metabolic versatility probably facilitates flexible responses to environmental conditions, contributing to the feast-and-famine lifestyle and widespread occurrence of this marine bacterium<sup>24,30</sup>. Sequencing of additional genomes may reveal whether strain-specific abilities translate to the existence of phylogenetic clades with distinct ecological boundaries, corresponding to larger eco-evolutionary concepts<sup>1,115,116</sup>. Our functional-ecological interpretation of the *A. macleodii* pangenome, illustrating the extent of eco-genomic differentiation within bacterial species, has broader implications for niche specialization, microbial interactions and biochemical roles of marine bacteria.

## Materials and Methods

**Isolation and sequencing of *Alteromonas macleodii* strains.** Strains BGP6, BGP9 and BGP14 were isolated from alginate-enriched seawater from the south, equatorial and north Pacific Ocean on expedition SO248 with RV *Sonne*<sup>117</sup>. The genomes of BGP strains, MIT1002 and EZ55 were sequenced *de novo* using PacBio II technology (Supplementary Methods). In addition, a number of published closed genomes were analyzed (Table S1).

**Pangenomic and phylogenetic analyses.** Core, accessory and unique genes (Table S2) were identified using anvio v5.2<sup>118</sup> following the pangenome workflow of Delmont and coworkers<sup>23</sup> with minbit parameter 0.5, MCL inflation parameter 10, Euclidean distance and Ward linkage, and NCBI-BLASTp for sequence similarity analysis (see Supplementary Methods for details). For phylogenetic analysis, 92 single-copy core genes (<https://help.ezbiocloud.net/ubcg-gene-set>) were identified, extracted and aligned using the UBCG pipeline<sup>119</sup> with *Alteromonas stellipolaris* LMG21861<sup>T</sup> as outgroup. The alignment was manually checked and submitted to

W-IQ-TREE<sup>120</sup> for calculating a maximum-likelihood phylogeny with 1000 bootstrap replicates and the GTR + G model determined by jModeltest 2<sup>121</sup>. Average nucleotide identities, polymorphic sites and a 16S rRNA gene similarity matrix were calculated using enveomics<sup>122</sup>, ParSNP/Gingr<sup>123</sup> and BioEdit<sup>124</sup>, respectively. Biosynthetic gene clusters and prophages were predicted using antiSMASH 4.0<sup>97</sup> and PHASTER<sup>125</sup>, respectively. CAZymes were predicted using dbCAN2<sup>126</sup> and abundances visualized using R package pheatmap<sup>127</sup>, only considering HMM hits with e-value  $<10^{-23}$  and  $>80\%$  query coverage. Genes were assigned to KEGG categories using KAAS and GhostKoala<sup>128,129</sup>. Annotations were checked using UniProtKB/Swiss-Prot<sup>130</sup> and Pfam<sup>131</sup>. Amino acid sequences of homoserine lactone synthases were aligned using MAFFT<sup>132</sup> followed by maximum-likelihood phylogeny using MEGA7<sup>133</sup> with 1000 bootstrap replicates and the LG + G model determined by ProtTest3<sup>134</sup>. Statistical analyses were done in R v3.5.2<sup>135</sup> within RStudio (<https://www.rstudio.com>). Reported significances refer to Wilcoxon rank-sum tests ( $p < 0.05$ ).

**Exometabolomics.** All cultivations were done in triplicate using SWM seawater minimal medium<sup>136</sup>. Each replicate was inoculated at 1% (v/v) with precultures grown in 10 mL SWM + 0.1% glucose for 24 h at 20 °C and 140 rpm (washed twice with sterile SWM and diluted to OD600 of 0.1 before inoculation). For exometabolomics, nine strains were inoculated in 50 mL SWM + 0.1% glucose at 0.5% (v/v) in triplicate. After incubation at 20 °C and 140 rpm until late exponential phase, a 20 mL subsample from each replicate was centrifuged for 20 min at 3500 g and 4 °C. In addition, three sterile media blanks were incubated and processed in the same manner. Exometabolites were purified from supernatants using solid phase cartridges<sup>137</sup> followed by ultrahigh-resolution mass spectrometry<sup>138,139</sup> on a 15 T Solarix Fourier transform ion cyclotron resonance mass spectrometer (FT-ICR-MS) in negative mode (Supplementary Methods). Only peaks present in two biological replicates were considered, and only if detected in technical duplicates measured per replicate. Furthermore, spectra were calibrated and denoised using strict procedures to ensure that only bacterial metabolites were evaluated (Table S3). Tentative identification of masses was done using databases MetaCyc<sup>140</sup> and KEGG Compounds via R package KEGGREST<sup>141,142</sup>.

**Degradation of different substrates.** Degradation of specific carbon sources was tested in SWM supplemented with phenol (final concentration 0.5 mM), toluene (1 mM), xylene (1 mM), sodium benzoate (2 mM), alpha-mannan (Carbosynth YM63069; 0.1% w/v), rhamnogalacturonan (Megazyme P-RHAM1; 0.1% w/v), or pectin (Fluka 76282; 0.1% w/v). Cultures were inoculated with precultures as described above and evaluated by photometry (OD600) or colony-forming units (log CFU mL<sup>-1</sup>) after plating serial dilutions on marine agar (cultures with aromatics subcultured twice before plating). In addition, strain 83-1 was tested for degradation of macroalgal tissue (Supplementary Methods). Briefly, healthy specimens of the brown macroalga *Ecklonia radiata* were incubated with strain 83-1 for 12 days and tissue degradation evaluated in comparison to a control without bacterial addition ( $n = 15$ ).

**Screening for bioactive secondary metabolites.** Siderophore production was tested with sterile-filtered supernatants of overnight cultures in iron-deplete vs. iron-replete minimal medium using a modified CAS assay<sup>143,144</sup> with 50 μM deferoxamine mesylate (DFOM) and sterile medium as positive and negative controls, respectively. Activity was quantified against a seven-point DFOM standard curve ( $R^2 = 0.981$ ). Production of HSLs was tested by streaking *Alteromonas* colony mass in parallel to the biosensor strains *Chromobacterium violaceum* CV026 and *Agrobacterium tumefaciens* A136 according to Ravn and coworkers<sup>99</sup>, with *Phaeobacter inhibens* DSM17395 as positive control.

**Co-culture and quantitative PCR of unique genes.** Quantitative PCR (qPCR) was performed using a LightCycler 480 (Roche, Switzerland) according to Berger and coworkers<sup>145</sup>. For a unique gene of each *A. maclodii* strain, primers were designed using the Roche Universal Probe Library and ordered from TIB MolBiol Germany (Table S5). After confirmation of primer specificity against target and non-target strains, selected strains were grown as mono- and co-cultures in triplicate (inoculated with precultures as described above) in SWM + 0.1% glucose at 100 rpm and 20 °C. DNA was extracted using the Master Pure RNA Purification Kit (Epicentre, Madison, WI) and amplified in 15 μL qPCR reactions (each 10 μL of LightCycler 480 Probes Master, 3 μL PCR-H<sub>2</sub>O, 400 nM of each primer, 200 nM of the respective UPL probe and 5 μL template adjusted to 10 ng μL<sup>-1</sup>). Cycling conditions were 95 °C for 10 min, 45 cycles (95 °C for 10 s, 60 °C for 30 s, 72 °C for 1 s) and 40 °C for 30 s. For each biological replicate, three technical PCR replicates were run. Growth was expressed as DNA equivalents in relation to a five-point DNA standard curve for each strain ( $R^2 > 0.98$ ).

**Biogeography and taxonomic relatives of unique genes.** Three genomic loci specific for strains MIT1002, 83-1 and 27126<sup>T</sup> (Table S6) were searched against TARA Ocean metagenomes using the Sequenceserved-based web application at <http://bioinfo.szn.it/tara-blast-server><sup>146</sup>. Detection was considered positive if at least one gene from two loci was detected with  $>99\%$  identity and  $>70\%$  query coverage. Furthermore, unique genes were searched against the NCBI RefSeq Protein database to identify the closest taxonomic relative.

### Data availability

Complete genomes have been deposited at EMBL-EBI under study PRJEB32335 and are also available at IMG<sup>147</sup> under accession numbers 2738541260, 2738541261, 2738541262, 2738541267 and 2785510739, respectively.

Received: 14 June 2019; Accepted: 23 December 2019;

Published online: 21 January 2020

## References

- Larkin, A. A. & Martiny, A. C. Microdiversity shapes the traits, niche space, and biogeography of microbial taxa. *Environ. Microbiol. Rep* **9**, 55–70, <https://doi.org/10.1111/1758-2229.12523> (2017).
- Farrant, G. K. *et al.* Delineating ecologically significant taxonomic units from global patterns of marine picocyanobacteria. *Proc. Natl. Acad. Sci. USA* **113**, E3365–E3374, <https://doi.org/10.1073/pnas.1524865113> (2016).
- Riley, M. A. & Lizotte-Waniewski, M. Population genomics and the bacterial species concept. *Methods Mol. Biol* **532**, 367–377, [https://doi.org/10.1007/978-1-60327-853-9\\_21](https://doi.org/10.1007/978-1-60327-853-9_21) (2009).
- Arevalo, P., VanInsberghe, D. & Polz, M.F. A Reverse Ecology Framework for Bacteria and Archaea in *Population Genomics: Microorganisms* (eds. Martin F. Polz & Om P. Rajora) 77–96 (Springer, 2019).
- Mira, A., Martín-Cuadrado, A. B., D'Auria, G. & Rodríguez-Valera, F. The bacterial pan-genome: a new paradigm in microbiology. *Int. Microbiol.* **13**, 45–57, <https://doi.org/10.2436/20.1501.01.110> (2010).
- Freese, H. M. *et al.* Trajectories and drivers of genome evolution in surface-associated marine *Phaeobacter*. *Genome Biol. Evol* **9**, 3297–3311, <https://doi.org/10.1093/gbe/evx249> (2017).
- Kashtan, N. *et al.* Single-cell genomics reveals hundreds of coexisting subpopulations in wild *Prochlorococcus*. *Science* **344**, 416–420, <https://doi.org/10.1126/science.1248575> (2014).
- Letzel, A.-C. *et al.* Genomic insights into specialized metabolism in the marine actinomycete *Salinispora*. *Environ. Microbiol* **19**, 3660–3673, <https://doi.org/10.1111/1462-2920.13867> (2017).
- López-Pérez, M., Martín-Cuadrado, A.-B. & Rodríguez-Valera, F. Homologous recombination is involved in the diversity of replacement flexible genomic islands in aquatic prokaryotes. *Front. Genet* **5**, 147, <https://doi.org/10.3389/fgene.2014.00147> (2014).
- Rodríguez-Valera, F., Martín-Cuadrado, A. B. & López-Pérez, M. Flexible genomic islands as drivers of genome evolution. *Curr. Opin. Microbiol.* **31**, 154–160, <https://doi.org/10.1016/j.mib.2016.03.014> (2016).
- Chan, A. P. *et al.* A novel method of consensus pan-chromosome assembly and large-scale comparative analysis reveal the highly flexible pan-genome of *Acinetobacter baumannii*. *Genome Biol.* **16**, 143, <https://doi.org/10.1186/s13059-015-0701-6> (2015).
- Heuer, H. & Smalla, K. Plasmids foster diversification and adaptation of bacterial populations in soil. *FEMS Microbiol. Rev.* **36**, 1083–1104, <https://doi.org/10.1111/j.1574-6976.2012.00337.x> (2012).
- López-Pérez, M., Ramon-Marco, N. & Rodríguez-Valera, F. Networking in microbes: conjugative elements and plasmids in the genus *Alteromonas*. *BMC Genomics* **18**, 36, <https://doi.org/10.1186/s12864-016-3461-0> (2017).
- González-Torres, P. & Gabaldón, T. Genome variation in the model halophilic bacterium *Salinibacter ruber*. *Front. Microbiol* **9**, 1499, <https://doi.org/10.3389/fmicb.2018.01499> (2018).
- Sun, Y. & Luo, H. Homologous recombination in core genomes facilitates marine bacterial adaptation. *Appl. Environ. Microbiol.* **84**, e0254 5–02517, <https://doi.org/10.1128/AEM.02545-17> (2018).
- Sniegowski, P. D. & Gerrish, P. J. Beneficial mutations and the dynamics of adaptation in asexual populations. *Philos. Trans. R. Soc. Lond. B* **365**, 1255–1263, <https://doi.org/10.1098/rstb.2009.0290> (2010).
- Kirchberger, P. C. *et al.* A small number of phylogenetically distinct clonal complexes dominate a coastal *Vibrio cholerae* population. *Appl. Environ. Microbiol.* **82**, 5576–5586, <https://doi.org/10.1128/AEM.01177-16> (2016).
- Hehemann, J.-H. H. *et al.* Adaptive radiation by waves of gene transfer leads to fine-scale resource partitioning in marine microbes. *Nat. Commun.* **7**, 12860, <https://doi.org/10.1038/ncomms12860> (2016).
- Yawata, Y. *et al.* Competition-dispersal tradeoff ecologically differentiates recently speciated marine bacterioplankton populations. *Proc. Natl. Acad. Sci. USA* **111**, 5622–5627, <https://doi.org/10.1073/pnas.1318943111> (2014).
- Ziemert, N. *et al.* Diversity and evolution of secondary metabolism in the marine actinomycete *Salinispora*. *Proc. Natl. Acad. Sci. USA* **111**, E1130–E1139, <https://doi.org/10.1073/pnas.1324161111> (2014).
- Patin, N. V., Duncan, K. R., Dorrestein, P. C. & Jensen, P. R. Competitive strategies differentiate closely related species of marine actinobacteria. *ISME J.* **10**, 478–490, <https://doi.org/10.1038/ismej.2015.128> (2015).
- Chase, A. B. *et al.* Microdiversity of an abundant terrestrial bacterium encompasses extensive variation in ecologically relevant traits. *mBio* **8**, e01809–01817, <https://doi.org/10.1128/mBio.01809-17> (2017).
- Delmont, T. O. & Eren, A. M. Linking pangenomes and metagenomes: the *Prochlorococcus* metapangenome. *PeerJ* **6**, e4320, <https://doi.org/10.7717/peerj.4320> (2018).
- López-Pérez, M. & Rodríguez-Valera, F. The family *Alteromonadaceae* in *The Prokaryotes* (eds Eugene Rosenberg *et al.*) 69–92 (Springer, 2014).
- Wu, S., Zhou, J., Xin, Y. & Xue, S. Nutritional stress effects under different nitrogen sources on the genes in microalga *Isochrysis zhangjiangensis* and the assistance of *Alteromonas macleodii* in releasing the stress of amino acid deficiency. *J. Phycol.* **51**, 885–895, <https://doi.org/10.1111/jpy.12328> (2015).
- Diner, R. E., Schwenck, S. M., McCrow, J. P., Zheng, H. & Allen, A. E. Genetic manipulation of competition for nitrate between heterotrophic bacteria and diatoms. *Front. Microbiol* **7**, 880, <https://doi.org/10.3389/fmicb.2016.00880> (2016).
- Lee, M. D. *et al.* The *Trichodesmium* consortium: conserved heterotrophic co-occurrence and genomic signatures of potential interactions. *ISME J.* **11**, 1813–1824, <https://doi.org/10.1038/ismej.2017.49> (2017).
- Mitulla, M. *et al.* Response of bacterial communities from California coastal waters to alginate particles and an alginolytic *Alteromonas macleodii* strain. *Environ. Microbiol.* **18**, 4369–4377, <https://doi.org/10.1111/1462-2920.13314> (2016).
- Taylor, J. D. & Cunliffe, M. Coastal bacterioplankton community response to diatom-derived polysaccharide microgels. *Environ. Microbiol. Rep* **9**, 151–157, <https://doi.org/10.1111/1758-2229.12513> (2017).
- López-Pérez, M. & Rodríguez-Valera, F. Pangenome evolution in the marine bacterium *Alteromonas*. *Genome Biol. Evol* **8**, 1556–1570, <https://doi.org/10.1093/gbe/evw098> (2016).
- Ivars-Martinez, E. *et al.* Comparative genomics of two ecotypes of the marine planktonic copiotroph *Alteromonas macleodii* suggests alternative lifestyles associated with different kinds of particulate organic matter. *ISME J.* **2**, 1194–1212, <https://doi.org/10.1038/ismej.2008.74> (2008).
- López-Pérez, M. *et al.* Genomes of surface isolates of *Alteromonas macleodii*: the life of a widespread marine opportunistic copiotroph. *Sci. Rep* **2**, 696, <https://doi.org/10.1038/srep00696> (2012).
- Neumann, A. M. *et al.* Different utilization of alginate and other algal polysaccharides by marine *Alteromonas macleodii* ecotypes. *Environ. Microbiol.* **17**, 3857–3868, <https://doi.org/10.1111/1462-2920.12862> (2015).
- Gonzaga, A. *et al.* Polyclonality of concurrent natural populations of *Alteromonas macleodii*. *Genome Biol. Evol* **4**, 1360–1374, <https://doi.org/10.1093/gbe/evs112> (2012).
- Kimes, N. E., López-Pérez, M., Ausó, E., Ghai, R. & Rodríguez-Valera, F. RNA sequencing provides evidence for functional variability between naturally co-existing *Alteromonas macleodii* lineages. *BMC Genomics* **15**, 938, <https://doi.org/10.1186/1471-2164-15-938> (2014).
- Chafee, M. *et al.* Recurrent patterns of microdiversity in a temperate coastal marine environment. *ISME J.* **12**, 237–252, <https://doi.org/10.1038/ismej.2017.165> (2018).
- Konstantinidis, K. T. & Tiedje, J. M. Genomic insights that advance the species definition for prokaryotes. *Proc. Natl. Acad. Sci. USA* **102**, 2567–2572, <https://doi.org/10.1073/pnas.0409727102> (2005).
- López-Pérez, M., Gonzaga, A. & Rodríguez-Valera, F. Genomic diversity of “deep ecotype” *Alteromonas macleodii* isolates: evidence for Pan-Mediterranean clonal frames. *Genome Biol. Evol* **5**, 1220–1232, <https://doi.org/10.1093/gbe/evt089> (2013).

39. López-Pérez, M. *et al.* Intra- and intergenomic variation of ribosomal RNA operons in concurrent *Alteromonas macleodii* strains. *Microb. Ecol.* **65**, 720–730, <https://doi.org/10.1007/s00248-012-0153-4> (2013).
40. MacLean, R. C. & San Millan, A. Microbial evolution: towards resolving the plasmid paradox. *Curr. Biol.* **25**, R764–R767, <https://doi.org/10.1016/J.CUB.2015.07.006> (2015).
41. Hou, S. *et al.* Benefit from decline: the primary transcriptome of *Alteromonas macleodii* str. Te101 during *Trichodesmium* demise. *ISME J.* **12**, 981–996, <https://doi.org/10.1038/s41396-017-0034-4> (2018).
42. Vargas, W. A., Weyman, P. D., Tong, Y., Smith, H. O. & Xu, Q. [NiFe] hydrogenase from *Alteromonas macleodii* with unusual stability in the presence of oxygen and high temperature. *Appl. Environ. Microbiol.* **77**, 1990–1998, <https://doi.org/10.1128/AEM.01559-10> (2011).
43. Fadeev, E. *et al.* Why close a bacterial genome? The plasmid of *Alteromonas macleodii* HOT1A3 is a vector for inter-specific transfer of a flexible genomic Island. *Front. Microbiol.* **7**, 248, <https://doi.org/10.3389/fmicb.2016.00248> (2016).
44. López-Pérez, M., Gonzaga, A., Ivanova, E. P. & Rodriguez-Valera, F. Genomes of *Alteromonas australica*, a world apart. *BMC Genomics* **15**, 483, <https://doi.org/10.1186/1471-2164-15-483> (2014).
45. Bryant, J. A., Sellars, L. E., Busby, S. J. W. & Lee, D. J. Chromosome position effects on gene expression in *Escherichia coli* K-12. *Nucleic Acids Res* **42**, 11383–11392, <https://doi.org/10.1093/nar/gku828> (2014).
46. Stocker, R. & Seymour, J. R. Ecology and physics of bacterial chemotaxis in the ocean. *Microbiol. Mol. Biol. Rev.* **76**, 792–812, <https://doi.org/10.1128/MMBR.00029-12> (2012).
47. Iwaki, H., Yamamoto, T. & Hasegawa, Y. Isolation of marine xylene-utilizing bacteria and characterization of *Halioxenophilus aromaticivorans* gen. nov., sp. nov. and its xylene degradation gene cluster. *FEMS Microbiol. Lett.* **365**, <https://doi.org/10.1093/femsle/fny042> (2018).
48. Berlendis, S. *et al.* First evidence of aerobic biodegradation of BTEX compounds by pure cultures of *Marinobacter*. *Appl. Biochem. Biotechnol.* **160**, 1992–1999, <https://doi.org/10.1007/s12010-009-8746-1> (2010).
49. Burlage, R. S., Hooper, S. W. & Saylor, G. S. The TOL (pWW0) catabolic plasmid. *Appl. Environ. Microbiol.* **55**, 1323–1328 (1989).
50. Medema, M. H., Takano, E. & Breitling, R. Detecting sequence homology at the gene cluster level with MultiGeneBlast. *Mol. Biol. Evol.* **30**, 1218–1223, <https://doi.org/10.1093/molbev/mst025> (2013).
51. Gutierrez, T. Marine, Aerobic Hydrocarbon-Degrading *Gammaproteobacteria*: Overview in *Taxonomy, Genomics and Ecophysiology of Hydrocarbon-Degrading Microbes* (ed. McGenity, T.) 1–10 (Springer, 2017).
52. Handley, K. & Lloyd, J. Biogeochemical implications of the ubiquitous colonization of marine habitats and redox gradients by *Marinobacter* species. *Front. Microbiol.* **4**, 136, <https://doi.org/10.3389/fmicb.2013.00136> (2013).
53. Hedlund, B. P. & Staley, J. T. Isolation and characterization of *Pseudoalteromonas* strains with divergent polycyclic aromatic hydrocarbon catabolic properties. *Environ. Microbiol.* **8**, 178–182, <https://doi.org/10.1111/j.1462-2920.2005.00871.x> (2006).
54. Green, D. H., Bowman, J. P., Smith, E. A., Gutierrez, T. & Bolch, C. J. S. *Marinobacter algicola* sp. nov., isolated from laboratory cultures of paralytic shellfish toxin-producing dinoflagellates. *Int. J. Syst. Evol. Microbiol.* **56**, 523–527, <https://doi.org/10.1099/ij.s.0.63447-0> (2006).
55. Gärdes, A., Iversen, M. H., Grossart, H.-P., Passow, U. & Ullrich, M. S. Diatom-associated bacteria are required for aggregation of *Thalassiosira weissflogii*. *ISME J.* **5**, 436–445, <https://doi.org/10.1038/ismej.2010.145> (2011).
56. Zyska-Haberecht, B., Niemczyk, E. & Lipok, J. Metabolic relation of cyanobacteria to aromatic compounds. *Appl. Microbiol. Biotechnol.* **103**, 1167–1178, <https://doi.org/10.1007/s00253-018-9568-2> (2019).
57. Kastman, E. K. *et al.* Biotic interactions shape the ecological distributions of *Staphylococcus* species. *mBio* **7**, e01157–01116, <https://doi.org/10.1128/mBio.01157-16> (2016).
58. Morris, J. J., Johnson, Z. I., Szul, M. J., Keller, M. & Zinser, E. R. Dependence of the cyanobacterium *Prochlorococcus* on hydrogen peroxide scavenging microbes for growth at the ocean's surface. *PLoS One* **6**, e16805, <https://doi.org/10.1371/journal.pone.0016805> (2011).
59. Biller, S. J., Coe, A., Roggensack, S. E. & Chisholm, S. W. Heterotroph interactions alter *Prochlorococcus* transcriptome dynamics during extended periods of darkness. *mSystems* **3**, e00040–18, <https://doi.org/10.1128/mSystems.00040-18> (2018).
60. Morris, J. J., Kirkegaard, R., Szul, M. J., Johnson, Z. I. & Zinser, E. R. Facilitation of robust growth of *Prochlorococcus* colonies and dilute liquid cultures by “helper” heterotrophic bacteria. *Appl. Environ. Microbiol.* **74**, 4530–4534, <https://doi.org/10.1128/AEM.02479-07> (2008).
61. Biller, S. J., Coe, A., Martin-Cuadrado, A.-B. & Chisholm, S. W. Draft genome sequence of *Alteromonas macleodii* strain MIT1002, isolated from an enrichment culture of the marine cyanobacterium *Prochlorococcus*. *Genome Announc.* **3**, e00967–00915, <https://doi.org/10.1128/genomeA.00967-15> (2015).
62. Biller, S. J., Coe, A. & Chisholm, S. W. Torn apart and reunited: impact of a heterotroph on the transcriptome of *Prochlorococcus*. *ISME J.* **10**, 2831–2843, <https://doi.org/10.1038/ismej.2016.82> (2016).
63. Fiore, C. L., Longnecker, K., Kido Soule, M. C. & Kujawinski, E. B. Release of ecologically relevant metabolites by the cyanobacterium *Synechococcus elongatus* CCMP 1631. *Environ. Microbiol.* **17**, 3949–3963, <https://doi.org/10.1111/1462-2920.12899> (2015).
64. Aharonovich, D. & Sher, D. Transcriptional response of *Prochlorococcus* to co-culture with a marine *Alteromonas*: differences between strains and the involvement of putative infochemicals. *ISME J.* **10**, 2892–2906, <https://doi.org/10.1038/ismej.2016.70> (2016).
65. Hennon, G. M. M. *et al.* The impact of elevated CO<sub>2</sub> on *Prochlorococcus* and microbial interactions with ‘helper’ bacterium *Alteromonas*. *ISME J.* **12**, 520–531, <https://doi.org/10.1038/ismej.2017.189> (2018).
66. Yelton, A. P. *et al.* Global genetic capacity for mixotrophy in marine picocyanobacteria. *ISME J.* **10**, 2946–2957, <https://doi.org/10.1038/ismej.2016.64> (2016).
67. Zubkov, M. V. & Tarran, G. A. Amino acid uptake of *Prochlorococcus* spp. in surface waters across the South Atlantic Subtropical Front. *Aquat. Microb. Ecol.* **40**, 241–249, <https://doi.org/10.3354/ame040241> (2005).
68. Seth, E. C. & Taga, M. E. Nutrient cross-feeding in the microbial world. *Front. Microbiol.* **5**, 350, <https://doi.org/10.3389/fmicb.2014.00350> (2014).
69. Pacheco, A. R., Moel, M. & Segrè, D. Costless metabolic secretions as drivers of interspecies interactions in microbial ecosystems. *Nat. Commun.* **10**, 103, <https://doi.org/10.1038/s41467-018-07946-9> (2019).
70. Seymour, J. R., Ahmed, T., Durham, W. M. & Stocker, R. Chemotactic response of marine bacteria to the extracellular products of *Synechococcus* and *Prochlorococcus*. *Aquat. Microb. Ecol.* **59**, 161–168, <https://doi.org/10.3354/ame01400> (2010).
71. Richardson, B. & Corcoran, A. A. Use of dissolved inorganic and organic phosphorus by axenic and nonaxenic clones of *Karenia brevis* and *Karenia mikimotoi*. *Harmful Algae* **48**, 30–36, <https://doi.org/10.1016/J.HAL.2015.06.005> (2015).
72. Scanlan, D. J. *et al.* Ecological genomics of marine picocyanobacteria. *Microbiol. Mol. Biol. Rev.* **73**, 249–299, <https://doi.org/10.1128/MMBR.00035-08> (2009).
73. Partensky, F. & Garczarek, L. *Prochlorococcus*: advantages and limits of minimalism. *Annu. Rev. Mar. Sci.* **2**, 305–331, <https://doi.org/10.1146/annurevmarine-120308-081034> (2009).
74. Koch, H. *et al.* Biphasic cellular adaptations and ecological implications of *Alteromonas macleodii* degrading a mixture of algal polysaccharides. *ISME J.* **13**, 92–103, <https://doi.org/10.1038/s41396-018-0252-4> (2019).
75. Levy, A. *et al.* Genomic features of bacterial adaptation to plants. *Nat. Genet.* **50**, 138–150, <https://doi.org/10.1038/s41588-017-0012-9> (2018).

76. Qiu, Z. *et al.* Future climate change is predicted to affect the microbiome and condition of habitat-forming kelp. *Proc. R. Soc. B* **286**, <https://doi.org/10.1098/rspb.2018.1887> (2019).
77. Marzinielli, E. M. *et al.* Continental-scale variation in seaweed host-associated bacterial communities is a function of host condition, not geography. *Environ. Microbiol.* **17**, 4078–4088, <https://doi.org/10.1111/1462-2920.12972> (2015).
78. Zhu, Y. *et al.* Genetic analyses unravel the crucial role of a horizontally acquired alginate lyase for brown algal biomass degradation by *Zobellia galactanivorans*. *Environ. Microbiol.* **19**, 2164–2181, <https://doi.org/10.1111/1462-2920.13699> (2017).
79. Lin, J. D., Lemay, M. A. & Parfrey, L. W. Diverse bacteria utilize alginate within the microbiome of the giant kelp *Macrocystis pyrifera*. *Front. Microbiol.* **9**, 1914, <https://doi.org/10.3389/fmicb.2018.01914> (2018).
80. Saha, M. & Weinberger, F. Microbial “gardening” by a seaweed holobiont: surface metabolites attract protective and deter pathogenic epibacterial settlement. *J. Ecol.* **107**, 2255–2265, <https://doi.org/10.1111/1365-2745.13193> (2019).
81. Duchêne, S. *et al.* Genome-scale rates of evolutionary change in bacteria. *Microb. Genomics* **2**, e000094, <https://doi.org/10.1099/mgen.0.000094> (2016).
82. Freese, H. M., Methner, A. & Overmann, J. Adaptation of surface-associated bacteria to the open ocean: a genomically distinct subpopulation of *Phaeobacter gallaeciensis* colonizes Pacific mesozooplankton. *Front. Microbiol.* **8**, 1659, <https://doi.org/10.3389/fmicb.2017.01659> (2017).
83. Postle, K. & Kadner, R. J. Touch and go: tying TonB to transport. *Mol. Microbiol.* **49**, 869–882, <https://doi.org/10.1046/j.1365-2958.2003.03629.x> (2003).
84. Fitzpatrick, T. B. *et al.* Two independent routes of *de novo* vitamin B biosynthesis: not that different after all. *Biochem. J* **407**, 1–13, <https://doi.org/10.1042/BJ20070765> (2007).
85. Tazzyman, S. J. & Bonhoeffer, S. Why there are no essential genes on plasmids. *Mol. Biol. Evol.* **32**, 3079–3088, <https://doi.org/10.1093/molbev/msu293> (2014).
86. Lau, B. T. C., Malkus, P. & Paulsson, J. New quantitative methods for measuring plasmid loss rates reveal unexpected stability. *Plasmid* **70**, 353–361, <https://doi.org/10.1016/j.plasmid.2013.07.007> (2013).
87. Grondin, J. M., Tamura, K., Déjean, G., Abbott, D. W. & Brumer, H. Polysaccharide Utilization Loci: fuelling microbial communities. *J. Bacteriol.* **199**, JB.00860–16, <https://doi.org/10.1128/JB.00860-16> (2017).
88. Tang, K., Lin, Y., Han, Y. & Jiao, N. Characterization of potential Polysaccharide Utilization Systems in the marine *Bacteroidetes Gramella flava* JLT2011 using a multi-omics approach. *Front. Microbiol.* **8**, 220, <https://doi.org/10.3389/fmicb.2017.00220> (2017).
89. Foran, E. *et al.* Functional characterization of a novel “ulvan utilization loci” found in *Alteromonas* sp. LOR genome. *Algal Res* **25**, 39–46, <https://doi.org/10.1016/j.algal.2017.04.036> (2017).
90. Koch, H., Freese, H. M., Hahnke, R., Simon, M. & Wietz, M. Adaptations of *Alteromonas* sp. 76-1 to polysaccharide degradation: a CAZyme plasmid for ulvan degradation and two alginolytic systems. *Front. Microbiol.* **10**, 504, <https://doi.org/10.3389/fmicb.2019.00504> (2019).
91. Kappelmann, L. *et al.* Polysaccharide utilization loci of North Sea *Flavobacteriia* as basis for using SusC/D-protein expression for predicting major phytoplankton glycans. *ISME J.* **13**, 76–91, <https://doi.org/10.1038/s41396-018-0242-6> (2019).
92. Pujalte, M. J., Sitjà-Bobadilla, A., Álvarez-Pellitero, P. & Garay, E. Carriage of potentially fish-pathogenic bacteria in *Sparus aurata* cultured in Mediterranean fish farms. *Dis. Aquat. Org* **54**, 119–126, <https://doi.org/10.3354/dao054119> (2003).
93. Helbert, W. Marine polysaccharide sulfatases. *Front. Mar. Sci* **4**, 6, <https://doi.org/10.3389/fmars.2017.00006> (2017).
94. Torrecillas, S., Montero, D. & Izquierdo, M. Improved health and growth of fish fed mannan oligosaccharides: potential mode of action. *Fish. Shellfish. Immunol.* **36**, 525–544, <https://doi.org/10.1016/j.fsi.2013.12.029> (2014).
95. Sheridan, P. O. *et al.* Polysaccharide utilization loci and nutritional specialization in a dominant group of butyrate-producing human colonic *Firmicutes*. *Microb. Genomics* **2**, e000043, <https://doi.org/10.1099/mgen.0.000043> (2016).
96. Hmelo, L. R. Quorum Sensing in marine microbial environments. *Annu. Rev. Mar. Sci* **9**, 257–281, <https://doi.org/10.1146/annurev-marine-010816-060656> (2017).
97. Blin, K. *et al.* antiSMASH 4.0—improvements in chemistry prediction and gene cluster boundary identification. *Nucleic Acids Res.* **45**, W36–W41, <https://doi.org/10.1093/nar/gkx319> (2017).
98. Doberva, M. *et al.* Large diversity and original structures of acyl-homoserine lactones in strain MOLA 401, a marine *Rhodobacteraceae* bacterium. *Front. Microbiol.* **8**, 1152, <https://doi.org/10.3389/fmicb.2017.01152> (2017).
99. Ravn, L., Christensen, A. B., Molin, S., Givskov, M. & Gram, L. Methods for detecting acylated homoserine lactones produced by Gram-negative bacteria and their application in studies of AHL-production kinetics. *J. Microbiol. Methods* **44**, 239–251, [https://doi.org/10.1016/S0167-7012\(01\)00217-2](https://doi.org/10.1016/S0167-7012(01)00217-2) (2001).
100. Doberva, M., Sanchez-Ferandin, S., Toulza, E., Lebaron, P. & Lami, R. Diversity of quorum sensing autoinducer synthases in the Global Ocean Sampling metagenomic database. *Aquat. Microb. Ecol.* **74**, 107–119, <https://doi.org/10.3354/ame01734> (2015).
101. Girard, L. *et al.* Evidence of a large diversity of N-acyl-homoserine lactones in symbiotic *Vibrio fischeri* strains associated with the squid *Euprymna scolopes*. *Microbes Environ.* **34**, 99–103, <https://doi.org/10.1264/jsme2.ME18145> (2019).
102. Tagliabue, A. *et al.* The integral role of iron in ocean biogeochemistry. *Nature* **543**, 51–59, <https://doi.org/10.1038/nature21058> (2017).
103. Sandy, M. & Butler, A. Microbial iron acquisition: marine and terrestrial siderophores. *Chem. Rev.* **109**, 4580–4595, <https://doi.org/10.1021/cr9002787> (2009).
104. Boiteau, R. M. *et al.* Siderophore-based microbial adaptations to iron scarcity across the eastern Pacific Ocean. *Proc. Natl. Acad. Sci. USA* **113**, 14237–14242, <https://doi.org/10.1073/pnas.1608594113> (2016).
105. Dinkla, I. J., Gabor, E. M. & Janssen, D. B. Effects of iron limitation on the degradation of toluene by *Pseudomonas* strains carrying the TOL (pWWO) plasmid. *Appl. Environ. Microbiol.* **67**, 3406–3412, <https://doi.org/10.1128/AEM.67.8.3406-3412.2001> (2001).
106. Tappin, A. D. & Millward, G. E. The English Channel: contamination status of its transitional and coastal waters. *Mar. Pollut. Bull.* **95**, 529–550, <https://doi.org/10.1016/j.marpolbul.2014.12.012> (2015).
107. Vital, M. *et al.* Gene expression analysis of *E. coli* strains provides insights into the role of gene regulation in diversification. *ISME J.* **9**, 1130–1140, <https://doi.org/10.1038/ismej.2014.204> (2015).
108. Waite, A. J. *et al.* Non-genetic diversity modulates population performance. *Mol. Syst. Biol.* **12**, 895, <https://doi.org/10.15252/msb.20167044> (2016).
109. Hibbing, M. E., Fuqua, C., Parsek, M. R. & Peterson, S. B. Bacterial competition: surviving and thriving in the microbial jungle. *Nat. Rev. Microbiol.* **8**, 15–25, <https://doi.org/10.1038/nrmicro2259> (2010).
110. Hansell, D. A. & Carlson, C. A. *Biogeochemistry of marine dissolved organic matter* (Academic Press, 2014).
111. Dang, H. & Lovell, C. R. Microbial surface colonization and biofilm development in marine environments. *Microbiol. Mol. Biol. Rev.* **80**, 91–138, <https://doi.org/10.1128/MMBR.00037-15> (2016).
112. Partensky, F., Hess, W. R. & Vaulot, D. *Prochlorococcus*, a marine photosynthetic prokaryote of global significance. *Microbiol. Mol. Biol. Rev.* **63**, 106–127 (1999).
113. Fuchsmann, C. A., Collins, R. E., Roca, G. & Brazelton, W. J. Effect of the environment on horizontal gene transfer between bacteria and archaea. *PeerJ* **5**, e3865, <https://doi.org/10.7717/peerj.3865> (2017).
114. Hoetzinger, M., Schmidt, J., Jezberova, J., Koll, U. & Hahn, M. W. Microdiversification of a pelagic *Polynucleobacter* species is mainly driven by acquisition of genomic islands from a partially interspecific gene pool. *Appl. Environ. Microbiol.* **83**, e02266–16, <https://doi.org/10.1128/aem.02266-16> (2017).

115. Shapiro, B. J. & Polz, M. F. Ordering microbial diversity into ecologically and genetically cohesive units. *Trends Microbiol.* **22**, 235–247, <https://doi.org/10.1016/j.tim.2014.02.006> (2014).
116. Cohan, F. M. Transmission in the origins of bacterial diversity, from ecotypes to phyla. *Microbiol. Spectr.* **5**, <https://doi.org/10.1128/microbiolspec.MTBP-0014-2016> (2017).
117. Simon, M. Functional diversity of bacterial communities and the geomicrobiome in the central and north Pacific (BacGeoPac). Cruise Report SO248, German Research Fleet Coordination Centre, University of Hamburg (2016).
118. Eren, A. M. *et al.* Anvi'o: an advanced analysis and visualization platform for 'omics data. *PeerJ* **3**, e1319, <https://doi.org/10.7717/peerj.1319> (2015).
119. Na, S.-I. *et al.* UBCG: Up-to-date bacterial core gene set and pipeline for phylogenomic tree reconstruction. *J. Microbiol.* **56**, 281–285, <https://doi.org/10.1007/s12275-018-8014-6> (2018).
120. Trifinopoulos, J., Nguyen, L.-T., Minh, B. Q. & von Haeseler, A. W-IQ-TREE: a fast online phylogenetic tool for maximum likelihood analysis. *Nucleic Acids Res.* **44**, W232–W235, <https://doi.org/10.1093/nar/gkw256> (2016).
121. Darriba, D., Taboada, G. L., Doallo, R. & Posada, D. jModelTest 2: more models, new heuristics and parallel computing. *Nat. Methods* **9**, 772, <https://doi.org/10.1038/nmeth.2109> (2012).
122. Rodriguez-R, L. M. & Konstantinidis, K. T. The enveomics collection: a toolbox for specialized analyses of microbial genomes and metagenomes. *PeerJ Preprints* **4**, e1900v1, <https://doi.org/10.7287/PEERJ.PREPRINTS.1900V1> (2016).
123. Treangen, T. J., Ondov, B. D., Koren, S. & Phillippy, A. M. The Harvest suite for rapid core-genome alignment and visualization of thousands of intraspecific microbial genomes. *Genome Biol.* **15**, 524, <https://doi.org/10.1186/s13059-014-0524-x> (2014).
124. Hall, T. A. BioEdit: a user-friendly biological sequence alignment editor and analysis program for Windows 95/98/NT. *Nucleic Acids Symposium Ser.* **41**, 95–98 (1999).
125. Arndt, D. *et al.* PHASTER: a better, faster version of the PHAST phage search tool. *Nucleic Acids Res.* **44**, W16–21, <https://doi.org/10.1093/nar/gkw387> (2016).
126. Zhang, H. *et al.* dbCAN2: a meta server for automated carbohydrate-active enzyme annotation. *Nucleic Acids Res.* **46**, W95–W101, <https://doi.org/10.1093/nar/gky418> (2018).
127. Kolde, R. Package 'pheatmap', <https://cran.r-project.org/web/packages/pheatmap/index.html> (2018).
128. Moriya, Y., Itoh, M., Okuda, S., Yoshizawa, A. C. & Kanehisa, M. KAAAS: an automatic genome annotation and pathway reconstruction server. *Nucleic Acids Res.* **35**, W182–W185, <https://doi.org/10.1093/nar/gkm321> (2007).
129. Kanehisa, M., Sato, Y. & Morishima, K. BlastKOALA and GhostKOALA: KEGG tools for functional characterization of genome and metagenome sequences. *J. Mol. Biol.* **428**, 726–731, <https://doi.org/10.1016/j.jmb.2015.11.006> (2016).
130. Boutet, E. *et al.* UniProtKB/Swiss-Prot, the manually annotated section of the UniProt KnowledgeBase: How to use the Entry View. *Methods Mol Biol* **1374**, 23–54, [https://doi.org/10.1007/978-1-4939-3167-5\\_2](https://doi.org/10.1007/978-1-4939-3167-5_2) (2016).
131. Potter, S. C. *et al.* HMMER web server: 2018 update. *Nucleic Acids Res.* **46**, W200–W204, <https://doi.org/10.1093/nar/gky448> (2018).
132. Katoh, K., Misawa, K., Kuma, K.-I. & Miyata, T. MAFFT: a novel method for rapid multiple sequence alignment based on fast Fourier transform. *Nucleic Acids Res.* **30**, 3059–3066, <https://doi.org/10.1093/nar/gkf436> (2002).
133. Tamura, K., Stecher, G., Peterson, D., Filipski, A. & Kumar, S. MEGA6: Molecular Evolutionary Genetics Analysis version 6.0. *Mol. Biol. Evol.* **30**, 2725–2729, <https://doi.org/10.1093/molbev/mst197> (2013).
134. Darriba, D., Taboada, G. L., Doallo, R. & Posada, D. ProtTest 3: fast selection of best-fit models of protein evolution. *Bioinformatics* **27**, 1164–1165, <https://doi.org/10.1093/bioinformatics/btr088> (2011).
135. R: A language and environment for statistical computing. R Foundation for Statistical Computing, Vienna, Austria (2018).
136. Zech, H. *et al.* Growth phase-dependent global protein and metabolite profiles of *Phaeobacter gallaeciensis* strain DSM 17395, a member of the marine *Roseobacter*-clade. *Proteomics* **9**, 3677–3697, <https://doi.org/10.1002/pmic.200900120> (2009).
137. Dittmar, T., Koch, B., Hertkorn, N. & Kattner, G. A simple and efficient method for the solid-phase extraction of dissolved organic matter (SPE-DOM) from seawater. *Limnol. Oceanogr. Methods* **6**, 230–235, <https://doi.org/10.4319/lom.2008.6.230> (2008).
138. Seidel, M. *et al.* Biogeochemistry of dissolved organic matter in an anoxic intertidal creek bank. *Geochim. Cosmochim. Acta* **140**, 418–434, <https://doi.org/10.1016/j.gca.2014.05.038> (2014).
139. Osterholz, H. *et al.* Deciphering associations between dissolved organic molecules and bacterial communities in a pelagic marine system. *ISME J.* **10**, 1717–1730, <https://doi.org/10.1038/ismej.2015.231> (2016).
140. Caspi, R. *et al.* The MetaCyc database of metabolic pathways and enzymes and the BioCyc collection of Pathway/Genome Databases. *Nucleic Acids Res.* **42**, D459–471, <https://doi.org/10.1093/nar/gkt1103> (2014).
141. Kanehisa, M., Furumichi, M., Tanabe, M., Sato, Y. & Morishima, K. KEGG: new perspectives on genomes, pathways, diseases and drugs. *Nucleic Acids Res.* **45**, D353–D361, <https://doi.org/10.1093/nar/gkw1092> (2017).
142. Tenenbaum, D. KEGGREST: client-side REST access to KEGG, <http://bioconductor.org/packages/release/bioc/html/KEGGREST.html> (2018).
143. Schwyn, B. & Neilands, J. B. Universal chemical assay for the detection and determination of siderophores. *Anal. Biochem.* **160**, 47–56, [https://doi.org/10.1016/0003-2697\(87\)90612-9](https://doi.org/10.1016/0003-2697(87)90612-9) (1987).
144. Alexander, D. B. & Zuberer, D. A. Use of chrome azurol S reagents to evaluate siderophore production by rhizosphere bacteria. *Biol. Fertil. Soils* **12**, 39–45, <https://doi.org/10.1007/BF00369386> (1991).
145. Berger, M., Neumann, A., Schulz, S., Simon, M. & Brinkhoff, T. Trophodithetic acid production in *Phaeobacter gallaeciensis* is regulated by N-acyl homoserine lactone-mediated quorum sensing. *J. Bacteriol.* **193**, 6576–6585, <https://doi.org/10.1128/JB.05818-11> (2011).
146. Priyam, A. *et al.* Sequenceserver: a modern graphical user interface for custom BLAST databases. *Mol. Biol. Evol.* **36**, 2922–2924, <https://doi.org/10.1093/molbev/msz185> (2019).
147. Chen, I. M. A. *et al.* IMG/M: integrated genome and metagenome comparative data analysis system. *Nucleic Acids Res.* **45**, D507–D516, <https://doi.org/10.1093/nar/gkw929> (2017).

## Acknowledgements

We thank Steven Biller, Allison Coe, Erik Zinser, Spiro Papoulis, Daniel Sher and Dikla Aharonovich for kindly sharing strains MIT1002, EZ55 and HOT1A3. Excellent technical assistance was provided by Katrin Klapproth, Matthias Friebe (FT-ICR-MS) and Cathrin Spröer (genome sequencing). We are grateful to captain, crew and scientists of RV *Sonne* expedition SO248; supported by grant BacGeoPac 03G0248A (German Ministry of Education and Research; BMBF). Francisco Rodriguez-Valera, Mario López-Pérez, Jutta Niggemann, Jan-Hendrik Hehemann and Kai Bischof are thanked for helpful suggestions. M.W. and H.F. were supported by German Research Foundation (DFG) through grants WI3888/1-2 and TRR 51/2-3 TA07, respectively. H.K. was supported by Volkswagen Foundation under VW-Vorab grant 'Marine Biodiversity across Scales' (MarBAS; ZN3112) and the Radboud Excellence Initiative. E.M. and P.S. received funding from the Australian Research Council (DP180104041).

### Author contributions

M.W. and H.K. designed the study. H.F. and J.O. carried out whole-genome sequencing, assembly and annotation. H.K., M.W., N.G. and M.B. carried out genome analyses and physiological experiments. B.N.O. and T.D. performed exometabolomic analyses. N.G., D.L. and M.B. designed and performed qPCR. G.Q., E.M., A.C. and P.S. designed and performed incubation experiments with live algae. H.K., M.W., H.F. and M.S. wrote the manuscript, with contributions from all authors.

### Competing interests

The authors declare no competing interests.

### Additional information

**Supplementary information** is available for this paper at <https://doi.org/10.1038/s41598-020-57526-5>.

**Correspondence** and requests for materials should be addressed to M.W.

**Reprints and permissions information** is available at [www.nature.com/reprints](http://www.nature.com/reprints).

**Publisher's note** Springer Nature remains neutral with regard to jurisdictional claims in published maps and institutional affiliations.



**Open Access** This article is licensed under a Creative Commons Attribution 4.0 International License, which permits use, sharing, adaptation, distribution and reproduction in any medium or format, as long as you give appropriate credit to the original author(s) and the source, provide a link to the Creative Commons license, and indicate if changes were made. The images or other third party material in this article are included in the article's Creative Commons license, unless indicated otherwise in a credit line to the material. If material is not included in the article's Creative Commons license and your intended use is not permitted by statutory regulation or exceeds the permitted use, you will need to obtain permission directly from the copyright holder. To view a copy of this license, visit <http://creativecommons.org/licenses/by/4.0/>.

© The Author(s) 2020

## Appendix 8

### **The polar night shift: Seasonal dynamics and drivers of Arctic Ocean microbiomes revealed by autonomous sampling**

Wietz M, Bienhold C, Metfies K, Torres-Valdes S, von Appen W-J, Salter I, Boetius A

*ISME Communications* (2021), 1:76



# The polar night shift: seasonal dynamics and drivers of Arctic Ocean microbiomes revealed by autonomous sampling

Matthias Wietz<sup>1,2</sup>, Christina Bienhold<sup>1,2</sup>, Katja Metfies<sup>3</sup>, Sinhué Torres-Valdés<sup>4</sup>, Wilken-Jon von Appen<sup>5</sup>, Ian Salter<sup>1,6</sup> and Antje Boetius<sup>1,2,7</sup>

© The Author(s) 2021

The Arctic Ocean features extreme seasonal differences in daylight, temperature, ice cover, and mixed layer depth. However, the diversity and ecology of microbes across these contrasting environmental conditions remain enigmatic. Here, using autonomous samplers and sensors deployed at two mooring sites, we portray an annual cycle of microbial diversity, nutrient concentrations and physical oceanography in the major hydrographic regimes of the Fram Strait. The ice-free West Spitsbergen Current displayed a marked separation into a productive summer (dominated by diatoms and carbohydrate-degrading bacteria) and regenerative winter state (dominated by heterotrophic Syndiniales, radiolarians, chemoautotrophic bacteria, and archaea). The autumn post-bloom with maximal nutrient depletion featured *Coscinodiscophyceae*, *Rhodobacteraceae* (e.g. *Amylibacter*) and the SAR116 clade. Winter replenishment of nitrate, silicate and phosphate, linked to vertical mixing and a unique microbiome that included *Magnetospiraceae* and *Dadabacteriales*, fueled the following phytoplankton bloom. The spring-summer succession of *Phaeocystis*, *Grammonema* and *Thalassiosira* coincided with ephemeral peaks of *Aurantivirga*, *Formosa*, *Polaribacter* and NS lineages, indicating metabolic relationships. In the East Greenland Current, deeper sampling depth, ice cover and polar water masses concurred with weaker seasonality and a stronger heterotrophic signature. The ice-related winter microbiome comprised *Bacillaria*, *Naviculales*, *Polarella*, *Chrysophyceae* and *Flavobacterium* ASVs. Low ice cover and advection of Atlantic Water coincided with diminished abundances of chemoautotrophic bacteria while others such as *Phaeocystis* increased, suggesting that Atlantification alters microbiome structure and eventually the biological carbon pump. These insights promote the understanding of microbial seasonality and polar night ecology in the Arctic Ocean, a region severely affected by climate change.

ISME Communications; <https://doi.org/10.1038/s43705-021-00074-4>

## INTRODUCTION

Microbes are fundamental for the marine biosphere and have been recognized as key components of global change biology [1]. Understanding the causes, complexity, and consequences of microbial community dynamics significantly benefits from continuous observations in the physicochemical context. Ocean time series are beginning to discern the temporal variability and environmental drivers of marine microbiomes from diurnal to decadal scales, but focusing on temperate and tropical waters to date [2–6]. In contrast, continuous records from the polar oceans are rare. Pioneering studies have identified variable numbers, activities, and communities of polar microbes over time and space [7–13] indicating considerable seasonal contrasts [14], yet with limited temporal or spatial resolution.

Due to the extreme winter conditions and remoteness, continuous observations covering the polar night have been seldom accomplished through shipboard expeditions, or performed in coastal areas [15, 16]. New autonomous technologies are a key advance for year-round studies in polar waters, recently

providing the first annual records in the Arctic and Antarctic Oceans [17, 18]. Such approaches can identify transition phases in the seasonal interplay between ocean physics and the ecosystem, for instance the onset of the spring bloom or the end of net growth. In this regard, the polar night is of key interest, when physical mixing [19, 20] and microbial activities [21, 22] replenish nutrients to fuel the subsequent phytoplankton bloom. Arctic phototrophic taxa are thought to overwinter in dormancy [23], responding rapidly when light returns [15, 24], but recent evidence suggests that primary production might already start from late winter [18]. However, microbial dynamics in the open Arctic Ocean during the polar night, especially in presence of sea ice, remain largely unknown.

Here, using an array of autonomous samplers and sensors, we portray microbial and oceanographic seasonality in the two major hydrographic regimes of the Fram Strait. This main deep-water gateway to the central Arctic Ocean harbors the northward, relatively warm and ice-free West Spitsbergen Current (WSC) and the southward, ice-covered and cold East Greenland Current

<sup>1</sup>Deep-Sea Ecology and Technology, Alfred Wegener Institute Helmholtz Centre for Polar and Marine Research, Bremerhaven, Germany. <sup>2</sup>Max Planck Institute for Marine Microbiology, Bremen, Germany. <sup>3</sup>Polar Biological Oceanography, Alfred Wegener Institute Helmholtz Centre for Polar and Marine Research, Bremerhaven, Germany. <sup>4</sup>Marine BioGeoScience, Alfred Wegener Institute Helmholtz Centre for Polar and Marine Research, Bremerhaven, Germany. <sup>5</sup>Physical Oceanography of the Polar Seas, Alfred Wegener Institute Helmholtz Centre for Polar and Marine Research, Bremerhaven, Germany. <sup>6</sup>Faroe Marine Research Institute, Tórshavn, Faroe Islands. <sup>7</sup>MARUM Center for Marine Environmental Sciences, University of Bremen, Bremen, Germany. ✉email: [matthias.wietz@awi.de](mailto:matthias.wietz@awi.de); [Antje.Boetius@awi.de](mailto:Antje.Boetius@awi.de)

Received: 8 June 2021 Revised: 3 November 2021 Accepted: 15 November 2021

Published online: 11 December 2021

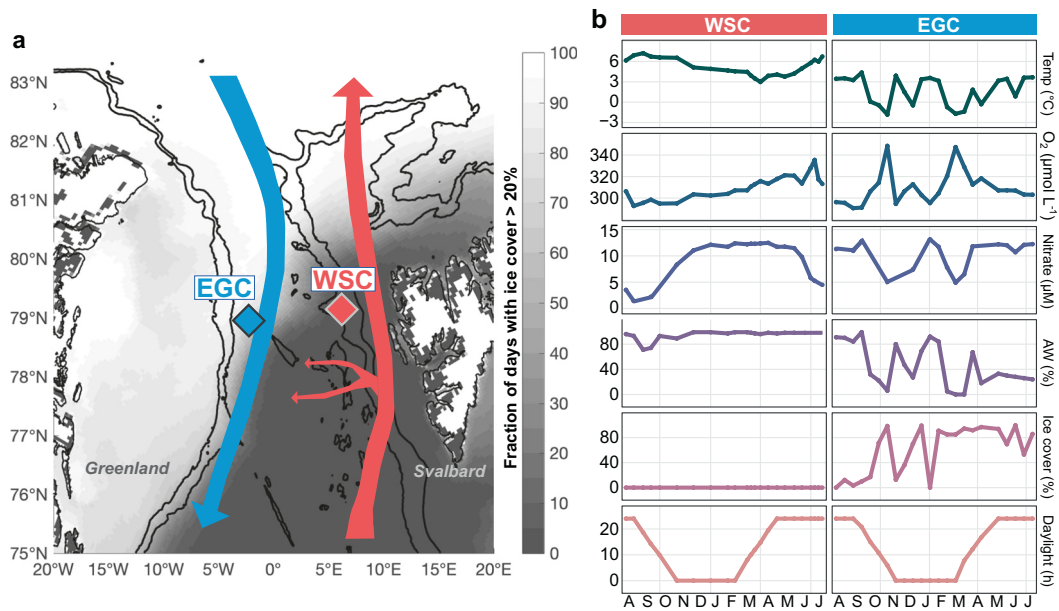


**Fig. 1 Study area and oceanographic conditions.** **a** Location of moored Remote Access Samplers in the East Greenland Current (EGC) and the West Spitsbergen Current (WSC) of Fram Strait, indicated in blue and red respectively. The small red arrows illustrate recirculation of Atlantic Water in central Fram Strait. The grayscale gradient indicates the fraction of days with average sea ice cover of >20%. **b** Water temperature ( $^{\circ}\text{C}$ ), concentrations of oxygen ( $\mu\text{mol L}^{-1}$ ) and nitrate ( $\mu\text{M}$ ), the proportion of Atlantic Water (%), sea ice cover (%), and daylight hours.

(EGC), with some recirculation in central Fram Strait across the marginal ice zone (Fig. 1a). Our study is embedded in the long-term HAUSGARTEN observatory studying primary production, benthopelagic coupling, and deep-sea ecology since the 1990s [25, 26]. The recent deployment of autonomous devices within the FRAM infrastructure program affords the unique opportunity for continuous year-round records. These considerably expand summertime observations of microbial diversity and activity in the WSC and EGC [27–32], shaped by a combination of sea ice cover, nitrate availability, and mixed layer depth [33, 34]. Annual records also help to understand the biological responses to the northward expansion of subarctic habitats, termed Atlantification, which propagates through the entire food web [35].

Here we investigated how polar day and night shape seasonality, expecting considerable differences between summer and winter microbiomes in both regions. We hypothesized that phototrophy- and heterotrophy-dominated periods in the WSC harbor markedly dissimilar microbial communities, whereas sea ice cover and polar water masses in the EGC sustain winter-type communities year-round. Our study illuminates fundamental principles of seasonality in Arctic microbial diversity, the ecological importance of the polar night, and potential effects of Atlantification. This evidence helps understanding natural variability and human impact in a region under severe threat by climate change [36, 37], with important implications for the present and future Arctic Ocean.

## MATERIALS AND METHODS

### Sampling approach

Within the framework of the FRAM marine observatory (<https://www.awi.de/en/expedition/observatories/ocean-fram.html>), Remote Access Samplers (RAS; McLane, East Falmouth, MA) were deployed in July 2016 on seafloor moorings F4-S-1 in the core WSC (79.0118 N–2.7938 E) and EGC-3 in the marginal ice zone (78.831 N–2.7938 E), constituting a fixed-point Eulerian approach (Fig. 1a). RAS deployment depth was 30 m (WSC) and 80 m (EGC; to avoid ice collisions). However, vertical movements in the water column resulted in variable actual sampling depths, with a mean of 40 m and 90 m in the WSC and EGC respectively (Supplementary Table 1). RAS

frames were equipped with 48 sterile sampling bags, each containing 700  $\mu\text{L}$  of saturated (7.5% w/v) mercuric chloride solution. At each programmed sampling event, two water samples of 500 mL were autonomously pumped an hour apart into individual sampling bags and fixed by mixing with mercuric chloride (0.01% final concentration). Upon recovery in August 2017, samples were immediately filtered through 0.22  $\mu\text{m}$  Sterivex cartridges (Millipore, Burlington, MA) and frozen at  $-20^{\circ}\text{C}$  until DNA extraction.

### DNA extraction and amplicon sequencing

DNA was extracted using the PowerWater kit (QIAGEN, Germany) according to the manufacturer's instructions, and quantified using Quantus (Promega, Madison, WI). 16S and 18S rRNA gene fragments were amplified using primers 515F–926R [38] and 528iF–964iR [29] respectively. Libraries were prepared according to the 16S Metagenomic Sequencing Library Preparation protocol (Illumina, San Diego, CA). rRNA gene fragments were sequenced using MiSeq technology in 2x300bp paired-end runs (Supplementary Methods).

### Sequence analysis

After primer removal using cutadapt [39], 16S and 18S rRNA reads were processed into amplicon sequence variants (ASVs) using DADA2 v1.14.1 [40] and classified using taxonomy databases Silva v138 [41] and PR<sup>2</sup> v4.12 [42] respectively (Supplementary Methods). After singleton removal, we obtained on average 62,000 16S rRNA and 99,000 18S rRNA reads per sample (Supplementary Table 2) sufficiently covering community composition (Supplementary Fig. 1). Sequences have been deposited in the European Nucleotide Archive under accession numbers PRJEB43890 (16S rRNA) and PRJEB43504 (18S rRNA) using the data brokerage service of the German Federation for Biological Data (GFBio) in compliance with MIxS standards.

### Mooring and satellite data

Temperature, depth, salinity, oxygen concentration, and oxygen saturation were derived from Seabird SBE37-ODO CTD sensors attached to the RAS, confirming consistent properties of the two water samples per date. Sensor measurements were averaged over 4 h around each sampling event, allowing to determine the relative proportions of Atlantic Water (AW) and Polar Water (PW) (Supplementary Methods). Relative proportions of >80% were considered as pure Atlantic or Polar Water respectively; and 20–80% as mixture of both. Physical sensors were manufacturer-calibrated

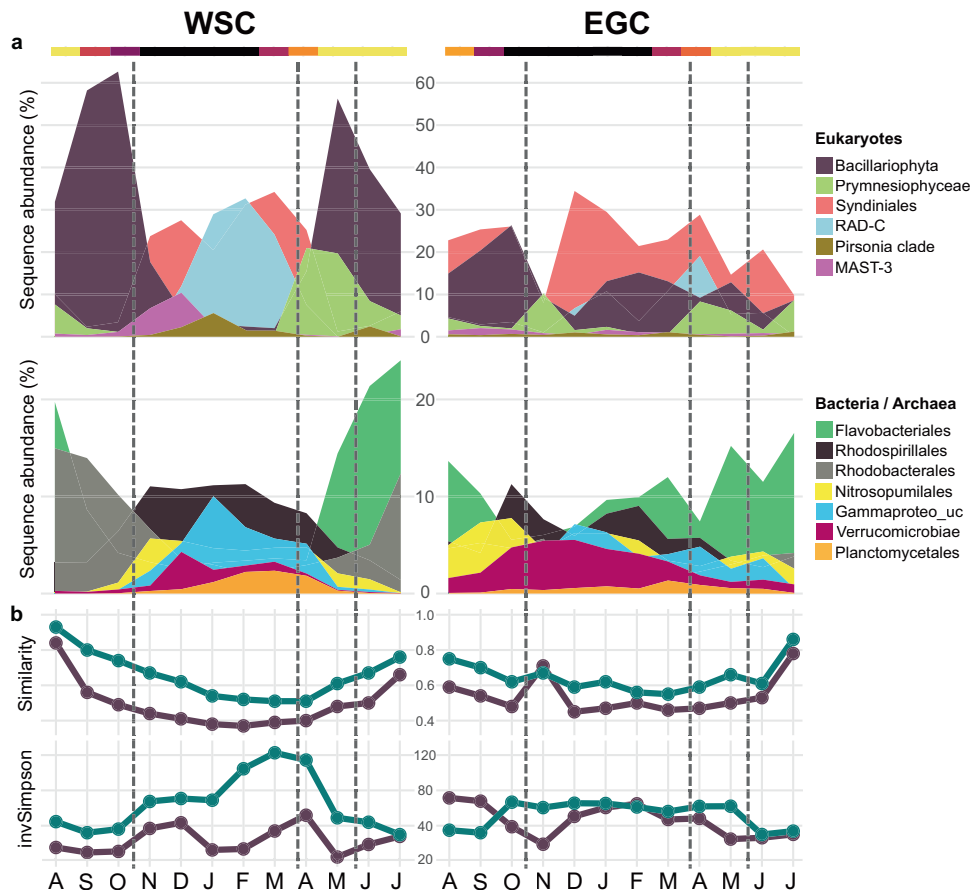


**Fig. 2** Year-round microbial community structure and turnover. **a** Relative sequence abundances (%) of eukaryotic, bacterial and archaeal taxa over the annual cycle. **b**, upper panel: Microbial community turnover (taxonomic similarities expressed as 1 minus Jensen-Shannon distance) compared to the first sampling event in relation to daylight hours (top color gradient). **b**, lower panel: Microbial alpha-diversity (inverse Simpson index). Eukaryotes: purple; bacteria and archaea: green. Lines indicate the seasonal boundaries defined by multivariate evaluation of physicochemical and microbial dynamics (Fig. 3).

and processed in accordance with <https://epic.awi.de/id/eprint/43137>. For chemical sensors (Sunburst SAMI-pH and Sunburst SAMI-CO<sub>2</sub>), the raw readouts are reported. Mooring data are available under <https://doi.pangaea.de/10.1594/PANGAEA.904565>. Sea ice and surface chlorophyll concentrations, derived from the AMSR-2 and Sentinel 3A OLCI satellites, were downloaded from the University of Bremen and the European Space Agency respectively, considering grid points within a radius of 15 km around the moorings.

### Nutrient quantification

Nitrate, nitrite, phosphate, and silicate were quantified using a QuAatro Seal Analytical segmented continuous-flow autoanalyser following standard colorimetric techniques. Accuracy was evaluated using KANSO LTD Japan Certified Reference Materials, with corrections applied as required. Following quality controls, results deemed questionable or of bad quality (quality flags 4 or 8 respectively) were excluded from further analyses (labeled NA in Supplementary Table 1). Nutrient data are available under <https://doi.pangaea.de/10.1594/PANGAEA.936749>.

### Statistical evaluation

Data analysis was done in R v4.1.1 implemented in RStudio (<https://rstudio.com>). In short, alpha-diversity and rarefaction curves were computed on raw ASV counts using R package iNEXT [43], excluding metazoan, chloroplast, and mitochondrial sequences. Subsequently, we only considered reads with  $\geq 3$  counts in  $\geq 2$  samples. Also, two samples from >200 m depth, when the RAS was pushed down by currents, were discarded to omit deep-water signatures. NMDS was performed using Bray-Curtis dissimilarities on Hellinger-transformed relative abundances. Seasons were defined based on multivariate patterning of oceanographic parameters and microbial community composition (Figs. 2, 3). Statistical differences

were computed by PERMANOVA or Kruskal-Wallis plus Bonferroni-corrected Dunn's post-hoc test as appropriate. Pairwise associations were assessed by Spearman correlations. Major R packages used were tidyverse, phyloseq, ampvis2, and PNWColors [44–47]. Code for reproducing workflow and figures is available at <https://github.com/matthiaswietz/RAS-1617>.

## RESULTS AND DISCUSSION

The present study elucidates microbial and oceanographic seasonality in the WSC and the EGC of Fram Strait using automated, year-round high-frequency sampling (Fig. 1a). For this purpose, seawater was autonomously collected and preserved in situ using moored Remote Access Samplers (RAS) in weekly to monthly intervals (Supplementary Table 1). In addition, sensors continuously measured depth, temperature, salinity, and oxygen, informing about oceanographic conditions including the proportions of Atlantic Water (AW) and Polar Water (PW). After recovery, water samples were subjected to amplicon sequencing of microbial communities and quantification of inorganic nutrients. Bacterial, archaeal, and eukaryotic amplicon sequence variants (ASVs) were then evaluated in the oceanographic context, including satellite-derived ice and chlorophyll concentrations (Supplementary Table 1).

### Major annual dynamics and drivers

Environmental conditions and microbial communities substantially differed over the year, but also between the two sampling sites (Fig. 1b, Supplementary Figs. 2, 3). At the WSC mooring,

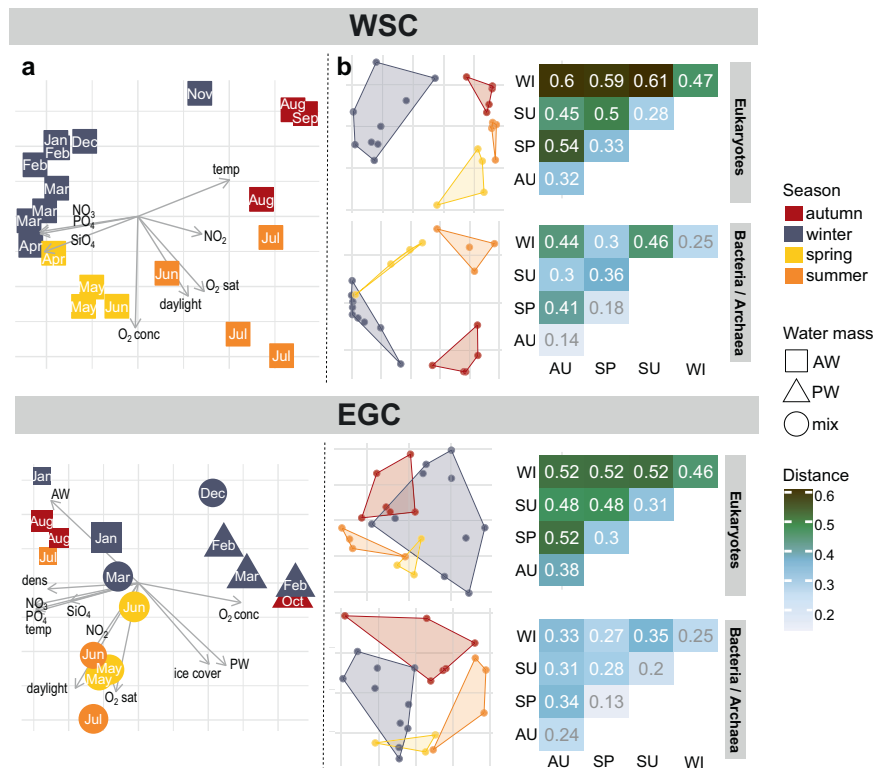


**Fig. 3 Microbial and environmental seasonality.** **a** Principal Component Analysis of environmental conditions. Components 1 and 2 explained 58/26% (WSC) and 60/14% (EGC) respectively, and hence the majority of physicochemical variability. For EGC, label size indicates percent ice cover. Only sampling events with complete environmental data were considered. **b** Non-metric multidimensional scaling of Hellinger-transformed relative ASV abundances (stress values 0.07, 0.03, 0.13, 0.1 from top to bottom) and corresponding Jensen-Shannon distances between and within seasons (larger numbers designate more dissimilar communities).

ice-free AW prevailed throughout the year, with water temperatures between 3.0 and 7.2 °C at sampling depth (Supplementary Table 1). Stratification in summer and mixing of the water column in winter [48, 49] corresponded to a mixed layer depth between 0 (July/August) and 270 m (February). At the EGC mooring, deployed at the edge of the marginal ice zone, water temperature varied between −1.8 and 4.4 °C. Intermittent advection of AW resulted in dynamic changes between polar (cold/ice-rich) and Atlantic (warmer/low-ice) conditions (Fig. 1b). PW-dominated periods showed a specific physicochemical and microbial signature, whereas AW advection resulted in greater similarities to the WSC (Supplementary Figs. 2, 3). This connection was strongest between AW proportions and bacterial composition (Spearman's  $\rho = 0.4$ ;  $p = 0.0008$ ). Hence, differences between the WSC and EGC correspond to different hydrography, ice cover as well as sampling depth. Earlier studies investigated the background of these vertical and horizontal contrasts in hydrography [33] and microbial composition [29].

This study focuses on the seasonal shifts in microbial communities. In both the WSC and EGC, communities markedly changed in composition and diversity over the annual cycle (Fig. 2a), illustrating dynamic microbiome structures year-round. Taxonomic dissimilarities to the first sampling event peaked around the March equinox before increasing again towards peak polar day (Fig. 2b), indicating light-driven temporal recurrence [50]. Notably, bacterial but not eukaryotic alpha-diversity correlated with daylight hours in both regions (Spearman's  $\rho = 0.6$ ,  $p < 0.006$ ).

### Microbial and environmental seasonality

We contextualized major patterns in microbial and physicochemical variability (Figs. 2–4) to delineate the four seasons: spring (mid-April to mid-June), summer (mid-June to late-July), autumn (August

to October), and winter (November to mid-April). Comparing all sampling events in the WSC and EGC, community structures largely clustered by season, with up to ~60% compositional dissimilarity to the other seasons respectively. Nonetheless, region-specific sub-clusters underlined the influence of hydrographic differences on microbiome composition (Supplementary Fig. 4). Seasonal contrasts in physicochemistry (Fig. 3a, Supplementary Table 3) and community composition (Fig. 3b, Fig. 4, Supplementary Fig. 5a) were most pronounced in the WSC, corroborated by season-specific correlations between microbial taxa and environmental parameters (Fig. 5). Weaker seasonality in the EGC corresponded to the combined influence of deeper sampling depth, sea ice cover, and the proportions of PW (Figs. 3b, 5). In line with recent metagenomic evidence, these patterns indicate a considerable degree of temporal specialization among Fram Strait microbiomes [51, 52], although the abundant SAR11 and SAR86 clades (constituting on average  $25 \pm 6\%$  and  $8 \pm 3\%$  of sequences, respectively) varied little over the year (Supplementary Fig. 5a).

In the WSC, daylight and temperature were significant drivers of eukaryotic variability (PERMANOVA,  $p < 0.001$ ), whereas bacterial composition varied mostly with temperature (PERMANOVA,  $p < 0.001$ ), comparable to the global TARA microbiome study [53]. Bacterial alpha-diversity peaked at the end of polar night (Fig. 2b) when water temperatures were lowest (Fig. 1b), underlining the day-night shift as key transition event. ASVs associated with Bacillariophyta (i.e. diatoms) and Flavobacteriales predominated from spring to autumn (Fig. 2a), presumably corresponding to metabolic interrelations through algal carbohydrates [54]. In contrast, heterotrophic eukaryotes (foremost Syndiniales and RAD-C radiolarians), archaea (Nitrosopumilales) and specific bacterial taxa (e.g., Rhodospirillales) prevailed in winter, with additional short-lived peaks of the diatom parasites *Pirsonia* and

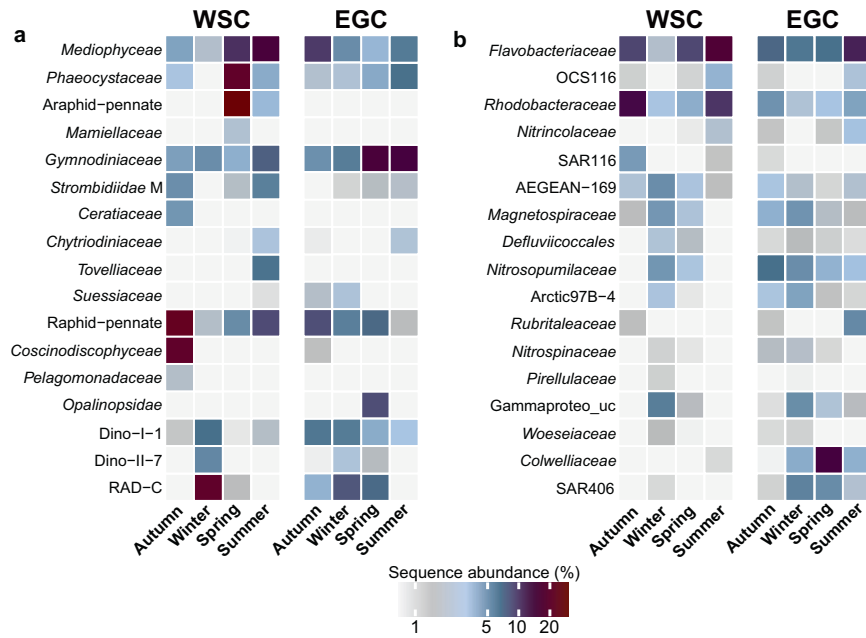


**Fig. 4 Microbes as indicators for seasons.** Relative sequence abundances of major microbial families by season and region (see Supplementary Fig. 5a for details).

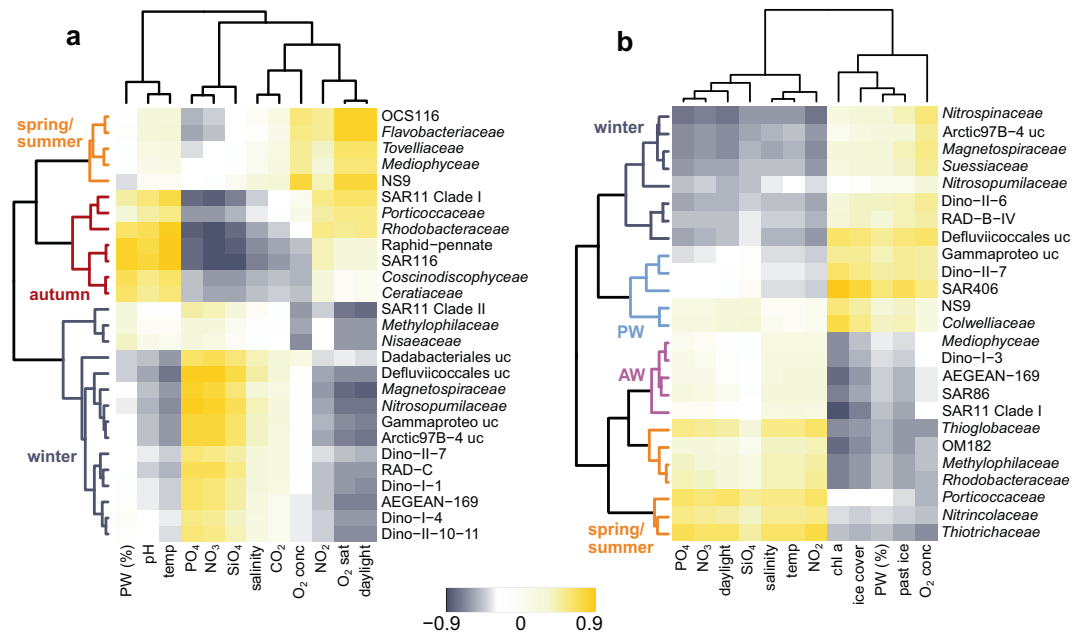


**Fig. 5 Environmental drivers of community structure.** Partial Least Square regression between environmental parameters and the abundance of microbial families, identifying seasonal groupings in the WSC (a) compared to both seasonal and polar/Atlantic-influenced groupings in the EGC (b). Only correlation coefficients  $> 0.5$  were considered. Temp: water temperature;  $O_2$  conc: oxygen concentration;  $O_2$  sat: oxygen saturation; PW: proportion of Polar Water; ice cover: percent ice cover on a given sampling event; past ice: percent ice cover integrated over the time between sampling events;  $CO_2$ : partial  $CO_2$  pressure.

MAST-3 (Fig. 2a). We consider these taxa as “microbial recyclers” persisting on detrital, inorganic or semi-refractory substrates. For instance, as detailed below, Nitrosopumilales are involved in ammonia oxidation and hence nitrate replenishment. The separation into photoautotrophy- and heterotrophy-driven periods of production and recycling was reflected in nutrient concentrations, with depletion in summer and replenishment during winter (Fig. 1b, Supplementary Table 1).

In the EGC, changes between polar and Atlantic conditions caused more variable community composition, turnover and

diversity. For instance, environmental conditions during AW advection in January resembled those in August (Figs. 1b, 3a). Daylight, temperature, hydrography and ice cover all contributed to microbial community structuring (PERMANOVA,  $p < 0.05$ ). This explained why some taxa correlate with seasonally changing environmental parameters, and some with polar or Atlantic conditions (Fig. 5). Constant proportions of photoautotrophic and heterotrophic eukaryotes year-round, with  $\sim 50\%$  lower diatom abundances than in the WSC (Fig. 2a, Supplementary Fig. 5b), illustrated a more heterotrophic food web largely

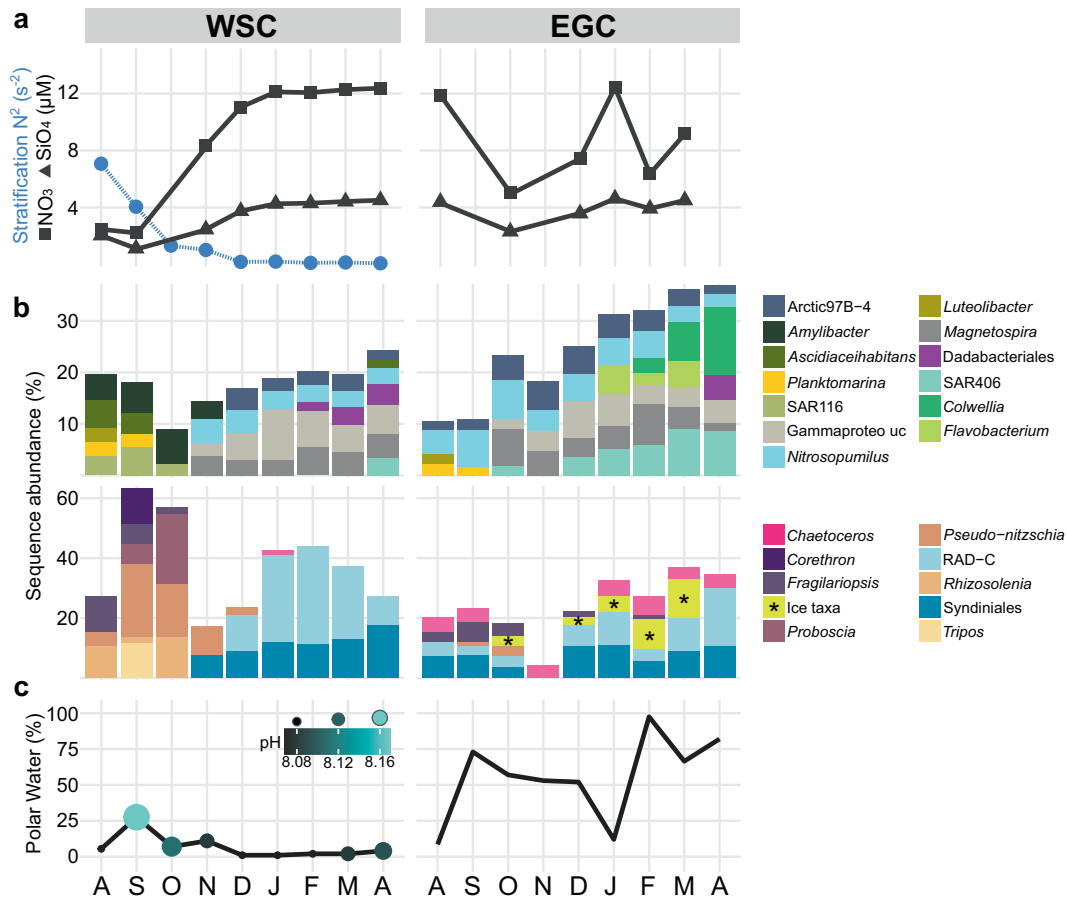


**Fig. 6 Autumn and winter dynamics.** **a** Concentrations of nitrate (squares) and silicate (triangles) in relation to stratification (blue; only available for the WSC). **b** Microbial genera with increased proportions in autumn or winter. “Winter-ice” eukaryotes are combined (marked by asterisks; see Supplementary Fig. 7a for abundances of each genus). **c** pH values (only available for the WSC) and proportions of Polar Water.

determined by sampling depth [55]. Sensor data available from autumn 2017 onwards show that <1% of photosynthetically active radiation reaches 80 m, impeding primary production. Furthermore, stratification in the upper ~50 m is strong [33, 34]. Detected phytoplankton sequences thus largely correspond to sinking cells from surface blooms and ice [56, 57]. In this context, high ice cover between May and July presumably repressed light availability and hence surface primary production, while stimulating the downward flux of ice-derived microbes. This combination of factors contributed to the weaker seasonality and temporal lag in the detection of certain phytoplankton taxa. For instance, *Phaeocystaceae* and *Mediophyceae* primarily occurred in summer/autumn (EGC) compared to spring/summer (WSC) respectively (Fig. 4). Nonetheless, our results indicate some overarching seasonal principles, especially during AW recirculation to the EGC. In the following, we present a detailed synopsis of seasonal patterns and specific events in chronological order from autumn 2016 to summer 2017.

### Autumn

Autumn in the WSC was characterized by nitrate, silicate and phosphate depletion and a specific community of *Coscinodiscophyceae*, *Ceratiaceae*, SAR116 and *Rhodobacteraceae* (Figs. 3, 4–6, Supplementary Table 3). These patterns illustrate a post-bloom state, with growing decay of summer phytoplankton [58] and concurrent increase in mixotrophic dinoflagellates [59]. The prevalence of *Corethron*, *Rhizosolenia* and *Proboscia* sequences (Fig. 6b, Supplementary Fig. 5b) matched microscopic cell counts [60], corroborating our amplicon-based results. Similar autumn

patterns in the Southern Ocean indicate bi-polar seasonal preferences of *Coscinodiscophyceae*, likely facilitated by their ability to overcome silicate limitation [61], use ammonium instead of nitrate [17], and resist grazing [62]. Appearance of chytrid fungi and *Labyrinthulaceae* at maximal nutrient depletion in October (Supplementary Fig. 6) indicates saprophytic activity on decaying algae [63, 64]. Up to 13-fold higher abundances of *Cand. Punciceispirillum*, other SAR116 members as well as *Ascidiaceihabitans*, *Amylibacter* and *Planktomarina* (Fig. 6b) were probably fueled by DMSP and senescence compounds from decaying phytoplankton [65, 66]. Detection of *Luteolibacter* from the *Rubritaleaceae* family (Fig. 5b) mirrored autumn in coastal Svalbard [67] and suggested ongoing particle formation, typical processes in ageing phytoplankton [68]. Overall, the average mixed layer depth of 17 m (Supplementary Table 3) suggests that microbial signals partially correspond to cells sinking from the shallow productive layer.

*Fragilariopsis* co-occurred in the WSC and the EGC during early autumn (Fig. 5b). We hypothesize that this typically ice-associated taxon was transported to the WSC by advection, considering the higher proportion of PW during this time (Fig. 6c). This event also covaried with higher pH, with potential metabolic effects on prevalent taxa such as *Pseudo-nitzschia* [69]. Otherwise, the EGC displayed quite different dynamics. Peaking diatom abundances characterized autumn as major photosynthetic period (Fig. 4, Supplementary Fig. 5b). We attribute this delay to the low ice cover (Fig. 1b, Supplementary Table 3) enhancing light penetration and stratification [70]. This combination presumably allowed an autumn surface bloom, becoming subsequently detectable at 80 m once phytoplankton cells sank.

## Winter

The WSC and EGC shared elevated abundances of *Magnetospiraceae*, *Nitrospinaceae*, the Arctic97B-4 clade and unclassified Gammaproteobacteria (Figs. 4, 5b), although their winter-summer contrasts were stronger in the WSC (average Kruskal-Wallis significance  $p \leq 0.003$  vs. 0.02 in the EGC). Furthermore, Dadabacteriales appeared from February (WSC) or late March (EGC) (Fig. 6) and might contribute to the recycling of organic matter [71]. Fundamental regional differences were the complete switch to heterotrophy in the WSC, compared to ice-related microbial signatures including persistent diatom signals in the EGC.

**Heterotrophic winter communities of the WSC.** The increase of Syndiniales, parasitic recyclers of phytoplankton biomass [72], in November marked the onset of winter (Supplementary Fig. 6). Bacterial diversification and nutrient replenishment (Figs. 2, 6) followed the breakdown of summer stratification, with maximal mixing of the water column in January (Fig. 6a). At this time, heterotrophic eukaryotes constituted ~70% of sequences and nutrient standing stocks were restored (Figs. 2a, 6a). The parallel decline of phototrophs to a combined relative abundance of <5% (Supplementary Fig. 5b) indicated complete mixing as one central turning point of the annual cycle [73, 74]. Notably, this also illustrates that only a small “seed bank” overwintered to initiate the following spring bloom. The upward transport of microbes during mixing likely enriched the community’s metabolic potential [75]. For instance, appearance of deep-water RAD radiolarians [76] possibly contributed to the recycling of phytoplankton biomass. Stratification potentially also influenced the temporal succession of different Syndiniales lineages over winter (Supplementary Fig. 6).

Winter bacteria and archaea likely contributed to nutrient replenishment. The co-occurrence of *Nitrosopumilaceae* and *Nitrospinaceae* (Figs. 4, 6b), the major drivers of marine nitrification, suggests an interactive niche with initial oxidation of ammonia or urea by *Nitrosopumilaceae* and subsequent nitrite oxidation by *Nitrospinaceae* [77]. In addition, the *Magnetospiraceae* family (Rhodospirillales) might recycle nitrogen by fixation and contribute to a yet underestimated nitrogen source [78, 79]. Furthermore, metaproteomic data indicate that *Magnetospiraceae* perform CO<sub>2</sub> fixation and thiosulfate oxidation [13]. Overall, genomic and metabolic evidence suggests consistent roles of *Nitrosopumilaceae*, *Nitrospinaceae*, and *Magnetospiraceae* during winter in both Arctic and Antarctic Oceans [80, 81]. Further potential recyclers are the *Pirellulaceae* and *Woeseiaceae* through ammonia oxidation and denitrification respectively [82, 83]. The winter niche of Defluviococcales was potentially fueled by stored glycogen or unsaturated aliphatics [84, 85]. Overall, the prevalence of diverse heterotrophic and chemoautotrophic taxa illustrates the polar night as important recycling phase before the spring bloom. Furthermore, the winter microbiome is not static, but responsive to certain stimuli such as mixing.

**An ice-related microbial loop in the EGC.** Unique to the EGC was the persistence of raphid-pennate diatoms and flavobacteria throughout winter (Fig. 4), contrasting their light-correlated seasonality in the WSC. We attribute these signals to ice melt and release of cells into the water, following intermittent water temperatures of >2 °C during AW advection in January (Fig. 1b). The diatoms *Bacillaria* and *Naviculales*, together with *Polarella* and *Chrysoephyceae* flagellates, constituted up to 15% of sequences between February and March (Fig. 6b, Supplementary Fig. 7a). All of these taxa occur in sea ice and the underlying water [56, 86], possibly constituting an ice-related microbial loop. Ice algae produce copious amounts of storage polysaccharides and extracellular polymeric substances, fueling bacterial growth in the underlying water [70, 87]. *Bacillaria* exudates are a valuable

nutrient source for bacteria [88], as is chrysolaminarin from diatoms and *Chrysoephyceae* [89]. Concurrently, *Chrysoephyceae* potentially also influenced organic matter cycling by preying on bacteria [90]. A *Flavobacterium* ASV constituted ~10% between January and March (Fig. 6b, Supplementary Fig. 7a), sharing >99% sequence similarity with *Flavobacterium frigidarium*, a psychrophilic genus with laminarinolytic abilities [91]. Detection of related sequences on ice-algal aggregates [92] supports a presumed niche of this ASV through utilization of ice-algal carbohydrates. Overall, such ice-fueled processes might explain signatures and activities of specific microbial taxa in the warming Arctic [93, 94].

An EGC-specific winter bacterium was the SAR406 clade, peaking at 9% sequence abundance in March and remaining detectable into summer. In addition, the frequently ice-associated genus *Colwellia* increased from February to abundances of >20% in mid-June (Figs. 6b, 7a). Both SAR406 and *Colwellia* markedly correlated with ice cover (Spearman’s  $\rho = 0.7$ ,  $p < 0.0004$ ), suggesting that ice cover sustained these winter-type taxa into summer. As SAR406 might participate in sulfur cycling [95], loss of sea ice might diminish the recycling of inorganic substrates.

## Spring and summer

**Microbial succession in the WSC.** Once daylight reached ~20 h in mid-April, the microbial system returned to a phototrophic state. The winter-spring transition occurred within few weeks, comparable to warmer Pacific waters [96]. The average mixed layer depth of >200 m until mid-June (Supplementary Table 3) likely facilitated strong phytoplankton growth. Eukaryotic composition changed ahead of bacterial communities, whose structure changed within four weeks after the primary photosynthetic peak (Supplementary Fig. 6). We observed three distinct bloom stages, featuring phototrophic pioneers (*Phaeocystis* and *Chaetoceros*) followed by araphid-pennate diatoms (*Grammonema*) and centric diatoms (*Thalassiosira*) (Fig. 7, Supplementary Fig. 8). A comparable three-stage bloom has been observed a year before in nearby Kongsfjorden [97]. The replacement of eukaryotic heterotrophs by photoautotrophs (Fig. 3b, Supplementary Fig. 6) suggests considerable energy fluxes around the winter-spring transition, with possible effects on benthopelagic coupling [98–100]. The early detection of *Aurantivirga* and SAR92 (Supplementary Fig. 6) matched observations during the Antarctic spring bloom [17], indicating comparable temporal niches at both poles. The *Grammonema* abundance of >50% in May coincided with peaking chlorophyll, potentially fueling intermittent peaks of *Formosa*, *Polaribacter*, and NS clades from family *Flavobacteriaceae* (Fig. 7a), comparable to diatom-flavobacteria relationships in temperate and Antarctic waters [54, 101].

*Thalassiosira* was specific for summer and the final bloom stage, when nitrate and phosphate declined and oxygen concentrations peaked (Fig. 7). The average mixed layer depth in summer was 23 m (Supplementary Table 3); hence, the RAS sampled just below the productive layer. The relative increase of mixotrophic flagellates (e.g., *Gyrodinium* and *Woloszynskia*) and concurrently decreasing chlorophyll indicates that trophic structure shifted towards heterotrophy. Increase of the roseobacter *Amylibacter* (formerly NAC11-7) to 15% sequence abundance emphasized the beginning transition to the autumn post-bloom where *Rhodobacteraceae* dominated (Fig. 4). We hypothesize concurrent generation of detritus particles, given the typical termination of diatom blooms by aggregation [68] and the association of *Amylibacter* with related particles [102]. Furthermore, the appearance of ectoparasitoid dinoflagellates such as *Chytriodinium* indicates beginning parasitism on diatoms and larger metazoans [103].

**Absence of major phototrophic peaks in the EGC.** Diatom abundances resembled those during winter (Supplementary Fig. 5b), with threefold lower chlorophyll concentrations than

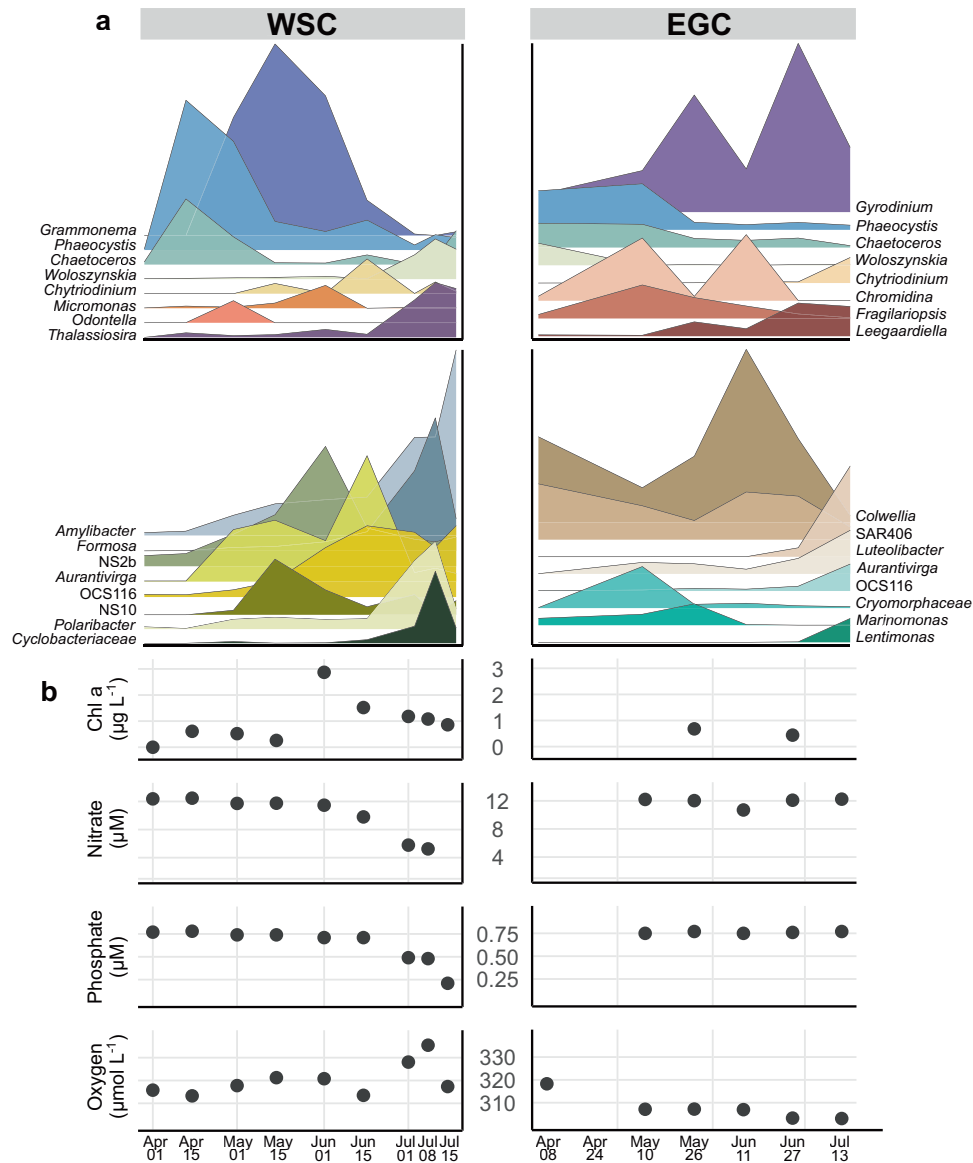


**Fig. 7 Spring and summer dynamics.** **a** Relative abundances of dominant eukaryotic and bacterial genera (see Supplementary Fig. 8 for detailed abundances). **b** Concentrations of chlorophyll, nitrate, phosphate and oxygen.

the WSC peak (Fig. 7b). *Fragilariopsis* and *Chaetoceros* together only constituted <10% of eukaryotic sequences, although nutrients were not limiting (Fig. 7b, Supplementary Table 3). Furthermore, *Phaeocystis* only reached 9% and hence a quarter of WSC proportions. These observations corroborate the influence of sampling depth, i.e. that phytoplankton sequences merely mirror preceding surface dynamics and export flux. This constant input of detrital material presumably also explains why Syndiniales prevailed over summer (Fig. 4), together with major peaks of the mixotrophs *Chromidina* (Ciliophora) and *Gyrodinium* (Dinoflagellata) that constituted up to 35% of eukaryote sequences. *Chromidina* is normally considered an animal parasite, suggesting yet undescribed free-living niches in the marginal ice zone. The prevalence of mixotrophy was underlined by the earlier detection of *Woloszynskia*, and twofold lower flavobacterial abundances compared to the WSC (Figs. 2a, 4b). Moreover, the typical phytoplankton associates OCS116, *Lentimonas* and *Luteolibacter* [104, 105] were only detected from mid-summer, following EGC-specific *Cryomorpaceae* and *Marinomonas* peaks (Fig. 7a). The presence of ice cover over summer, likely resulting in continuous

input of ice-derived substrates, indicates further differences in trophic structure. Ice substrates presumably fueled the major peak of *Colwellia*, which can efficiently grow on organic matter from sea ice [70].

### ECOLOGICAL CONCLUSIONS

This first assessment of microbial seasonality in the Fram Strait by autonomous sampling identified marked seasonal contrasts, distinct transition events, as well as dynamic variability linked to polar vs. Atlantic conditions. The characterization of bloom stages, ephemeral abundance peaks, and polar night characteristics promotes the understanding of the drivers and timescales of microbial seasonality in ice-covered and ice-free Arctic waters. These insights yield a number of fundamental ecological conclusions, with implications for the present and future Arctic Ocean.

1. We identified major dynamics and drivers of microbiome structure in the Arctic Ocean: marked seasonal contrasts

related to daylight, temperature and stratification in the euphotic zone of the ice-free WSC, compared to weaker seasonality related to ice cover, proportions of polar/Atlantic water masses and sampling depth in the EGC.

2. Dynamics in the WSC illustrate key principles of microbial seasonality in the ice-free, open Arctic Ocean: *Phaeocystis* as daylight pioneer followed by pennate diatoms and maximum chlorophyll concentrations when mixed layer depth was still >200 m (spring); declining nitrate and shift towards centric diatoms and mixotrophic flagellates upon increasing stratification (summer); minimum nutrients and highest temperatures when *Coscinodiscophyceae* diatoms and oligotrophic bacteria prevailed (autumn); and chemoautotrophic microbial recyclers and nutrient replenishment during vertical mixing (winter). Comparable observations have been made in a year-round study using Niskin-based sampling [11], illustrating that autonomous techniques provide results consistent with traditional approaches while considerably increasing temporal resolution. Moreover, our results remarkably overlap with a RAS-based study in the open Southern Ocean, which also reports *Coscinodiscophyceae* in autumn, *Aurantivirga* and SAR92 as first bacterial responders, and *Amylibacter* at the summer-autumn transition [17]. This suggests fundamental “bi-polar” patterns of microbial seasonality, only discernable by autonomous sampling.
3. The EGC exhibited combined effects of depth, ice cover and variable polar/Atlantic water masses, with a strong heterotrophic signature year-round. Seasonality and similarities to the WSC scaled with the extent of AW advection. At a maximum speed of  $0.25 \text{ m s}^{-1}$  [106], water from the WSC can reach the EGC within ~2 weeks, underlining how quickly hydrographic regimes can change and influence community composition. Polar-dominated conditions extended the duration and abundance of winter taxa such as SAR406 and *Colwellia*, with surface phytoplankton growth mainly detected during low ice in autumn. Periods of low ice coincided with higher abundances of *Phaeocystis*, *Thalassiosira*, OCS116 and *Aurantivirga* (Supplementary Fig. 7b). These dynamics are sentinels of how the future EGC might shift from an ice- to a light-driven habitat [107], presumably affecting the fate of phytoplankton blooms and the biological carbon pump [57, 108, 109]. Elevated photosynthesis and resulting higher amounts of organic substrates might accelerate the microbial loop [110], inducing the remineralization of ice-derived organic matter at the expense of chemoautotrophic metabolisms [70, 111].
4. Atlantification of the Arctic may enhance early blooms of *Phaeocystis* [15, 27] and alter biogeochemical fluxes, considering the associated production of TEP that serves as microbial substrate, microhabitat and downward vehicle of organic matter. In case stratification becomes stronger and more permanent with increasing temperatures, winter-time convection might diminish and deep-water “recycling taxa” disappear from the winter assemblage, with yet unknown ecological consequences.

In conclusion, the demonstrated seasonal microbiome dynamics and drivers contribute to the understanding of Arctic ecosystem functioning over polar day and night. This evidence is particularly relevant considering the anticipated impact of climate change on polar regions.

## REFERENCES

1. Cavicchioli R, Ripple WJ, Timmis KN, Azam F, Bakken LR, Baylis M, et al. Scientists' warning to humanity: microorganisms and climate change. *Nat Rev Microbiol*. 2019;17:569–86.

2. Bunse C, Pinhassi J. Marine Bacterioplankton seasonal succession dynamics. *Trends Microbiol*. 2017;25:494–505.
3. Buttigieg PL, Fadeev E, Bienhold C, Hehemann L, Offre P, Boetius A. Marine microbes in 4D—using time series observation to assess the dynamics of the ocean microbiome and its links to ocean health. *Curr Opin Microbiol*. 2018;43:169–85.
4. Gilbert JA, Steele JA, Caporaso JG, Steinbrück L, Reeder J, Temperton B, et al. Defining seasonal marine microbial community dynamics. *ISME J*. 2012;6:298–308.
5. Cram JA, Chow C-ET, Sachdeva R, Needham DM, Parada AE, Steele JA, et al. Seasonal and interannual variability of the marine bacterioplankton community throughout the water column over ten years. *ISME J*. 2015;9:563–80.
6. Auladell A, Barberán A, Logares R, Garcés E, Gasol JM, Ferrera I. Seasonal niche differentiation among closely related marine bacteria. *ISME J*. 2021.
7. Alonso-Saez L, Sanchez O, Gasol JM, Balague V, Pedros-Alio C. Winter-to-summer changes in the composition and single-cell activity of near-surface Arctic prokaryotes. *Environ Microbiol*. 2008;10:2444–54.
8. Rokkan Iversen K, Seuthe L. Seasonal microbial processes in a high-latitude fjord (Kongsfjorden, Svalbard): I. Heterotrophic bacteria, picoplankton and nano-flagellates. *Polar Biol*. 2011;34:731–49.
9. Grzymalski JJ, Riesenfeld CS, Williams TJ, Dussaq AM, Ducklow H, Erickson M, et al. A metagenomic assessment of winter and summer bacterioplankton from Antarctica Peninsula coastal surface waters. *ISME J*. 2012;6:1901–15.
10. Pedrós-Alió C, Potvin M, Lovejoy C. Diversity of planktonic microorganisms in the Arctic Ocean. *Prog Oceanogr*. 2015;139:233–43.
11. Wilson B, Müller O, Nordmann E-L, Seuthe L, Bratbak G, Øvreås L. Changes in marine prokaryote composition with season and depth over an Arctic polar year. *Front Mar Sci*. 2017;4:95.
12. Sandaa R-A, E Storesund J, Olesin E, Lund Paulsen M, Larsen A, Bratbak G, et al. Seasonality drives microbial community structure, shaping both eukaryotic and prokaryotic host–viral relationships in an Arctic marine ecosystem. *Viruses*. 2018;10:715.
13. Williams TJ, Long E, Evans F, Demaere MZ, Lauro FM, Raftery MJ, et al. A metaproteomic assessment of winter and summer bacterioplankton from Antarctica Peninsula coastal surface waters. *ISME J*. 2012;6:1883–900.
14. Freyria NJ, Joli N, Lovejoy C. A decadal perspective on north water microbial eukaryotes as Arctic Ocean sentinels. *Sci Rep*. 2021;11:8413.
15. Assmy P, Fernández-Méndez M, Duarte P, Meyer A, Randelhoff A, Mundy CJ, et al. Leads in Arctic pack ice enable early phytoplankton blooms below snow-covered sea ice. *Sci Rep*. 2017;7:40850.
16. Hegseth EN, Assmy P, Wiktor JM, Wiktor J, Kristiansen S, Leu E, et al. Phytoplankton seasonal dynamics in Kongsfjorden, Svalbard and the adjacent shelf. In: Hop H, Wiencke C (eds). *The ecosystem of Kongsfjorden, Svalbard*. 2019. Springer International Publishing, Cham, pp 173–227.
17. Liu Y, Blain S, Crispi O, Rembauville M, Obernosterer I. Seasonal dynamics of prokaryotes and their associations with diatoms in the Southern Ocean as revealed by an autonomous sampler. *Environ Microbiol*. 2020;22:3968–84.
18. Randelhoff A, Lacour L, Marec C, Leymarie E, Lagunas J, Xing X, et al. Arctic mid-winter phytoplankton growth revealed by autonomous profilers. *Sci Adv*. 2020;6:eabc2678.
19. Randelhoff A, Reigstad M, Chierici M, Sundfjord A, Ivanov V, Cape M, et al. Seasonality of the physical and biogeochemical hydrography in the inflow to the Arctic Ocean through Fram Strait. *Front Mar Sci*. 2018;5:224.
20. Berge J, Renaud PE, Darnis G, Cottier F, Last K, Gabrielsen TM, et al. In the dark: a review of ecosystem processes during the Arctic polar night. *Prog Oceanogr*. 2015;139:258–71.
21. Müller O, Wilson B, Paulsen ML, Rumińska A, Armo HR, Bratbak G, et al. Spatiotemporal dynamics of ammonia-oxidizing thaumarchaeota in distinct arctic water masses. *Front Microbiol*. 2018;9:24.
22. Johnsen G, Leu E, Gradinger R. Marine micro- and macroalgae in the polar night. In: Berge J, Johnsen G, Cohen JH (eds). *Polar night marine ecology: life and light in the dead of night*. 2020. Springer International Publishing, Cham, pp 67–112.
23. Vader A, Marquardt M, Meshram A, Gabrielsen T. Key Arctic phototrophs are widespread in the polar night. *Polar Biol*. 2014;38:13–21.
24. Leu E, Mundy CJ, Assmy P, Campbell K, Gabrielsen TM, Gosselin M, et al. Arctic spring awakening—steering principles behind the phenology of vernal ice algal blooms. *Prog Oceanogr*. 2015;139:151–70.
25. Soltwedel T, Bauerfeind E, Bergmann M, Bracher A, Budaeva N, Busch K, et al. Natural variability or anthropogenically-induced variation? Insights from 15 years of multidisciplinary observations at the arctic marine LTER site HAUSGARTEN. *Ecol Indic*. 2016;65:89–102.
26. Nöthig E-M, Ramondenc S, Haas A, Hehemann L, Walter A, Bracher A, et al. Summertime chlorophyll a and particulate organic carbon standing stocks in surface waters of the Fram Strait and the Arctic Ocean (1991–2015). *Front Mar Sci*. 2020;7:350.

27. Nöthig E-M, Bracher A, Engel A, Metfies K, Niehoff B, Peeken I, et al. Summertime plankton ecology in Fram Strait—a compilation of long- and short-term observations. *Polar Res.* 2015;34:23349.
28. Engel A, Bracher A, Dinter T, Endres S, Grosse J, Metfies K, et al. Inter-annual variability of organic carbon concentration in the Eastern Fram Strait during summer (2009–17). *Front Mar Sci.* 2019;6:187.
29. Fadeev E, Salter I, Schourup-Kristensen V, Nöthig E-M, Metfies K, Engel A, et al. Microbial communities in the east and west Fram Strait during sea ice melting season. *Front Mar Sci.* 2018;5:429.
30. von Jackowski A, Grosse J, Nöthig E-M, Engel A. Dynamics of organic matter and bacterial activity in the Fram Strait during summer and autumn. *Philos Trans R Soc Math Phys Eng Sci.* 2020;378:20190366.
31. Metfies K, Bauerfeind E, Wolf C, Sprong P, Frickenhaus S, Kaleschke L, et al. Protist communities in moored long-term sediment traps (Fram Strait, Arctic)—preservation with mercury chloride allows for PCR-based molecular genetic analyses. *Front Mar Sci.* 2017;4:301.
32. Cardozo-Mino MG, Fadeev E, Salman-Carvalho V, Boetius A. Spatial distribution of Arctic bacterioplankton abundance is linked to distinct water masses and summertime phytoplankton bloom dynamics (Fram Strait, 79°N). *Front Microbiol.* 2021;12:658803.
33. Richter ME, von Appen W-J, Wekerle C. Does the East Greenland Current exist in the northern Fram Strait? *Ocean Sci.* 2018;14:1147–65.
34. Tuerena RE, Hopkins J, Buchanan PJ, Ganeshram RS, Norman L, von Appen W-J, et al. An Arctic strait of two halves: the changing dynamics of nutrient uptake and limitation across the Fram Strait. *Glob Biogeochem Cycles.* 2021;35:e2021GB006961.
35. Polyakov IV, Pnyushkov AV, Alkire MB, Ashik IM, Baumann TM, Carmack EC, et al. Greater role for Atlantic inflows on sea-ice loss in the Eurasian Basin of the Arctic Ocean. *Science.* 2017;356:285–91.
36. Lannuzel D, Tedesco L, van Leeuwe M, Campbell K, Flores H, Delille B, et al. The future of Arctic sea-ice biogeochemistry and ice-associated ecosystems. *Nat Clim Change.* 2020;10:983–92.
37. Carter-Gates M, Balestrieri C, Thorpe SE, Cottier F, Baylay A, Bibby TS, et al. Implications of increasing Atlantic influence for Arctic microbial community structure. *Sci Rep.* 2020;10:19262.
38. Parada AE, Needham DM, Fuhrman JA. Every base matters: assessing small subunit rRNA primers for marine microbiomes with mock communities, time series and global field samples. *Environ Microbiol.* 2016;18:1403–14.
39. Martin M. Cutadapt removes adapter sequences from high-throughput sequencing reads. *EMBnetjournal* 2011;17:10–2.
40. Callahan BJ, McMurdie PJ, Rosen MJ, Han AW, Johnson AJA, Holmes SP. DADA2: High-resolution sample inference from Illumina amplicon data. *Nat Methods.* 2016;13:581–3.
41. Quast C, Pruesse E, Yilmaz P, Gerken J, Schweer T, Yarza P, et al. The SILVA ribosomal RNA gene database project: improved data processing and web-based tools. *Nucleic Acids Res.* 2013;41:D590–596.
42. Guillou L, Bachar D, Audic S, Bass D, Berney C, Bittner L, et al. The Protist Ribosomal Reference database (PR2): a catalog of unicellular eukaryote Small Sub-Unit rRNA sequences with curated taxonomy. *Nucleic Acids Res.* 2013;41:D597–D604.
43. Hsieh TC, Ma KH, Chao A. iNEXT: an R package for rarefaction and extrapolation of species diversity (Hill numbers). *Methods Ecol Evol.* 2016;7:1451–6.
44. Wickham H, Averick M, Bryan J, Chang W, McGowan LD, François R, et al. Welcome to the Tidyverse. *J Open Source Softw.* 2019;4:1686.
45. McMurdie PJ, Holmes S. phyloseq: an R package for reproducible interactive analysis and graphics of microbiome census data. *PLOS ONE.* 2013;8:e61217.
46. Andersen KSS, Kirkegaard RH, Karst SM, Albertsen M. ampvis2: an R package to analyse and visualise 16S rRNA amplicon data. *bioRxiv.* 2018.
47. Lawlor J. PNWColors: A Pacific Northwest inspired R color palette package. 2020 <https://github.com/jakelawlor/PNWColors>.
48. von Appen W-J, Schauer U, Hattermann T, Beszczynska-Möller A. Seasonal cycle of mesoscale instability of the west Spitsbergen Current. *J Phys Oceanogr.* 2016;46:1231–54.
49. Wekerle C, Wang Q, von Appen W-J, Danilov S, Schourup-Kristensen V, Jung T. Eddy-resolving simulation of the Atlantic water circulation in the Fram Strait with focus on the seasonal cycle. *J Geophys Res Oceans.* 2017;122:8385–405.
50. Giner CR, Balagué V, Krabberød AK, Ferrera I, Reñé A, Garcés E, et al. Quantifying long-term recurrence in planktonic microbial eukaryotes. *Mol Ecol.* 2019;28:923–35.
51. Royo-Llonch M, Sánchez P, Ruiz-González C, Salazar G, Pedrós-Alió C, Sebastián M, et al. Compendium of 530 metagenome-assembled bacterial and archaeal genomes from the polar Arctic Ocean. *Nat. Microbiol.* 2021;6:1561–74.
52. Priest T, Orellana LH, Huettel B, Fuchs BM, Amann R. Microbial metagenome-assembled genomes of the Fram Strait from short and long read sequencing platforms. *PeerJ.* 2021;9:e11721.
53. Sunagawa S, Coelho LP, Chaffron S, Kultima JR, Labadie K, Salazar G, et al. Structure and function of the global ocean microbiome. *Science.* 2015;348:1261359.
54. Teeling H, Fuchs BM, Becher D, Klockow C, Gardebrecht A, Bennis CM, et al. Substrate-controlled succession of marine bacterioplankton populations induced by a phytoplankton bloom. *Science.* 2012;336:608–11.
55. Monier A, Comte J, Babin M, Forest A, Matsuoka A, Lovejoy C. Oceanographic structure drives the assembly processes of microbial eukaryotic communities. *ISME J.* 2015;9:990–1002.
56. Leeuwe M, van, Tedesco L, Arrigo KR, Assmy P, Campbell K, Meiners KM, et al. Microalgal community structure and primary production in Arctic and Antarctic sea ice: a synthesis. *Elem Sci Anth.* 2018;6:4.
57. Fadeev E, Rogge A, Ramondenc S, Nöthig E-M, Wekerle C, Bienhold C, et al. Sea ice presence is linked to higher carbon export and vertical microbial connectivity in the Eurasian Arctic Ocean. *Commun Biol.* 2021;4:1–13.
58. Wasmund N, Göbel J, von Bodungen B. 100-years-changes in the phytoplankton community of Kiel Bight (Baltic Sea). *J Mar Syst.* 2008;73:300–22.
59. Stoecker DK, Lavrentyev PJ. Mixotrophic plankton in the polar seas: a pan-Arctic review. *Front Mar Sci.* 2018;5:292.
60. Lampe V, Nöthig E-M, Schartau M. Spatio-temporal variations in community size structure of Arctic protist plankton in the Fram Strait. *Front Mar Sci.* 2021;7:579880.
61. Brichta M, Nöthig E-M. The role of life cycle stages of diatoms in decoupling carbon and silica cycles in polar regions. In: Proceedings of SCAR Open Science Conference Bremen, Germany. 2004.
62. Not F, Siano R, Kooistra WHCF, Simon N, Vaulot D, Probert I. Diversity and ecology of eukaryotic marine phytoplankton. In: Pignaneau G (ed). *Advances in botanical research.* 2012. Academic Press, pp 1–53.
63. Raghukumar S. Ecology of the marine protists, the Labyrinthulomycetes (Thraustochytrids and Labyrinthulids). *Eur J Protistol.* 2002;38:127–45.
64. Scholz B, Guillou L, Marano AV, Neuhauser S, Sullivan BK, Karsten U, et al. Zoospore parasites infecting marine diatoms—a black box that needs to be opened. *Fungal Ecol.* 2016;19:59–76.
65. Choi DH, Park K-T, An SM, Lee K, Cho J-C, Lee J-H, et al. Pyrosequencing revealed SAR116 clade as dominant dddp-containing bacteria in oligotrophic NW Pacific Ocean. *PLOS One.* 2015;10:e0116271.
66. Wemheuer B, Wemheuer F, Hollensteiner J, Meyer F-D, Voget S, Daniel R. The green impact: bacterioplankton response toward a phytoplankton spring bloom in the southern North Sea assessed by comparative metagenomic and meta-transcriptomic approaches. *Front Microbiol.* 2015;6:805.
67. Delpech L-M, Vonnahme TR, McGovern M, Gradinger R, Præbel K, Poste A. Terrestrial inputs shape coastal bacterial and archaeal communities in a high Arctic fjord (Isfjorden, Svalbard). *Front Microbiol.* 2021;12:614634.
68. Alldredge AL, Gotschalk CC. Direct observations of the mass flocculation of diatom blooms: characteristics, settling velocities and formation of diatom aggregates. *Deep Sea Res Part A. Oceanogr Res Pap.* 1989;36:159–71.
69. Lundholm N, Hansen PJ, Kotaki Y. Effect of pH on growth and domoic acid production by potentially toxic diatoms of the genera *Pseudo-nitzschia* and *Nitzschia*. *Mar Ecol Prog Ser.* 2004;273:1–15.
70. Underwood GJC, Michel C, Meisterhans G, Niemi A, Belzile C, Witt M, et al. Organic matter from Arctic sea-ice loss alters bacterial community structure and function. *Nat Clim Change.* 2019;9:170–6.
71. Graham E, Tully BJ. Marine Dada bacteria exhibit genome streamlining and phototrophy-driven niche partitioning. *ISME J.* 2021;15:1248–56.
72. Clarke LJ, Bestley S, Bissett A, Deagle BE. A globally distributed Syndiniales parasite dominates the Southern Ocean micro-eukaryote community near the sea-ice edge. *ISME J.* 2019;13:734–7.
73. Randelhoff A, Sundfjord A, Reigstad M. Seasonal variability and fluxes of nitrate in the surface waters over the Arctic shelf slope. *Geophys Res Lett.* 2015;42:3442–9.
74. García FC, Alonso-Sáez L, Morán XAG, López-Urrutia Á. Seasonality in molecular and cytometric diversity of marine bacterioplankton: the re-shuffling of bacterial taxa by vertical mixing. *Environ Microbiol.* 2015;17:4133–42.
75. Jousset A, Bienhold C, Chatzinotas A, Gallien L, Gobet A, Kurm V, et al. Where less may be more: how the rare biosphere pulls ecosystems strings. *ISME J.* 2017;11:853–62.
76. Giner CR, Pernice MC, Balagué V, Duarte CM, Gasol JM, Logares R, et al. Marked changes in diversity and relative activity of picoeukaryotes with depth in the world ocean. *ISME J.* 2020;14:437–49.
77. Lehtovirta-Morley LE. Ammonia oxidation: ecology, physiology, biochemistry and why they must all come together. *FEMS Microbiol Lett.* 2018;365:fny058.
78. Williams TJ, Lefevre CT, Zhao W, Beveridge TJ, Bazylinski DA. *Magnetospira thiophila* gen. nov., sp. nov., a marine magnetotactic bacterium that represents a novel lineage within the *Rhodospirillaceae* (Alphaproteobacteria). *Int J Syst Evol Microbiol.* 2012;62:2443–50.
79. von Friesen LW, Riemann L. Nitrogen fixation in a changing Arctic Ocean: an overlooked source of nitrogen? *Front Microbiol.* 2020;11:596426.

80. Alonso-Saez L, Waller AS, Mende DR, Bakker K, Farnelid H, Yager PL, et al. Role for urea in nitrification by polar marine archaea. *Proc Natl Acad Sci USA*. 2012;109:17989–94.
81. Martínez-Pérez C, Greening C, Zhao Z, Lappan RJ, Bay SK, De Corte D, et al. Lifting the lid: nitrifying archaea sustain diverse microbial communities below the Ross Ice Shelf. *Cell Rev*. 2020; <https://ssrn.com/abstract=3677479> or <https://doi.org/10.2139/ssrn.3677479>.
82. Mohamed NM, Saito K, Tal Y, Hill RT. Diversity of aerobic and anaerobic ammonia-oxidizing bacteria in marine sponges. *ISME J*. 2010;4:38–48.
83. Mussmann M, Pjevac P, Kruger K, Dykma S. Genomic repertoire of the *Woeiseiaceae*/JTB255, cosmopolitan and abundant core members of microbial communities in marine sediments. *ISME J*. 2017;11:1276–81.
84. Burow LC, Kong Y, Nielsen JL, Blackall LL, Nielsen PH. Abundance and ecophysiology of *Deffluviococcus* spp., glycogen-accumulating organisms in full-scale wastewater treatment processes. *Microbiology*. 2007;153:178–85.
85. Lucas J, Koester I, Wichels A, Niggemann J, Dittmar T, Callies U, et al. Short-term dynamics of North Sea Bacterioplankton-dissolved organic matter coherence on molecular level. *Front Microbiol*. 2016;7:321.
86. Stecher A, Neuhaus S, Lange B, Frickenhaus S, Beszteri B, Kroth PG, et al. rRNA and rDNA based assessment of sea ice protist biodiversity from the central Arctic Ocean. *Eur J Phycol*. 2016;51:31–46.
87. Lalonde C, Nöthig E-M, Somavilla R, Bauerfeind E, Shevchenko V, Okolodkov Y. Variability in under-ice export fluxes of biogenic matter in the Arctic Ocean. *Glob Biogeochem Cycles*. 2014;28:571–83.
88. Hoffmann K, Hassenrück C, Salman-Carvalho V, Holtappels M, Bienhold C. Response of bacterial communities to different detritus compositions in Arctic deep-sea sediments. *Front Microbiol*. 2017;8:266.
89. Kappelmann L, Krüger K, Hehemann J-H, Harder J, Markert S, Unfried F, et al. Polysaccharide utilization loci of North Sea *Flavobacteriia* as basis for using SusC/D-protein expression for predicting major phytoplankton glycans. *ISME J*. 2019;13:76–91.
90. Izaguirre I, Unrein F, Schiaffino MR, Lara E, Singer D, Balagué V, et al. Phylogenetic diversity and dominant ecological traits of freshwater Antarctic Chryso-phyceae. *Polar Biol*. 2021;44:941–57.
91. Humphry DR, George A, Black GW, Cummings SP. *Flavobacterium frigidarium* sp. nov., an aerobic, psychrophilic, xylanolytic and laminarinolytic bacterium from Antarctica. *Int J Syst Evol Microbiol*. 2001;51:1235–43.
92. Rapp JZ, Fernández-Méndez M, Bienhold C, Boetius A. Effects of ice-algal aggregate export on the connectivity of bacterial communities in the central Arctic Ocean. *Front Microbiol*. 2018;9:1035.
93. Ardyna M, Mundy CJ, Mayot N, Matthes LC, Oziel L, Horvat C, et al. Under-ice phytoplankton blooms: shedding light on the “invisible” part of Arctic primary production. *Front Mar Sci*. 2020;7:608032.
94. Alonso-Sáez L, Zeder M, Harding T, Perenthaler J, Lovejoy C, Bertilsson S, et al. Winter bloom of a rare betaproteobacterium in the Arctic Ocean. *Front Microbiol*. 2014;5:425.
95. Hawley AK, Nobu MK, Wright JJ, Durno WE, Morgan-Lang C, Sage B, et al. Diverse Marinimicrobia bacteria may mediate coupled biogeochemical cycles along eco-thermodynamic gradients. *Nat Commun*. 2017;8:1507.
96. Berdjeb L, Parada A, Needham DM, Fuhrman JA. Short-term dynamics and interactions of marine protist communities during the spring–summer transition. *ISME J*. 2018;12:1907–17.
97. Singh A, Divya DT, Tripathy SC, Naik RK. Interplay of regional oceanography and biogeochemistry on phytoplankton bloom development in an Arctic fjord. *Estuar Coast Shelf Sci*. 2020;243:106916.
98. Engel A, Piontek J, Metfies K, Endres S, Sprong P, Peeken I, et al. Inter-annual variability of transparent exopolymer particles in the Arctic Ocean reveals high sensitivity to ecosystem changes. *Sci Rep*. 2017;7:4129.
99. Nejtgaard JC, Tang KW, Steinke M, Dutz J, Koski M, Antajan E, et al. Zooplankton grazing on *Phaeocystis*: a quantitative review and future challenges. *Biogeochemistry*. 2007;83:147–72.
100. Lampitt RS, Salter I, Johns D. Radiolaria: major exporters of organic carbon to the deep ocean. *Glob Biogeochem Cycles*. 2009;23:GB1010.
101. Luria CM, Amaral-Zettler LA, Ducklow HW, Rich JJ. Seasonal succession of free-living bacterial communities in coastal waters of the western Antarctic Peninsula. *Front Microbiol*. 2016;7:1731.
102. Taylor JD, Cunliffe M. Coastal bacterioplankton community response to diatom-derived polysaccharide microgels. *Environ Microbiol Rep*. 2017;9:151–7.
103. Gómez-Gutiérrez J, Kawaguchi S, Nicol S. Epibiotic suctorians and enigmatic ecto- and endoparasitoid dinoflagellates of euphausiid eggs (Euphausiacea) off Oregon, USA. *J Plankton Res*. 2009;31:777–85.
104. Cardman Z, Arnosti C, Durbin A, Ziervogel K, Cox C, Steen AD, et al. Verruc-microbia: candidates for polysaccharide-degrading bacterioplankton in an Arctic fjord of Svalbard. *Appl Environ Microbiol*. 2014;80:3749–56.
105. Landa M, Blain S, Harmand J, Monchy S, Rapaport A, Obernosterer I. Major changes in the composition of a Southern Ocean bacterial community in response to diatom-derived dissolved organic matter. *FEMS Microbiol Ecol*. 2018;94:fy034.
106. Fahrbach E, Meincke J, Østerhus S, Rohardt G, Schauer U, Tverberg V, et al. Direct measurements of volume transports through Fram Strait. *Polar Res*. 2001;20:217–24.
107. Comeau AM, Li WK, Tremblay JE, Carmack EC, Lovejoy C. Arctic Ocean microbial community structure before and after the 2007 record sea ice minimum. *PLOS ONE*. 2011;6:e27492.
108. Lalonde C, Bauerfeind E, Nöthig E-M, Beszczynska-Möller A. Impact of a warm anomaly on export fluxes of biogenic matter in the eastern Fram Strait. *Prog Oceanogr*. 2013;109:70–7.
109. Dybwad C, Assmy P, Olsen LM, Peeken I, Nikolopoulos A, Krumpen T, et al. Carbon export in the seasonal sea ice zone north of Svalbard from winter to late summer. *Front Mar Sci*. 2021;7:525800.
110. Glud RN, Rysgaard S, Turner G, McGinnis DF, Leakey RJG. Biological- and physical-induced oxygen dynamics in melting sea ice of the Fram Strait. *Limnol Oceanogr*. 2014;59:1097–111.
111. Shiozaki T, Iijichi M, Fujiwara A, Makabe A, Nishino S, Yoshikawa C, et al. Factors regulating nitrification in the Arctic Ocean: potential impact of sea ice reduction and ocean acidification. *Glob Biogeochem Cycles*. 2019;33:1085–99.

## ACKNOWLEDGEMENTS

We thank Jana Bäger, Theresa Hargesheimer, Rafael Stiens, and Lili Hufnagel for RAS operation; Daniel Scholz for RAS and sensor operations and programming; Normen Lochthofen, Janine Ludszuweit, Lennard Frommhold, and Jonas Hagemann for mooring operation; Jakob Barz and Swantje Rogge for DNA extraction and library preparation; Halina Tegetmeyer for quality control and sequencing of 16S rRNA amplicons; and Laura Wischnewski for nutrient analysis. Christiane Hassenrück, Stefan Neuhaus, Pier L. Buttigieg, Magda Cardozo-Mino and Andrew B. Collier contributed bioinformatic assistance. We thank Eva-Maria Nöthig for constructive discussions and the entire FRAM team for excellent collaboration. The captain, crew and scientists of RV Polarstern cruises PS99 and PS107 are gratefully acknowledged. Ship time was provided under grants AWI\_PS99\_00 and AWI\_PS107\_05. This project has received funding from the European Research Council (ERC) under the European Union's Seventh Framework Program (FP7/2007-2013) research project ABYSS (Grant Agreement no. 294757) to AB. Additional funding came from the Helmholtz Association, specifically for the FRAM infrastructure and from the Max Planck Society.

## AUTHOR CONTRIBUTIONS

MW performed sequence analysis, statistical evaluation, and wrote the paper. CB contributed to sampling design, data interpretation and data management. KM provided eukaryotic sequence data and contributed to data interpretation. STV performed nutrient quantification and quality control. WJvA contributed quality-controlled oceanographic data, and coordinated the mooring operations. IS and AB designed the autonomous sampling and mooring strategy. All authors contributed to the final manuscript.

## FUNDING

Open Access funding enabled and organized by Projekt DEAL.

## COMPETING INTERESTS

The authors declare no competing interests.

## ADDITIONAL INFORMATION

**Supplementary information** The online version contains supplementary material available at <https://doi.org/10.1038/s43705-021-00074-4>.

**Correspondence** and requests for materials should be addressed to Matthias Wietz or Antje Boetius.

**Reprints and permission information** is available at <http://www.nature.com/reprints>

**Publisher's note** Springer Nature remains neutral with regard to jurisdictional claims in published maps and institutional affiliations.



**Open Access** This article is licensed under a Creative Commons Attribution 4.0 International License, which permits use, sharing, adaptation, distribution and reproduction in any medium or format, as long as you give appropriate credit to the original author(s) and the source, provide a link to the Creative Commons license, and indicate if changes were made. The images or other third party material in this article are included in the article's Creative Commons license, unless indicated otherwise in a credit line to the material. If material is not included in the article's Creative Commons license and your intended use is not permitted by statutory regulation or exceeds the permitted use, you will need to obtain permission directly from the copyright holder. To view a copy of this license, visit <http://creativecommons.org/licenses/by/4.0/>.

© The Author(s) 2021

## Appendix 9

### **Atlantic water influx and sea-ice cover drive taxonomic and functional shifts in Arctic marine bacterial communities**

Priest T, von Appen W-J, Oldenburg E, Popa O, Torres-Valdés S, Bienhold C, Metfies K, Boulton W, Mock T, Fuchs B, Amann R, Boetius A, Wietz M

*The ISME Journal* (2023), 17:1612–1625

## ARTICLE OPEN



# Atlantic water influx and sea-ice cover drive taxonomic and functional shifts in Arctic marine bacterial communities

Taylor Priest<sup>1</sup>✉, Wilken-Jon von Appen<sup>2</sup>, Ellen Oldenburg<sup>3</sup>, Ovidiu Popa<sup>3</sup>, Sinhué Torres-Valdés<sup>2</sup>, Christina Bienhold<sup>1,4</sup>, Katja Metfies<sup>5</sup>, William Boulton<sup>6,7</sup>, Thomas Mock<sup>6</sup>, Bernhard M. Fuchs<sup>1</sup>, Rudolf Amann<sup>1</sup>, Antje Boetius<sup>1,4,8</sup> and Matthias Wietz<sup>1,4</sup>✉

© The Author(s) 2023

The Arctic Ocean is experiencing unprecedented changes because of climate warming, necessitating detailed analyses on the ecology and dynamics of biological communities to understand current and future ecosystem shifts. Here, we generated a four-year, high-resolution amplicon dataset along with one annual cycle of PacBio HiFi read metagenomes from the East Greenland Current (EGC), and combined this with datasets spanning different spatiotemporal scales (Tara Arctic and MOSAIC) to assess the impact of Atlantic water influx and sea-ice cover on bacterial communities in the Arctic Ocean. Densely ice-covered polar waters harboured a temporally stable, resident microbiome. Atlantic water influx and reduced sea-ice cover resulted in the dominance of seasonally fluctuating populations, resembling a process of “replacement” through advection, mixing and environmental sorting. We identified bacterial signature populations of distinct environmental regimes, including polar night and high-ice cover, and assessed their ecological roles. Dynamics of signature populations were consistent across the wider Arctic; e.g. those associated with dense ice cover and winter in the EGC were abundant in the central Arctic Ocean in winter. Population- and community-level analyses revealed metabolic distinctions between bacteria affiliated with Arctic and Atlantic conditions; the former with increased potential to use bacterial- and terrestrial-derived substrates or inorganic compounds. Our evidence on bacterial dynamics over spatiotemporal scales provides novel insights into Arctic ecology and indicates a progressing Biological Atlantification of the warming Arctic Ocean, with consequences for food webs and biogeochemical cycles.

*The ISME Journal* (2023) 17:1612–1625; <https://doi.org/10.1038/s41396-023-01461-6>

## INTRODUCTION

The Arctic Ocean is experiencing unprecedented changes as a result of climate warming, progressing nearly four times faster than the global average [1]. Of particular significance is the rapid decline in sea-ice extent and thickness [2, 3], with future projections indicating frequent ice-free summers by 2050 [4]. In the Eurasian Arctic, accelerated rates of sea-ice decline are associated with increasing volume and heat content of inflowing Atlantic water (AW) [5]. The expanding influence of AW in the Arctic Ocean, termed Atlantification, not only impacts hydrographic and physicochemical conditions, but also provides avenues for habitat range expansion of temperate organisms [6, 7].

The impact of climate change on biological communities has become increasingly apparent across the Arctic Ocean in recent decades. Elevated primary production in shelf seas has been attributed to declining sea-ice extent and increasing phytoplankton biomass [8], particularly in the Eurasian Arctic where Atlantification is driving a poleward expansion of temperate

phytoplankton [7, 9]. Concurrently, phytoplankton phenologies are also changing, with secondary autumnal blooms now occurring in seasonally ice-covered areas [10]. This will have major consequences for the organic matter pool of the Arctic Ocean. Sea-ice dynamics play an important role in the availability of nutrients and organic matter in surface waters and the transport of carbon to the deep-sea [11–13]. At sea-ice margins, strong melt events result in intense stratification, which traps organic material in surface waters and delays vertical export [11].

Considering their role as primary degraders of organic matter and mediators of biogeochemical cycles, assessing the consequences of such changes for bacterial communities is essential to understand and predict alterations to ecosystem functioning. Recent studies have documented distinctions in bacterial communities between Atlantic- and Arctic-derived waters [14], and between sea-ice and seawater [15]. In addition, sea ice-derived dissolved organic matter (DOM) has been shown to stimulate rapid responses by bacterial taxa and significantly alter communities in incubation experiments [16, 17]. However, in order to gain

<sup>1</sup>Max Planck Institute for Marine Microbiology, Bremen 28359, Germany. <sup>2</sup>Physical Oceanography of the Polar Seas, Alfred Wegener Institute Helmholtz Centre for Polar and Marine Research, Bremerhaven 27570, Germany. <sup>3</sup>Institute for Quantitative and Theoretical Biology, Heinrich Heine University Düsseldorf, Düsseldorf 40225, Germany. <sup>4</sup>Deep-Sea Ecology and Technology, Alfred Wegener Institute Helmholtz Centre for Polar and Marine Research, Bremerhaven 27570, Germany. <sup>5</sup>Polar Biological Oceanography, Alfred Wegener Institute Helmholtz Centre for Polar and Marine Research, Bremerhaven 27570, Germany. <sup>6</sup>School of Environmental Sciences, University of East Anglia, Norwich Research Park, Norwich NR4 7TJ, United Kingdom. <sup>7</sup>School of Computing Sciences, University of East Anglia, Norwich Research Park, Norwich NR4 7TJ, United Kingdom. <sup>8</sup>MARUM – Center for Marine Environmental Sciences, University of Bremen, Bremen 28359, Germany. ✉email: [tpriest@mpi-bremen.de](mailto:tpriest@mpi-bremen.de); [matthias.wietz@awi.de](mailto:matthias.wietz@awi.de)

Received: 19 September 2022 Revised: 6 June 2023 Accepted: 15 June 2023

Published online: 8 July 2023

a deeper understanding of potential shifts in Arctic Ocean microbial ecology, communities need to be studied over high-resolution temporal scales and across natural environmental gradients such as the Arctic–Atlantic interface.

The Fram Strait, the main deep-water gateway between the Arctic and Atlantic Oceans, is a key location for conducting long-term ecological research over environmental gradients and under changing conditions [18]. Fram Strait harbours two major current systems; the East Greenland Current (EGC), transporting polar water (PW) southwards, and the West Spitsbergen Current (WSC), transporting AW northward. The EGC accounts for the export of ~50% of freshwater and ~90% of sea-ice from the central Arctic Ocean and carries Arctic hydrographic signatures [19]. Large-scale recirculation of AW into the EGC continuously occurs, although the magnitude varies across latitudes and over time [20, 21]. The mixing of AW and PW in the marginal ice zone (MIZ) creates different hydrographic regimes reflective of Arctic, mixed and Atlantic conditions, which can harbour unique bacterial compositions [14, 22]. It has been predicted that future Atlantification of the Arctic may result in a shift towards temperate, Atlantic-type communities [14]. However, further assessments of microbial population dynamics across spatiotemporal scales are needed to validate such hypotheses.

Here, we performed a high-resolution analysis of the temporal variation of bacterial taxonomy and function in the MIZ (2016–2018) and the core-EGC (2018–2020), covering the full spectrum of ice cover, daylight and hydrographic conditions. Our study is embedded in the “Frontiers in Arctic Marine Monitoring” (FRAM) ocean observing framework that employs mooring-attached sensors and autonomous Remote Access Samplers (RAS) to continuously monitor physicochemical parameters and biological communities in the Fram Strait. We analysed four-year 16S rRNA gene amplicon data supplemented with an annual cycle of PacBio HiFi read metagenomes, expanding a previous assessment of microbial dynamics over a single annual cycle in the EGC [23]. We hypothesise that high AW influx and low sea-ice cover result in communities dominated by chemoheterotrophic populations that taxonomically and functionally resemble those of temperate ecosystems. Our study provides essential insights into the impact of changing conditions on microbial ecology and biogeochemical cycles in the Arctic Ocean.

## METHODS

### Seawater collection and processing

Autonomous sample collection and subsequent processing proceeded as previously described [23]. Briefly, RAS (McLane, East Falmouth, MA) were deployed over four consecutive annual cycles between 2016 and 2020, with deployments and recoveries occurring each summer (2019–2020 mooring recovered in 2021). From 2016 to 2018, RAS were deployed in the MIZ (78.83° N –2.79° E) and from 2018 to 2020 in the core-EGC (79° N –5.4° E), with average sampling depths of 80 and 70 m, respectively. The depths were chosen to prevent contact with moving ice overhead. In weekly to fortnightly intervals (Supplementary Table S1), ~1 L of seawater was pumped into sterile plastic bags and fixed with mercuric chloride (0.01% final concentration). After RAS recovery, water was filtered onto 0.22 µm Sterivex cartridges directly frozen at –20 °C until DNA extraction.

### Amplicon sequencing and analysis

DNA was extracted using the DNeasy PowerWater kit (Qiagen, Germany), followed by amplification of 16S rRNA gene fragments using primers 515F–926R [24]. These primers perform well at recovering marine mock communities, and were recently suggested as optimal for studying Arctic microbial communities [24, 25]. Sequencing was performed on a MiSeq platform (Illumina, San Diego, CA) using 2 × 300 bp paired-end libraries according to the “16S Metagenomic Sequencing Library Preparation protocol” (Illumina). Reads were subsequently processed into amplicon sequence variants (ASVs) using DADA2 and the SILVA v138 database [26–28]. Analysis and plotting were performed in RStudio [29], primarily using the vegan [30], limma [31], mixOmics [32], ggplot2 [33] and

ComplexHeatmap [34] packages. Briefly, community composition was compared using Bray-Curtis dissimilarities and distance-based redundancy analysis (dbRDA) with the functions *decostand* and *dbRDA* in *vegan*, and visualised using *ggplot2*. The influence of environmental variables on community dissimilarity was determined through a stepwise significance test on the dbRDA using the *ordiR2step* and *anova.cca* functions in *vegan*. ASVs were assigned to distribution groups based on the frequency of detection over time.

Co-occurrence networks were calculated for MIZ and core-EGC samples separately using the packages *segmentTier* [35] and *igraph* [36]. Oscillation signals were calculated for each ASV per year based on Fourier transformation of normalised abundances and compared using Pearson's correlations. Only statistically significant positive correlations were retained (adjusted *p*-value < 0.05 after correction using the FDR method [37]). Using a network robustness analysis, a correlation coefficient of 0.7 was determined as a strong co-occurrence. Below this value, removal of a single node would cause network disruption. Networks were constructed using the co-occurrences that passed the above thresholds, and visualised in Cytoscape [38] with the Edge-weighted Spring-Embedded Layout. Values of centrality and node betweenness were calculated using *igraph*.

### PacBio metagenome sequencing

Nine samples from the 2016–2017 annual cycle in the MIZ were selected for metagenomic sequencing, using the same DNA as for amplicon sequencing. Sequencing libraries were prepared following the protocol “Procedure & Checklist – Preparing HiFi SMRTbell Libraries from Ultra-Low DNA Input” (PacBio, Menlo Park, CA) and inspected using a FEMTOpuse. Libraries were sequenced on 8M SMRT cells on a Sequel II platform for 30 h with sequencing chemistry 2.0 and binding kit 2.0. The sequencing was performed together with samples of another project, such that seven samples were multiplexed per SMRT cell. On average, this resulted in 268,000 reads per metagenome, with an N50 of 6.8 kbp.

### Taxonomic and functional annotation of HiFi reads

The 2.4 million generated HiFi reads were processed through a custom taxonomic classification and functional annotation pipeline. The classification pipeline followed similar steps to previously published tools, but with some modifications. A local database was constructed based on protein sequences from all species-representatives in the GTDB r202 database [39]. Prodigal v2.6.3 [40] was used to predict open reading frames (ORFs) on HiFi reads, which were subsequently aligned to the GTDB-based database using Diamond blastp v2.0.14 [41] with the following parameters: `--id 50 --query-cover 60 --top 5 --fast`. After inspection of the hits, a second filtering step was performed: percentage identity of >65% and an *e*-value of <1<sup>–10</sup>. Using Taxonkit v0.10.1 [42], the last common ancestor (LCA) algorithm was performed, resulting in a single taxonomy for each ORF. A secondary LCA was subsequently performed for all ORFs from the same HiFi read, generating a single taxonomy for each read. Functional annotation of HiFi reads was performed using Prokka [43] followed by a series of specialised databases. This included using blastp v2.11.0 [44] or HMMscan (HMMER v3.2.1) [45] against dbCAN v10 [46], CAZy (release 09242021) [47], SulfAtlas v1.3 [48], the Transporter Classification [49], MEROPS [50] and KEGG [51] databases along with sets of Pfam HMM family profiles for SusD and TonB-dependent transporter genes. Functional gene counts were normalised by the average sequencing depth of 16 universal, single-copy ribosomal protein genes per sample [52] – providing “per genome” counts. Genes enriched under high- and low-ice cover conditions were identified using ALDEx2 [53].

### Metagenome-assembled genome recovery

In order to maximise the recovery of metagenome-assembled genomes (MAGs), metagenomes were clustered into two groups based on dissimilarity in ASV composition of the corresponding amplicon samples. Samples were individually assembled using metaFlye v2.8.3 (parameters: `--meta --pacbio-hifi --keep-haplotypes --hifi-error 0.01`). Contigs with a length of <10 kbp were removed and the remaining contigs were renamed to reflect the sample of origin. Contigs from each group were concatenated into a single file. Coverage information, necessary for binning, was acquired through read recruitment of raw reads from all metagenomes to the contigs using Minimap2 v2.1 [54], using the ‘map-hifi’ preset. Contigs were binned using Vamb v3.0.2 [55] in multisplit mode using three different sets of parameters (set1: `-l 32 -n 512 512`, set2: `-l 24 -n 384 384`, set3: `-l 40 -n 768 768`). Completeness and contamination estimates of bins were determined using CheckM v1.1.3 [56], and those with >50% completeness were

manually refined using the interactive interface of Anvi'o v7 [57]. A consensus set of refined MAGs with non-redundant contigs was obtained using DASTool v1.1.1 [58]. The consensus MAGs were de-replicated at 99% average nucleotide identity using dRep v3.2.2 [59] (parameters: -comp 50 -con 5 -nc 0.50 -pa 0.85 -sa 0.98), resulting in 47 population-representative MAGs. A phylogenetic tree was reconstructed that also incorporated MAGs recently published from the Fram Strait [22], following a procedure outlined previously [52]. Briefly, 16 single-copy universal ribosomal protein genes were identified in each MAG using HMMsearch against the individual Pfam HMM family profiles and aligned using Muscle v3.8.15 [60]. Alignments were trimmed using TrimAl v1.4.1 [61], concatenated, and submitted to FastTree v2.1.0 [62]. The tree was visualised and annotated in iTOL [63].

### Classification, abundance and distribution of MAGs

A dual taxonomic classification of MAGs was performed using single-copy marker and 16S rRNA genes. Firstly, MAGs were assigned a taxonomy using the GTDBtk tool v1.7.0 [64] with the GTDB r202 database. Secondly, extracted 16S rRNA gene sequences were imported into ARB [65], aligned with SINA [66] and placed into the SILVA SSU 138 Ref NR99 reference tree using ARB parsimony. Those containing a 16S rRNA gene were linked to ASV sequences through competitive read recruitment using BBMap of the BBtools programme v35.14, with an identity threshold of 100%.

The distribution of MAGs across the Arctic Ocean were determined through recruitment of reads from the herein generated metagenomes and published datasets from the Tara Arctic and MOSAiC expeditions (Supplementary Table S11). Counts of competitively mapped reads were converted into the 80% truncated average sequencing depth, TAD80 [67]. Relative abundance was then determined as the quotient between the TAD80 and the average sequencing depth of 16 single-copy ribosomal protein genes. Ribosomal proteins were identified following the same procedure outlined above, and their sequencing depth estimated using read recruitment with minimap2 (for PacBio-derived metagenomes) and BBMap (for Illumina-derived metagenomes).

### Mooring and satellite data

Bacterial community data was placed into context using in situ measured environmental parameters (Supplementary Table S1). Temperature, depth, salinity and oxygen concentrations were measured using Seabird SBE37-ODO CTD sensors and chlorophyll *a* concentration was measured using a WET Labs ECO Triplet sensor, all attached to the RAS. Sensor measurements were averaged over 4 h around each sampling event. The relative proportions of AW and PW were determined as described previously [23]. Physical sensors were manufacturer-calibrated and processed in accordance with <https://epic.awi.de/id/eprint/43137>. Mooring-derived data are published under PANGAEA accession 904565 [68], 941159 [69], and 946539 [70]. Sea-ice concentrations, derived from the AMSR-2 satellite, were downloaded from <https://seaice.uni-bremen.de/sea-ice-concentration-amrs2>, and averaged over a 15 km radius around the moorings.

## RESULTS

The amplicon dataset incorporates samples (>0.2 µm fraction) collected at weekly to fortnightly intervals in the MIZ (2016–2018) and central EGC (core-EGC; 2018–2020) between 70 and 90 m depth (Supplementary Table S1). The two locations were selected in order to capture the full spectrum of water mass and sea-ice conditions. The core-EGC was characterised by year-round dense ice cover (hereon abbreviated as “high ice”) and PW conditions. In contrast, the MIZ featured variable, generally lower ice cover (hereon abbreviated as “low ice”) and periodic AW influx (Fig. 1). To visually portray this variability, animated GIFs were created for current velocities (Supplementary Fig. S1) and sea-ice cover (Supplementary Fig. S2) over the four-year period. Combining the high-resolution data from both mooring locations allowed for the assessment of bacterial community dynamics over time and in relation to Arctic- and Atlantic-dominated conditions.

### Bacterial community and population dynamics over time

The amplicon dataset encompasses 12.5 million quality-filtered reads in 84 samples, with an average of 134,588 reads per sample. A total of 4083 ASVs (Supplementary Table S2) were recovered,

which were initially used in a taxonomy-independent approach to assess community dynamics over environmental gradients (Fig. 2). A dbRDA with stepwise significance testing identified AW proportion, daylight and past ice cover (average ice cover of the days preceding the sampling event) as the significant factors constraining compositional variation (model  $R^2 = 0.23$ ,  $p = 0.001$ ). AW proportion explained 13% of the variation in bacterial community dissimilarity, compared to 6% for daylight and 4% for past ice cover.

Assessing ASV dynamics at the two mooring locations over time revealed several distinct patterns. In total, 75% of the ASVs were detected at both mooring sites (i.e. shared), whilst 16% and 9% were unique to the MIZ and core-EGC respectively. The frequency of detection and maximum relative abundance of shared ASVs exhibited a strong positive linear relationship, i.e., those identified in more samples also reached higher maximum relative abundances (Fig. 3a). To better understand the structuring of communities and distinguish between ecologically different fractions, we categorised ASVs into three groups: (a) Resident (Res-ASVs), present in >90% of samples, (b) Intermittent (Int-ASVs), present in 25–90% of samples, and (c) Transient (Trans-ASVs), present in <25% of samples (Supplementary Table S3). Res-ASVs represented a small fraction of the diversity (231 ASVs) but the largest proportion of the sampled bacterial communities (43–87% relative abundance). In comparison, the 1943 Int-ASVs constituted 12–53% and the 1909 Trans-ASVs 0.4–9.3% of relative abundances. Presence of a dominant resident microbiome, represented by a minority of ASVs, is consistent with multiannual observations in the Western English Channel and Hawaiian Ocean time-series [71, 72].

Temporal dynamics of the three community fractions was linked to changes in AW proportion, evidenced by negative correlations for the resident (Pearson's coefficient:  $-0.29$ ,  $p < 0.05$ ) and transient fractions (Pearson's coefficient:  $-0.36$ ,  $p < 0.01$ ) compared to positive correlations for the intermittent fraction (Pearson's coefficient:  $0.37$ ,  $p < 0.01$ ). This is reflected in the more stable temporal dynamics at the core-EGC with less AW influence, compared to the MIZ (Fig. 3c). In addition, the transient fraction was positively correlated with ice cover (Pearson's coefficient:  $0.26$ ,  $p < 0.05$ ).

The dynamics of the three community fractions were supported by co-occurrence networks computed at ASV level (Supplementary Fig. S3). The MIZ network contained more ASVs and more significant co-occurrences compared to the core-EGC, primarily driven by Int-ASVs. There were 283 more Int-ASVs in the MIZ than in the core-EGC network, and the number of connections per ASV was nine-fold higher. In contrast, Trans-ASVs were threefold more numerous and exhibited threefold more connections per ASV in the core-EGC compared to the MIZ network (Fig. 3b and Supplementary Information). Res-ASVs were comparable in number in both networks.

The resident microbiome was phylogenetically diverse, incorporating both abundant and rare community members. Res-ASVs were assigned to 61 families and 79 genera, with the *Flavobacteriaceae* ( $n = 15$ ), *Magnetospiraceae* ( $n = 13$ ), *Marinimicrobia* ( $n = 11$ ), SAR11 Clade I ( $n = 21$ ) and SAR11 Clade II ( $n = 17$ ) harbouring the largest diversity. Maximum relative abundances of Res-ASVs ranged from 0.04 to 13.9%, with the most prominent being affiliated with SAR11 Clade Ia (asv1; 14%), *Polaribacter* (asv6; 14%), *Aurantivirga* (asv7; 12%), SUP05 (asv2; 12%), SAR92 (asv16; 11%) and SAR86 (asv3; 9%). Pronounced fluctuations of the intermittent community coincided with AW influx in the MIZ. Int-ASVs were more phylogenetically diverse than Res-ASVs, encompassing 254 genera, and included rare and abundant populations that reached 0.004–36% maximum relative abundance. The most diverse taxa included the SAR11 Clade II ( $n = 148$ ), *Marinimicrobia* ( $n = 129$ ), NS9 Marine Group ( $n = 78$ ), AEGEAN-169 ( $n = 73$ ), and SAR86 ( $n = 47$ ). Those with largest relative abundances were

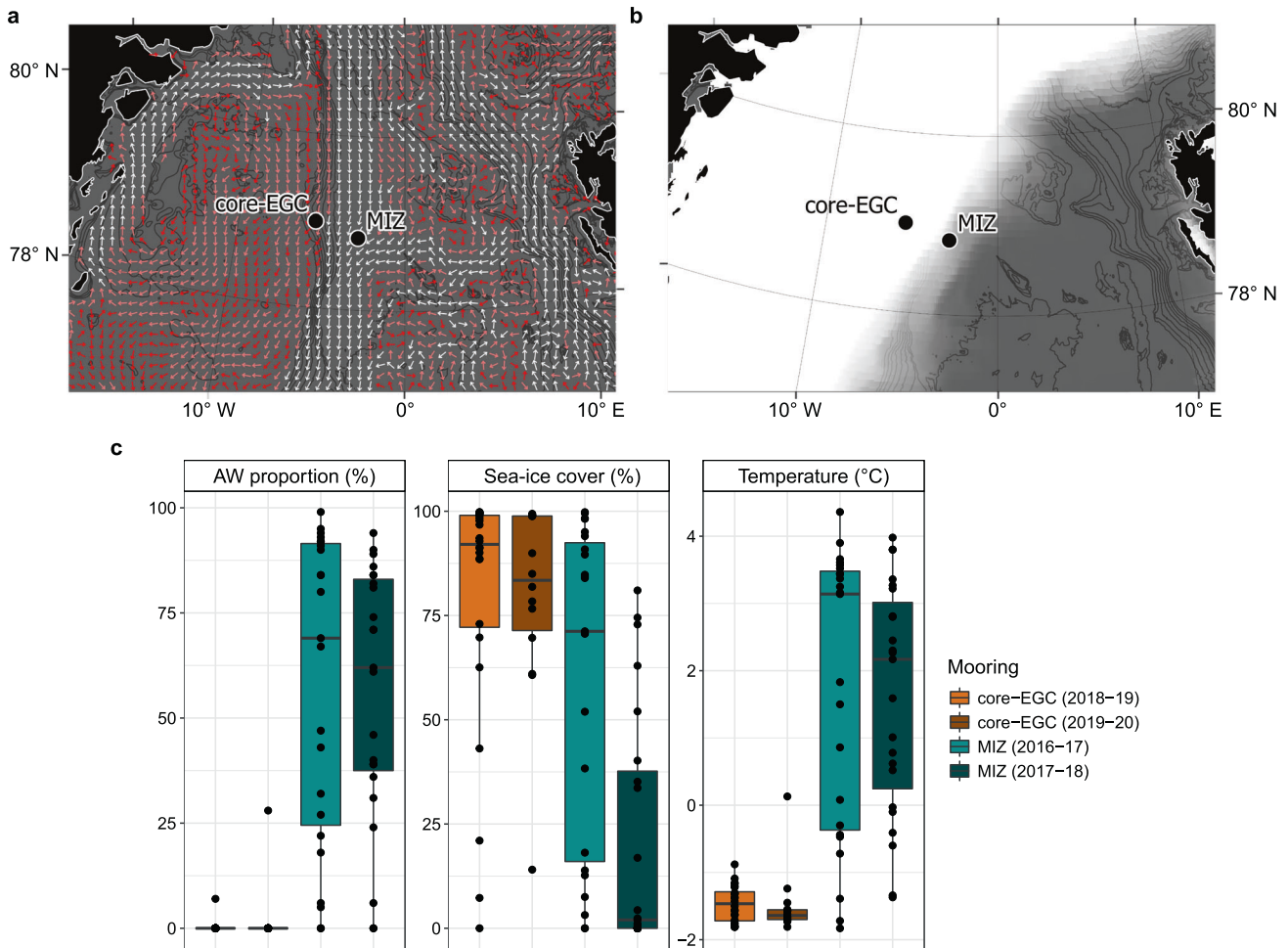


**Fig. 1** Location of seafloor moorings and environmental conditions in the MIZ (2016–2018) and core-EGC (2018–2020). **a** Example representation of monthly average (January 2020) current velocities at the approximate depth of sampling (78 m). White and dark red arrows indicate strongest and weakest velocities, respectively. **b** Example representation (December 2019) of sea-ice cover. Increasing opacity of white colour reflects increasing sea-ice cover (pure white = 100%). Current and sea-ice data were obtained from copernicus.eu under 'ARCTIC\_ANALYSIS\_FORECAST\_PHY\_002\_001\_a'. **c** Variation in AW proportion, ice cover and water temperature at the two moorings. The bathymetric map was made using data from [GEBCO](#).

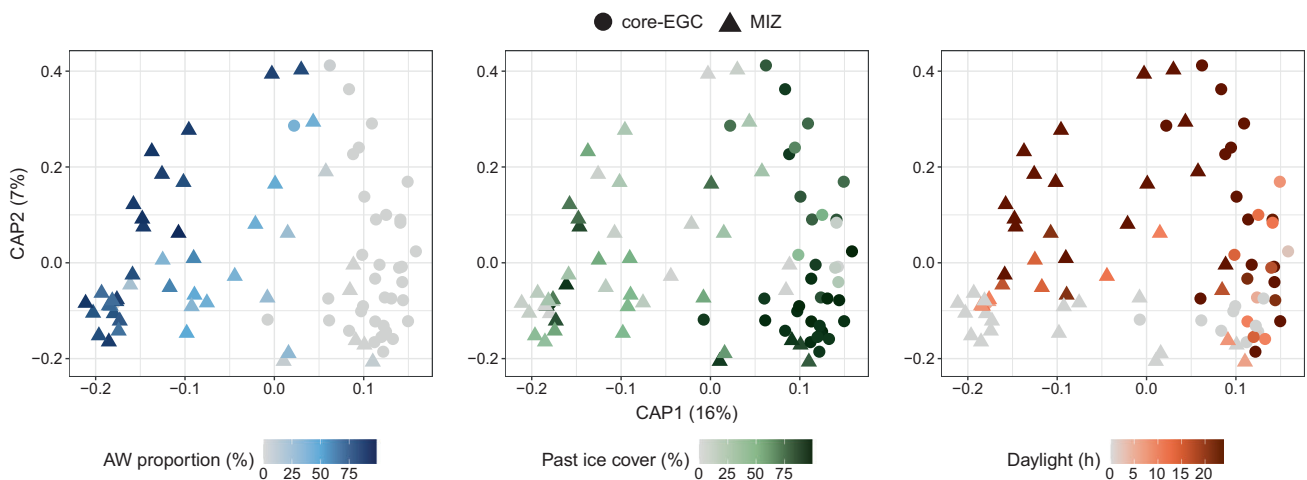


**Fig. 2** Community structure across water mass, sea-ice and daylight conditions. Distance-based redundancy analysis based on Bray-Curtis dissimilarities of community composition along with AW proportion (blue), past ice cover (green) and daylight (orange) as constraining factors. The factors were selected using a stepwise significance test and combined into a single model ( $R^2 = 0.1$ ,  $p = 0.01$ ) that constrains 14% of the total variation. For ease of interpretation, the environmental conditions are visualised individually on the same ordination.

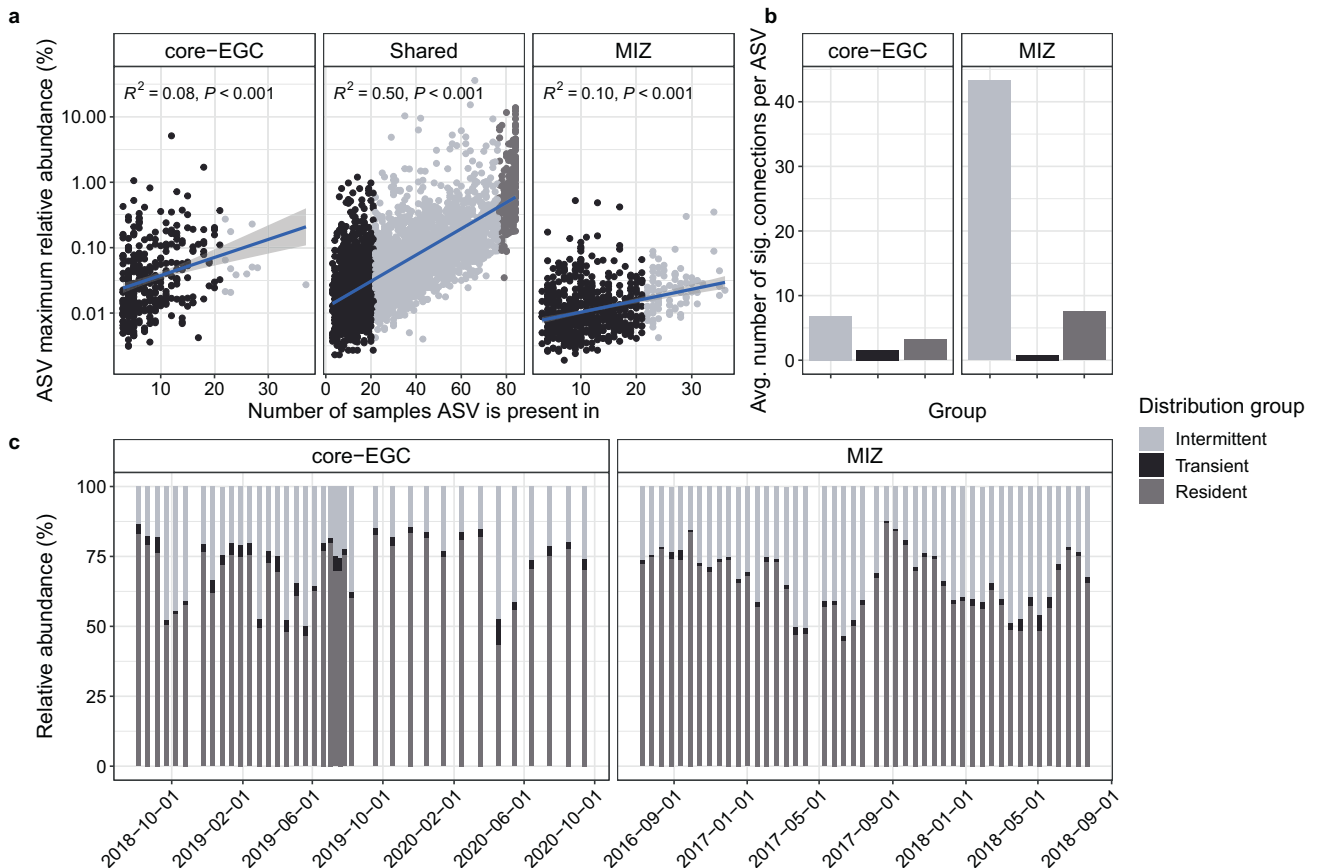


**Fig. 3 Distribution dynamics and co-occurrence of ASVs.** **a** Occurrence of ASVs across samples in relation to their maximum relative abundances, along with categorisation into resident, intermittent and transient. **b** Average number of connections within the co-occurrence networks for resident, intermittent and transient ASVs. **c** Relative abundance dynamics of resident, intermittent and transient ASVs over time.

affiliated with *Colwellia* (asv10; 36%), *Luteolibacter* (asv24; 15%), *Flavobacterium* (asv140; 10%), and *Polaribacter* (asv206; 10%). The resident and intermittent community fractions shared 71 genera, constituting 90% of the genus-level diversity of the resident microbiome. Hence, compositional changes over temporal scales relate to dynamics on the (sub-)species level.

#### Taxonomic signatures of distinct environmental conditions

A sparse partial least squares regression analysis (sPLS) identified 430 ASVs that were associated with distinct environmental conditions. Based on similar, significant correlations (Pearson's coefficient  $> 0.4, p < 0.05$ ) to environmental parameters, the ASVs were grouped into eight distinct clusters (Fig. 4a and Supplementary Table S3), each comprising unique taxonomic signatures (Fig. 4b). The three largest clusters encompassed 88% of the ASVs, and were distinguishable based on their associations to different water mass and ice cover conditions. Clusters C1 and C2 represent AW conditions, with C1 also being associated with low-ice cover. In contrast, cluster C8 represents PW conditions under high-ice cover. In accordance with the distribution dynamics described above, the AW-associated clusters comprised a higher proportion of Int-ASVs, 51–88%, compared to ~50% Res-ASVs in PW-associated clusters. Five smaller clusters (C3–C7) correspond to polar day and night under different ice cover and water mass conditions. Comparing the most prominent ASVs ( $>1\%$  relative abundance) of each cluster revealed unique taxonomic signatures at the genus level (Fig. 4b). For instance, *Amylibacter*, SUP05 and AEGEAN-169 are signatures of the AW-associated, low-ice cluster C1, whereas SAR324, NS2b and *Magnetospira* are signatures of the PW-associated, high-ice cluster C8. Overall, this pattern underlines

that water mass and ice cover have the largest influence on microbial community structure, with a smaller number of ASVs being influenced by daylight and seasonality.

#### MAGs and comparison to other Arctic datasets

Nine PacBio HiFi read metagenomes spanning one annual cycle in the MIZ yielded 43 manually refined, population-representative MAGs, delineated at 99% ANI (Supplementary Table S4). The MAGs were of medium- and high-quality according to MIMAG standards [73], exhibited low fragmentation (average number of contigs = 33), and  $>80\%$  contained at least one complete rRNA gene operon. MAGs covered a broad phylogenetic diversity, including 35 genera, 27 families and nine classes (Supplementary Fig. S4). For deeper ecological insights, we contextualised ASV dynamics with MAGs to link distribution with metabolic potential. Of the 27 ASVs linked to a MAG through competitive read recruitment (100% identity threshold), 18 were associated with sPLS clusters and thus distinct environmental conditions – these are hereon referred to as “signature populations” (Supplementary Table S5). Signature populations included some of the most abundant ASVs, such as asv6-*Polaribacter* and asv7-*Aurantivirga* from cluster C4 (polar day-associated) and asv18-SAR86 from cluster C8 (high-ice, PW-associated).

To corroborate the associations of signature populations with distinct environmental conditions, we assessed their spatiotemporal dynamics across the Arctic Ocean. This comparison included an additional 59 metagenomes as well as 1184 MAGs and metagenomic bins from the Fram Strait [22], the Tara Arctic expedition (TARA) [74], and the MOSAiC expedition [75]. Combined, these datasets provide an extensive geographical and seasonal coverage, from above the continental shelf in summer to the central basin in

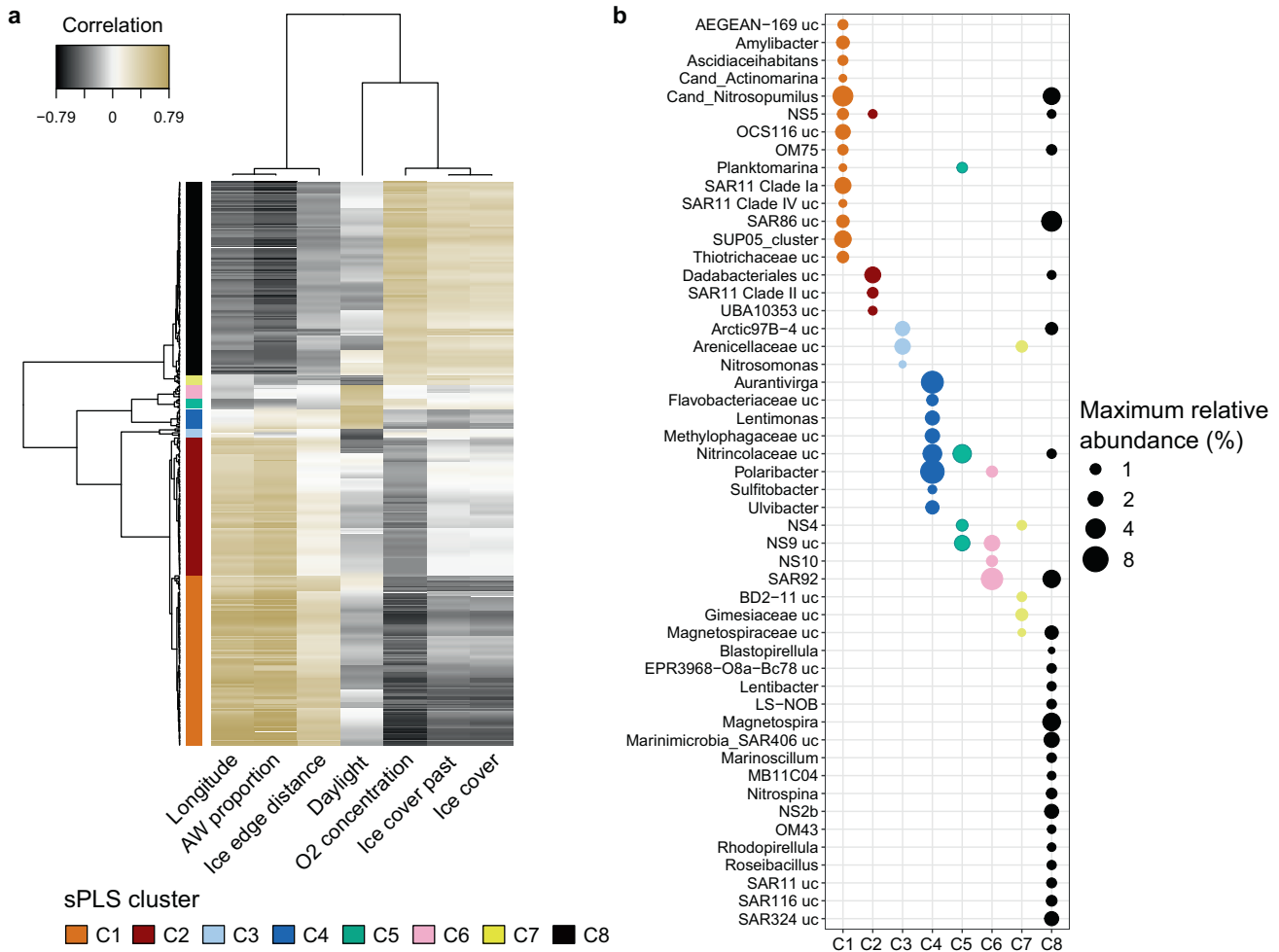


**Fig. 4** Sparse partial least square regression (sPLS) linking community structure and environmental parameters. **a** Heatmap showing eight major sPLS clusters, encompassing 430 ASVs with significant correlations to environmental conditions. **b** Representation of the most prominent genera per cluster. ASVs with <1% relative abundance were excluded, whilst the remaining were grouped by genus and the maximum abundance of each genus shown. Due to high collinearity with AW proportion, temperature and salinity were excluded. Thresholds: coefficients > 0.4,  $p < 0.05$ .

winter. Combining the MAG datasets resulted in 843 species-level clusters at 95% ANI (Supplementary Table S6). Each dataset comprised a mixture of unique and shared species (Fig. 5a), but there were no cosmopolitan species. Of the MAGs recovered in this study, hereon termed FRAM\_EGC MAGs, 42% were unique species. However, these results are influenced by differences in dataset size, sequencing platforms and analysis pipelines, e.g. co-assembly (TARA) vs. single sample assembly (FRAM and MOSAiC).

FRAM\_EGC MAGs were among the most abundant and widely detected (Supplementary Table S7) across the Fram Strait and Arctic Ocean, constituting 0.02–58% of bacterial communities. Their distribution across the wider Arctic supported the dynamics observed in the EGC; e.g. residents (associated with a Res-ASV) were more widely detected than intermittent or transient populations (Fig. 5b, Supplementary Figs. S5 and S6). Three of the resident FRAM\_EGC MAGs, one assigned to OM182 (UBA9659) and two to *Thioglobus*, were detected in >90% of all metagenomes. One of these species did not have a MAG representative in the other Arctic datasets, highlighting that our study contributes novel genomic information towards a better understanding of Arctic Ocean microbial ecology. Furthermore, the dynamics of signature-population MAGs across the Arctic supported their association with distinct environmental conditions. MAGs from cluster C8 (high-ice and PW) and C7 (high-ice

and polar night) reached higher relative abundances in mesopelagic depths (TARA) and during polar night (MOSAIC) (Fig. 5c). In contrast, a higher relative abundance of C4 and C6 (polar day) MAGs occurred in surface water collected during summer (TARA).

### Functional potential of Atlantic and Arctic signature populations

Connecting ASV temporal dynamics and MAG functional potential facilitated predictions on the ecology of signature populations within the context of environmental conditions. Of particular interest were the signature populations of Atlantic (cluster C1) and Arctic (cluster C8) conditions, as they could provide insights into how bacterial community structure and function may shift in the future Arctic Ocean. Comparing the functional potential of MAGs revealed that Atlantic and Arctic signature populations clearly differ in substrate metabolism. In short, signature populations of Arctic conditions harboured genes for autotrophy and the utilisation of bacterial- and/or terrestrial-derived compounds, compared to Atlantic signature populations that were functionally connected to phytoplankton-derived organic substrates. Ecological descriptions of all signature populations and functional gene tables are provided in Supplementary Information and Supplementary Files S1, respectively.

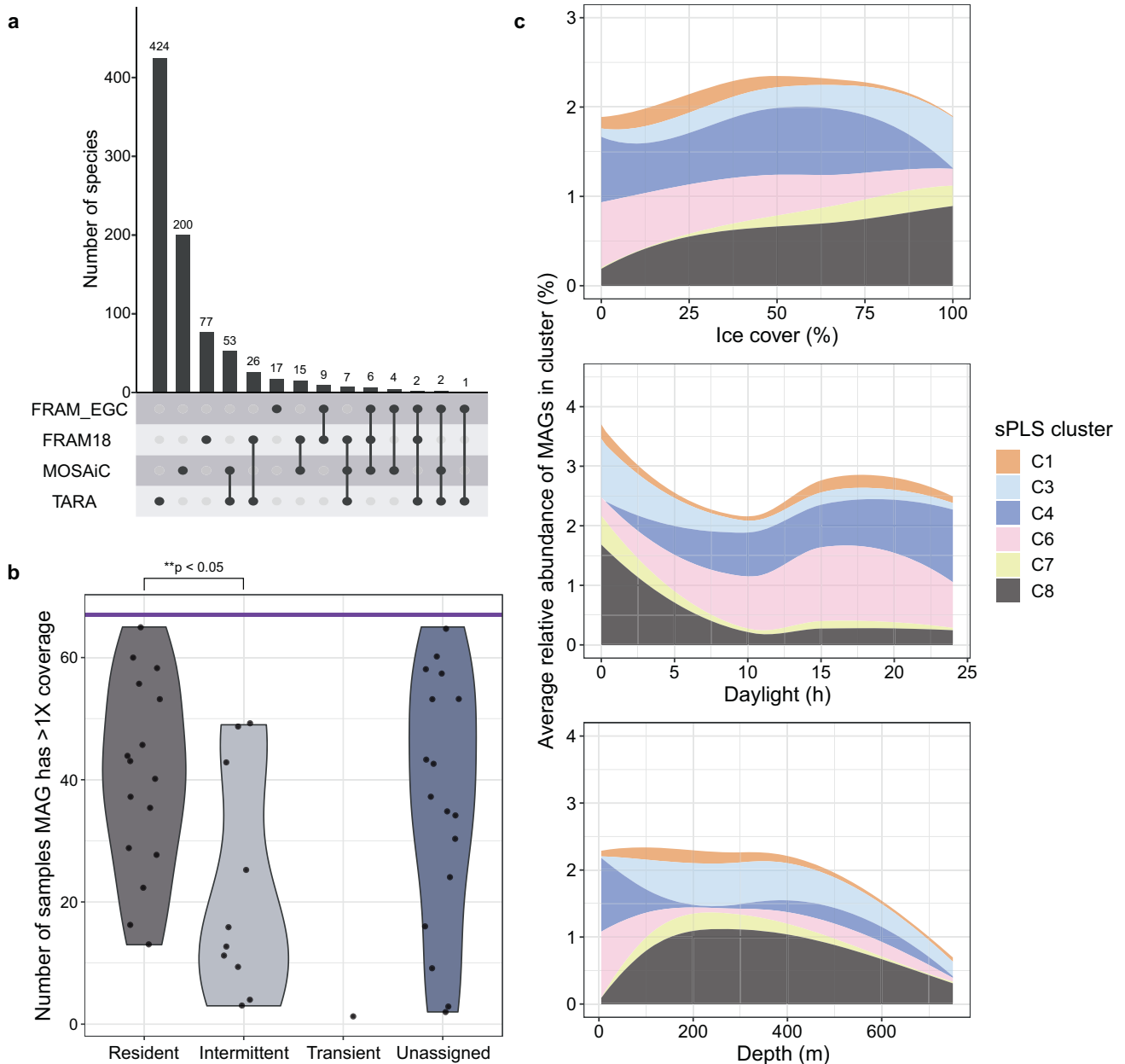


**Fig. 5 Comparison and dynamics of MAGs across the Fram Strait and Arctic Ocean.** We compared metagenome-assembled genomes (MAGs) generated in this study (FRAM\_EGC), and from samples previously collected in the Fram Strait (FRAM18) [23], in the Arctic Ocean during summer (TARA) [34], and in the Arctic Ocean during winter (MOSAIC) [35]. **a** Number of shared and unique species across the four MAG datasets, determined by comparisons at 95% average nucleotide identity threshold. **b** Number of metagenomes in which FRAM\_EGC MAGs were detected with at least 1× coverage. The horizontal purple line represents the total number of samples ( $n = 67$ ). **c** Average relative abundance of sPLS clusters (Fig. 4) across different ice cover, daylight and depth values determined by read recruitment from Arctic Ocean and Fram Strait metagenomes to the respective FRAM\_EGC MAGs. The ~4000 m sample from MOSAIC was not included.

**Atlantic signature populations.** Atlantic signature populations included *Thiotrichaceae* (asv45), OM182 (asv130) and SAR86 (asv157) from the *Gammaproteobacteria* (Fig. 6). Although all three populations were more abundant in the MIZ, differences were observed in their temporal dynamics (asv45 peaking during polar day, asv157 peaking during polar night, and asv130 showing minimal seasonality). The asv45 and asv130 populations both harboured genes for the degradation of phytoplankton-derived organic compounds. For asv45-*Thiotrichaceae*, this included the capacity to oxidise methanethiol (MTO gene) and the downstream reaction products, sulfide (*dsrAB* and *soeABC*) and formaldehyde (H4-MPT-dependent oxidation pathway), which could provide

carbon, sulfur and energy. The asv130-OM182 population encoded a more diverse substrate metabolism, with the capacity to use dissolved organic sulfur (DOS) and nitrogen (DON) compounds, such as taurine and methylamine, as well as carbon monoxide (CO) as supplemental energy source. The capacity to store and use elemental sulfur was evidenced by a polysulfide reductase and flavocytochrome *c*-sulfide dehydrogenase. Together with its flagellar machinery, this suggests a motile, heterotrophic, carboxydovorous lifestyle.

**Arctic signature populations.** Arctic signature populations included *Nitrospina* (asv118), OM75 (asv163), SAR86 (asv18) and

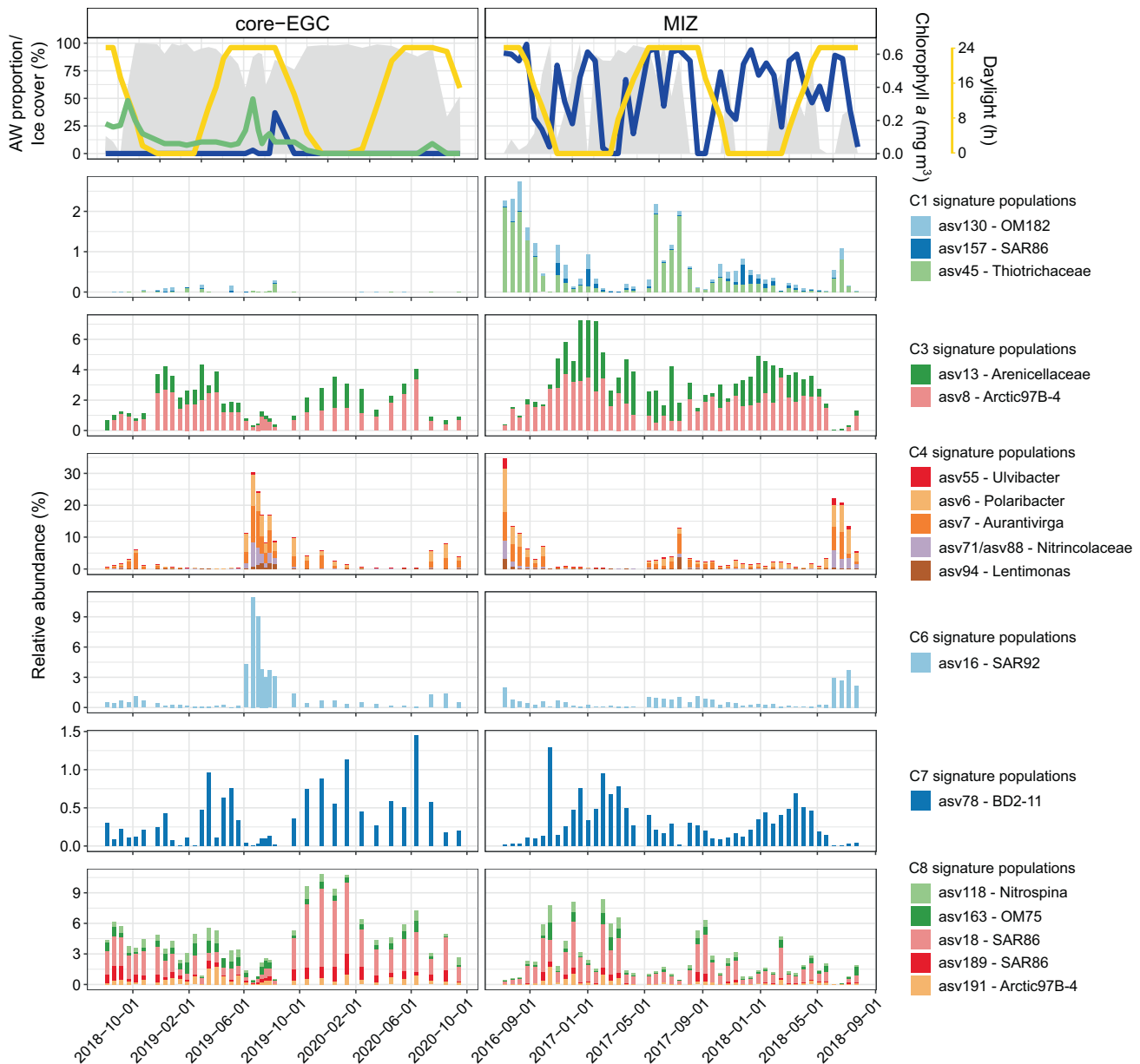


**Fig. 6 Temporal dynamics of signature populations.** Signature populations were identified as ASV representatives from sPLS clusters that a corresponding MAG was recovered for (based on 100% identity threshold competitive read recruitment). The temporal dynamics visualised are derived from ASV data. The missing chlorophyll data in 2016–2018 is due to the lack of a sensor on the MIZ mooring.

asv189) and Arctic97B-4 (asv191) affiliated with cluster C8, as well as BD2-11 (asv78) affiliated with cluster C7 (high-ice and polar night) (Fig. 6). Their metabolic potential and predicted ecological role varied considerably. The most prominent population (asv18-SAR86), reaching 8% relative abundance, harboured a heterotrophic metabolism with the capacity to gain supplemental energy through a green-light proteorhodopsin. Although similar to other SAR86 members [76, 77], asv18-SAR86 has an enriched repertoire of peptidases ( $n = 19$ ) compared to carbohydrate-active enzymes ( $n = 7$ ), as well as genes for D-amino acid metabolism.

Two of the Arctic signature populations were affiliated with enigmatic taxa, including the Arctic97B-4 (*Verrucomicrobiae*; *Pedospharaceae*) and BD2-11 (*Gemmatimonadota*). Arctic97B-4 was shown to be enriched in the particle-attached fraction in the Southern Ocean [78] and in subsurface waters [79, 80]. In comparison, BD2-11 has largely been observed in terrestrial and freshwater environments or in deep-sea sediments [81]. The

genomic content of the Arctic97B-4 population indicated a motile chemomixotrophic lifestyle with the capacity to fix carbon, assimilate sulfate, and synthesise the vitamins riboflavin and biotin. This population encoded a high number of CAZymes (23 genes) and sulfatases (84 genes). The most numerous CAZyme gene families are involved in animal glycan degradation, such as sialic acids (GH33). The BD2-11 population encodes genes for inorganic and organic compound metabolism, including aerobic denitrification (*nap*, *nirk*) and the metabolism of taurine, hypotaurine, D-amino acids, dicarboxylic acids and halogenated haloaliphatic compounds.

#### Whole-community functional shifts with contrasting environmental conditions

The raw HiFi reads contained 17.6 million ORFs (Supplementary Table S8), with 54% being assigned a function and 92% a taxonomy. Expectedly, taxonomic classifications varied in

resolution, with 92% of genes assigned to a kingdom and 37% to a genus (Supplementary Fig. S7). Evident taxonomic shifts over the annual cycle included higher proportions of *Bacteroidia* during polar day and low-ice cover; compared to *Verrucomicrobiae*, BD2-11 and *Marinimicrobia* under polar night and high-ice cover, in agreement with ASV dynamics. A dissimilarity analysis of community functionality separated samples into two distinct clusters, with ice cover being the only statistically significant factor between the two (F-statistic = 12.6,  $p = 0.009$ ) (Supplementary Fig. S8). A total of 1088 differentially abundant genes were identified between the two clusters, with 328 and 845 genes enriched under high- and low-ice conditions, respectively.

**Enriched functions under different ice-cover regimes.** In agreement with Arctic and Atlantic signature populations, the enrichment of genes under high- and low-ice cover suggested differences in substrate utilisation (Supplementary Fig. S9). Low-ice communities were enriched in genes involved in the utilisation of phytoplankton-derived carbohydrates as well as DON and DOS compounds, including dimethylsulfoniopropionate (DMSP), taurine, sulfoquinovose and methylamine (Fig. 7). In addition, glycoside hydrolase families involved in the degradation of laminarin,  $\alpha$ -galactose- and  $\beta$ -galactose-containing polysaccharides (GH16, GH36, GH42 and GH8), and genes related to the metabolism of mono- and disaccharides, such as D-xylose, glucose and rhamnose, were enriched (Fig. 7). All of these compounds have been related to phytoplankton production [82] and can act as carbon, nitrogen and sulfur sources for heterotrophic microbes [83, 84].

Under high-ice cover, 50% fewer genes were enriched, and they were mostly related to the recycling of bacterial cell wall carbohydrates, proteins, amino acids, aromatics and ketone compounds (Fig. 7). Reduced phytoplankton productivity under high-ice cover and during polar night [23] limits the availability of fresh labile organic matter, which would necessitate alternative growth strategies. For instance, the enrichment of an assimilatory nitrate reductase gene (*nap*) indicates a need for utilising inorganic nitrogen compounds. Enrichment of GH109 and GH18 involved in peptidoglycan and chitin degradation [85], along with genes for D-amino acid degradation, indicate an increased reliance on recycling of bacterial-derived organic matter. Furthermore, we observed an enrichment in genes for the degradation of aromatic and ketone compounds, such as phenylpropionate (Fig. 7).

## DISCUSSION

In recent decades, the Atlantic influence in the Arctic Ocean has expanded, a process termed Atlantification [5, 6]. Atlantification encompasses the multi-faceted physicochemical impacts of northward-flowing AW, such as accelerated sea-ice decline, weakened water column stratification and altered nutrient availability. Although its impact on microbial communities has been postulated [14], we provide the first high-resolution analysis over a natural mixing zone between outflowing PW and inflowing AW in Fram Strait to assess potential ecological implications. We show that sea-ice cover and AW influx have a considerable impact on the composition, structure and functionality of bacterial communities. Densely ice-covered PW harboured a temporally stable, resident microbiome capable of using versatile substrates, with an enriched potential to degrade bacterial- and terrestrial-derived substrates as well as inorganic compounds. In contrast, low ice cover and high AW influx coincided with seasonally fluctuating populations that are functionally linked to phytoplankton-derived organic matter. We further identified bacterial signatures of distinct environmental conditions in the EGC (Fig. 8), showed the consistency of these patterns across the wider Arctic Ocean, and assessed ecological roles through MAG-based functional gene content. Our combined

population- and community-level evidence suggests a future “Biological Atlantification” of the Arctic Ocean.

## Bacterial communities under different water mass and ice cover regimes

The pronounced impact of AW influx reflects the role of water masses as physical barriers to and conduits of dispersion for planktonic organisms. Influx events thus result not only in physicochemical changes, but also the mixing of microbial communities. How the microbiomes are reshaped under these events is a function of the degree of influx as well as the size (in number), competitive fitness and physiological adaptations of individual populations. Our dataset reveals that large influx events over short timescales can lead to the “replacement” of populations, evidenced by the dominance of AW-derived populations (Int-ASVs) in the MIZ. In contrast, the core-EGC, with rare occurrences of AW influx, harboured a temporally stable resident community that is adapted to polar conditions and constantly seeded from southward-flowing PW. However, the continual detection of the resident community in the MIZ indicates that even large influx events do not result in complete community turnover. Although the hydrological dynamics assessed here are more rapid than the gradually proceeding Atlantification of other Arctic regions, northward advection of organisms and subsequent replacement has already been documented for phyto- and zooplankton [7, 9, 86].

In addition to AW influx, bacterial communities were significantly impacted by sea-ice cover, which reflects its integral role in shaping Arctic Ocean ecosystems. Of particular significance is the influence of sea ice on water column stratification and organic matter availability. Sea ice supports rich biological communities that contribute significantly to Arctic Ocean primary production and the pool of organic matter [87, 88]. The melting of sea ice results in the release of dissolved and particulate organic matter, which heterotrophic bacteria can be highly responsive to [16, 17, 89]. However, ice-derived meltwater also induces rapid and strong stratification of the water column, which can reduce the mixed layer depth to as little as 5 m [11]. This shallow mixed layer can support prolonged phytoplankton blooms, but also trap the produced organic carbon, delaying vertical export [11]. In contrast, ice-free conditions result in a deeper mixed layer, shorter but more pronounced phytoplankton blooms and a higher response of grazers [11], potentially contributing to an increased availability of organic carbon to communities below. Considering the sampling depth in this study (70–80 m), the bacterial communities likely experienced an indirect influence from sea ice, through its impact on mixed layer depth, mixing and the vertical export of surface water production.

AW influx and sea-ice cover are intrinsically linked in the Eurasian Arctic. Consequently, the majority of signature populations were associated with either Arctic (high-ice and low-AW) or Atlantic (low-ice and high-AW) conditions. Furthermore, these populations were metabolically distinguishable, with Arctic signature populations harbouring genes for chemoautotrophy and the utilisation of bacterial and/or terrestrial-derived compounds. In the Beaufort Sea and Canadian Arctic, heterotrophic *Alphaproteobacteria* (*Rhodobacterales* and *Rhodospirillales*) and SAR324 (Chloroflexi) were shown to encode [90] and transcribe [91] pathways for the degradation of terrestrial-derived aromatic compounds. Similarly, Royo-Llonch et al. [74] described a number of bacteria as Arctic habitat specialists with versatile metabolisms, including the potential for autotrophy and denitrification. In this study, we found further examples of specific adaptations to Arctic Ocean conditions. For instance, the asv18-SAR86 population appears adapted towards proteinaceous and bacterial-derived compounds, with a reduced capacity for carbohydrate degradation compared to other SAR86 [76, 77]. In addition, the asv78-BD2-11 population encodes the capacity to use diverse inorganic and

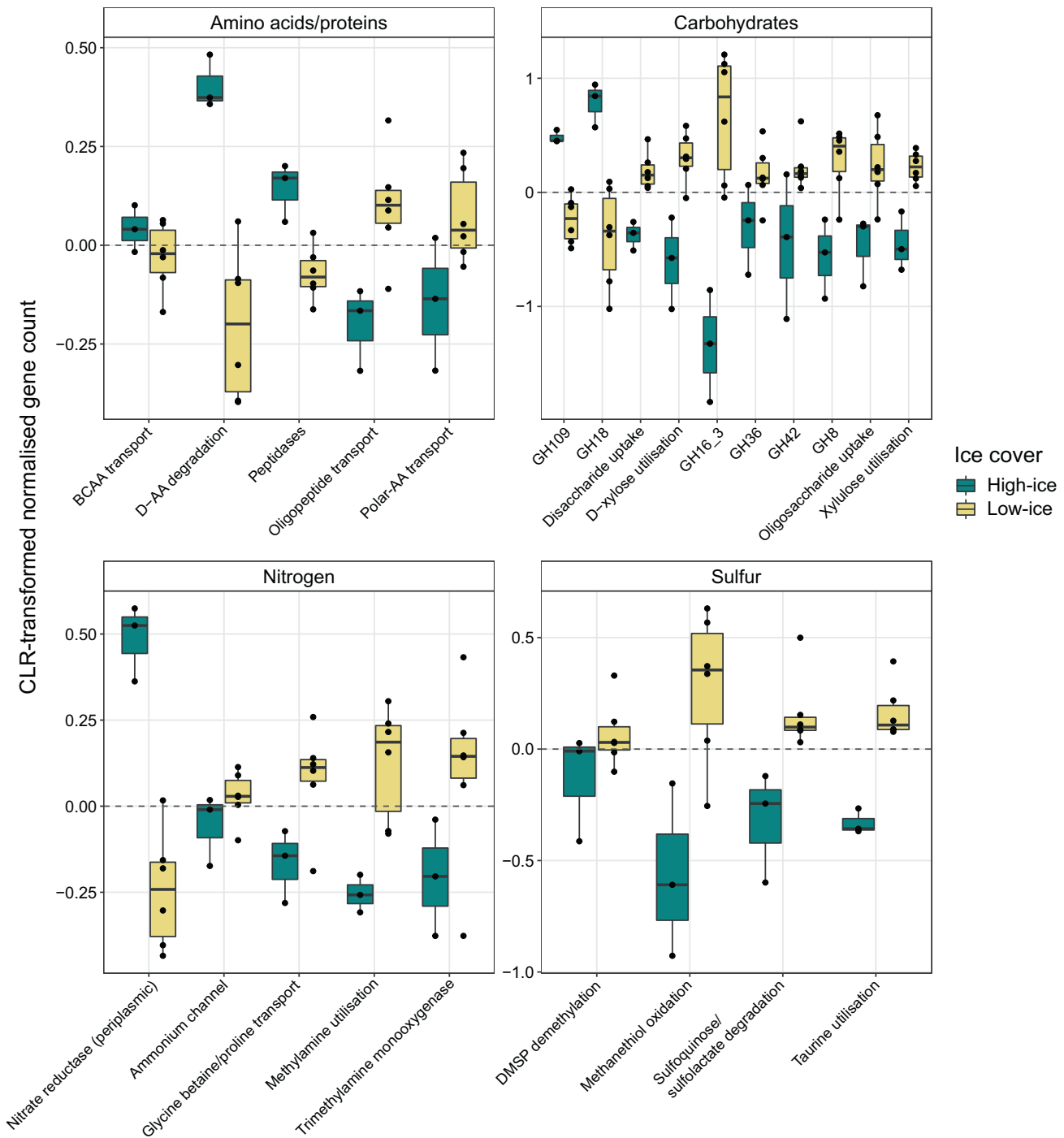


**Fig. 7** Selected genes involved in the metabolism of organic and inorganic compounds enriched under high- and low-ice conditions. Enrichment is displayed as centred-log ratio transformed normalised gene counts. Where several genes of a single pathway or mechanism were identified as enriched, they were grouped into one and the term ‘utilisation’ used (e.g. “taurine utilisation” indicates the uptake and degradation of taurine). When single genes were identified, the corresponding gene names are included. AA amino acids, BCAA branched-chain amino acids, GH glycoside hydrolase.

organic substrates, indicating a high degree of metabolic flexibility. The metabolic distinctions of Arctic signature populations illustrate evolutionary adaptations to the unique hydrological and physicochemical conditions. The Arctic Ocean is characterised by a comparatively large terrestrial and riverine influence [92, 93] and experiences a short productive season with a single phytoplankton bloom, compared to biannual bloom events in temperate oceans. This results in an organic matter pool rich in terrestrial-derived material, up to 33% in the case of DOM

[94], which has likely contributed to the enrichment of distinct metabolic potentials.

Atlantic signature populations featured a closer relation to labile, phytoplankton-derived organic matter. For example, the *asv45-Thiotrichaceae* population harbours genes for the degradation of methanethiol and its downstream reaction products. Methanethiol originates from DMSP demethylation [95], an osmoprotectant produced by phytoplankton. DMSP concentrations in the Arctic Ocean are spatially heterogeneous and

influenced by water mass and sea ice, with highest concentrations in areas with AW inflow [96] where its availability is tightly coupled to chlorophyll [96, 97]. Methanethiol concentrations would thus be elevated in AW during polar day. Similarly, the concentration of CO and its production by phytoplankton is also elevated in temperate compared to Arctic water masses [98]. The asv130-OM182 population encodes genes for CO degradation, as well as a capacity to use DOS compounds and store sulfur that may contribute to sustaining its more stable temporal dynamics in the MIZ. Given that previous reports of such a metabolism are restricted to members of the *Roseobacter* clade [99], the asv130-OM182 population may contribute to connecting carbon and sulfur cycles.

### Connectivity and structuring of bacterial communities across the Arctic

The identification of signature populations not only highlights ecological distinctions associated with different environmental regimes, but also aids in elucidating patterns in dispersal and connectivity in the Arctic Ocean. Although microbial species have been previously associated with certain depth layers and regions in the Arctic [74], this is the first study to evidence tight associations of populations with specific conditions over seasonally and geographically resolved scales. For example, polar day signatures found in the MIZ between 2016 and 2018 were also abundant in surface waters above continental shelves during the summer of 2013 (TARA). In addition, the here identified polar night and high-ice signature populations, which are of particular significance due to limited sampling of these conditions, were also abundant in the central Arctic during winter (MOSAIC). The consistency in dynamics of signature populations over space and time indicates a strong connectivity between Arctic regions, which is in agreement with the relatively short residence times of upper water layers [100]. Consequently, local environmental forcing is likely the key process shaping microbial communities. Furthermore, the prevalence of Arctic winter signatures in mesopelagic depths during summer suggests that solar- and meltwater-induced stratification contribute to shaping bacterial distribution.

In the core-EGC, where conditions are temporally stable, we identified a persistent, resident community fraction. The temporal stability of resident populations in the core-EGC, their variable dynamics in the MIZ, and low detection rate across summer Arctic samples suggests an adaptation to high-ice and PW conditions. However, in order to persist, the populations must be continually seeded from southward-flowing PW, underlining high dispersal and connectivity in the Arctic. Although the presence of a persistent

community fraction has been reported from the Western English Channel and Hawaiian Ocean time-series [71, 72], this is the first such description from the Arctic. It is also a feature likely restricted to the central Arctic and core-EGC, as bacterial communities of continental shelf and peripheral regions are exposed to more dynamic conditions and stronger seasonal forcing.

### Biological Atlantification and future Arctic Ocean bacterial communities

Considering population- and community-level dynamics in concert with contrasting environmental conditions, we predict a Biological Atlantification of Arctic Ocean bacterial communities. Biological Atlantification will be driven by northward advection of populations, coupled with shifting physicochemical conditions from expanding AW influence as well as its associated effects on primary producers and higher trophic levels. There are two underlying mechanisms; “replacement” through advection, mixing and species sorting (as outlined above), and physiological or evolutionary adaptation. We hypothesise that replacement will be more commonplace for bacteria with narrow ecological niches due to their sensitivity to change. In addition, replacement is more likely to occur in the central Arctic and above Eurasian shelves. With ice-free summers predicted by 2050, the central Arctic is shifting to a seasonally dynamic environment. This will reduce the niche space of bacteria that are adapted to permanent ice cover, while benefitting those adapted to conditions of the shelf and peripheral regions. Similarly, the Eurasian shelves will experience the immediate impact of Atlantification along with the northward expansion of temperate species. In short, we envision a net shift in bacterial distribution from shelf regions to the central Arctic, and from the North Atlantic onto the Eurasian Arctic shelves. However, adaptation will also play a role in the reshaping of communities, but will likely be more commonplace among bacteria with wider ecological niches and higher competitive fitness that are less vulnerable to changing conditions (Fig. 8).

### DATA AVAILABILITY

The 16S rRNA gene sequences are available at EBI-ENA under PRJEB43890 (2016–17), PRJEB43889 (2017–18), PRJEB54562 (2018–19), and PRJEB54586 (2019–20). Individual sample accessions are provided in Supplementary Table S9. The metagenomic sequence data and MAGs generated are available at EBI-ENA under PRJEB52171 (accessions provided in Supplementary Table S10). Tara Arctic data are available under PRJEB9740. MOSAiC accession numbers are shown in Supplementary Table S11. Functional gene annotations for all signature populations are provided in Supplementary Files S1. Physicochemical parameters are available under PANGAEA accessions 904565 [68], 941159 [69], and 946539 [70].

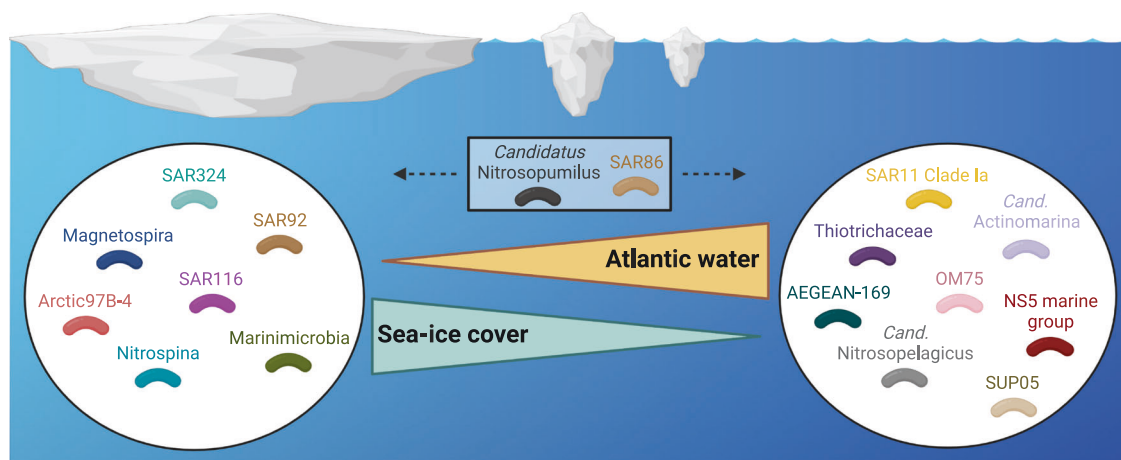


**Fig. 8 Bacterial communities under contrasting AW influx and ice cover conditions.** Illustration showing the ten taxonomic groups with highest average relative abundances under Atlantic vs. Arctic conditions, derived from the relative abundances of Int-ASVs (sPLS cluster C1) and Res-ASVs (sPLS cluster C8), respectively. Figure was generated using Biorender.com.

## CODE AVAILABILITY

Bioinformatic code for reproducing analyses and generating figures, along with necessary data files, is available at [https://github.com/tpriest0/FRAM\\_EGC\\_2016\\_2020\\_data\\_analysis](https://github.com/tpriest0/FRAM_EGC_2016_2020_data_analysis).

## REFERENCES

- Rantanen M, Karpechko AY, Lipponen A, Nordling K, Hyvärinen O, Ruosteenoja K, et al. The Arctic has warmed nearly four times faster than the globe since 1979. *Commun Earth Environ*. 2022;3:1–10.
- Kwok R. Arctic sea ice thickness, volume, and multiyear ice coverage: losses and coupled variability (1958–2018). *Environ Res Lett*. 2018;13:105005.
- Arctic Monitoring and Assessment Programme (AMAP). Snow, water, ice and permafrost in the Arctic (SWIPA). Oslo; 2017. <https://www.amap.no/documents/doc/snow-water-ice-and-permafrost-in-the-arctic-swipa-2017/1610>.
- Notz D, SIMIP Community. Arctic sea ice in CMIP6. *Geophys Res Lett*. 2020;47:e2019GL086749.
- Årthun M, Eldevik T, Smedsrud LH, Skagseth Ø, Ingvaldsen RB. Quantifying the influence of Atlantic heat on Barents Sea ice variability and retreat. *J Clim*. 2012;25:4736–43.
- Polyakov IV, Pnyushkov AV, Alkire MB, Ashik IM, Baumann TM, Carmack EC, et al. Greater role for Atlantic inflows on sea-ice loss in the Eurasian Basin of the Arctic Ocean. *Science*. 2017;356:285–91.
- Oziel L, Baudena A, Ardyna M, Massicotte P, Randelhoff A, Sallée J-B, et al. Faster Atlantic currents drive poleward expansion of temperate phytoplankton in the Arctic Ocean. *Nat Comm*. 2020;11:1–8.
- Lewis KM, Dijken GL, van, Arrigo KR. Changes in phytoplankton concentration now drive increased Arctic Ocean primary production. *Science*. 2020;369:198–202.
- Neukermans G, Oziel L, Babin M. Increased intrusion of warming Atlantic water leads to rapid expansion of temperate phytoplankton in the Arctic. *Glob Change Biol*. 2018;24:2545–53.
- Ardyna M, Arrigo KR. Phytoplankton dynamics in a changing Arctic Ocean. *Nat Clim Chang*. 2020;10:892–903.
- von Appen W-J, Waite AM, Bergmann M, Bienhold C, Boebel O, Bracher A, et al. Sea-ice derived meltwater stratification slows the biological carbon pump: results from continuous observations. *Nat Commun*. 2021;12:7309.
- Rapp JZ, Fernández-Méndez M, Bienhold C, Boetius A. Effects of ice-algal aggregate export on the connectivity of bacterial communities in the central Arctic Ocean. *Front Microbiol*. 2018;9:1035.
- Fadeev E, Rogge A, Ramondenc S, Nöthig E-M, Wekerle C, Bienhold C, et al. Sea ice presence is linked to higher carbon export and vertical microbial connectivity in the Eurasian Arctic Ocean. *Commun Biol*. 2021;4:1–13.
- Carter-Gates M, Balestreri C, Thorpe SE, Cottier F, Baylay A, Bibby TS, et al. Implications of increasing Atlantic influence for Arctic microbial community structure. *Sci Rep*. 2020;10:19262.
- Yergeau E, Michel C, Tremblay J, Niemi A, King TL, Wyglinski J, et al. Metagenomic survey of the taxonomic and functional microbial communities of sea-water and sea ice from the Canadian Arctic. *Sci Rep*. 2017;7:42242.
- Niemi A, Meisterhans G, Michel C. Response of under-ice prokaryotes to experimental sea-ice DOM enrichment. *Aquat Micro Ecol*. 2014;73:17–28.
- Underwood GJC, Michel C, Meisterhans G, Niemi A, Belzile C, Witt M, et al. Organic matter from Arctic sea-ice loss alters bacterial community structure and function. *Nat Clim Change*. 2019;9:170–6.
- Soltwedel T, Bauerfeind E, Bergmann M, Bracher A, Budaeva N, Busch K, et al. Natural variability or anthropogenically-induced variation? Insights from 15 years of multidisciplinary observations at the Arctic marine LTER site HAUS-GARTEN. *Ecol Indic*. 2016;65:89–102.
- Serreze MC, Barrett AP, Slater AG, Woodgate RA, Aagaard K, Lammers RB, et al. The large-scale freshwater cycle of the Arctic. *J Geophys Res Oceans*. 2006;111:C11010.
- de Steur L, Hansen E, Mauritzen C, Beszczynska-Möller A, Fahrbach E. Impact of recirculation on the East Greenland Current in Fram Strait: results from moored current meter measurements between 1997 and 2009. *Deep Sea Res Part I Oceanogr Res Pap*. 2014;92:26–40.
- Hofmann Z, von Appen W-J, Wekerle C. Seasonal and mesoscale variability of the two Atlantic water recirculation pathways in Fram Strait. *J Geophys Res Oceans*. 2021;126:e2020JC017057.
- Priest T, Orellana LH, Huettel B, Fuchs BM, Amann R. Microbial metagenome-assembled genomes of the Fram Strait from short and long read sequencing platforms. *PeerJ*. 2021;9:e11721.
- Wietz M, Bienhold C, Metfies K, Torres-Valdés S, von Appen W-J, Salter I, et al. The polar night shift: seasonal dynamics and drivers of Arctic Ocean microbes revealed by autonomous sampling. *ISME Commun*. 2021;1:1–12.
- Parada AE, Needham DM, Fuhrman JA. Every base matters: assessing small subunit rRNA primers for marine microbiomes with mock communities, time series and global field samples. *Environ Microbiol*. 2016;18:1403–14.
- Fadeev E, Cardozo-Mino MG, Rapp JZ, Bienhold C, Salter I, Salman-Carvalho V, et al. Comparison of two 16S rRNA primers (V3–V4 and V4–V5) for studies of Arctic microbial communities. *Front Microbiol*. 2021;12:637526.
- Quast C, Pruesse E, Yilmaz P, Gerken J, Schweer T, Yarza P, et al. The SILVA ribosomal RNA gene database project: improved data processing and web-based tools. *Nucleic Acids Res*. 2013;41:590–6.
- Callahan BJ, McMurdie PJ, Rosen MJ, Han AW, Johnson AJA, Holmes SP. DADA2: High-resolution sample inference from Illumina amplicon data. *Nat Methods*. 2016;13:581–3.
- Yilmaz P, Parfrey LW, Yarza P, Gerken J, Pruesse E, Quast C, et al. The SILVA and “All-species Living Tree Project (LTP)” taxonomic frameworks. *Nucleic Acids Res*. 2014;42:643–8.
- RStudio Team. RStudio: Integrated development of R. 2020. PBC, Boston, MA.
- Oksanen J, Blanchet FG, Friendly M, Kindt R, Legendre P, McGlinn D, et al. Vegan community ecology package version 2.5-7. 2020. <https://github.com/vegandevs/vegan>.
- Ritchie ME, Phipson B, Wu D, Hu Y, Law CW, Shi W, et al. limma powers differential expression analyses for RNA-sequencing and microarray studies. *Nucleic Acids Res*. 2015;43:e47.
- Le Cao K-A, Rohart F, Gonzalez I, Dejean S. mixOmics: omics data integration project. 2016. R package version 6.1.1. <https://www.bioconductor.org/packages/release/bioc/html/mixOmics.html>.
- Wickham H. ggplot2: elegant graphics for data analysis. New York: Springer; 2016.
- Gu Z, Eils R, Schlesner M. Complex heatmaps reveal patterns and correlations in multidimensional genomic data. *Bioinformatics*. 2016;32:2847–9.
- Machné R, Murray DB, Stadler PF. Similarity-based segmentation of multidimensional signals. *Sci Rep*. 2017;7:12355.
- Csárdi G, Nepusz T, Traag V, Horvát S, Zanini F, Noom D, Müller K. igraph: Network analysis and visualization in R. R package version 1.5.0, 2023. <https://CRAN.R-project.org/package=igraph>.
- Benjamini Y, Hochberg Y. Controlling the false discovery rates: a practical and powerful approach to multiple testing. *J R Stat Soc, B Stat Methodol*. 1995;57:289–300.
- Shannon P, Markiel A, Ozier O, Baliga NS, Wang JT, Ramage D, et al. Cytoscape: a software environment for integrated models of biomolecular interaction networks. *Genome Res*. 2003;13:2498–504.
- Parks DH, Chuvochina M, Rinke C, Mussig AJ, Chaumeil P-A, Hugenholtz P. GTDB: an ongoing census of bacterial and archaeal diversity through a phylogenetically consistent, rank normalized and complete genome-based taxonomy. *Nucleic Acids Res*. 2022;50:785–94.
- Hyatt D, Chen G-L, LoCascio PF, Land ML, Larimer FW, Hauser LJ. Prodigal: prokaryotic gene recognition and translation initiation site identification. *BMC Bioinform*. 2010;11:119.
- Buchfink B, Xie C, Huson DH. Fast and sensitive protein alignment using DIAMOND. *Nat Methods*. 2015;12:59–60.
- Shen W, Ren H. TaxonKit: a practical and efficient NCBI taxonomy toolkit. *J Genet Genomics*. 2021;48:844–50.
- Seemann T. Prokka: rapid prokaryotic genome annotation. *J Bioinform*. 2014;30:2068–9.
- Camacho C, Coulouris G, Avagyan V, Ma N, Papadopoulos J, Bealer K, et al. BLAST+: architecture and applications. *BMC Bioinform*. 2009;10:421.
- Eddy SR. Accelerated profile HMM searches. *PLoS Comput Biol*. 2011;7:e1002195.
- Zhang H, Yohe T, Huang L, Entwistle S, Wu P, Yang Z, et al. dbCAN2: a meta server for automated carbohydrate-active enzyme annotation. *Nucleic Acids Res*. 2018;46:95–101.
- Lombard V, Golaconda Ramulu H, Drula E, Coutinho PM, Henrissat B. The carbohydrate-active enzymes database (CAZy) in 2013. *Nucleic Acids Res*. 2014;42:490–5.
- Barbeyron T, Brillet-Guéguen L, Carré W, Carrière C, Caron C, Czjzek M, et al. Matching the diversity of sulfated biomolecules: creation of a classification database for sulfatases reflecting their substrate specificity. *PLoS ONE*. 2016;11:e0164846.
- Saier MH Jr, Reddy VS, Moreno-Hagelsieb G, Hendargo KJ, Zhang Y, Iddamsetty V, et al. The transporter classification database (TCDB): 2021 update. *Nucleic Acids Res*. 2021;49:D461–D467.
- Rawlings ND, Barrett AJ, Thomas PD, Huang X, Bateman A, Finn RD. The MEROPS database of proteolytic enzymes, their substrates and inhibitors in 2017 and a comparison with peptidases in the PANTHER database. *Nucleic Acids Res*. 2018;46:624–32.
- Aramaki T, Blanc-Mathieu R, Endo H, Ohkubo K, Kanehisa M, Goto S, et al. KofamKOALA: KEGG ortholog assignment based on profile HMM and adaptive score threshold. *J Bioinform*. 2020;36:2251–2.
- Hug LA, Baker BJ, Anantharaman K, Brown CT, Probst AJ, Castelle CJ, et al. A new view of the tree of life. *Nat Microbiol*. 2016;1:1–6.

53. Fernandes AD, Reid J, Macklaim JM, McMurrough TA, Edgell DR, Gloor GB. Unifying the analysis of high-throughput sequencing datasets: characterizing RNA-seq, 16S rRNA gene sequencing and selective growth experiments by compositional data analysis. *Microbiome* 2014;2:15.
54. Li H. Minimap2: pairwise alignment for nucleotide sequences. *J Bioinform.* 2018;34:3094–3100.
55. Nissen JN, Johansen J, Allesøe RL, Sønderby CK, Armenteros JJA, Grønbech CH, et al. Improved metagenome binning and assembly using deep variational autoencoders. *Nat Biotechnol.* 2021;39:555–60.
56. Parks DH, Imelfort M, Skennerton CT, Hugenholtz P, Tyson GW. CheckM: assessing the quality of microbial genomes recovered from isolates, single cells, and metagenomes. *Genome Res.* 2015;25:1043–55.
57. Eren AM, Esen ÖC, Quince C, Vineis JH, Morrison HG, Sogin ML, et al. Anvi'o: an advanced analysis and visualization platform for 'omics data. *PeerJ.* 2015;3:e1319.
58. Sieber CMK, Probst AJ, Sharrar A, Thomas BC, Hess M, Tringe SG, et al. Recovery of genomes from metagenomes via a dereplication, aggregation and scoring strategy. *Nat Microbiol.* 2018;3:836–43.
59. Olm MR, Brown CT, Brooks B, Banfield JF. dRep: a tool for fast and accurate genomic comparisons that enables improved genome recovery from metagenomes through de-replication. *ISME J.* 2017;11:2864–8.
60. Edgar RC. MUSCLE: multiple sequence alignment with high accuracy and high throughput. *Nucleic Acids Res.* 2004;32:1792–7.
61. Capella-Gutiérrez S, Silla-Martínez JM, Gabaldón T. trimAl: a tool for automated alignment trimming in large-scale phylogenetic analyses. *J Bioinform.* 2009;25:1972–3.
62. Price MN, Dehal PS, Arkin AP. FastTree 2 – approximately maximum likelihood trees for large alignments. *PLoS ONE.* 2010;5:e9490.
63. Letunic I, Bork P. Interactive tree of life (iTOL) v4: recent updates and new developments. *Nucleic Acids Res.* 2019;47:256–9.
64. Chaumeil P-A, Mussig AJ, Hugenholtz P, Parks DH. GTDB-Tk: a toolkit to classify genomes with the Genome Taxonomy Database. *J Bioinform.* 2020;36:1925–7.
65. Ludwig W, Strunk O, Westram R, Richter L, Meier H, Yadukumar, et al. ARB: a software environment for sequence data. *Nucleic Acids Res.* 2004;32:1363–71.
66. Pruesse E, Peplies J, Glöckner FO. SINA: accurate high-throughput multiple sequence alignment of ribosomal RNA genes. *Bioinformatics.* 2012;28:1823–9.
67. Orellana LH, Francis TB, Ferraro M, Hehemann J-H, Fuchs BM, Amann RL. Verucomicrobiota are specialist consumers of sulfated methyl pentoses during diatom blooms. *ISME J.* 2022;16:630–41.
68. von Appen W-J. Physical oceanography and current meter data (including raw data) from FRAM moorings in the Fram Strait, 2016–2018. PANGAEA; 2019. <https://doi.org/10.1594/PANGAEA.904565>.
69. Hoppmann M, von Appen W-J, Monsees M, Lochthofen N, Bäger J, Behrendt A, et al. Raw physical oceanography, ocean current velocity, bio-optical and biogeochemical data from mooring HG-EGC-5 in the Fram Strait, July 2018 - August 2019. PANGAEA; 2022. <https://doi.org/10.1594/PANGAEA.941159>.
70. Hoppmann M, von Appen W-J, Barz J, Bäger J, Bienhold C, Frommhold L et al. Raw physical oceanography, ocean current velocity, bio-optical and biogeochemical data from mooring HG-EGC-6 in the Fram Strait, August 2019 - June 2021. PANGAEA; 2022. <https://doi.org/10.1594/PANGAEA.946539>.
71. Gilbert JA, Field D, Swift P, Newbold L, Oliver A, Smyth T, et al. The seasonal structure of microbial communities in the Western English Channel. *Environ Microbiol.* 2009;11:3132–9.
72. Eiler A, Hayakawa D, Rappé M. Non-random assembly of bacterioplankton communities in the subtropical North Pacific Ocean. *Front Microbiol.* 2011;2:140.
73. Bowers RM, Kyrpides NC, Stepanauskas R, Harmon-Smith M, Doud D, Reddy TBK, et al. Minimum information about a single amplified genome (MISAG) and a metagenome-assembled genome (MIMAG) of bacteria and archaea. *Nat Biotechnol.* 2017;35:725–31.
74. Royo-Llonch M, Sánchez P, Ruiz-González C, Salazar G, Pedrós-Alió C, Sebastián M, et al. Compendium of 530 metagenome-assembled bacterial and archaeal genomes from the polar Arctic Ocean. *Nat Microbiol.* 2021;6:1561–74.
75. Mock T, Boulton W, Balmonte J-P, Barry K, Bertilsson S, Bowman J, et al. Multionics in the central Arctic Ocean for benchmarking biodiversity change. *PLoS Biol.* 2022;20:e3001835.
76. Hoarfrost A, Nayfach S, Ladau J, Yooshep S, Arnosti C, Dupont CL, et al. Global ecotypes in the ubiquitous marine clade SAR86. *ISME J.* 2020;14:178–88.
77. Francis B, Urich T, Mikolasch A, Teeling H, Amann R. North Sea spring bloom-associated Gammaproteobacteria fill diverse heterotrophic niches. *Environ Microbiome.* 2021;16:15.
78. Milici M, Vital M, Tomasch J, Badewien TH, Giebel H-A, Plumeier I, et al. Diversity and community composition of particle-associated and free-living bacteria in mesopelagic and bathypelagic Southern Ocean water masses: evidence of dispersal limitation in the Bransfield Strait. *Limnol Oceanogr.* 2017;62:1080–95.
79. Pajares S. Unraveling the distribution patterns of bacterioplankton in a mesoscale cyclonic eddy confined to an oxygen-depleted basin. *Aquat Micro Ecol.* 2021;87:151–66.
80. Chun S-J, Cui Y, Baek SH, Ahn C-Y, Oh H-M. Seasonal succession of microbes in different size-fractions and their modular structures determined by both macro- and micro-environmental filtering in dynamic coastal waters. *Sci Total Environ.* 2021;784:147046.
81. Mujakić I, Piwosz K, Koblížek M. Phylum Gemmatimonadota and its role in the environment. *Microorganisms.* 2022;10:151.
82. Ksionzek KB, Lechtenfeld OJ, McCallister SL, Schmitt-Kopplin P, Geuer JK, Geibert W, et al. Dissolved organic sulfur in the ocean: biogeochemistry of a petagram inventory. *Science.* 2016;354:456–9.
83. Landa M, Burns AS, Roth SJ, Moran MA. Bacterial transcriptome remodeling during sequential co-culture with a marine dinoflagellate and diatom. *ISME J.* 2017;11:2677–90.
84. Moran MA, Durham BP. Sulfur metabolites in the pelagic ocean. *Nat Rev Microbiol.* 2019;17:665–78.
85. Beier S, Bertilsson S. Bacterial chitin degradation—mechanisms and ecophysiological strategies. *Front Microbiol.* 2013;4:149.
86. Ershova EA, Kosobokova KN, Banas NS, Ellingsen I, Niehoff B, Hildebrandt N, et al. Sea ice decline drives biogeographical shifts of key *Calanus* species in the central Arctic Ocean. *Glob Change Biol.* 2021;27:2128–43.
87. Arrigo KR. Sea ice as a habitat for primary producers. In: Thomas DN (ed). *Sea ice*, 3rd ed. Wiley & Sons, New York, 2017. p. 352–69.
88. Fernández-Méndez M, Wenzhöfer F, Peeken I, Sørensen HL, Glud RN, Boetius A. Composition, buoyancy regulation and fate of ice algal aggregates in the central Arctic Ocean. *PLoS ONE.* 2014;9:e107452.
89. Piontek J, Galgani L, Nöthig E-M, Peeken I, Engel A. Organic matter composition and heterotrophic bacterial activity at declining summer sea ice in the central Arctic Ocean. *Limnol Oceanogr.* 2021;66:S343–S362.
90. Colatrinario D, Tran PQ, Guéguen C, Williams WJ, Lovejoy C, Walsh DA. Genomic evidence for the degradation of terrestrial organic matter by pelagic Arctic Ocean Chloroflexi bacteria. *Commun Biol.* 2018;1:90.
91. Grevesse T, Guéguen C, Onana VE, Walsh DA. Degradation pathways for organic matter of terrestrial origin are widespread and expressed in Arctic Ocean microbiomes. *Microbiome.* 2022;10:237.
92. Jones BM, Arp CD, Jorgenson MT, Hinkel KM, Schmutz JA, Flint PL. Increase in the rate and uniformity of coastline erosion in Arctic Alaska. *Geophys Res Lett.* 2009;36:L03503.
93. Gondeev VV, Martin JM, Sidorov IS, Sidorova MV. A reassessment of the Eurasian river input of water, sediment, major elements, and nutrients to the Arctic Ocean. *Am J Sci.* 1996;296:664–91.
94. Opsahl S, Benner R, Amon RMW. Major flux of terrigenous dissolved organic matter through the Arctic Ocean. *Limnol Oceanogr.* 1999;44:2017–23.
95. Kiene RP. Production of methanethiol from dimethylsulfoniopropionate in marine surface waters. *Mar Chem.* 1996;54:69–83.
96. Uhlig C, Damm E, Peeken I, Krumpen T, Rabe B, Korhonen M, et al. Sea ice and water mass influence dimethylsulfide concentrations in the central Arctic Ocean. *Front Earth Sci.* 2019;7:179.
97. Park K-T, Lee K, Yoon Y-J, Lee H-W, Kim H-C, Lee B-Y, et al. Linking atmospheric dimethyl sulfide and the Arctic Ocean spring bloom. *Geophys Res Lett.* 2013;40:155–60.
98. Conte L, Szopa S, Séférian R, Bopp L. The oceanic cycle of carbon monoxide and its emissions to the atmosphere. *Biogeosciences.* 2019;16:881–902.
99. Luo H, Moran MA. Evolutionary ecology of the marine *Roseobacter* clade. *Microbiol Mol Biol Rev.* 2014;78:573–87.
100. Ekwurzel B, Schlosser P, Mortlock RA, Fairbanks RG, Swift JH. River runoff, sea ice meltwater, and Pacific water distribution and mean residence times in the Arctic Ocean. *J Geophys Res Oceans.* 2001;106:9075–92.

## ACKNOWLEDGEMENTS

We thank Jana Bäger, Theresa Hargesheimer, Rafael Stiens and Lili Hufnagel for RAS operation; Daniel Scholz for RAS and sensor operations and programming; Normen Lochthofen, Janine Ludszuweit, Lennard Frommhold and Jonas Hagemann for mooring operation; Jakob Barz, Swantje Ziemann and Anja Batzke for DNA extraction and library preparation, and Bruno Huettel, Christian Woehle and the technicians at the Max Planck Genome Centre in Cologne for metagenome sequencing. The captain, crew and scientists of RV Polarstern cruises PS99.2, PS107, PS114, PS121 and PS126 are gratefully acknowledged. We thank Oliver Ebenhöf and Eva-Maria Nöthig for helpful discussions. Ian Salter made essential contributions during the early phase of FRAM.

## AUTHOR CONTRIBUTIONS

TP performed ASV and metagenomics analysis. MW processed amplicon raw data into ASVs and coordinated the data analysis. TP and MW wrote the paper. WJvA contributed quality-controlled oceanographic data, and coordinated the mooring operations. EO and OP performed network analyses. STV provided quality-controlled chlorophyll data. CB, KM and AB co-designed and coordinated the autonomous sampling and mooring strategy, and contributed to interpretation of the results. TM and WB provided access and background information on MOSAiC data, and contributed to interpretation of the results. BMF and RA contributed to interpretation of the results and development of the story. All authors contributed to the final manuscript.

## FUNDING

Open Access funding enabled and organized by Projekt DEAL. This project has received funding from the European Research Council (ERC) under the European Union's Seventh Framework Program (FP7/2007-2013) research project ABYSS (Grant Agreement no. 294757) to AB. Additional funding came from the Helmholtz Association, specifically for the FRAM infrastructure, and from the Max Planck Society.

## COMPETING INTERESTS

The authors declare no competing interests.

## ADDITIONAL INFORMATION

**Supplementary information** The online version contains supplementary material available at <https://doi.org/10.1038/s41396-023-01461-6>.

**Correspondence** and requests for materials should be addressed to Taylor Priest or Matthias Wietz.

**Reprints and permission information** is available at <http://www.nature.com/reprints>

**Publisher's note** Springer Nature remains neutral with regard to jurisdictional claims in published maps and institutional affiliations.



**Open Access** This article is licensed under a Creative Commons Attribution 4.0 International License, which permits use, sharing, adaptation, distribution and reproduction in any medium or format, as long as you give appropriate credit to the original author(s) and the source, provide a link to the Creative Commons license, and indicate if changes were made. The images or other third party material in this article are included in the article's Creative Commons license, unless indicated otherwise in a credit line to the material. If material is not included in the article's Creative Commons license and your intended use is not permitted by statutory regulation or exceeds the permitted use, you will need to obtain permission directly from the copyright holder. To view a copy of this license, visit <http://creativecommons.org/licenses/by/4.0/>.

© The Author(s) 2023

# Diplom

## PhD

**Matthias Wietz**

Global patterns of marine bacterioplankton diversity and characterization of bioactive *Vibrionaceae* isolates

**GRADEN ER TILDELT DEN**  
DEGREE AWARDED

**20. april 2011**  
20 April 2011

**VÆRTSINSTITUT**  
DEPARTMENT

**Fødevareinstituttet**  
National Food Institute

**VEJLEDERE**  
SUPERVISORS

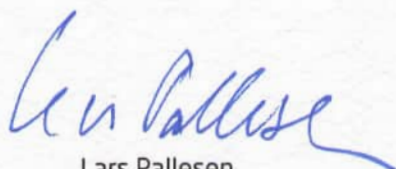
Professor Lone Kirsten Gram

**BEDØMMELSESDVALG**  
ASSESSMENT COMMITTEE

Professor Søren Molin  
Professor James Grant Burgess  
Professor Meinhard Simon

**CPR-NR.**  
DATE OF BIRTH

**021080-3629**  
2 October 1980



Lars Pallesen  
**Rektor**  
President



Martin P. Bendsøe  
**Dekan**  
Dean



**Matthias Wietz**

021080-3629



Danmarks Tekniske Universitet

Indehaveren af dette diplom  
har gennemført en ph.d.-uddannelse, udført det krævede forskningsarbejde og er tildelt ph.d.-  
graden.

Technical University of Denmark

The holder of this diploma  
has been awarded a PhD degree upon completion of a research project as well as the required  
course work.

Ecole Polytechnique du Danemark

Le titulaire de ce diplôme  
s'est vu décerner le grade universitaire de docteur à l'issue de la formation suivie et du projet  
de recherche mené à bien pour l'obtention du grade universitaire de docteur (PhD)

Dänemarks Technische Universität

Der Inhaber / Die Inhaberin dieser Urkunde  
hat ein PhD-Studium absolviert und eine Forschungsarbeit vorgelegt. Er / Sie ist berechtigt,  
den Titel "PhD" zu führen.

Bilag til diplom/diploma supplement

Ph.d.-kontor/PhD-Office

## **Curriculum vitae**

Matthias Wietz, PhD

Born 2<sup>nd</sup> October 1980 in Mülheim an der Ruhr, Germany

### ***Academic career***

04/2024 – 03/2026	Research Scientist (Institute for Chemistry and Biology of the Marine Environment, University of Oldenburg)
10/2018 – 12/2023	Research Scientist (Alfred Wegener Institute for Polar and Marine Research & Max Planck Institute for Marine Microbiology)
10/2013 – 09/2018	Temporary Principal Investigator (Institute for Chemistry and Biology of the Marine Environment, University of Oldenburg)
10/2012 – 09/2013	Postdoctoral Scientist (Scripps Institution of Oceanography, University of California San Diego)
09/2011 – 09/2012	Postdoctoral Scientist (Institute for Chemistry and Biology of the Marine Environment, University of Oldenburg)
02/2008 – 06/2008	Visiting Scientist at Aarhus University (Denmark)
11/2007 – 04/2011	PhD studies (Technical University of Denmark)
05/2006 – 03/2007	MSc thesis (Australian Institute of Marine Science)
07/2004 – 04/2006	Student Assistantship (Max Planck Institute for Marine Microbiology)
10/2001 – 06/2006	Diploma studies in Biology (University of Bremen). Major subjects: Marine Biology, Genetics, Biochemistry

### ***Third-party funding, fellowships and awards***

- AWI DataHub Information Infrastructure program (€100.000 | 2024)
- SPP 1158 Antarctic Research; German Research Foundation (€233.800 | 2023)
- AWI Award for Science Communication (together with AWIs4Future; €2000 | 2020)
- Sequencing Grant; German Research Foundation (€30.000 | 2016)
- Temporary Principal Investigator; German Research Foundation (€177.600 | 2015)
- Conference travel grant; German Academic Exchange Service (€2000 | 2015)
- Research Scientist fellowship; University of Oldenburg (€30.000 | 2015)
- Conference travel grant; German Academic Exchange Service (€2300 | 2014)
- Temporary Principal Investigator; German Research Foundation (€172.300 | 2012)
- Postdoc stipend USA; German Academic Exchange Service (€31.320 | 2012)
- Travel grant; German Academic Exchange Service (€500 | 2006)

### ***Academic services***

- Chair, Gordon Research Seminar “Marine Molecular Ecology” (2017)
- Discussion Leader, Gordon Research Conference “Marine Molecular Ecology” (2017)
- Young Ambassador, International Society for Microbial Ecology (2016–present)

- Council Member, Association of Polar Early Career Scientists (2015–2016)
- Discussion Leader, Gordon Research Seminar “Marine Molecular Ecology” (2015)
- Reviewer for European Research Council, French National Research Agency, Dutch Research Council / Netherlands Polar Programme, National Research Council of Italy, German-Israeli Scientific Cooperation
- Reviewer for PNAS, ISME J, Environ Microbiol, Mol Ecol, Front Microbiol, Sci Rep, FEMS Microbiol Ecol, Aquat Microb Ecol, Prog Oceanogr, Limnol Oceanogr, mSystems, mSphere, Syst App Microbiol, Microbiology, Polar Biol, Microbiome, PLOS ONE, BMC Genomics, Marine Drugs, MicrobiologyOpen, Curr Microbiol, New Biotechnol, Environ Sci Pollut Res, J Mar Sci Engin, Heliyon, Peer Community in Microbiology
- Editor, Frontiers Research Topic “Socio-Ecology of Microbes in a Changing Ocean”
- Scientific Advisor, [Seafields Solutions Ltd.](#) (CO<sub>2</sub> sequestration via *Sargassum* algae)

### **Academic networking and memberships**

- ORCID: <https://orcid.org/0000-0002-9786-3026>
- GoogleScholar: <https://scholar.google.com/citations?user=pDhsWwMAAAAJ>
- ResearchGate: <https://www.researchgate.net/profile/Matthias-Wietz>
- Peer-review record: <https://publons.com/a/396211>
- Bioinformatics code: <https://github.com/matthiaswietz>
- ShinyApp “polaDNAexplorer” for dataset visualization: <https://polardnaexplorer.awi.de>
- International Society for Microbial Ecology (ISME), Association of Polar Early Career Scientists (APECS), Association for General and Applied Microbiology (VAAM)

### **Fieldwork**

- Arctic Ocean / North Pole; RV *Polarstern* (2023)
- Svalbard / Ny-Alesund; AWIPEV station (2021 & 2022)
- Arctic Ocean / Fram Strait; RV *Polarstern* (2019)
- Biological Department Helgoland (2017)
- Pacific Ocean / New Zealand to Alaska; RV *Sonne* (2016)
- Atlantic Ocean / Chile to Germany; RV *Polarstern* (2012)
- Southern Ocean / Antarctica; RV *Polarstern* (2011)
- Arctic Ocean / North Pole; RV *Oden* (2009)
- Coral Sea; RV *Cape Ferguson* (2006)
- North Sea; RV *Heincke* (2005)

### **Invited presentations**

- University Center of Svalbard (2022)
- University of Oldenburg (2022)
- University of Tromsø (2019)
- MIMAS2 Symposium “Microbial Interactions in Marine Systems”, Greifswald (2018)
- GEOMAR Helmholtz Centre for Marine Research, Kiel (2018)
- Workshop “Biogeochemistry of Marine Polysaccharides”, HWK Delmenhorst (2016)
- Young Investigator Session, Gordon Conference “Marine Molecular Ecology” (2015)
- Max Planck Institute for Marine Microbiology Bremen (2015)
- Technical University of Denmark (2014)

### ***Outreach and science communication***

- Jury member of "[Ideenlauf](#)" 2022 (citizen science initiative of German Government)
- Core team member of [AWIs4Future](#) (regional group of Scientists4Future)
- Organizer and co-moderator of "[Sitting Room Science](#)" (scientific livestreams on YouTube), with own presentations on [Arctic time-series](#) and [ocean-atmosphere coupling](#)
- Scientific advice for children's book "[Die Tiefseetaucherin](#)"
- Audiovisual contribution to exhibition "[Change Now](#)" (Maritime Museum Bremerhaven)
- Live interview with Kepler Gymnasium Freiburg (2022)
- Live interview from Svalbard research station for "Science & Shopping" (2021)
- Science communication via Radio Bremen, newspapers (Weser-Kurier, Nordseezeitung), websites ([wissenschaftskommunikation.de](#)) and social media (AWI "[Coffee Break](#)")
- Broadcasting *frost flower* research (e.g. National Geographic, television, school textbooks)
- Presentation of research to the public ("Ocean's Day" at University of Oldenburg, 2015)
- Introduction to ship research for high school students on RV Polarstern (2012)

## **Eidesstattliche Versicherung**

Hiermit versichere ich, dass ich die vorliegende Habilitation selbständig und ohne fremde Hilfe erstellt habe. Alle Quellen wurden ausdrücklich gekennzeichnet. Dabei wurden alle Regeln der guten wissenschaftlichen Praxis beachtet, unter Berücksichtigung der „Ordnung über die Grundsätze zur Sicherung guter wissenschaftlicher Praxis an der Carl-von-Ossietzky Universität“.

Des Weiteren versichere ich, dass ich keine früheren Anträge auf Zulassung zu Habilitation gestellt habe.

Oldenburg, den 30. Januar 2024

Matthias Wietz